DIGITAL PROCESSING OF SATELLITE IMAGES FOR GEOLOGICAL APPLICATIONS WITH EXAMPLES FROM NORTH-EAST SCOTLAND AND NORTH-WEST MALAYSIA

Thesis

Submitted in fulfilment of the

requirement of the degree of

Doctor of Philosophy

at the

Department of Environmental Science

University of Stirling

by

Juhari bin Mat Akhir

May 1990

DISTORTED PAGES IN ORIGINAL

ACKNOWLEDGEMENT

I want to express my deepest appreciation to those who helped me in writing this research. Firstly to my supervisors, Professor Michael F. Thomas, Head, Department of Environmental Science, University of Stirling, to whom I feel a deep gratitude for his persistent supervision and support, thoughtful comments and constructive criticism throughout my period of study, and to Dr Alistair. I. Watson, Lecturer, Department of Environmental Science, University of Stirling, whose help, encouragement and supervision particularly in digital image processing work were invaluable to accomplishing the thesis.

I also owe sincere gratitude to the staff of the University with special mention to; Rob Isbister and Rob Marshall, Computing Advisory Unit, for helping me a lot to solve computing problems in early part of the study; Mary Smith, Cartographer, Department of Environment Science, who produced most of the original colour photographs from slides; and Graham Brown, Technician, AVA Unit, who printed most of the original black and white photographs.

I am indebted to Mr Dunbar, Mrs Fortune and Mr Artchison, Air Photo Unit, Scottish Development Office, Edinburgh, for allowing me to use the facilities and access to the Photo-lab during preliminary photo-interpretation work. With many thanks

to Mr Will, British Geological Survey, Edinburgh, for allowing me to consult geological maps, and publications and for giving information about drift mapping work.

The willingness of my colleague, Dr Ibrahim Abdullah, to search and send many publications related to the study was also highly appreciated and a great help. The assistance of my friends, Haji Mad Sidin Ahmad Ishak in reading all the captions and Abdul Ghani Shafei for allowing me to use his printer for final printing of the thesis, is greatly appreciated. I would also like to thank my friend, Abdul Manan Ali, for his friendship and help in different ways.

With many thanks to the Universiti Kebangsaan Malaysia for giving me a study leave and opportunity to undertake the research, and for the generous financial support for my family. I would like also to thank the Government of Malaysia through her Public Service Department for providing me a scholarship for the study.

I am also indebted to all members of my family for their kindness and support while completing this thesis. Last but not least, my wife Rohayah deserves a special thank-you for the understanding, patience and unquestioning support particularly in difficult moments.

DEDICATION

To my father, Hj Mat Akhir Mk Lela,

and to the memory of my beloved mother,

Hajjah Lijah Hj Yusof (1925-1989).

And to my wife, Rohayah,

to my daughters Sarah Farhana and Najlaa Raihana, and

to my son, Azri Hanif

who are my inspirations.

TABLE OF CONTENTS

page

Acknowledgments ii

Dedication iv

Table of Contents v

List of Figures x

List of Photographs xxiii

List of Tables xxvii

Abstract xxxii

CHAPTER 1: Introduction

1.1 Brief history of remote sensing 3

1.2 Previous works on geological remote sensing 6

1.3 Study areas 11

1.4 Research objectives and methods 18

CHAPTER 2: Physiography and general geology of study areas

2.1 Introduction 23

2.2 The Lochindorb area

2.2.1 Physiography 27

2.2.2 General geology 32

2.3 The Loch Tummel area

2.3.1 Physiography 45

2.3.2 General geology 49

2.4 The Kedah-Perak area

2.4.1 Physiography 58

2.4.2 General geology 63

2.5 Summary 69

CHAPTER 3: Basic principles of remote sensing

3.1 Introduction 71

3.2 Electromagnetic radiation and its properties

3.2.1 Physical characteristics of electromagnetic radiation 72
3.2.2 Atmospheric effects on electromagnetic radiation 80
3.3 Spectral reflectance of earth surface materials
3.3.1 Spectral reflectance of vegetation 87
3.3.2 Spectral reflectance of soils .. 89
3.3.3 Spectral reflectance of water bodies 91
3.3.4 Spectral reflectance of geology .. 92
3.4 Geobotany 94
3.5 Summary 99

CHAPTER 4: Remote sensing system, data acquisition and image processing system
4.1 Introduction 101
4.2 The Landsat satellites
4.2.1 Landsat multi-spectral scanner .. 105
4.2.2 Landsat thematic mapper 109
4.3 Digital image data format 111
4.4 Interactive digital processing system
4.4.1 Digital image analysis display (DIAD) system 113
4.5 Aerial photographs and aerial photo-interpretation 117
4.6 Summary 119

CHAPTER 5: Digital image processing
5.1 Introduction 121
5.2 Preprocessing of remotely sensed data
5.2.1 De-striping method 125
5.2.2 Resampling 126
5.2.3 Atmospheric correction 127

5.3 Enhancement techniques
5.3.1 Contrast enhancement 130
5.4 The derivation of synthetic channels
5.4.1 Arithmetic operation 135
5.4.2 Principal components analysis .. 140
5.4.3 Discriminant analysis 142
5.4.4 Colour display 145
5.5 Filtering techniques
5.5.1 Low-pass filter 149
5.5.2 High-pass filter 150
5.5.3 Nondirectional filter 151
5.5.4 Directional filter 152
5.6 Summary 153

CHAPTER 6: General assessment and comparison of geological information content of the image processing and image products
6.1 Introduction 155
6.2 General assessment of image processing and image products
6.2.1 Unprocessed image 156
6.2.2 Contrast enhancement of original band images 157
6.2.3 Colour composites 170
6.2.4 Principal components analysis .. 185
6.2.5 Discriminant analysis 210
6.2.6 Ratioing 227
6.2.7 Filtering techniques 245
6.2.8 Other processed images 257
6.3 Comparison of the geological information content of enhanced image products 261
6.4 Summary 275

CHAPTER 7: Interpretation of the image processing: lithological and surface material mapping

7.1 Introduction 276

7.2 Surface material mapping of the Lochindorb area 292

7.2.1 Colour association and image-characteristics of cover types .. 298

7.2.2 Photo-characteristics of cover types 303

7.2.3 The interpreted maps and their comparison with the published maps 305

7.2.4 Summary 313

7.3 Geological mapping of Kedah-Perak area .. 313

7.3.1 Colour association and image-characteristics of geological units 315

7.3.2 The interpreted maps and their comparison with the published map 316

7.3.3 Summary 337

CHAPTER 8: Interpretation of the image processing: lineament mapping and analysis

8.1 Introduction 338

8.1.1 Recognition and terminology of lineaments 341

8.2 Data selection and approach in delineation of lineaments 344

8.3 Lineament mapping and analysis of Loch Tummel area

8.3.1 General lineament pattern and distribution 349

8.3.2 Lineament length and frequency .. 365

8.3.3 Summary 370

8.4 Lineament mapping and analysis of Kedah-Perak area
8.4.1 Lineaments and orientation 371
8.4.2 Lineaments and fracture analysis .. 392
8.4.3 Lineaments and rock type 399
8.4.4 Lineaments and mineral deposits .. 404
8.4.5 Summary 408

CHAPTER 9: Conclusions and recommendations
9.1 General remarks on geological remote sensing 409
9.2 Mapping lithology and superficial deposits from satellite images 412
9.2.1 Concluding remarks on the superficial deposits mapping of the Lochindorb area 415
9.2.2 Concluding remarks on the lithological mapping of the Kedah-Perak area .. 423
9.3 Mapping lineament from satellite imagery 430
9.3.1 Concluding remarks on the lineament analysis of the Loch Tummel area .. 432
9.3.2 Concluding remarks on the lineament analysis of the Kedah-Perak area .. 435
9.4 Future recommendations
9.4.1 Geological remote sensing in Scotland (U.K.): lithological mapping .. 437
9.4.2 Geological remote sensing in Malaysia: lithological mapping 444
9.4.3 Geological remote sensing: lineament mapping 447

References 450

LIST OF FIGURES

1.1 Location map of the study areas in Scotland:
A = the Lochindorb Area and B = the Tummel Area 12

1.2 Location map of the study area in Kedah-Perak, Malaysia: A = Sub-area 1 and B = Sub-area 2 .. 14

2.1 Major geological faults in Scotland 24

2.2 Structural outline of the Malaysia Peninsula .. 26

2.3 Topography and drainage of the Lochindorb area 29

2.4 Map of the solid geology in the Lochindorb area 33

2.5 Map of the superficial deposits in the Lochindorb area 34

2.6 Topography and drainage of the Loch Tummel area 48

2.7 Simplified geological map of the Loch Tummel area 53

2.8 Sketch-map of the South Central Highlands showing major faults and area occupied by the study area 57

2.9 Drainage and main topographical peaks of the Kedah-Perak sub-area 1 60

2.10 Drainage and main topographical peaks of the Kedah-Perak sub-area 2 61

2.11 Simplified map of the solid geology in the Kedah-Perak sub-area 1 64

2.12 Simplified map of the solid geology in the Kedah-Perak sub-area 2 65

3.1 Electromagnetic spectrum 74

3.2 Spectral distribution of the energy radiated from black bodies of several temperatures 79

3.3 Solar irradiance at the top of the atmosphere and at sea level 81

3.4 Radiation transmission through the atmosphere by radiant energy of different wavelengths 83

3.5 Idealized spectral reflectance curve for vigorous vegetation, soil and water 88

3.6 Spectral reflectance curves of four surface types: volcanic rocks, altered latite, limonitic volcanics, and tan soil or rhyolite 94

3.7 Simplified spectral reflectance curves for healthy and stressed or senescent vegetation in the visible and near infrared parts of the electromagnetic spectrum 98

4.1 Multi-spectral scanner system (MSS) on Landsat 1, 2, and 3 107

4.2 Arrangement of scan lines and pixels in Landsat MSS and TM images 107

4.3 Path - row coordinates in the Landsat Worldwide Reference System (WRS) for the area around United Kingdom 108

4.4 Schematic layout of the DIAD 68K system 115

4.5 Flow diagram showing the sequence of steps used in processing the MSS computer-compatible tapes and a number of image products generated 118

5.1. Hypothetical reflectance curves showing how ratios enhance minor variations in the curve 137

5.2 Suppression of illumination differences on a ratio image 137

5.3 Elliptical scatter pattern for a hypothetical data set consisting of multi-spectral channels X_1 and X_2. The principal component analysis creates a new set of coordinate axes by a rotation and translation such that the first (Y_1) component accounts for most of the variability. The second axis (Y_2) is chosen orthogonal to the first 143

5.4 Flow diagram showing the general sequence of steps involved in processing the Landsat data in the discriminant analysis 144

6.1 Unprocessed image of the Landsat MSS (band 7) data for the Kedah-Perak sub-area 1 158

6.2 Linear contrast stretched of Landsat MSS (band 7), Lochindorb area 158

6.3 Linear contrast stretched of individual Landsat TM bands, Lochindorb area 159-161

6.4 Linear contrast stretched of Landsat MSS (band 7), Loch Tummel area 163

6.5 Linear contrast stretched of five individual Landsat TM (band 1, 3, 4, 5, and 7) images, Loch Tummel area 163-165

6.6 Linear contrast stretched of individual Landsat MSS bands, Kedah-Perak sub-area 1 167-168

6.7 Several colour composite combination of the Lochindorb area from the Landsat TM data . 175-178

6.8 Standard colour composite combination (band 4 = blue, band 5 = green, and band 7 = red) of Landsat MSS data, Lochindorb area 182

6.9 Colour composite combination of band 7 (blue), band 5 (green) and 4 (red) of the TM data of the Loch Tummel area 182

6.10 MSS band colour composite of the Kedah-Perak sub-area 1 (A) and sub-area 2 (B) 184

6.11 Percentage of variance represented by (A) the six PC images of the Lochindorb area from the Landsat TM data, and (B) the four PC images of the Kedah-Perak sub-area 1 from the Landsat MSS data .. 187

6.12 PC images of the Lochindorb area 189-191

6.13 PC images of the Kedah-Perak sub-area 1 .. 195-196

6.14 TM principal component colour composites of the Lochindorb area 203-204

6.15 MSS principal component colour composite of the Lochindorb area 208

6.16 MSS principal component colour composites of the Kedah-Perak sub-area 1 208-209

6.17 Discriminant function images of the Lochindorb 213-215

6.18 Discriminant function images of the Kedah-Perak sub-area 1 219-220

6.19 TM discriminant function colour composites of the Lochindorb area 225-226

6.20 MSS discriminant function colour composite of the Kedah-Perak sub-area 1 226

6.21 Examples of the TM ratio images of the Lochindorb area 231-235

6.22 Examples of the MSS ratio images of the Kedah-Perak sub-area 1 235-237

6.23 TM band-ratio colour composites of the Lochindorb area 241-242

6.24 MSS band-ratio colour composites of the Kedah-Perak sub-area 1 242-243

6.25 Edge-enhanced images for the MSS band 7 and TM band 5 of the Loch Tummel area 248

6.26 Laplacian add-back filtered images for the Loch Tummel area: (A) MSS band 7 and (B) TM band 5 249

6.27 Edge-enhanced image for the MSS band 7 of the Kedah-Perak sub-area 1 250

6.28 Laplacian add-back filtered image for the Kedah-Perak sub-area 1 250

6.29 Directional filtered images for the Lochindorb area: (A) MSS band 7 and (B) TM band 5 253

6.30 Directional filtered images for the Loch Tummel area: (A) MSS band 7 and (B) TM band 5 254

6.31 Directional filtered images for the Landsat MSS band 7 of the Kedah-Perak sub-area 1 .. 255-256

6.32 TM band (7-4) image of the Loch Tummel area .. 259

6.33 Negative images of TM band 5 of the Loch Tummel area and MSS band 7 of the Kedah-Perak area 259-260

7.1 Surface material map of the Lochindorb based on visual interpretation of the TM image products 283

7.2 The Quaternary map of the Lochindorb area, reduced from the Quaternary map of the United Kingdom 294

7.3 Surface material map of the Lochindorb based on visual interpretation of the TM image products 296

7.4 Map of the superficial deposits of part of the Lochindorb area 297

7.5 TM band-ratio colour composite of the Lochindorb area 299

7.6 TM discriminant function colour composite of the Lochindorb area 300

7.7 TM bands 1-3-4 colour composite combination of the Lochindorb area 301

7.8 Surface material map of part of the Lochindorb area based on the TM imagery, aerial photograph and field visits 302

7.9 Superficial deposits map of the Lochindorb area, Scotland .. .. in-folder

7.10 MSS band-ratio colour composite of the Kedah-Perak sub-area 1 319

7.11 MSS principal component colour composite of the Kedah-Perak sub-area 1 320

7.12 MSS bands 4-5-7 colour composite combination of the Kedah-Perak sub-area 1 321

7.13 Slightly simplified map of the solid geology in the Kedah-Perak sub-area 1 322

7.14 Geological interpretation of the Kedah-Perak sub-area 1 based on the Landsat MSS imagery 323

7.15 MSS band-ratio colour composite of the Kedah-Perak sub-area 2 326

7.16 MSS principal component colour composite of the Kedah-Perak sub-area 2 327

7.17 MSS band colour composite of the Kedah-Perak sub-area 2 328

7.18 Slightly simplified map of the solid geology in the Kedah-Perak sub-area 2 329

7.19 Geological interpretation of the Kedah-Perak sub-area 2 based on the Landsat MSS imagery 330

8.1 Laplacian add-back filtered images for the Loch Tummel area: (A) MSS band 7 and (B) TM band 5 350-351

8.2 Edge-enhanced images for the MSS band 7 and TM band 5 of the Loch Tummel area 352-353

8.3 Lineament map of the Loch Tummel area derived from the lands at MSS images 354

8.4 Lineament map of the Loch Tummel area derived from the Landsat TM images 355

8.5 Rose diagrams of the lineament calculated by both length as well as number of observation on the MSS and on the TM data, Loch Tummel area 357-358

8.6 Rose diagrams of frequency of Landsat lineaments and mapped faults in southern Highland of Scotland 382

8.7 Mapped fault in the Loch Tummel area. The interpreted fault lines depicted on the Landsat and TM as well as on aerial photographs are also shown 353

8.8 Rose diagrams of the Landsat MSS and TM lineaments with different length groups of the Loch Tummel area 368

8.9 Linear contrast stretched of Landsat MSS band 7 of the Kedah-Perak sub-areas 1 and 2 .. 372-373

8.10 Laplacian add-back filtered images of the Landsat MSS band 7 for the Kedah-Perak sub-areas 1 and 2 374-375

8.11 Lineament and circular feature map of the Kedah-Perak sub-area 1 derived from the Landsat MSS images 376

8.12 Lineament and circular feature map of the Kedah-Perak sub-area 2 derived from the Landsat MSS images 377

8.13 Rose diagrams of the lineament calculated by both length as well as number of observation on the Landsat MSS for the Kedah-Perak area 379

8.14 Rose diagrams of the Landsat MSS lineaments of different length groups of Kedah-Perak area .. 380-381

8.15 Rose diagrams of the Landsat MSS lineaments with more than 2 km length and mapped faults of the Kedah-Perak area 384-386

8.16 The structural trendlines of the Northwest domain of the Malaysia Peninsular 387

8.17 Mapped faults in the Kedah-Perak sub-area 1 .. 390

8.18 Mapped faults in the Kedah-Perak sub-area 2 .. 391

8.19 Potential fracture orientations as a result of east-west directed maximum compression 394

8.20 Seven morphotectonic domains of Peninsular Malaysia 395

8.21 Relationship between the rock types and density of lineaments depicted on Landsat MSS of the Kedah- Perak sub-areas 1 and 2 401-402

8.22 The relationship between the mineral deposits and lineament density as depicted on the Landsat MSS images of the Kedah-Perak sub-area 2 .. 406

8.23 The distribution of mineral deposits and intrusive igneous rock (granite) in Kedah-Perak sub-area 2 407

LIST OF PHOTOGRAPHS

2.1 The smooth-flowing slopes characteristic of boulder-clay deposits, at background, are replaced by a very irregular surface forms consist of simple linear ridges or complexes of ridges, hollows and mounds of hummocky-moraine in the valley-floors in the middle .. 31

2.2 Low-relief to hummocky terrain formed by the morainic drift which is believed was deposited by the glacier from the south and sent a lobe of ice toward the north into the study area through this pass 31

2.3 The pelitic gneiss belt of the Central Highland Division ('Old' Moine), forms a higher ground an main ridges in the area 38

2.4 Exposure of psammites and semi-pelites with subordinate quartzite of the Grampian Division ('Young' Moine) 39

2.5 Boulder clay deposits are widely distributed throughout the area and form an almost continuous veneer over the land surface 41

2.6 The typical appearance of the boulder clay deposit in the area, consists of a stiff, stony clay with well-glaciated stones which retain the ice marks, and usually has a yellow or fawn-colour 41

2.7 The typical appearance of the sand and gravel deposit, generally consisting partly of fine sand, partly of stratified sand and fine gravel, and partly of gravel with no regular arrangement, however, it generally well rounded and are not striated 43

2.8 Peat deposits are exposed along the drained channel 43

2.9 The wilderness of basin peat spreads over a very large area of nearly flat plain terrain and overlies the metamorphic rocks of the Grampian Division ('Young' Moine) 44

2.10 Fresh-water alluvium deposits form a few patches of flat surface around the Lochindorb 46

2.11 The Schiehallion, the most conspicuous hill in the area, is underlain by the metamorphic rocks (mainly quartzite) of the Dalradian 46

2.12 The Grampian Division ('Young' Moine) forms rather massive, long rolling slopes and ridges, and has a nearly flat terrain whereas the Dalradian forms a rugged topography with obvious hills and peaks 50

7.1 Glacial deposits are dominated by members of the Heather family (Ericaceae) 282

7.2 Small communities of Gorse which often form dense clumps or thickets on the boulder clay deposits 282

7.3 Boulder clay deposits are dominated by Cross-leave Heath (Bog Heather) in the wetter areas and thicker peat deposits 283

7.4 Most of the improved land areas are underlain by glacial sand and gravel deposits 283

7.5 Alluvium, confined mainly along main drainage channels, is uniformly covered by mixed green and grasses and forms the most important areas of grazing and cultivation 285

7.6 Cover-types on the thick Bog Mosses: (A) purple grass-moor, Cotton-grass and Bog Heather, (B) a variety of Rushes, and (C) note that the area is poorly drained 285-286

7.7 Active screes comprise of lichen-covered angular rock fragments and become increasingly grassed down slope (A), and a thin cover of fescue grass with variable amount of bracken occur on stabilised screes (B) 288

7.8 More than 50% of the exposed bedrock are lichen covered, on top of that, the bedrock in the area is covered by thin heather and grass 289

7.9 Field view of general correlation between landform: surface deposits: vegetation cover over the area 290

7.10 Mixture of grasses in area mapped as alluvium whereas from remote sensing view and field observation the area is classified as peat deposit 311

LIST OF TABLES

2.1 The geological formations and groups of rock occurring within the Lochindorb area 36

2.2 Subdivision of the Moine of the Morar region, Invernesshire 36

2.3 The geological formations and groups of rock occurring within the Loch Tummel area 51

2.4 The stratigraphic successions of the Dalradian in Central Perthshire, including the Loch Tummel area 54

2.5 The geological formations and groups of rock occurring within the Kedah-Perak area 66

2.6 Soil types present in the Kedah-Perak sub-area 2 and their derivation 68

3.1 Wavelengths and frequencies used in satellite remote sensing 75

3.2 Types of atmospheric scatter 81

4.1 Operation periods and characteristics of the Landsat-1 to -5 mission 103

4.2 Landsat-1 to -3 satellite and multi-spectral scanner wavebands 103

4.3 Landsat-4 and -5 satellite and thematic mapper wavebands 104

4.4 Landsat Multi-spectral scanner and thematic mapper bands and their principal applications 110

4.5 The characteristics of the MSS and TM data in the study 112

4.6 The characteristics of the vertical aerial photographs used for the Lochindorb area .. 119

6.1 Means an standard deviation (A) and correlation matrix (B) of the Lochindorb TM 512 x 512 subscene 172

6.2 Optimum Index Factor (OIF) values for the images of the Lochindorb 512 x 512 subscene 173

6.3 Eigenvectors and percentage of the variability of the original data set in the principal component images of the Lochindorb TM 512 x 512 subscene 186

6.4 A: correlation matrix, and B: eigenvectors and percentage of the variability of the original data set in the principal component images of the Kedah-Perak MSS 1024 x 1024 subscene .. 193

6.5 Eigenvectors (A), eigenvalues and discriminating power (B) in the discriminant analysis of the Lochindorb TM 512 x 512 subscene 212

6.6 Eigenvectors (A), eigenvalues and discriminating power in the discriminant analysis (B) of the Kedah-Perak MSS 1024 x 1024 subscene (subarea 1) 218

6.7 Comparison of the geological information content of TM imagery of the Lochindorb area 264

6.8 Comparison of the geological information content of MSS imagery of the Kedah-Perak area 285

6.9 Comparison of the structural information content of TM imagery of the Loch Tummel area 273

7.1 Colour associations, image characteristics and field observation of the main surface deposits and bedrock of the Lochindorb area 304

7.2 Photo-characteristics of the main surface deposits, bedrock an their cover-types of the Lochindorb area 305

7.3 Percentage of the surface material deposits and bedrock in the Lochindorb area 308

7.4 Colour associations and other image characteristics of rock-types of the Landsat MSS for the Kedah-Perak area 317

7.5 Correlation between the image units and the mapped units for the Kedah-Perak area 335

8.1 The azimuthal distribution of lineaments for both Landsat MSS and TM of the Loch Tummel area 380

8.2 The photo-characteristics, geological correlation with the map and interpretation of a new (major) lineament trends on the Landsat TM and MSS images of the Loch Tummel area 386

8.3 Percentage frequency of lineaments for Landsat TM and MSS of the Loch Tummel area 386

8.4 The azimuthal distribution of lineament derived from Landsat MSS of the Kedah-Perak area 382

8.5 Structural strikes in Peninsular Malaysia .. 386

8.6 Several interpreted fracture types in the Kedah-Perak area 388

9.1 List of ATM bands with approximate equivalent with Landsat Thematic Mapper, Landsat Multi-spectral Scanner and SPOT 439

ABSTRACT

This study describes the use of Landsat MSS and TM for geological applications in two Scottish areas: Lochindorb and Loch Tummel; and one Malaysian area: Kedah-Perak. The areas are poorly exposed and highly vegetated.

The data were digitally processed with the objective of producing more interpretable images. The processes include contrast enhancement, ratioing, subtraction, principal component analysis, discriminant analysis, filtering, the combination of images as colour composites, and producing negative images of the data.

Geological interpretation of the most informative images was undertaken by visual interpretation.

In the Lochindorb area, Landsat MSS imagery did not prove useful for superficial deposits mapping, and the resolution offers by the TM is still not sufficient for semi-detailed mapping at scale 1:50,000. The combination of TM imagery and aerial photographs, however, made the mapping task easier and produced "better" map.

In the Kedah-Perak area, textural information is more important than spectral information for lithological interpretation and many image units correlate well with major mapped rocks.

Lineaments are well expressed on Landsat imagery and are mapped for the Loch Tummel and Kedah-Perak areas. The lineament maps for both areas confirm many mapped faults and reveal a new prominent lineaments (probably faults). For the Loch Tummel area, the relative merits of TM versus MSS data were examined. Both produced similar results regarding major lineament orientations, but the TM provides a good improvement over the MSS in the ability to map lineaments. For both areas, lineaments appear to be correlated with geomorphology (lithology), and with the occurrence of ore deposits and probably geologic structure for the Kedah-Perak area.

Landsat imagery can be used to aid lithological mapping in Malaysia, but has not proved useful for Scotland (U.K.) because of different objectives and constraints. However, Landsat imagery is an effective tool in mapping lineaments for both areas.

CHAPTER 1

INTRODUCTION

The name remote sensing, was first used in the early 1960's with reference to a new scientific field (Fisher, 1975). Nowadays, remote sensing is a very commonly used term and has become one of the fastest-growing, most exciting and powerful techniques in many field of studies. Although the term is largely self explanatory, to define remote sensing is not a simple matter and still open for discussion (Fussel et al., 1987; Curran, 1987), and more than one author has at least alluded to the fact that there is no single, concise, and universally accepted definition of remote sensing (e.g., Reeves, 1975; Lintz and Simonett, 1976 and Richason, 1978), but general definition runs: *Remote sensing is the acquiring of data about an object without touching it* (e.g., Holz, 1973; Lintz and Simonett, 1976; Siegal and Gillespie, 1980; Barrett and Curtis, 1982). This definition, like many others, is short, simple, general, and memorable but, unfortunately, not wholly adequate. Short (1982), and others (e.g., Reeves, 1975; Gustafson, 1982; Sabin, 1987) gives a good definition of remote sensing as *the acquisition of data and derivative information about objects or materials (targets) located at the Earth's surface or in its atmosphere by using sensors mounted on platforms located at a distance from*

the targets to make measurements (usually multi-spectral) of interactions between the targets and the electromagnetic radiation.

In the broader definition, gravity and magnetic measurements together with other techniques are also included in remote sensing. However, the most versatile and commonly used of these sources of information, and the majority of remotely sensed data collected for geographic application, are the result of sensors that record electromagnetic energy (Siegal and Gillespie, 1980; Jensen, 1986), while other measurements like magnetism, gravity and radioactivity which are frequently made from aircraft are considered airborne geophysical surveys rather than remote sensing (Sabin, 1987). Throughout this work, therefore, remote sensing is referred and restricted to the use of electromagnetic radiation sensors to record data of the environment, the representation of the results in the form of an image (Watson, 1984), which can be processed, analyzed and interpreted to yield useful information, in this study about geological information. The numerous recent definitions of the field found in the literature, support the contention that remote sensing still is a new and rapidly developing technique.

Apart from a short historical review of remote sensing, in the remainder of this introduction, previous geological remote sensing works will also be discussed. This is followed by the general view of the study area, and the chapter will end with the discussion about research aims and methods.

1.1 Brief history of remote sensing

Remote sensing began with the invention of photography in the Nineteenth Century. At the beginning, aerial photographs were taken from a balloon and after that kites were being used, and then in early 1900s the first aerial photograph was taken from a plane. Airplanes greatly stimulated aerial photography because they provided more reliable and much more controllable platforms compare with balloons or kites.

The capability of photography, apart from its military use, was readily appreciated. The civilian need for aerial photography was increased dramatically between World War I and II for use in geology, forestry, agriculture, cartography etc., and this led to the development of cameras, films and also interpretation equipment or instruments. New films were developed which are able to record not only visible wavelength but also extended to either side in the electromagnetic spectrum, and can produce colour photographs in addition to black-and-white. In addition to aerial photography, other aerial reconnaissance devices, namely thermal infrared and active microwave systems, were also developed during World War II.

The development of unmanned and manned earth satellites began in the late 1950s, and in 1960 saw the first meteorological satellite (Tiros I) launched to provide an orbital view of the Earth. From here started a new era of remote sensing, where further development include, for example, a development of high spatial resolution sensors for land application, operational data collection of atmospheric

information, and the experimentation with new sensors in a variety of wavelengths.

The first satellite designed specifically to collect data of the earth's surface and resources was the Earth Resource Technology Satellite (ERTS-1), which was launched by NASA on July 23, 1972. This event marked the beginning of a completely new era in the approach to the study of a number of scientific disciplines including geology and earth resources. With the launch of Landsat 2 on January 22, 1975, the name of the series was changed from ERTS to Landsat, the latest of which called Landsat 5 and was launched on March, 1984 and is still operating now. Since then many new satellites and sensors have been developed, e.g. SPOT (*Systeme Pour l'Observation de la Terre*) program by the French Government, where the first satellite in this series, SPOT-1 was launched on February 21, 1986, and the Marine Observation Satellite MOS-1 by the Japanese Government was successfully launched on February 19, 1987. Numerous satellite systems are currently being planned by countries throughout the world in order to find out more and more about our environment.

Apart from these satellites which record wavelengths in the visible and infra-red part of electromagnetic spectrum there are other imaging systems which obtain data from different wavelengths, for example radar (either airborne or spaceborne) imaging systems which record data from the microwave region. Radar is an acronym for *radio detection and ranging*, hence as its name implies, radar was developed as a means of using radio waves to detect the presence of objects

and determine their range or position. There are several radar systems such as Doplar radar, plan position indicator radar (PPI) and side-looking radar or airborne radar (SLR or SLAR). However, only SLAR is appropriate to remote sensing application because the PPI system has rather poor spatial resolution while the Doplar radar is a nonimaging radar system. SLAR was first developed for military reconnaissance purposes in the early 1950s. In addition to nearly all-weather operating capability, SLAR is an ideal military reconnaissance system because it is an active, day-or-night imaging system. With an improvement in nonmilitary capabilities, SLAR has evolved into a powerful tool in remote sensing for acquiring natural resource data. Perhaps the largest single boost to the development of applications of radar imaging will be the increased availability of image data from spaceborne systems as in the case of MSS where the launched of Landsat precipitated a boom in the application of space MSS imagery. Radar remote sensing from space began with the launched of Seasat in 1978 and continued with the Shuttle Imaging Radar (SIR) experiments in the 1980s. Radar images from the satellite and spaceborne experiments have revealed interesting patterns, for example about ocean bottom configurations and about underlying bedrock structure to a certain depth (Lillesand and Kiefer, 1987). Radar imagery, however, is currently neither as available nor as well understood as other image products. Notwithstanding this, experience to date suggests that radar imagery, particularly that acquired from satellite platforms, will play an

increasing important role particularly in geological remote sensing application. Consequently, a few satellites planned for launch, for example by the European Space Agency (ERS-1), the Canadian government (Radarsat) and the National Space Development Agency of Japan (JERS-1) are designed to have the radar system on board.

Some basic characteristics of the Landsat is discussed in Chapter 4 (section 4.2). For a comprehensive review of the history of remote sensing, see Fisher (1975) and Simonett (1983), and for the description about other satellites, see Colwell (1983), Lillesand and Kiefer (1987), and Mather (1987).

1.2 Previous works on geological remote sensing

The use of remote sensing techniques in geology to complement geological mapping and mineral exploration have been used for more than a half century. The first airborne ascent for a purely geological purpose took place in 1898, when Albert Heim made a balloon flight over the Alps and the Jura mountains to construct geological cross sections and maps (Mekel, 1978). At the beginning, the use of the techniques, however, have been largely limited to the interpretation of standard black and white aerial photography (Smith, 1943; Johnstone, 1953; Colwell, 1960; Ray, 1960; Miller, 1961; Allum, 1966; Bandat, 1962; and Lattman and Ray, 1965).

These successful photo interpretation techniques in geology have more recently been extended for use with other remote sensing data such as satellite photography. The

earliest indications of the potential value of satellite photography for terrestrial studies were revealed in the geologic experiments using photographs obtained from the Viking and Aerobee rockets (Lowman, 1965). Later, geologic evaluation of Mercury, Gemini, Nimbus and Apollo photographs reaffirmed this potential (Meer Mohr, 1969; Allum, 1970; Lathram, 1972; Lowman, 1973).

The launch of Landsat in 1972 presented geologists with the first opportunity to map large regions of the world. During the past decade images from the Landsat Multi-spectral Scanner (MSS) have been the most appropriate satellite image for use in environmental, dynamic, and geological problems (William and Carter, 1976; Short, 1982). They demonstrated that Landsat images in geological problems were effective, especially for detection of large-scale geologic structures previously unknown and not recognizable on aerial photographs, and also, they indicated that images were useful in preparation of structural maps of regional scale because of their broad coverage under the same conditions. Consequently, many articles have been published on the findings of Landsat images for geological studies. At the beginning most applications, however, have relied mainly on photo interpretation of these synoptic views, i.e by visual interpretation of single or several black-and-white images, rather than on multi-spectral reflectance analysis (Meer Mohr, 1974; Viljoen et al, 1975; Halbouty, 1976; Welby, 1976, Sesören, 1976; MÜhlfeld, 1976; Iranpanah, 1977; Kayan and Klemas, 1978; Barzegar, 1979; Drury and Holt, 1980; Kujansuu

and Koho, 1982; Ahmed, 1983). The development of technology including computer and image processing equipment, however, has changed the trend toward more computer assisted analysis of Landsat MSS (Podwysocki et al, 1977; Condit and Chavez, 1979; Blodget and Brown, 1982; Podwysocki et al, 1983; Rothery, 1985; Guha and Mallick, 1985; Belliss et al, 1985; Warner, 1985; Berhe and Rothery, 1986; Rothery, 1987a; Shazly, 1987; Maude, 1987). More recently, the remote sensing community in geology has gradually shifted its attention away from Landsat MSS imagery to the use of Landsat Thematic Mapper (TM) imagery, which has a wider choice of spectral band and higher resolution as compared with Landsat MSS, (Podwysocki et al., 1983; Drury, 1986a; Davis et al, 1987; Sultan et al., 1987; Rothery, 1987b; Tibaldi and Ferrari, 1988; Kaufmann, 1988; Bagheri and Kiefer, 1989), and most recently, working with images from other platforms, especially SPOT which offers higher spatial resolution than TM (Lunden and Wester, 1988; Styles, 1988). Some of the process and the enhancement techniques as well as the type of images used by the previous workers are mentioned and discussed in the Chapter 5.

Because radar wavelengths are so long they are not affected by the relatively small cloud particles and radar can therefore penetrate clouds and this means that the system can 'see' the ground surface in cloudy conditions. This is one of the advantages of the radar remote sensing systems over others and of great benefit especially in the cloudy mid-latitude and tropical areas like Malaysia. Consequently, apart from the above developments, quite substantial amounts of geological

remote sensing works are carried out by using radar images especially for structural analysis in the mid-latitude and tropical areas which always have a cloud cover (Berlin et al, 1980; Boorder, 1981; Koopmans, 1983; Sabin Jr, 1983; Isiorho, 1984; Blom et al., 1984; Wadge and Dixon, 1984; McDonough and Martin-Kaye, 1984; Nielsen and Stern, 1985; Schultejann, 1985; Koopmans, 1986; Mackenzie and Ringrose, 1986; Borengasser and Taranik, 1988, Alizai and Ali, 1988). In addition to that, a few geological remote sensing works have been carried out using airborne multi-spectral scanner data which has moderately high spectral and spatial resolution than MSS, TM, SPOT and Radar images (Drury, 1986b; Greenbaum, 1987; Smithurst et al., 1987; Saraf et al., 1989). The availability of these two data sources, particularly the airborne multi-spectral scanner, are not worldwide, and hence only a few areas are covered by the data, because at present it is available on experimental basis only.

The best results of geological remote sensing works stem from areas of strong erosion and minimal superficial cover, where bedrock structures exert a strong control over topography at all scales (Drury and Holt, 1980; Chavez, 1983; Marrs and Raines, 1984; Rothery and Drury, 1984). Consequently most published geological studies based on (satellite) remotely sensed images concern of nonvegetated or sparsely vegetated arid and semi-arid environments (Rowan et al., 1974; Viljoen et al., 1975; and many others as quoted before), and more humid and temperate areas where vegetation is in natural communities (Talvitie, 1979; Raines and Wynn,

1982; Kujansuu and Koho, 1982; Brooks and McDonnell, 1983). On the other hand, apart from lineament mapping and analysis (Johnson and Frost, 1977, Tjia and Zaiton Harun, 1975; Drury, 1986a; Parsons and Yeary, 1986; Almashoor and Tjia, 1987; Black, 1987; Maude, 1987; Ringrose and Davenport, 1988), there are very few examples indeed of published geological studies based on satellite remotely sensed images for humid, temperate areas with comparatively poorly exposure, extensive drift cover, highly vegetated and strongly affected by man's influence like Great Britain (Abdelhamid and Vaughan, 1988). It is known that a tropical rain forest zone like Malaysia with a combination of dense vegetation together with thick soil cover, greatly reduces the value of the imagery for geological application, hence will give disappointing results, particularly for lithological mapping. Such terrain, therefore, has been largely ignored by remote-sensing geologists. Unfortunately, these highly vegetated regions, like many others, have to be studied, and surveyed and cannot be neglected simply because of the difficulties which may be encountered when involving satellite remote sensing work. There are at least two reasons for doing this. Firstly, the satellite image, which has broad coverage under the uniform conditions, is the best alternative for those areas which are highly vegetated, poorly exposed and hard-to-reach and where field work is difficult or impossible. Secondly, over two-third of the land surface of the world is covered with vegetation (Draeger and Lauder (1967) quoted by Brooks, 1972), and since developed areas with less natural vegetation will

already have been explored more thoroughly than remoter regions, and because arid or semi-arid regions will have obvious outcrops, it is likely that most of the world's remaining mineral resources will be hidden beneath vegetation, such as the belt of tropical forest. For this reason alone, and with the world's increasing needs for raw materials, these areas are now required to be surveyed and explored, and without doubt the remote sensing technique is the best method for this, at least for the preliminary or reconnaissance stage. This study was carried out in order to use and to assess the usefulness of available satellite remote sensing data for geological applications for such areas (poorly exposed and highly vegetated).

1.3 Study areas

Two areas were chosen for the present study. The first area is located in the Grampian Highland Region, Northeast of Scotland, which is divided into two sub-areas (see Fig. 1.1). The second area covers parts of Perak and Kedah State, Northwest of Malaysia, that is near the border between Malaysia and Thailand (see Figure 1.2) which is also divided into two sub-areas.

The first sub-area is around Lochindorb, northwest of a small town called Grantown-on-Spey (just outside the area), covers approximately 200 km^2, between longitudes 3^0 32' W to 3^0 47' W and latitude 57^0 21' N to 57^0 29' N. It corresponds to the southeast area in the Ordnance Survey (1:50,000),

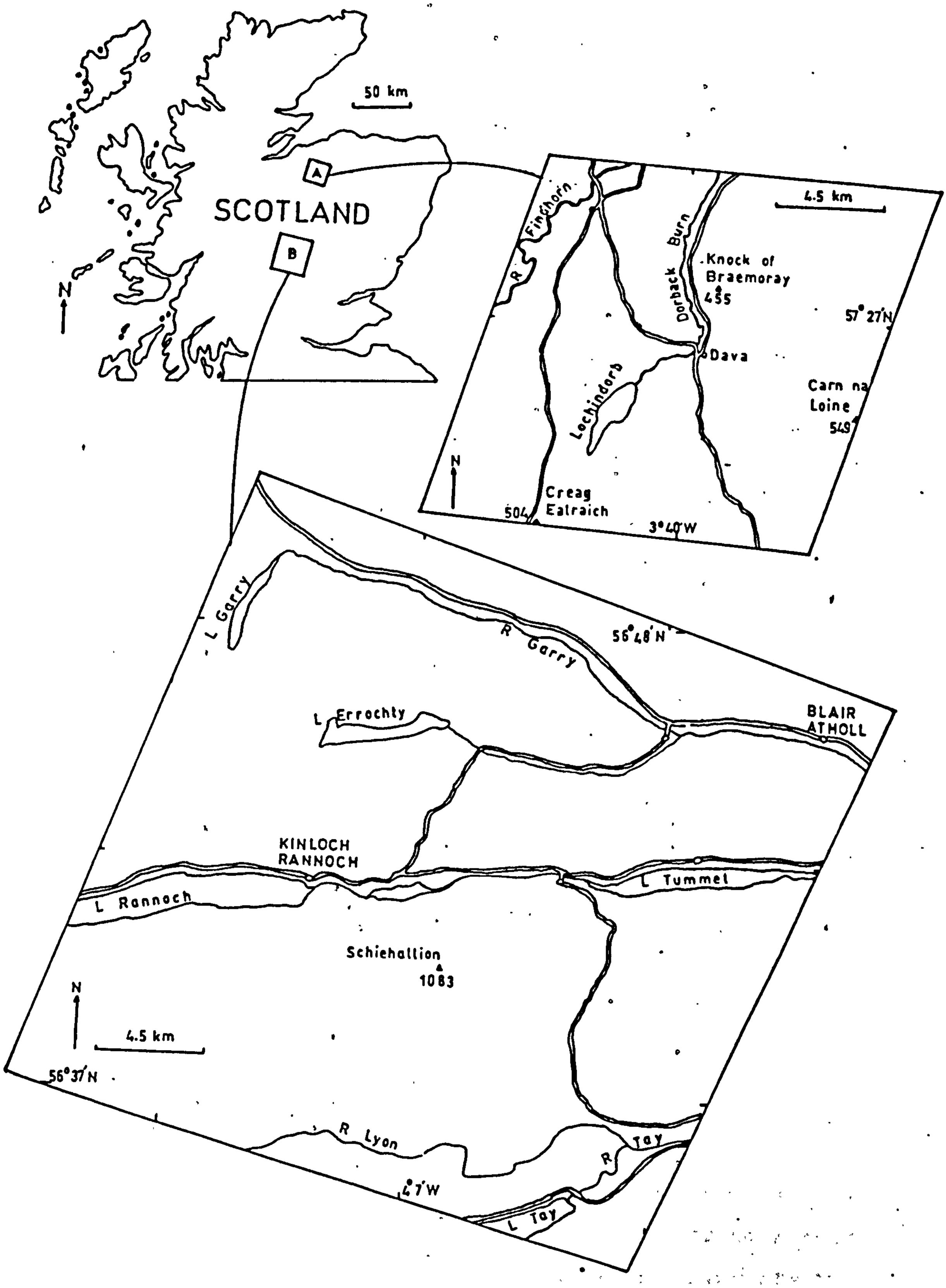

Figure 1.1 Location map of the study areas in Scotland: A = the Lochindorb Area and B = the Loch Tummel Area.

topographic map sheet 27, and on the British Geological Survey the area occupies the southeast part of Sheet 84, (1:63,360) and south part of Sheet 84E (drift map), (1:50,000). The second, is located around Loch Tummel, Loch Tay, Loch Rannoch and Loch Garry which covers approximately 500 km^2 between longitude 3^0 49' W to 4^0 24' W and latitude 56^0 34' N to 56^0 52' N. This sub-area is covered by the Ordnance Survey, (1:50,000) topographic map sheets 42, 43 and 52, and corresponds with the British Geological Survey map sheet 54E, (1:50,000) and sheet 55, (1:63,360). Throughout this work, the first and second sub-areas are called the Lochindorb and Loch Tummel areas, respectively.

The second area, called Perak-Kedah area, occupies an area of approximately 4600 km^2 between longitude 100^0 50' E to 101^0 50' E and latitude 5^0 25' N to 6^0 25' N. It consists of two sub-areas which are called sub-area 1 and sub-area 2, respectively (Figure 1.2).

These areas were chosen for a number of reasons particularly to correspond with the objectives of the study (section 1.4).

Lochindorb area

a. Apart from aerial photographs (approx. scale 1:25,000) and Landsat MSS, the most important thing is that the area is also covered by Landsat TM data, and was the only area in Scotland which is covered by reasonably good quality of Landsat TM scenes to Oct. 1986 archived by the National Remote Sensing Centre. The use of these data

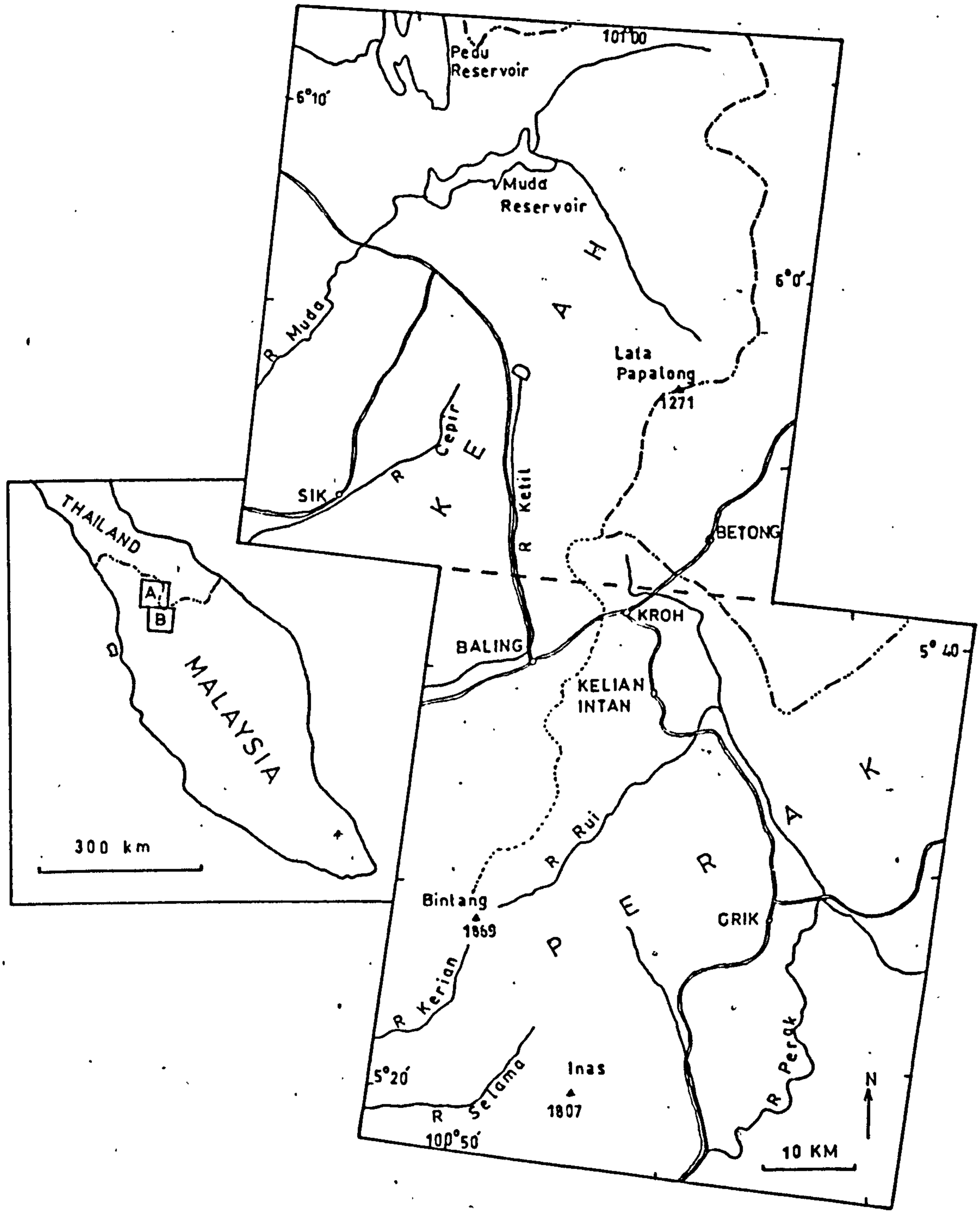

Figure 1.2 Location map of the study area in Kedah-Perak, Malaysia: A = Sub-area 1 and B = Sub-area 2.

for geological application for this particular area can therefore be evaluated.

b. Lithologically the area is not so varied and there are just two metamorphic rock units, namely psammites and semi-pelites with subordinate quartzites and coarse-grained psammitic and siliceous gneisses, interbanded with belts of quartzite and pelitic gneiss, and igneous rock unit, mainly granite, represented (Horne, 1923; BGS, 1954; and Allison et al., 1988). However, there is variety and substantial cover of superficial deposits, like freshwater alluvium, glacial and fluvio-glacial deposits (till, moraines and morainic drift, fluvio-glacial sand and gravel and morainic gravel) and peat (BGS, 1978). As there is such variety between superficial deposits, it was hoped that some differentiation might be observed between them in some processed, remotely sensed images.

c. Beside the solid geologic map (1:63,360), both the Drift edition map of the area (1:50,000) and a soil map (1:63,360) are available for the area. These published data will be used as a reference and as control data in the study.

Loch Tummel area

a. As in the Lochindorb area, in addition to aerial photographs and Landsat MSS, the area is covered by Landsat TM. A comparative study of lineament analysis from different remote sensing data can be performed.

b. It contains a diversity of topography, so it is a more appropriate one for lineament mapping and analysis.

c. A solid geological map (1:63,360) which shows several faults (BGS, 1967), and also a major fault map (Smith, 1961), a Landsat MSS lineament and fault maps of the area (Johnson and Frost, 1977) are available. This made it possible to compare these data with the result of the study.

Perak-Kedah area

a. Up till now only two scenes of Landsat MSS with low percentage of cloud cover and good quality cover parts of Malaysia, and this area is covered by the better of the two. The availability of this scene, means that it can be processed and used for geological work for this tropical region (which most of the time covered by cloud and thus making it difficult to use this type of data).

b. A lineament map of a very small part to the east of the area (Almashoor and Tjia, 1987) and to the south-east of the area (Tjia and Zaiton Harun, 1985) has been made through interpreting hard copy false colour composite and black and white band 7 from the Landsat MSS image, respectively. In addition, Raj (1982) has used Landsat MSS image to make a reappraisal of the Bok-Bak fault zone which runs through the study area and Lai (1987) has compiled a lineament map for an area to the west of the sub-area 1 through interpretation of the standard hard copy of Landsat MSS image. Apart from that, all

geological work in the area (lithological and structural), mostly at local scale have been done based on photo-interpretation of aerial photographs, and no work either at regional or local scale has been published based on digitally processed Landsat MSS data. So, this work is a first attempt to digitally process the Landsat MSS data for the area and to use it for geological application. It is hoped, particularly lineament mapping and analysis which is carried out for the area will give a regional geological picture of the area and act as a guide for more detailed investigations.

c. The area is poorly exposed, hard-to-reach, and underpopulated area where field work is difficult or impossible. Consequently, the geology (lithology) for a large areas in the region so far is studied by using conventional black and white aerial photographs for limited areas and with few field traverses. The Landsat image which has broad coverage under the same condition is possibly the best alternative available in order to get geological information, including lithology, in such difficult areas. Therefore, the study is the first opportunity in applying the Landsat MSS data, which was digitally processed, for lithological mapping for a part of the Peninsular Malaysia area. It is hoped, the outcome of this study will show either that satellite data is a useful tool and can be used for geological application of the area or vice versa due to certain factors such as

dense forest, thick soil cover or perhaps related to the quality and spatial resolution of the data.

1.4 Research objectives and methods

The main aim of this study is to use and to assess the usefulness of available remote sensing data (Landsat MSS and TM) for geological interpretation for the two study areas which belong to different environments and experienced different geological history (see Chapter 2), but both areas are humid, poorly exposed, highly vegetated and strongly affected by man's influence. Specific objectives include:

Lochindorb area

a. To demonstrate the usefulness of multi-spectral remote sensing data, particularly Landsat TM data for geological applications for part of Scotland (glaciated temperate zone).
b. To evaluate a suite of digital enhancement techniques and data products for feature interpretation of the area.
c. To prepare a surface material map based on digitally processed remote sensing data and aerial photographs, and to make comparison with the published map.

Loch Tummel area

a. To examine whether the potential offered by Landsat TM, with its higher spatial resolution than Landsat MSS, would provide a large improvement in the ability to map lineaments.

Perak-Kedah area

a. To examine the usefulness of Landsat MSS data for geologic application, particularly lineament mapping, for this particular area.

b. To produce a regional lineament map and to compare it with the existing geological map.

c. To examine the relationship between image characteristics particularly texture with geological unit (based on published map). To produce a lithological map based on the image characteristics and to compare it with the published map.

In order to achieve the said objectives, the following steps and methods were taken:

Lochindorb area

a. Various image enhancement techniques were applied to the Landsat MSS and TM data with the objective of producing images which best discriminate the geologic units that exist in the study area. Enhanced images which were found to discriminate geologic units best in other areas by previous workers were recreated where possible for comparison and an evaluation of these images made for the study area. These include contrast enhancement, combination of visible and reflected infrared data as false colour composites and as ratios and principal component analysis. In addition, discriminant images

(Watson, per. com., 1987) are also produced for this purpose. The enhancement techniques used and their processed images are discussed in chapters 5 and 6 respectively.

b. The general assessment and geological evaluation of digitally processed and enhanced data products are carried out in terms of their photo characters, enhancement of subtle images and feature identification, and presented in the Chapter 6.

c. The surface material map was prepared based on information from processed images combined with data from conventional aerial photo interpretation, and with limited field visits. The usefulness of remote sensing data for this purpose is examined by comparison between this map with the existing map. Relationships between various spectral responses and other photo characteristics with the corresponding cover types was determined during field visits which were carried out in early August 1988 to early November 1988, and in May 1989.

Loch Tummel area

a. Several methods were used in order to enhance linear features in Landsat MSS and TM data. These include arithmetic operation, edge enhancement and filtering. All the techniques and their results are discussed and presented in Chapters 5 and 6 respectively, and lineament

mapping and analysis is carried out on images within which linear features are best shown.

b. The lineament maps prepared from Landsat MSS and TM are compared in terms of frequencies, orientations and lengths of lineaments. The result of this analysis is discussed in the Chapter 8 and compared with published data.

Perak-Kedah area

a. As for the Lochindorb area, the Landsat MSS data of this area have also gone through similar enhancement techniques with the objective of producing images which best enhance the geologic units in the area. The relationship between image characteristics and geological units is examined, and the possibility of using this relationship together with lineament characteristics for general lithological mapping of the area is proposed (Chapter 7). The lithological map was compiled based on this relationship and compared with the published map (Chapter 8).

b. The Landsat MSS data of this area have also gone through various processes in order to enhance linear features. The best images were chosen for use in preparing the lineament map (Chapter 8).

c. The lineament map was analyzed and compared with the geological map. The relationship between the lineaments and geologic structures (faults), lineament and rock-

types and its potential usefulness in mineral exploration are discussed in Chapter 8.

CHAPTER 2

PHYSIORAPHY AND GENERAL GEOLOGY OF STUDY AREAS

2.1 Introduction

Both study areas, the Lochindorb and the Loch Tummel areas of the Scottish Grampian Highlands form the central part of a regional structural unit, the Grampian High (Ziegler, 1982), and are located between two major geological faults, the Great Glen Fault on the north and the Highland Boundary Fault on the south (Figure 2.1). Therefore the area belongs to a complex fracture-zone, along which movements, not all affecting the total length, have taken place from Arenig - Lower Ordovician (or perhaps earlier) times to Tertiary times (Anderson and Owen, 1980). Although the Grampians represent the highest land in Britain, the study areas are by no means all mountainous, rather they contain a diversity of topography, including both upland and lowland areas, and topographically they form part of the Grampian surface (Gemmell, 1975). Apart from small areas which are formed by the intrusive igneous rocks, the remainder of the area is occupied by metamorphic rocks, the Moine and Dalradian. The description of the rocks in Scotland has been given by many workers: Johnstone (1966), Rayner (1976), Whittow (1977), and Anderson and Owen (1980) described the rocks in the Grampian Highland, Scotland, while Barrow et

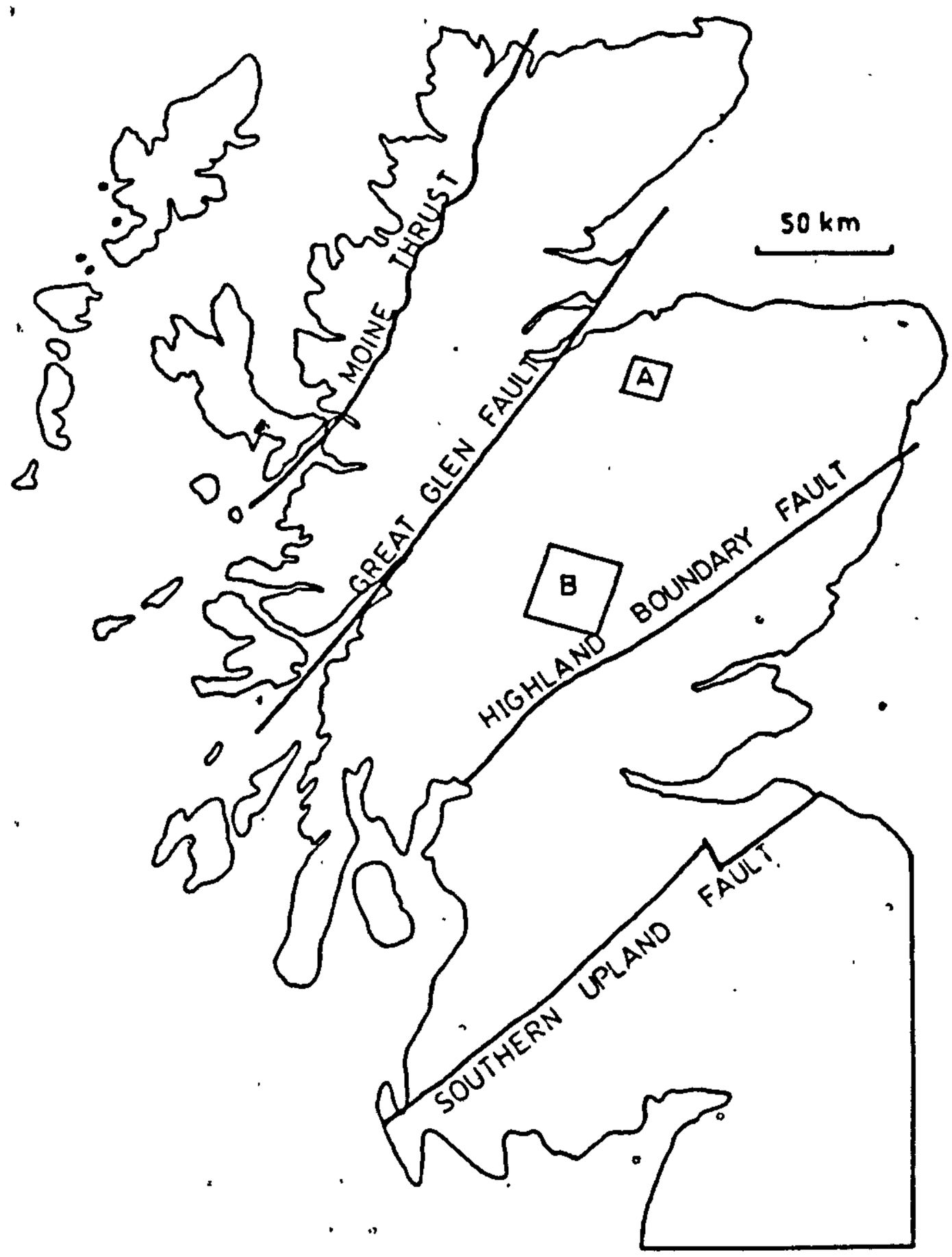

Figure 2.1 Major geological faults in Scotland (after Baird, 1988). The study areas (A and B) are located between the two of the major faults.

al. (1905) and Horne (1923) described the rocks which occur in the Loch Tummel and Lochindorb areas, respectively. More recently, Johnson (1983) has given an authoritative statement of the rocks in Scotland, while Piasecki (1980) has described the Moine rocks of the Central Highlands of Scotland. The solid rock is overlain by various Recent superficial (drift) deposits including boulder clay (till), fluvio-glacial sands and gravels, peat, alluvium and scree, and therefore rock exposures are very limited and consist only of approximately 5% to 10% of surface area; mostly restricted to the main ridges. Apart from superficial deposits, the area is covered by substantial vegetation cover probably exceeding 90 per cent overall. In general terms the area experiences climatic conditions which are surprisingly mild (mean temperature of between 3^0C and 4^0C in January and 13^0C and 15^0C in July) in relation to its latitudinal position (57^0N) and receives more than 1,000 mm of precipitation per year (Price, 1983). Because of its low potential evapotranspiration rate of only about 400 mm (Price, 1983), a large proportion of the soils are waterlogged for long periods and anaerobic conditions prevail and commonly lead to peat formation.

The Perak-Kedah area, belongs to the western zone of structural outline of the Malaysian Peninsula (Figure 2.2), which has a sinuous trend of the regional strike (trends shown by the strikes of bedding, fold axes and by the elongation of plutonic bodies) (Gobbett and Tjia, 1973). The area comprises mainly hilly and mountainous terrain except in the northwest parts where it is mainly lowlying. Generally, the mountainous

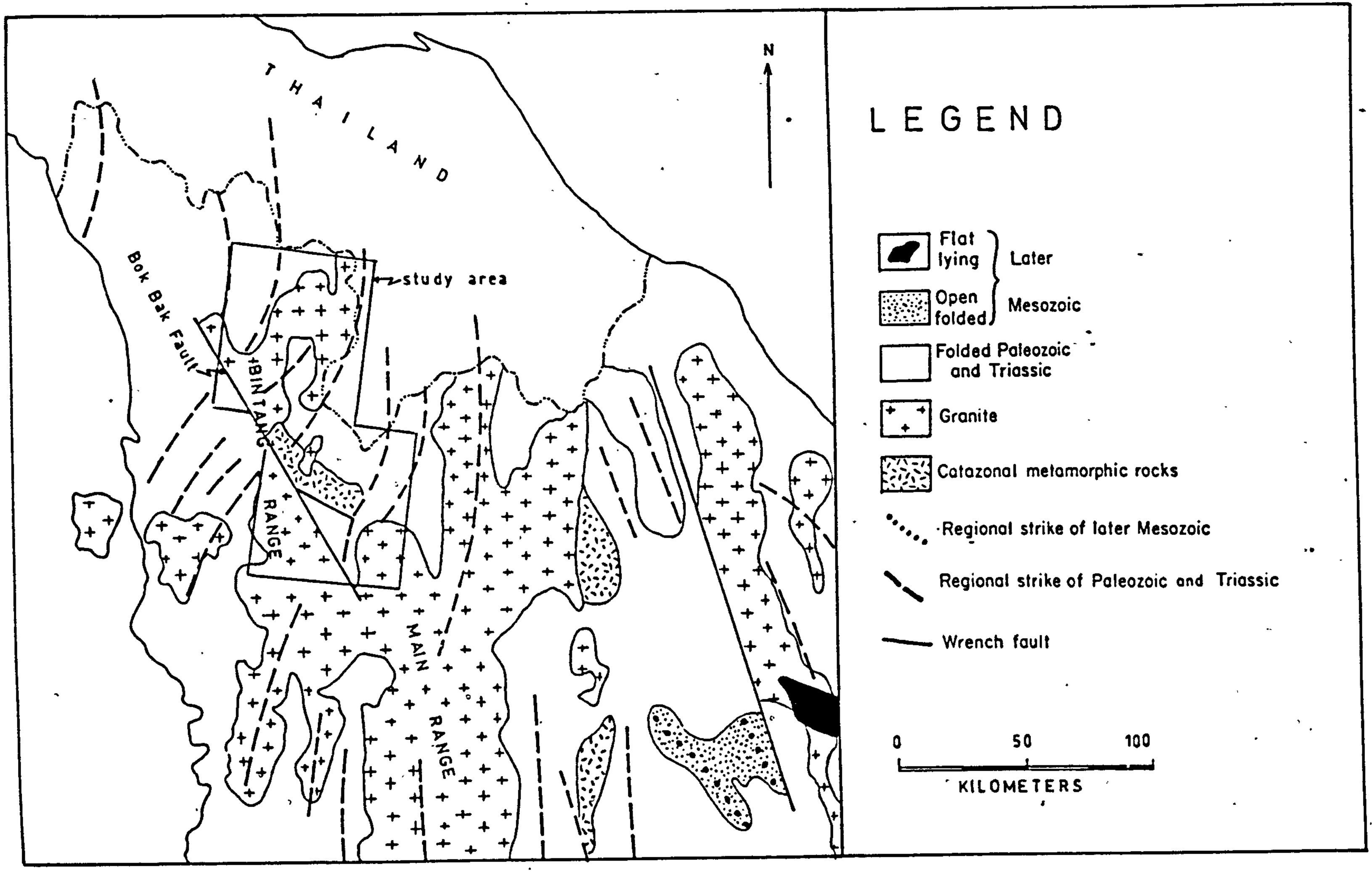

Figure 2.2 Structural outline of the Malaysia Peninsula (after Gobbett and Tjia, 1973). Study area is included in the western zone of the outline which has a sinuous trend of the regional strike.

and rugged hilly areas are underlain by intrusive igneous rocks, areas of subdued relief are underlain by metamorphic rocks, whereas the lowland areas are underlain by sedimentary rocks. Because of its equatorial latitudinal situation (5^0N), the area is subject to a humid tropical climate which is characterized by uniform, fairly high temperatures varying from about 30^0C to 40^0C, and copious rain fall with an average of approximately 2200 mm annually, fairly evenly distributed throughout most of the years (Burton, 1970; Jones, 1970). The area is almost completely covered by tropical rain forest and agricultural plantation. Apart from that, tropical weathering of bedrock leads to an accumulation of a blanket of residual material overlying the unweathered bedrock. Generally, this forms a relatively thick mantle of soil and subsoil which occur almost over entire area.

Further discussions about physiography and general geology for each of the study area are the subjects of the following sections.

2.2 The Lochindorb area

2.2.1 Physiography

Topographically, the area can be divided into two groups. The southern and northeastern parts of the area comprise a dissected portion of the Highland tableland, which slope north and northwestward to the lowland fertile areas of the Findhorn and its tributaries (Figure 2.3). The highlands show a general tendency for the ridges and hill tops to reach up to a more or less uniform level of about 450 to nearly 500 m with a number

of peaks, for example, Creag Liath (450 m), Craig Tiribeg (486 m) and Carn Ruigh Chorrach (484 m). The area between the Dorback burn and the River Divie forms a bleak moorland where the Knock of Braemoray (455 m) is its most prominent feature (Figure 2.3).

The whole area is bounded by two main rivers, the Findhorn on the northwest and the Spey (just outside on the southeast) respectively. However, most of the area is drained by the Findhorn's tributaries like the River Divie (its largest affluent), Dorback Burn and Anaboard Burn where their courses are northerly (Figure 2.3). This direction corresponds with the general topographical slope of the area and there is no indication that the direction of the drainage in the area is structurally controlled. About 4.5 km southeast of Lochindorb, a well-marked depression occurs which follows the course of the Anaboard burn northwards to the Dorback valley. Hinxman (1915) found that this depression is continuous with the hollow which runs southwards to the valley of the Dulnan (out side of the study area in the south) and this hollow is interpreted as a probable early pre-Glacial course of the River Dulnan northwards into the present valley of the Dorback and Anaboard burn. The Lochindorb is the largest water body within the area, with a maximum depth of 51 feet but nearly one-half of its floor being covered by less than 10 feet of water (Hinxman, 1910). Its waters are to a large extent retained by the thick glacial deposits. The remaining lochs which are much smaller in size and depth lie in hollows in the

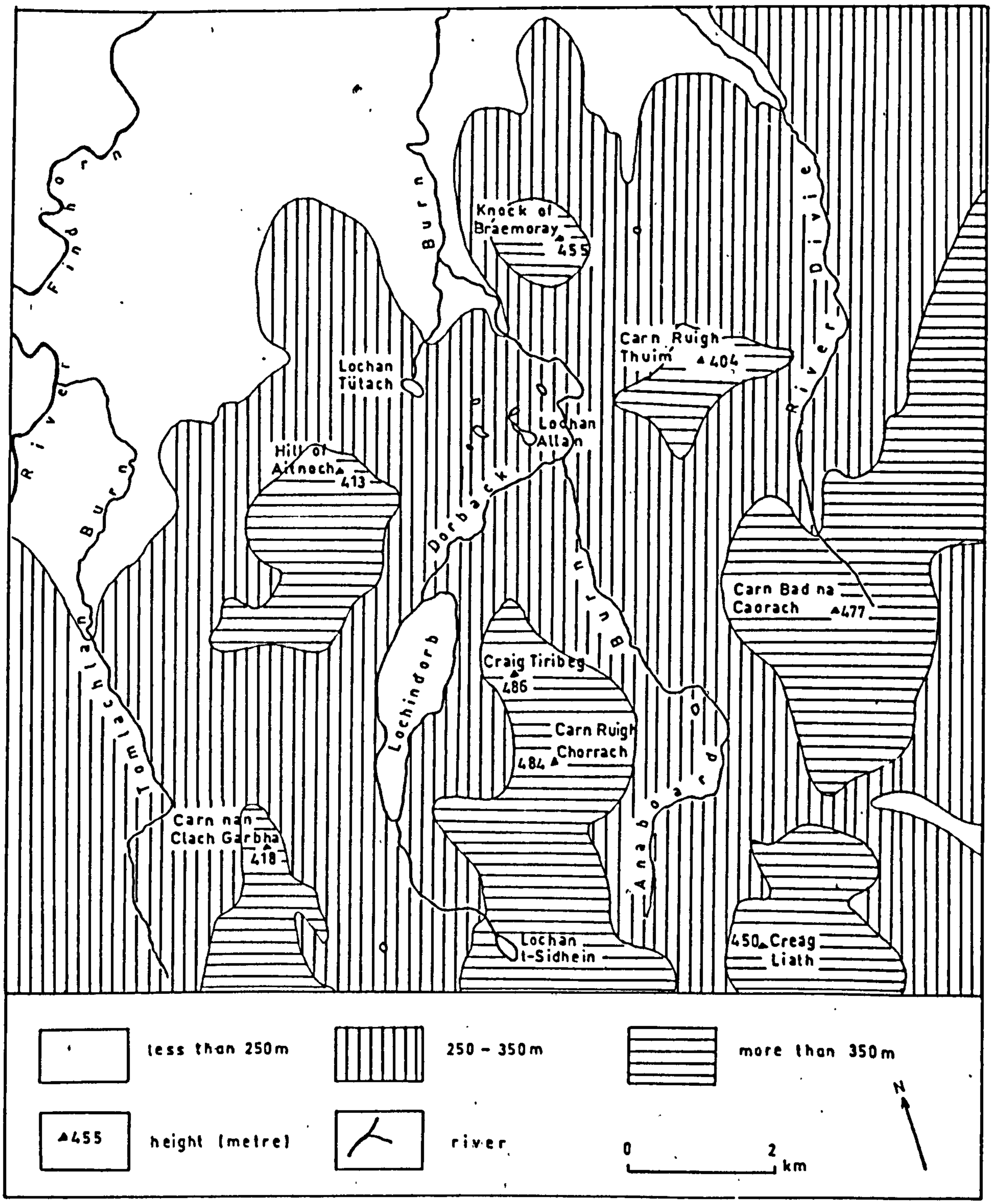

Figure 2.3 Topography and drainage of the Lochindorb area.

superficial deposits, especially at the centre of the area. Among these are Loch Allan and Loch Tutach (Figure 2.3).

The features of surface relief due to glacial action are mainly those of accumulation. In the upland region boulder-clay or till-plain/sheet fills the tributary valleys, depressions in the bedrock and sweeps over the cols, leaving only the hill tops bare of glacial materials which are classified as rock and podzols or as rock, rankers, podzols and occasional peat (Soil Survey of Scotland, 1976). The smooth-flowing slopes characteristic of till deposits are replaced by very irregular surface forms which consist of simple linear ridges or complexes of ridges, hollows and mounds of hummocky-terrain of fluvio-glacial deposits in the valley-floors like those of the Dorback and Anaboard burns (Photograph 2.1). These areas generally correspond to peaty podzol soils and basin peat deposits (Soil Survey of Scotland, 1976). Similar topography also occurs on hill slopes of higher areas which are covered by morainic drift (Photograph 2.2).

The area consists predominantly of moorlands (more than 80% of total land area), woodland (about 10%) and a small area of agricultural land and improved land. The moorlands are dominantly covered by a mixture of heather, grasses, sedges, mosses and a variable proportion of brackens. Generally, lush grasses only dominate the well-drained areas underlain by alluvium, fescue grass occur in areas which underlain well drained till on higher topography, heather and grasses cover

Photograph 2.1 The smooth-flowing slopes characteristic of till deposits, at background, are replaced by a very irregular surface forms consisting simple linear ridges or complexes of ridges, hollows and mound of fluvio-glacial deposits in the valley-floors in the middle. Most of the flat areas, at foreground, are occupied by the peat deposits. Location: 360010 (3.5 km to the east of the Lochindorb and 3 km to the south of Dava.

Photograph 2.2 Low-relief to hummocky terrain formed by the morainic drift which is believed was deposited by the glacier from the south (foreground) and sent a lobe of ice toward the north (background) into the study area through this pass. Note the sides of the pass are terraced with this fluvio-glacial deposits. Location: The pass of Beum a' Chlaidheimh (305937).

the areas underlain by peat which covers almost the entire area, while mixtures of grasses, heather, sedges and mosses cover the thick peat deposits in peat bog or water saturated depressions, whereas bracken is restricted to areas of coarse stabilised scree but show no preference for any particular rock type (discussion about cover-types on the surface deposits will be given in the Chapter 6). The general species distribution, however, has been modified locally by grazing patterns, cultivation, reafforestation and burning. The woodland consists of both coniferous and deciduous trees which occur mainly in the lowland area of the Findhorn and also on higher areas of the Spey. Agriculture is concentrated along the alluvial terraces in the Findhorn valley and in the lower reaches of Dorback burn, River Divie, the Spey's tributaries and also around the Lochindorb. Most of the improved land areas are situated in the areas which are underlain by fluvio-glacial sand and gravel deposits, hence it has a similar cover-type as the alluvial deposits, while the rest of the upland area is used for sheep grazing and grouse shooting.

2.2.2 General geology

The geological formations and groups of rocks occurring within the area are presented in the Table 2.1 , and their distributions over the area are shown in Figure 2.4 and 2.5.

The Moine-like rocks which extend from the Great Glen Fault in the west to the base of the Late Precambrian Dalradian Supergroup (Allison et al., 1988), which cover the Lochindorb area and part of the Loch Tummel area, were known for some

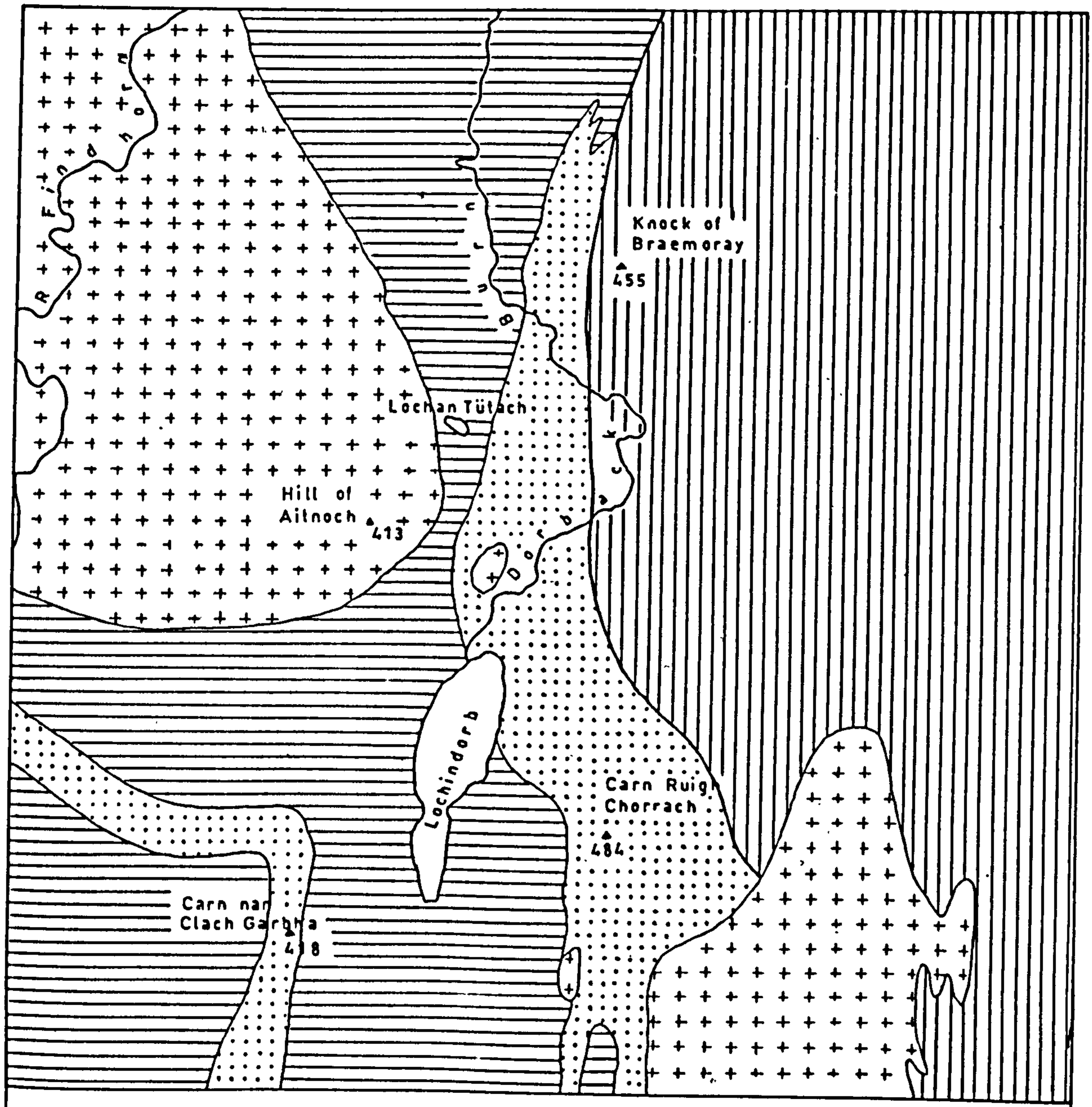

Figure 2.4 Map of the solid geology in the Lochindorb area (slightly simplified) (after Horne, 1923; BGS, 1954 and Allison et al., 1988).

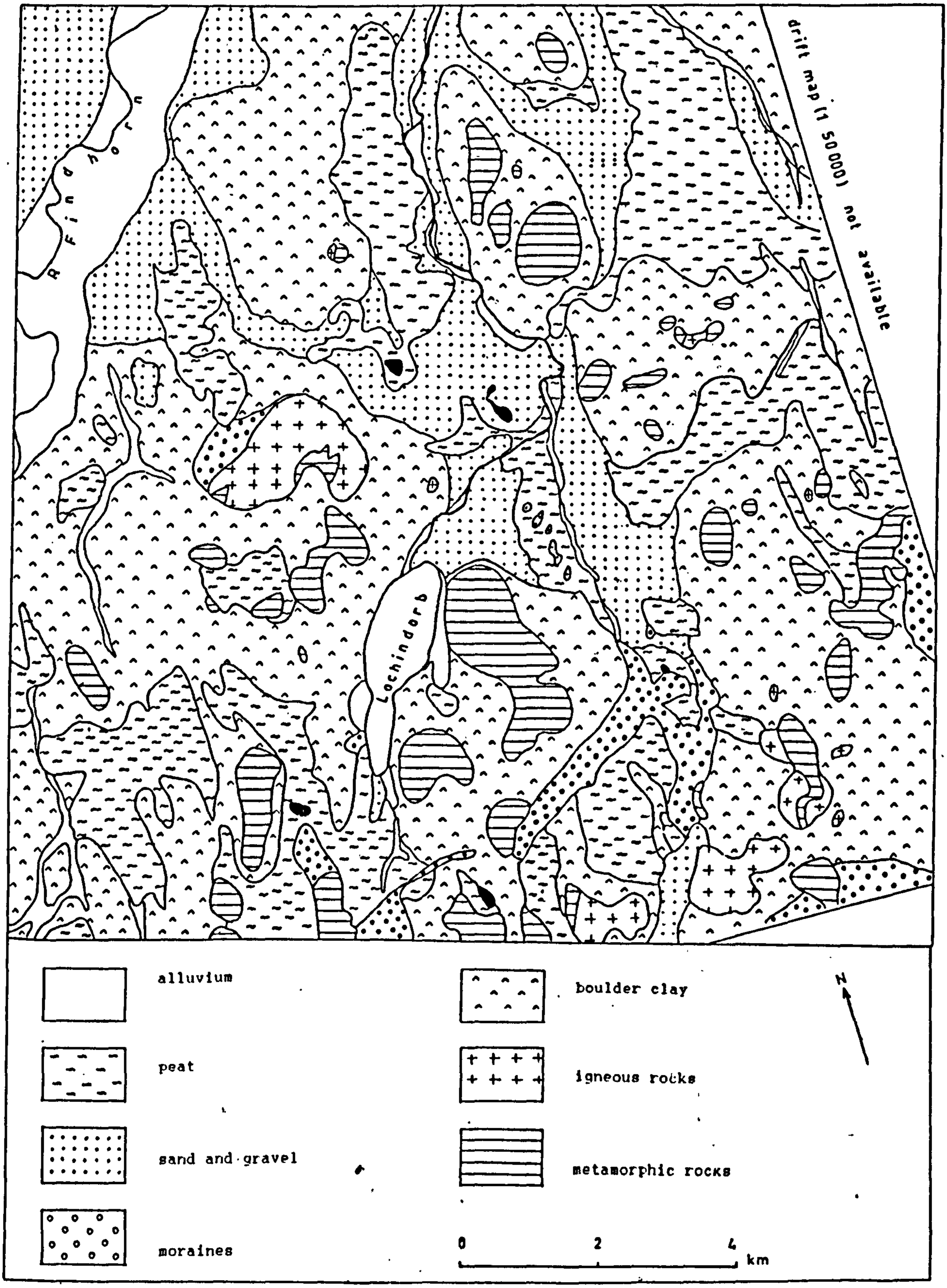

Figure 2.5 Map of the superficial deposits in the Lochindorb area (slightly simplified) (after BGS, 1978).

time as the 'Central Highland Granulites' (Hinxman et al., 1915 and Horne, 1923). Following Anderson (1956) the rocks were subdivided into psammites, then regarded as possible correlatives of the Moine Series, and pelites thought to be possible infolds within the Moine of the Lowermost Dalradian (Johnstone, 1966 and Harris and Pitcher, 1975). Recent work (Piasecki and Van Breemen, 1979a ,1979b; Piasecki, 1980) suggests, however, that these rocks are much more complex and in part significantly older than previously suspected, and may be subdivided into two: Central Highland Division and Grampian Division. About 75% of the area is occupied by the metamorphic rocks which belong to the Central Highland Division and Grampian Division of the Moine Series of the Geological Survey (Figure 2.4). Large parts of the area are underlain by the Central Highland Division which consists mainly of coarse-grained psammitic and siliceous gneisses, interbanded with belts of quartzite and pelitic gneiss (Piasecki, 1980). The Grampian Division which occupies about half of the area in the east, comprises a thick sequence of psammites and semi-pelites with subordinate quartzites (Piasecki, 1980). The relative uniformity of deposits over great vertical thicknesses (maximum thickness of about 600 m) suggests that they probably represent the metamorphism of sediments deposited in the shallow water of a slowly subsiding area of late Pre-Cambrian age (Johnstone, 1966; Rayner, 1976; Anderson and Owen, 1980, and Whittow, 1977). Although local stratigraphic successions have been erected in several areas (Johnstone et al., 1969 and Johnstone, 1975) (Table 2.2), lateral facies changes are

RECENT and PLEISTOCENE	Freshwater alluvial terraces at different levels Peat Glacial sand and gravel Moraines and morainic drift Boulder-clay
IGNEOUS ROCKS INTRUSIVE	Granite with local basic modification
METAMORPHIC ROCKS	Psammites and semi-pelites with subordinate quartzites - GRAMPIAN DIVISION ('Young Moine') Psammitic and siliceous gneisses, interbanded with belts of quartzite and pelitic gneiss - CENTRAL HIGHLAND DIVISION ('Old Moine')

Table 2.1 The geological formations and groups of rock occuring within the Lochindorb area (adapted from Horne, 1923 and Allison et al., 1988).

LOCH EIL DIVISION	Loch Eil Psammite
GLENFINNAN DIVISION	Glenfinnan Striped Schist Lochailort Pelite
MORAR DIVISION	Upper Morar Psammite Morar (striped and pelitic) Schist Lower Morar Psammite Basal Pelite

Table 2.2 Subdivision of the Moine of the Morar region, West Invernesshire (after Johnstone, 1975).

common and further work will be necessary before any well-defined stratigraphy is applied throughout the divisions (Allison et al., 1988). Because of the difficulty of establishing their stratigraphy and structure (Anderson and Owen, 1980), they have been mapped on a lithological basis only (Horne, 1923; Johnstone, 1966; Allison et al., 1988). The rock exposures of the Central Highland Division have been recognised in several areas, particularly on the higher ground or ridges like the Craig Tiribeg (360985), Carn Ruigh Chorrach (347990) and Creag Ealraich (305943) (Photograph 2.3). The units of the Grampian Division have been recognised in a few places like the area around Huntly's Cave (360048), at Knock of Braemoray (417012) and Carn Bad na Caorach (355032) (Photograph 2.4).

About 25% of the area is occupied by intrusive igneous rocks, granites which were intruded into the metamorphic rocks between 400 and 350 million years ago (Rayner, 1976), that are associated with the Caledonian Orogeny (Johnstone, 1966). In the area, the granites occur around the Hill of Aitnoch (395965), Carn Luig (320020) (Figure 2.4).

As mentioned earlier, the widespread covering of drift (till, moraihic gravel and fluvio-glacial sand and gravel) particularly in the lowland area has concealed the solid rocks over wide areas. Furthermore, a large portion of the area is covered by peat (Figure 2.5). Apart from that, the lowland belt especially along the Findhorn, River Divie and Dorback Burn is covered by freshwater alluvium.

Photograph 2.3 The pelitic gneiss belt of the Central Highland Division ('Old' Moine), forms a higher ground and main ridges in the area. Note that the outcrop is highly covered by vegetation as well as lichen. Location: Craig Tiribeg (360985).

Photograph 2.4

Exposure of psammites and semi-pelites with subordinate quartzite of the Grampian Division ('Young' Moine). This rock unit generally forms nearly equal height of ground with no obvious ridges or peaks. Note that the outcrop is almost completely covered by vegetation. Glacial deposits, mainly made up of morainic drift, formed the mounds in the middle and right hand side of the photograph. Location: Huntly's Cave (358046).

Till deposits are widely distributed throughout the area (Figure 2.5), filling the hollows sometimes to a depth of several tens of meter (Horne, 1923), and can be traced across cols exceeding more than 400 m in height. Hence they form an almost continuous veneer over the land surface (Photograph 2.5). The typical deposit consists of a stiff, stony clay with well-glaciated stones retaining the ice marks, and usually has a yellow or fawn-colour (Photograph 2.6). In some places, the intercalation of fluvio-glacial sands and gravels in the tills has been observed (Horne, 1923)..

South of Lochindorb, the till is overlain by gravelly morainic matter, which includes stones that are similar to those found in the till. However, the striated blocks are less common and many of the stones are well rounded and waterworn. Crampton, in Horne (1923) believed that this material was deposited by the Dulnan glacier (from the south of the area), which appears to have sent a lobe of ice through the pass of Beum a' Chlaidheimh (305907) where its sides were terraced with gravelly moraines (Photograph 2.2) which spread out over the plain to the north (Figure 2.5).

In addition to the till and moraines, fluvio-glacial sands and gravels also occupy quite extensive areas (Figure 2.5). The materials of the deposits vary in character, consisting partly of fine sand, partly of stratified sand and fine gravel, and partly of gravel with no regular arrangement. However, the stones are generally well rounded and are not striated (Photograph 2.7). They cover an area in the NE of Lochindorb, and also along the courses of the River Divie and

Photograph 2.5 Till deposits are widely distributed throughout the area and form an almost continuous veneer over the land surface. The smooth-rolling ground of the Grampian Division at the background is covered by the deposits. Peat deposits occupy over the valley-floor (wet area) in the middle and the nearly flat plain (more dry area) at foreground. Location: from Badahad (376045) looking toward Carn Ruigh Thuim (395025).

Photograph 2.6

The typical appearance of the till deposits in the area, consists of a stiff, stony clay with well-glaciated stones which retain the ice marks, and usually has a yellow or fawn-colour. Note this peaty podzols soil with heather cover occurs on top of the till deposits. Location: along the track between Badahad and Dava.

the Dorback burn. These deposits generally form prominent ridges and mounds with terraced platforms and numerous peaty flats (Photograph 2.1). Between Dava and Aitnoch stretches a smooth, nearly level plain of sand and gravel with occasional mounds of sand and gravel and with round or irregular-shaped hollows occupied by lochans like Loch Allan, Loch Tutach etc. These lochs are probably of the nature of 'kettle holes' (Hinxman, 1915). The sorting and stratification in these sediment indicate deposition from water, and their irregular morphology is indicative of a variety of ice-contact environments. Collectively these sediments are known as kame complexes and are considered to be fluvio-glacial in origin.

Peat is a partially decomposed mass of vegetation which, in this area, started to form soon after the ice retreated and is continuing to form today (Price, 1983). About 40% of the area is covered with a mantle of peat, and almost all of this area is classified as basin peat (raised moss and low moor stages) and only a very small area southwest of the Carn nan Clach Garbha (346945) is classified as blanket peat (hill peat) (Soil Survey of Scotland, 1976). The thickness of the peat is variable, from less than 1 m to may be up to 6 m or more (Johnstone, 1966; Soil Survey of Scotland, 1976) (Photograph 2.8). It covers considerable tracts in the areas traversed by the River Divie and Dorback burn, and fills basin-shape hollows among the moraines and fluvio-glacial sands and gravels in area southwest of Dava as far as Carr Mor in the south (Photograph 2.1). An area to the southwest and west of Lochindorb is also covered by substantial amounts of

Photograph 2.7 The typical appearance of the sand and gravel deposit, generally consisting partly of fine sand, partly of stratified sand and fine gravel, and partly of gravel with no regular arrangement, however, the layer clasts are generally well rounded and are not striated. Location: Little Aitnoch (408966).

Photograph 2.8

Peat deposits are exposed along the drained channel. The thickness of the exposed deposit is about 1.5 m. Location: Along the road between Lochindorb and Carn nan Clach Garbha.

Photograph 2.9

The wilderness of basin peat spreads over a very large areas of nearly flat plain terrain and overlies the metamorphic rocks of the Grampian Division ('Young' Moine). The areas covered by the peat deposits are fairly open habitats, however, a few trees do occur and survive, and in the area far at the background, the area is invaded by shrub and Birch trees which may indicate that the peat deposits here have reached the final stage in the formation of Histosols (peat). Location: Moidach More (420030).

peat. To the south of the Moidach More (430030), peat spreads over the nearly flat plain terrain, and is marked as 'deep peat' on the map (BGS, 1978) (Photograph 2.9).

The fresh-water alluvium is confined mainly to the Findhorn where it forms a flat surface, and to narrow strips along the courses of the River Divie and Dorback burn which are incised into the fluvio-glacial sands and gravels. Other alluvial patches occur around Lochindorb. The deposits are usually under cultivation (Photograph 2.10).

Once again, apart from solid rocks, the wide-spread covering of drift and peat may also conceal dislocations in the area due to geological faults. Previous study has shown that dislocations within the area are only of minor importance (Horne, 1923).

2.3 The Loch Tummel area

2.3.1 Physiography

The topography and drainage of the area are illustrated by Figure 2.6. In general the terrain of the region is mountainous throughout. The most striking topographical feature is the great ridge at the centre of the area which commences in Ben Vrackie (840 m), a few kilometres to the east of the area, and continues in a south-westerly direction to and far beyond, Ben Lawers (1214 m), just a few kilometres tc the southwest of the area. This ridge, the great structural axis of the area, is due exclusively to geological structure (Barrow et al., 1905). Meall Tairneachan (787 m) is one of the peaks in the ridge which separates the Tay valley from

Photograph 2.10 Fresh-water alluvium deposits form a few patches of flat surface around the Lochindorb. The deposits are usually cultivated. In the area, large flat areas of the deposits also occur along the Findhorn valley, and form narrow strip along other channels.

Photograph 2.11 The Schiehallion, the most conspicuous hill in the area, is underlain by the metamorphic rocks (mainly quartzite) of the Dalradian. The Tummel Valley (foreground), is covered by extensive alluvial deposits and forms one of the few places in the area which are suitable for agricultural activities.

River Tummel. West of the Meall Tairneachan range rises Schiehallion (1083 m), the most conspicuous hill in the area, which forms a near-perfect cone and is isolated from the surrounding hills on every side (Photograph 2.11). The mountainous terrain continues to the north of Schiehallion and culminates at Beinn a' Chuallaich (891 m). To the west of Schiehallion, the high ground in the south-west area includes Carn Mairg (1042 m), Carn Gorm (1029 m), Meall Garbh (932 m) and Geal Charn (790 m), and forms the eastern portion of the mountain chain which lies between Loch Rannoch and River Lyon. Between Loch Tay and the river Lyon is situated Drummond Hill (455 m). In contrast, the northern half of the area, north of Loch Rannoch-north of River Tummel-west of River Tilt, forms massive, long rolling slopes and ridges, and has a summit level of about 550 m and nearly flat terrain except in the north-west corner of the area where it forms part of the south-west end of the Grampian Mountains (Figure 2.6).

A large part of the area falls within the catchment basin of the Garry which flows from the north-west to the east corner. Other main rivers are the Tay and the Lyon in the south, and the Tummel in the middle of the area (Figure 2.6) which flow approximately in an east-west direction. Two other rivers are the Errochty in the centre and the Tilt in the extreme north-east of the area. The Tilt valley, with its high steep sides and narrow bottom, and also forms a sharp line of demarcation between the mountain relief of the Dalradian mass on its eastern side with a more uniform terrain and somewhat featureless plateau lands of the 'Young' Moinian of the

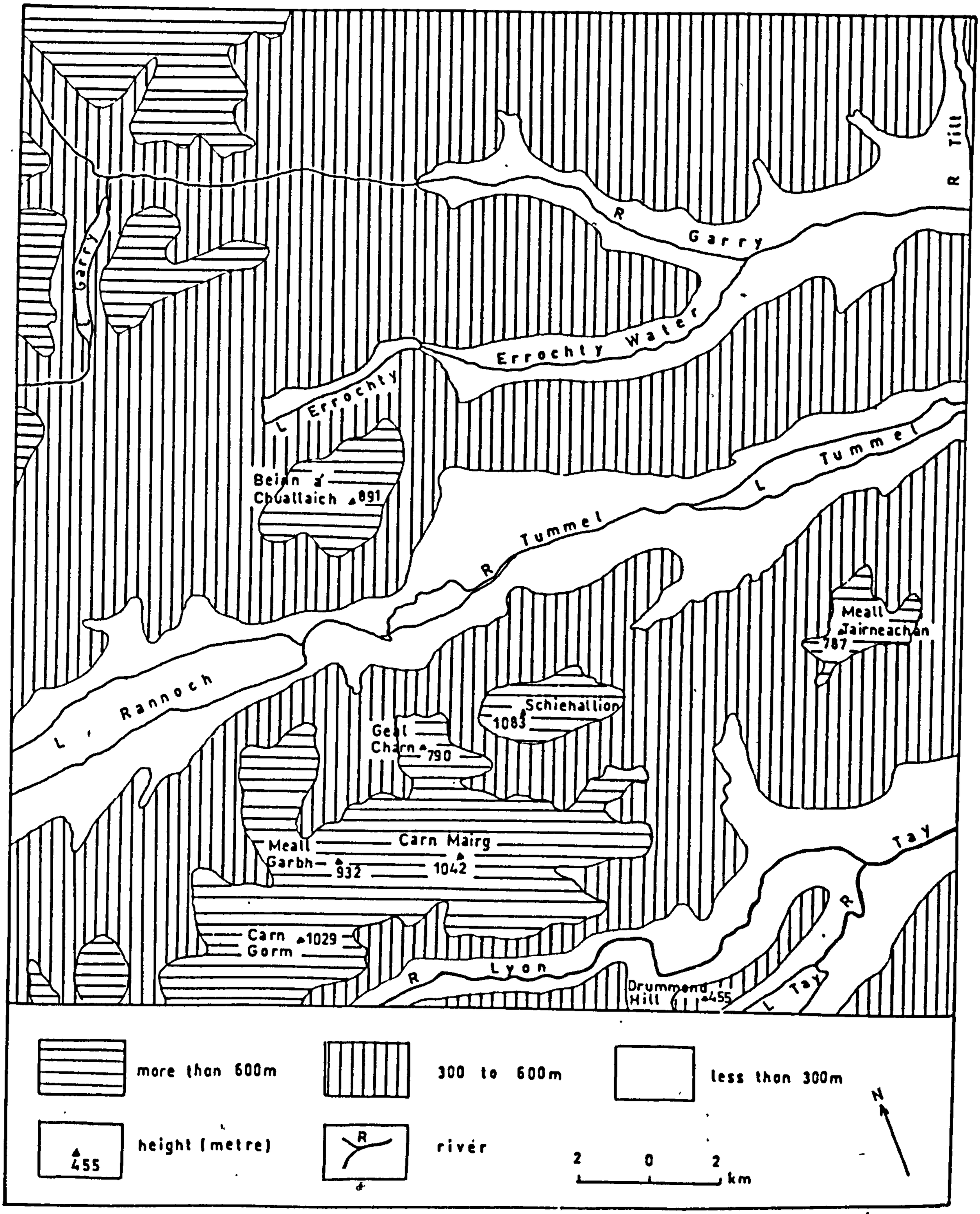

Figure 2.6 Topography and drainage of the Loch Tummel area.

Grampian Division to the west, presents a very striking feature. The course of this river has been determined by the important line of fracture which traverses the River Tilt and is continued south-westward across the area (Barrow et al., 1905).

Loch Rannoch, Loch Tummel, Loch Errochty, Loch Garry and part of Loch Tay are the large water bodies in the area (Figure 2.6). Apart from that, a few small lakes are scattered over the area and classed either as rock-basins or drift-impounded lochs (Barrow et al., 1905).

A considerable area of ground to the south of the Rannoch, north and north-west of the Tummel, north and north-east of the Tay is covered by woodland. The cultivated ground being for the most part restricted to the bottom and lower flanks of the main valleys like the Tay, the Tummel and the Lyon (Photograph 2.12), and consequently these are the well populated areas. Apart from that, the greater part of the area is moorland particularly in the northern side. The higher ground is either bare rock or thickly covered with turf, heather, bracken, and peat (Photograph 2.12).

2.3.2 General geology

Apart from the Moinian Metamorphic assemblages (like in the Lochindorb area), the main rock formations within the area are Dalradian Metamorphic assemblages (Anderson, 1948), which were intruded by granitic magma when they were orogenically deformed and regionally metamorphosed during Caledonian period (Johnson and Frost, 1977). The geological formations and

Photograph 2.12

The Grampian Division ('Young' Moine) forms rather massive, long rolling slopes and ridges, and has a nearly flat terrain (nearly similar summit level) whereas the Dalradian forms a rugged topography with obvious hills and peaks. Both areas, however, are largely overlain by the glacial deposits (mainly till and moraine) which are covered by mixtures of turf, heather and bracken which give similar cover-types for different underlain bedrock. Agricultural activity is concentrated on the extensive alluvial deposits along the Tummel valley.

RECENT and POST-TERTIARY	Alluvium Peat Glacial deposits, mainly boulder clay and moraines
IGNEOUS ROCKS	Granite, epidiorite and porphyrite sills
METAMORPHIC ROCKS	Quartzite, limestone, pelite, schist, slate and schistose - DALRADIAN Psammite and semi-pelite with subordinate quartzite - GRAMPIAN DIVISION ('Young Moine')

Table 2.3 The geological formations and groups of rock occuring within the Loch Tummel area (adapted from Barrow et al., 1905 and Allison et al., 1988).

groups of rocks occurring within the area are presented in Table 2.3 and their distribution in the area is illustrated in Figure 2.7.

The general rock types of the Moines series which belong to the Grampian Division (Piasecki and Van Breeman, 1979b) or commonly termed the Central Highland Granulites or Central Highland Psammitic Group (Anderson and Owen, 1980) in the area are quartzo-micaceous gneiss and grey granulites quartz-schists where an evenly colour-banded granulitic gneiss is the dominant member of the series (Barrow et al., 1905). Their structures are complex and multiple, incorporating several superimposed fold systems. However, they appear to be a tendency for the larger folds (isoclinal), to strike generally north-east and south-west, with the long limbs of the folds inclined to south-east (Peach and Horne, 1930; Rayner, 1976). About half of the area is underlain by the Moinian which covers almost all the area between the Tummel and the Garry, west of the Loch Tay Fault (Figure 2.7). However, away from the stream and road cut, rock exposures are rare because large areas are obscured by drift cover.

The metamorphic rocks of the Dalradian cover the other half of the area (Figure 2.7). In contrast with the Moinian, the Dalradian Assemblage is characterized by a greater diversity of sediments which were accumulated during the later phase of the geosyncline (Whittow, 1982) of the late pre-Cambrian to Lower Cambrian (Rayner, 1976; Whittow, 1977, Johnson, 1983). The stratigraphic succession of the Dalradian in Central Perthshire, including this area is presented in

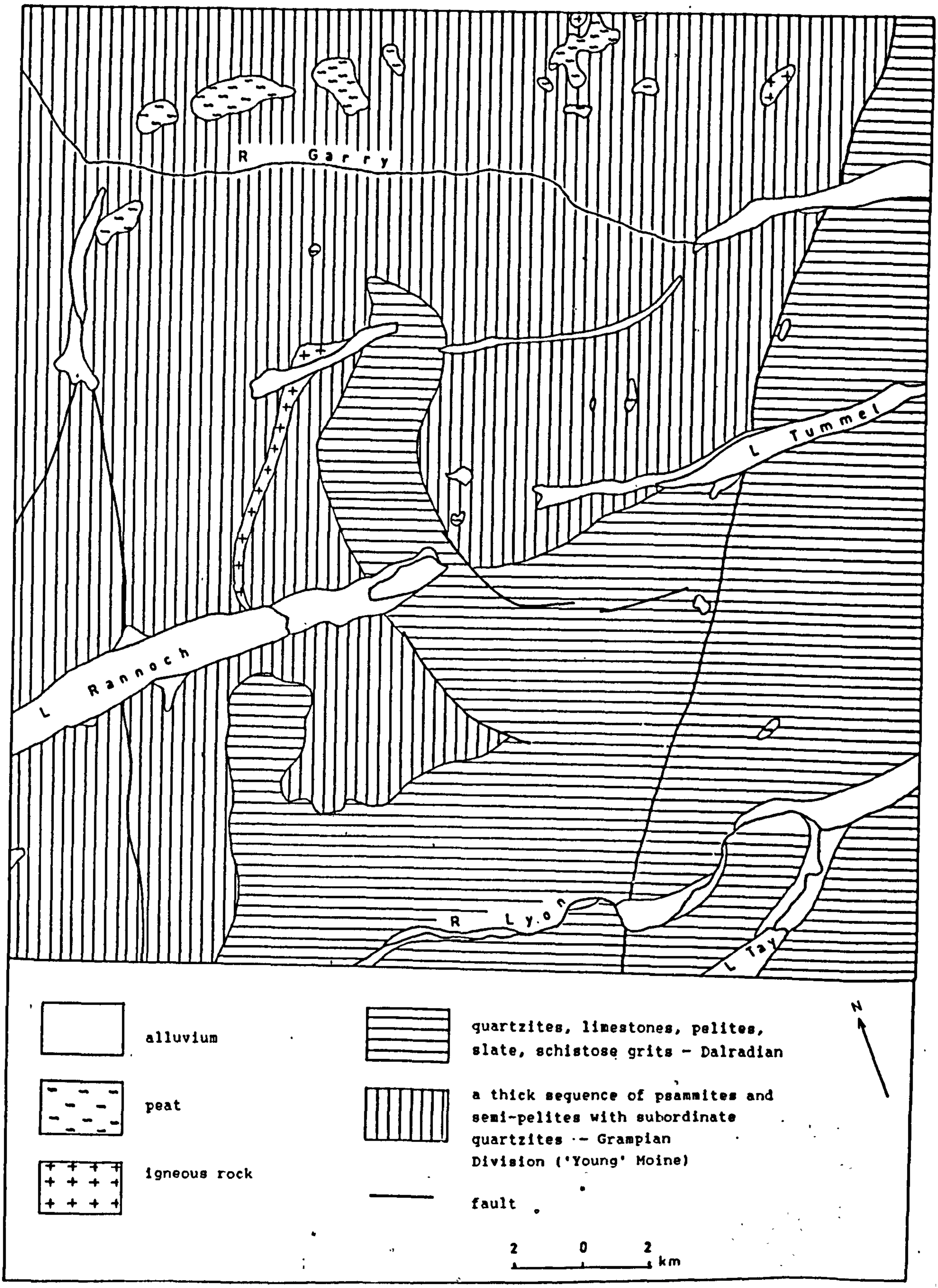

Figure 2.7 Simplified geological map of the Loch Tummel area (after BGS, 1964, 1967 and 1974).

UPPER PSAMMITIC GROUP	Leny Grits Green Beds	SOUTHERN HIGHLAND GROUP	UPPER DALRADIAN
PELITIC GROUP	Pitlochry Schists Dunkeld Slates		
UPPER CALCAREOUS GROUP	Loch Tay Limestone		
LOWER PSAMMITIC GROUP	Ben Lui Schists		
PELITIC AND CALCAREOUS GROUP	Ben Lawers Schists	ARGYLL GROUP	LOWER DALRADIAN
CARBONACEOUS GROUP	Ben Eagach Schist		
QUARTZITIC GROUP	Central Highland Quartzite Series		
LOWER CALCAREOUS GROUP	Schichallion Boulder Bed Blair Atholl Series		
PELITIC and QUARTZITIC (transition group)	Schists and Quartzites of Rannoch	APPIN GROUP	
Grampian Division ('Young Moine')			

Table 2.4 The stratigraphic successions of the Dalradian in Central Perthshire, including the Loch Tummel area (adopted from Johnstone, 1966 and Johnson, 1983).

Table 2.4. The earlier part of the sequence is probably of shallow-water, possibly shelf-sea origin based on the presence of well-sorted and current-bedded (?shallow water) quartzites, limestones and pelites, whereas the later part of the sequence may well be of deep-water origin which is characterized by thick beds of slate and schistose grits in which graded-bedding is well preserved (Johnstone, 1966; Rayner, 1976). The amount of deformation the rocks have undergone does not allow thicknesses to be estimated. However, Rayner (1976) stated that it may have reached many thousands of meters, perhaps over 9000 m. Until now, no firm conclusions can be arrived at as to whether the Dalradian rocks lie completely conformably on the Moinian Assemblage, disconformably on it, or are to some extent diachronous with the upper Moinian rocks (Johnstone, 1966). However there are grounds for believing that the Moines are composed of old and young parts, and the young Moines (Grampian Division) which are widespread in the Grampian Highland, including this area, pass up without significant break into the Dalradian (Johnson, 1983).

Only a small proportion of the area is covered by igneous rocks (Figure 2.7). A small granite boss pierces the schists to the west of Glen Tilt, and several small laccoliths of epidiorite are found at Meall Garbh in Glen Lyon, Trinafour (NE of Loch Rannoch) and Loch Kinardochy (west of Meall Tairneachan), while many epidiorite sills are scattered all through the Schiehallion complex and the schists in the Tay valley (Barrow et al., 1905). To the north-east between Loch Rannoch and Loch Errochty, a well marked sill of porphyrite

forms a prominent feature in the landscape rising in a series of steep escarpments.

As in the Lochindorb area, large parts of this area are also covered by glacial deposits which were grouped as till and moraines (Barrow et al., 1905) which conceal the solid rocks as well as the structures. Beside that, the lowland belt particularly along the Tay, Lyon and Tummel is covered by extensive alluvial deposits. In comparison with the Lochindorb area, this area is poorly supplied with peat with only a number of small peat mosses scattered over the area (Figure 2.7).

The Dalradian rocks, which were subjected to metamorphism and structural deformation during the Caledonian Orogeny, were thrown into major recumbent folds (Johnson, 1983). The axes of these folds run in a general NE-SW, ENE-WSW or E-W. The area is traversed by several major wrench faults, notable among these are the Loch Tay Fault and the Tyndrum Fault which have a north-easterly trend, while the Killin Fault is directed more north-north-easterly (Smith, 1961; Johnson and Frost, 1977) (Figure 2.8). The Loch Tay Fault crosses the area in a NE-SW direction between west of Loch Tay and Glen Tilt. Parts of the Tyndrum Fault and the Killin Fault cross the area in a NE-SW and NNE-SSW direction respectively, between Loch Garry and to the south of Loch Rannoch. Johnson and Frost (1977) describe these faults in the Grampian Highland as follow:

a. Loch Tay Fault (025^0 - 040^0) - this can be traced for 80 km across Dalradian, Moines and Granites. Estimated slip is 6 - 8 km, sinistral, it displaces fold axes and

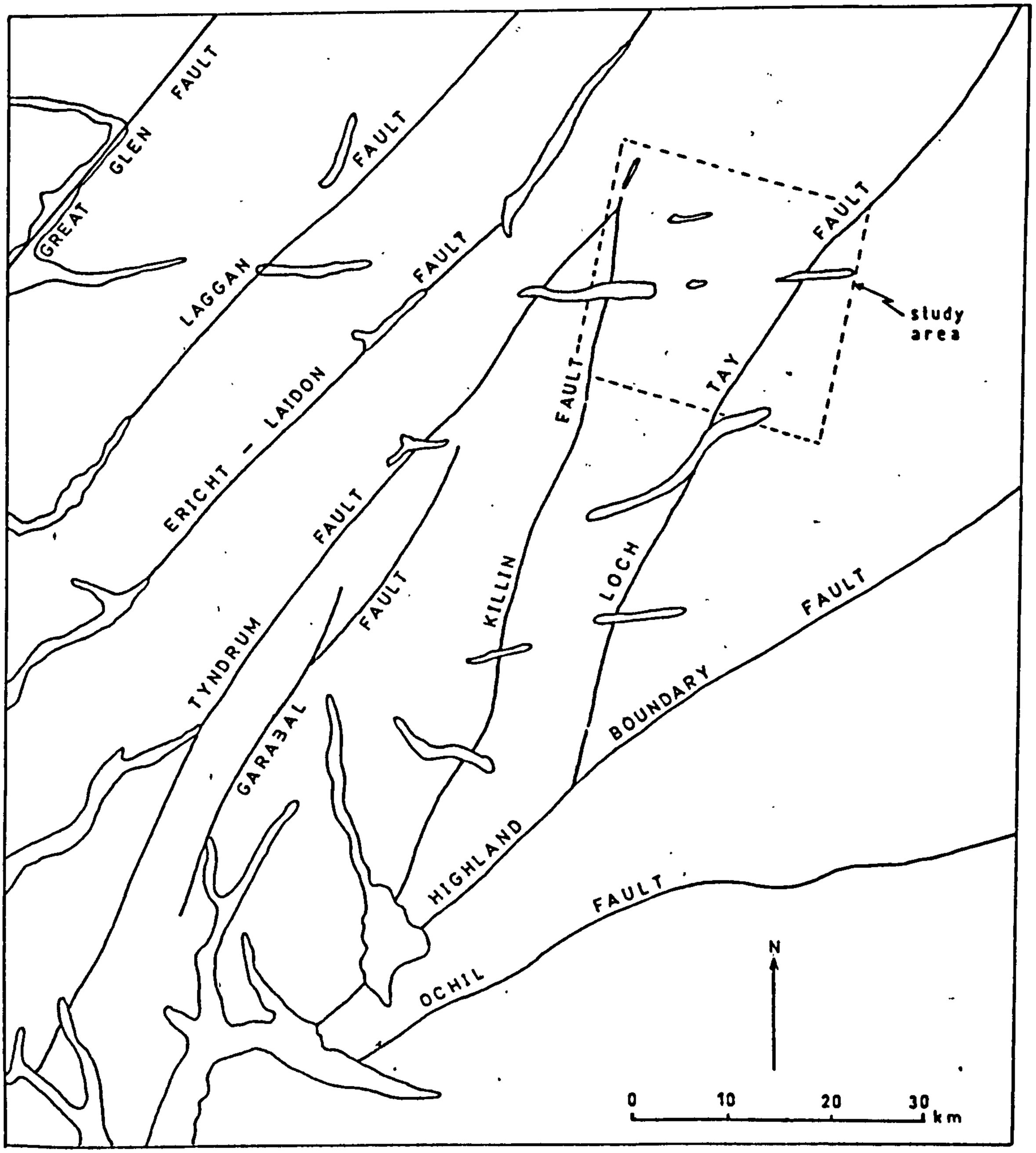

Figure 2.8 Sketch-map of the South Central Highlands showing major faults and area occupied by the study area (after Smith, 1961 and Johnson and Frost, 1977).

metamorphic zones. In the southwest, near the Highland Boundary Fault, it passes into a series of splays, along which limited sinistral slip is evident.

b. Tyndrum Fault (030^0) - this can be traced for 60 km across Moines, Dalradian and Granites. It is clearly seen as a high angle fault (70^0) on hillsides. No estimates of slip are given. The fault line has been mineralised.

c. The Killin Fault (020^0) - this can be traced for about 60 km, a dip of 70^0 has been measured. A zone of shattered rock some 100 m across is found along the middle part of the fault. The zone is cut by Lower Devonian intrusives.

Beside that, a large fault bounds the Schiehallion complex, and a few minor faults that shift the outcrops of the epidiorite sills, green beds and the Loch Tay limestone around Loch Tay are observed (Barrow et al., 1905).

2.4 The Perak-Kedah area

2.4.1 Physiography

In general the well-forested terrain of the region is hilly to mountainous. The main peaks are the Bintang (1869 m), Inas (1807 m) and Baubak (1203 m) which form the northern end of the Bintang Range in the north, while the Besar (1754 m) forms the northern tip of the Main Range in the eastern side of the area (Figure 2.10). Generally, this high terrain is underlain by the granite mass of Bintang and the Main Range, and the difference in elevation is due mainly, if not entirely, to differential erosion (Jones, 1970). That is to say the granites are relatively more resistant to tropical weathering

and erosion than are the other rocks (Burton, 1970). The topography of these granites is characterized by steep valley walls, numerous waterfalls and rapids which indicate a late youthful stage of erosion (Tjia, 1973). Slopes are normally of only moderate steepness and therefore retain a good cover of soil. Some portions of the granite appear to have been considerably affected by hydrothermal alteration (Jones, 1970), and in such areas weathering and erosion have progressed more rapidly to produce undulating terrain of less pronounced relief. In the central area, surrounded by the mountainous and highly dissected hilly area, the topography is more subdued with less elevated peaks like the Papulut (728 m), Kenderong (1227 m), Kobeh (898 m) and Gagang (773 m) (Figure 2.10). This area is underlain mainly by metamorphic rocks. In the northwest and west, the area is represented by a low to gently undulating country with occasional prominent parallel ridges which extend uninterrupted for several kilometres, running in a north-easterly direction. This particular terrain is underlain mainly by sedimentary rocks and the parallel ridges are formed from the strike ridges of a resistant unit of the underlying rocks.

Large parts of the area, particularly in the south and east, are drained by the Perak River, which flows in the northeast-southwest direction, and by its tributaries. The Muda River drains the northwestern and western part of the sub-area 1 and the Rui River drains the central part of the sub-area 2, respectively (Figure 2.9 and 2.10). The granitic terrain especially the Bintang granite is deeply dissected by

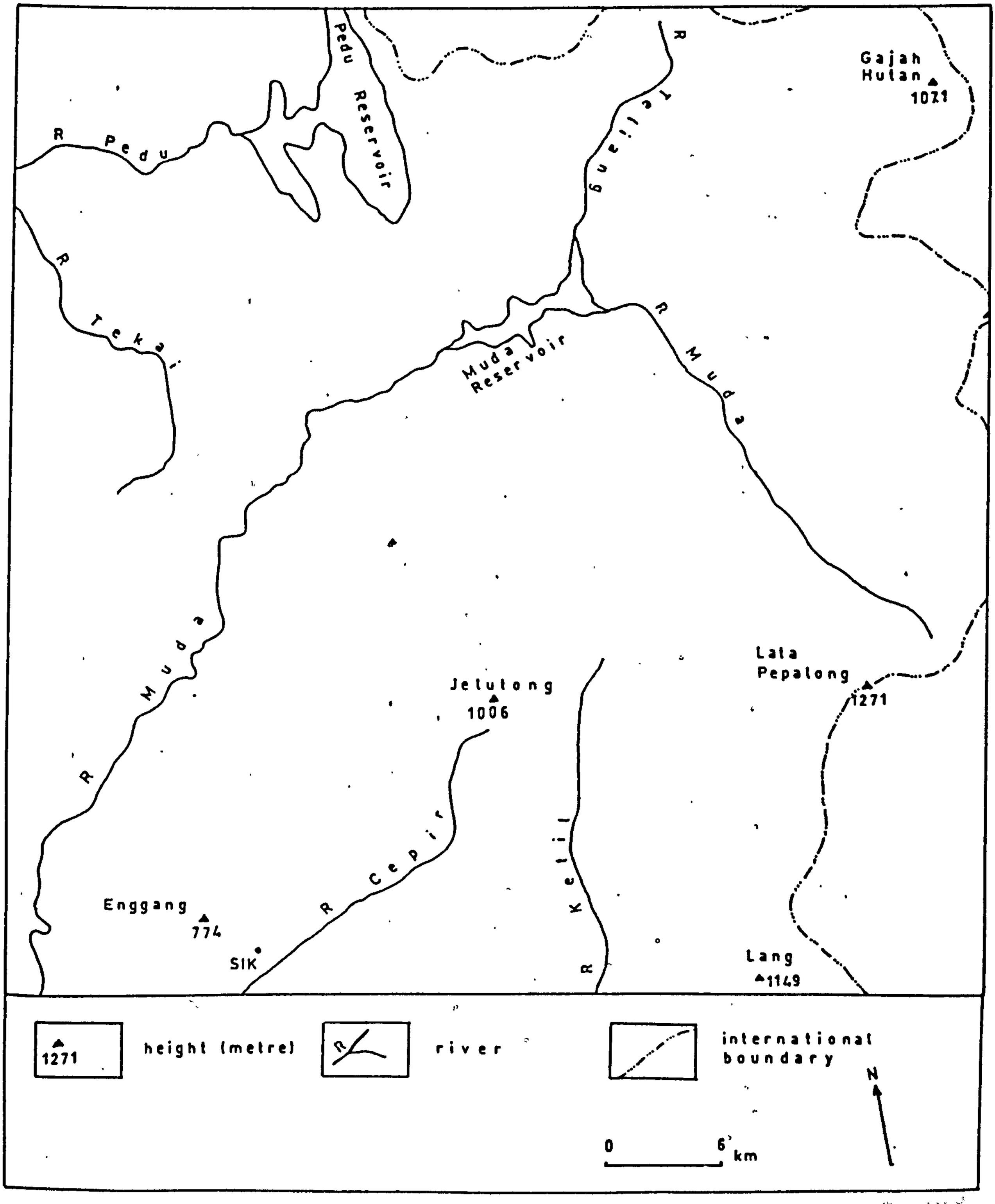

Figure 2.9 Drainage and main topographical peaks of the Kedah-Perak sub-area 1.

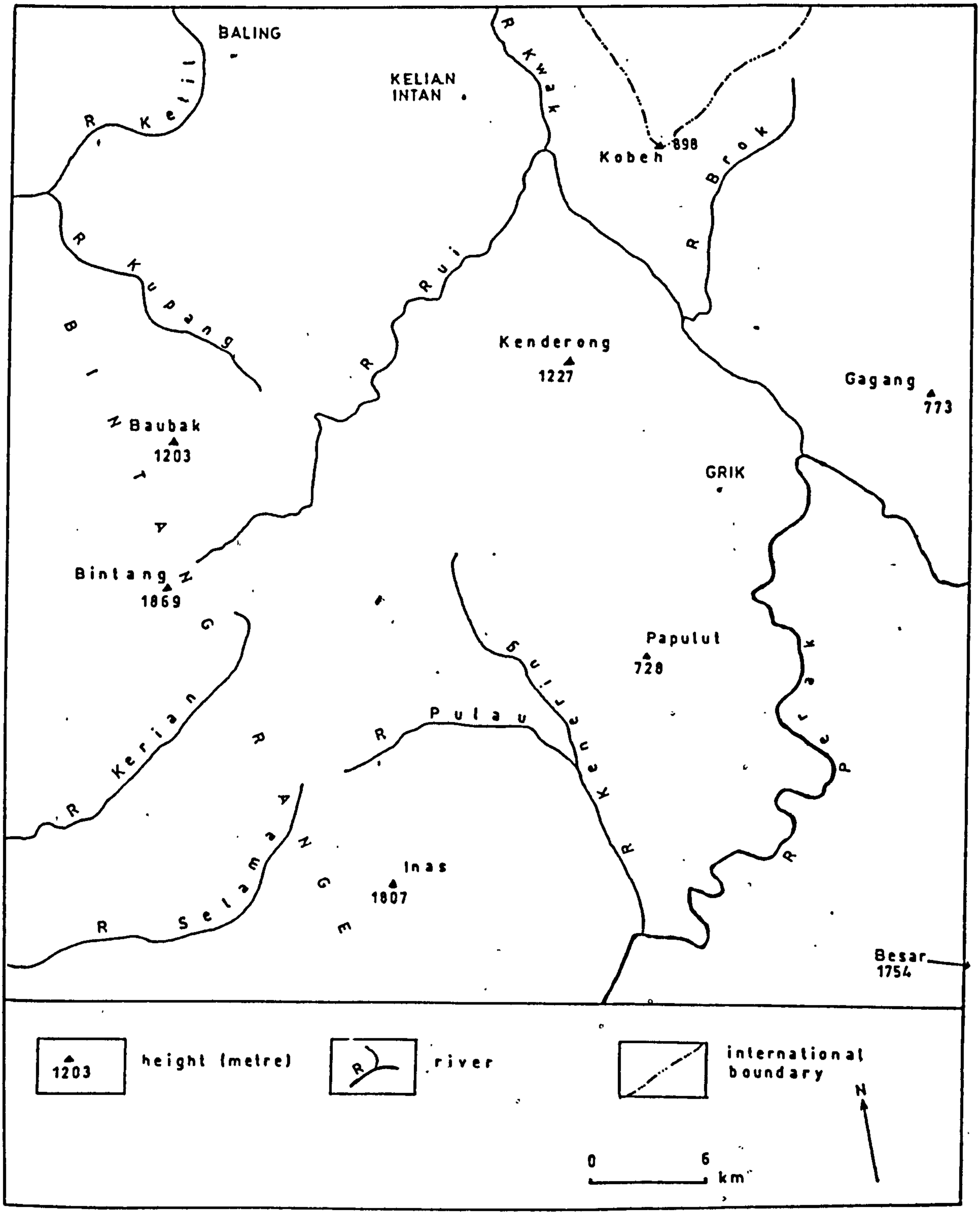

Figure 2.10 Drainage and main topographical peaks of the Kedah-Perak sub-area 2.

a close network of valleys. The drainage pattern in the granitic region follows no well defined pattern but in places rectangular, angulate and parallel patterns do occur, indicating the influence of fracture zones (joints and faults) in the granite (Jones, 1970; Tjia, 1973; Courtier, 1974). Drainage channels in the central area, to a large extent, have developed along two main directions of faulting particularly in areas underlain by granite, with mean directions of 323^0 and 032^0 (Burton, 1970). In the north, the Pedu and Muda Reservoirs form large water bodies in the area (Figure 2.9).

The primary jungle of the Malay Peninsula, characteristic of a humid tropical climate, is of the type known as tropical evergreen rain forest. A large proportion of the area, irrespective of terrain and rock type, is covered by this virgin forest. However, in Pulau Langkawi, limestone areas support only a low scrubby vegetation with occasional high trees, whereas in contrast, the igneous or sedimentary areas are covered by high dark-green forest (Jones, 1981). Only a small area of forest has been cleared for agriculture or developed for urban purposes. The cultivation of rice predominately on the alluvial flats which occur along the drainage channels of Perak, Ketil and Muda, whereas the adjoining higher ground (lower hill-slopes) is devoted mainly to the production of rubber, together with a few other minor crops. The settlements in the area are the small towns of Baling, Grik, Sik and Kelian Intan, whereas the rest of the population is scattered along the main road and the major

drainage of the area as far up-stream as it has been found possible to cultivate rice.

2.4.2 General geology

Figure 2.11 and 2.12 show a generalized geologic map of the area covered by the image. The figures are a slightly simplified version of the 1: 500,000 Geological Map of Peninsular Malaysia (Geological Survey of Malaysia, 1985). The map shows that most of the area is underlain by metamorphic rocks of Silurian-Ordovician age which belong to the Baling Formation and were interpreted as representing the geanticlinal rocks of the Malayan Lower Palaeozoic Geosyncline (Hutchison, 1973), and intrusive igneous rocks of Lower Cretaceous-Middle Lower Jurassic (Hutchison, 1973) or Late Triassic (Geological Survey of Malaysia, 1985). Apart from these, the sedimentary rocks of Triassic age which are commonly affected by low grade regional metamorphism (Geological Survey of Malaysia, 1985) of the Semanggul Formation (Burton, 1973) and of Cretaceous-Jurassic age (Geological Survey of Malaysia, 1985) of the Tembeling Formation (Burton, 1973) occupy the northwestern corner of the area. Table 2.5 gives additional detail of the rock units in the area.

Small deposits of Recent river alluvium are present along the meander belt of the Perak, Ketil and Muda River, and in the lower valleys of their main tributaries. These consist of unconsolidated mixtures of mud, silt, sand, and gravel, providing limited areas of flat land suitable for agriculture,

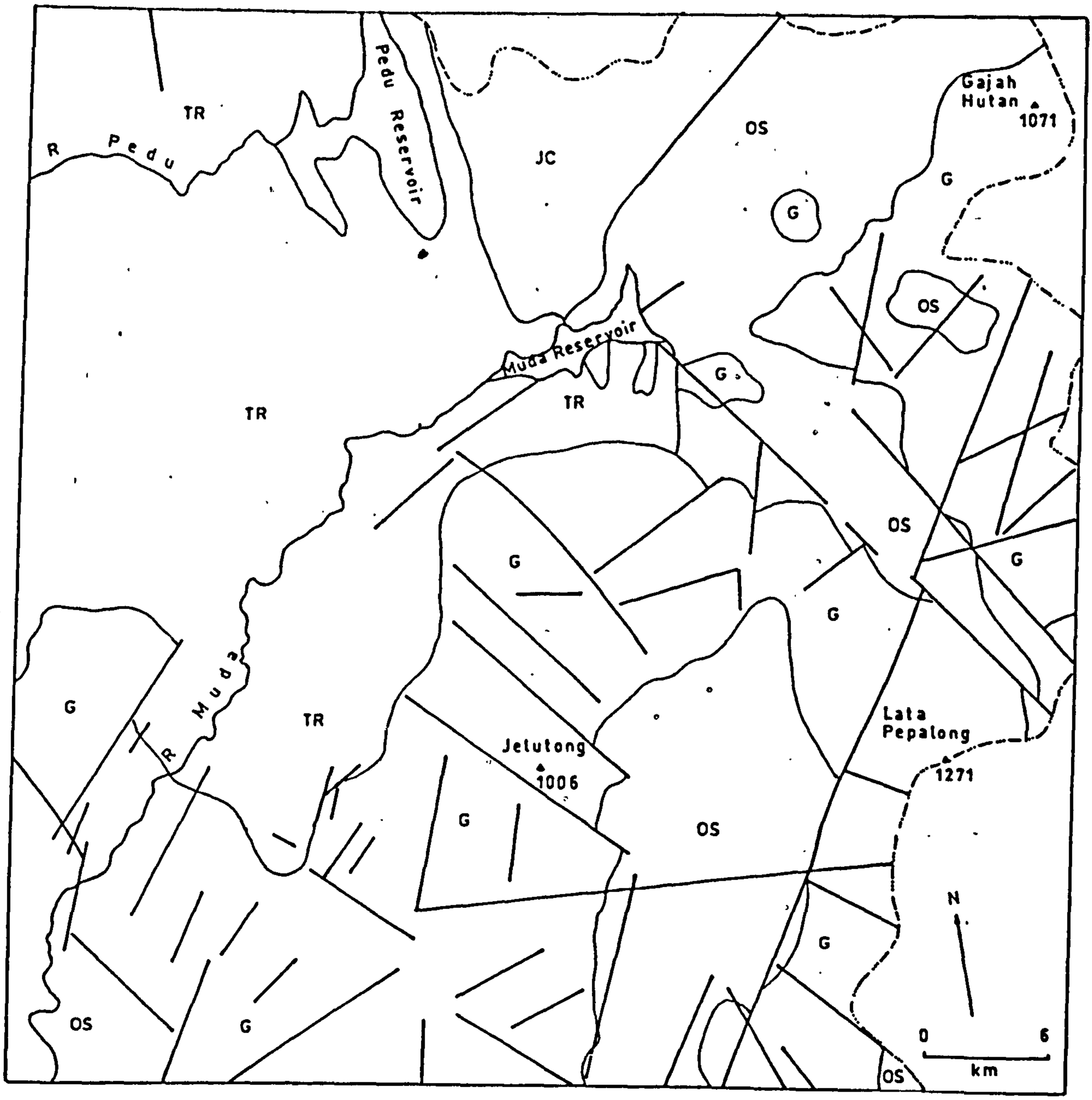

Figure 2.11 Simplified map of the solid geology in the Kedah-Perak sub-area 1 (after Geological Survey of Malaysia, 1985).

Key for Figure 2.11 and 2.12

T	TERTIARY: Isolated continental basin deposits of Late Tertiary age: shale, sandstone, conglomerate and minor coal seams.
JC	CRETACEOUS - JURASSIC: Continental deposits of thick, cross-bedded sandstone with subordinate conglomerate and shale/mudstone.
TR	TRIASSIC: Interbedded sandstone, siltstone and shale; widespread volcanics, mainly tuffs of rhyolitic to dacitic composition. Limestone, conglomerate and chert locally prominent.

Figure 2.12 Simplified map of the solid geology in the Kedah-Perak sub-area 2 (after Geological Survey of Malaysia, 1985).

Key for Figure 2.11 and 2.12 (continued)

OS	SILURIAN – ORDOVICIAN: Schist, phyllite, slate and limestone. Minor intercalations of sandstone and volcanics.
G	Mainly JURASSIC: Acid intrusive (undifferentiate), but mainly granite.

——— Geological fault

~ Geological boundary

AGE		FORMATION	DESCRIPTION
CENOZOIC	QUATERNARY Recent	Alluvium	Small unconsolidated fluviatile deposits consisting of mixture of gravel, sand, and silt
			POSSIBLE UNCONFORMITY
	QUATERNARY Holocene to ? Pleistocene	Alluvium	Pre-Recent alluvial river terrace deposits
	LATE TERTIARY TO QUATERNARY	Lawin Basin Deposits	Loosely consolidated, poorly bedded gravel, grit, sand, and silt deposits in a fluviatile-deltaic-lacustrine
			UNCONFORMITY
MESOZOIC	Believed to be mainly JURASSIC but possibly ranging from CRETACEOUS to TRIASSIC	Granite and Differentiates	Mainly granite composition, fina-grained to coarse-grained, porphyritic to non-porphyritic types; adamellite and grahodiorite composition
			PROBABLE UNCONFORMITY
	CRETACEOUS - JURASSIC	Tembeling Formation	Conglomerate, feldspathic and quartzitic sandstone, grey and reddish shale and mudstone
	TRIASSIC	Semanggol Formation	Alternating sandstone, siltstone, and shale, interbedded with chert
			UNCONFORMITY
PALAEOZOIC	SILURIAN - ORDOVICIAN	Baling Formation	Calc-Silicate Facies: Hornfels Argillaceous Facies: Various argillites Quart-biotite hornfels Volcanic Facies: rhyolite tuff Limestone Facies: Marble Arenaceous Facies: Calcareous quartzite and Quartzite

Table 2.5 The geological formations and groups of rock occuring within the Kedah-Perak area (adopted from Burton, 1970; Jones, 1970 and Gobbett et al., 1973

mainly rice-growing and grazing. Besides Recent alluvium, it has been reported that pre-Recent alluvium deposits occur in the area close to the present river channels and are commonly in the form of terraces, 3 to 10 m in height above the present flood plains (Burton, 1970). The formation is partly consolidated and closely resembles the Older Alluvium of Johore and Singapore (Burton, 1964), which is composed of material of coarse character including sandy gravel, gravelly sand and gravelly silt. In addition to the superficial deposits forming the alluvial plain and river terraces, a number of exposures of semi-consolidated and poorly bedded gravel, grit, sand and silt of the Tertiary basin deposits occur in the sub-area 2, underlying an area roughly 2.5 kilometres in diameter (Jones, 1970) (Figure 2.12). Apart from all these Quaternary and Tertiary deposits, the weathering of bedrock under tropical conditions forms a relatively thick mantle of soil which occurs almost everywhere in the area, however, on steeper slopes the residual material is continually washed down slope, hence the soil cover is very thin, leaving occasional patches of bare rock. Where little or no transport has been involved, the composition of soils is usually directly related to the parent rock. The general description of several soil types which are present in the area and their derivation is presented in Table 2.6.

Figure 2.2 shows an outline of the structure of the Malay Peninsula. It is clearly shown that the study area belongs to the western zone of structural outline of the Malay Peninsula. Further, Tjia (1972, 1978) placed the area in the

PARENT MATERIAL	SOIL DESCRIPTION/CHARACTERISTIC
Rhyolite tuff	Pale-coloured, stiff, shallow, poorly structured, silty clay loams with unfavourable physical characteristics, a very high content of free quartz, and low inherent fertility.
Shale and phyllite	Heavy textured, moderately well-structured soils of good depth and colour except for sporadic lateritic developments in which the laterite normally occurs within 3 feet of the surface. Average to slightly above average fertility.
Quartzite	Fine sandy loam or fine sandy clay loam of good depth, well-drained, and of loose consistency: Average fertility.
Limestone	Very limited thicknesses of red lateritic clayey soils which develop close to the foot of limestone cliffs.
Granite	Medium and coarse sandy clay loams with very deep uniform profiles developed on the less steeply sloping topography, and shallow bouldery profiles in the steeper areas. The soils of the deeper profiles are of above average fertility, but those on the steep slopes are unsuitable for agriculture.
Basin deposits	Coarse-textured pebbly soils of low fertility.
Alluvium	Usually loamy in texture with variable drainage characteristics and relatively high fertility.

Table 2.6 Soil types present in the Kedah-Perak sub-area 2 and their derivation (Source: notes by Panton in Jones, 1970).

morphotectonic domains 1 and 3 (Figure 8.20) which have various structural trends caused by compression in several directions during certain geologic ages (Table 8.5). Apart from that, it has been reported that there was also an east-west compression during Early Mesozoic in the west of the area (Burton,1965; Tjia, 1971) which may have influenced the structural trends of the area. The major elements of the structural pattern in the area are large fractures and faults which appear to have occurred during brittle phase deformation in Post Triassic (Hutchison, 1973) or in Jurassic to Early Tertiary times (Tjia, 1978). One of the major faults in Malay Peninsula, the Bok Bak Fault (Figure 2.2), runs in the northwest-southeast direction in the southwest of the area. It is a strike-slip fault which runs in a N 30 W direction, 80 km long and 10 km wide and at least 55 km aggregate left lateral displacement (Burton, 1965, 1970; Tjia, 1978). Recent study suggests that the length of the Bok Bak Fault is much more than previously stated (Raj, 1982). There are numerous other major lineaments (topographic and geological) in the area particularly in the granite, and it is likely that many of these lineaments, especially the longer ones are probably faults or fault zones as interpreted in the Chapter 8.

2.5 Summary

The general physiography and geology of the study areas is outlined. Although the areas belong to a different climatic zone (the Lochindorb and Loch Tummel areas of Scotland represent the temperate zone while the Kedah-Perak area of

Malaysia experiences the tropical climate), they have in common certain physiographical and geological attributes:

a. All areas receive copious annual precipitation.

b. Almost all areas are covered by dense vegetation, and human influence affects the distribution of natural vegetation in certain areas.

c.. The areas are poorly exposed.

The Kedah-Perak area, however, is not covered by glacial and peat deposits as occurs in both of the Scottish areas.

There is a close relationship between the topography and the rock types of the areas. The Lochindorb and Loch Tummel areas contain lowlands with long rolling slopes and ridges, that have a nearly uniform level and are mostly underlain by the Moines (mainly composed of a thick and monotonous psammitic and pelitic rocks). The southern half of the Loch Tummel area, which is mountainous throughout, is underlain by the Dalradian which is characterized by a greater diversity of rocks including quartzites and limestones. Generally, for the Kedah-Perak area, mountainous and highly dissected terrain, subdued topography with less elevated peaks, and low to gently undulating topography are generally related to the granite, metamorphic rocks and sedimentary rocks, respectively.

Structurally, the Lochindorb area is not important to this study. Several major faults (which have been described in detail by previous workers) traverse across the Loch Tummel, with the Loch Tay Fault which runs in NE-SW direction being the longest. The Bok Bak Fault, which runs in NW-SE direction is the major geological structure in the Kedah-Perak area.

CHAPTER 3

BASIC PRINCIPLES OF REMOTE SENSING

3.1 Introduction

Remote sensing, as defined in Chapter 1, comprises the measurement and recording of electromagnetic radiation (EMR), reflected or emitted from the earth surface and atmosphere, by a sensor above earth surface and the relating of such measurements to the nature and distribution of Earth surface materials (Curran, 1985; Mather, 1987). Normally, this gives rise to some form of imagery which is further processed and interpreted to produce useful information for application in many fields including geology. Therefore, the main objective of remote sensing is to extract environmental and natural resources data related to the earth. The information about the object which is recorded by remote sensing actually represents the final result of interaction between EMR with the earth's surface (the amount and characteristics of radiation reflected or emitted is dependent upon the characteristics of the objects on the earth surface) and atmosphere (EMR passing through the atmosphere is distorted and scattered). From this point of view, the key to designing remote sensing systems, defining their use, understanding and interpreting the resultant images, lies in the way in which EMR is generated,

propagated and modified (Curran, 1985). Detailed description of this subject matter including complex mathematics is given in many texts particularly Suits (1983), Smith (1983) and Chahine (1983) and a general overview of the subject is discussed in several standard texts, such as Curran (1985), Lo (1986), Sabin (1987), Lillesand and Kiefer (1987), Drury (1987) and Mather (1987).

In order to outline the subject, basic consideration about the properties of EMR will be discuss in this chapter, and this is followed by a discussion of its interaction with atmosphere as well as earth surface. General discussion about the interaction between EMR with earth surface materials is given in section 3.3. Finally the chapter will end with a brief discussion about geobotany, the relationship between a plant and geologic materials like soil and rock in remote sensing context.

3.2 Electromagnetic radiation and its properties

3.2.1 Physical characteristics of electromagnetic radiation

The source of EMR is either from the Sun's reflected light, or the Earth's emitted heat, or from an artificial source like microwave radar. This is measured and recorded by a sensor that may be in the form of a radiometer or a camera on board a platform such as an aircraft or a satellite. EMR occurs as a continuum of wavelengths and frequencies called the electromagnetic spectrum (EMS), from short wavelength with high frequency waves, for example ultraviolet to long

wavelength with low frequency waves, for example radio waves (Figure 3.1). The EMS used in remote sensing extends from about 0.4 μm, the ultra violet region, to about 50 cm, the microwave region. The most important wavelengths used in remote sensing are, however, the visible and near infrared radiation in the wavebands 0.4 μm to 2.3 μm, infrared radiation in the wavebands 3 μm to 5 μm and from 8 μm to 14 μm, and the microwave region, from 5 mm to 500 mm (Lo, 1986; Lillesand and Kiefer, 1987). Although these names are assigned to specific regions in the EMS, it must be noted, that, there is no clear cut dividing lines between one spectral region and the others.

EMR is a form of energy transfer from one medium to another by the means of radiation. This energy behaves in accordance with the basic wave theory and moves equally in a sinusoidal fashion at the velocity of light, 3×10^{10} cm sec^{-1}. The wave consists of two force fields, electric (vertical) and magnetic (horizontal), which move perpendicularly to each other and to the direction of wave propagation. The wave can be measured in terms of the wavelength, λ, in micrometers (μm), which is the distance from one wave peak to the next, or its frequency, f, in hertz (H_z), which is the number of wave peaks passing a fixed point in space in a given time. Since c is constant (velocity of light), either wavelength or frequency can be used to describe a particular wave as they are related inversely as shown by the equation:

$$c = f\lambda \quad \text{or} \quad f = \frac{c}{\lambda}$$

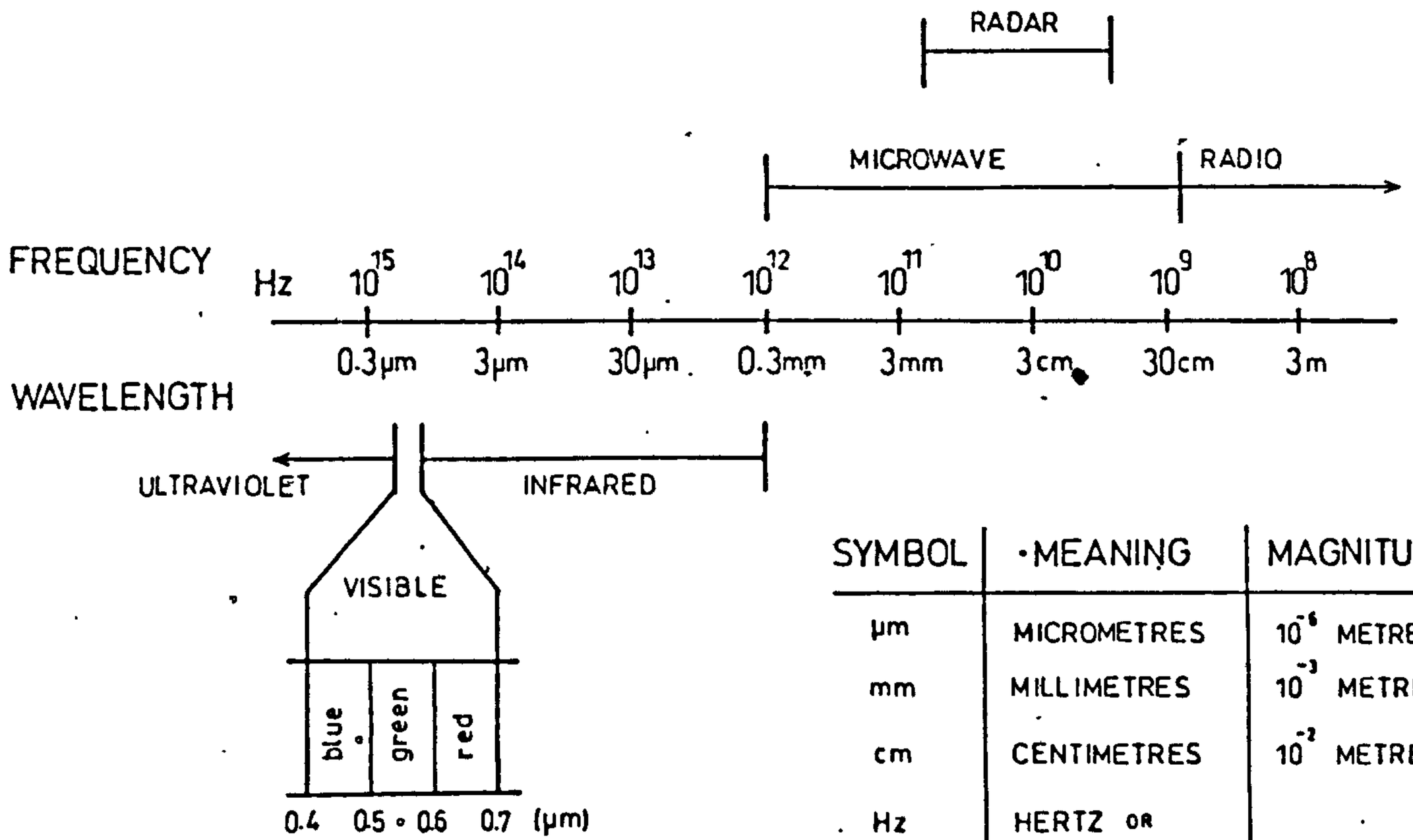

SYMBOL	MEANING	MAGNITUDE
μm	MICROMETRES	10^{-6} METRES
mm	MILLIMETRES	10^{-3} METRES
cm	CENTIMETRES	10^{-2} METRES
Hz	HERTZ OR CYCLES/SEC	

Figure 3.1 Electromagnetic spectrum (after Cornillon, 1982)

From this relationship, as the wavelength becomes shorter then more waves pass a point in a given time so the frequency is greater. In remote sensing, particularly for systems working in visible and infrared wavelengths, it is most common to categorize electromagnetic waves by their wavelength location within EMS rather than their frequency. For the systems working in microwave remote sensing, however, both wavelength and frequency are commonly employed (Table 3.1).

TYPE	WAVELENGTH		FREQUENCY	EXAMPLE
Visible	0.4- 0.7μm	400- 700nm	-	SPOT HRV
Near Infrared	0.7- 1.5μm	700- 1500nm	-	NOAA AVHRR
Middle Infrared	1.5- 2.3μm	1500- 2300nm	-	Landsat TM
Thermal Infrared	8.5-12.5μm	8500-12500nm	-	Meteosat
Microwave	10-300mm		1-12.5GHz	
K-band	11-17mm		18-26.5GHz	
X-band	24-38mm		8-12.5GHz	
C-band	38-75mm		4- 8GHz	ERS-1
L-band	150-300mm		1-2GHz	Seasat

$1\mu m = 10^{-6}m$ (one millionth of a metre)
$1nm = 10^{-9}m$ (one billionth of a metre)
Frequency $v = c^{-1}$ [GHz(10^9 cycles sec^{-1})]

Table 3.1 Wavelengths and frequencies used in satellite remote sensing (adopted from Harris, 1987 and Lillesand and Kiefer, 1987).

Based on the recently developed particle theory (quantum mechanics), radiation is considered not only to exhibit wave like properties, but also particle like properties. Specifically, the theory suggests that EMR is composed of many discrete units called quanta or photons, and energy of radiation (E), thus the energy of a quantum is related to the frequency (f) and a constant value known as Planck's constant (P) which is 6.6256×10^{-34} J sec such that:

$$E = Pf$$

Alternatively, the amount of energy of the waveform can be related to its amplitude (the maximum distance attained by the wave from its mean position). By combining and substituting the above quantum model equation of EMR with the wave model equation of EMR, one can relate the particle and wave properties of EMR as:

$$E = \frac{Pc}{\lambda}$$

Thus, the energy of a quantum is inversely related to wavelength and directly with the frequency. This means, the greater the energy, the shorter its wavelength and the higher its frequency.

Beside the sun, the most obvious EMR source exploited in remote sensing system, all bodies with temperature above zero degrees Kelvin (0 K = -273^0C) continuously emit some form of EMR over a broad range of wavelengths, therefore they are also

sources of EMR. How much is emitted and the distribution of the emitted radiation at each wavelength across the EMS is not uniform. In other words, every object emits a characteristic set of radiation waves which is related to its surface temperature. The total amount of radiation emitted by a black body - an ideal radiator or a perfect emitter (a hypothetical body which absorbs and reemits all the radiation incident upon it) is expressed by the Stefan-Boltzmann law, which states that

$$W = \sigma T^4$$

where,

W = total radiant emmitance from the surface of material, Watts (W) m^{-2}

σ = Stefan-Boltzmann constant, 5.6697×10^{-8} W m^{-2} $^0K^{-4}$.

T = absolute temperature (degree K) of the emitting material

Therefore, the radiant energy emitted by an object increases very rapidly with increases in temperature. This means, the energy emitted from an object is primarily a function of its temperature. But for a real object, the equation becomes

$$W = \sigma T^4 \Omega$$

where Ω is the emissivity of the body which lies between 0 and 1 (Ω for black body is 1).

Just as the total energy emitted by an object varies with temperature, the spectral distribution of the emitted energy also varies. Its absolute temperature, however, will determine the spectral distribution and the dominant wavelength or wavelengths at which it emits the maximum amount of energy. As the absolute temperature of a body changes, the dominant wavelength is also displaced according to Wien's Displacement Law,

$$\lambda_{max} = \frac{a}{T}$$

where,

λ_{max} = wavelength of maximum spectral radiant emittance, μm

a = a constant, 2898 μm K

T = temperature, K

Thus, the hotter the object the shorter the dominant wavelength. The relationship for a black body is shown graphically in Figure 3.2. The area under each curve represents the total radiation flux per metre^2 or emittance of an object at each temperature. In other words the higher the temperature of the radiator, the greater the amount of energy it emits. Spectral distribution of energy radiated from a black body at 6000 K and 300 K closely approximates the Sun's and the Earth's spectral distribution curves, respectively. Thus, the Sun has much higher total emitted energy compared to the Earth, and the dominant wavelength for the Sun and the Earth is about 0.5 μm (green light in visible region) and 9.7

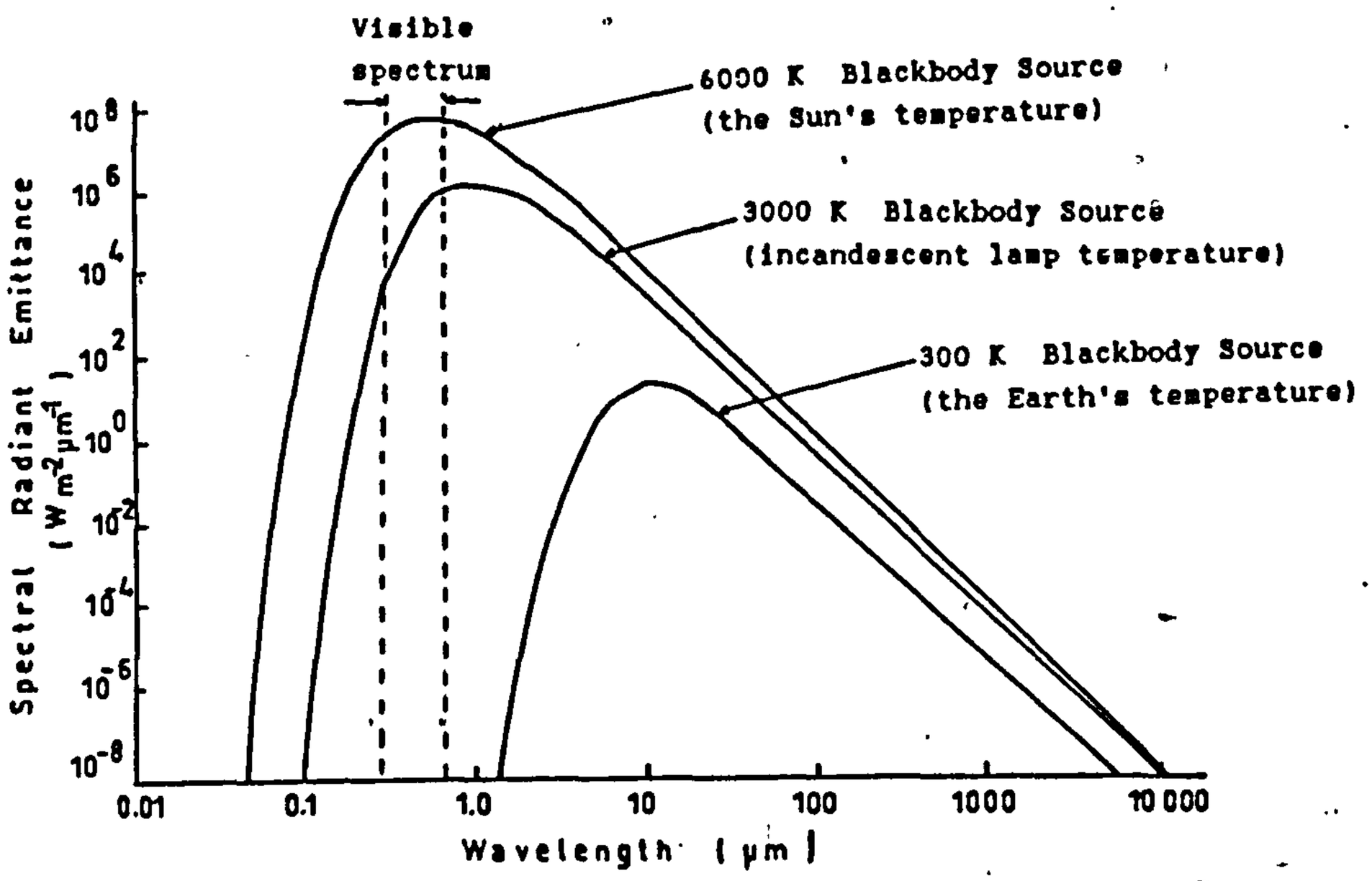

Figure 3.2 Spectral distribution of energy radiated from blackbodies of several temperatures. Note that spectral emittance, W , is the energy emitted from an area of 1 m^2 per unit wavelength interval. Total radiant emittance, W, is given by the area under the spectral emittance curves (Source: Slater, 1980).

μm (thermal infrared region) of the EMS, respectively. This explains why the Sun radiates visible and thermal wavelengths strongly while the Earth radiates thermal infrared wavelengths weakly (Barrett and Curtis, 1982).

There are two types of remote sensing system. First, the systems which are concerned with the EMR reflected from the Earth's surface receive radiation derived mainly from the Sun and are called passive systems such as Landsat, SPOT and AVHRR. On the other hand, the active systems are those systems which supply their own source of energy, the most widely used active systems being radar which uses transmission and detection of the microwave energy which is reflected back to a sensor by the earth surface.

3.2.2 Atmospheric effects on electromagnetic radiation

Virtually the whole of the EMS is available for use in remote sensing. However, whatever the source, the EMR has to travel through the atmosphere to some extent, with higher platforms such as satellites the detected radiation has passed through the whole layer of the earth atmosphere twice, whereas from an aircraft, which is much lower, the radiation detected has passed through a significantly lesser amount of atmosphere. During this passage, EMR interacts with particulate matter suspended in the atmosphere (water droplets, dust and smoke) and with the molecules of the constituent gases (oxygen, nitrogen, ozone, carbon dioxide and water vapour). This interaction will alter the radiation's characteristics, such as intensity and spectral distribution, and the main effects caused by the atmosphere are scattering and absorption (Figure 3.3). Therefore, an understanding of how EMR interacts with atmosphere is needed prior to any interpretation task on remotely sensed image.

Scattering

Scattering is the result of interaction between EMR and suspended particles or gas molecules which are present in the atmosphere. Scattering causes changes in direction and intensity of EMR, giving spurious results at the sensors. The amount of scattering depends on the wavelength and the size of the particles involved in the atmosphere. There are three main types of scattering (Table 3.2):

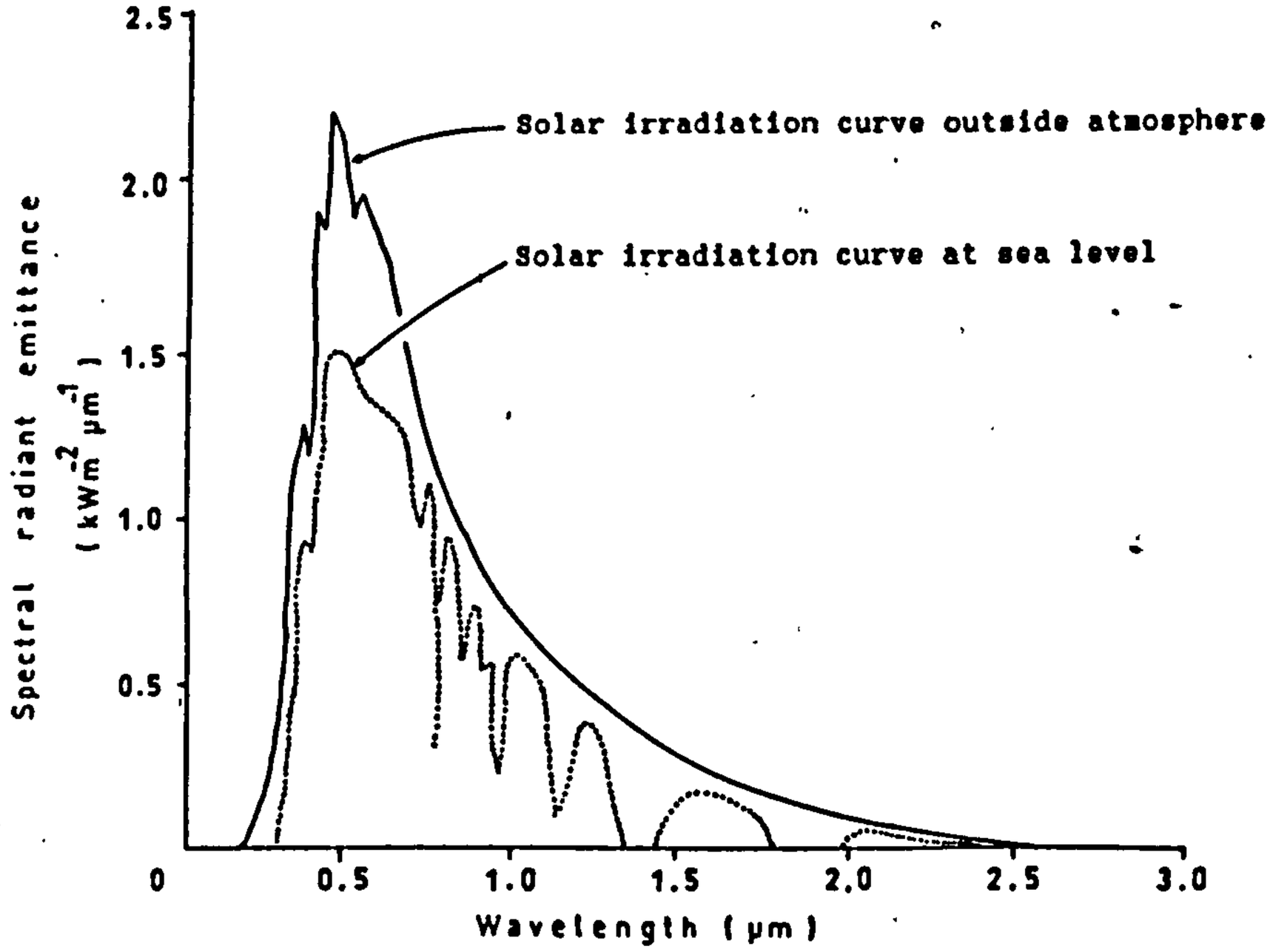

Figure 3.3 Solar irradiance at the top of the atmosphere (solid line) and at sea level (dotted line). Differences are due to atmospheric effects as discussed in the text (Source: Chahine, 1983).

TYPE OF SCATTER	SIZE OF EFFECTIVE ATMOSPHERIC PARTICLES	TYPE OF EFFECTIVE ATMOSPHERIC PARTICLES	SCATTER	EFFECT OF SCATTER ON VISIBLE AND NEAR VISIBLE LENGTHS
Rayleigh	Smaller than the wavelength of radiation. Usually $< 0.1\lambda$	Gas molecules	Molecule absorbs high energy radiation and re-emits. Scatter is inversely proportional to fourth power of wavelength	Affects short visible wavelengths, resulting in haze in photography, skylight and blue skies
Mie	Same size as the wavelength of radiation	Spherical particles of water vapour, fumes and dust	Physical scattering under overcast skies	Affects long visible wavelengths
Non-selective	Larger than the wavelength of radiation	Water droplets and dust	Physical scattering by fog and cloud	Affects all visible wavelengths equally, resulting in white fog and clouds

Table 3.2 Types of atmospheric scatter (after Curran, 1985).

a. Rayleigh scatter - this occurs when the EMR interacts with particles smaller than its own wavelength such as molecules of oxygen and nitrogen. Its intensity is inversely proportional to the fourth power of the wavelength, hence the effect of Rayleigh scattering increases dramatically at shorter wavelengths.

b. Mie scatter - this occurs when the particle diameters, for example vapour and dust, are approximately the same size as the EMR wavelengths. This effects EMR with wavelength longer than that of blue light.

c. Non-selective scatter - occurs when the particles in the atmosphere are larger than the EMR wavelengths, such as water droplets and ice fragments. White cloud is the result of this type of scatter, where all wavelengths of visible light are scattered in equal amounts.

Absorption

Absorption occurs when the EMR is absorbed by gas molecules, and the most efficient absorbers present in the atmosphere are water vapour (H_2O), carbon dioxide (CO_2), oxygen (O_2) and ozone (O_3). They normally absorb radiation at specific wavelengths of the EMS called absorption bands. Therefore, this can effect the portion of the spectrum looked at. In addition it implies that only some wavelengths in the EMS are not or less absorbed and are available for surveillance. The wavelength regions in the EMS where the absorption effect is not so significant, which means the atmosphere is more transmissive of EMR, are known as atmospheric windows (Figure 3.4). Wavelength regions

at 3 to 5 μm and 8 to 14 μm are examples of the atmospheric windows. Hence, the remote sensing systems are designed to utilize the wavelengths in the atmospheric windows.

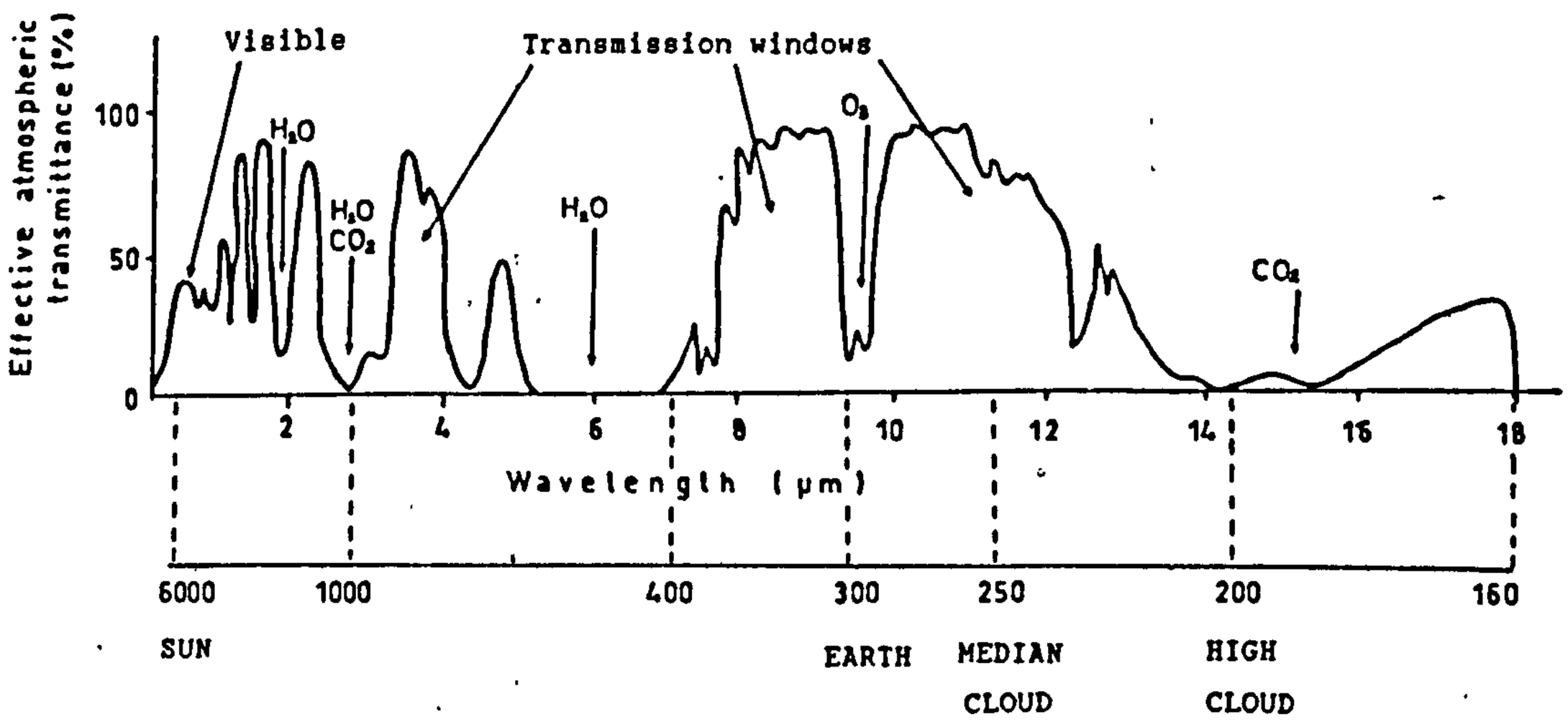

Figure 3.4 Radiation transmission through the atmosphere by radiant energy of different wavelengths (after Lo, 1986).

3.2.3 Interaction with the surface

When the EMR eventually reaches the earth's surface it is further modified through interaction with features on the surface. Various fractions of the EMR incident on the surface are reflected, absorbed and/or transmitted. The amount of energy reflected, absorbed or transmitted will depend on the type of material the energy is incident on. Therefore, if the

proportion of the source energy that is reflected, absorbed or transmitted is highly different for different materials on the earth surface, then these differences can be used to identify and distinguish materials based on their spectral properties.

Reflection

The amount of reflection of the EMR depends on surface roughness or smoothness of the material, and the relative size of the irregularities and the wavelengths. If the high variation of the surface is less than the wavelength of the incident EMR, then the surface behaves as a smooth reflector where radiation is reflected without being scattered; the angle of incidence remaining equal to the angle of reflectance. This type of surface is termed as specular reflector. On other hand, when the surface irregularities are greater than wavelengths, the surface will appear rough and behaves as a Lambertian (diffuse) reflector which will reflect the incident radiation uniformly in all direction.

Most earth surface features lie somewhat in between the specular and diffuse reflectors. The reflectivity of a surface is known as the reflection coefficient or albedo. The albedo of a surface is the percentage of the radiation which is reflected back towards space (Barrett and Curtis, 1982; Lo, 1986).

Absorption

Not all the incident energy on the earth's surface is scattered or reflected, instead it may be absorbed or retained

by the materials. The absorbed energy may be re-emitted as radiation of a different wavelength. For example, the solar energy absorbed at the earth's surface is re-emitted from the Earth at much longer wavelengths as thermal energy. This emitted energy forms another source of EMR for remote sensing, apart from geothermal energy which is emitted from the interior of the Earth.

Transmission

Some of the incident radiation may be transmitted through the features. The transmission properties of a material depends on the material and wavelength. The transmittance of a target (or a medium like the atmosphere) is defined as the ratio of the radiation at a certain distance within it to the incident radiation (Barrett and Curtis, 1982).

In general, the total interaction and interrelationship between energy and the earth's surface for passive remote sensing can be simplified as (Lo, 1986):

$$E_D(\lambda) = E_I(\lambda) - [E_A(\lambda) + E_T(\lambda) + E_R(\lambda)] + E_E(\lambda)$$

where,

$E_D(\lambda)$ = total energy detected.

$E_I(\lambda)$ = source or incident energy.

$E_A(\lambda)$ = absorbed energy

$E_T(\lambda)$ = transmitted energy

$E_R(\lambda)$ = reflected energy

$E_E(\lambda)$ = emitted energy

3.3 Spectral reflectance of earth surface materials

The reflectance characteristics of earth's surface materials may be quantified by measuring the proportion of incident energy that is reflected. This is measured as a function of wavelength and is called spectral reflectance or spectral response, Γ and is mathematically defined as (Lillesand and Kiefer, 1987):

$$\Gamma = \frac{E_R(\lambda)}{E_I(\lambda)} \times 100$$

where $E_R(\lambda)$ and $E_I(\lambda)$ are equal to reflected energy from the object and incident energy upon the object, respectively at wavelength λ , and spectral reflectance is expressed as a percentage.

The spectral reflectance of individual earth surface features when measured throughout the EMS are unique to the surface feature (Figure 3.5). Apart from feature types, spectral reflectance will also be influenced by two factors, namely temporal and spatial effects. Temporal effects are any factors that change the spectral response over time such as sun azimuth, sun elevation and state of growth of the vegetation. The spatial effects are any factors that change the spectral response of a feature at a certain time, in different locations such as variation in the state of health in the vegetation cover. Therefore, although an individual feature may be characterized by a specific spectral response, often referred to as spectral signature. However, because of

many external and internal factors, the same feature may appear variable, hence the signatures are only relatively distinguishable but they are not necessarily unique. To illustrate the point, vegetation, soil, water, and rock, will be discussed.

3.3.1 Spectral reflectance of vegetation

Over two-thirds of the land surface of the world is covered with vegetation (Lyon, 1977), therefore, it must not be neglected when dealing with geological application of remote sensing and mineral exploration programs. The most important point to note is that vegetation has a relatively low reflectance in the visible part of the EMS and relatively high reflectance in the near infrared part (Tucker, 1979), whereas other surface features like soil, water and rock, commonly have similar or small changes in reflectance in both wavelengths (Harris, 1987) (Figure 3.5). Therefore, the shape of the spectral reflectance curve can be used to distinguish vegetated and non-vegetated areas on remotely-sensed imagery. This difference also means that even a small amount of vegetation will alter the spectral signatures of other surface materials such as soil and rock.

A plant uses the sun's energy to change inorganic nutrients into organic compounds through the process of photosynthesis. The plant's requirements for the suns energy varies with the season according to the plants growth stage and associated with these changes are shifts in the spectral reflectance (Curran, 1980). Other factors such as leaf and

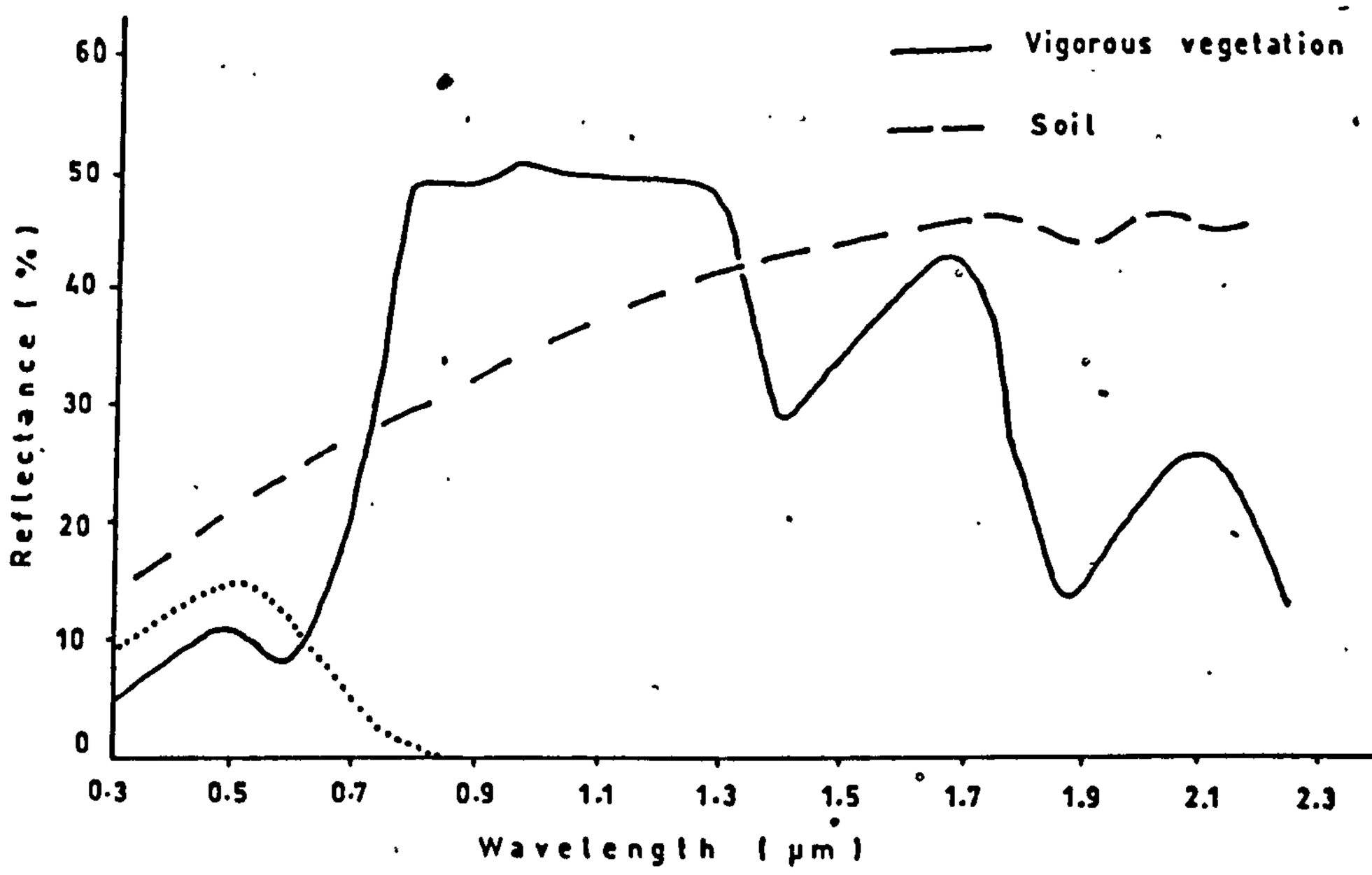

Figure 3.5 Idealized spectral reflectance curve for vigorous vegetation, soil and water (after Mather, 1987).

canopy geometry, plant physiology, soil type, solar angle and climate conditions have an effect on the reflectance, absorbance and transmittance properties of a vegetation (Jensen, 1983; Curran, 1985).

Different parts of the spectrum are affected by the differences in leaf structure. A function of chlorophyll is to absorb radiation by the photosynthesis process, and this is indicated by absorption bands of about 0.45 μm (blue light) and and 0.68 μm (red light) (Drury, 1987). However, there is a slight rise in reflectance at about 0.55 μm (green light), i.e. the portion of the visible band which is not absorbed, and this results in the green appearence of healthy leaves

(Myers, 1983). The 0.7 to 1.35 - μm region shows high reflectance and low absorption, and this is controlled mainly by the leaf's internal structure, namely the spongy mesophyll layer (Gausman, 1974; Myers, 1983). The combined effects of leaf pigments and physiological structure give all healthy green leaves their characteristic reflectance properties: low reflectance of blue and red light, medium reflectance of green light and high reflectance of near infrared radiation. At three major water absorption bands at wavelengths of 1.4 μm, 1.9 μm and 2.7 μm, and two minor water absorption bands at wavelength of 0.96 μm and 1.1 μm (Figure 3.4), cause leaf reflectance to decrease (Curran, 1985). Apart from that, this phenomenon is also affected by leaf structure and the water concentration in the tissue (Barrett and Curtis, 1982).

For a stressed or senescent leaf, because its chlorophyll pigment decays away, the ability to absorb blue and red light decreases, and as a result, the amount of visible light reflected increases. Similarly, as the spongy mesophyll layer contracts, the density of air space decreases and so the reflectance of near infrared radiation also decreases (see Figure 3.7) (Myers, 1983).

3.3.2 Spectral reflectance of soils

A large proportion of the EMR incident upon a soil surface is either reflected or absorbed, and little is transmitted. Soil reflectance depends on many factors such as its moisture content, organic content, texture, structure and iron oxide content, and these factors are complex, variable, and

interrelated (Hoffer, 1978; Smith, 1983; Wright and Birnie, 1986; Lillesand and Kiefer, 1987). However, the reflectances of the majority of soils are similar, and soil reflectance curves exhibit a gentle increase with increasing wavelength (Figure 3.5) (Smith, 1983; Curran, 1985; Mather, 1987).

General spectral reflectance of soils can be summarised as;

a. Dry soils are normally brighter than wet soils at the same wavelength, because the presence of soil moisture considerably reduces the surface reflectance of soil (Bowers and Hanks, 1965; Jensen and Hodgson, 1983).

b. Soil reflectance decreases as organic matter content increases (Page, 1974 as quoted by Curran, 1985; Smith, 1983).

c. Usually, soil reflectance also decreases with increasing iron-oxide content (Smith, 1983).

d. Some soils, for example clays, which have a smooth texture (depending on the proportion of sand, silt and clay particles) and strong structure (the arrangement of sand, silt and clay particles into aggregates) which leads to a rough surface on ploughing, and also poorly drained, resulting in high moisture content will have a rather low reflectance. On the other hand, a sandy soil which has a rough texture, low structure - smooth surface and well drained, resulting in low moisture content will have high reflectance properties (Bower and Hanks, 1965).

3.3.3 Spectral reflectance of water bodies

The majority of the EMR incident upon water is not reflected but absorbed or transmitted (Figure 3.5). In visible wavelengths, little (5 per cent) is reflected and the majority is transmitted (Curran, 1985). In the near infrared, the reflectance of deep and clear water is virtually none, and as a result, water bodies can be distinguished easily from other surface features. However, the spectral reflectance of water is affected by three main factors: i.e. the depth of the water, the materials within the water and the surface roughness of the water which is summarised below:

a. For depths greater than 40 m, all visible radiation is absorbed, hence, it appears dark (Drury, 1987). In shallow water, apart from the water, some of the radiation is reflected from the bottom of the waterbody, therefore, it is often the underlying materials in shallow streams and lakes that determine the waterbody's reflectance properties (Curran, 1985; Mather, 1987).

b. The presence of materials suspended in the water, suchsa non-organic and organic materials, will increase the apparent reflectance of visible light from water.

c. A water body with a rough surface will have high reflectance, whereas if the surface is smooth its reflectance will be very high or very low depending upon the position of the sensor.

3.3.4 Spectral reflectance of rocks

About 70% of the earth's land surface is vegetated and underlying rocks cannot be seen directly, therefore, geological use of remotely sensed data relies to a considerable extent upon knowledge of the spectral reflectance curves of vegetation (Rowan, 1975; Lillesand and Kiefer, 1987). This means, in most cases the spectral reflectance curves of rocks and minerals cannot be used directly to infer the lithology of the area. Consequently, many studies have been published on the uses of geobotanical anomalies in order to infer and determine the location of certain type of mineral deposits which may be related to certain rock types, for example see Lyon (1977), Hoffer (1978) and Curran (1980). Further discussion about geobotany will be given in section 3.4. For areas where rocks are well exposed, for example in semi-arid and arid areas, the spectral reflectance curves of rocks and minerals may be used directly in order to infer the lithology of the study area, for example see Rothery, (1987a and 1987b), Davis et al., (1987). This is not the case for the study areas in this work where the area is almost completely vegetated.

Reflectance of rocks and minerals depends on both factors namely surface external effects such as surface roughness, and internal effects such as its composition (Smith, 1983). From a remote sensing perspective, probably the most exhaustive work relating to the measurement of reflectance properties for minerals and mineral complexes is the work which was carried out by Hunt and co-workers, e.g. Hunt et al (1973), (1974a),

1974b), (1975) and (1976). They indicated from their study that rock-forming minerals have unique spectral reflectance curves and the presence of absorption features in these curves is diagnostic of the presence of certain mineral types. Rowan et al. (1974) recognized limonitic alteration based on the typical absorption bands in the 0.4 - 0.6 μm and 0.8 - 1.0 μm. Clay minerals are identified by decreasing spectral reflectance beyond 1.6 μm while carbonate and silicate minerals can be determined from the presence of absorption bands at about 2.0 - 2.5 μm (Hunt et al., 1971). Despite these general relationships, unfortunately, the spectral characteristics of most rock types do not have as distinctive a curve (Figure 3.6) as that for vegetation, hence the identification of rocks and minerals, in most cases, remains difficult (Williams, 1983).

In addition to the effects of atmospheric scattering and absorption, weathering is the major difficulty involved in the identification of rocks and minerals from the properties of spectral reflectance. The reason is that weathering produces a surface layer which is different in composition from the parent rock, and this will alter the measured spectral reflectance (Williams, 1983). Furthermore, the rocks and minerals may only be detected if they are sufficiently abundant (well exposed) and their spectral features are strong enough and different from their surrounding features.

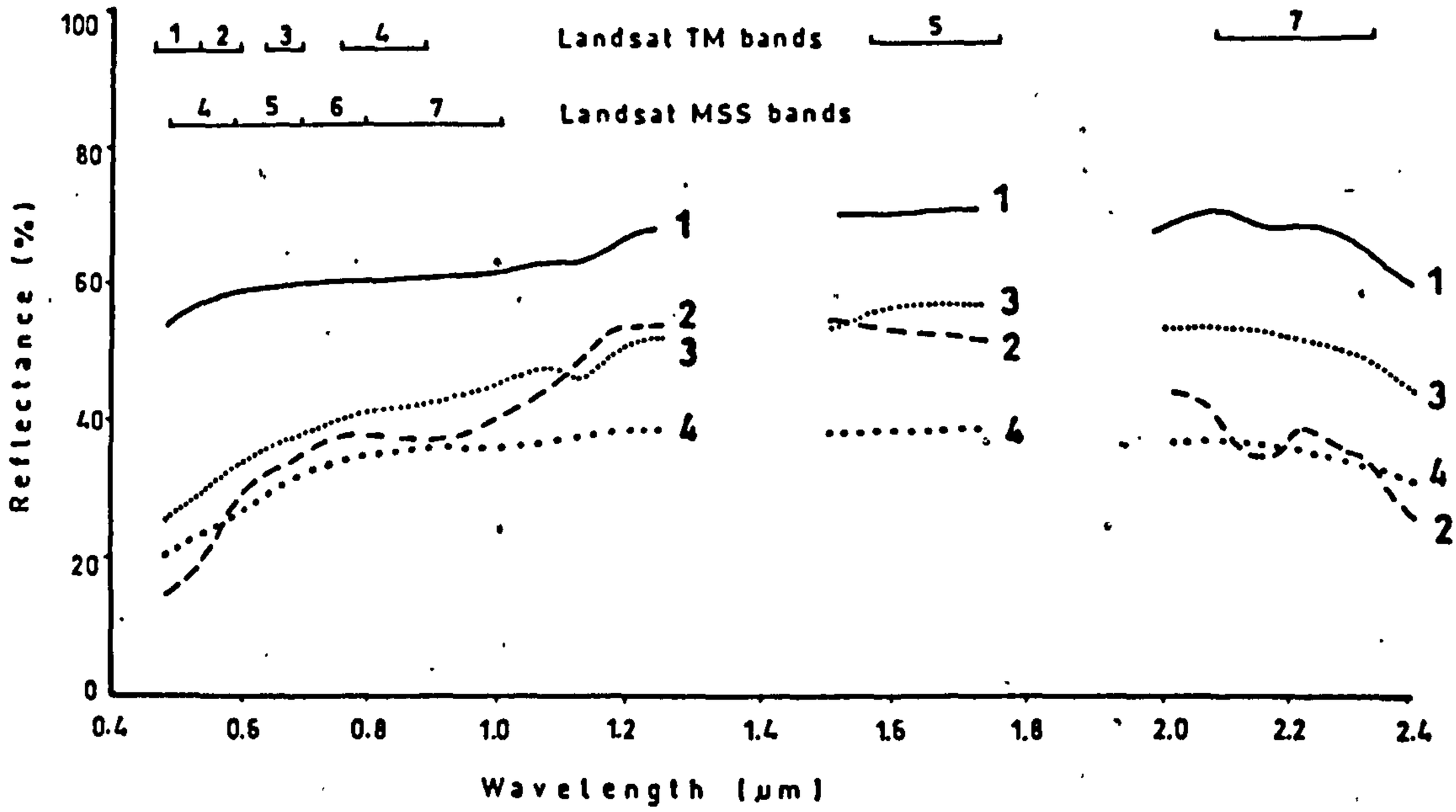

Figure 3.6 Spectral reflectance curves of four surface types: (1) volcanic rocks, (2) altered latite, (3) limonitic volcanics, (4) tan soil or rhyolite. The data were collected with a field reflectance spectrometer. (After Williams, 1983).

3.4 Geobotany

Two important methods in mineral exploration where vegetation is used as a guide to mineralization are biogeochemistry and geobotany. Biogeochemical methods of exploration depend on the chemical analysis of plants or humus to obtain evidence of mineralization in the substrate, whereas geobotanical methods involve a "visual" survey of the vegetation cover in order to detect mineralization (Brooks, 1972). Geobotany, therefore, is the analysis of electromagnetic radiation reflected and emitted from vegetation in order to infer geological

differences of the landscape (Raines and Canney, 1980) which can be measured or detected through some form of remote sensing technique. This analysis is necessary and important because much of the land surface of the earth is covered by vegetation which means the surface geology cannot be sensed directly, and must be obtained via an analysis of the vegetation cover. With the increasing needs for raw materials, reliance on direct observation is not viable, hence methods of investigating geology prospects, despite vegetation cover, need to be investigated and developed to satisfy the demands for raw materials. The basis of geobotany is the relationship between the nutrient requirements of the plants and what is available in the soil; and the physical properties of the soil. In addition, there is an underlying assumption that there is a relationship between soil formation and the underlying lithology (Raines and Canney, 1980). Hence, geobotanical techniques are particularly successful in getting indirect geological information where the local rock type has a distinct effect upon the soil as well as the vegetation, see Rowan (1975), Goetz et al., (1983), Morrisely et al. (1984) and many studies also indicate that geobotanical anomalies of an area can be used as a good guide to reveal the effects of certain mineralisation, the presence of mineral deposits, and to infer and determine the location of certain type mineral deposits, for example see Longshaw and Gilbertson (1975), Milton et al. (1983), Collins et al. (1983), Darch and Barber (1983), Sabin (1987).

Different plants require different nutrients in varying amounts. The nutrients available to a plant depend on the soil which in turn depends on the parent material and the soil forming processes. However, not all the nutrients present in the soil are available for plant uptake due to certain physical factors of the soil. Nutrients are not the only factor affecting plants, they are dependant on a whole range of parameters available within the environment, hence, it would seem impossible to observe the influence of geology in such a complex situation. However, in several cases this influence can still be observed, as in the above mentioned studies.

The study of geobotany can be classified into three conceptual approaches: the study of plant communities including characteristic floras and specific indicator species, the study of vegetation density including the extreme case of complete absence of vegetation, and the study of plant morphology (Raines and Canney, 1980). Geobotanical anomalies may be expressed in four main ways (as defined by Goetz et al. (1983) and Mather (1987);

a. Anomalous distribution of species and/or plant communities.

b. Stunted growth and/or decreased percentage ground cover.

c. Alteration of leaf pigment complexes, physiologic process that causes yellowing or chlorosis, altered transpiration rate.

d. Anomalous phonological cycles that cause early foliage change or senescence in autumn, alteration of flowering periods, or late leaf flush in spring.

Because these anomalies can occur over the growing season and the overall condition of vegetation may also vary from year to year due to climatic fluctuation, it is important that remote sensing data are collected at several times during the year and over several years (Williams, 1983; Lillesand and Kiefer, 1987).

If an area contains high concentrations of heavy metals in the soils particularly Ni, Cu, Cr, Co and Pb, then the area may become toxic to plants (Williams, 1983; Sabin, 1987). The effects of this metal toxicity on the plants can be seen in many ways. For example the plant growth may be stunted (Raines and Canney, 1980), or deformed (Lyon, 1975), or found in reduced number and in severe cases barren spots may occur (Williams, 1983). On the other hand, indicator plants, the plants that grow preferentially on outcrops and soils enriched in certain elements, may be found exclusively or in large numbers in mineralized areas. For example, Cannon (1960) found that a small blue-flowered mint, *Acrocephalus robertii* grows only on copper bearing rocks in the Katanga region of Zaire. Another effect is chlorosis which is a yellowing of the normal green leaves and is cause by an excess of heavy metals like Cu, Zn, Mn, Pb, and some others that interferes with chlorophyll production (Raines and Canney, 1980; Sabin, 1987). The high pH associated with calcareous soils on carbonate

rocks also limits nutrient availability such as iron, phosphorus, manganese, boron, copper and zinc to certain plant species (Williams, 1983). Several workers have measured the reflectance of various plants under the influence of heavy metals stress (Horler et al., 1980a; Horler et al., 1980b; Birnie and Francica, 1981; Labovitz et al., 1985; Yost and Wenderoth, quoted by Harris (1987) and Sabin (1987). They generally conclude that the result of heavy metal stress is an increased reflectance in the visible part of the EMS and contrasting effect occurs in the near infrared which is associated with a decrease in the chlorophyll content and changes in the internal leaf structure of the stressed leaves, respectively (Figure 3.7). Furthermore, there are many other effects on plants caused by the high concentration of heavy metals, hydrocarbons and soil moisture that have been reported, but are beyond of the scope of this study.

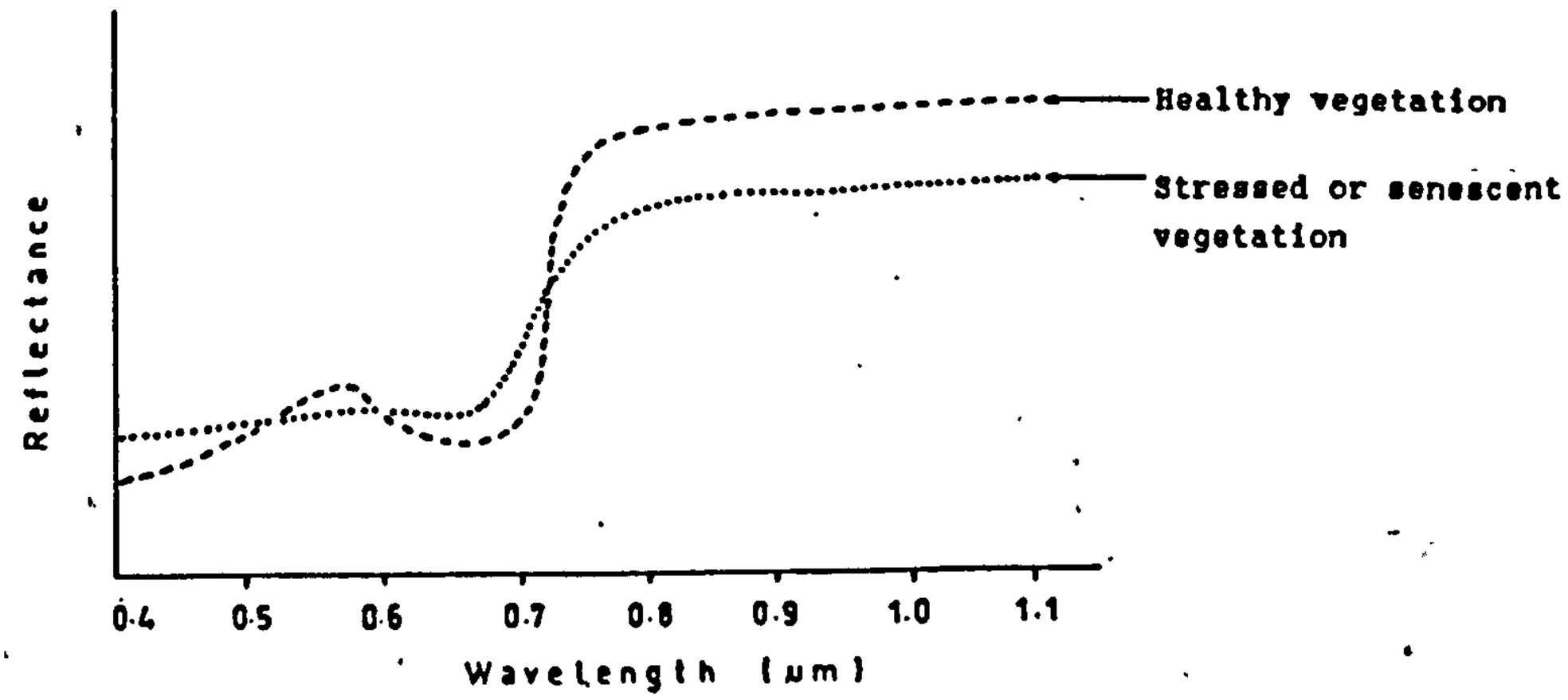

Figure 3.7 Simplified spectral reflectance curves for healthy and stressed or senescent vegetation in the visible and near infrared parts of the electromagnetic spectrum (adapted from Harris, 1987).

One important point must be noted, that it would be unwise to suggest that all the changes in plants are related to lithological units or mineral deposits (heavy metals) because they can also be caused by a variety of environmental factors or by disturbance. However, the results of a number of studies do show that the identification of such anomalies in the vegetation community of an area can be a valuable sign of the presence of mineral deposits. This means that the geology of an area can have an effect on the vegetation. Some of these anomalies can be detected through some form of remote sensing. For example, although the identification of individual plants may be beyond the resolvable limits of most remote sensor systems, both aerial photographs and satellite imagery can record vegetation species composition. Plant density and physiological changes of a vegetation type are represented as image or photo tone, texture, and pattern in the photographs or images and these can be interpreted.

3.5 Summary

Basic principles of remote sensing have been discussed in this chapter. The main purpose of remote sensing technique is to get data (environmental and natural resources) related to the earth based on the spectral characteristics. Therefore, the basic principle of applied remote sensing is that all earth-surface elements are separable on the basis of their spectral reflection characteristics, or in other words, the spectral reflectance characteristics throughout the electro-magnetic spectrum are unique to specific object/element. In reality,

however, many factors such as the atmospheric effects on EMR, the interaction between EMR and features on the earth's surface, cover-types which mask the underlying features, temporal and spatial effects make the situation more difficult. Consequently, the same element, for example soils, may show different spectral characteristics, or may show similar to others, for example rocks, hence the spectral signatures are no longer unique. Large areas of the earth's surface are vegetation covered. Through the assumption which has been proven for certain areas, that there is a relationship between vegetation - soil - underlying lithology, hence, it has proved possible to infer geological distribution. Through this understanding, we will appreciate some of the problems encountered in the design and application of the remote sensing systems.

CHAPTER 4

REMOTE SENSING SYSTEM, DATA ACQUISITION AND IMAGE PROCESSING SYSTEM.

4.1 Introduction

A large numbers of satellites for remote sensing have been launched since 1960. A complete list and detailed description of these satellite remote sensing systems can be found in Cornillon (1982), Elachi (1983), Allison and Schnapf (1983), Freden and Gordon (1983), Curran (1985), Jensen (1986) and Harris (1987). In this chapter, however, the Landsat satellite system with multi-spectral scanner (MSS) and the thematic mapper (TM) sensors will be outlined. They are the most widely used by the geographical and geological communities (Short, 1982; Mather, 1987) and the Landsat system will probably continue to provide an extensive collection of remote sensor data (Jensen, 1986). Freden and Gordon (1983) give details of the Landsat platforms, orbits, and imaging systems. The data from Landsat is made available to use in the study on computer magnetic tape. The basic characteristics of this data is discussed in section 4.3. The data, which is in a digital format, is processed using a digital image processing system. Basic characteristics of the system used in this study, is the subject of section 4.4. At the end (section 4.5), a general

discussion about aerial photo-interpretation which has been carried out is presented.

4.2 The Landsat satellites

Landsat is the result of the earth resources programme developed by the National Aeronautical and Space Administration (NASA) in the USA. The first satellite was launched on 22 July 1972 as ERTS-1 (Earth Resources Technology Satellite) and was later renamed Landsat 1 (Freden and Gordon, 1983). It represented the first unmanned satellite specifically designed to acquire data about earth resources on a systematic, repetitive, medium resolution, multi-spectral basis (Lillesand and Kiefer, 1987). Since then, five Landsat satellites have been launched. Table 4.1 highlights the chronological launch, retirement and other characteristics of the Landsat 1 through Landsat 5 mission. Because Landsat 1, 2, 3 were so similar in their operation, as were Landsat 4 and 5, they are termed first and second generation of Landsat, respectively (Lo, 1986; Sabin, 1987; Harris, 1987). All the Landsat satellites were launched into repetitive, circular, sun-synchronous, near-polar orbits. There are differences, however, in term of altitude, orbits per day, times of crossing the Equator etc between these two Landsat generations (Table 4.2 and 4.3).

In the context of this section on data acquisition, the type of imaging systems carried by Landsat, the nature and quality of remote sensor data is an interesting point for discussion. There are three imaging systems onboard Landsat

SATELLITE	LAUNCHED	RETIRED	RBV bands	MSS bands	TM bands	ORBIT
Landsat 1	July 1972	January 1978	1,2,3	4,5,6,7	None	18 day/900 km
Landsat 2	January 1975	July 1983	1,2,3	4,5,6,7	None	18 day/900 km
Landsat 3	March 1978	September 1983	A,B,C,D	4,5,6,7,8[a]	None	18 day/900 km
Landsat 4	July 1982	-	None	1,2,3,4[b]	1,2,3,4,5,6,7	16 day/705 km
Landsat 5	March 1984	-	None	1,2,3,4[b]	1,2,3,4,5,6,7	16 day/705 km

[a] Band 8 (10.4-12.6μm) failed shortly after launched

[b] For simplicity, we use only the Landsat-1 to -3 MSS band numbers here (4,5,6,and 7) for the Landsat-5 MSS data of the Lochindorb and Loch Tummel (see Table 4.5) througout this study.

Table 4.1 Operation periods and characteristics of the Landsat-1 to -5 missions (Source: NOAA, 1986).

MULTISPECTRAL SCANNER		LANDSAT-1 TO -3 SATELLITE
Channel	Waveband (μm)	
		Orbit: near-polar, Sun-synchronous
4	0.5 - 0.6	Altitude: 919 km nominal
5	0.6 - 0.7	Inclination: 99.09^0
6	0.7 - 0.8	Period : 103 minutes
7	0.8 - 1.1	Equatorial crossing time: 0930
		Repeat cycle: 18 days
Spatial resolution: 80 m		
Radiometric resolution: 6 bits (64 levels)		
Swath width: 185 km		

Table 4.2 Landsat-1 to -3 satellite and multispectral scanner wavebands (after Mather, 1987).

THEMATIC MAPPER		LANDSAT-4 AND -5 SATELLITE
Channel	Waveband (μm)	
		Orbit: near-polar, Sun-synchronous
1	0.45 - 0.52	Altitude: 705 km
2	0.52 - 0.60	Inclination: 98.2^0
3	0.63 - 0.69	Period: 99 minutes
4	0.75 - 0.90	Equatorial crossing time: 0945
5	1.55 - 1.75	Repeat cycle: 16 days
6	10.40-12.5	
7	2.08 - 2.35	
Swath width: 185 km		
Spatial resolution: 30 m (band 6: 120 m)		
Radiometric resolution: 8 bits (256 levels)		

Table 4.3 Landsat-4 and -5 satellite and thematic mapper wavebands (after Mather, 1987).

satellites namely return beam vidicon (RBV) cameras, multi-spectral scanners (MSS) and thematic mapper (TM). However, the following discussion will be focused only on the multi-spectral scanner and the thematic mapper system.

4.2.1 Landsat multi-spectral scanner

The Landsat multi-spectral scanner system (MSS) was the major imaging system placed on each of the five Landsat satellites. It is a line scanning device which uses an oscillating mirror to continuously scan a swath 185 km wide of the earth surface in a west-east direction across the ground track of the spacecraft (Figure 4.1). As the satellite moves forward so quickly it is necessary to record six scan lines for each sweep of the mirror, hence necessitating the use of 24 detectors, 6 in each of the 4 wavebands . This permits the ground coverage rate to be achieved at one-sixth the single-line scan rate, resulting in improved system response characteristics (Lillesand and Kiefer, 1987). The MSS system recorded in four different spectral bands: two in the visible spectrum at 0.5 to 0.6 μm (green) and 0.6 to 0.7 μm (red), and two in the near infrared at 0.7 to 0.8 μm and 0.8 to 1.1 μm, which are designated as bands 4, 5, 6, and 7 (because the RBV subsystem included bands 1, 2, and 3 (Table 4.1). On Landsat 3, the MSS had an added band 8 (10.4 to 12.6 μm - thermal infrared band).

The scan mirror oscillates back and forth through an angular displacement of about 2.9^0 to give total field of view of 11.6^0 for Landsat 1, 2, and 3, and 14.9^0 for Landsat 4 and 5. At the 913 km and 705 km altitude of the first generation and second generation, respectively, this has resulted in a swath width of 185 km for each orbit. The spatial resolution of the sensor is determined by the diameter of each optical fibre which is 0.086 mrad and at the 913 km altitude this

instantaneous field of view (IFOV) produces a ground resolution element of approximately 79 x 79 m. During each scan, the analog signal is sampled every 9.95 μs along a 185 km line, which is corresponding to 57 m on the ground. This means that the individual sampled element relates to an area of 79 m in the direction of satellite motion and 57 m in the across-track direction. This nominal dimension of 57 x 79 m area is called a Landsat picture element or pixel. Therefore, although the radiation measurement is made from a 6241 m^2 area each pixel is reformatted as if the measurement is made from a 4503 m^2 area. The analog signal from each detector is converted to a 0 - 63 range of digital number (DN) (6 bits precision) by an onboard analog-to-digital converter. The data is then rescaled to other ranges in subsequent ground processing, eg. band 4 - 6 are scaled to a range of 0 - 127 (7 bits) and 0 - 63 (6 bits) for band 7, and is output to film or to computer compatible tape (CCT). In both cases the data is used in the range 0 - 255 (8 bits precision), but only 64 different real levels are possible in the data. Each Landsat MSS scene is "cut" from the continuous swath of an orbit so that it covers approximately a 185 x 185 km area with 10% endlap. A typical scene contained exactly 2340 scan lines with 3240 pixels per line or 2340 x 3240 pixels per band. Because of the rotation of the Earth during the scanning process from the top to the bottom of the scene, the scene is a parallelogram in shape (Figure 4.2A). Location for each scene can be specified by its path-row co-ordinates in the Landsat Worldwide Reference System (WRS) (Figure 4.3).

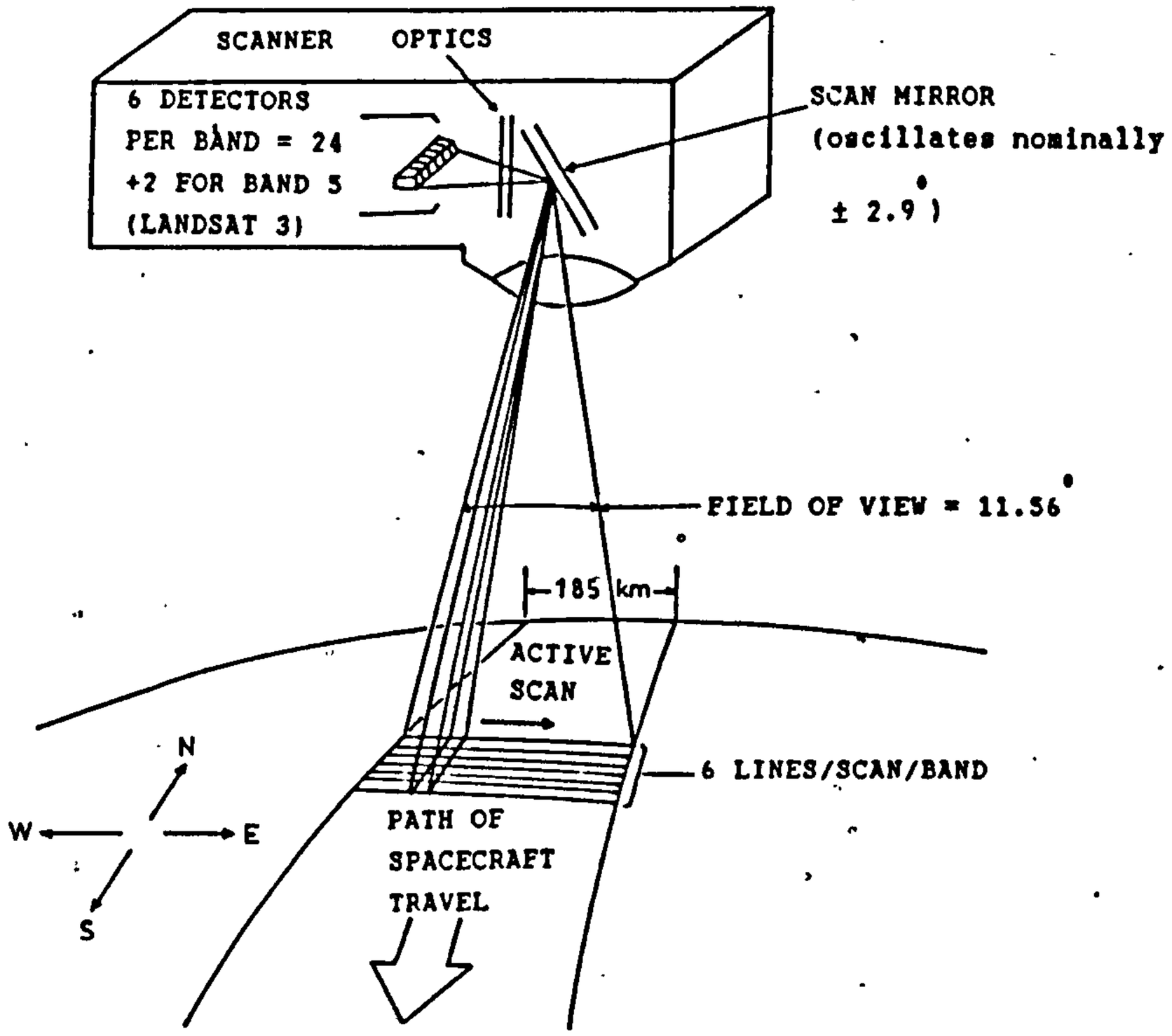

Figure 4.1 Multispectral scanner system (MSS) on Landsat 1,2, and 3 (adopted from Teranik, 1978).

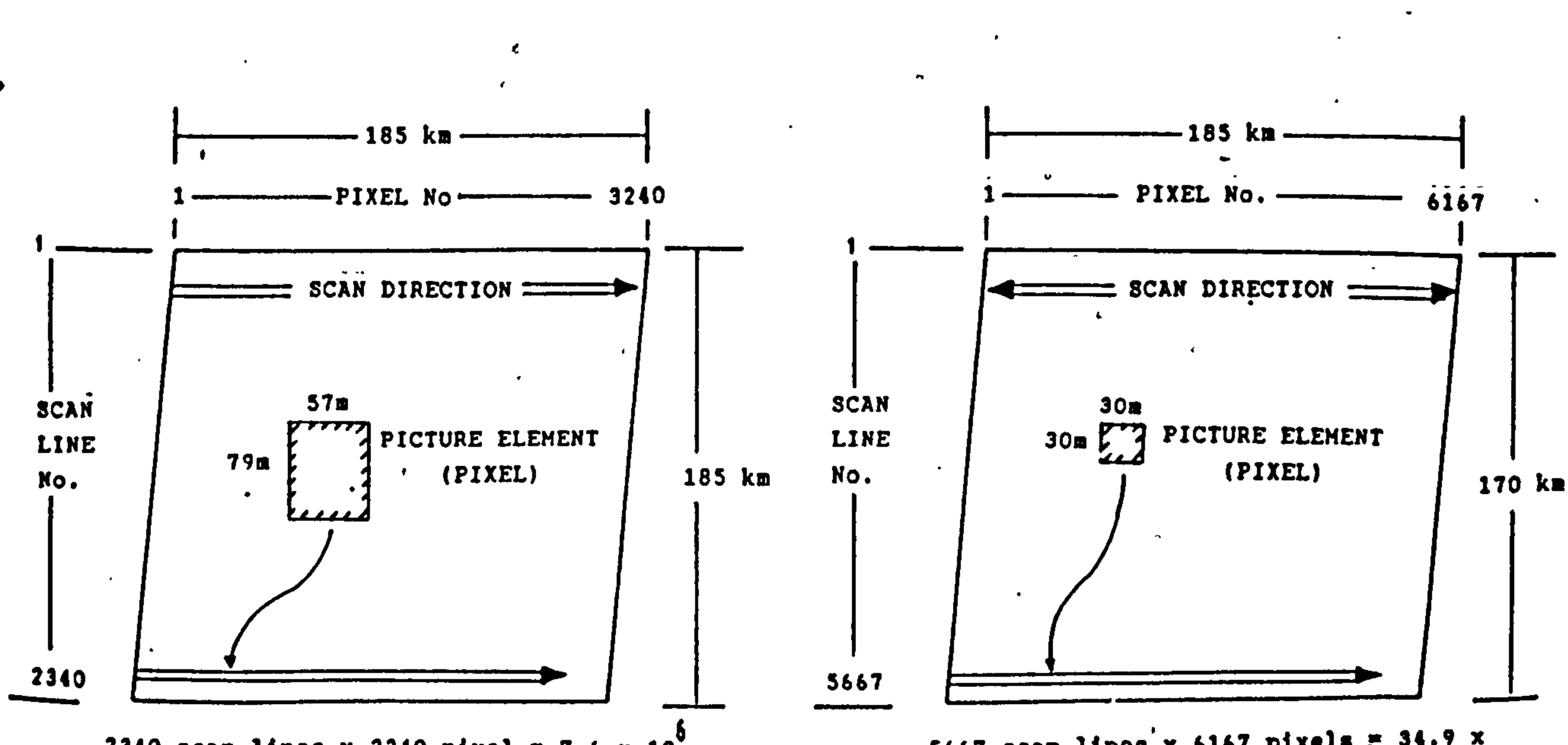

Figure 4.2 Arrangement of scan lines and pixels in Landsat MSS and TM images (after Sabin, 1987).

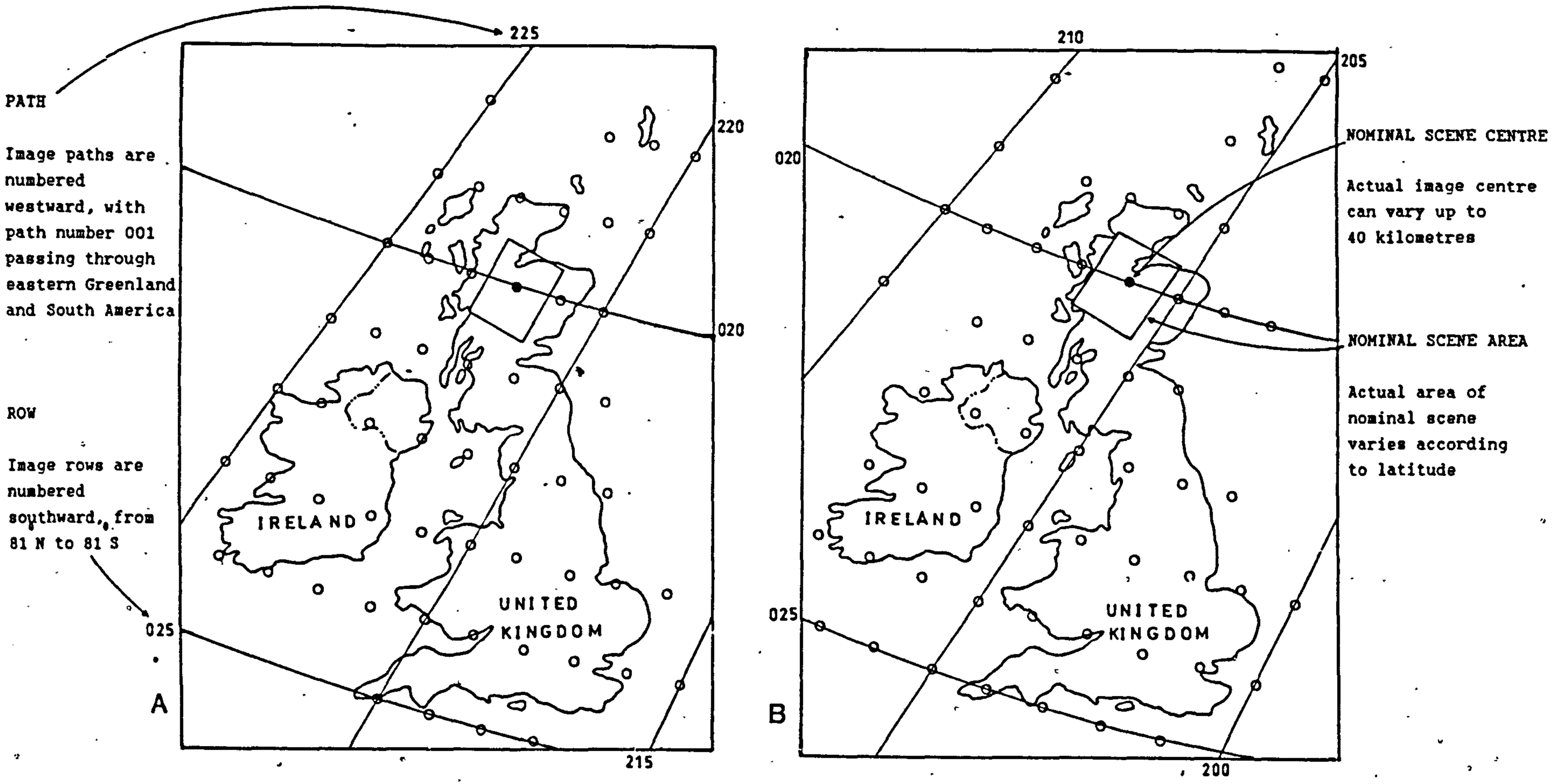

Figure 4.3 Path - row coordinates in the Landsat Worldwide Reference System (WRS) for the area around United Kingdom. A = Landsat 1, 2, and 3 coverage maps and B = Landsat 4 and 5 coverage maps. Solid scene centres on the maps indicate the scenes used in the study.

Since the launch of Landsat 1, the MSS sensor has undergone very little change. First, on Landsat 3 the MSS was extended to include a band 8 which recorded thermal infrared band of 10.4 - 12.5 μm and a pixel size of 237 x 237 m but it failed shortly after launch. Second, for Landsat 4 and 5, the spatial resolution (IFOV) of the MSS images is decreased to 82 x 82 m and the field of view was increase to 14.9^0 to compensate with their lower orbit. Lastly, for Landsat 4 and 5, MSS bands are numbered as band 1, 2, 3, and 4 instead of band 4, 5, 6, and 7.

Principal applications of Landsat MSS bands are given in Table 4.4. The characteristics of Landsat MSS data used in this study are shown in Table 4.5.

4.2.2 Landsat thematic mapper

In addition to the four bands MSS, Landsat 4 and 5 also carry onboard a new generation of sensor called Landsat thematic mapper (TM), which has a high spatial and spectral resolution, and with an improved radiometric sensitivity. Like the MSS, it is also a line scanner but it does not employ fibre optic as does the MSS. Generally TM works on the same basic principle as the MSS, however it differs from the MSS in the following;

a. There are 7 spectral bands (Table 4.3).

b. The IFOV is 30 m except for the thermal infrared band (band 6) where it is 120 m (Figure 4.2B).

c. The scanning mirror collects data on both the forward and reverse scans.

MSS Spectral Bands and Principal Application

Band 4 (0.5-0.6 μm)	can be used in coastal region to assess the depth and turbidity of water and also suspended sediment loads, delineation of shoals and reefs in shallow water.
Band 5 (0.6-0.7 μm)	is best for showing topographic and cultural features such as drainage patterns, roads and towns.
Band 6 (0.7-0.8 μm)	shows certain tonal contrasts which reflect a variety of land uses, vegetation studies and delineating boundaries between landforms, land and water.
Band 7 (0.8-1.1 μm)	is best suited for vegetation and land-water separation, provides the best penetration of atmospheric haze.

Landsat TM Bands and Principal Application

Band 1 (0.45-0.52 μm)	maximum penetration of water, useful for bathymetric mapping in shallow water (mapping coastal water), soil and vegetation separation, differentiating coniferous and deciduous species.
Band 2 (0.52-0.60 μm)	measurement of visible green reflectance peaks to assess vigour of vegetation.
Band 3 (0.63-0.69 μm)	important for discriminating between plant species by chlorophyll absorption measurements.
Band 4 (0.76-0.90 μm)	delineation of water bodies, determination of biomass content and mapping shorelines.
Band 5 (1.55-1.75 μm)	measurement of vegetation and soil moisture, differentiation of clouds from snow.
Band 6 (10.4-12.5 μm)	thermal mapping, plant heat stress analysis, soil moisture determination.
Band 7 (2.08-2.35 μm)	potential for discrimination rock types and mapping hydrothermally altered rocks associated with mineral deposits.

Table 4.4 Landsat Multi-spectral scanner and thematic mapper bands and their principal applications (Sources: Freden and Gordon (1983), National Remote Sensing Centre (1987) and Sabin (1987).

d. There are 16 detectors per band except for band 6 which has 4 detectors.

e. The data are digitized on an 8 bit (0 - 255) scale before transmission.

The orbit and coverage of Landsat 4 and 5 are slightly different from those for the earlier Landsat (Table 4.3). Differences in its orbital inclination and nominal altitude resulting a slightly different path and row designation in the WRS, therefore a separate WRS map is required to select images obtained by the second generation of Landsat (Figure 4.3B).

Principal applications of Landsat TM bands are shown in Table 4.4. The characteristics of Landsat TM data used in this study are given in Table 4.5.

4.3 Digital image data format

Data from satellites including Landsat are stored on CCT's. Unfortunately, there is no worldwide standard format for such tapes. Therefore before a tape can be read the number of tracks and the data density on the tape and the format of the image data must be discovered. Once known, suitable algorithms can be used in the computer in order to read the data and to convert it from one format to another.

Digital numbers (DN's) or pixel values (PV's) for a pixel are recorded on-board in the range of 0 - 63 (6 bits), however, the range is commonly expanded to 0 - 255 (8 bits), therefore, the data is recorded on either 7- or 9-track CCT's (one additional track is used for parity check (Short, 1982)).

DATA	SATELLITE	PATH/ROW	SUN ELEVATION	SUN AZIMUTH	CLOUD COVER	DATE	AREA
MSS	Landsat-5	205/20	22	158	0%	24 April 1984	Lochindorb
MSS	Landsat-5	205/20	22	158	0%	24 April 1984	Loch Tummel
TM	Landsat-5	206/20 Q-2	19	162	10%	27 October 1985	Lochindorb
TM	Landsat-5	206/20 Q-4	19	162	30%	27 October 1985	Loch Tummel
MSS	Landsat-3	137/56	43	128	10%	10 January 1979	Kedah-Perak

NOTE: ↑ = Quarter scene no.2
↓ = Quarter scene no.4

Table 4.5 The characteristics of the MSS and TM data used in the study.

The data is recorded on CCT's with data density of either 800, 1600 or 6250 bits per inch (BPI) and the most common formats for storing the data are band sequential (BSQ) and band interleaved by line (BIL) (Short, 1982; Jensen, 1986; Mather, 1987). In BSQ, all data for a single band covering the entire scene is written on one file, whereas for BIL the data for the bands is written line by line on the same tape (Short, 1982; Jensen, 1986). The Landsat MSS and TM data used in the study are recorded on nine-track CCT's with data density on the tape of 1600 BPI and stored in BSQ format.

4.4 Interactive digital processing system

Once the remotely sensed data are in a digital format it is possible to analyze them using a digital image processing system. In fact, there are a lot of these systems available at present time as listed by Short (1982) and Jensen (1986) which provide the hardware and software ready for digital image processing task. A typical image processing system consists of four main components (Harris, 1987): a magnetic tape drive, storage disk, processing units and video display or monitor. In addition, a camera or film writer or printer is used to capture the display image. The system is attached to a main computer such as VAX, IBM etc.

4.4.1 Digital image analysis display (DIAD) systems

The DIAD (Digital Image Analysis and Display) is the image processing system used in this study which is based at Department of Environmental Science, University of Stirling, U.K. The system has been designed for interactive digital analysis of remotely sensed imagery including Landsat data. Apart from that, the DIAD system is also suitable for processing digital imagery from a variety of sources such as aerial sensors, meteosat receivers and framegrabbers (DIAD, 1988). The DIAD hardware is a flexible general purpose image processing unit that is controlled by the DIAD software packages which are available in various operating systems. The System used in this study is for the UCSD P-System DIAD software, version 3.2, on Sage IV and running on the DIAD 68K hardware (DIAD, 1988) and is connected to the micro-VAX

computer. Before this, the system was attached to a host computer, VAX 11/780. Schematic layout of the system is shown in Figure 4.4. The system, includes tape drive, storage disk, micro-VAX computer, colour monitor, cursor control, keyboard and monitor and image processing unit.

The operation of the DIAD is made very simple by means of an interactive 'menu' system. The commands appear on the terminal screen and the appropriate one is selected by means of the keyboard, and the command is executed using the appropriate sequence. Hard copies of the image in this work were obtained by screen photography.

Some of the application programs used in the study are not available in the DIAD software package. These software, some of which have been mentioned particularly in Chapter 5, were developed by Dr. A. Watson at the University of Stirling.

Further information on the operation and organisation of the DIAD can be found in the DIAD Systems User's Manual.

The general procedure for use of the DIAD system in order to get digital data as an image display on the colour monitor is as follows:

a. Load an appropriate magnetic tape (which contains original data) into tape drive and copy the data to a storage disk in computer.

b. The systems can only display 512 pixels across the screen, so that only a portion of a scene can be viewed at once (in full detail), though it is possible to show a degraded version by omitting a proportion of the pixels. For example, algorithm QLOOK (Watson, per. comm.,

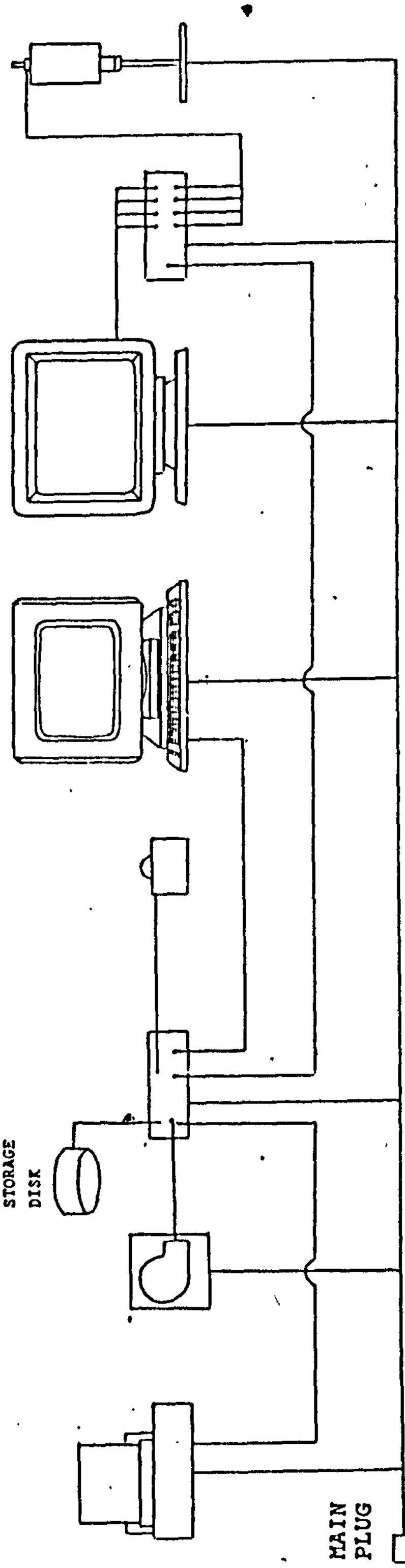

Figure 4.4 Schematic layout of the DIAD 68K system (adopted from 'DIAD, 1988).

1987) is able to display the whole of the Landsat MSS scene by taking a sample, of every sixth pixel per line and every sixth line. Such a display is useful to get a first glance of the scene and assess image quality, cloud cover and for selecting an area for study.

c. The WINDOW and FSMOOTH programs (Watson, per. comm., 1987) can be used to extract a specified subscene which covers the study area and to remove a striping effect in the image, respectively. For Landsat MSS data, a program called RESAM (Watson, per. comm., 1987) was used to resample the image so that each pixel was at 58 m x 58 m, in order to get a square shape of subimage and to utilize all the information contained in the original data.

d. Furthermore, subscene image data had to be run through the BI program (Watson, per. comm., 1987) which changed the data format from BSQ to BIL (section 4.3).

All the general procedures so far outlined are carried out on the micro-VAX computer. Once processed, the data is available to transfer to the DIAD System for image display on the colour monitor or for further manipulation of the data. However, for some of the digital image processing techniques which have been discussed in Chapter 5, the data has to be processed in the VAX computer because the DIAD System does not offer the algorithms which are needed in this work. A general sequence of program execution as applied to a Landsat MSS data in this work is shown in Figure 4.5.

4.5 Aerial photographs and aerial photo-interpretation

Beside Landsat MSS and TM data, the Lochindorb area is also covered by aerial photographs. The characteristics of the photographs are shown in Table 4.6. Photo-geology, that is to obtain geological information through the study and analysis of aerial photographs is very well known, well established and has been discussed in many texts (Ray, 1960; Miller, 1961; Bandat, 1962; Lattman and Ray, 1965; Allum, 1966; Mekel, 1978). Standard procedures of aerial photo-interpretation for the area have been carried out in this study in order to obtain geological information. Generally, the work involved can be divided into three stages. First, photo-interpretation and the preparation of a preliminary map based on the elements of aerial photo-interpretation such as tone, texture, pattern etc., and also information from the processed remotely sensed images of the area. This was followed by short field visits to several sites in the area to compare geological features with their photo-images and to see whether the preliminary interpretation is confirmed or should be revised or reinterpreted. Then, a final map was prepared. The result of this work for the Lochindorb area will be discussed in the Chapter 7.

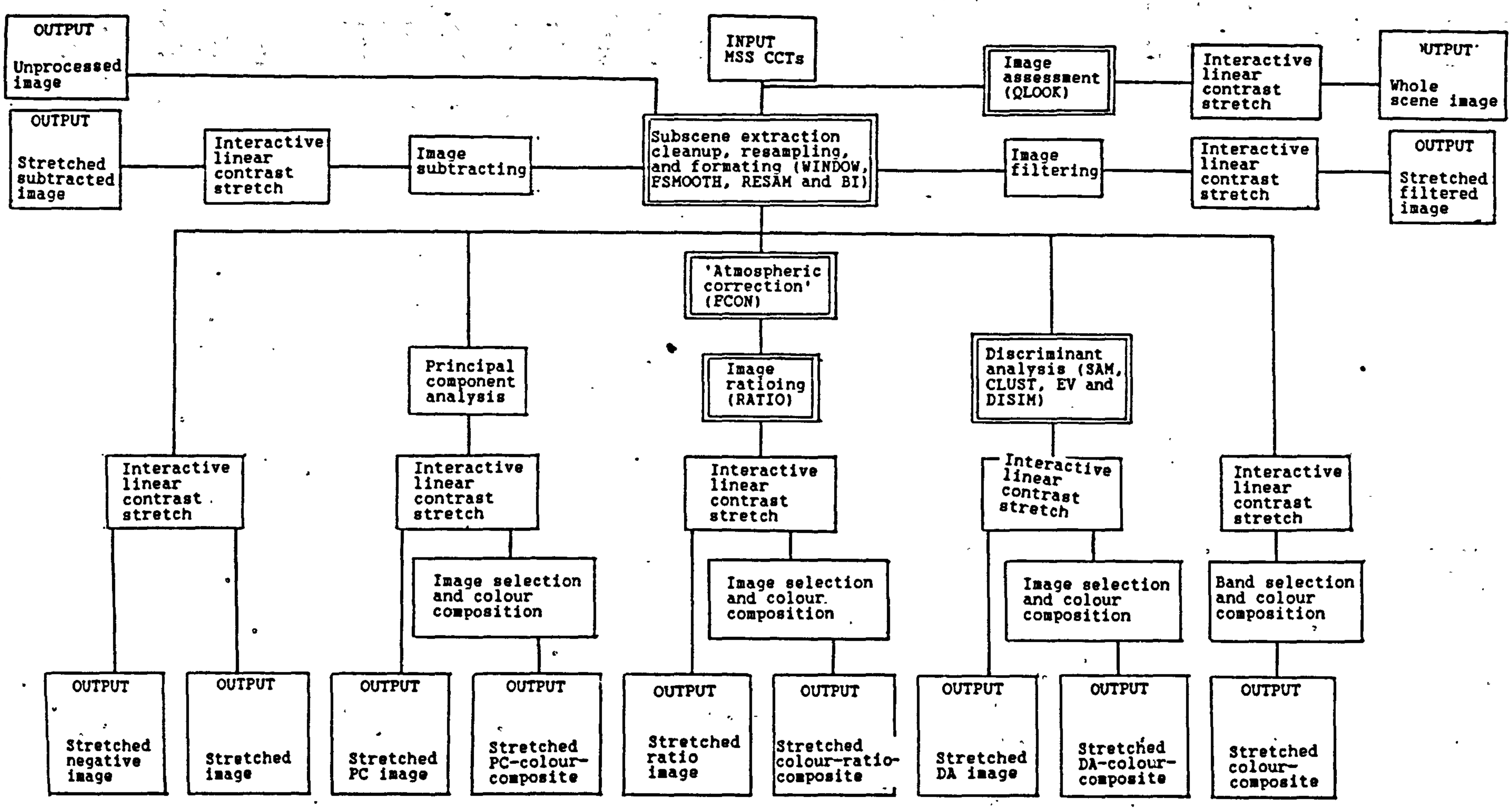

Figure 4.5 Flow diagram showing the sequence of steps used in processing the MSS computer-compatible tapes and a number of image products generated. The steps in double line boxes are carried out on computer using certain algorithms (in brackets) before the processed data are being transferred to the DIAD System.

SORTIE NO.	PHOTO. NO.	SCALE	TYPE	DATE
OS/67/164	293-300	1: 25,000	B&W	11.6.1967
OS/64/183	034-039	1: 30,000	B&W	02.9.1964
OS/64/183	065-070	1: 30,000	B&W	02.9.1964

Table 4.6 The characteristics of the vertical aerial photographs used for the Lochindorb area.

4.6 Summary

The Landsat systems (MSS and TM) are summarized in this chapter. The Landsat data are widely available and commonly used nowadays, and most likely will continue as a main source of remotely sensed data. The TM data has higher resolution, both spectral and spatial, than the MSS. The TM band 7 (2.08-2.35 μm) has been said to have a potential for discrimination of different rock types. Hence it may offer an improvement compared to MSS data for geological study.

One major disadvantage of the Landsat system is that it can be very difficult to provide cloud-free and snow-free (for Scotland) data for the study areas because of the frequent occurrence of clouds. The scenes chosen for this study are the best data available for the Scottish area to Oct. 1986, and for the Malaysia area to July 1988. For Scottish examples, the

choice of dates for both areas was unfortunate because they do not coincide with the acquisition period which has been reported useful for geological study in the region. The season of acquisition is less important for Malaysian examples which are covered by ever-green forest.

CHAPTER 5

DIGITAL IMAGE PROCESSING

5.1 Introduction

The majority of the satellite images, including Landsat MSS and TM, provide data in a digital form on Computer Compatible Tapes (CCTs) (Southworth, 1985). Only at a later stage are these digital numbers (DNs) processed and converted into photographic form. Although good quality images like enlarged prints or transparencies and false colour composites are available from the primary distributor like EROS Data Centre in U.S.A., or photographically processed (Best and Smith, 1978; Dean and Spencer, 1982; Shazly, 1987), processing of the digital tapes has proven to be effective for the production of better quality imagery necessary for geologic interpretation (Rowan et. al., 1974; Rowan, 1975; Siegal and Abrams, 1976; Condit and Chavez, Jr., 1979; Blodget and Brown, 1982; and Rothery, 1985).

All steps involved in converting and processing DNs to photographic form cause successive degradation of the image quality (NASA, 1977; Short. 1982). Therefore, in the working product, the integrity of the original picture elements (pixels) is lost and the finest details are missing (Rothery, 1985). In addition, the range of grey levels recorded on film or print is narrow, and as a result, only a small part of the

spectral information contained in the multi-spectral satellite data is shown in the standard film products (Blodget and Brown, 1982). As an alternative to photographic reproduction, the satellite images data is available in digital format on magnetic tapes which are much more amenable to computer assisted analysis (reprocessing and manipulation), allowing the full resolution (both spatial and spectral) of pixel data to be maintained from step to step throughout the computer processing (Jensen, 1986).

Today, thousands of scenes of the earth have been taken and thousands more will be taken tomorrow by satellite remote sensing systems. This means that satellite remote sensing produces very large quantities of digital data. For example, a single Landsat TM scene covering a ground area of 170 km x 185 km contains 273 Megabytes of data and occupies seven magnetic tapes when written at a tape density of 1600 bits per inch (Harris, 1987). Clearly there is a data mountain in satellite remote sensing (from Landsat MSS, SPOT, AVHRR and others), and at the moment digital processing is the only practical way of handling, processing and manipulation these vast amount of data.

The human eye is excellent at interpreting images, that is interpreting spatial attributes of an image and is capable of selectively considering obscure or subtle features. However, the eye is poor at discriminating the slight radiometric or spectral differences that may characterize such features (Harris, 1987). Furthermore, our eyes restrict us to interpreting at a combination of at most three bands of data.

Many satellite data contain more than three bands (for example, seven bands available for Landsat TM and four bands for Landsat MSS). Therefore, we only can look at a selection of any three of these bands at one time in a colour combination, this means that the remaining bands are not used. But, by means of digital image processing, there are methods of data compression where a larger number of bands can be combined together to produce new set of image. In principal components analysis, for example, a high percentage of the total variance can be compressed into the first component, making it a very effective single band for visual interpretation. Further, the first three components which usually contain approximately more than 95 per cent of the total variance can be viewed as a coloured image (Moik, 1980; Byrne et al, 1980; Lillesand and Kiefer, 1987).

Apart from this, many techniques which are employed in manipulation or processing satellite data are only possible through digital image processing and could not be achieved by visual interpretation alone. This does not mean that the traditional photo interpretation technique for satellite imagery is not useful or that digital image prccessing is superior to visual image analysis. The computer is much more adept at storing and manipulating a such tedious information and is capable and useful for enhancing the subtle radiometric or spectral details which should be used prior to the visual interpretation task.

General reviews of digital image processing of satellite data were given by Moik (1980), Hord (1982) and Jensen (1986);

whereas basic digital image processing for geological purposes was reviewed by Bernstein and Ferneyhough (1975), Robinson and Carroll (1977), Condit and Chavez (1979) and Gillespie (1980). The uses of digital image processing in geology can be found, for example, in Rowan et al. (1974), Rowan (1975), Geotz et al. (1975), Blodget and Brown (1982) and Williams (1983).

In this chapter, the basic idea and purpose of several digital image processing techniques which are related to geological remote sensing and have been used in this study will be discussed. In addition, a series of statistical techniques will be used to evaluate the amount and distribution of information contained in a few of the image data sets.

5.2 Preprocessing of remotely sensed data

In their raw form, remotely sensed data received from satellites may contain errors and anomalies. These various errors and anomalies may be traced to four groups of effects: platform, sensor, scene and atmospheric effects (Short, 1982). These deficiencies may have an impact on the result of image analysis. Hence, a series of corrective operations that remove or reduce these errors are usually necessary, and these operations are termed preprocessing because, quite logically, they are carried out prior to any use of the data (Jensen, 1986; Mather, 1987). Some corrections are carried out at the ground receiving station at Goddard's IPF and since 1979 these processed tapes sent to the EROS Data Centre are subjected to further computer processing before products are sent to the

users (Short, 1982). Despite this fact, there is often still a need for further preprocessing. It is a little difficult to decide what should be included in the preprocessing method because the definition of what is or is not a deficiency in the data will, to a large extent, depend on the use to which those data are to be put (Mather, 1987). In this work a few preprocessing methods are employed to the remotely sensed data of the study areas.

5.2.1 De-striping method

The Landsat MSS has six detectors that record the changing light intensities in four spectral regions, while the TM has 16 detectors functioning during each scan, measuring electromagnetic energy in six spectral regions (excluding thermal band). These detectors are carefully calibrated, but the response of some detectors may drift and may cause several detector anomalies including line dropouts, striping and line start problems.

After all the unprocessed images of the study areas were observed, it was found that none of them showed any line dropout or line start problems, but they do have striping problems. Although it does not seriously hamper use of the imagery in photo interpretation, this striping is a distinct cosmetic blemish and may be distracting, and furthermore it may influence computer identification and classification of features (Short, 1982). Therefore it was decided to remove this anomaly for all the data.

The raw data were run through a program called FSMOOTH (Watson, per. com., 1987) (Figure 4.5) the function of which is to eliminate the stripe. The first step is to calculate the average pixel value (PV) per scan for the whole subscene. Then, the average PV for each scan line is compared with this scene average. Any scan line deviating from the average by more than a designated threshold value is identified as a stripe line. Each of the pixels of a stripe line are corrected by subtracting the difference between the line average and the image average. This procedure is repeated until no scan line deviating from the scene average by more than a given threshold value remains. By this way the effect of periodic striping on the images can be removed or minimized.

5.2.2 Resampling

The nominal pixel size for Landsat MSS is 79 m x 57 m and for TM data, except for the thermal band, is 30 m x 30 m. In order to display a subscene, say 512 lines times 512 columns, it is necessary with MSS data to resample its pixel size in order to get a square image. In this study, Landsat MSS data were passed through a program called RESAM (Watson, per. com., 1987) (Figure 4.5) which resampled each pixel size at 58m x 58m. As a result, a square subscene of the study area is produced, and this resampling process also removes aspect ratio distortion of the data (rectangular pixel) (Condit and Chavez, 1979). The resampling process is not applied to the Landsat TM data because it already has a square pixel shape, and consequently will produce square subscene images.

5.2.3 Atmospheric correction

The interaction of EMR with atmospheric gases and particles (section 3.2.2) can produce notable variations in the radiance levels recorded by a remote sensor. The effect of atmospheric scattering (both Rayleigh and Mie scattering - section 3.2.2) is negatively related to wavelength. For Landsat MSS data, for example, the atmospheric scattering of green (band 4) has the highest effect, that is about four times greater than the scattering of infrared (band 6) radiation (Jensen, 1986). Atmospheric scattering gives rise to an additional radiance from the atmosphere itself that increases the overall brightness level at shorter wavelengths (haze) which causes low image contrast, so atmospheric conditions constitute a second source of error in image interpretation (Robinson and Carroll, 1977), after surface noise. The scattering decreases significantly at the wavelengths of bands 6 and 7, but absorption by water vapour increases, and hence attenuates the brightness of surface features as well as sky brightness induced by scattering. Fortunately digital processing of the bulk data can eliminate or minimize these effects and produce more accurate reflectance values. This removal is carried out in several ways. Sophisticated techniques rely on direct meteorological measurements fed into models for calculating the expected atmospheric spectroradiances under specific weather conditions (Dozier and Frew, 1981). This way is nearly always impractical when working with a given scene, since contemporaneous weather data, even if available, are usually

insufficient (Short, 1982). A simple correction cannot be applied for the absorption (Thomas et al., 1987), but a 'correction' can be included for the atmospheric scattering by far simpler methods such as histogram adjustment, regression adjustment and by shadowed pixel adjustment (Jensen, 1986; Sabin, 1987; and Drury, 1987). All methods are based on the fact that the infrared band is essentially free of atmospheric effects, whereas the visible band is strongly influenced by them. The histogram adjustment technique has been tried in this work because dense shadowed areas are less prominent for the Lochindorb area (due to less topographic relief); and the regression adjustment requires many more passes through the digital data than using the histogram adjustment, but whithout any guarantee that it will provide superior results (Jensen, 1986).

The raw data were run through a program called HIS (Watson, per. comm., 1988), the function of which is to list the amount of pixel in every DN interval. The histograms of the original data have to be plotted and studied. The data were run through an algorithm called FCON (Watson, per. comm., 1988), the function of which is to assign the minimum pixel values for each band to zero by subtracting all pixel values for each band from its minimum value (from histogram) and after that through the HIS program to list the number of pixels in every DN interval. This means that the original histograms were shifted to the left so that zero values appear in the data, and the effect of atmospheric scattering will be minimized. All the operations were carried out in the VAX

computer and cannot be done interactively through the DIAD System, therefore the process is slow. Generally, the resulting images do show good contrast, however, the operation enhances the shadow (in black and white or in colour composite images), hence some information which present in shadowed areas (by the scattering effect of the atmosphere) tends to disappear in the shadow. For this reason, the operation is carried out only for the ratioing technique (section 5.4.1) because as mentioned in section 3.2.2, the effects of scattering increase inversely with wavelength, so the two channels will be unequally affected by scattering, hence, the computed ratio will thus be a biased estimate of the true ratio.

5.3 Enhancement techniques

Enhancement is a process of altering the appearance of an image so that the interpreter can extract more information (Sabin, 1987). Here, enhancement simply means the transformation of the data to make subtle grey-scale differences, which are not readily detectable with the naked eye, into 'more obvious contrast. The techniques to be described, however, are said by some interpreters to vary in utility (Hord, 1982), and to a degree, enhancement must be regarded as an art (Boulter, 1979). The process, which is intended to improve the interpretability of an image, for example by increasing the apparent contrast between features in the scene, is performed on image data prior to visual interpretation tasks. Although trends toward classification,

thematic mapping and analysis of data by computer are evident in current usage of satellite data for many disciplines, for most geological works, the reliance on visual interpretation of imagery remains at the core of much interpretive methodology. In this case, enhanced images of the scenes of interest become powerful tools in the analytical approaches traditionally used in this disciplines (e.g. see Rowan et al, 1977; Siegal and Gillespie, 1980; Williams, Jr, 1983; Sabin, 1987; Drury, 1987).

There are several enhancement procedures or techniques currently available which may be employed with digital image data. This section will provide an introduction to the major contrast enhancement techniques that are used in this work., and relate these to enhancing the quality of images for improved visual interpretation.

5.3.1 Contrast enhancement.

In many cases, if the pixel values (PVs) or brightness values (BVs) or digital numbers (DNs) of satellite data are to be displayed in their original form, only a small range of grey values will be used, so the display images would have such a low contrast. This means that it would be difficult to differentiate between objects with a slightly different PV. The primary reason is due to the sensitivity range of remote sensors in the satellite system which was designed to accommodate or to record a wide range of PV (eg. from 0 to 127 or 0 to 256), or to record a wide range of earth surface illumination conditions (eg. from a poorly illuminated black

basalt plateau, possible represented as PV of 0, to well illuminated snow, possibly represented as PV 127 or 256). In reality there are very few scenes of satellite images, that have a brightness range of the full sensitivity range of the detectors, so the resulting images show a low contrast.

Beside this consideration, a relatively low contrast image is also due to the characteristics of earth surface materials which reflect and emit electromagnetic energy very similarly.

If the range of the grey levels of the data could be altered so as to fit or occupy the entire range of the sensors then the contrast between the dark and light areas of the image would be improved giving more detail. It is fortunate that this problem can be overcome in many ways. Although there are some differences of detail between these methods, generally this task is carried out by same principle, by expanding or altering the recorded PVs so that they will cover or utilise the full range of the display device. This process can be done either by photographic or by digital methods (Best and Smith, 1978; Dean. and Spencer, 1982; Shazly, 1987). The digital methods, however, may be more satisfactory than photographic techniques for contrast enhancement because of the precision and wide variety of processes that can be applied to the imagery (Jensen, 1986). In this work, the digital methods namely linear contrast and histogram contrast are employed to improve the contrast of the remotely sensed data.

Linear contrast stretch

This is the simplest contrast enhancement method (Sabin, 1987; Drury, 1987). In its basic form the technique involves the mapping of the PVs from the observed range PV_{min} to PV_{max} to the full range of the display device (for example 0-255, which is the range of values representable in an 8-bit display device). The brightness values are scaled in various ways, for example the PV_{min} (low end value) maps to a value of 0 and PV_{max} (high end value) maps to a value of 255 or the lower 5% of the pixels value are assigned to 0 and the upper 5% are assigned to 255, whereas those values lying between PV_{min} and PV_{max} or $PV_{5\%}$ and $PV_{95\%}$ are distributed linearly between these extremes (Jensen, 1986). Values other than these, of course, could be used, for example the analyst might elect to choose the $PV_{10\%}$ and $PV_{90\%}$ or any other.

All images in this study have been linearly contrast stretched using the algorithm for contrast stretching which is available in the DIAD Software Suite. To perform this linear contrast enhancement, first the analyst examines the image histogram or image data and determines the minimum and maximum PVs in the image, PV_{min} and PV_{max} respectively. The original image data is loaded into the DIAD System and displayed (one band for each time) in their original PV values. By using contrast stretching algorithm in the DIAD System (option RAMP CONTRAST STRETCH in KEYPAD MENU), this low contrast image can be improved. The System will ask for the lower and upper value of the pixel, and by entering these values the System will display an image which is linearly contrast stretch based on

these lower and upper limit. This interactive process (by changing input value of the lower and upper limit) finally will display an image which is good in contrast according to the analyst's needs. For a colour image such as a false colour composite image , separate linear contrast stretch is applied to each component image before combining or displaying it in colour. The linear contrast stretch, apart from its simplicity and common use in digital image enhancement, also greatly improves the contrast of most of the original PVs (Jensen, 1986; Sabin, 1987). In most cases this technique is sufficient to produce an image of high quality, and enhanced images of single bands or false colour images comprising three contrast stretched bands can then be interpreted geologically with a fair measure of success (e.g. Drury, 1987), and this is the case for the images in this study.

Histogram equalisation contrast stretch

This is one of the most useful of the non-linear enhancement techniques which can be applied to low contrast image data and applies the greatest enhancement to the middle, most highly populated range of PVs in the image, with extreme compression in the less densely populated low and high pixel tails (Jensen, 1986; Drury, 1987; Sabin, 1987). Gonzalez and Wintz (1977) and Jensen (1986) give more detail explanation on this enhancement technique. Its underlying principle is straightforward, the original histogram has to be redistributed or in other words the PVs are assigned to the display values based on their frequency of occurrence so that

each histogram class in the displayed image contains an approximately equal number of pixels. First, the number of output classes of the displayed image (for example in this work was 32) into which the pixels are to be redistributed is specified. In this study, the raw image data was passed through a program called HISTEQ (Watson, per.com., 1988) which assigns approximately equal numbers of pixels to each of the output classes, and this means that the original histogram has been redistributed to produce a more or less uniform population density of pixels for each output class.

This particular contrast enhancement was selected and carried out with the aim to get better image contrast. Generally, the resulting images do show good contrast. However, because this operation is non interactive, and slow, and does not give better results than the simple linear stretch, only the linear stretch was used.

5.4 The Derivation of Synthetic Channels

A Synthetic Channel (Image) is regarded as any image that is produced from more than one of the basis bands, for example the Band Ratio and Principal Component Images (Thomas et al., 1987). The resulting image may have properties which make it more useful than the original single bands. This kind of operation is carried out on multiband image sets which may consist of a single multi-spectral image of an area or it may also operate on a number of images of the same area taken at different times (a multitemporal image set).

5.4.1 Arithmetic operation

Two or more bands, either multi-spectral or multitemporal can be combined together by one of several arithmetic operations like division and subtraction.

Image division

The process of numerically dividing the PVs in one image by the corresponding PVs in another image is well known as ratioing, and it is one of the most commonly used in digital image processing of remotely sensed data (Goetz and Billingsley, 1974; Geotz et al., 1975; Podwysocki et al, 1977; Robinson and Carroll, 1977; Condit and Chavez, 1979; Moik, 1980, Short, 1982; Williams, Jr, 1983; Jensen, 1986; Sabin, 1987; Drury, 1987; Mather, 1987).

Ratio images are also widely used in geological interpretation of remotely sensed data because of their great utility in analyzing the spectral aspect of certain types of ground features. Rowan et al. (1974) used three Landsat MSS band ratios (b4/b5, b5/b6 and b6/b7 ratios in blue, yellow and magenta, respectively) to generate a false colour composite image of a semi arid region in Nevada, and this composite ratio image was said to allow better visual discrimination between altered rock types. Raines and Wynn (1982) generated and used a colour ratio composite Landsat MSS image (b4/b5, b4/b6 and b6/b7 ratios in red, blue, and green, respectively) which allowed for the mapping of some ultramafic areas, that would have otherwise been missed and was useful in subdividing the ultramafic units near Crescent City, California. The

ratio-contrast stretch image of Landsat MSS bands 4/5, 5/6 and 6/7 projected through blue, green and red filters, respectively, provides the greatest capability for rock discrimination in Western Saudi Arabia (Blodget and Brown, 1982). A colour ratio composite of 24-channel Bendix multi-spectral scanner which is very similar to Landsat TM bands 5/1, 3/4 and 5/7 ratios in blue, green and red, respectively, successfully distinguished most types of altered rocks from unaltered rocks in Utah (Podwysocki et al., 1983). The Landsat MSS (4/5)/(6/7) ratio and also a colour ratio composite of bands 4/5, 6/7 and (4/5)/(6/7) ratios as red, blue and green, respectively, was successfully applied to maximize the difference between limonitic rocks and vegetation (Segal, 1983). Drury (1986b) stated that the best combination for the airborne thematic mapper data to be used in a red-green-blue colour composite is 5/3, 9/3 and 10/7 respectively, which is equivalent to Landsat TM ratios 3/2, 5/2 and 7/4, and they should produce a wide spread of colours related to vegetation types during any season and be useful for visual discrimination.

The band ratio technique is an effective method to enhance spectral differences or colour differences (Figure 5.1), and effectively removes the effect of variable degrees of brightness caused by the environmental factors like topographic condition and shadow, and suppresses differences in albedo variation (Figure 5.2) (Rowan et al., 1974, Rowan et al., 1977; Condit and Chavez, Jr., 1979, Drury, 1987; Sabin, 1987).

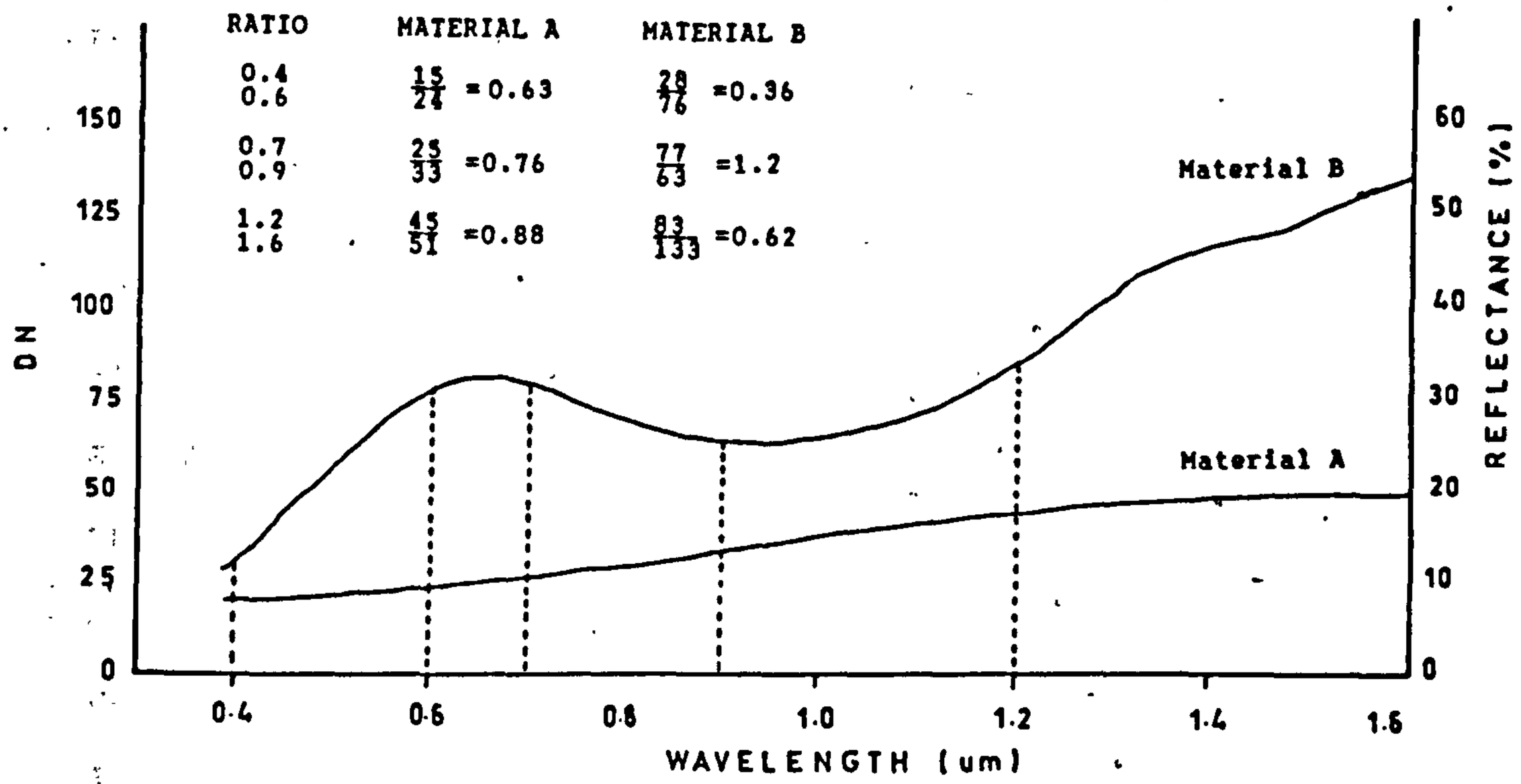

Figure 5.1 Hypothetical reflectance curves showing how ratios enhance minor variations in the curve (adopted from Prost, 1980).

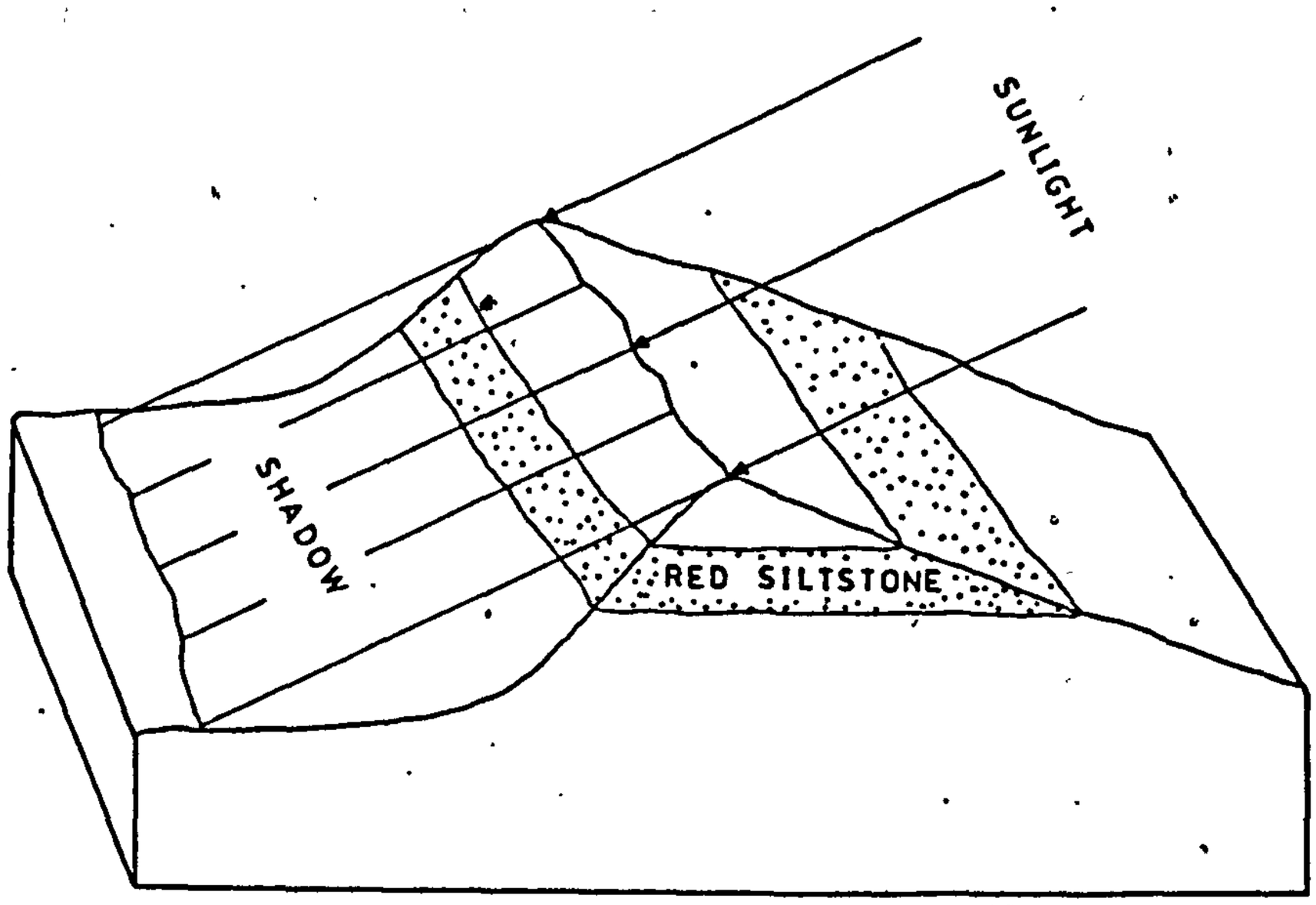

SILTSTONE REFLECTANCE

ILLUMINATION	TM BAND 3	TM BAND 1	RATIO 3/1
Sunlight	94	42	2.24
Shadow	76	34	2.23

Figure 5.2 Suppression of illumination differences on a ratio image (after Sabin, 1987).

The mathematical form for band ratioing is of the format

$$PV_{i,j,r} = PV_{i,j,k} / PV_{i,j,l}$$

where $PV_{i,j,r}$ is the output ratio value for the pixel at row i, column j; $PV_{i,j,k}$ is the pixel value at same location in band k; and $PV_{i,j,l}$ is the pixel value in band 1. The computation, however, is not always simple and this simple form of image ratio is not very effective due to several limitations. These limitations are: when $PV_{i,j,l} = 0$ and when $PV_{i,j,k}$ is less than $PV_{i,j,l}$. In the first case, $PV_{i,j,r}$ becomes infinity or unbounded, and in the second condition, the results are compressed into the grey-level less than 1. Fortunately, there are several alternatives available to overcome this problem. For example by simply giving any $PV_{i,j}$ with a value of 0 with the value of 1, or by adding a small value (e.g., 0.1) to the denominator if it equal zero, and to represent the range of the function in a linear fashion and to encode the ratio values in a standard 8-bit format (values from 0 to 255), normalising functions are applied (Jensen, 1986). Another approach is to use the following function such as outlined by Hord (1982):

$$PV_{i,j,r} = R \arctan (PV_{i,j,k} / PV_{i,j,l})$$

Here $PV_{i,j,r}$ ranges from 0 to 1.57R; the multiplying constant R may be adjusted to suit the characteristics of the output devices. For an 8-bit device, the constant R is set equal to 162.34, and the ratio $PV_{i,j,r}$ can take upon itself any value from

0 to 255. Several ratio images have been generated in this study through an algorithm called RATIO (Watson, per. comm., 1988) (Figure 4.5) which used the above approach outlined by Hord (1982).

Image subtraction

One of the main purposes of subtracting a pair of co-registered images of the same area taken from different times is, to assess the degree of change that has taken place between the dates of imaging (Mather, 1987). Therefore the operation will become important, for instance when working with dynamic geological work like mapping lava flows, flooding and landslides where the changes may happen between the dates of imaging. In this respect, the image subtraction operation is perhaps not so important in this work which deals with static rather than dynamic geology. However, Black (1987) found that an image which was generated from image subtraction of band 7 and band 4 of Landsat TM was very useful for mapping brittle structure in the Applecross Peninsula, Scotland. Consequently, this operation is carried out in this study for Loch Tummel and Perak-Kedah data for the same purpose, to enhance linear features. The algorithm for this operation is available in the DIAD System (ARITHMETIC AND LOGIC in ENHANCEMENT MENU) (Figure 4.5), and it uses this mathematical formula;

$$(b1 - b2 + 255) / 2$$

where b1 and b2 are the input bands.

5.4.2 Principal components analysis

A false colour composite (FCC) is arguably the most effective means of visual presentation of multichannel images and survey data (Canas and Barnett, 1985). Although the optimum index factor (OIF), section 5.4.4, (Chavez et al., 1982) provides an easily-computed guide to potentially useful band combinations, colour images are generally displayed by selecting three of the available bands for red-green-blue colour presentation devices (e.g. three bands out of seven on the Landsat TM data). This means only a portion of the acquired data can be displayed in one standard FCC, and the use of any three band composite will inevitably result in a loss of information contained in the remaining bands. It could be better if more bands (preferably, if possible, all bands of data) could be effectively displayed at one time, allowing more information to be presented and interpreted in a single display. Therefore some means of combining or compressing the information of a number of bands of data into just two or three images with minimum loss of information needs to be employed.

The data compression technique known as principal components analysis (PCA), also referred to as the eigenvector transformation, the Hotelling transformation and the Karhunen-Loève transformation (Singh and Harrison, 1985), is a technique that provides a systematic means of reducing the dimensionality of multichannel image data and offers the opportunity of displaying a greater proportion of the original variance in a single image and/or in a new set of component

images that are uncorrelated with each other (Bernstein et al., 1984; Canas and Barnett, 1985; Greenbaum, 1987). Thus, PCA is a statistical technique that transforms a multivariate data set consisting of intercorrelated variables into a data set consisting of variables that are uncorrelated linear combinations of the original variables (Ingebritsen and Lyon, 1985). The ability of the technique to reduce the number of bands of the data set that must be analyzed to produce usable results is an important economic consideration. Moreover, the potential information recoverable from the transformed data is just as good as that from the original data (Anuta, 1977; Haralick and Fu, 1983; Canas and Barnett, 1985). PCA has proven to be of significant value in the analysis of remotely sensed data (Jensen, 1986) and the resulting new principal component images are more interpretable than the original data (Byrne et al., 1980; Moik, 1980), and have been widely used in geological interpretation (Jacobberger et al., 1983; Rothery; 1985; Drury, 1986b; Black, 1987; Greenbaum, 1987).

In this study, PCA images of the Lochindorb and Kedah-Perak areas are generated by using the PCA algorithm in the DIAD System (option COVARIANCE MATRIX and LINEAR COMBINATION in ENHANCEMENT MENU) (Figure 4.5). A detailed description of the statistical procedures used to derive principal component transformation is beyond the scope of this work, but it can be found, for example in Mather (1976), Anuta (1977), Gillespie, 1980; Short (1982), Billingsley (1983) and Thomas et al (1987). Therefore only basic discussion of the technique will be given.

In a geometric sense, PCA fits a new set of coordinate axes to the data, choosing as the first new axis or component an orientation which coincides with the line along which the data has the greatest spread or will maximize the variance accounted for by this axis (Figure 5.3). The second principal component, which is at right angle to the first, is a line along which the data has the second largest variation. In space with more than two dimensions (Landsat TM data has six dimensions excluding one dimension of thermal band), the process will continue to define axes, the third, fourth, fifth and sixth, components which contain decreasing amounts of the scene variance found in the data set. Because successive components are chosen to be orthogonal to all previous ones, the data they contain are uncorrelated. Tables 6.3 (Chapter 6) summarises the salient statistics involved the process to produce principal component images of the Landsat TM of the Lochindorb area.

5.4.3 Discriminant analysis

Similar to the PCA, discriminant analysis is often used as a data-compression technique, that is to reduce the number of bands (for example, for Landsat TM, from 7 to 2 or 3 bands) which contain usable results for visual interpretation. While the PCs are chosen in such a way that the first PC expresses the maximum possible proportion of the variance in the original data set, in the discriminant analysis the first axis expresses the maximum number of spectral clusters (classes)

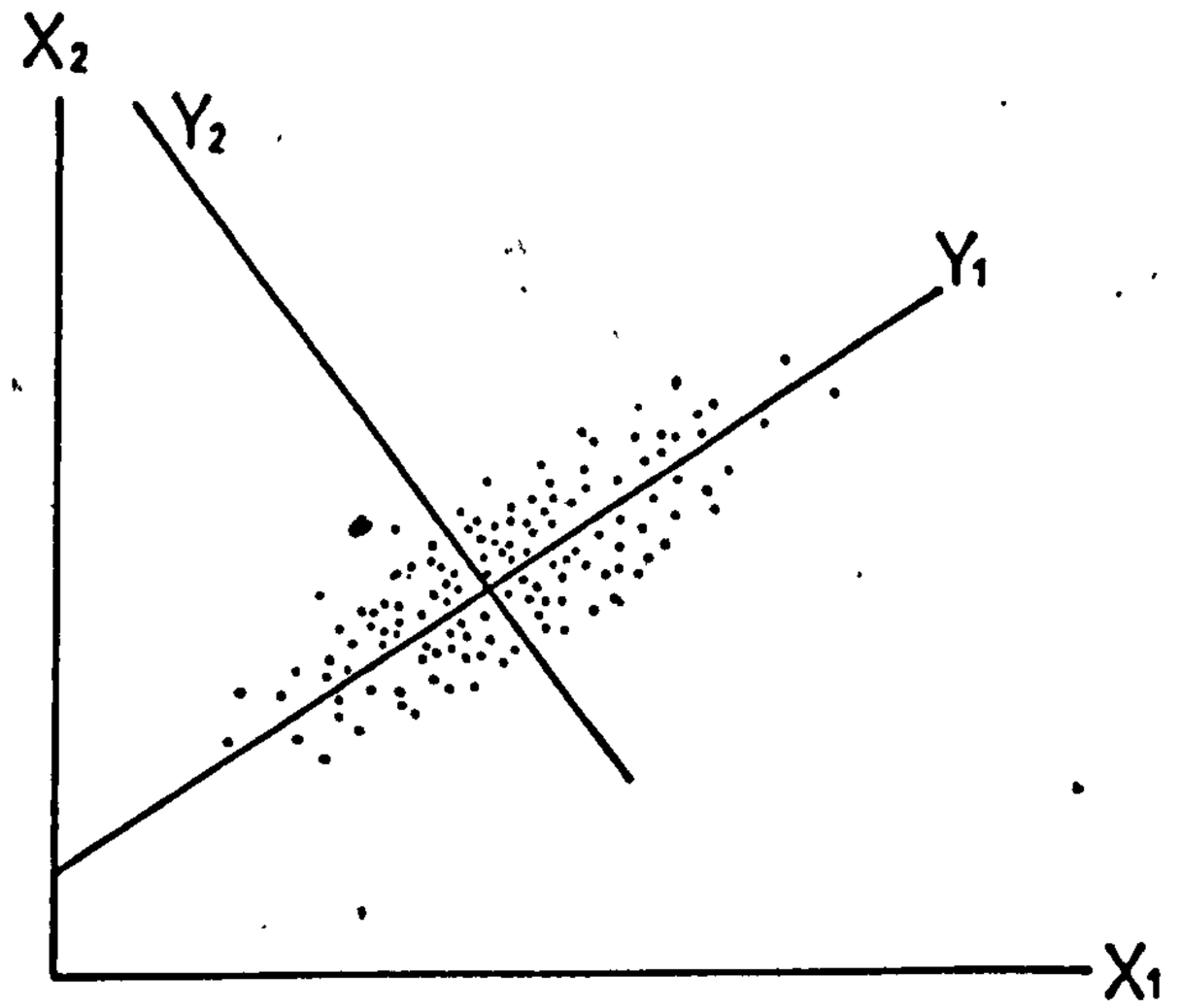

Figure 5.3 Elliptical scatter pattern for a hypothetical data set consisting of multispectral channels X_1 and X_1. The principal component analysis creates a new set of coordinate axes (components) by a rotation and translation such that the first (Y_1) component accounts for most of the variability. The second axis (Y_2) is chosen orthogonal to the first. This concept can be extended to multi-dimensional space, with each succeeding component axis being orientated orthogonal to the earlier ones and accounting for less and less variation (after Podwysocki et al., 1977).

which can be discriminated. Therefore, discriminant analysis provides one means of separating spectral classes (groups of pixels) along new axes (Lo, 1986; Harris, 1987).

In this study, the Landsat TM data of the Lochindorb and the Landsat MSS data of the Kedah-Perak area were processed through an algorithm called SAM, CLUST, EV and DISIM (Watson, per. comm., 1988) (Figure 4.5) in order to produce discriminant images of the area. Figure 5.4 shows general idea of the process.

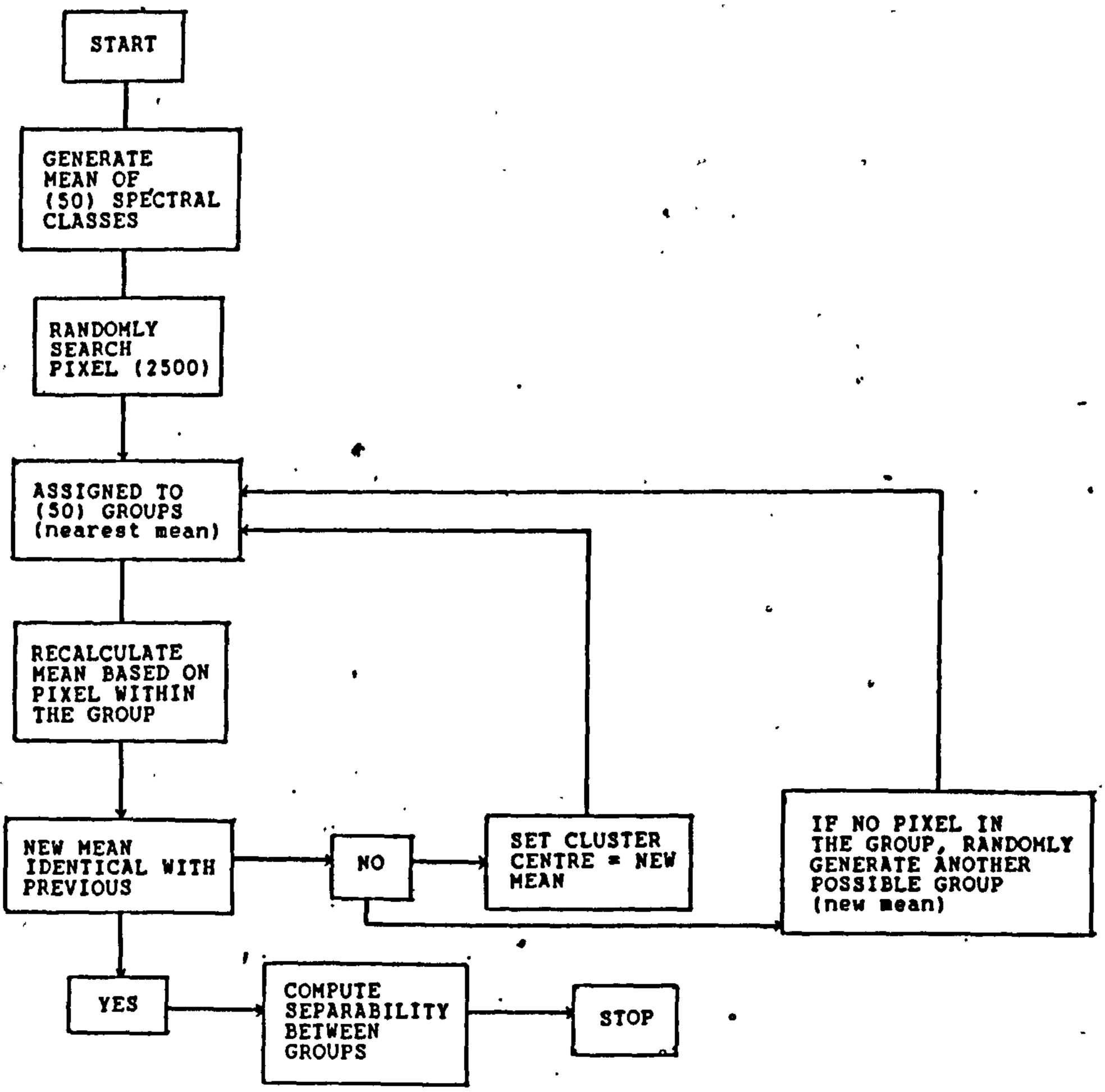

Figure 5.4 Flow diagram showing the general sequence of steps involved in processing the Landsat data in the discriminant analysis (Watson, per. com., 1988).

5.4.4 Colour display

In addition to black and white images of single bands, either processed or unprocessed, therefore, colour images can be generated by assigning a colour to each of three images and either optically or digitally superimposing the results. For example, to produce the so-called standard Landsat MSS false colour composite, MSS 4 (green band) was displayed as blue, MSS 5 (red band) was displayed as green and MSS 7 (near infrared band) was displayed as red. The same method can be applied to other images, for example PCA, such that any three of the components can be assigned with blue, green and red to create a principal component colour composite which often depicts more subtle differences in colour shading and distribution than the tradítional or standard colour composite images (Jensen, 1986). Like PCA, ratio images may be combined to produce a colour composite image. The colour variations of the ratio colour images express more geologic information and have greater contrast between units than do the conventional colour images (Sabin, 1987).

Apart from the colour infrared composite (standard false colour composite), is possible to create other colour images with different band combinations. For Landsat TM data, for example, a natural colour image can be created by assigning bands 1,2,3 with blue, green and red, respectively. The question may arise about how to identify and to produce the optimum colour composite from the Landsat TM data with seven bands. Chavez et al. (1982) devised a statistic, which they called the optimum index factor (OIF), to rank three ratio

combinations from Landsat MSS data, that provides a measure of the uncorrelated information content of all possible three band combinations. The OIF can be applied to any set of interdependent variables (Chavez and Berlin, 1984) and is calculated for each three band combination by dividing the sum of the standard deviations (representative of the total spectral range of the bands) by the sum of the absolute values of the correlation coefficients (providing a measure of data redundancy):

$$OIF = \sum_{i=1}^{3} \sigma_i \Big/ \sum_{j=1}^{3} |r_j|$$

where σ_i is the standard deviation of band i and $|r_j|$ is the absolute value of the correlation coefficient between any two of the three bands. Based on this statistic, the combination having the largest OIF value should have the most information (total variance) with the least amount of duplication (Chavez and Berlin, 1984), and often three band combinations that are within 2 to 3 rankings of each other appear similar in colour composite form, because there is little difference in their total information content (Chavez et al., 1982). Whilst the OIF is a convenient, easily-computed guide to useful band combination, the results will not necessarily give a precise indicator of geological information content and give the most suitable image for qualitative interpretation (Greenbaum, 1987; Crósta and Moore, 1989), and an empirically selected image sometimes is more useful than OIF for certain areas (Hunt et al., 1986; Crósta and Moore, 1989). Therefore, the

band combinations used in this study to produce false colour composites were selected empirically as well as by the OIF. In addition, colour composite images were also produced based on the distribution statistics of the data (section 6.2.3).

The correlation matrix and standard deviations of the Landsat TM data of Lochindorb area are shown in Table 6.1 (Chapter 6) and the OIF ranking for triple band TM combinations (excludes the thermal infrared band) of the area are presented in Table 6.2 (Chapter 6).

5.5 Filtering techniques

Filtering provides a means of improving images by suppressing or enhancing certain spatial frequencies, directions and textures (Rosenfeld and Kak, 1976). Many interpreters, particularly geologists, are concerned with recognizing linear features in images (Moore and Waltz, 1983; Sabin, 1987). Linear features may represent rock types with different resistances to erosion or perhaps tectonic weaknesses such as faults, fractures or joints. Therefore, lineament mapping is valuable in geological applications of remotely sensed data for producing regional structure and tectonic maps as well as for mineral exploration (as quoted in the Chapter 8).

On images, few linear features are shown by pronounced differences in brightness, whereas in many cases they are marked by subtle brightness or gradational boundaries so they are vague and difficult to define and map. Although by manipulating contrast, linear features can be enhanced, this method is not specific for linear features (Sabin, 1987;

Drury, 1987). A technique called filtering has been developed to enhance linear features, and the most common filter used in image processing is termed two-dimensional convolution (Drury, 1987), a process of evaluating the weighted neighbouring pixel values (Rosenfeld and Kak, 1976). The technique has been used to enhance linear features for geological interpretation (e.g. see Moore and Waltz, 1983; Drury, 1986a; Sabin, 1987; Maude,. 1987). In this work, this technique which can be categorized as low pass, high pass, directional and nondirectional filter (Holdermann et al., 1978; Sabin, 1987) was used to enhance or detect linear features for Landsat MSS and TM for Loch Tummel and Landsat MSS for Kedah-Perak area.

Convolution of an image involves the following procedures (Lillesand and Kiefer, 1987):

a. A moving window is established which contains an array of coefficients or weighting factors. Such arrays are referred to as operators or kernels and they are normally an odd number of pixels in size (e.g., 3 x 3, 5 x 5, 7 x 7).

b. The kernel is moved through the original image and the PV at the centre of the kernel in a second (convoluted). output image is obtained by multiplying each coefficient in the kernel by the corresponding PV in the original image and adding all the resulting products. This operation is performed for each pixel in the original image.

In this study only a 3 x 3 pixel kernel size is available and therefore was used by choosing option CONVOLUTION FILTER in

ENHANCEMENT MENU of the DIAD system (Figure 4.5). Option FILTER CONSTRUCTION in the same menu is selected first to construct a 3 x 3 filter matrix (kernel) and a weighting. In the convolution processes, as the kernel is moved over the image, each pixel value under the filter is multiplied by the corresponding value in the kernel. The nine products are added together and then divided by the weighting, and the resultant value is placed into the image to replace the pixel at the centre of the filter.

5.5.1 Low pass filter

A linear spatial filter that deemphasizes or blocks the high spatial frequencies (large area changes in brightness) or in other words it enhances low spatial frequencies is called a low frequency or low pass filter. Therefore, the original data will result in a low frequency filtered image which appears smooth, defocussed or blurred, hence the filter is known as a smoothing or defocussing filter (Curran, 1985). Such image smoothing is useful for removing periodic "salt and pepper", and suppression of banding and "speckle" in remotely sensed images (Curran, 1985; Jensen, 1986).

The smoothed images were generated by selecting option SMOOTH DISPLAY in ENHANCEMENT MENU of the DIAD System. This smooths the image by passing a filter over the display by replacing each pixel with either the mean, mode or median of the histogram of the surrounding 3 x 3 box of pixels (DIAD, 1988). The result of this smoothing process shows that the high spatial frequencies are blocked or deemphasized and low

spatial frequencies are enhanced. In this study the process was used to suppress high frequencies detail in several images which are processed through nondirectional filter to make the image appear continuous, less "noisy" and shows clearer definition for linear features.

5.5.2 High pass filter

A linear spatial filter that enhances high spatial frequencies and deemphasizes the slowly varying components is called a high pass filter. The processed image is more "sharpened" and "edge enhanced", consequently the filter is known as a "sharpening" or "edge enhancement" filter (Short, 1982). The data in this study were passed through the filter by choosing option EDGE ENHANCEMENT DISPLAY in the ENHANCEMENT MENU of the DIAD System. This sharpens the image by passing a filter over the display, and the function used is:

$$out = 3 * in - 2 * m$$

Where out is the new pixel value, in is the original pixel value, and m is either the mean, mode or median of the histogram of the surrounding 3 x 3 box of pixels (DIAD, 1988). This process was used in order to get its overall effect which is to "sharpen" all boundaries, and to increase the apparent resolution in the image (Short, 1982).

5.5.3 Nondirectional filter

A filter that will enhance or detect linear features without regard to their directions is called a nondirectional filter (Sabin, 1987). The most common high pass nondirectional filter is termed the Laplacian convolution filter (Jensen, 1986; Mather, 1987; Sabin, 1987). The directional filter (section 5.5.4) is generally preferred for finding lines, whereas the Laplacian is more useful in edge and boundary detection (Jensen, 1986). Several 3 x 3 Laplacian filters (and weights) are given below (Pratt, 1978; Jensen, 1986; Drury, 1987; Mather, 1987):

$$\text{filter A} = \begin{matrix} 0 & 1 & 0 \\ 1 & -4 & 1 \\ 0 & 1 & 0 \end{matrix} \qquad \text{filter B} = \begin{matrix} -1 & -1 & -1 \\ -1 & 8 & -1 \\ -1 & -1 & -1 \end{matrix}$$

$$\text{filter C} = \begin{matrix} 1 & -2 & 1 \\ -2 & 4 & -2 \\ 1 & -2 & 1 \end{matrix} \qquad \text{filter D} = \begin{matrix} 1 & -2 & 1 \\ -2 & 5 & -2 \\ 1 & -2 & 1 \end{matrix}$$

Often, a Laplacian edge enhancement is added back to the original image directly, using the following filter (Bernstein, 1983; Mather, 1987; Thomas et al., 1987) to produce the best enhancement of high frequency detail (this was chosen by Jensen (1986) in his analysis of urban and wetland areas):

$$\text{filter E} = \begin{matrix} 0 & -1 & 0 \\ -1 & 5 & -1 \\ 0 & -1 & 0 \end{matrix}$$

The non-directional filters were applied to Landsat MSS and TM data for Loch Tummel and Perak-Kedah areas to generate nondirectional edge enhanced images for delineating lineaments for the areas (Chapter 8).

5.5.4 Directional filter

Both low pass and high pass filters are nondirectional filters because they suppress or enhance linear features having any orientation in an image. On the other hand, directional filters are used to enhance specific linear trends in an image. In the environmental sciences high pass spatial filters are the most popular kind of directional filter as a result of their ability to enhance high spatial frequencies (edges) in a particular direction (Curran, 1985). This technique proved to be of particular value in the enhancement of features with a preferred orientation, including geological linear features (lineaments) (Moore and Waltz, 1983; Jensen, 1986; Drury, 1987; Maude, 1987; Mather, 1987) by using the following 3 x 3 directional filters (examples are for east-west enhancement):

$$\text{filter F} = \begin{matrix} -1 & -1 & -1 \\ 0 & 0 & 0 \\ 1 & 1 & 1 \end{matrix} \qquad \text{filter G} = \begin{matrix} -1 & -2 & -1 \\ 0 & 0 & 0 \\ 1 & 2 & 1 \end{matrix}$$

$$\text{filter H} = \begin{matrix} -1 & -1 & -1 \\ 2 & 2 & 2 \\ -1 & -1 & -1 \end{matrix} \qquad \text{filter I} = \begin{matrix} -1 & -2 & -1 \\ 2 & 4 & 2 \\ -1 & -2 & -1 \end{matrix}$$

The above filters were first tried to perform two dimensional edge detection processes (two dimensional convolution) to produce directional edge enhanced images in east-west and north-south directions. The filter which generates best edge detection images will be used to produce directional edge enhancement images in two other directions: northeast-southwest and northwest-southeast, for the Loch Tummel and Kedah-Perak areas, to be used in lineament mapping and analysis (Chapter 8).

5.6 Summary

Digital image processing is extremely broad and it often involves procedures which can be mathematically complex. However, in this chapter, only a brief and general introduction to this subject is given, and furthermore, only the techniques which are related to geological remote sensing and which have been used in this study are outlined. Several others classification menus, namely cluster classifier (DIAD, 1988), box (parallelepiped) classifier and maximum likelihood (Lillesand and Kiefer, 1987), which are available in the DIAD System have been tried in this study, but none of them were able to produce consistent and useful results for geological interpretation. The common reason is that the geology of any region can be extremely complex in form and relation, and mixtures of materials are more common than pure components. The spectral response of a region depends upon a number of interrelated factors including rock type, weathering, attitude as well as soil-vegetation cover, shadow, moisture content,

man-induced vegetation and cultural effects, thus making geological targets strongly inhomogeneous. Consequently it is very difficult and less successful to use the automated classification techniques to distinguish differences among rock types (Siegal and Abrams, 1976; Abraham, 1980; Blodget and Brown, 1982; Guha and Mallick, 1985; Drury, 1986b) than for mapping vegetation and land cover (Anderson et al., 1976; Bauer et al., 1979; Bradbury et al., 1985; Watson, 1978). For this reason they were not used in the present study. Therefore, the discussion of the topic is not given. In addition, the OIF, a statistical method used to evaluate the amount and distribution of information contained in the images is also discussed.

CHAPTER 6

GENERAL ASSESSMENT AND COMPARISON OF GEOLOGICAL INFORMATION CONTENT OF THE IMAGE PROCESSING AND IMAGE PRODUCTS

6.1 Introduction

Several digital image processing techniques were mentioned and discussed in the Chapter 5, and in general they are very useful for storing and manipulating such huge data sets and are capable of enhancing the subtle details which should be used prior to the visual interpretation task. In this respect, therefore the processed images were first assessed in terms of their image-characteristics and their general information content (section 6.2). Based on the general assessment, a few selected images, which showed useful geologic features and/or enhance the geologic information of the study areas were chosen and then compared in terms of their geological information content.

6.2 General assessment of the image processing and image products

In this section a general assessment of the image processing and image products for the Lochindorb (which will be used as an example of surface material mapping) and the Kedah-Perak (which will be used as an example for lithological mapping)

areas will be carried out in terms of their photo-characteristics (grey tone or colour), enhancement of subtle images and feature identification capability. General assessment for other features like relief, drainage, cultural and overall tone-texture on each image are also described. The TM data set of the Loch Tummel area is much effected by the atmospheric attenuation (as previously mentioned in section 4.2.2 in the Chapter 4), and as will be shown, several processed images produce spurious results. Due to this fact coupled with the geological features of the area (as described in Chapter 2 and in section 7.1) and also the objective of the study for the area (lineament analysis), the TM data for the Loch Tummel were not processed as for the Lochindorb area but were processed with the aim of enhancing the lineaments. Thus for lineaments, only the results for the Loch Tummel and the Kedah - Perak areas will be given.

6.2.1 Unprocessed images

The unprocessed image of each band for the study areas was viewed on the DIAD for a preliminary comparison. On the monitor screen the images appeared very dark in most cases, some features, though hazy, could be seen in certain images particularly the ones which recorded information in longer wavelengths (for example TM bands 7, 5 and 4 and MSS bands 7 and 6). However not much detail could be seen on the subsequent prints as they came out so dark. One such image is shown in Figure 6.1. This is of MSS band 7, but despite the fact that it displays the least effect of atmospheric

interference compared with MSS bands 4, 5, 6, the image is still very dark and low contrast, and apart from a few major lineaments, not much detail can be discerned: A simple linear contrast stretch of the same sub-scene was carried out and the result is shown in Figure 6.6 D. There is much greater contrast in tone hence it displays more detail. These images show that through a simple process of contrast stretching an image is more accessible to analysis and interpretation.

6.2.2 Contrast enhancement of original band images

Linear contrast stretches of the TM sub-scene images of the Lochindorb area are shown in Figure 6.3. This figure illustrates the dramatic improvement in resolution from the MSS's IFOV of 79 x 79 m (Figure 6.2) to the TM's IFOV of 30 x 30 m, also the characteristic appearance of the various bands is illustrated. Band 1 displays a great deal of atmospheric interference which affects the overall quality of the image greatly. Despite its lower contrast, however, spectral variations which are related to cover types still can be observed on the image. These atmospheric effects decrease toward the longer wavelength images. Apart from water bodies and shadowed areas, dark tones in the north-west and south-east corners of the area particularly in the TM bands 5 and 7 are due to forest cover. Green grass and agricultural land show very high reflectance in TM band 4, hence they appear as very light tones. Other mixed vegetation covers show as light grey to dark grey in all images. Topographic relief as well as drainage are best expressed in TM bands 5 and 7. Cultural

MSS Band 7 (0.8-1.1 μm)

Figure 6.1 Unprocessed image of the Landsat MSS (band 7) data for the Kedah-Perak sub-area 1. Despite the least effect of atmospheric interference it displays, the image is still very dark and very low contrast.

MSS Band 7 (0.8-1.1 μm)

Figure 6.2 Linear contrast stretched of Landsat MSS (band 7), Lochindorb area. Scale 1:160,000. The image is the best compared with other three bands (4,5, and 6), however because of its low resolution, not much details can be resolved compared with the TM images of the same area (Figure 6.3).

A Band 1 (0.45-0.52 μm)

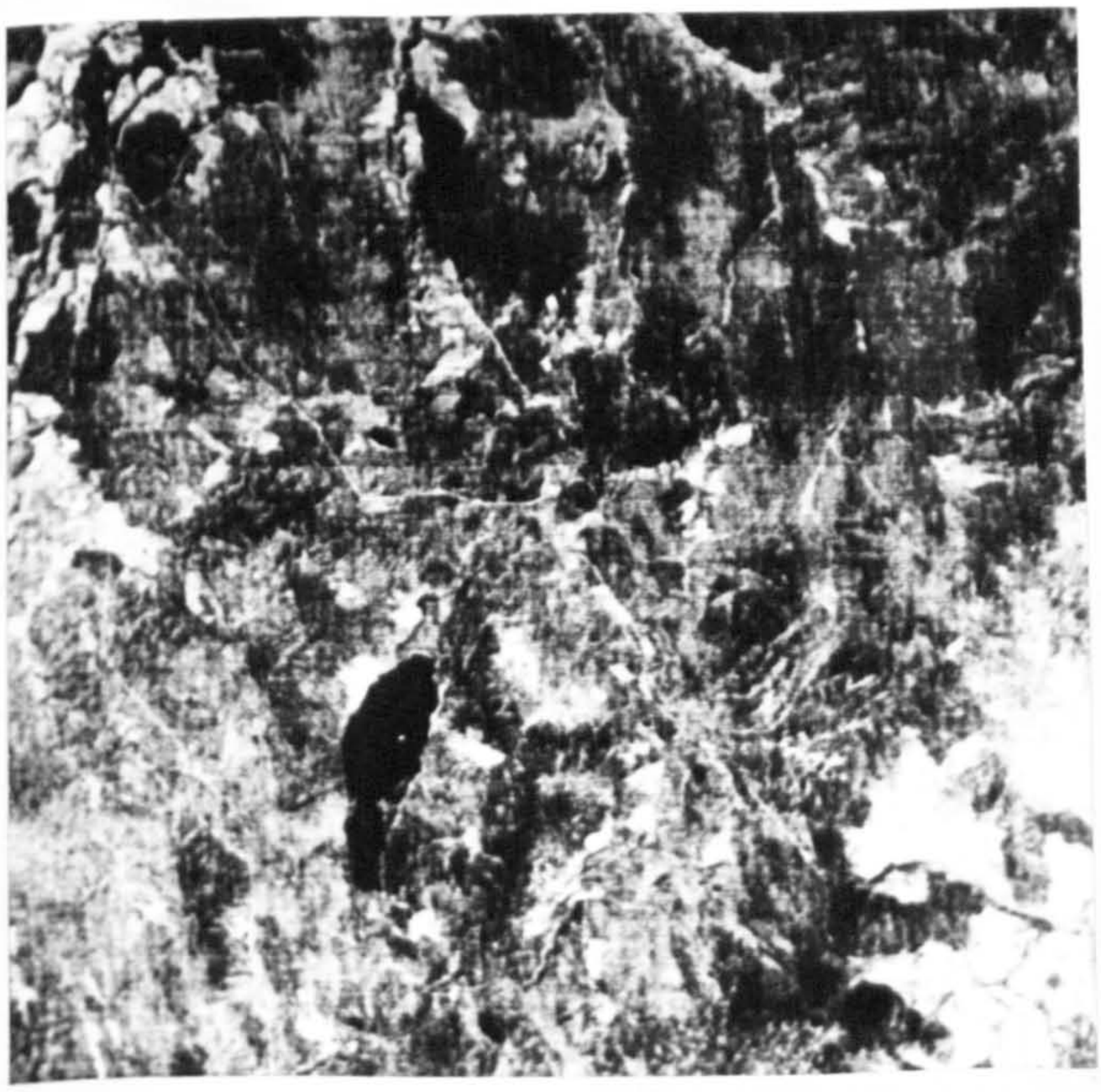

B Band 2 (0.52-0.60 μm)

Figure 6.3 Linear contrast stretches of individual Landsat TM bands, Lochindorb area. Note the dramatic improvement in resolution from the MSS data (Figure 6.2) and also the characteristics appearance of the bands. Scale 1:160,000.

C TM Band 3 (0.63-0.69 μm)

D TM Band 4 (0.76-0.90 μm)

Figure 6.3 (continue)

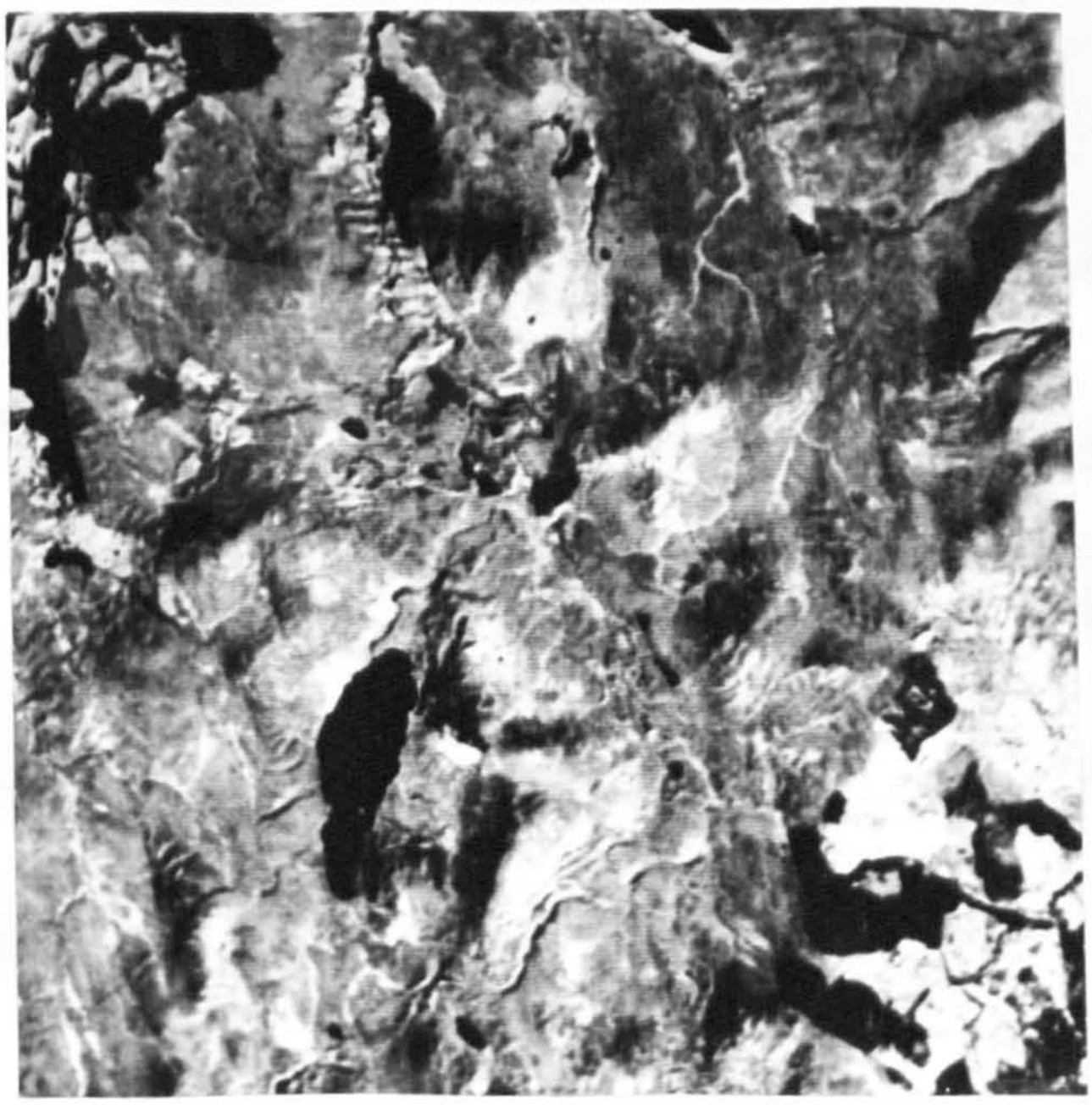

E TM Band 5 (1.55-1.75 μm)

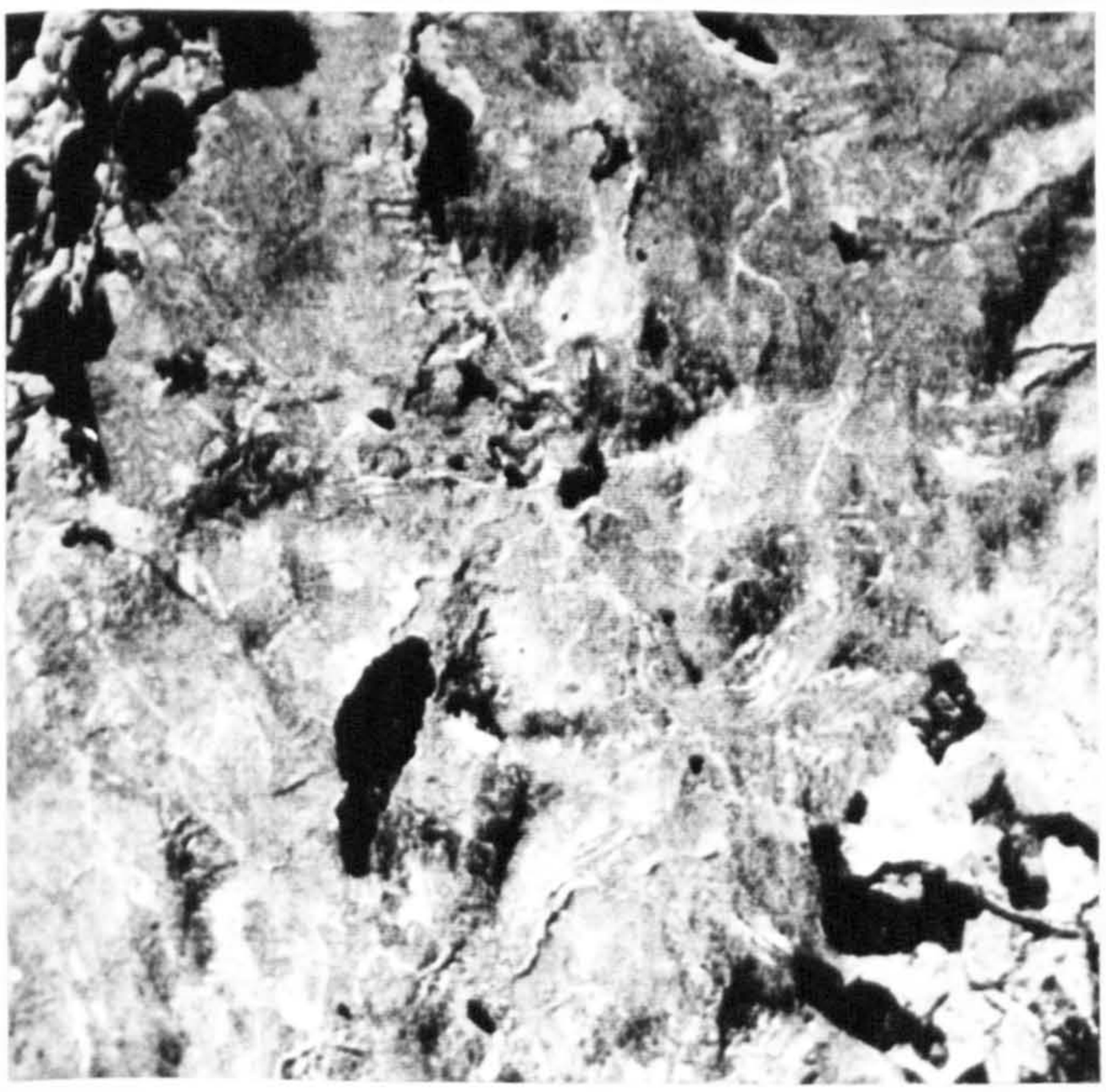

F TM Band 7 (2.08-2.35 μm)

Figure 6.3 (continue)

features such as main roads are best represented on TM bands 1 and 2. Although the quality of the images in general is good for interpretation purposes, it was very difficult to identify any of the surface material deposits and bedrock in the area. Apart from alluvial deposits which are confined to main drainage channels (generally appearing as light tones in all images because of its green grass cover or agricultural land areas), it was hardly possible to get any information about glacial and peat deposits or bedrock of the area based on their photo-elements on these images. Therefore further band combinations and enhancements of the data are needed in order to identify and discriminate these categories.

Linear contrast stretches of the TM sub-scene image of the Loch Tummel, show similar characteristics in terms of photo-character and the atmospheric effect with the Lochindorb TM sub-scene, however the affect of atmospheric interference is higher than on the Lochindorb sub-scene as shown in Figure 6.5 as well as previously indicated in section 4.2.2 in the Chapter 4. Among these images, it is evident that the TM band 5 (mid-infrared) (Figure 6.5D) and the MSS band 7 (near-infrared) (Figure 6.4) of the Loch Tummel show the best contrast and sharpest definition of geological features, compared with the other bands. These two bands therefore were chosen as the data source for the extraction of lineaments (Chapter 8) as well as for further processing for lineament enhancement (section 6.2.7) of the area.

Linear contrast stretches of the MSS sub-scene images of the Kedah-Perak area are shown in Figure 6.6. Generally the

MSS Band 7 (0.8-1.1 μm)

Figure 6.4 Linear contrast stretched of Landsat MSS (band 7), Loch Tummel area. Despite of its low resolution compared with the TM (Figure 6.5), several major lineaments can be seen quite clearly. Note that many linear features are well enhanced with the existence of snow cover on the hilly areas. Scale: 1:320,000.

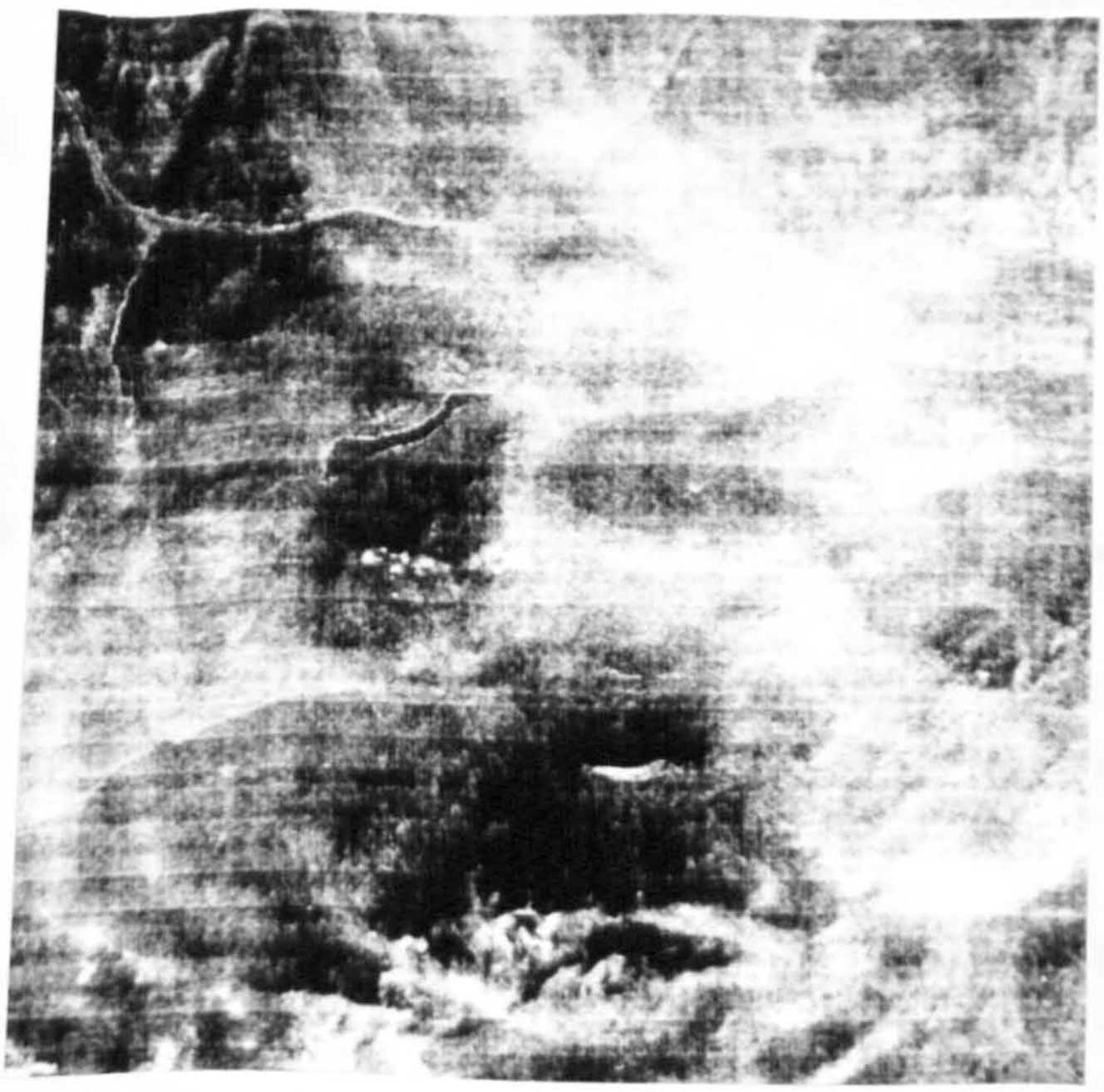

A TM Band 1 (0.45-0.52 μm)

Figure 6.5 Linear contrast stretched of five individual Landsat TM (band 1,3,4,5, and 7) images, Loch Tummel area. Scale 1:320,000. The atmospheric interference is higher than that on the Lochindorb area (compare Figure 6.5A and B with Figure 6.3A and C). The effect is decreased toward the longer wavelength band.

B TM Band 3 (0.63-0.69 μm)

C TM Band 4 (0.76-0.90 μm)

Figure 6.5 (continued)

D TM Band 5 (1.55-1.75 μm)

E TM Band 7 (2.08-2.35 μm)

Figure 6.5 (continued)

MSS bands 4 and 5 are similar in representation of photo-elements and geological information content. The MSS band 5, however, shows maximum tonal contrast and is less effected by atmospheric interference, hence it is of better quality than band 4. Apart from water bodies and shadows, other dark tones due to vegetation cover are prevalent in these bands. In this area, vegetation cover helps in defining the major geological boundaries. The effect of vegetation is less whereas relief impression and drainage are more pronounced in the near-infrared of the MSS bands 6 and 7. These bands thus enhance the photo-characteristics of rock units, specifically the resistant ones, which occur in vegetated areas. These two bands are similar in nature, but in general the MSS band 7 is better for overall lithological interpretation and lineament pattern analysis. In addition to that, the MSS band 7 also shows surface-water bodies more prominently than the MSS band 6. For these reasons, the MSS band 7 was chosen and used as one of the data sources in the extraction of lineaments (Chapter 8) and for further processing for lineament enhancement (section 6.2.7), of the area.

Two groups of (lithologic) unit may be delineated based on their vegetation cover on the MSS band 5 (Figure 6.6B). The first unit (A) has a dense vegetation cover and hence appears as a dark tone and based on the published map (Geological Survey of Malaysia, 1985), the unit is generally underlain by the granite, sandstone/conglomerate and metamorphic rocks, and the second unit (B) which has less or no vegetation cover and is shown as a light grey or light tone is generally

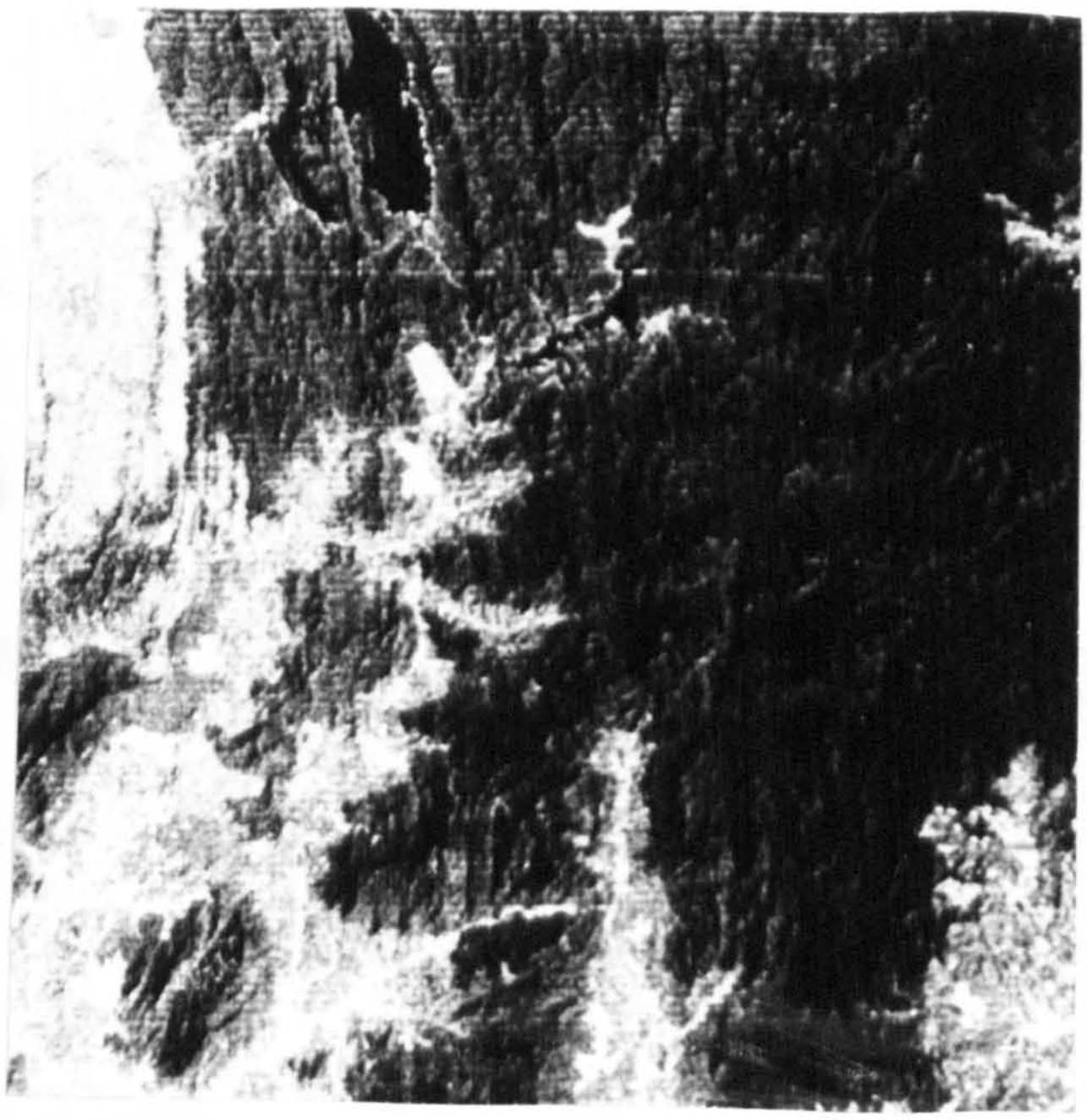

A MSS Band 4 (0.5-0.6 μm)

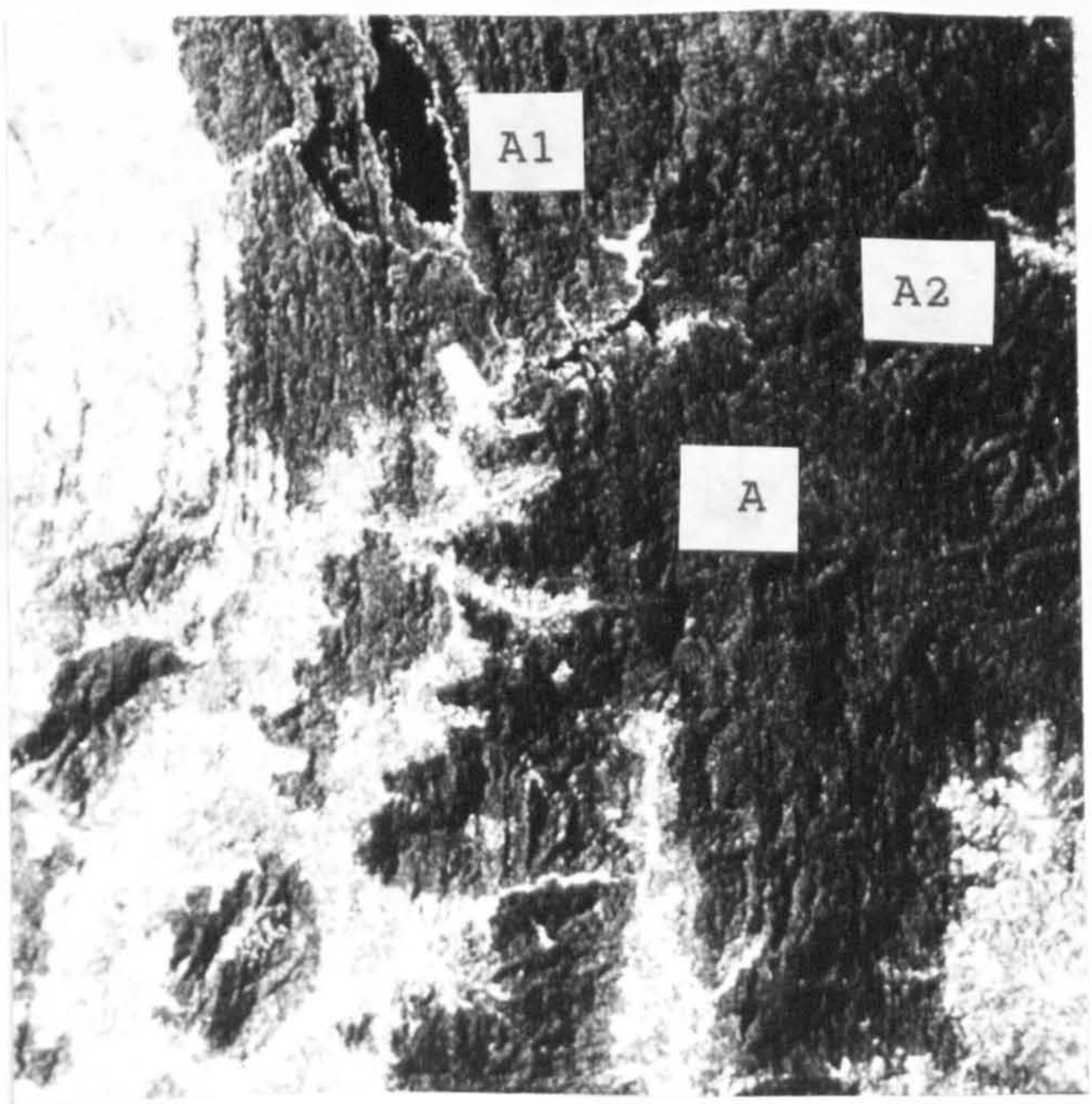

B MSS Band 5 (0.6-0.7 μm)

Figure 6.6 Linear contrast stretched of individual Landsat MSS bands, Kedah-Perak sub-area 1. The MSS band 5 shows maximum tonal contrast between vegetated and non-vegetated areas, whereas surface-water bodies and lineament pattern are best shown in the band 7. Scale 1:600,000.

C (MSS Band 6 (0.7-0.8 μm)

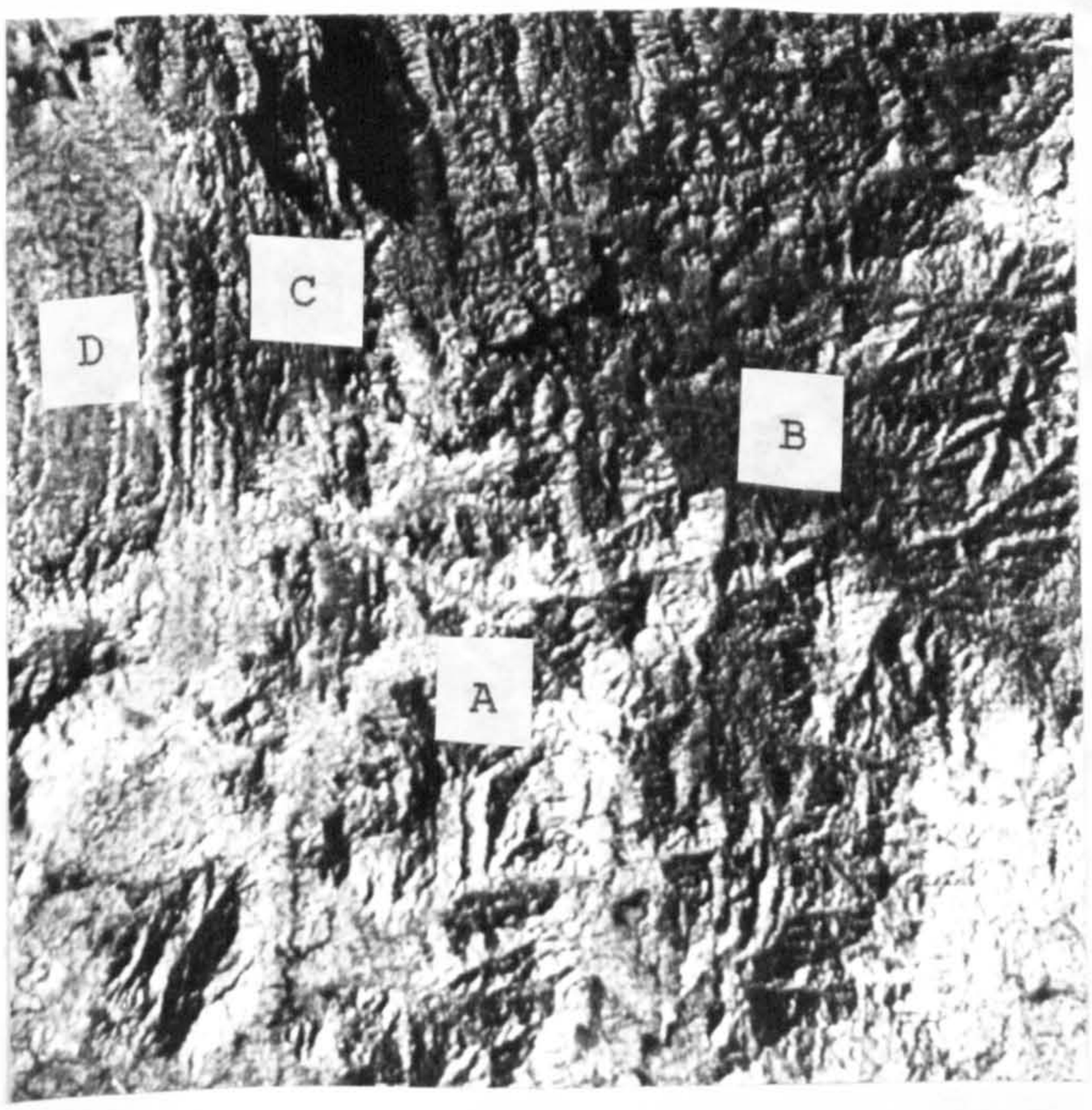

D (MSS Band 7 (0.8- 1.1 μm)

Figure 6.6 (continued)

underlain by shale-siltstone which has a very limited cover of alluvial deposits. Furthermore by close examination of the image, it seems to be possible to identify two units, A1 and A2 in unit A, where A1 which mainly corresponds to the sandstone-conglomerate terrain shows a lighter tone than A2 which mainly consists of granite and metamorphic rocks. Based on photo-characteristics on band 7 (Figure 6.4 D), four main (lithological) units of the area may be identified which show the following photo-element characteristics, although their boundaries are not very well defined:

a. Granite (A): grey tone, highly dissected terrain, generally high relief and appears to have rather rough texture..

b. Metamorphic rocks (B): dark grey tone, much less dissected terrain, subdued relief and generally smooth texture.

c. Sandstone/conglomerate (C): grey tone, forms high relief but less dissected than granitic terrain and moderate texture. Its occasionally prominent parallel strike ridges which can be observed in certain areas makes the differentiation between unit C and A possible. Shale-siltstone (D): light grey tone, low to moderate relief and very fine texture.

d. Alluvial deposits: grey tone, low relief, smooth texture, occurred in very limited areas along river channels.

Several major lineaments which correspond with faults in the published map are fairly clearly shown in the MSS band 7 (Figure 6.6 D), and some of them can easily be traced. In

general these images show that through a simple technique of linear contrast stretching they can give results useful for providing general geological information in the area. Nevertheless, better techniques are needed with an aim to get better images which may give better discrimination among the lithological units as well as display lineament better in the area.

6.2.3 Colour composites

For rock-type and surface material discrimination, information provided by spectral characteristics of the terrain are important and multi-spectral colour composite images may be very useful. The results from statistical methods (Chavez et al., 1982; Sheffield, 1985) (section 5.4.4) do not necessarily produce the most suitable images for interpretation (Greenbaum, 1987; Crósta and Moore, 1989). Furthermore, combinations of TM bands used by previous authors cannot be guaranteed to give useful results for different areas with different geology (Crósta and Moore, 1989). In this study, therefore, band combinations used to display images in colour for the TM sub-scene of the Lochindorb area were produced by (a) the Optimum Index Factor (OIF) (Chapter 5, section 5.4.4), (b) by examination of the distribution statistics of the data, and (c) by empirically selection in order to get the best combination for the area.

Application of the OIF criteria to the Lochindorb thematic data set (excluding the thermal band) resulted in the 20 combinations summarised in Table 6.2. Table 6.1(A) shows

the standard deviations and between-band correlation coefficients which were used in the OIF. Based on the OIF, a three-band combination using bands 1, 4, and 5 should provide the optimum colour composite with bands 1, 4, and 7, and 3, 4, and 5 just about as good. The higher value OIF combinations include one of the visible bands (TM 1, 2, or 3) and one of the longer-wavelength infrared bands (TM 5 or 7) together with TM band 4. The TM band 4 was present in all the first seven rankings (Table 6.2). The higher value OIF means that the combination has the higher total spectral range (higher sum of the standard deviation) and the lower data redundancy (lower sum of correlation coefficient) and vice versa. At the bottom end of the rankings, combinations consist of bands from the visible portion of the spectrum with bands 1, 2, and 3 'colour' combination being the second lowest. This information gives a useful guide in selecting the most suitable bands for three-band colour composites and then the analyst has to decide what colour to assign each band (blue, green, or red) in the colour composites. For the top rank OIF combination with bands 1, 5, and 4, a display in blue, green and red respectively produced good colour composite as shown in Figure 6.7 A. Topographic relief and main drainage channels are better represented. Water bodies are shown as black while bare fields appear pale blue. The boundary between different types of grass which is represented in different shades of orange, is not well defined. Forested areas are displayed as dark-brown to dark-red. Although the image shows good colour

A. MEANS AND STANDARD DEVIATIONS FOR TM BANDS FOR THE LOCHINDORB 512 X 512 SUBSCENE

	TM Spectral Band					
	1	2	3	4	5	7
Mean	39.93	15.04	14.34	26.22	24.28	9.14
Std. Dev.	1.85	1.40	1.73	6.42	6.30	2.25

B. LOWER TRIANGLE CORRELATION MATRIX FOR TM BANDS IN THE LOCHINDORB 512 X 512 SUBSCENE

TM band	1	2	3	4	5	7
micrometer	0.45-0.52	0.52-0.60	0.63-0.69	0.76-0.90	1.55-1.75	2.08-2.35
1	1.0000					
2	0.5902	1.0000				
3	0.5156	0.7695	1.0000			
4	0.4484	0.6520	0.5792	1.0000		
5	0.4799	0.6785	0.7594	0.7691	1.0000	
7	0.4475	0.6471	0.7323	0.6002	0.8731	1.0000

Table 6.1 Means and standard deviation (A) and correlation matrix (B) of the Lochindorb TM 512 x 512 subscene.

Combination	Σstandard deviation (A)	$\Sigma\lvert$correlation coefficient$\rvert$ (B)	OIF (A/B)	Ranking
1-4-5	14.57	1.68	8.67	1
1-4-7	10.52	1.50	7.01	2
3-4-5	14.45	2.09	6.91	3
2-4-5	14.12	2.09	6.76	4
4-5-7	14.97	2.23	6.71	5
1-3-4	10.00	1.53	6.54	6
1-2-4	9.67	1.68	5.76	7
1-5-7	10.40	1.81	5.75	8
1-3-5	9.88	1.76	5.61	9
3-4-7	10.40	1.90	5.47	10
1-2-5	9.55	1.75	5.46	11
2-4-7	10.07	1.90	5.30	12
2-3-4	9.55	1.99	4.80	13
2-5-7	9.95	2.20	4.52	14
3-5-7	10.28	2.36	4.36	15
2-3-5	9.43	2.21	4.27	16
1-3-7	5.83	1.71	3.41	17
1-2-7	5.50	1.78	3.09	18
1-2-3	4.98	1.88	2.64	19
2-3-7	5.38	2.15	2.50	20

For standard deviation and correlation, see Table 6.1(A) and (B) respectively.

Table 6.2 Optimum Index Factor (OIF) values for the TM images of the Lochindorb 512 x 512 subscene.

variation, however, colour differences between glacial (dark-brownish orange) and peat (yellowish pale blue) deposits are not clear, hence it is difficult to observe and to discriminate between the two. Figure 6.7 shows several OIF colour composite combinations and their comparative assessment is given in Table 6.7 (section 6.3).

From Table 6.1(B) (lower triangle correlation matrix for the TM bands in the Lochindorb 512 x 512 sub-scene), it is apparent that high correlations exist between several of the bands indicating a high level of information redundancy (strong correlation between band 5-7, 1-2-3, and band 4 shows high correlation with band 5 as well as band 3). This structure of data provides the first clue as to which three-band combinations are likely the most informative: one band from each of the two groups which show high correlation (1-2-3 and 5-7) together with band 4. In Table 6.1 (A) , the TM band 4 shows the overall highest standard deviation (that is range of DN's) which may indicate it to have more tonal variation hence good discriminating power. Based on this, of the highly correlated visible bands (1-2-3), the band 3 contains the most information, and between infrared bands (5-7), the band 5 contains the most information. Based on the distribution statistics of the data, therefore, the TM bands 3, 4, and 5 should produce a combination which contains the most information. The result of this combination is shown in Figure 6.7B with band 3, 5, and 4, displayed in blue, green and red respectively. This combination is placed third in the

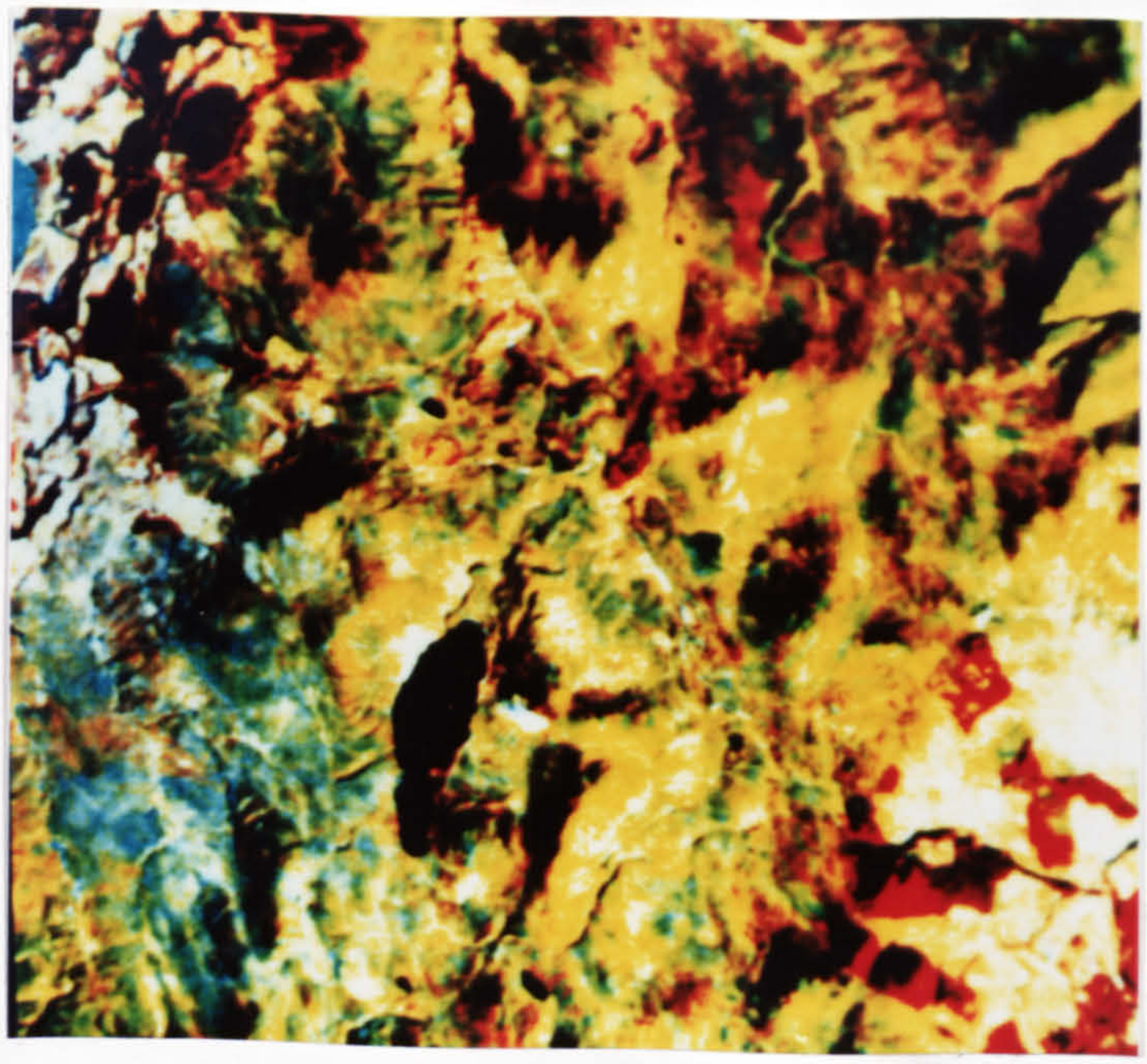

A TM 1(B)-5(G)-4(R) - ranked first

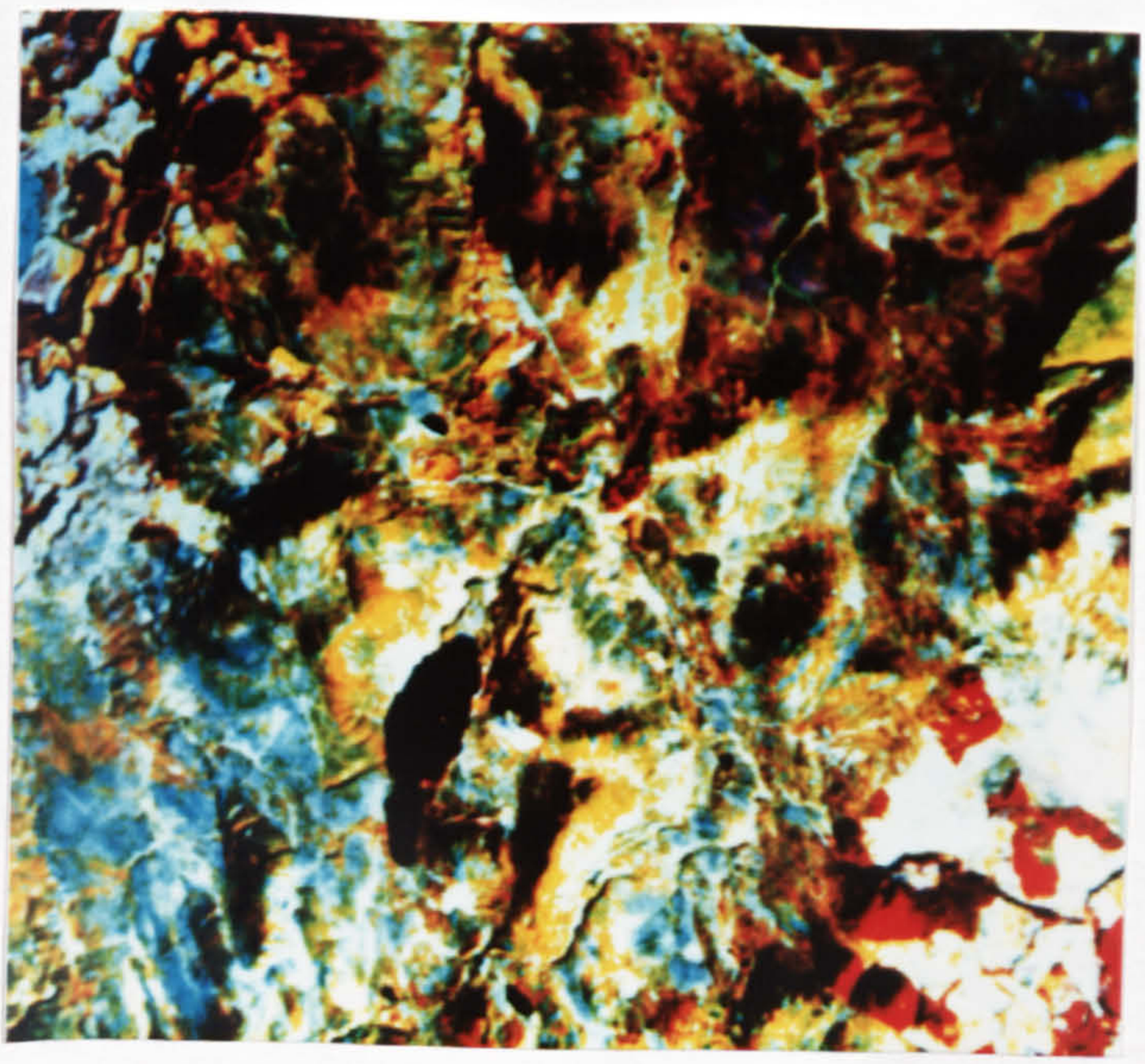

B TM 3(B)-5(G)-4(R) - ranked third

Figure 6.7 Several colour composite combinations of the Lochindorb area from the Landsat data. The ranking for each of the image is based on the Optimum Index Factor (OIF) value. Scale 1:160,000.

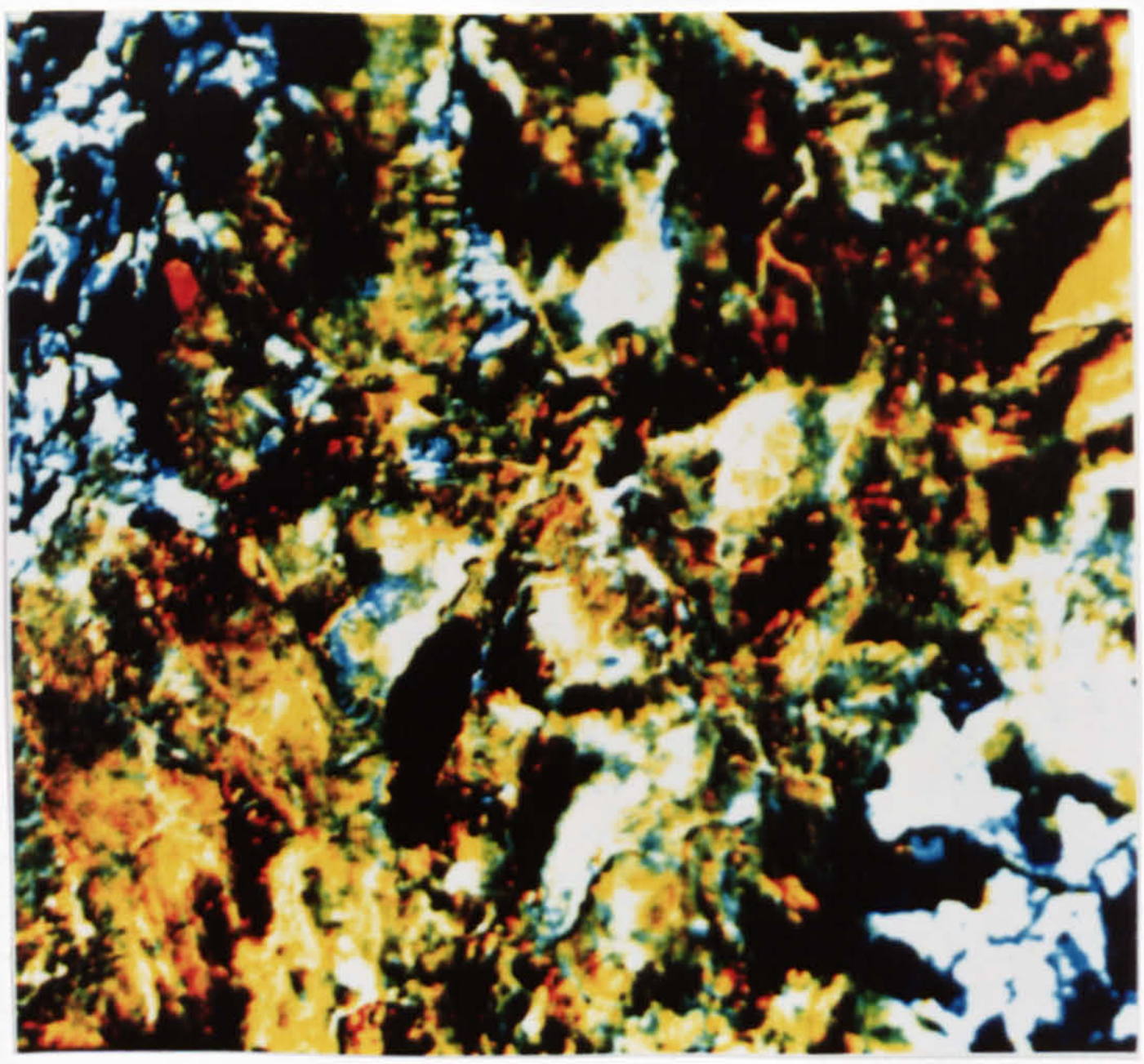

C TM 4(B)-5(G)-7(R) - ranked fifth

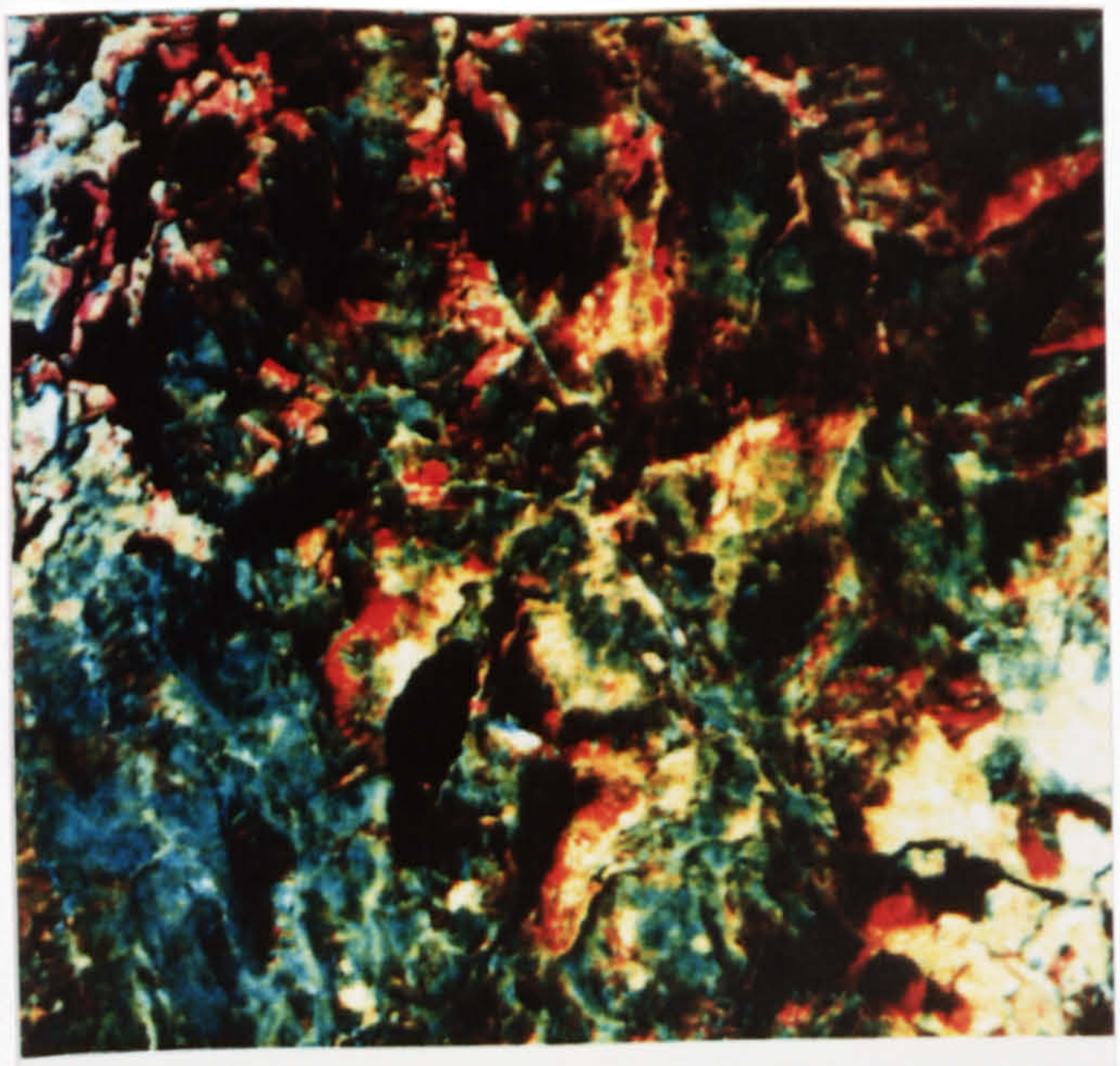

D TM 1(B)-3(G)-4(R) - ranked sixth

Figure 6.7 (continued)

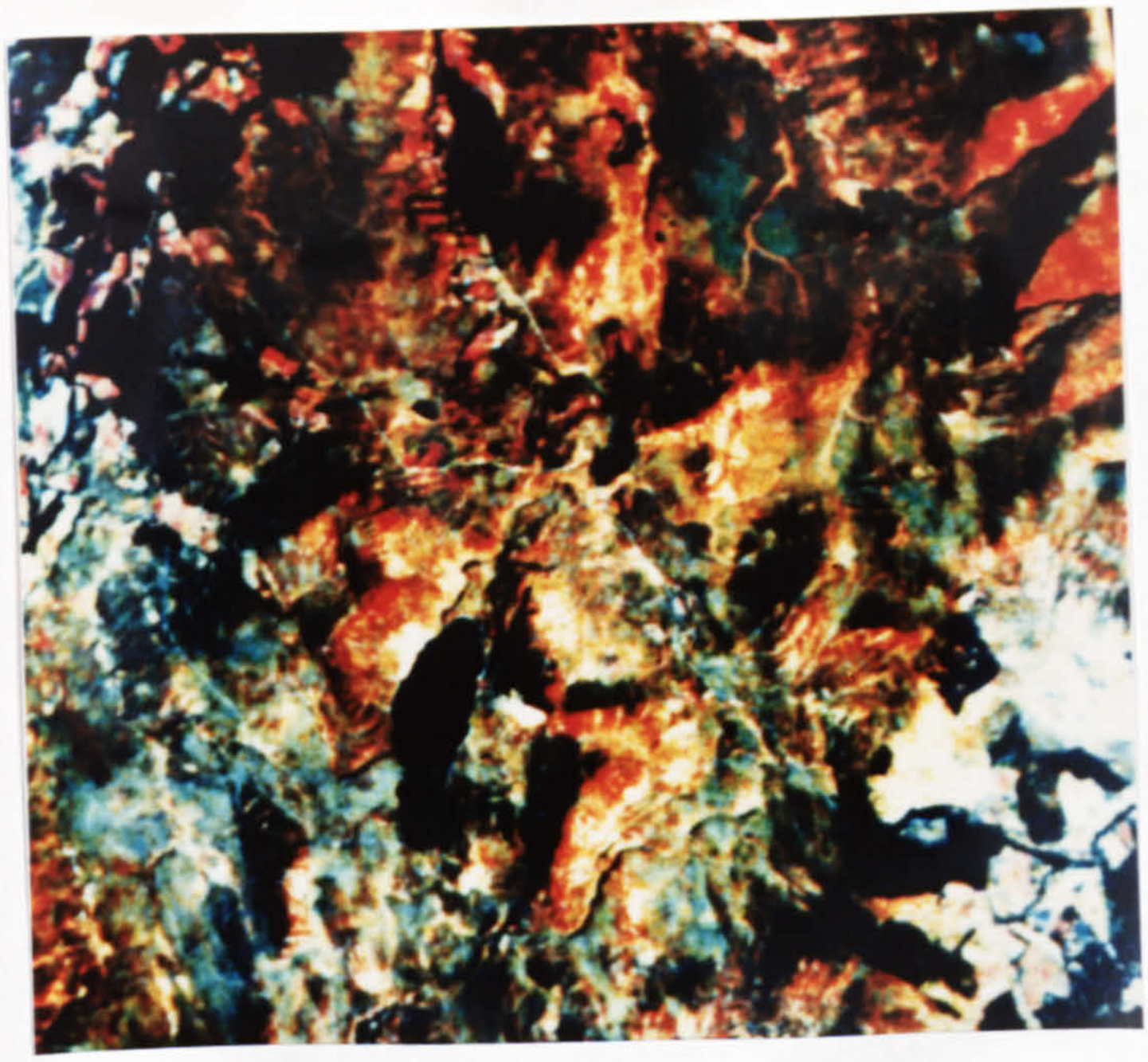

E TM 1(B)-3(G)-5(R) - ranked ninth

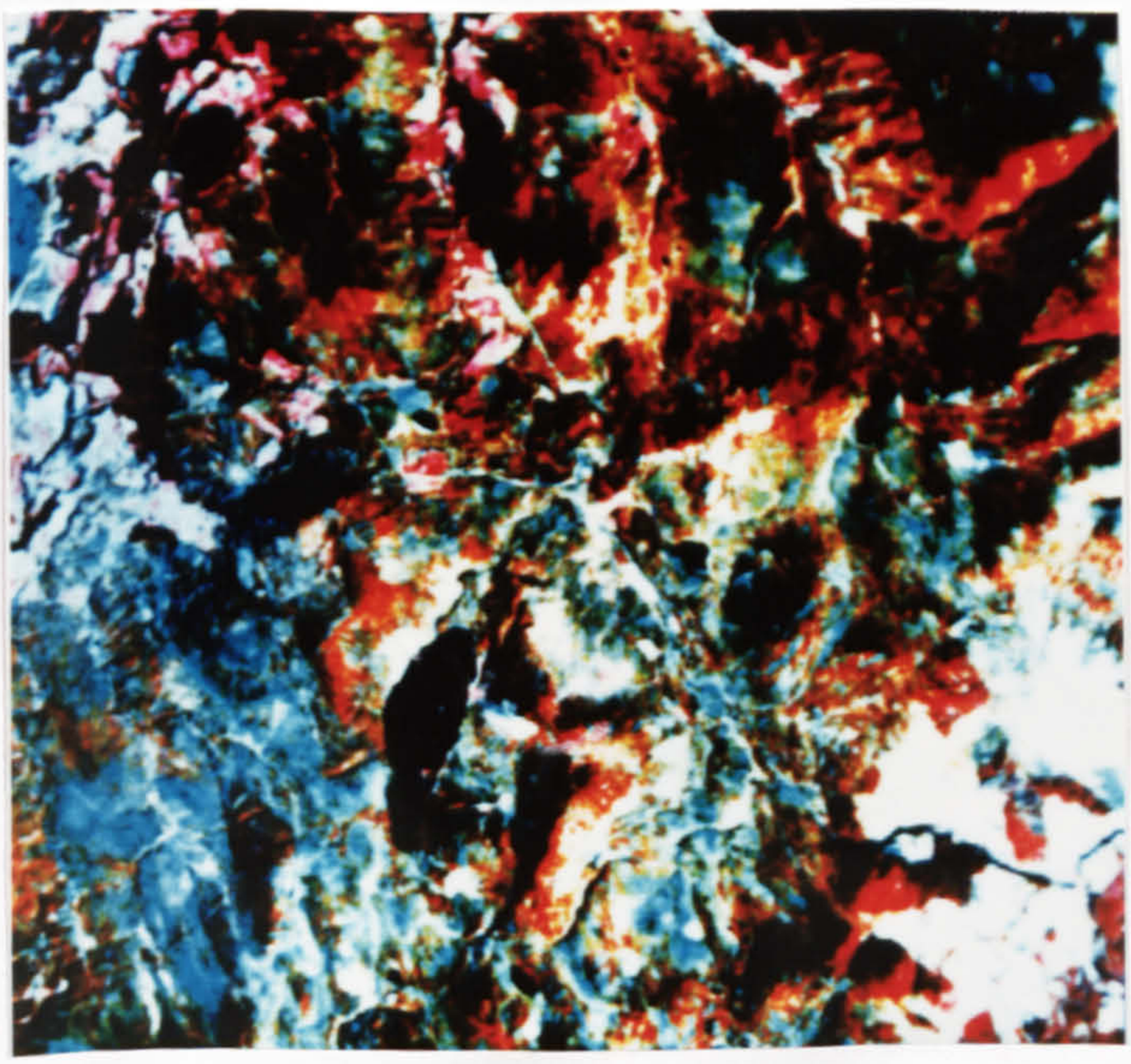

F TM 2(B)-3(G)-4(R) - ranked thirteenth

Figure 6.7 (continued)

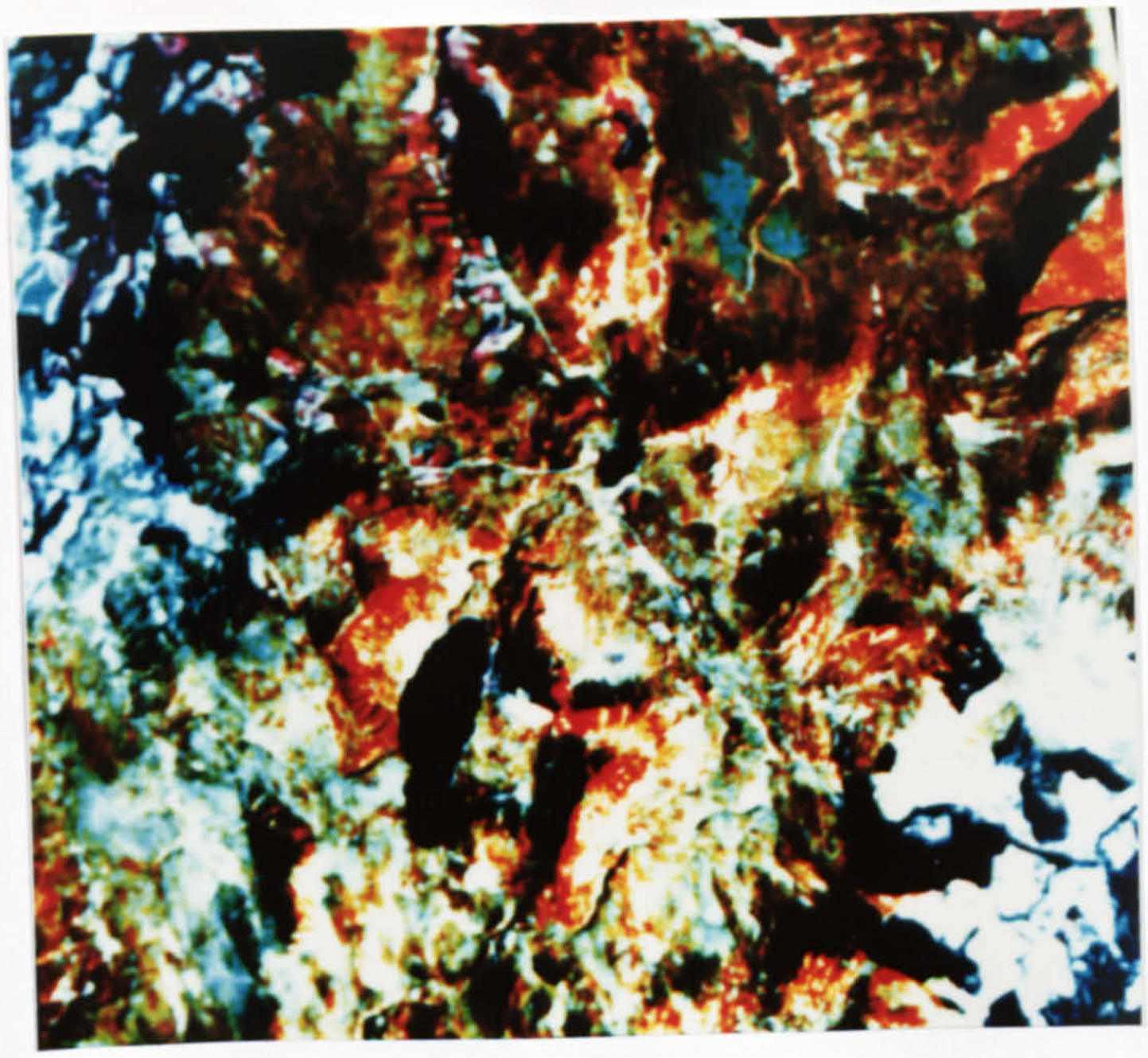

G TM 2(B)-3(G)-5(R) - ranked sixteenth

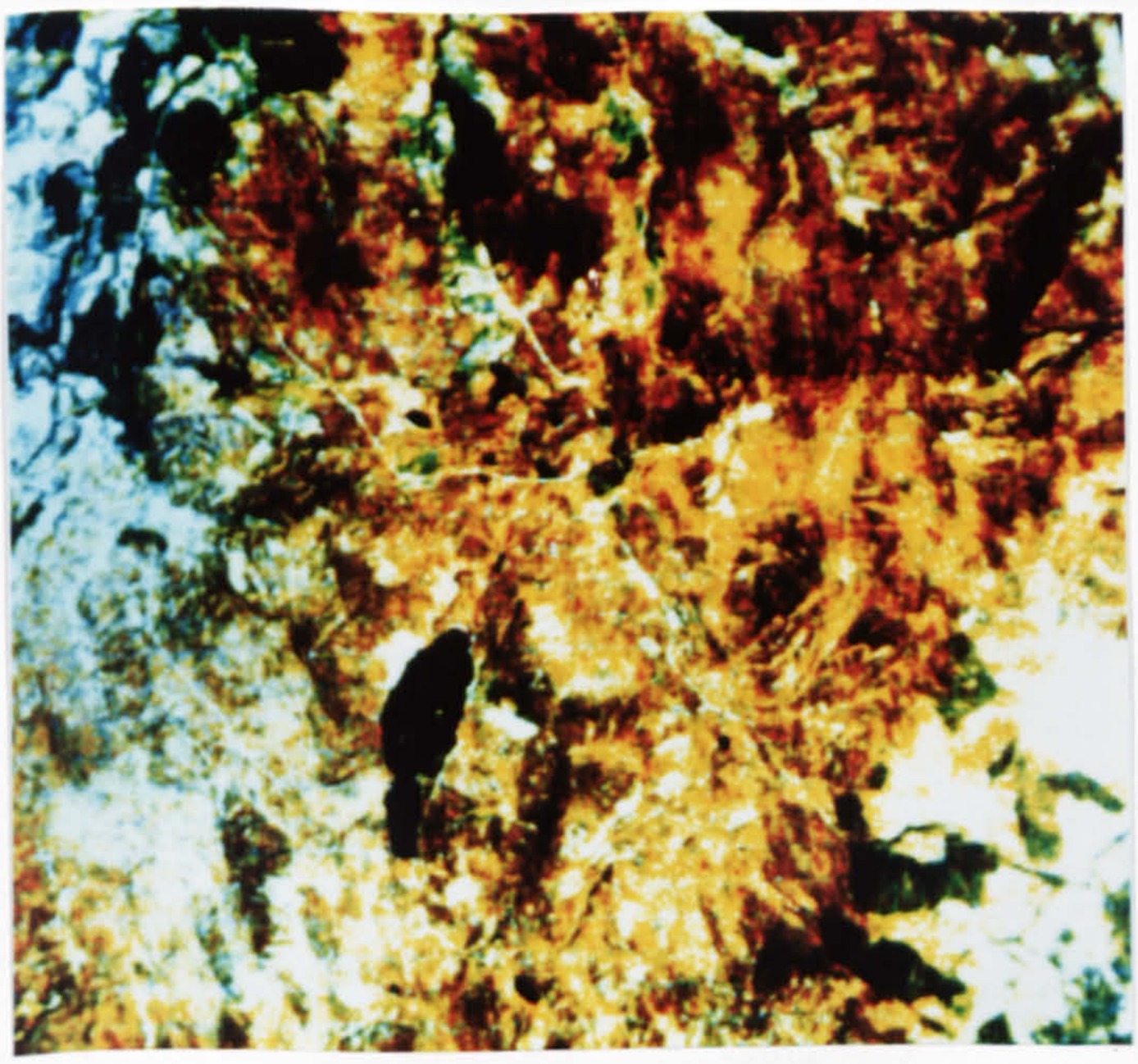

H 1(B)-2(G)-3(R) - ranked nineteenth

Figure 6.7 (continued)

OIF ranking (Table 6.2). Generally the image has a good contrast, and has a wide range of brightness. Peat deposits are clearly shown as bluish-green. Alluvial deposits with green grass cover appear as bright-orange. Glacial deposits appear as a mixture of bright to pale yellow and dark to light orange brown. Bedrock which is associated with higher topography is shown as a dark tone mainly due to the shadow effect. Forested areas appear as dark red to bright red whereas water bodies appear black. Its comparative assessment of geological information content is given in Table 6.7 (section 6.3).

Apart from the said methods, the band combination used in this study for the TM data of the Lochindorb area was selected empirically on the basis of experimentation and interpretative experience. First, the bands chosen for combination were selected by comparing each of the six contrast stretched TM band images (Figure 6.3) in terms of spectral variation related to cover types and the ability of individual bands to distinguish between the major surface material deposits shown on the published geological map. It was found that none of the individual bands shows any clear sign where major surface material deposits in the area may be discriminated. However bands 1, 3, 4 and 5 (Figure 6.3) did show relatively more tonal/spectral variations within, as well as between, cover types. These four bands were then displayed in four combinations of three to get the most useful band combination and making use of the human eye's sensitivity to colour changes. The colour composite with the bands 1, 3, and 4,

displayed in blue, green and red respectively was found the best colour composite combination to offer better discrimination between the main cover types which are related to surface material deposits in this area. The resulting image is shown in Figure 6.7D. Generally peat deposits in saturated areas which appear yellowish blue-green are well defined. Glacial deposits are shown as brown, orange-brown, pink and light pink, and alluvial deposits are represented by bright brown to pink. Bedrock which is confined to higher ground is mainly associated with dark brown areas. Forested areas appear dark red-brown while water bodies are shown as black. Overall the image shows good relief impression and main drainage channels are also well displayed. Notwithstanding, the discrimination between bedrock-glacial deposits and between peat (more drier areas)-glacial deposit are still confused. Its comparative assessment is presented in Table 6.7 (section 6.3). Although this combination is placed sixth in the OIF rankings, Table 6.2, it displays a much better colour composite combination and gives slightly better results than other combinations in discriminating the main surface materials in this study area. This indicates that in the cool temperate climate of Britain, where spectral response mainly comes from vegetation, the OIF will not necessarily be a valid indicator of geological information content.

Figure 6.8 displays the MSS colour composite for the Lochindorb area. The low resolution of the data is evident, so that not much information can be extracted from it and the image looks defocused at scale of 1: 160,000.

Because the effect of atmospheric interference is more severe in the TM data of the Loch Tummel sub-scene compared with the TM data for the Lochindorb sub-scene (as mentioned in section 4.2.2 in the Chapter 4) particularly for the bands 1, 2, and 3, therefore only bands which record information in longer wavelength, such as TM bands 7, 5, and 4, which are much less effected by atmospheric interference are used to produce false colour composite combinations. Several colour combinations were tried by using these three bands, and it was found that the TM bands 7, 5, and 4, displayed in blue, green and red respectively produce a good false colour image as shown in Figure 6.9. In the image, apart from forested areas which appear red, alluvial deposits are shown as orange pink, and mixtures of turf, heather and bracken on rolling topography are represented by greyish pale blue. The rest of colour variation is controlled by the position of the terrain in respect to the sun rather than bedrock or surface materials. As a result, the brighter tones represent the area which faces the sun and the darker tones (shadow areas) represent the area facing away from the sun. The image, therefore, is very difficult and very much less useful to interpret. Notwithstanding this, a few major lineaments which correspond to the geological faults can be observed. Topographic relief is well enhanced and main drainage channels are also well displayed. But it must be noted that water bodies which appear black may be confused with the shadow areas.

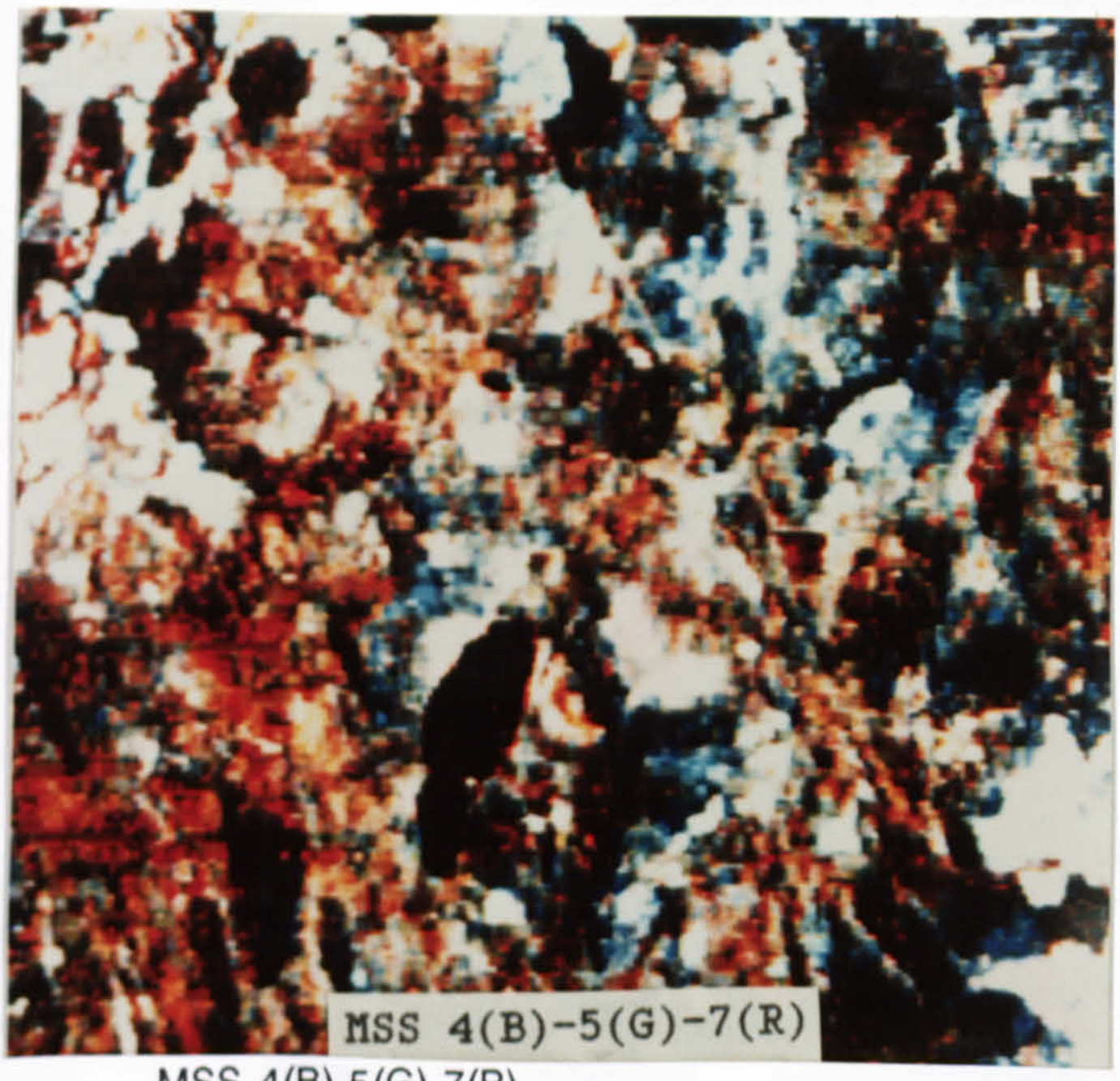

MSS 4(B)-5(G)-7(R)

Figure 6.8 Standard colour composite combination (band 4 = blue, band 5 = green, and band 7 = red) of Landsat MSS data, Lochindorb area. Because of its low resolution, not much detail can be depicted, and furthermore the image look blurred after enlargement to this scale, 1:160,000.

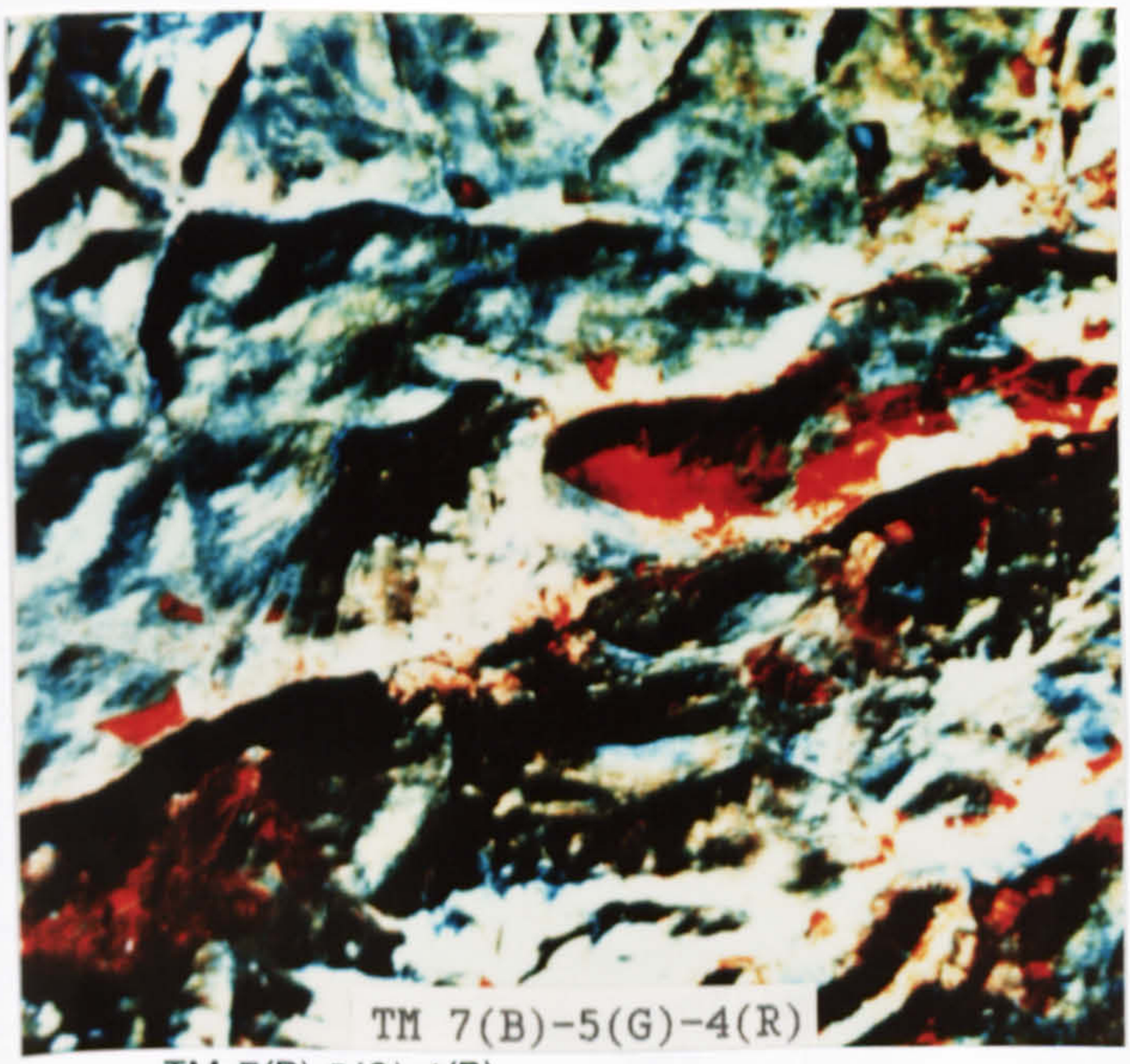

TM 7(B)-5(G)-4(R)

Figure 6.9 Colour composite combination of band 7 (blue), band 5 (green) and 4 (red) of the TM data of the Loch Tummel area. Most of the colour variations particularly in the brighter and darker areas are controlled by the position of the terrain in respect to the sun rather than geological materials. Combination using other bands (1, 2, and 3) was not possible because of the severe atmospheric effect in the data. Scale 1:320,000.

For MSS data with only 4 bands it is much easier and there is no difficulty in choosing a three band combination, and the most common combination uses bands 4, 5, and 7 and is displayed in blue, green and red respectively. The colour-infrared composite for the MSS data of the Kedah-Perak area was prepared by using the same band and colour combination where contrast stretches of the MSS bands 4, 5, and 7 were assigned to blue, green and red colours respectively in the DIAD system. This colour composite which is normally referred to as a standard false colour composite is shown in Figure 6.10. Relief impression is better exhibited in this composite, and drainage as well as lineament patterns are well expressed. It is very useful for discrimination of vegetated areas, where vegetation appears red in this composite, because of the high reflectivity of vigorous vegetation in the MSS band 7 (near-infrared). Generally the darkest red, and therefore the densest vegetation (forest), occurs in the hilly areas. Additional red tinges are apparent on the lowland areas, where these sparsely and less densely vegetated areas cannot be detected easily on the black-and-white stretched MSS images. Water bodies appear as black and shallow water areas as blue, whereas bare fields appear white to bluish white. Generally, the colour-infrared composite appears to offer some improvement over the stretched MSS images for discrimination of rock types in the area. The boundary between areas which are underlain by the sandstone/conglomerate and by the granite-metamorphic rocks is still confused. Notwithstanding,

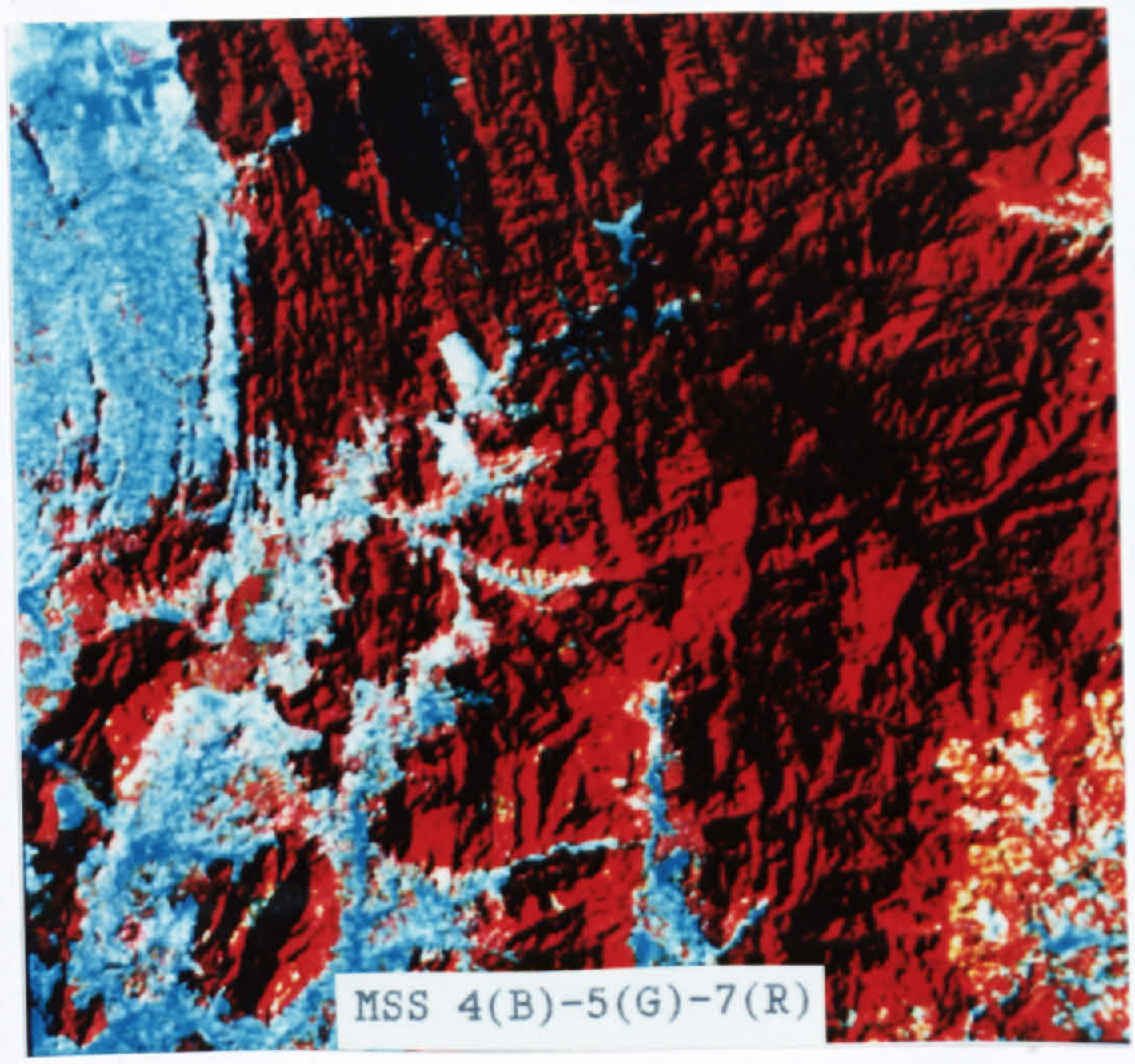

A MSS 4(B)-5(G)-7(R)

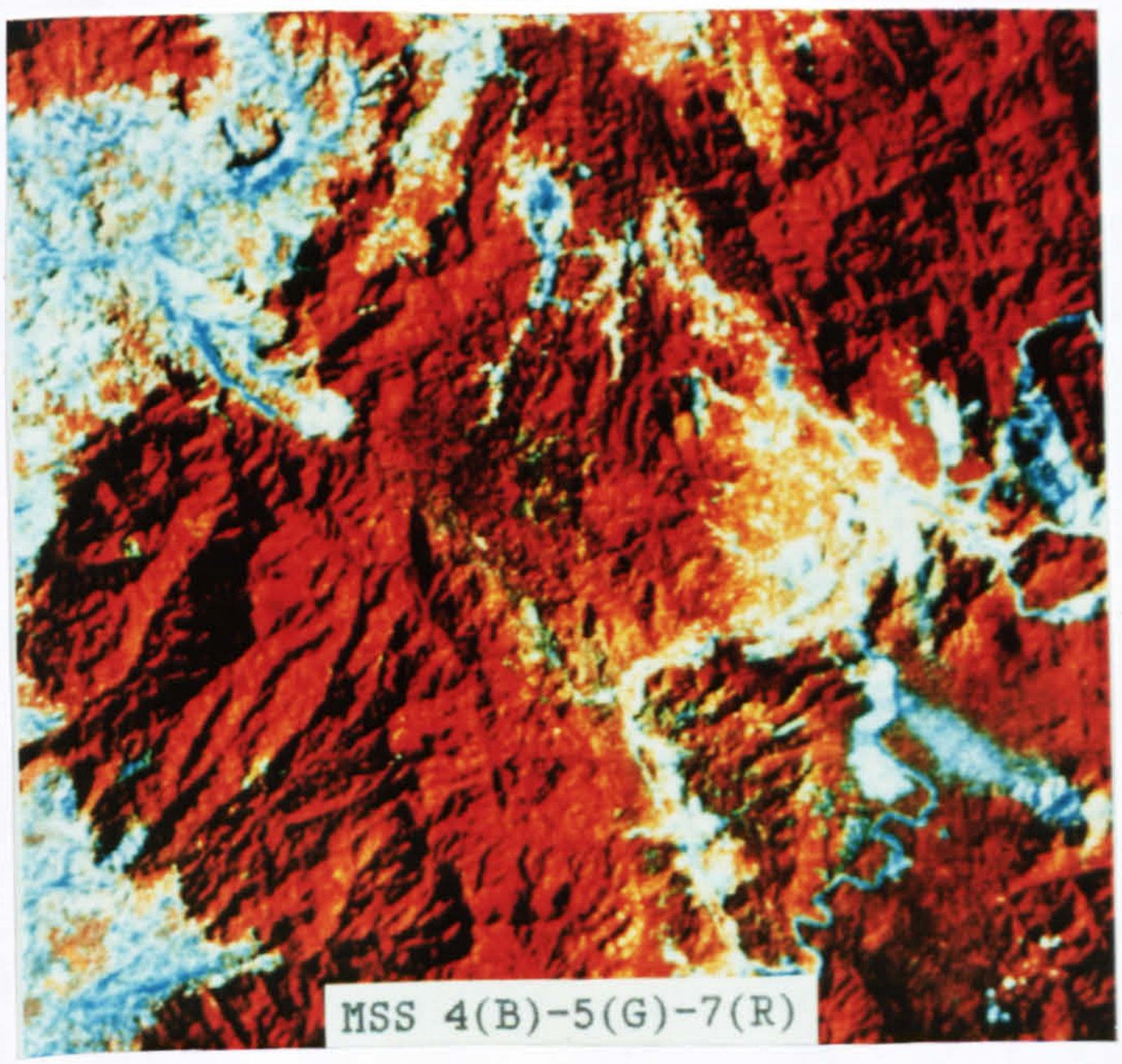

B MSS 4(B)-5(G)-7(R)

Figure 6.10 MSS band colour composite of the Kedah-Perak sub-area 1 (A) and sub-area 2 (B). Note that a very large area is covered by dense vegetation (tropical forest) which is corresponding to the red colour on the images. Scale 1:600,000.

one major improvement in the colour composite over the black-and-white images is that the boundary between the granite terrain and the metamorphic rock terrain is better defined (Figure 6.10A). The metamorphic rock areas are represented by dark-red colours while the granite appears as red. Other image characteristics like texture and relief are similar as in the black-and-white images. Combination of the MSS bands 4, 5, and 6 in blue, green and red respectively was also produced but it did not offer any new improvement over the standard false colour composite.

6.2.4 Principal component analysis

The principal component analysis (PCA) was done on the DIAD using all four channels of MSS and six channels of TM data for the Lochindorb and four channels of MSS for the Kedah-Perak areas. Tables 6.3 and 6.4 summarise the salient statistics involved in the production of PC images for both areas. It can be seen visually that the first PC contains more information than the following ones with the amount of information decreasing with each component. This also can be seen numerically by the percentage of variance (the concentration of variability in the data in orthogonal directions) represented by each component (Table 6.3 and 6.4 B) as graphically shown in Figure 6.11 and indicated for each PC image in Figure 6.12 and 6.13, where nearly 78 per cent and over 83 per cent of the variability in the data lies in the direction defined by the first PC of the MSS sub-scene of Kedah-Perak and the TM sub-scene of Lochindorb, respectively.

For each case there is a sharp decrease from PC1 to PC2 and again from PC2 to PC3 so the first and the second PC account for most of the available variance.

Line 1 of Table 6.3 and 6.4(B) give the relationship between the first PC and the original bands image and so on. For the Lochindorb area, the eigenvector matrix shows that the PC1 has positive loadings for all bands, higher contributions (loadings) from the TM band 4 and 5 and very small contributions from the rest of the original data set. The equal positive loadings have been interpreted as a brightness component in the transformation of the data (Robinove , 1982 quoted by Williams, Jr, 1983). This confirms that the PC1

PC	% Variance	Spectral Band					
		1	2	3	4	5	7
1	83.129	0.1041	0.1135	0.1431	0.6777	0.6731	0.2083
2	11.175	0.0385	0.0273	0.1561	-0.4271	0.5951	0.3011
3	2.889	0.8423	0.3532	0.3249	-0.0411	-0.2352	0.0574
4	1.361	-0.5031	0.3939	0.6169	0.0445	-0.2771	0.3640
5	0.975	0.1101	-0.1641	-0.4186	0.0704	-0.2348	0.8518
7	0.471	-0.1142	0.8244	-0.5421	-0.0588	0.0741	-0.0675

Table 6.3 Eigenvectors (principal component loadings) and percentage of the variability of the original data set in the principal component images of the Lochindorb TM 512 x 512 subscene.

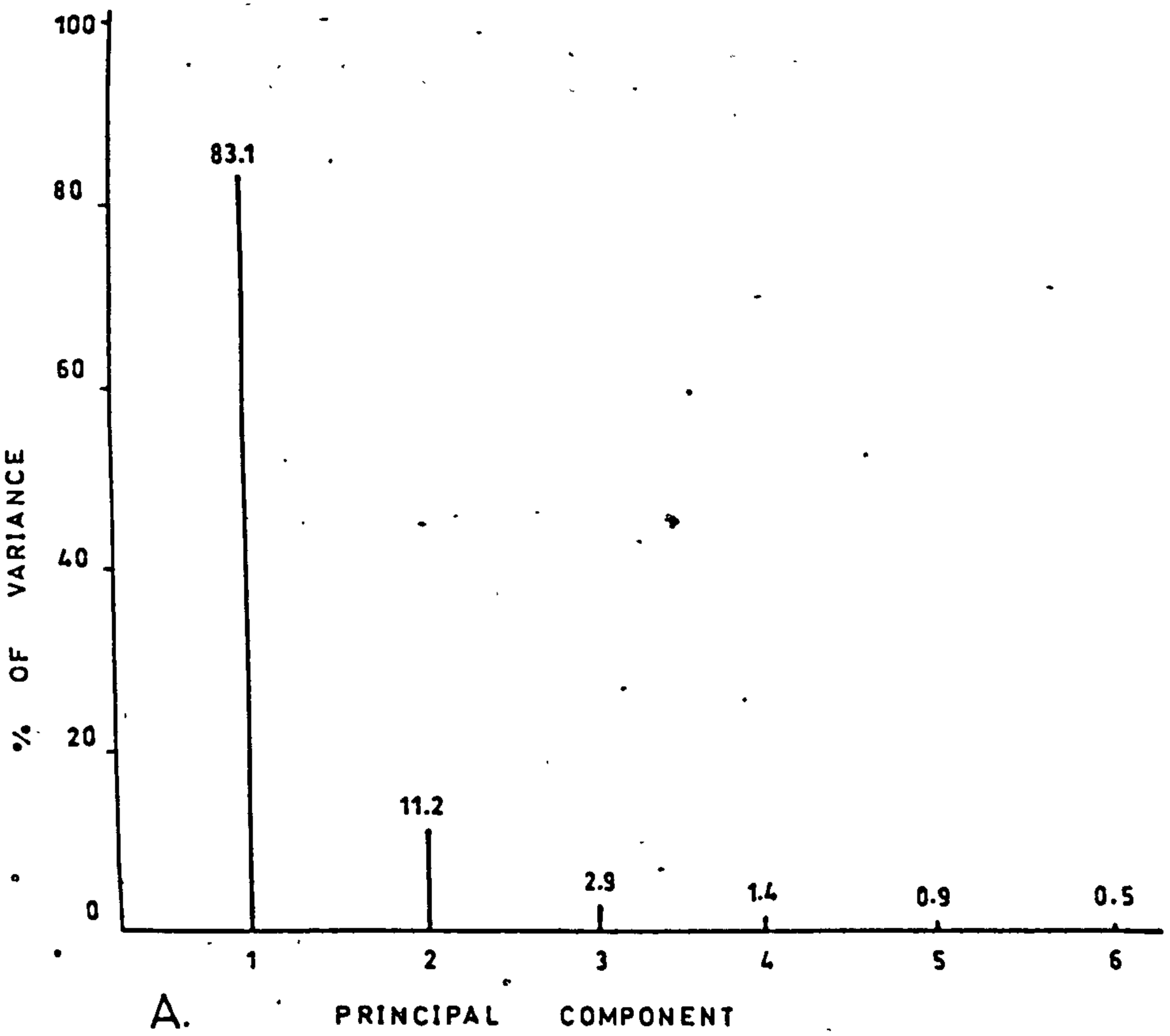

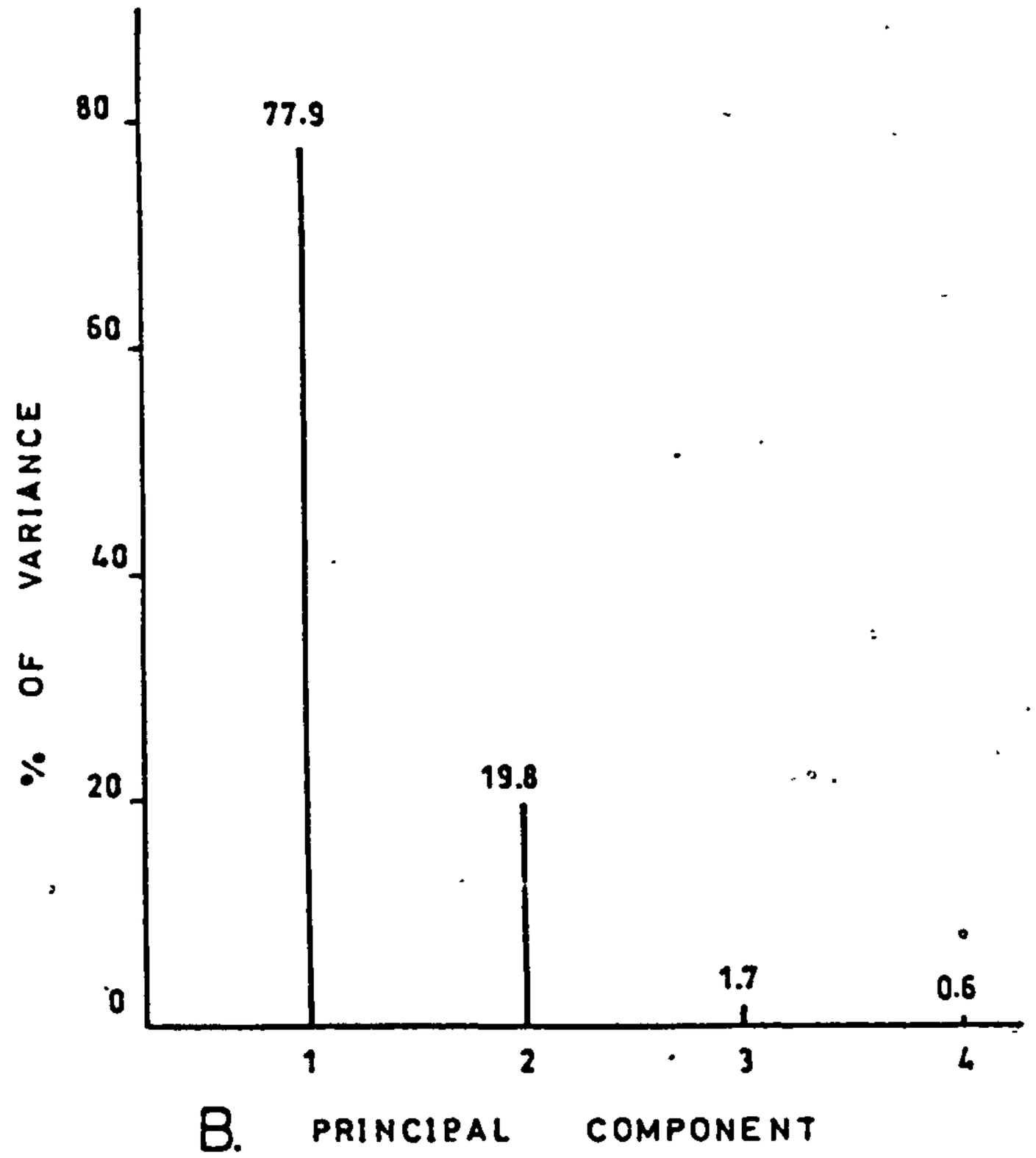

Figure 6.11 Percentage of variance represented by (A) the six PC images of the Lochindorb area from the Landsat TM data, and (B) the four PC images of the Kedah-Perak subarea 1 from the Landsat MSS data.

more or less represents a weighted average of bands 4 and 5, indeed its image is similar to those of the two bands (compare Figure 6.12A with Figure 6.3 D and E). PC2 (line 2 of Table 6.3) contains high positive loadings of band 5 and small positive loadings of band 7 contrasted against a nearly equal high negative loading of band 4. Basically, this component contrasts band 7 and particularly band 5 against band 4, and it was suggested that materials showing strong contrasts between these two pairs of bands will be emphasised in the resultant image (Williams, Jr, 1983). Therefore the materials that exhibit the strongest contrast will show the greatest separation in grey tones on the image. Between them, the PC1 and PC2 account for over 94 per cent of the variability in the original six-band data set (Figure 6.11 A). A further nearly 3 per cent is contributed by the PC3 which contains positive loadings of TM bands 1, 2, and 3 where band 1 contributes most (Table 6.3 and Figure 6.11A). The contribution from other bands is insignificant because their loadings are nearly zero. The PC3 therefore is a brightness component of visible bands and it appears similar to the band 1 which contributes most. Despite its lower percentage of variance, the main roads, which are better expressed on the visible bands than on the infrared images, crossing the area are more evident on this PC than on any other PC. PC4 contains a larger positive loading of TM band 3 and relatively small positive loadings of TM band 2 and band 7 contrasted against a large negative loading of TM band 1 (Table 6.3). It accounts for slightly more than 1 per

A PC 1 IMAGE (83.1%)

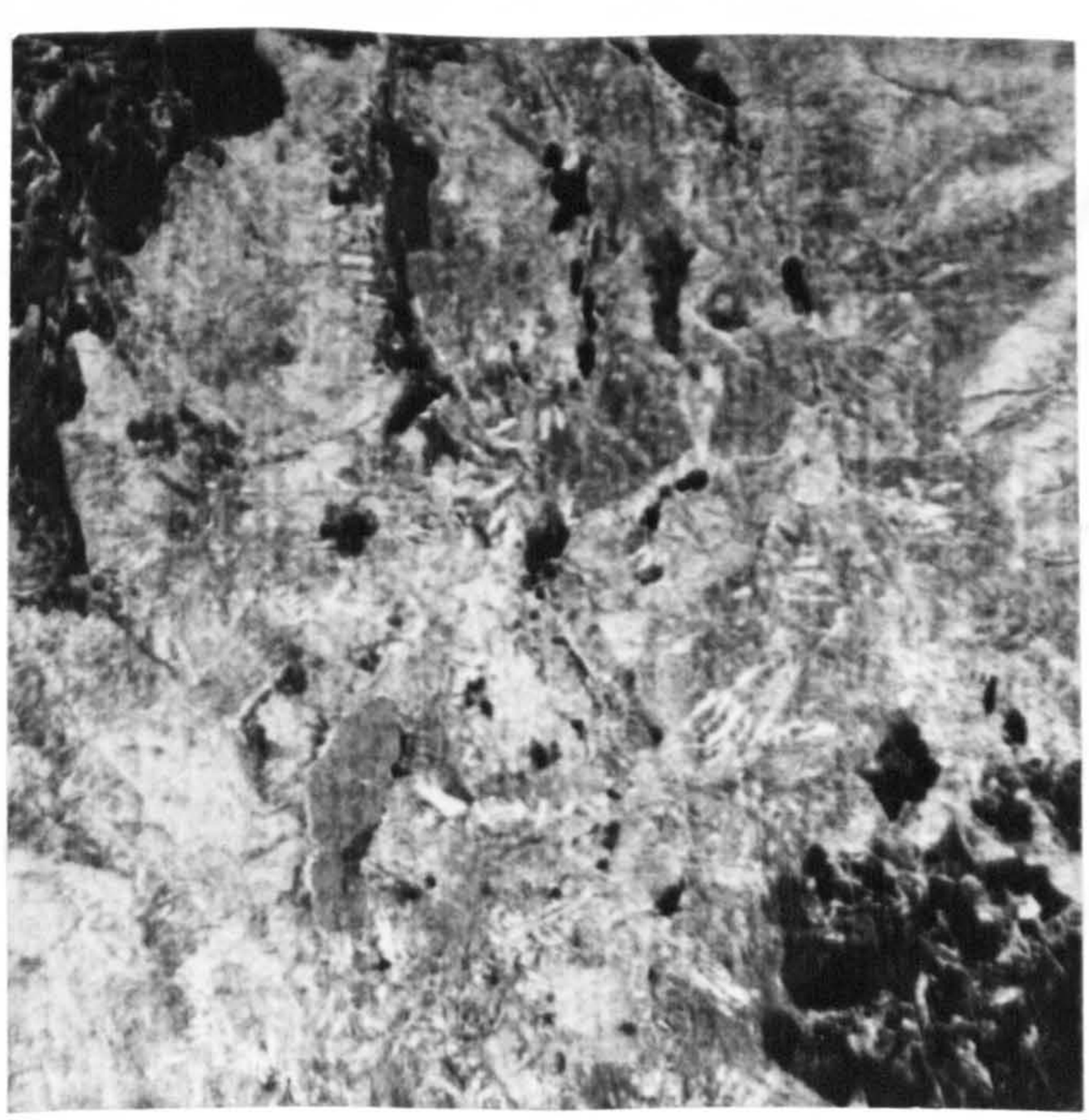

B PC 2 IMAGE (11.2%)

Figure 6.12 PC images 1-7 (A-F) of the Lochindorb area. The PC images are generated from the six visible and reflected IR bands of the Landsat TM image. Percentage of variance represented by each PC image in shown.

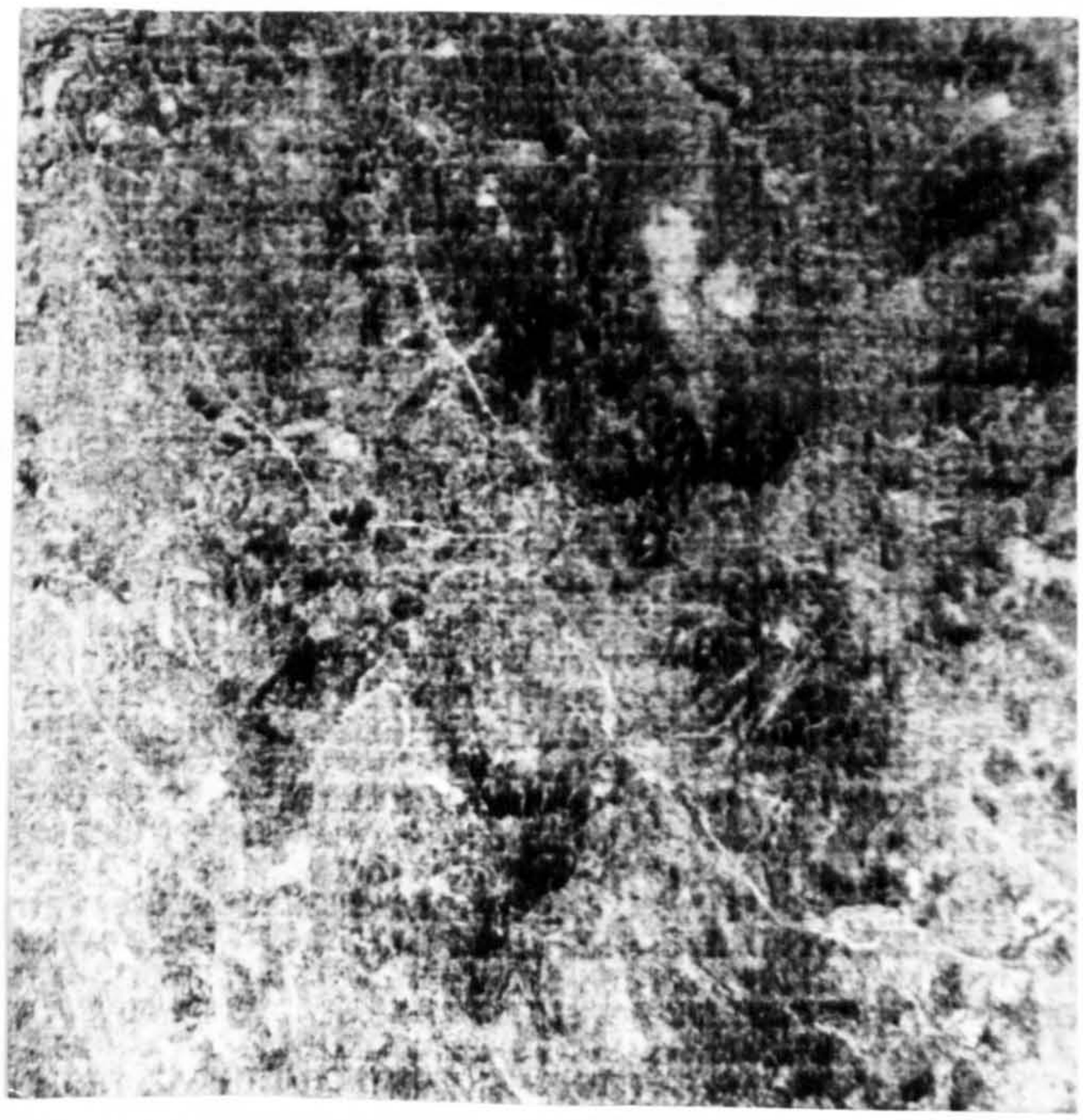

C PC 3 IMAGE (2.9%)

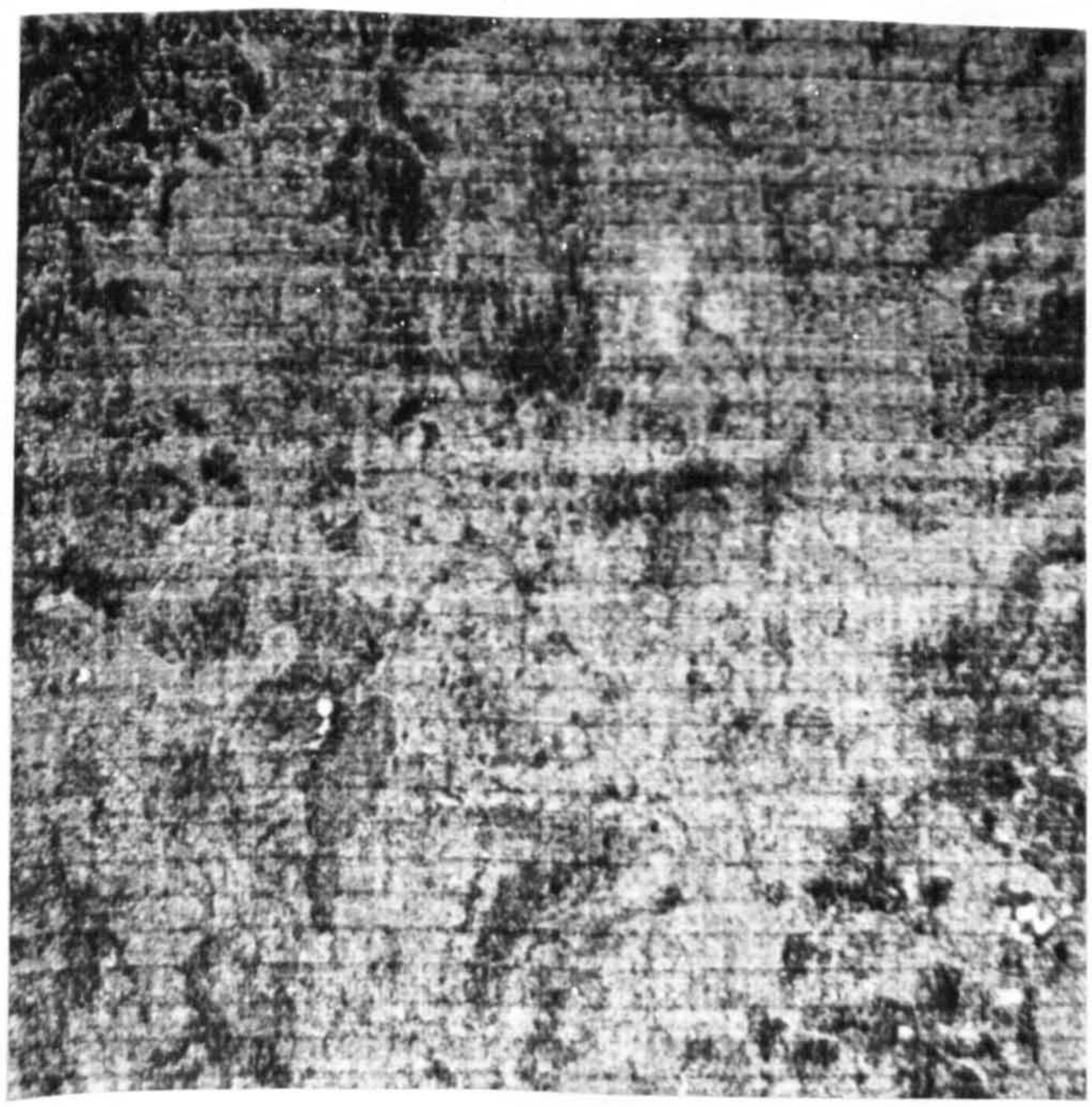

D PC 4 IMAGE (1.4%)

Figure 6.12 (continued)

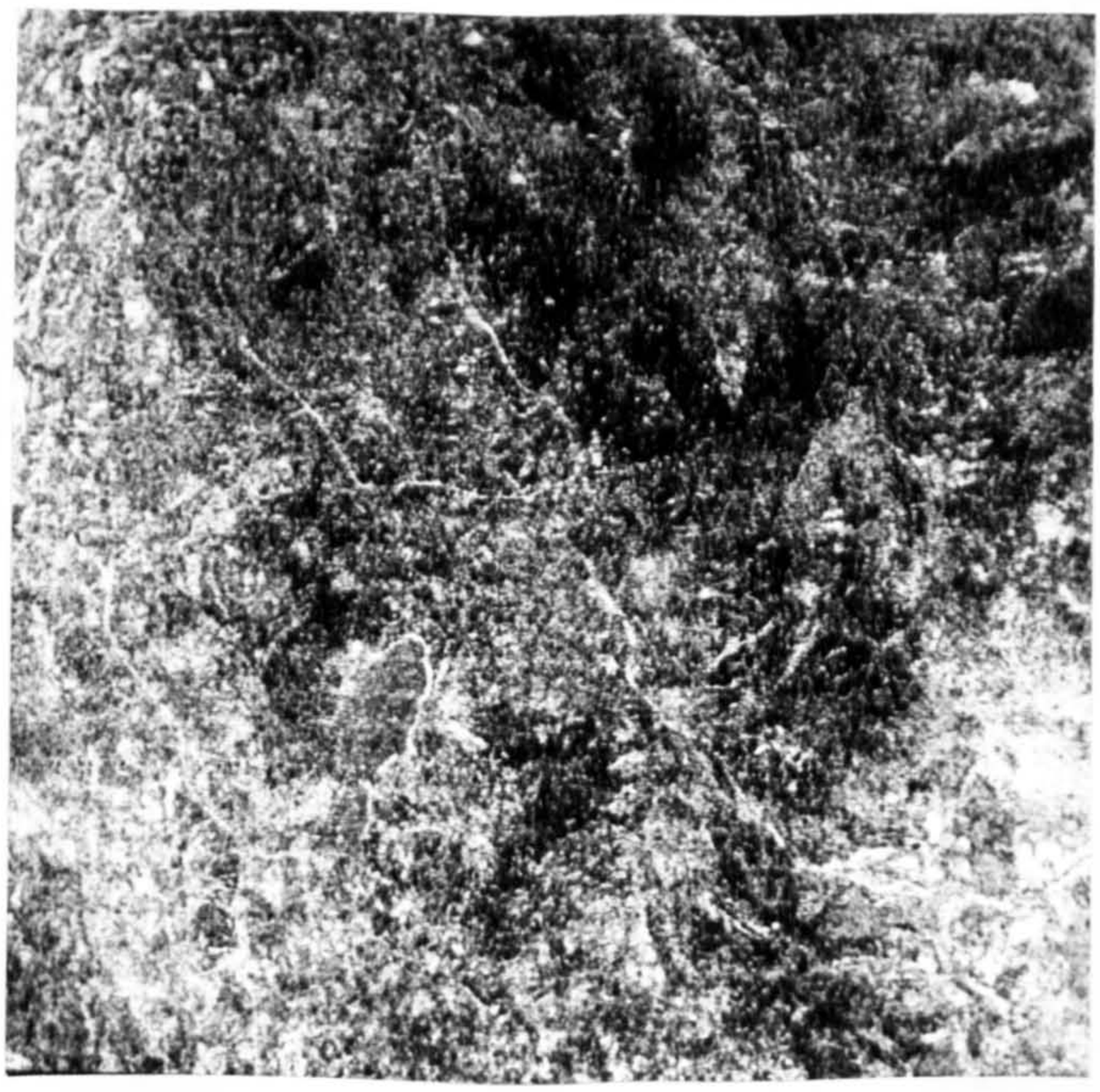

E PC 5 IMAGE (0.9%)

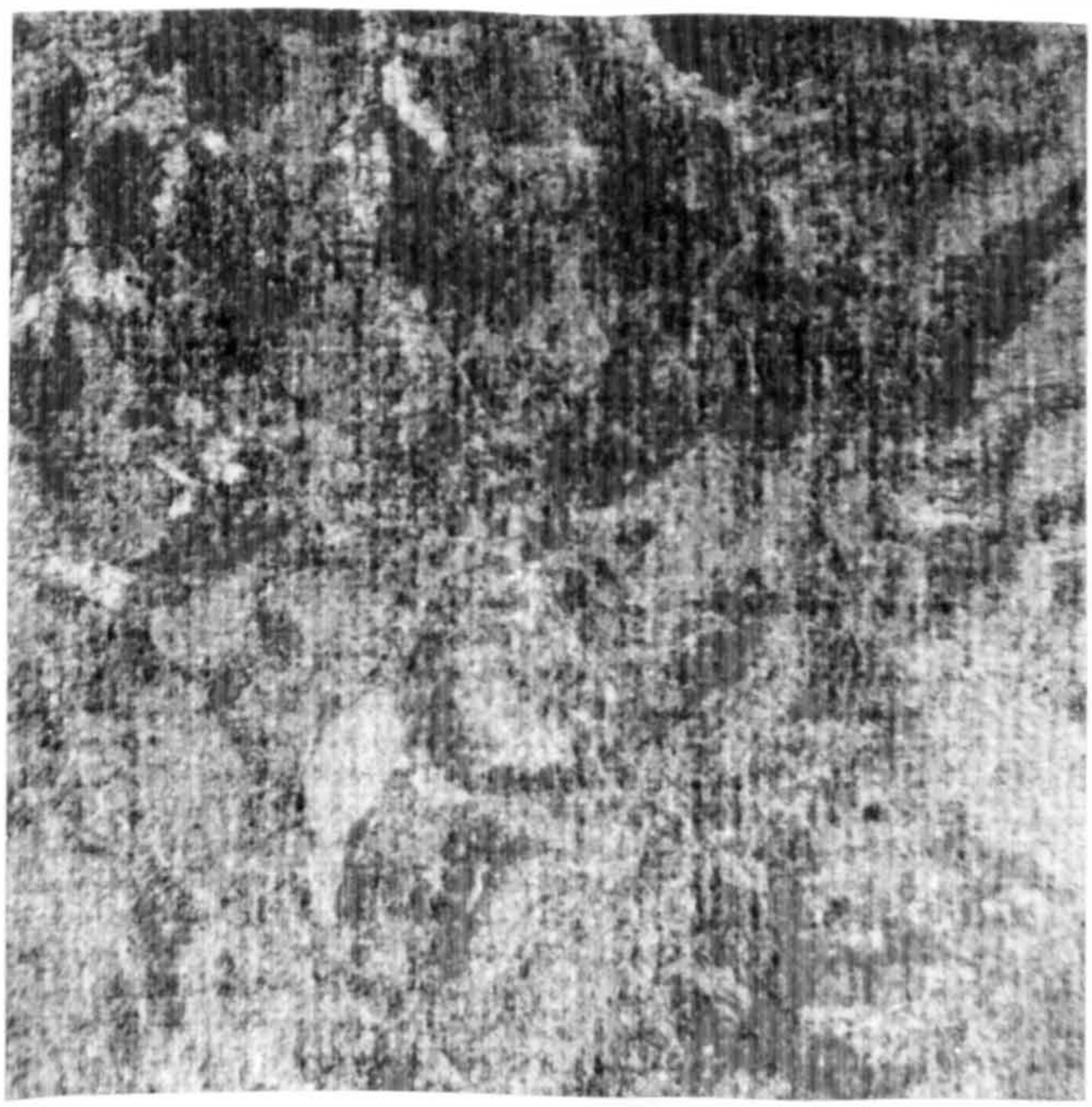

F PC 6 IMAGE (0.5%)

Figure 6.12 (continued)

cent of the total sub-scene variance (Figure 6.11A). Basically this component will enhance materials which show strong contrast between these two pairs of bands particularly between the TM bands 1 and 3, and bare fields or areas with thin grass or sparse vegetation (which appear as white) are well depicted in this component. PC5, accounting for less than 1 percent of the total sub-scene variance, contains a large positive loading of TM band 7 contrasted against a negative loading of TM band 3. The resultant image shows more tonal variation for the materials which have similar grey tone in both bands 7 and 3 (Figure 6.12E). PC6 contains a large positive loading of TM band 2 and negative loading of TM band 3 and accounts for about 0.5 percent of the total sub-scene variance. Because of the lack of variance in the lower-order PC images particularly in the PC6 and PC5, generally they do not show much contrast; display no additional information, and consist mainly of the unassigned sources of variation (noise). Notwithstanding, these lower-order components may show better distinction between certain cover types (Townshend, 1984). Therefore it seems important to check all the PC images by eye, rather than rely solely upon figures of merit for their information content.

For the MSS sub-scene of the Kedah-Perak area, the PC1 accounting for nearly 78 per cent of the total sub-scene variance (Figure 6.11B), has positive loadings for all bands, dominated by the MSS band 5, followed by bands 4 and 6, and small contributions from band 7 (Table 6.4 B). Higher contributions from these bands indicates (as was inferred from

A. LOWER TRIANGLE CORRELATION MATRIX FOR MSS BANDS IN THE KEDAH-PERAK SUBAREA 1

MSS band	4	5	6	7
micrometer	0.5-0.6	0.6-0.7	0.7-0.8	0.8-1.1
4	1.0000			
5	0.9266	1.0000		
6	0.6361	0.5495	1.0000	
7	0.4309	0.3377	0.9246	1.0000

B. EIGENVECTORS (PRINCIPAL COMPONENT LOADINGS) DERIVED FROM THE CORRELATION MATRIX, AND PERCENTAGE OF THE VARIABILITY IN THE PRINCIPAL COMPONENT IMAGES

PC	% Variance	Spectral Band			
		4	5	6	7
1	77.901	0.4508	0.7558	0.4304	0.2007
2	19.817	-0.1378	-0.4575	0.7010	0.5295
3	1.660	0.8690	-0.4680	-0.0139	-0.1598
4	0.623	0.1501	0.0195	-0.5686	0.8086

Table 6.4 A: correlation matrix, and B: eigenvectors and percentage of the variability of the original data set in the principal component images of the Kedah-Perak MSS 1024 x 1024 subscene.

the correlation matrix) that there is considerable overlap in the information carried by the different bands. The image produced by the first PC (Figure 6.13A) summarizes the brightness information that is common to these three bands or it can be thought of as a weighted average of these MSS bands. The second PC (Figure 6.13B) contains negative loadings of MSS band 5 contrasted against a nearly equal positive loading of MSS band 7 and more positive loading of MSS band 6. A negative loadings of band 4 for this component is insignificant because its loading is nearly zero. In this component therefore materials showing strong contrast between the red and near-infrared bands, for example agricultural areas which have less dense vegetation cover, will be emphasised. The PC2 accounts for nearly 20 per cent of the variability in the original four-band data set (Figure 6.11B). PC3 contains a large positive loading of band 4 contrasted against smaller negative loading of band 5. The contribution of near-infrared bands 6 and 7 is insignificant. The third component is interpreted as defining materials that have a strong contrast between bands 4 and 5 as compared to materials that exhibit little contrast between these two bands. The resultant image shows that only water bodies (shown as light tone because of its higher contrast in these two bands) and bare fields (appear as black because of its low/nil contrast between these two bands) are emphasised or well depicted. Other areas which have slight contrast between these two bands appear in grey shades. The PC3 contains less than 2 per cent of the total sub-scene variance (Table 6.4 B). PC4 accounts for less than 1 per cent

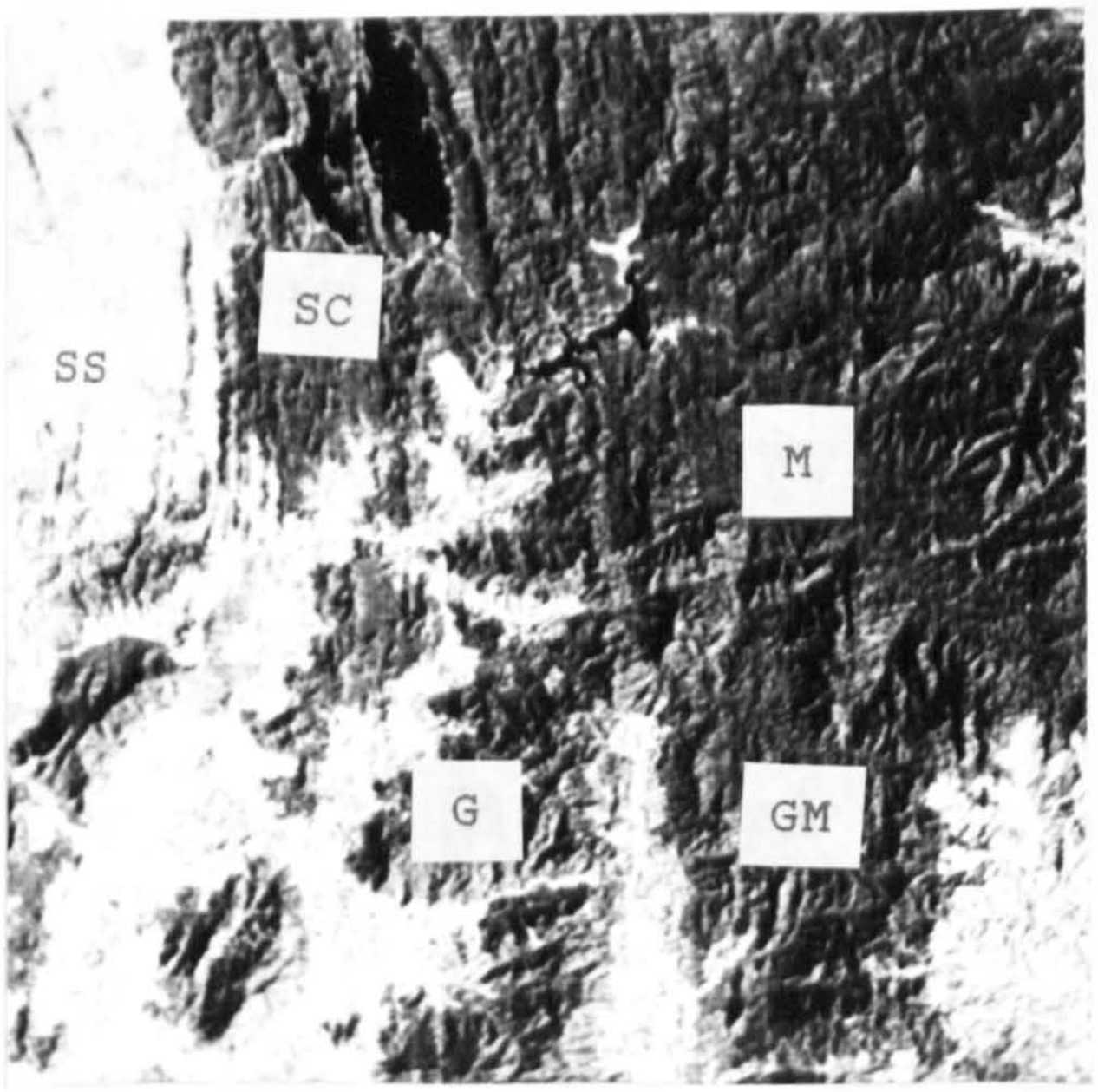

A PC 1 IMAGE (77.9%)

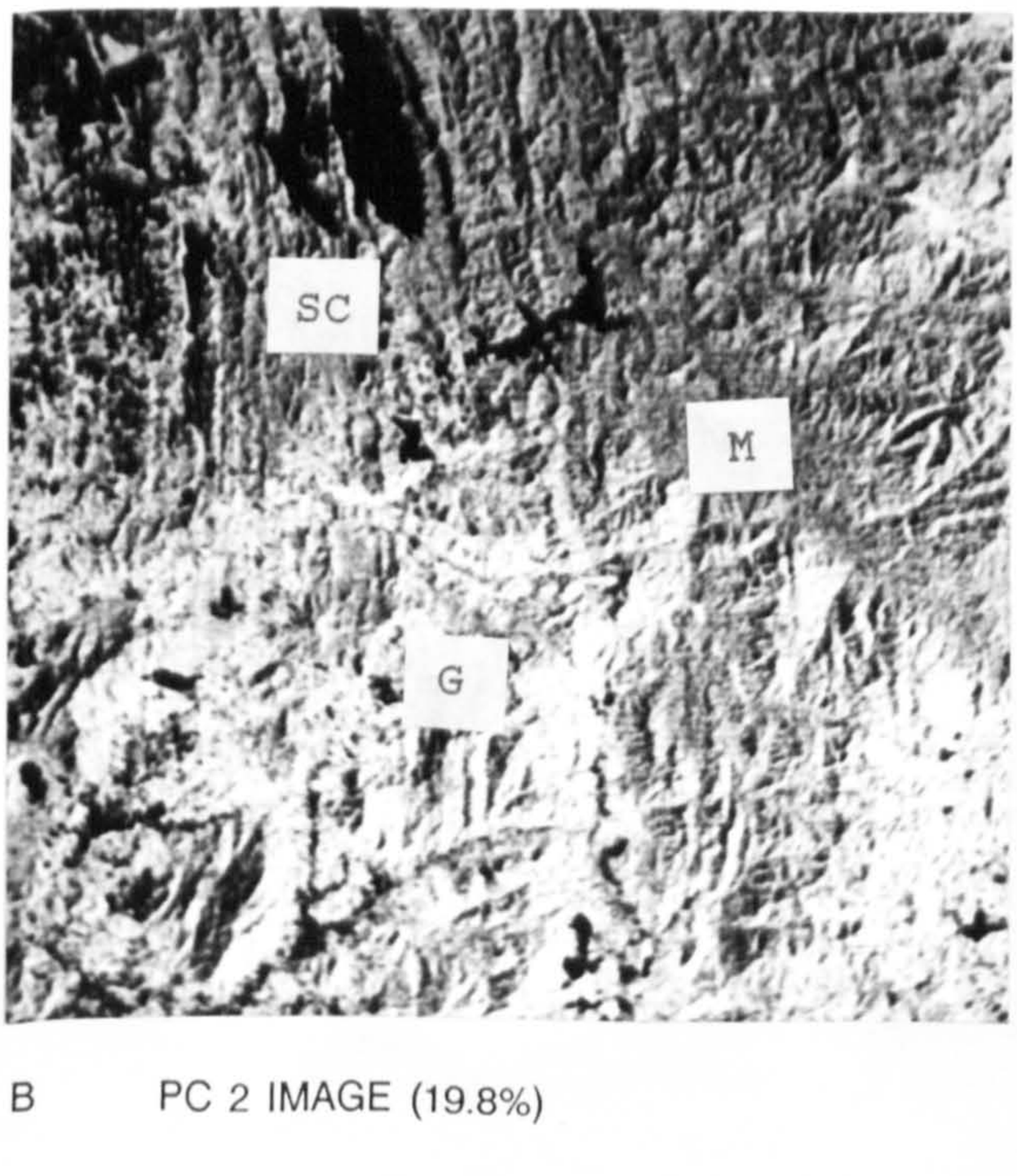

B PC 2 IMAGE (19.8%)

Figure 6.13 PC images 1-4 (A-D) of the Kedah-Perak sub-area 1. The PC images are generated from the four visible and reflected IR bands of the Landsat MSS image. Percentage of variance represented by each of the four PC images is shown. Scale 1:300,000.

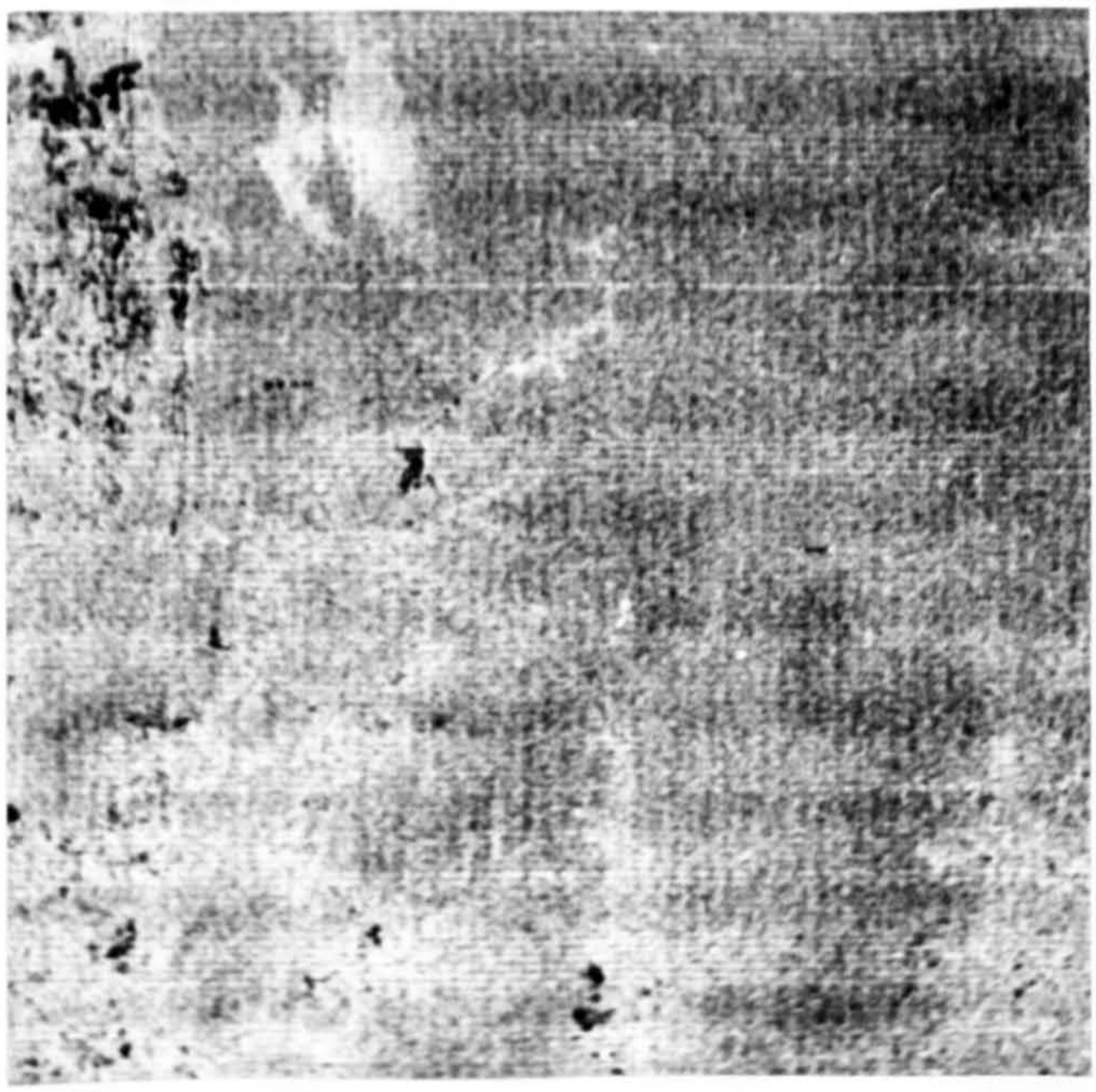

C PC 3 IMAGE (1.7%)

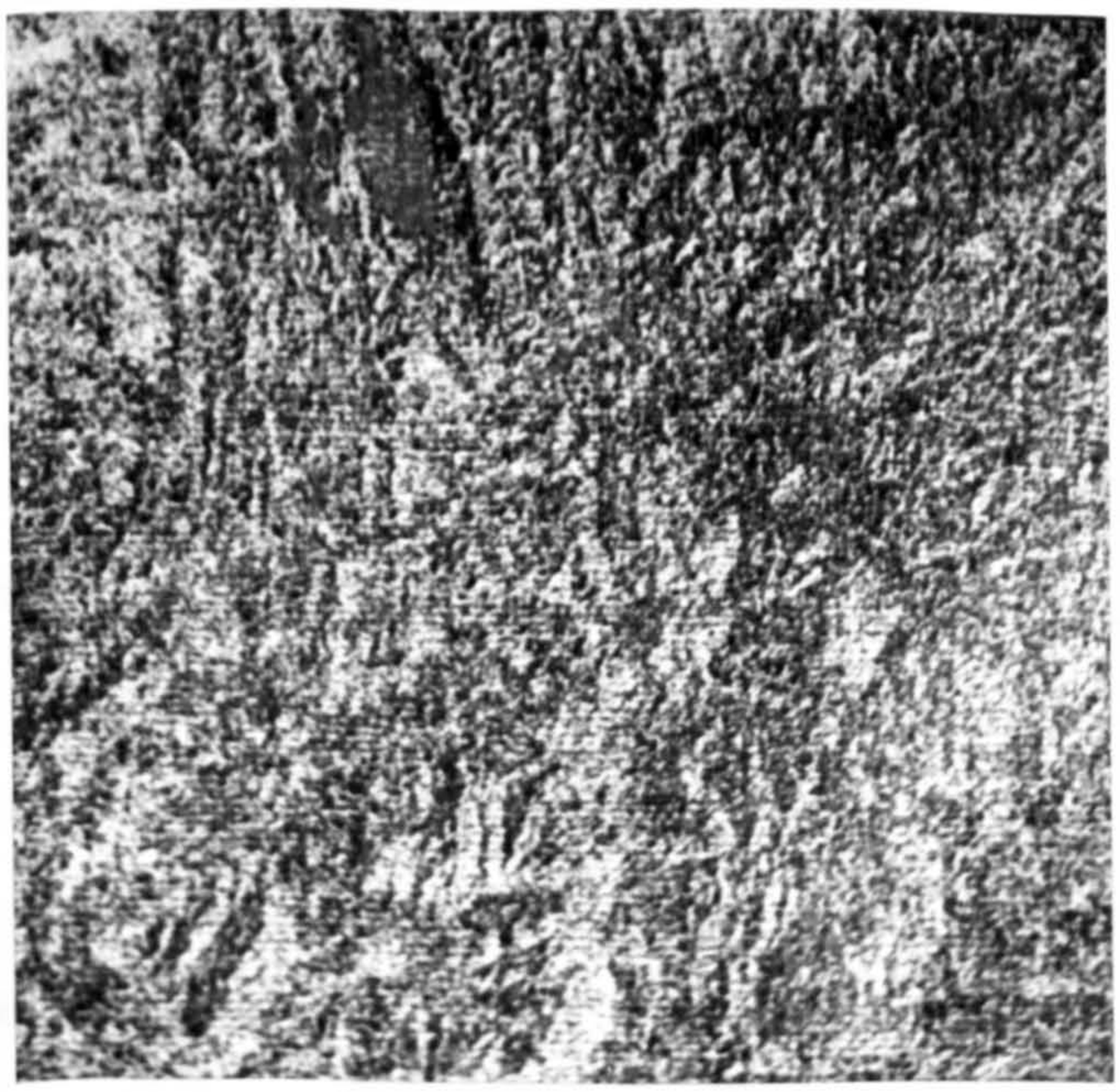

D PC 4 IMAGE (0.6%)

Figure 6.13 (continued)

of the total sub-scene variance, and contains a larger positive loading of MSS band 7 contrasted against slightly smaller negative loading of band 6 (Table 6.4 B). Contribution from the two other bands is insignificant. Although it contains very little information, it may highlight vegetation with perhaps some contribution from limonite (iron mineral variation) (Williams, Jr, 1983). The resultant image (Figure 6.13D), however, because of the lack of variance, does not show much contrast and clearly contains many of the unassigned sources of variation (noise).

Individual principal components

Figures 6.12A and B show the PC1 and PC2 of the TM sub-scene of the Lochindorb area. Generally the PC1 shows average brightness component of band 4 and band 5 where four categories of grey tone can be seen: very dark grey (black), dark-grey, grey and very light grey (white). Bright green grasses and other grassland areas which appear as very light tones on both the TM bands 4 and 5, also appear as light tones on the PC1 image and are very well defined. The grass area is mainly related to alluvial deposits and occasionally to improve land on the fluvio-glacial sand and gravel deposits. The forested (coniferous) area showing very dark grey tones, is also very well expressed. The dark grey tone (due to shadow effect) is related to higher terrain where the bedrock generally can be found. The rest of the terrain which has a grey tone is covered by various cover types. Glacial and peat deposits which are related to this grey tone category cannot

be differentiated on this image. The main drainage channels and surface-water bodies are well represented on the PC1. However, in some places it was difficult to differentiate between water bodies, some forested areas and shadows because all of them appear black. Despite its very high perlcentage variance (more than 83 percent), the identification of cover types is very limited where certain features, including the differences between the peat and glacial deposits, were masked by the more dominant brightness pattern in the PC1. The PC2, although it contains much less percentage variance, shows the contrast between the TM band 4 and band 5 which may emphasise certain features. It is evident that areas which are covered by forest and grass (shown as black and white respectively in both TM bands 4 and 5) appear just as black (deemphasised) in the PC2 image, whereas other areas which show variation in grey tones in the TM bands 4 and 5 appear in different tonal variation (emphasised). On other hand, because of its lesser contrast on TM band 4 and band 5 the peat areas show better separation in light grey shades on the PC2. Areas which are related to the glacial deposits appear as grey (because of its higher contrast than the peat in the TM bands 4 and 5). Generally the identification of these two main themes is good, however the glacial deposits can be confused with the bedrock because both of them show similar grey tones. Other PC images, because of their lower percentage of variance content, generally show a lack of tonal variation, and provide little additional information to the first two components. However, a few of them, for example the PC5 (Figure 6.12E), although it

shows low contrast, its tonal pattern (the darker patches) shows a close relationship with the peat deposits in the area, and the darker patches in the PC4 (Figure 6.12D) are closely related to the higher ground areas where the bedrock usually occurs.

The PC1 and PC2 for the MSS sub-scene of the Kedah-Perak area are displayed in Figures 6.13A and B. The PC1 is related to the brightness that is common to the MSS bands 4, 5 and 6, however it looks similar to the MSS band 5 which contributes most. The contribution from the MSS band 4 has resulted in the tonal differences between the sandstone/conglomerate (SC) and granite/metamorphic (GM) areas being much less pronounced than on the MSS band 5. On the other hand, the contribution by the MSS band 6 into this component has made topographic relief better expressed and has therefore enhanced the boundary between the granite (G) and the metamorphic rock area (M). Lowland and agricultural areas which have much less or no vegetation cover are shown as white to light grey tones and are mainly related to siltstone and shale (SS). PC2 has emphasised the materials which have strong contrast between the red and near-infrared bands. The resultant image shows that the area which is mainly related to the granite is better emphasised than any other areas. This may be related to its vegetation cover which has strong contrast between the red and near-infrared bands, hence it offers a means of separation from other rock units. In addition to that, a higher contribution particularly from the MSS band 6 makes its overall tone much lighter (except for water bodies and other

wet or damp areas which appear black), and relief impression, image texture as well as lineament patterns are all well displayed. This makes the boundary between the granite (G - coarse texture) and the metamorphic rocks (M - smooth texture) more pronounced. By observing the linear feature patterns, it may be possible to delineate the boundary between the granite (G - coarse texture and multidirectional linear features) and the sandstone/conglomerate (SC - medium texture and parallel linear features) on this component. For the PC3 and PC4, it was found that both of them do not show much contrast and display no additional information, and between them the PC4 (which shows the contrast between the MSS band 6 and band 7), although it has the lowest variance content however depicts linear features better than the PC3.

Comparative geological assessment for some of the PC images for both areas is given in Table 6.7 and 6.8 (section 6.3).

Principal component combinations

Colour composites of principal component combinations give a different perspective of the participating components. With the colour factor now involved there can be many combinations processed to enhance the different features. Six PC images from TM data (excluding the thermal band), for example, can be combined in groups of three, and will produce 20 possible image combinations. In order to make the process of investigating these combinations more objective and inexpensive, it was decided not to try and examine all those

possible in this study. On the contrary, the principal component combinations for the TM sub-scene of the Lochindorb area were tried and displayed, based on the total percentage of variance in each combination and also based on the ability of the PC images to discriminate the surface materials of the area.

Based on the total variance in each combination, the PC1-PC2-PC3, PC1-PC2-PC4, and PC1-PC3-PC4 combinations are among the highest where each combination contains approximately 97, 95, and 87 per cent of the total sub-scene variance respectively (Figure 6.11A). Based on this criterion, it was hoped that these top three combinations would produce better images (because of their high variance content) for visual interpretation. The single image in each combination was assigned to different primary colours with the aim of getting a better colour composite combination for interpretation. After examining all the possible colour combinations, it was found that the combination of the PC4-PC1-PC2 and PC3-PC2-PC1, displayed in blue, green and red respectively produced good colour composites. For the PC1-PC3-PC4, several colour combinations have been tried but they did not give better colour composites. The best colour combination in this group is the combination of the PC4-PC3-PC1, displayed in blue, green and red respectively.

Figure 6.14A shows the TM combination of the PC2-PC1-PC4 in red, green and blue respectively for the Lochindorb area. This PC image in combination contains over 95 per cent of the variability in the original six-band data set. In terms of

information content of the PC combinations in a single image, this is the second highest. The relief impression as well as drainage are fairly well pronounced. In the image, bare fields are shown as pale yellow, the forested area appears very dark bluish red and water bodies appear brownish red. Green grass which has a very light tone in PC1 appears bright green in this colour composite and it was very well defined. That it is closely related to alluvial deposit is evident from its distribution which is confined to the main river valleys. Generally thick peat which appear reddish orange can be identified on the basis of its colour association. However, its boundary with the glacial deposits which occupy most of the rest of the area and appear as mixtures of pale brownish blue, reddish brown, yellow and pale green is not clearly defined. Bedrock which is associated with higher ground is shown as dark reddish brown and may be confused with the glacial deposits. The second combination where PC3, PC2 and PC1 are displayed in blue, green and red respectively, is shown in Figure 6.14B. It contains the highest percentage of the total sub-scene variance, with over 97 per cent. Generally, although it gives different colours, it contains similar information to the previous combination, and does not contain any additional information, except that this colour combination offers better separation between shadow areas (appear pale bluish green) and water bodies (appear very dark greenish blue). This information, however has been seen in many other colour composites before. The distinction between peat deposits (appear pale green to pale yellowish green) and

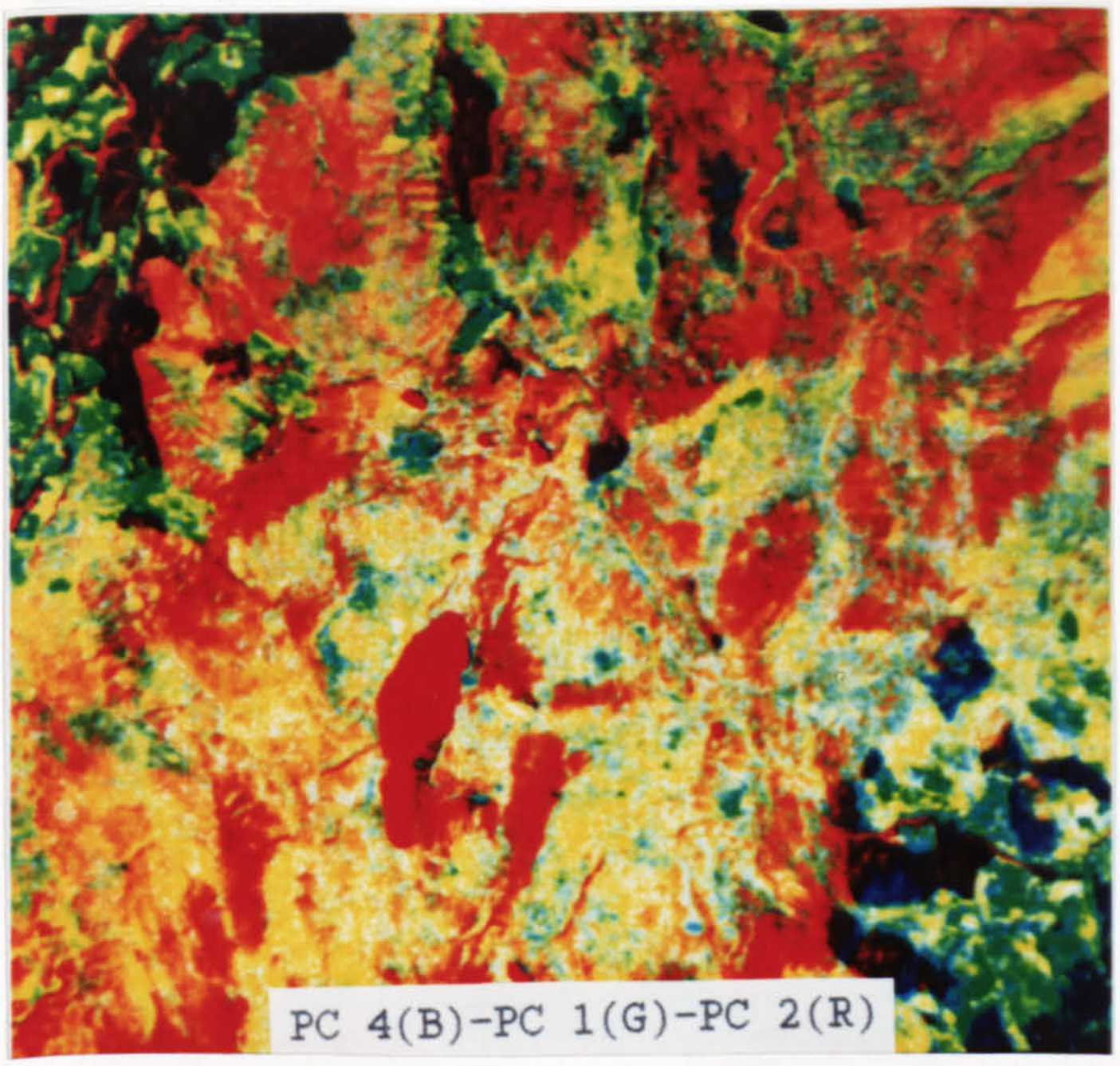

A PC 4(B)-PC 1(G)-PC 2(R)

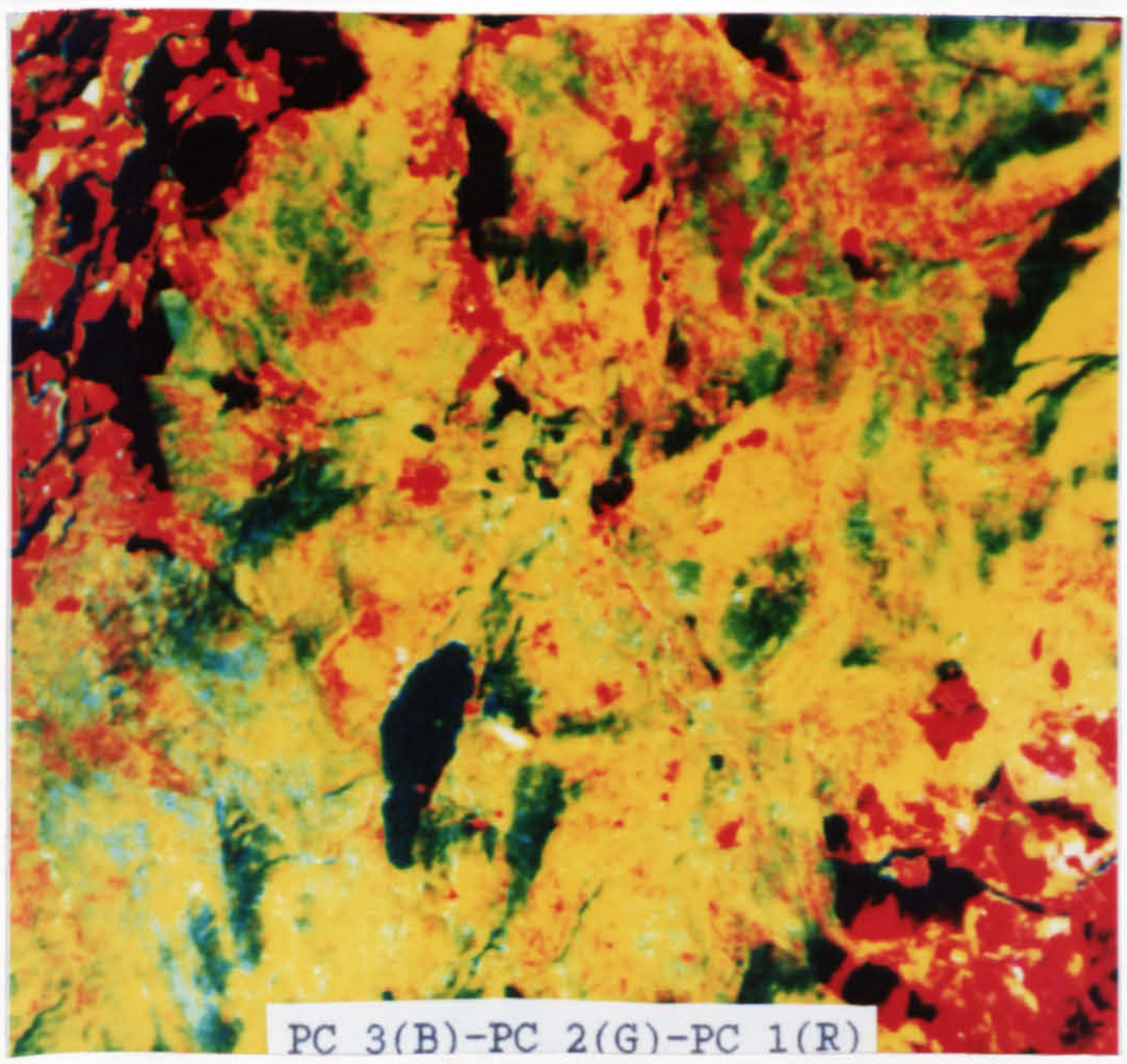

B PC 3(B)-PC 2(G)-PC 1(R)

Figure 6.14 TM principal component colour composites of the Lochindorb area (A-D). The combinations are chosen based on variance content (A and B) and the ability of the PC image to discriminate the surface material deposits in the area (C and D). Scale 1:160,000.

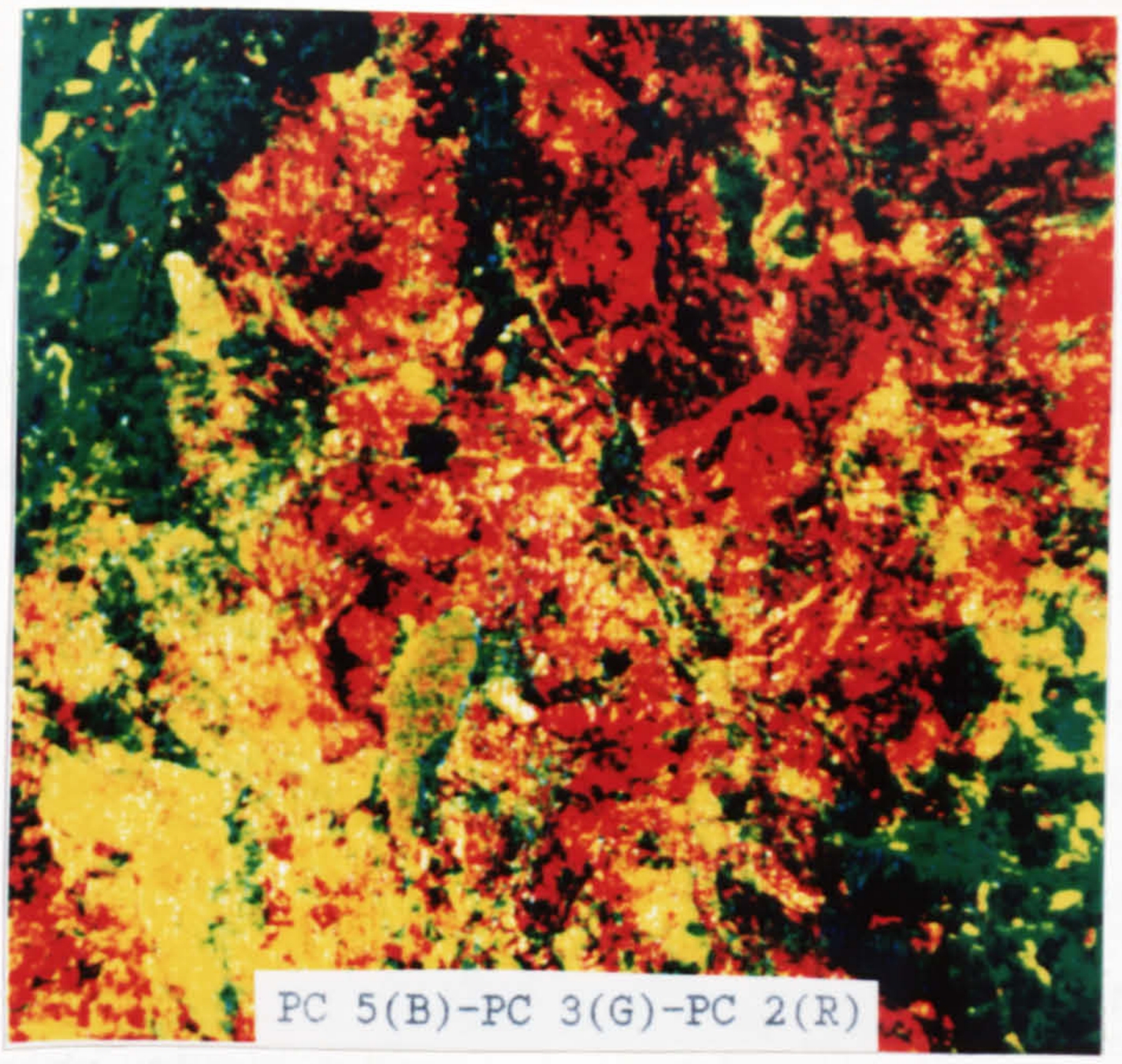

C PC 5(B)-PC 3(G)-PC 2(R)

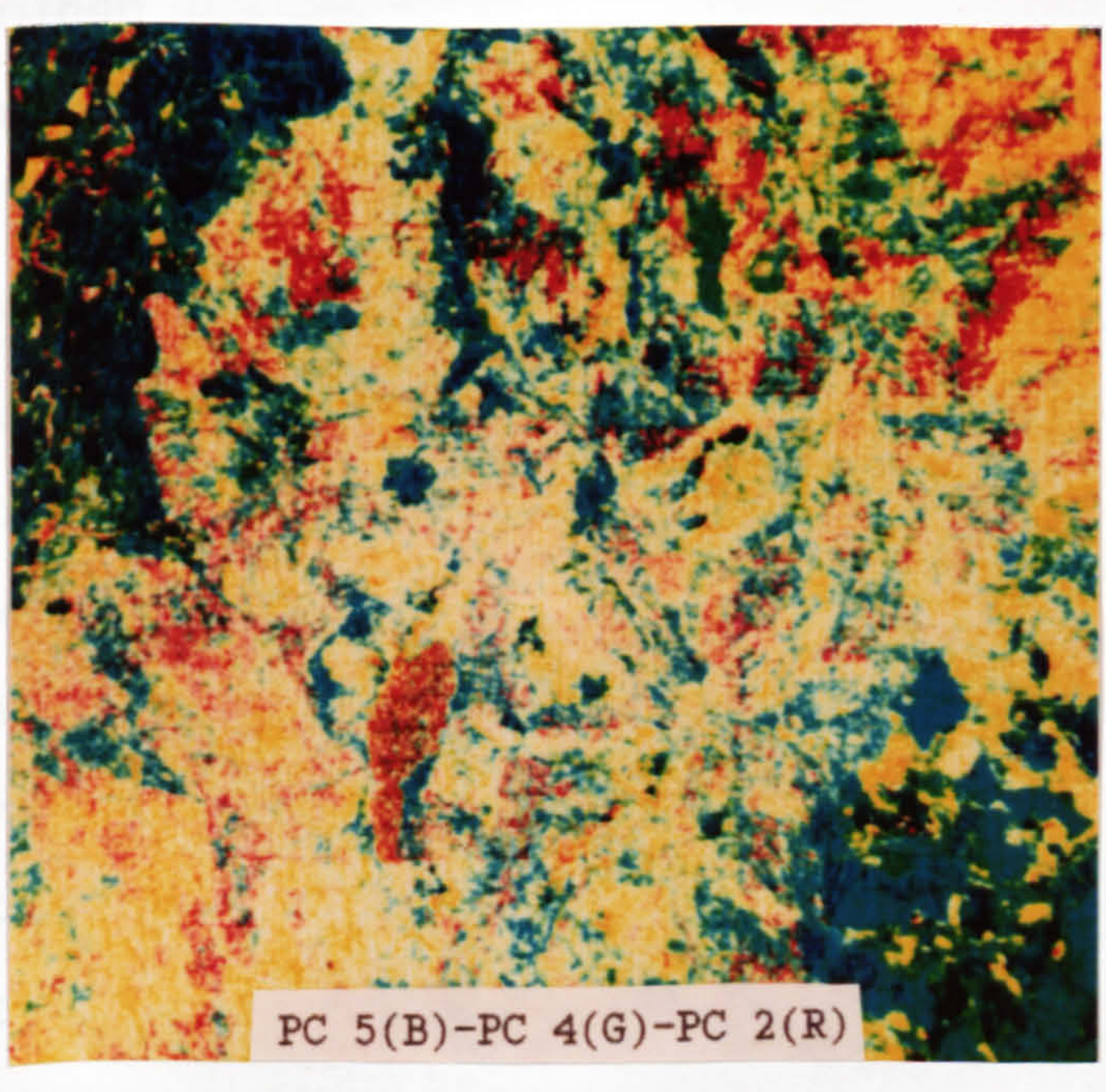

D PC 5(B)-PC 4(G)-PC 2(R)

Figure 6.14 (continued)

glacial deposits (appear reddish orange, darker reddish orange and darker orange red) is less clear in the PC3-PC2-PC1 combination than in the PC4-PC1-PC2. Probably the contribution from the PC4 which displays the contrast particularly between TM band 1 and TM band 3 makes better separation between the two deposits. Other PC combinations for the Lochindorb area were tried, for example the combination of the PC4, PC3 and PC1. The combination, although it has high variance content, does not contain any new information to the previous two.

Beside the variance content, the PC combinations were also tried based on their ability to discriminate the surface material deposits in the area. For this, every single PC image was examined and compared visually in order to find out among them the one which offers the best discrimination between the two main deposits: peat and glacial. As mentioned earlier, among the lower-order PC images, the PC5 and PC4 do show tonal variations which are closely related to the peat and higher ground area, respectively. Beside that, the PC3 also shows good tonal variation in relation to the two main deposits. These three PC images together with the PC2 which shows the best tonal variations among them, therefore were chosen and combined (three images at one time) to produce a few colour composites. It was found that the PC5-PC3-PC2 and PC5-PC4-PC2 combinations which were displayed in blue, green and red respectively produce good colour composites. The result of the PC5-PC3-PC2 colour composite combination is shown in Figure 6.14C. In this image, the forested and grass areas appear green to bluish green and are very well defined. Bare fields

or areas with thin grasses are shown as pale yellow to yellow. The peat deposits in saturated areas are represented by pale orange to reddish orange and may be distinguished from the glacial deposits which appear mainly as dark reddish purple. Figure 6.14D shows the PC5-PC4-PC2 colour composite combination. The image does not offer any better separation between the main deposits in the area. Despite that, the higher ground areas where generally the bedrock may be found are better depicted in the image. Notwithstanding, the areas do not entirely correspond to the bedrock because of the shadow effect and cover type, (as an example, some areas of the glacial deposit which cover by dense heather also show similar colour, that is pale brown).

PC3-PC2-PC1 combination of MSS data of the Lochindorb is shown in Figure 6.15. Although the image does show good colour variation, as in other MSS images for the area, the image is difficult to interpret or extract any information at enlarged scale of 1: 160,000.

Only four combinations of three PC images are possible for the MSS data set of Kedah-Perak area, these are the PC1-PC2-PC3, PC1-PC2-PC4, PC1-PC3-PC4 and PC2-PC3-PC4, and because of this, all of them were tried with different colour combinations. It was found that the combination of the PC3, PC2 and PC1 which are assigned to blue, green and red respectively gives the best colour composite and is shown in Figure 6.16A. This combination has about 99 per cent, the highest of the total variability in the original data set. Topographic impression, drainage and lineament pattern are

better displayed. In this PC combination bare fields which appear bright red (due to their lighter tone in the PC1) are very well depicted. Water bodies which are displayed as dark blue are clearly shown and colour variations within water bodies are also well displayed. Almost all the remaining areas appear green due to the light tone of vegetated areas on the PC2, generally the darker colour is associated with the denser forest. Agricultural areas appear pale green. The combination appears to offer little improvement over the false colour composite for the discrimination of rock type. For example, the metamorphic rocks which appear as dark green colour and smooth texture are more enhanced, and therefore their boundary with the granite and the sandstone/conglomerate which appears green to pale green and with a coarse texture is better expressed. Apart from that, strike ridges on the sandstone/conglomerate terrain are better displayed, hence they may be used to differentiate this unit from the other two: the granite and metamorphic rocks. The combination of the PC4-PC1-PC2 displayed as blue, green and red respectively produces an almost similar result, although with different colours than the first combination. However, the metamorphic rock which appears as a deeper pink in this combination is seen to be distinguished from the surrounding areas which appear a brighter pink (Figure 6.16B). This combination contains 98 per cent of the variability in the original data set. Third combination where the PC4-PC3-PC2 are assigned to blue, green and red respectively also produced a good colour

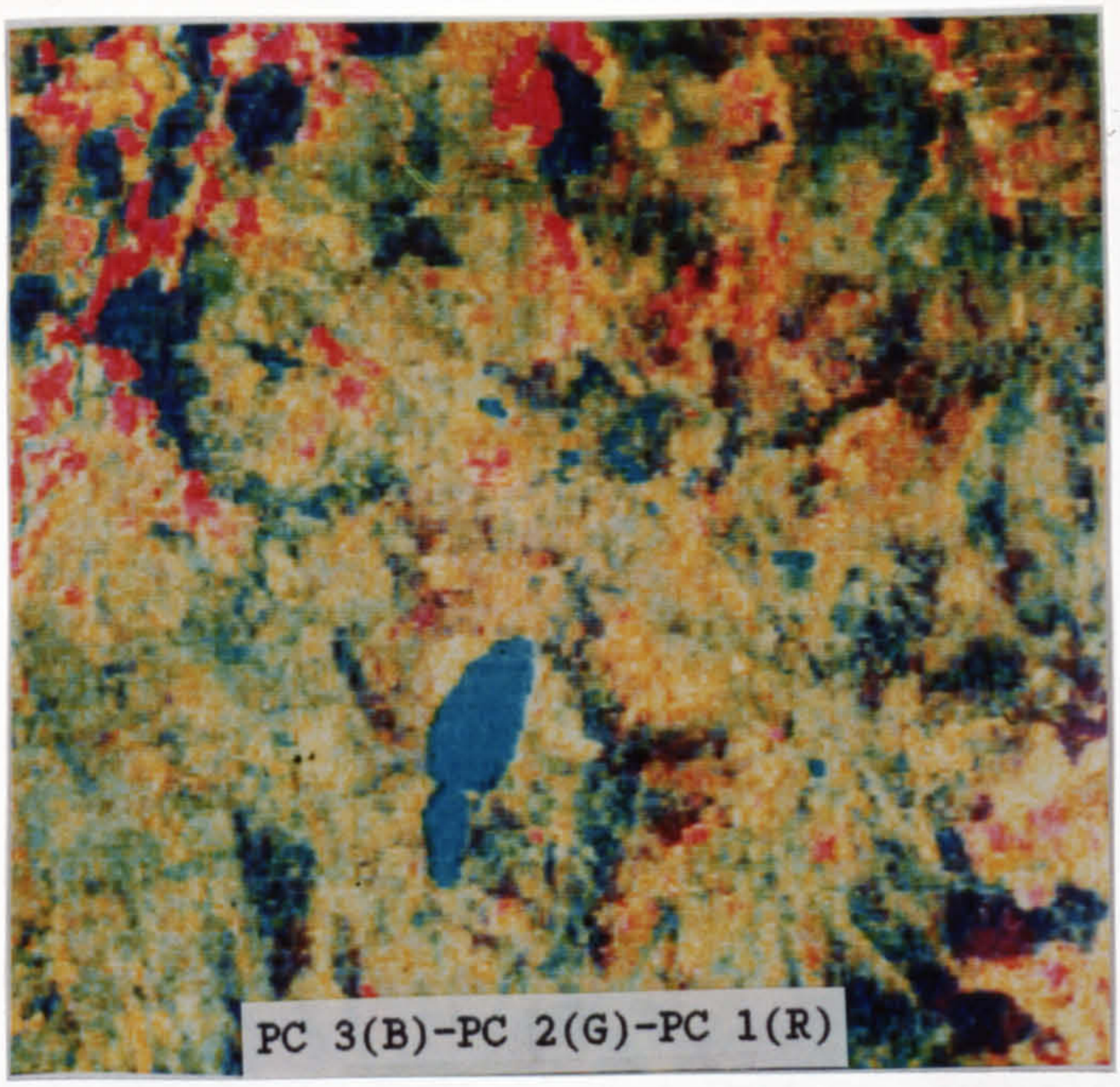

PC 3(B)-PC 2(G)-PC 1(R)

Figure 6.15 MSS principal colour composite of the Lochindorb area. Scale 1:160,000.

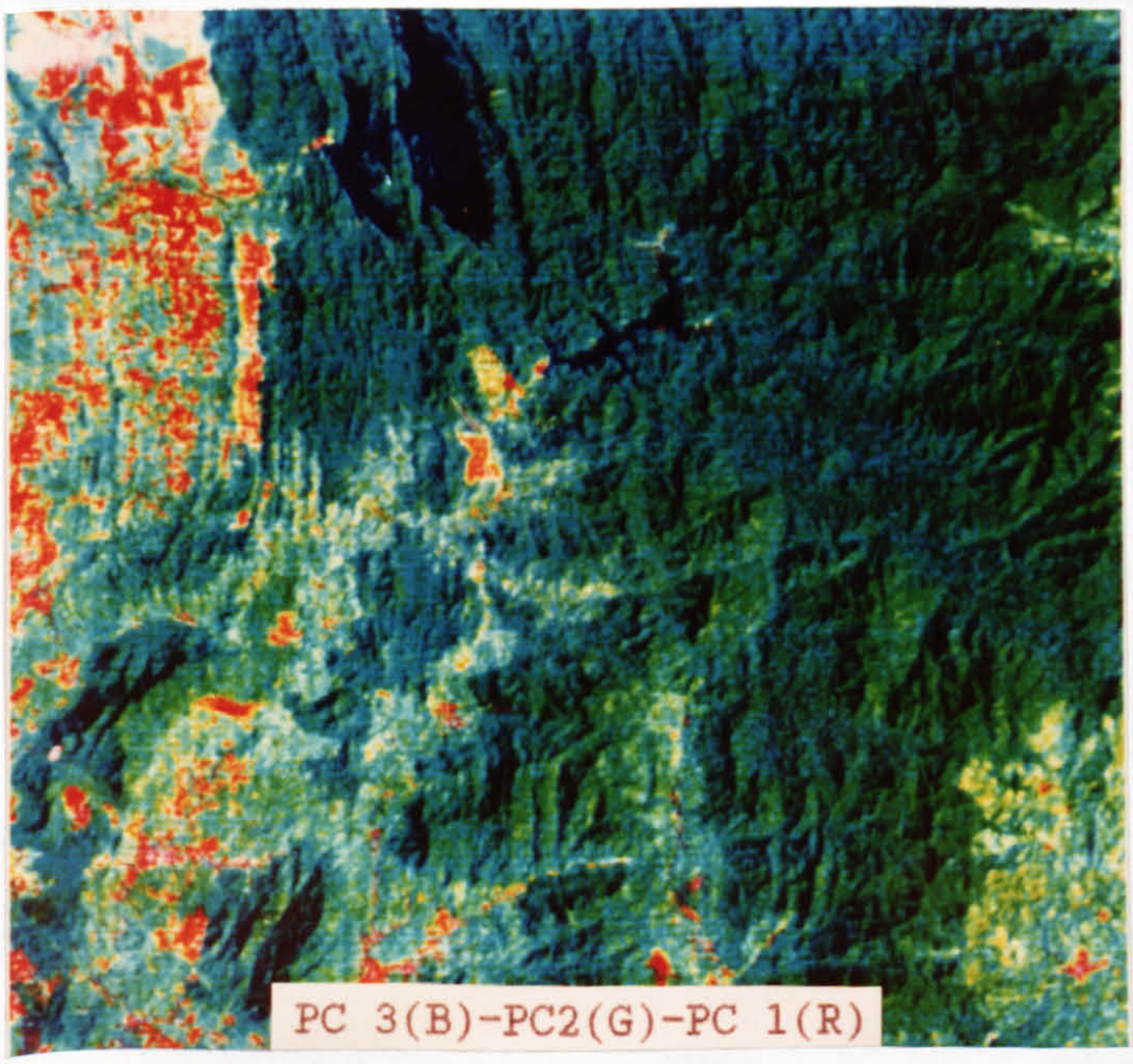

A PC 3(B)-PC 2(G)-PC 1(R)

Figure 6.16 MSS principal colour composites (A-C) of the Kedah-Perak sub-area 1. Scale 1:160,000.

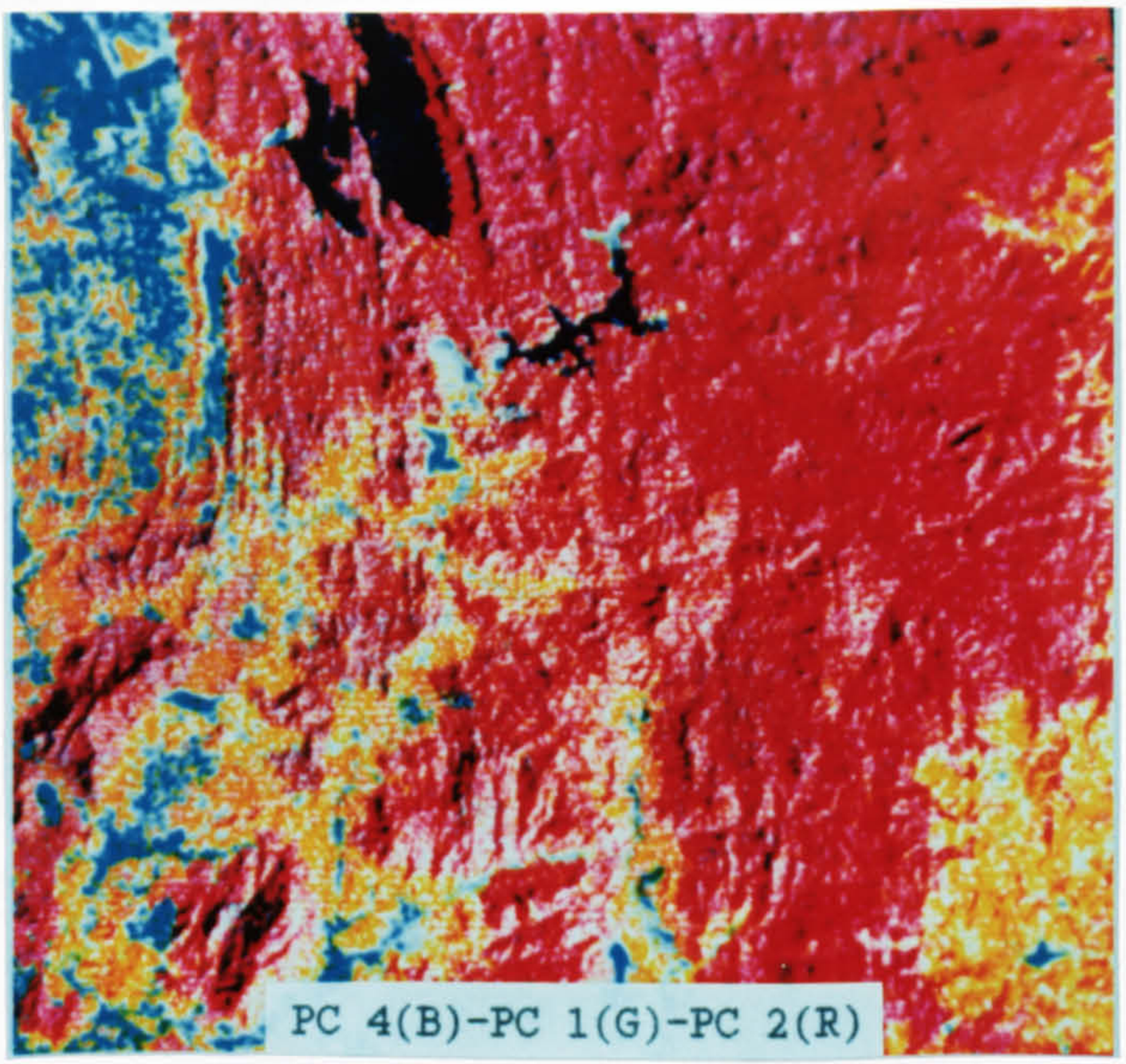

B PC 4(B)-PC 1(G)-PC 2(R)

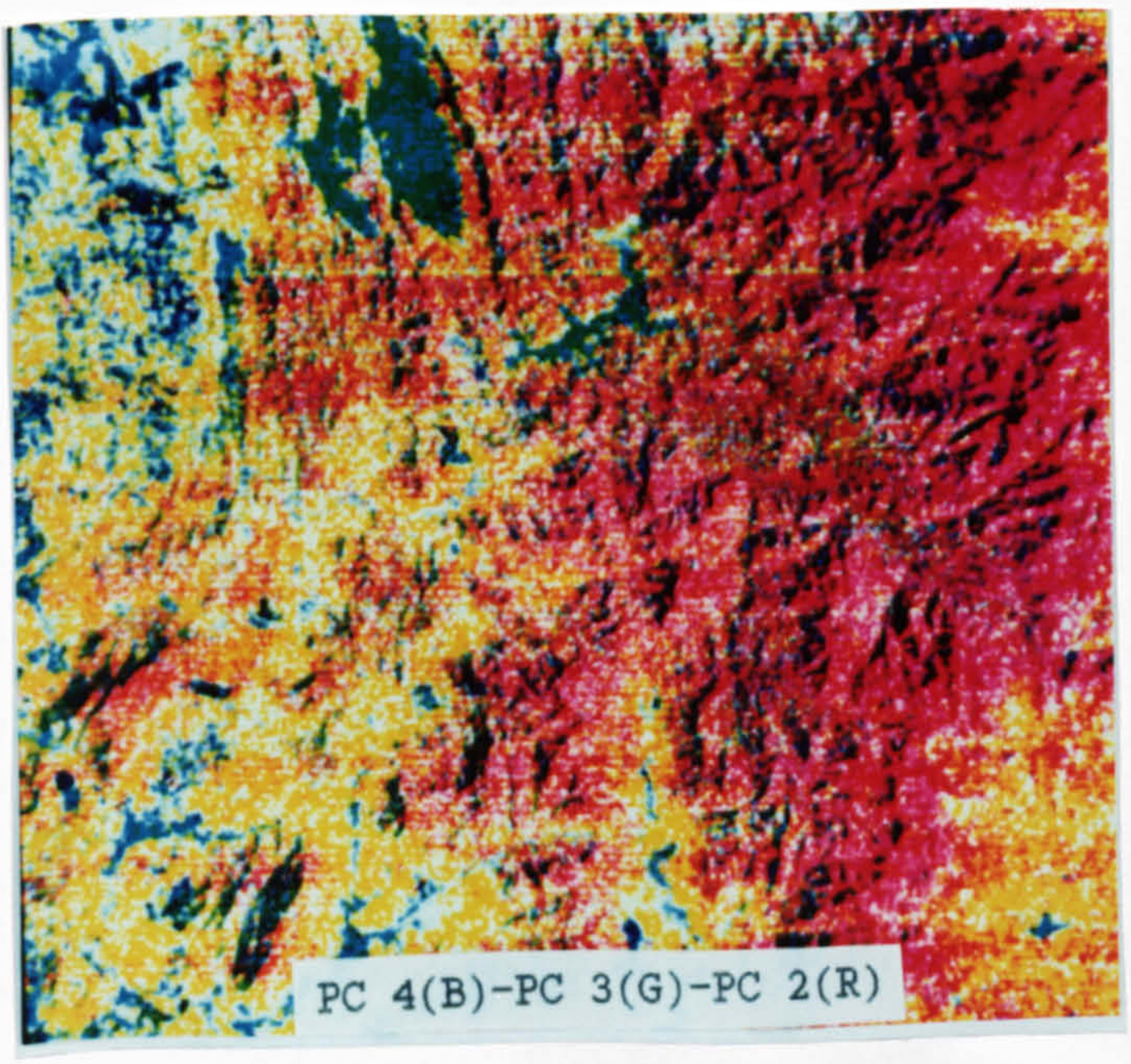

C PC 4(B)-PC 3(G)-PC 2(R)

Figure 6.16 (continued)

composite (Figure 6.16C). Although its information content (its total variance) is much lower than the previous combinations (i.e. only 22 per cent), it displays better colour variations which are related to the main lithologies. For example, the granite appears as reddish purple, the sandstone/conglomerate as orange purple, and the metamorphic rocks correspond to the dark orange purple colour. Notwithstanding, because of its total variance is very low so the definition between these colour variations is poorly displayed. Bare fields appear blue, agricultural areas as orange, while water bodies appear green in the image. Relief impression, main drainage, and lineaments are much less pronounced here than in the previous combinations.

One other combination (PC1-PC3-PC4) of the MSS data set for Kedah-Perak area was also tried with different colour combinations but they do not offer any additional information or display new features or produce better colour composites.

For a comparative assessment of a few of the PC combinations refer to Table 6.7 and 6.8 in section 6.3.

6.2.5 Discriminant analysis

The discriminant analysis (DA) was carried out for the TM data set of Lochindorb and the MSS data set of Kedah-Perak area. The data were processed through several computer programs (Chapter 5, section 5.4.3) and the processed data were transferred to the DIAD for final display. The DA analysis of the TM sub-scene of Lochindorb and the MSS sub-scene of Kedah-

Perak areas using 40 spectral classes produced the results shown in Table 6.5 and 6.6 respectively.

Table 6.5(B) shows that 62 per cent of the variability in the data lies in the direction defined by the discriminant function (DF) 1. The eigenvector matrix (Table 6.5 A) shows that the DF1 of the TM image set of Lochindorb is defined by a small positive coefficient or eigenvector of TM band 1 and a nearly equal negative coefficient of TM band 2. Contributions from other TM bands are nearly zero, and are insignificant. This pattern is difficult to interpret, although the coefficients seem to relate to TM bands in which reflectance is the norm for green vegetation (Mather, 1987), and it was also suggested that materials showing contrast between the two bands, in this case the TM bands 1 and 2, will be enhanced in the resultant image (Williams, Jr, 1983) (Figure 6.17A). The DF2 represents nearly 33 per cent of the discriminating power (Figure 6.17B). The eigenvectors or coefficients show that this function is dominated by TM band 3, the visible red band. As the coefficient for TM3 is positive it follows that darker tones on the image relate to areas of higher reflectance in the visible red (Mather, 1987), the grass areas in this case. The third DF (Figure 6.17 C), which represents slightly over 2 per cent of the discriminating power, has a high negative eigenvector for TM band 3 and a lower positive value on TM band 7. It shows that the lighter tones on the image relate to areas of low reflectance in the TM bands 3 and 7, and vice versa.

A. EIGENVECTOR (DISCRIMINANT FUNCTION LOADINGS) IN THE DISCRIMINANT ANALYSIS OF THE LOCHINDORB TM 512 X 512 SUBSCENE

DF	SPECTRAL BAND					
	1	2	3	4	5	7
1	0.18545	-0.20054	-0.06387	0.01196	-0.00779	0.04700
2	0.17819	-0.28373	0.65892	0.13132	-0.10227	0.15857
3	0.18242	-0.14650	-0.76227	0.03750	-0.04756	0.55839
4	0.19849	-0.25168	-0.35482	-0.08717	0.37459	-0.63554
5	-0.06438	0.06025	-0.19378	0.38665	-0.20871	-0.11575
6	0.30726	0.00566	-0.03476	-0.13462	-0.30806	-0.07955

B. EIGENVALUES AND DISCRIMINATING POWER IN THE DISCRIMINANT ANALYSIS OF THE LOCHINDORB TM 512 X 512 SUBSCENE

DF	EIGENVALUE	DISCRIMINATING POWER (%)	CUMMULATIVE OF DISCRIMINATING POWER (%)
1	10.52188	62.07	62.07
2	5.58970	32.98	95.05
3	0.39546	2.33	97.38
4	0.34090	2.01	99.39
5	0.08349	0.49	99.89
6	0.01916	0.11	100.00

Table 6.5 Eigenvectors (A), eigenvalues and discriminating power (B) in the discriminant analysis of the Lochindorb TM 512 x 512 subscene.

A DF IMAGE 1 (62.1%)

B DF IMAGE 2 (33.0%)

Figure 6.17 DF images 1-6 (A-F) of the Lochindorb area. The DF images are generated from six visible and IR bands of the Landsat TM image. Percentage of discriminant power represented by each DF image is shown. Scale 1:160,000.

C DF IMAGE 3 (2.3%)

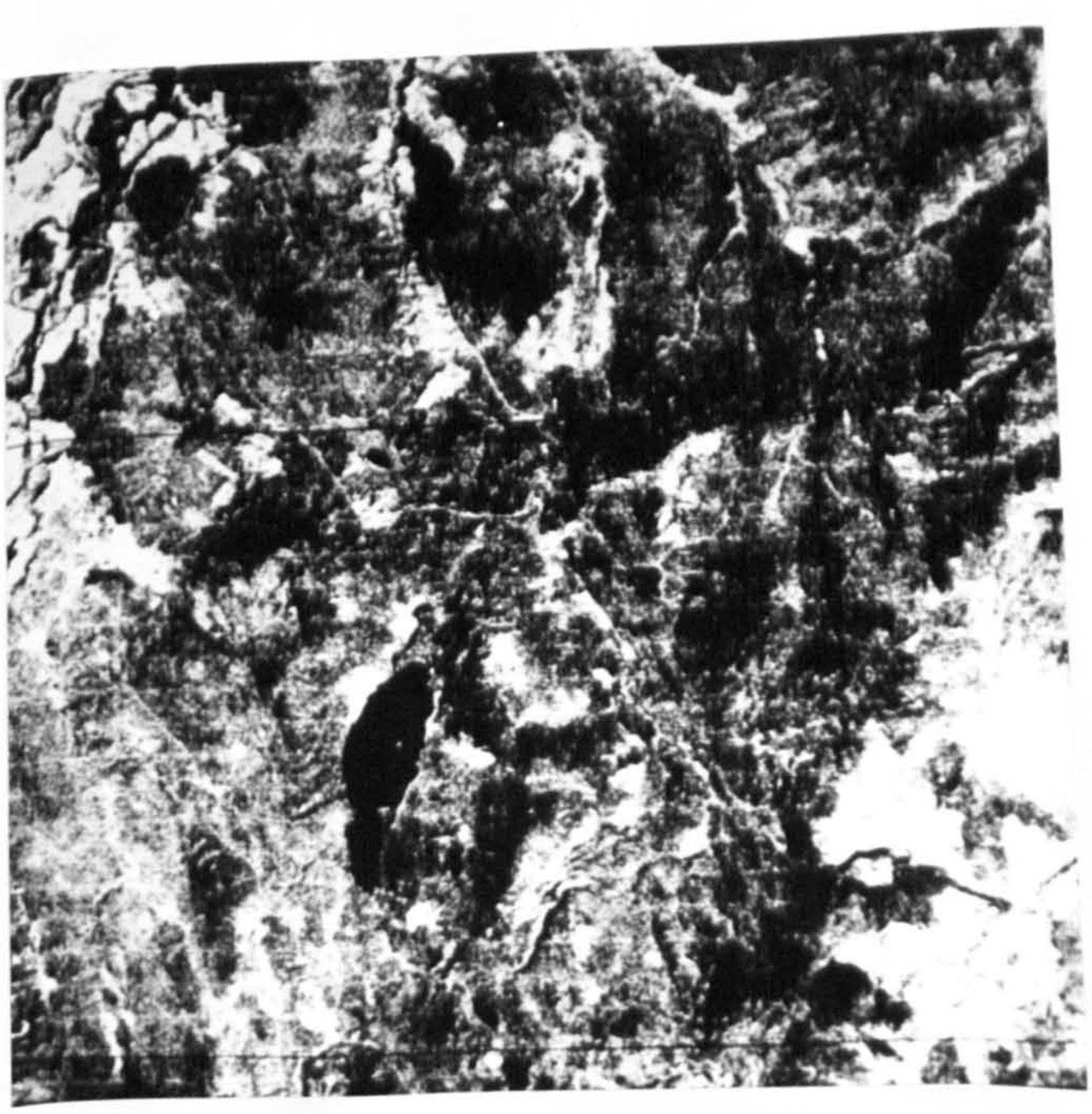

D DF IMAGE 4 (2.0%)

Figure 6.17 (continued)

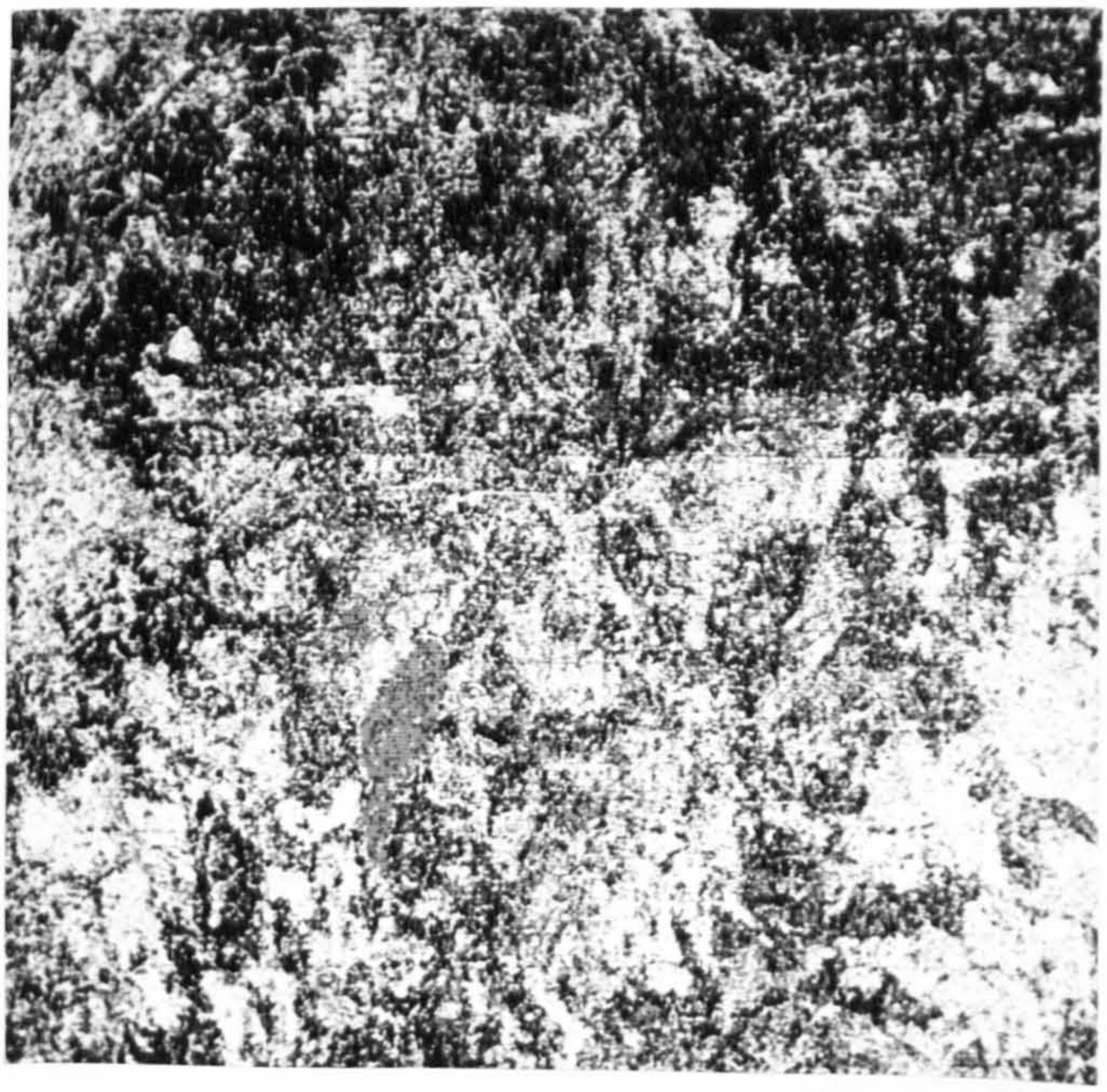

E DF IMAGE 5 (0.5%)

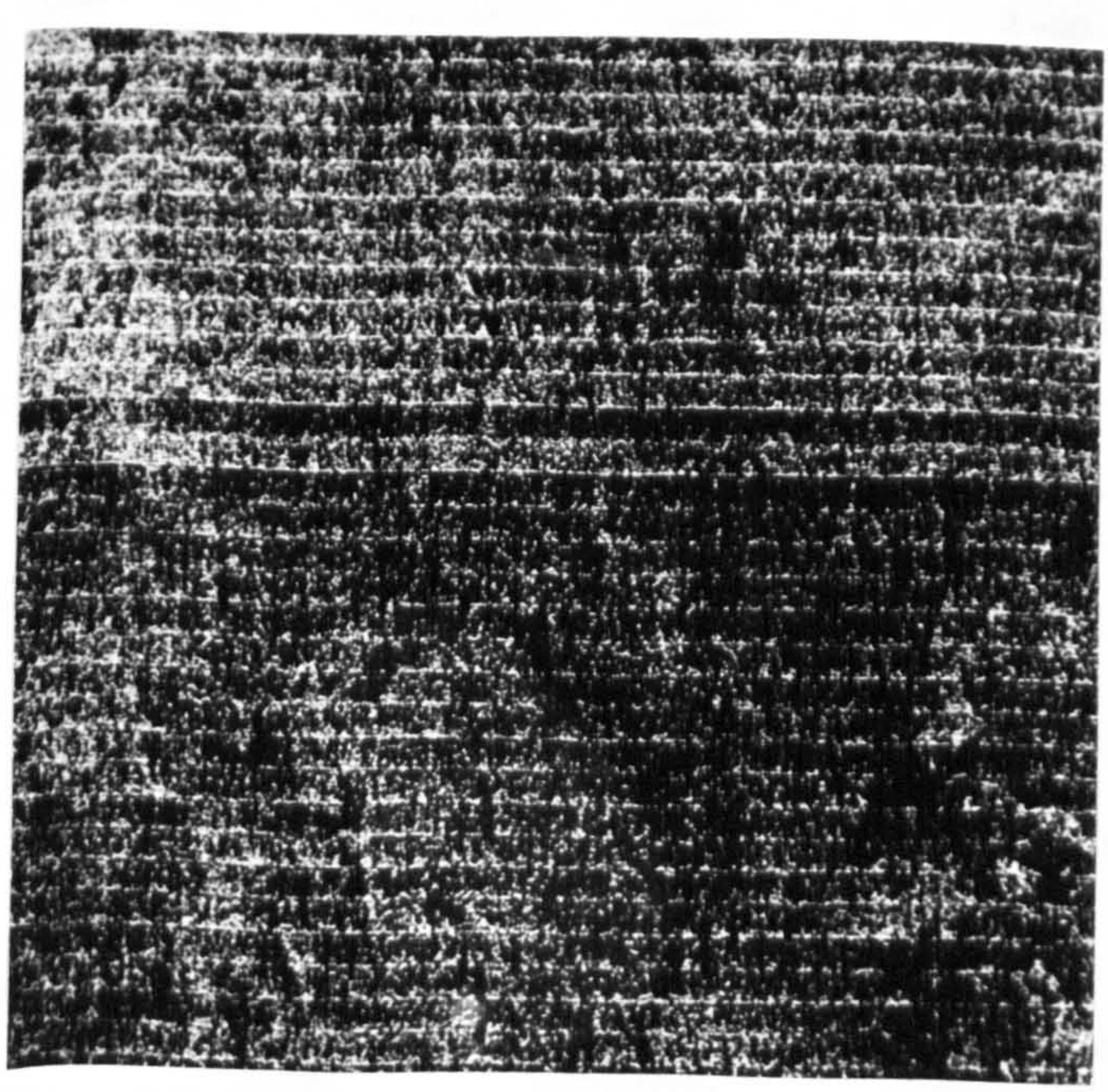

F DF IMAGE 6 (0.1%)

Figure 6.17 (continued)

Therefore, again the water bodies appear as lighter tones and the grass areas as darker tones. In the DF3 image, however, areas within the upland generally show more tonal variations, hence it offers better separation between different cover types, than was the case with DF 1 and 2. The eigenvalues in the Table 6.5(B) show that over 97 per cent of the discriminating power (the capability to distinguish statistically between the 40 spectral classes) is concentrated in the first three DFs. Combination of these first three DFs as a false colour composite would allow the simultaneous assessment of information content, and furthermore its differences and similarities are often more revealing here rather than separately assessed. The DFs 4-6 are noisy (Figure 6.17D, E, F); indeed, it would be very difficult to extract any meaningful conclusions particularly from the DF6 and 5. As mentioned earlier in the discussion of the principal components analysis that the lower-order components may contain useful information and they therefore should not be discarded on the basis either of low discriminating power (as measured by the relative size of the corresponding eigenvalue) or of inferences drawn from the vector of coefficients. All the DFs were examined visually, it is seen that the lower-order DFs contain significantly less information than the lower-order PCs, and they do not show clear tonal variations which may be related to certain cover types.

The eigenvectors show that the first DF image of the Kedah-Perak area is contributed by MSS bands 4 and 7 (positive sign) while MSS band 6 has a nearly-equal coefficient of the

opposite sign (Table 6.6 A). The DF1 (Figure 6.18A) represents nearly 64 per cent of the discriminating power (Table 6.6 B), where the separation between vegetated and non-vegetated areas is very well shown. DF2 which contains nearly 33 per cent of the discriminating power (Table 6.6 B), and is dominated by MSS band 7 (Figure 6.18B). As the coefficient for MSS band 7 is negative it follows that lighter tones on the image relate to areas of low reflectance in the near-infrared (Mather, 1987). The third DF (Figure 6.18C) is defined predominantly by MSS bands 4-6. MSS band 4 has the single highest coefficient, while MSS band 6 has a nearly-equal, and MSS band 5 has a slightly smaller, coefficient of the opposite sign. The positive coefficients (from MSS bands 5 and 6) may be related to the spectrum where absorption is the norm for green vegetation (Mather, 1987). The DF3 represents nearly 3 per cent of the discriminating power. As in the lower-order of the DF images for the Lochindorb area, the DF4 for the Kedah-Perak, with less than 0.5 per cent of discriminating power, hardly shows any information.

Individual discriminant images

Only a few of the DF images for both area will be discussed because they contain more information (higher percentage of discriminating power), show good contrast and better quality than other DF images which give no additional information.

Figure 6.17A shows DF1 of the TM data for the Lochindorb area. On the basis of visual inspection of Figure 6.17A it appears that the darkest (water bodies) and the lightest

A. EIGENVECTORS (DISCRIMINANT FUNCTION LOADINGS) IN THE DISCRIMINANT ANALYSIS OF KEDAH-PERAK MSS 1024 X 1024 SUBSCENE (SUBAREA 1)

DF	SPECTRAL BAND			
	4	5	6	7
1	0.15537	-0.04978	-0.17518	0.23940
2	0.12798	-0.15808	0.49123	-0.71765
3	-0.36508	0.18018	0.29933	0.02203
4	0.00134	0.22338	-0.13692	-0.22605

B. EIGENVALUES AND DISCRIMINATING POWER IN THE DISCRIMINANT ANALYSIS OF KEDAH-PERAK MSS 1024 X 1024 SUBSCENE (SUBAREA 1)

DF	EIGENVALUE	DISCRIMINATING POWER (%)	CUMMULATIVE OF DISCRIMINATING POWER (%)
1	9.82418	63.98	63.98
2	5.04294	32.84	96.83
3	0.42582	2.77	99.60
4	0.06116	0.39	100.00

Table 6.6 Eigenvectors (A), eigenvalues and discriminating power in the discriminant analysis (B) of the Kedah-Perak MSS 1024 x 1024 subscene (subarea 1).

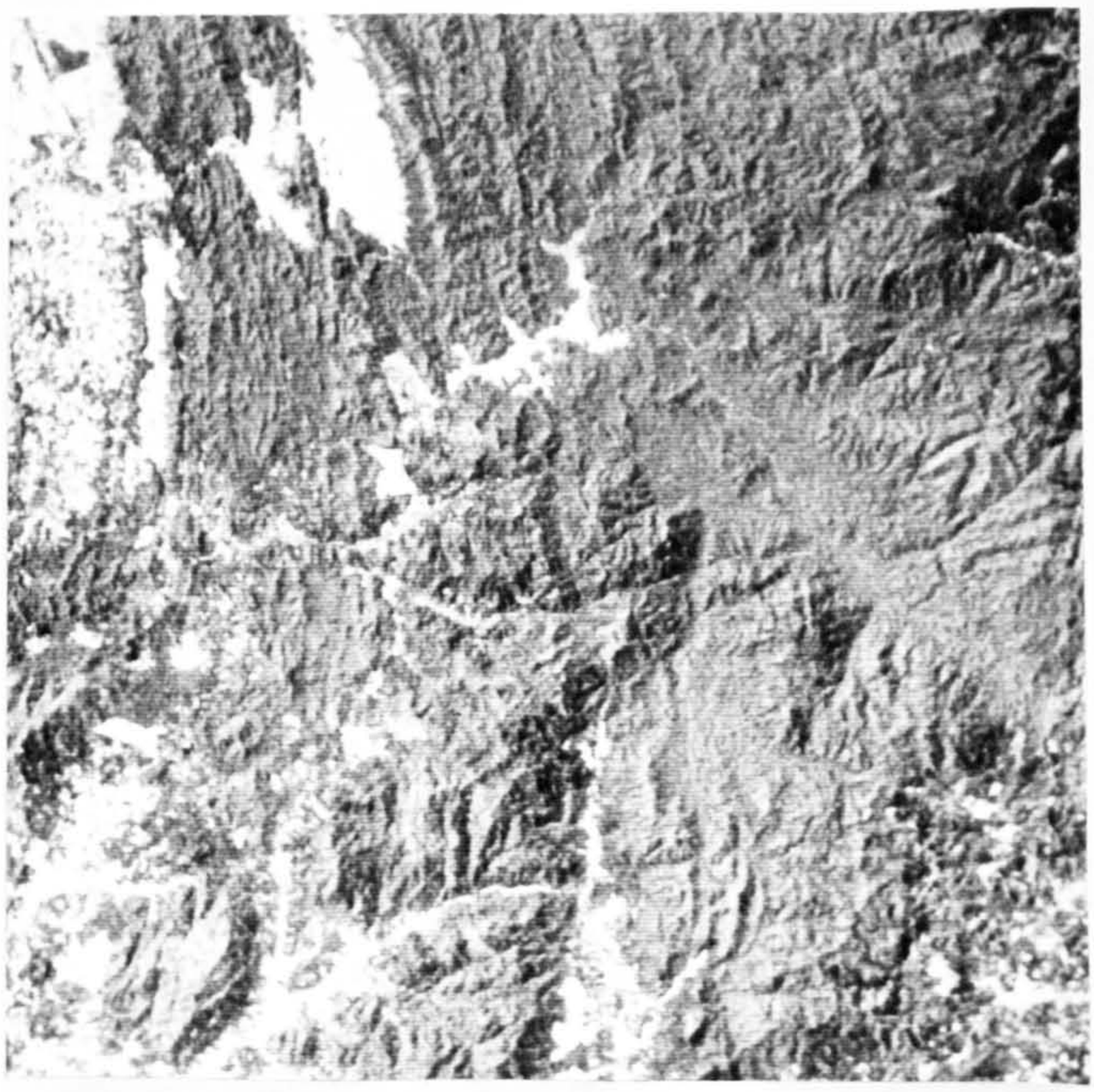

A DF IMAGE 1 (64.0%)

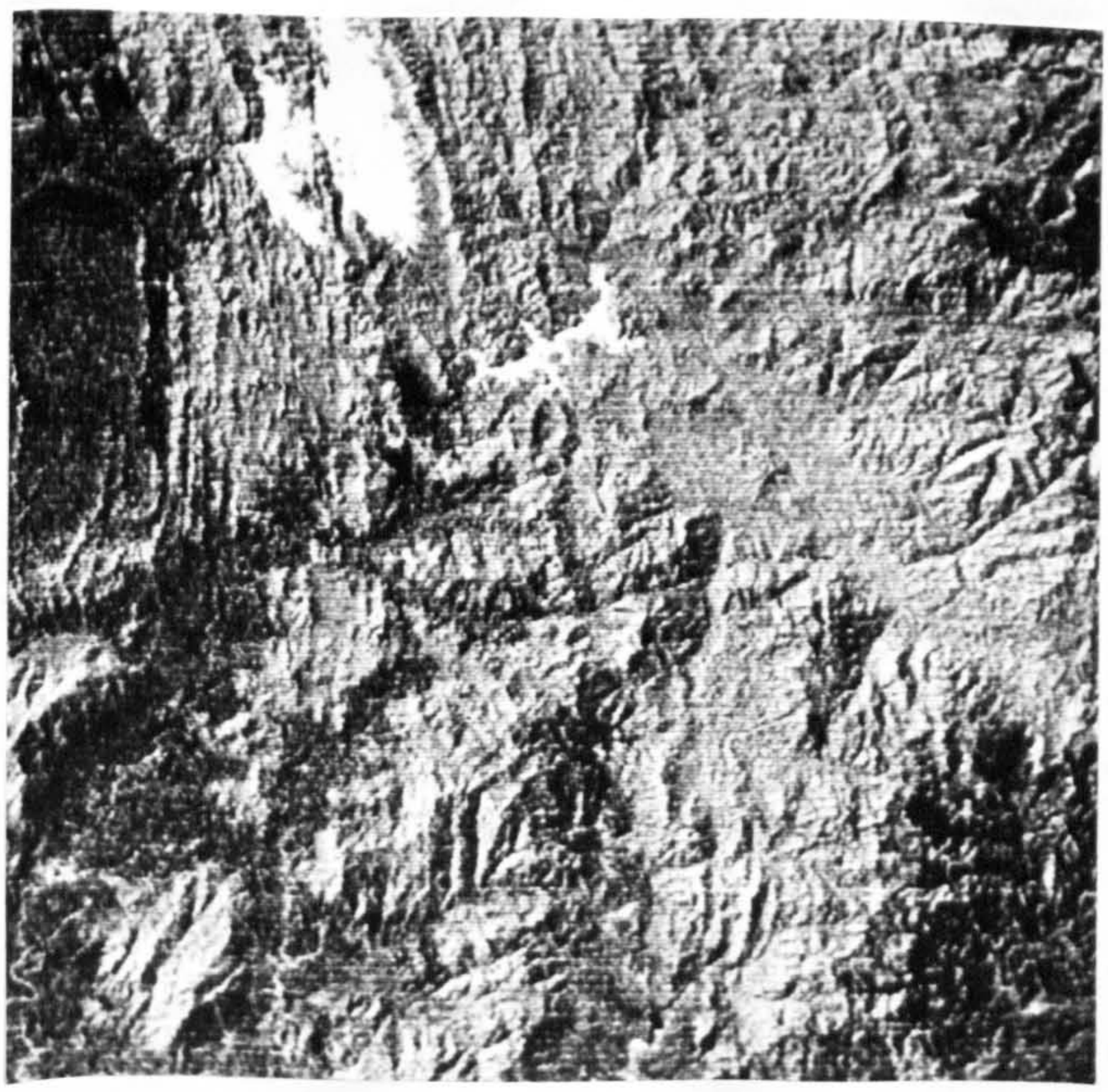

B DF IMAGE 2 (32.8%)

Figure 6.18 DF images 1-4 (A-D) of the Kedah-Perak sub-area 1. The DF images are generated from four visible and IR bands of the Landsat MSS image. Percentage of discriminant power represented by each DF image is shown. Scale 1:600,000.

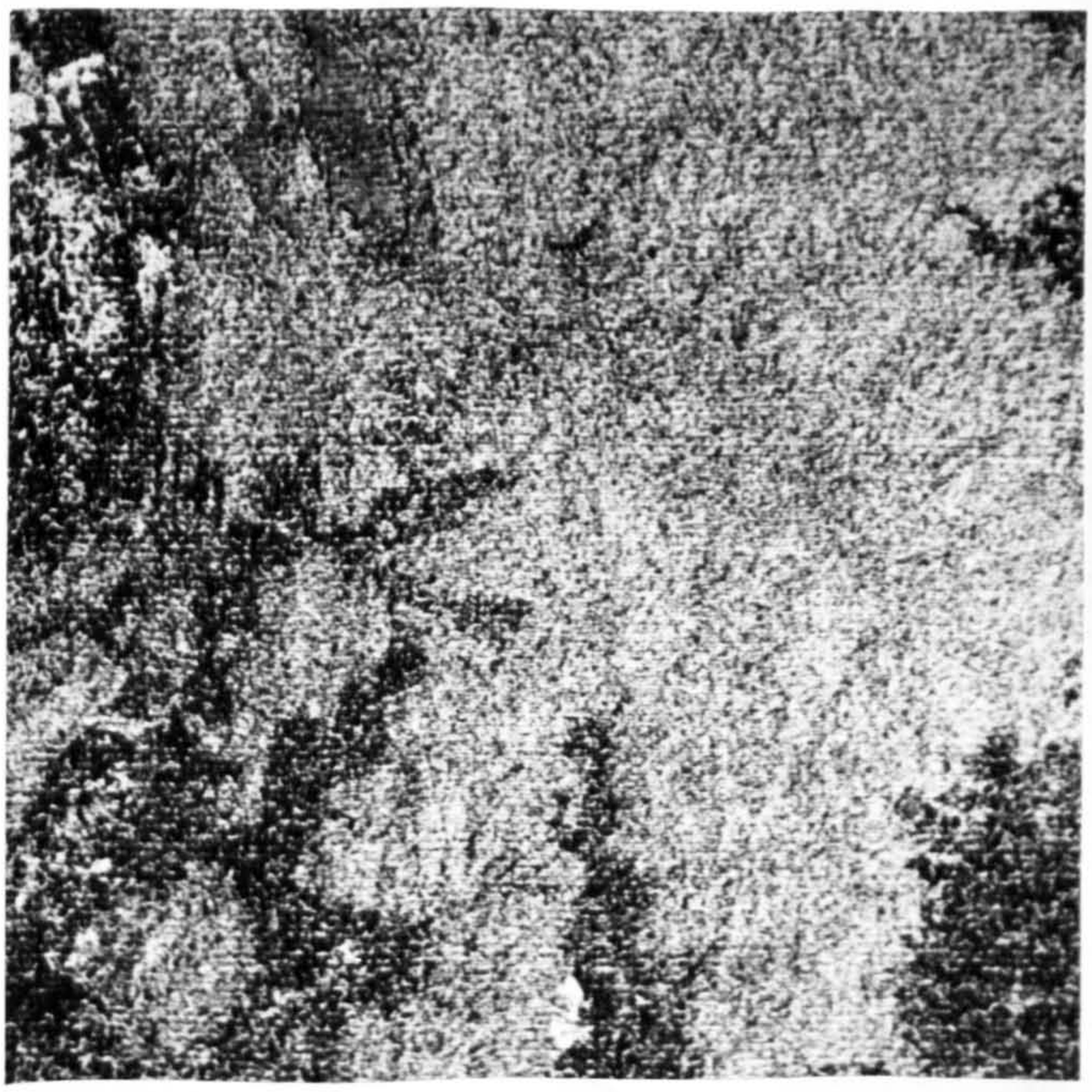

C DF IMAGE 3 (2.8%)

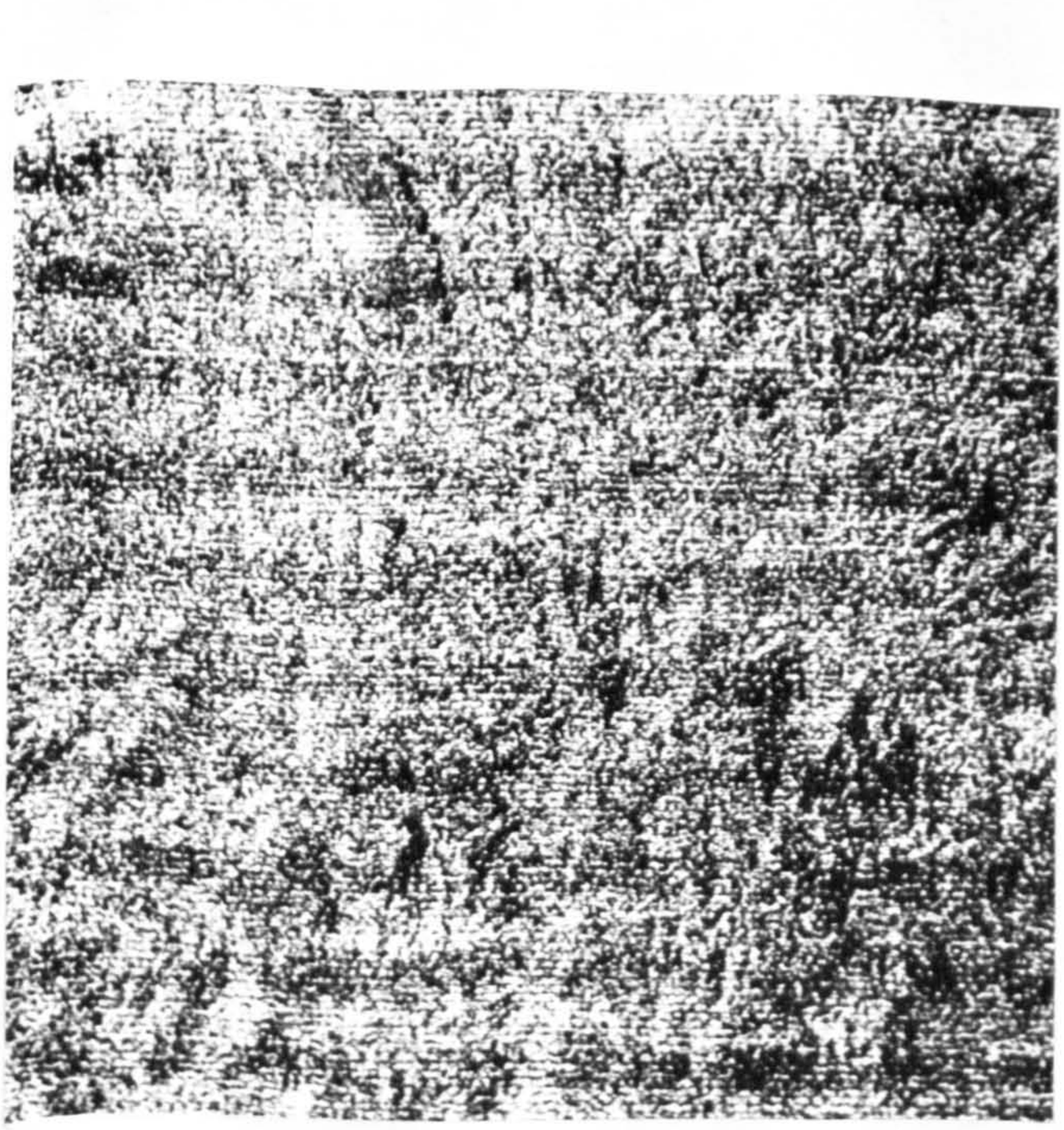

D DF IMAGE 4 (0.4%)

Figure 6.18 (continued)

(grass areas) areas both in the TM bands 1 and 2 (Figure 6.3A and B), appear as opposite tones in the DF1 image, hence it may be confusing as the water areas are bright rather than dark. Other areas (mostly related to the peat and glacial deposits) which have slight tonal variation in the TM bands 1 and 2 appear in different shades of grey tone. Impression of relief is less pronounced, however the main drainage channels are well depicted because of the darker tone of the grass alongside the channels. Generally it shows very good tonal variation and contrast, but, apart from green grass and other grass areas which appear black, other cover types, are not well depicted hence their boundaries are poorly defined if they are delimited purely on the basis of their grey tone.

The second DF image is given in Figure 6.17B. Generally DF2 is very similar to the DF1 in terms of relief impression, cultural features and drainage, however the DF2 shows better contrast and offers better discrimination of cover types than the DF1. For example, the peat deposit which appears as light grey can be separated to a certain degree from the glacial deposit which appears as dark grey tones. The identification of other cover types and their boundaries is still difficult and poorly defined. The DF3 is shown in Figure 6.17C. Generally it has less contrast and more noise than the first two functions. Despite that, the peat deposits which generally correspond to the dark grey tones are much better depicted here than on the DF1 or DF2.

DF1 for Kedah-Perak area is shown in Figure 6.18A. Roughly, it has only two grey tones: (a) dark grey for

vegetated areas, and (b) white for non-vegetated areas, wetter areas with thin vegetation cover and water bodies. Therefore the image is good, particularly, for separating vegetated and non-vegetated terrain. Apart from that, although relief impression, lineaments and photo-characteristic (texture) are fairly well displayed, those features which can be used to separate different lithological units are better enhanced on other data products. The DF2 image for the same area is shown in Figure 6.18B. The image shows better relief impression than the DF1, however it also does not offer better separation between rock types or enhance any new feature which was not known before. The DF3-4 are noisy, hence it would be difficult to extract any meaningful conclusion from them. Therefore, individual images of the DFs seem to have no benefit for the interpretation of this area where larger parts are covered by dense vegetation cover.

Combinations of discriminant images

Like other processed images, the individual discriminant analysis images were combined to produced colour composites with an aim to see whether they can offer better discrimination between various geological units or enhance certain features of interest in the study areas. There are many possible colour composite combinations which can be produced. The Combinations of DFs in this study, however, were chosen and tried on the basis of the percentage of the discriminating power of the individual function and also their ability to differentiate between various cover types which are

related to the surface deposits. After examining visually all the DFs, it was found that the first four DFs of the TM data for the Lochindorb, and the first three DFs of the MSS data for the Kedah-Perak areas show good tonal variations (which are generally related to cover types) as well as containing a higher percentage of the discriminating power. These DFs therefore were chosen and used to produce false colour images. Other lower-rank DFs did not fulfil the criteria, hence were not used in the colour composite combinations.

For the Lochindorb area, the combination consists of DF3, DF2, and DF1 displayed as blue, green and red respectively as shown in Figure 6.19A. The combination, which represents slightly over 97 per cent of the discriminating power of the spectral classes in this sub-scene (Table 6.6 B), generally shows better separation between the two main surface deposits: peat deposits appear as yellow and glacial deposits appear as purple. The mixture of cover types which are related to the two deposits is shown as a mixture of purple and yellow. The green grass cover which is mainly associated with the alluvial deposits alongside the main drainage channels, and the improved land area underlain by glacial deposits, appear dark blue. Bedrock areas which are generally closely associated with higher ground areas appear whitish yellow, water bodies are shown as white, and bare fields appear greenish yellow to green. Relief impression and drainage, however are less pronounced. Water bodies and wet areas which appear white can be confused with the shadow areas which are associated with high relief. It is to be noted that, the peat deposits which

appear yellow are better depicted in this colour combination than in any other composite images. Two other combinations were tried by using the same DF images but with different colour combinations (Figure 6.19B and C). For all combinations, they are similar in terms of discriminating power (information content). However, the colour combination can affect the image quality for feature identification. For example, the area covered by green grass is better depicted in the DF 2(B), DF 3(G) and DF 1(R) combination than in the other two. The result of the assessment of geological information content of the images (section 6.3) reflects the colour combination effect. Other combinations involving the DF4 were also tried but they did not offer any better discrimination between the main deposits and cover types.

DF combination for the MSS data set of Kedah-Perak area is presented in Figure 6.20 with DF3, DF2 and DF1 displayed in blue, green and red respectively. Although the combination contains more than 99 per cent of the discriminating power of the spectral classes (Table 6.6 B), and shows good colour variation, it is evident that the combination did not offer any new information or give better discrimination between lithological units in the area than previous images. The main obvious reason is that the area is dominated by the monotonous dense forest cover over large areas which offer no or only very small spectral differences to be depicted and shown in the image. The only feature which can be seen clearly is the agricultural land where it shown as mixtures of brown-yellow

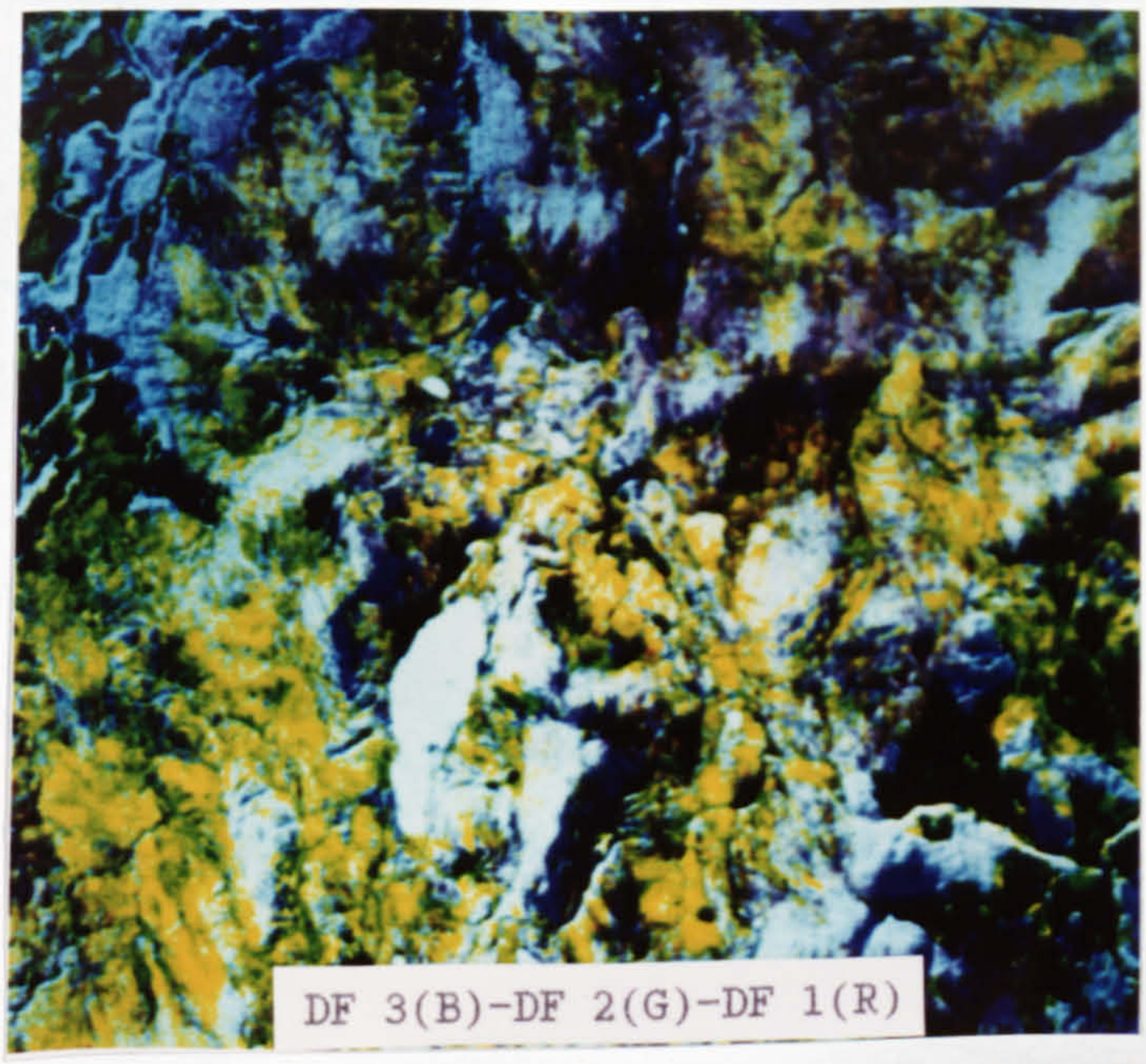

A DF 3(B)-DF 2(G)-DF 1(R)

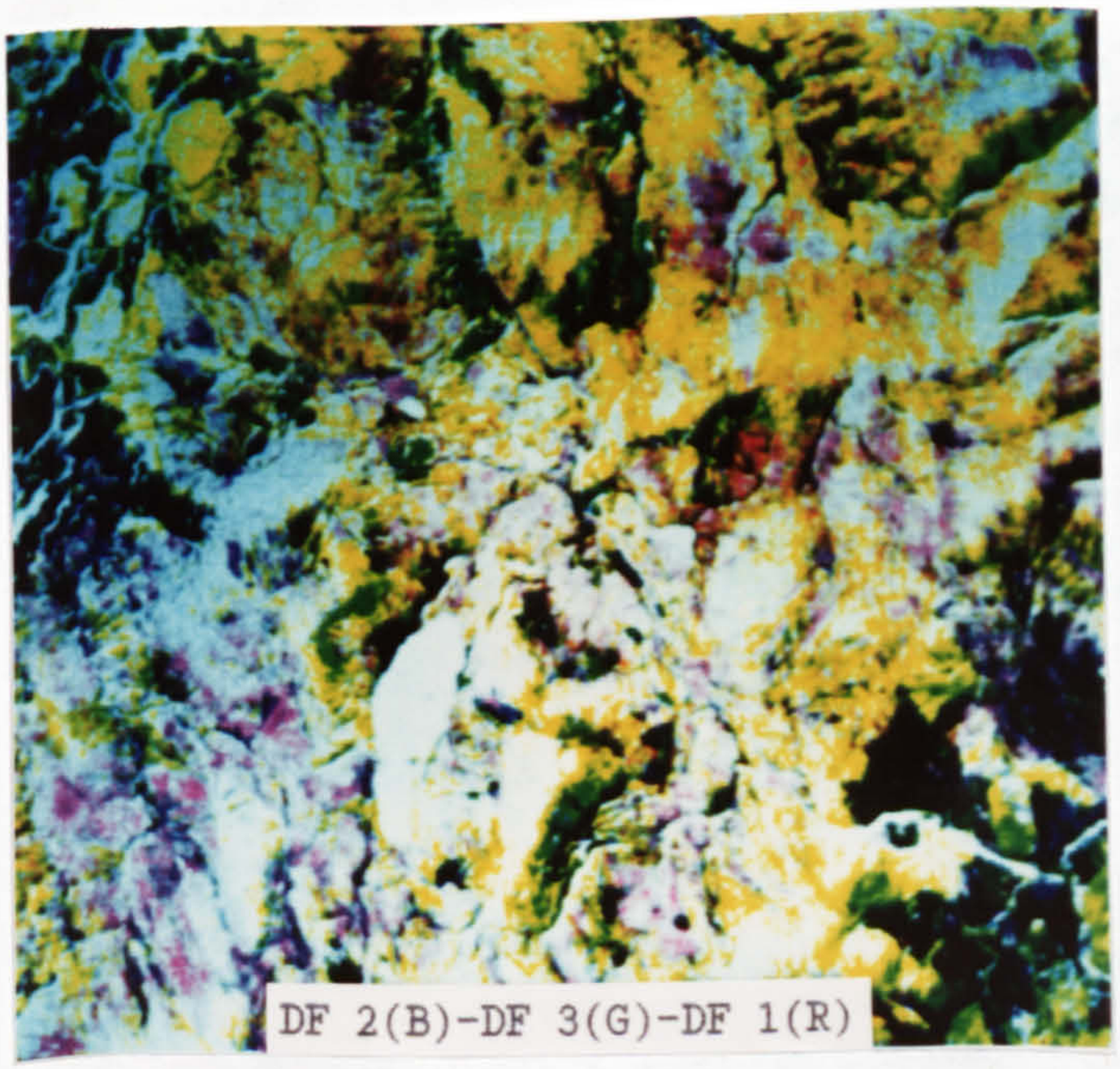

B DF 2(B)-DF 3(G)-DF 1(R)

Figure 6.19 TM discriminant function colour composites of the Lochindorb area (A-C). The images show that colour combination can affect the image quality for feature identification. Scale 1:160,000.

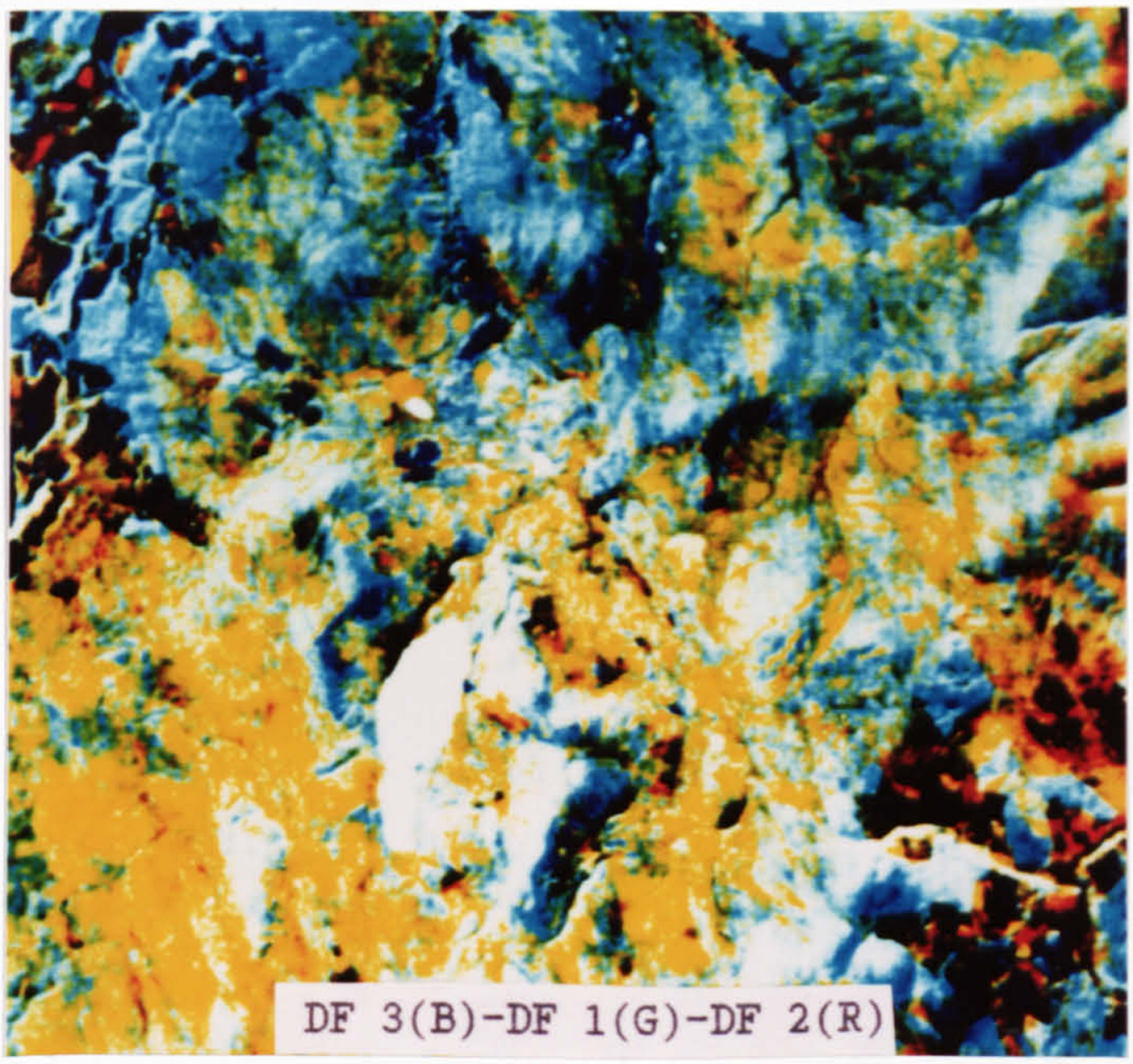

C DF 3(B)-DF 1(G)-DF 2(R)

Figure 6.19 (continued)

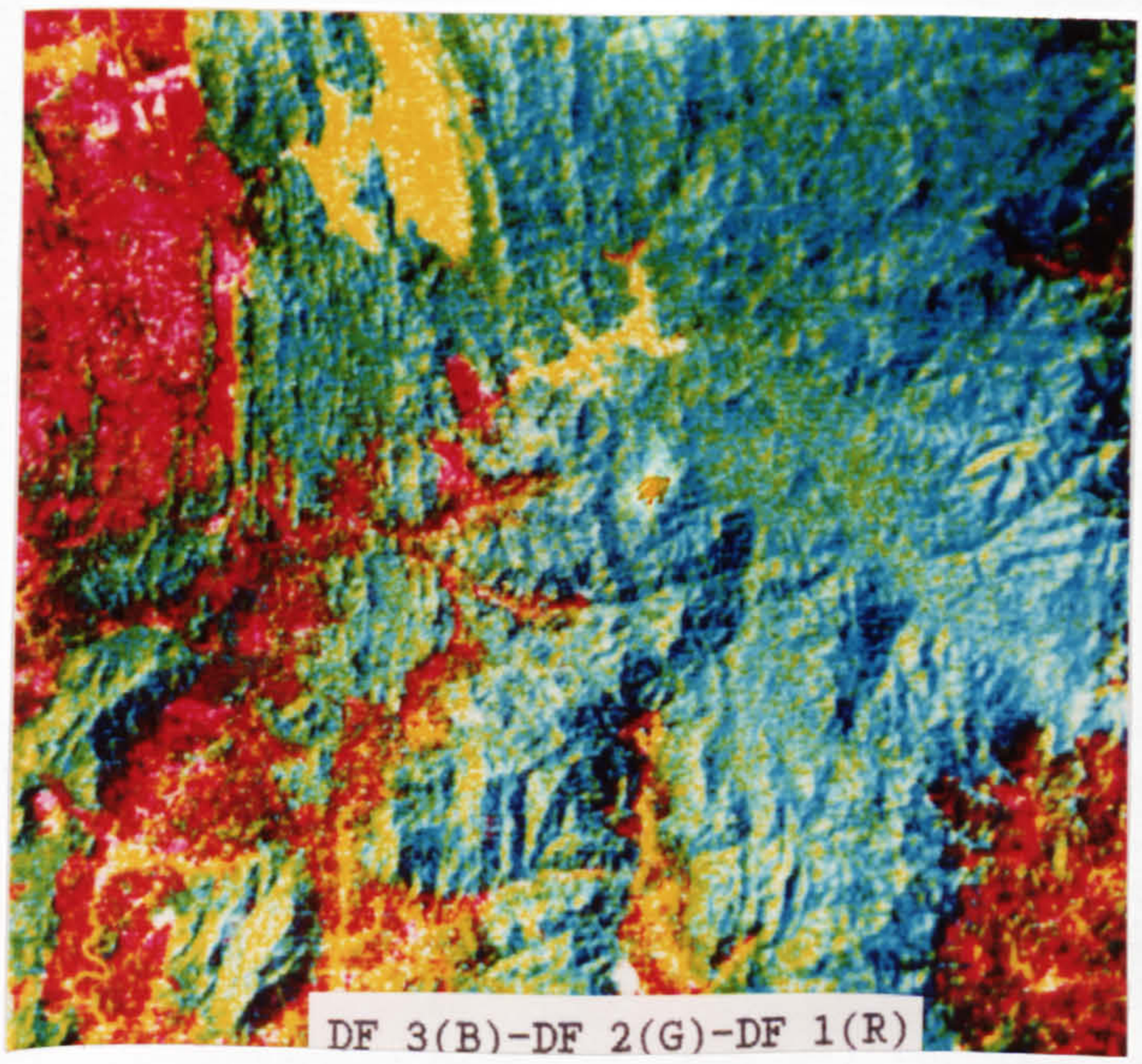

DF 3(B)-DF 2(G)-DF 1(R)

Figure 6.20 MSS discriminant function colour composite of the Kedah-Perak sub-area 1. DF 1 displayed as red, DF 2 as green and DF 3 as blue. Scale 1:600,000.

and pink in contrast with yellow for water bodies, reddish pink for bare fields and yellowish blue for forested areas. Although there are differences in terms of texture and relief between different rock types, these features are better expressed on several previous images. The first three DFs were also assigned to different colour combinations but the resultant colour composites did not show any new feature or offer better separation between rock types in the area.

6.2.6 Ratioing

Obviously there are a large number of combinations that can be made within the original data set. The number of ratios is given by the formula: N(N-1), where N = number of channels. This amounts to 12 ratios for the Landsat satellite MSS, or six if their inverse permutations are not counted. These ratios can be combined in groups of three for colour composites, and using the four Landsat bands for example, this produces 20 possible ratio combinations without the use of inverse permutations, or 220 if they are included. Furthermore, each of the ratio composites should be investigated in several colour combinations, hence, the previously mentioned ratio combinations are several times higher. The combination numbers are much higher for the TM with 6 bands (excluding the thermal band). If all the possible ratio combinations were investigated by trial and error this would make the process expensive, tedious and confusing. There are a few methods to overcome this difficulty including use of the optimal index factor (OIF) (Chavez et al., 1982), or by

deciding which spectral features are important to the study (Drury, 1986b; Drury,1987). Because of the nature of both study areas which are very highly vegetated and the lack of varying contents of minerals (for the Lochindorb area), therefore the OIF is not necessarily a valid indicator for the study area (section 6.2.3), and furthermore only spectral features from the vegetation prevail in the study areas, and not from the geological units such as rock types or surface deposits. Therefore, in the time allotted, various ratios in the study areas were tried and chosen based on the ability of every individual ratio image to distinguish between several known cover types or show better tonal variations which are related to the surface deposits or rock types in the study areas, rather than based on the OIF or spectral measurement of the original data set. Although ratioing alone is adequate to show large differences, such as those between the visible and near-infrared bands for vigorous vegetation, stretching is also necessary for adequate enhancement of the typically subtle spectral reflectance differences found among most geologic materials. Used in combination, ratioing and stretching provide additional means for enhancing spectral differences, however, as will be shown, because the areas are highly vegetated the ratioed images are a complicated mixture of spectral signatures so the discrimination between the features is still not clear. In the ratioed images the darkest areas occurred when the denominator of the ratio was greater than the numerator, and conversely for the lighter areas, when the denominator was less than the numerator. The largest

differences in reflectance between MSS bands for vegetation, for example, are shown in the image ratios 5/6 and 5/7 (vegetation very dark) (Figure 6.22D) and for ratio 4/5 (vegetation very light) (Figure 6.22B). The ratios and ratio combinations which show some interesting features and/or enhanced the geologic information of the area are here discussed.

Individual ratio images

All possible ratio images, 30 ratio images for the TM data set of Lochindorb and 12 ratio images for the MSS data set of Kedah-Perak areas, were produced in this study. They were examined visually and it was found that only a few of them did show good tonal variations which are seen to be related to certain geological features. These are the TM bands 2/1, 3/1, 3/4, 4/5, 7/1, and 7/4 for the TM sub-scene of the Lochindorb area (Figure 6.21), and the MSS bands 4/5, 4/6, 4/7, 5/6, 5/7, and 6/7 for the MSS sub-scene of the Kedah-Perak area (Figure 6.22).

The ratio images of TM bands 3/4 and/or 4/3 are used to assess the amount of green biomass present. This is because the ratios collate the red part of the spectrum where there is a high chlorophyll pigment absorption (TM band 3 ranges from 0.63 - 0.69 μm) and the near-infrared section (TM band 4 ranges from 0.76 - 0.90 μm) where there is a high reflection of the leaves due to their cellular structure (Eldvidge and Lyon, 1985). Green grass and other grass areas appear as black to very dark grey tones and stand out clearly on the TM bands

3/4 ratio image (Figure 6.22I). Generally the areas which are underlain by the peat deposits and covered by shrubs, birch trees, purple grass moor and dense heather are therefore lighter than the surrounding glacial deposits which are covered by mixture of heather, fescue grass and other grass types, hence their boundary is fairly well displayed. Bare fields show lighter tones than the area which is underlain by peat deposits, however the separation between them is confused. The peat areas show higher reflectance in the TM band 5 than on the TM band 4, while the glacial deposits areas have the opposite in the two bands. Therefore the subtle tonal variations between the two deposits are much better in the TM bands 4/5 ratio than on the original TM band 4 or 5 where the peat appears very dark grey or black whereas the glacial deposits are shown as light grey (Figure 6.21C). The vegetated areas which have higher reflectance on the TM band 4 than on the TM band 5 are clearly shown as very light grey or white in the ratio image. Ratio of TM bands 5/7 is widely used in the discrimination of altered and unaltered rocks (Harris, 1987) because 1.66 μm is the maximum reflectance of many geological materials like carbonate and hydrous minerals and the 2.22 μm region is a reflectance minimum (absorption) especially in hydroxyl and silicate minerals (Eldvidge and Lyon, 1985). This ratio combination helps detect the absorption associated with certain materials, hence it was hoped this ratio might show something of the lithology or the vegetation and soil over it.

A TM BANDS 2/1

B TM BANDS 3/1

Figure 6.21 Examples of the TM ratio images of the Lochindorb area (A-I). Scale 1:160,000.

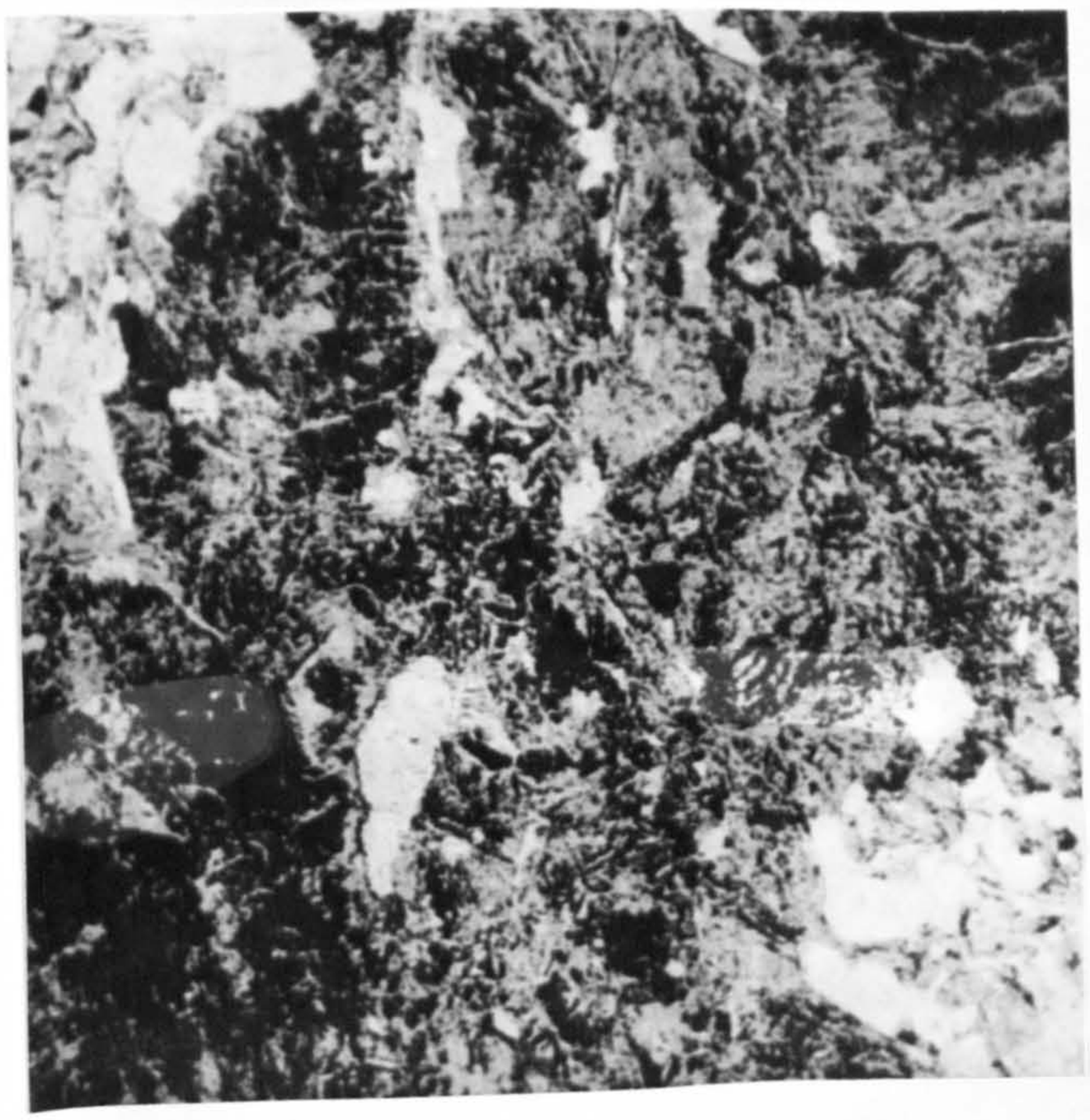

C TM BANDS 4/5

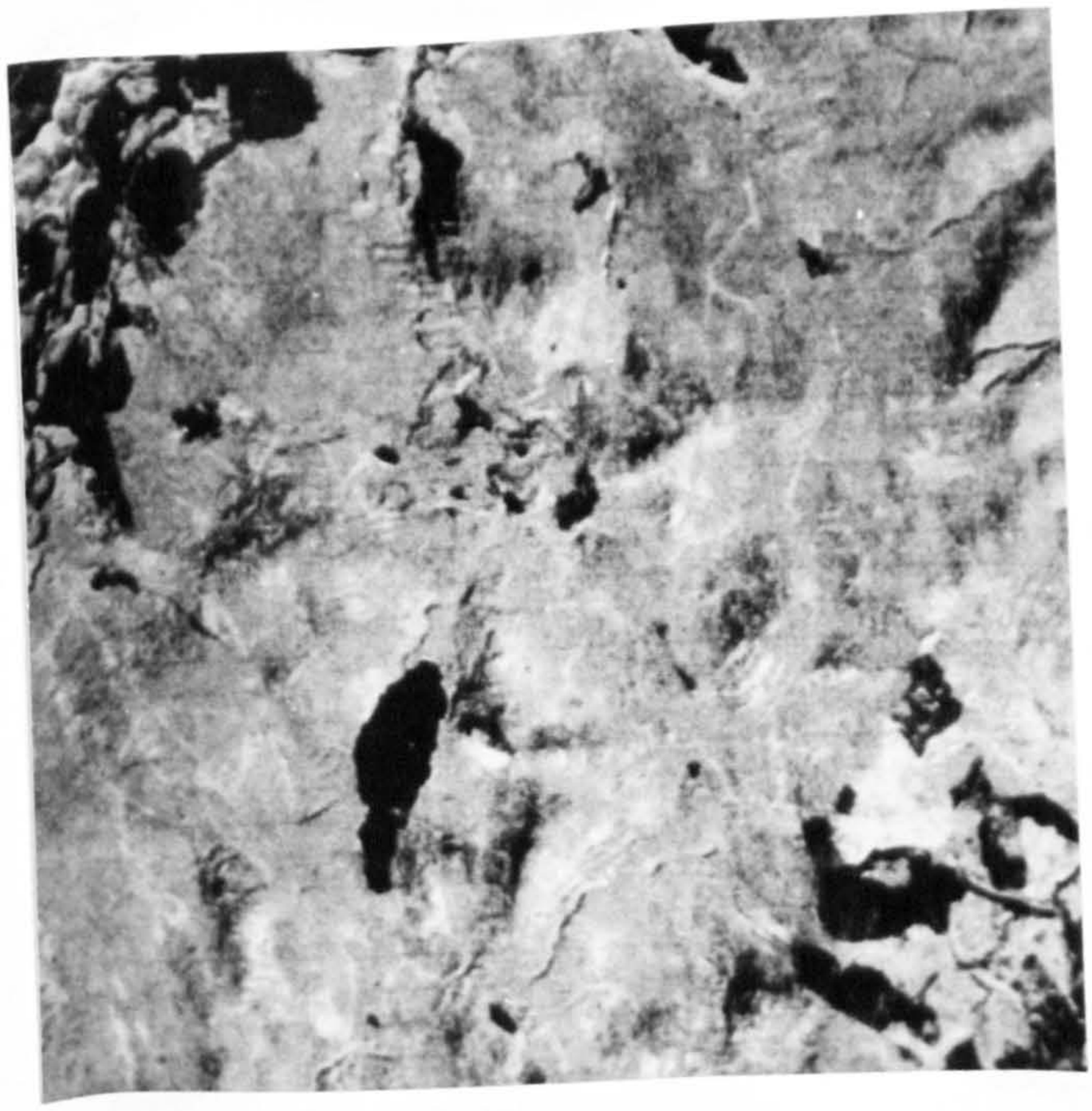

D TM BANDS 7/1

Figure 6.21 (continued)

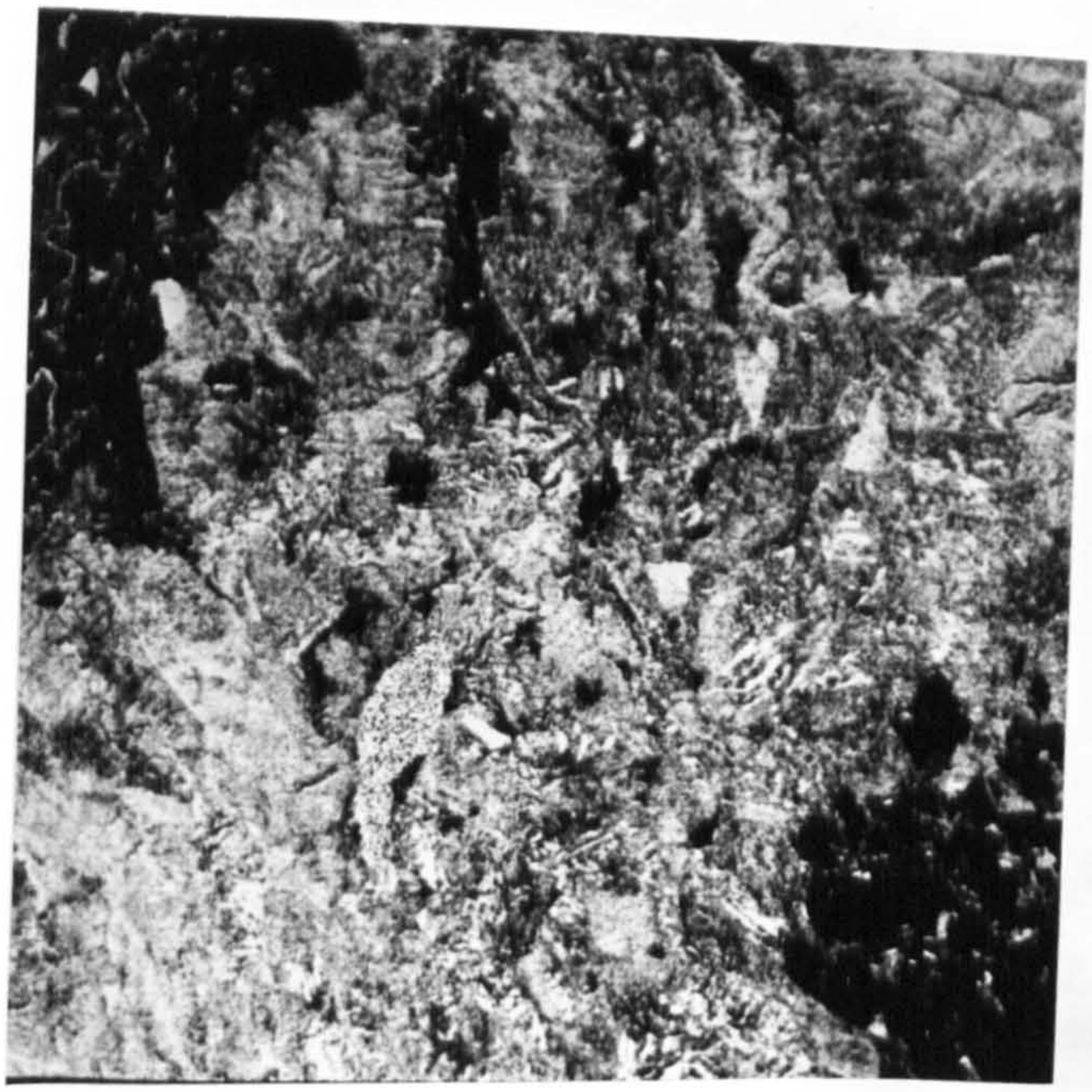

E TM BANDS 7/4

F TM BANDS 5/7

Figure 6.21 (continued)

G TM BANDS 7/2

H TM BANDS 4/2

Figure 6.21 (continued)

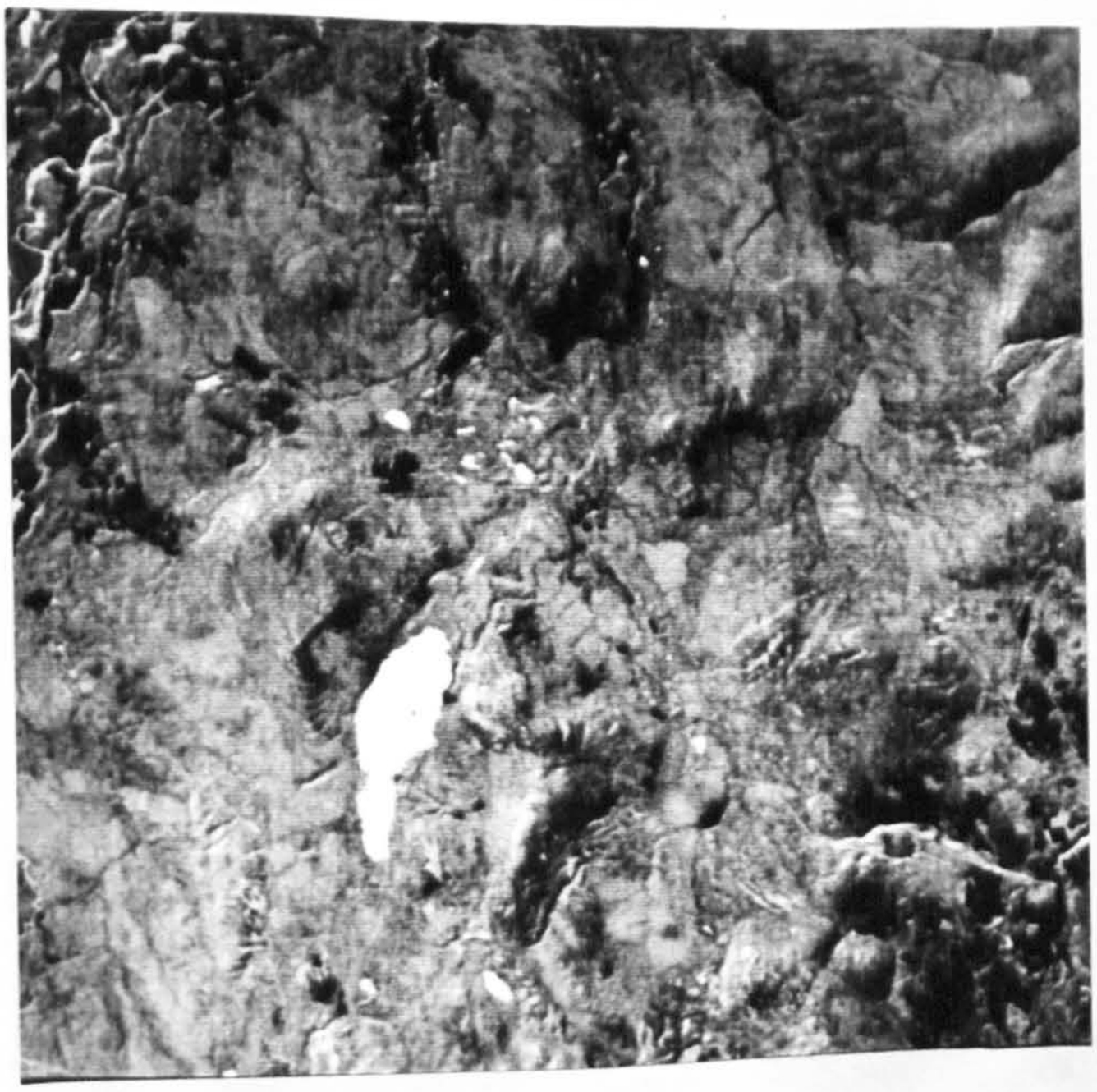

I TM BANDS 3/4

Figure 6.21 (continued)

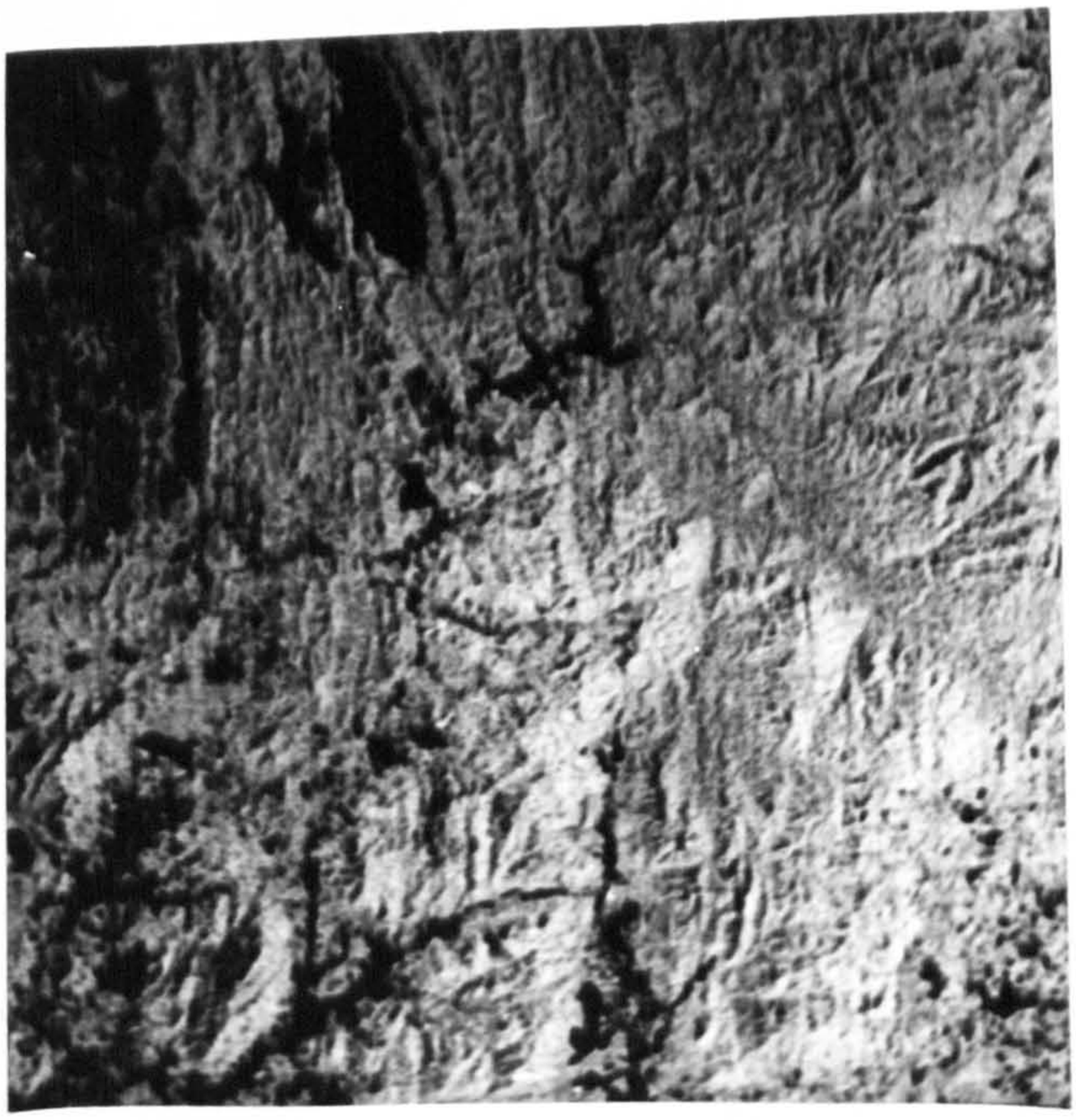

A MSS BANDS 7/5

Figure 6.22 Examples of the MSS ratio images of the Kedah-Perak sub-area 1 (A-E). Scale 1:160,000.

B MSS BANDS 4/5

C MSS BANDS 4/6

Figure 6.22 (continued)

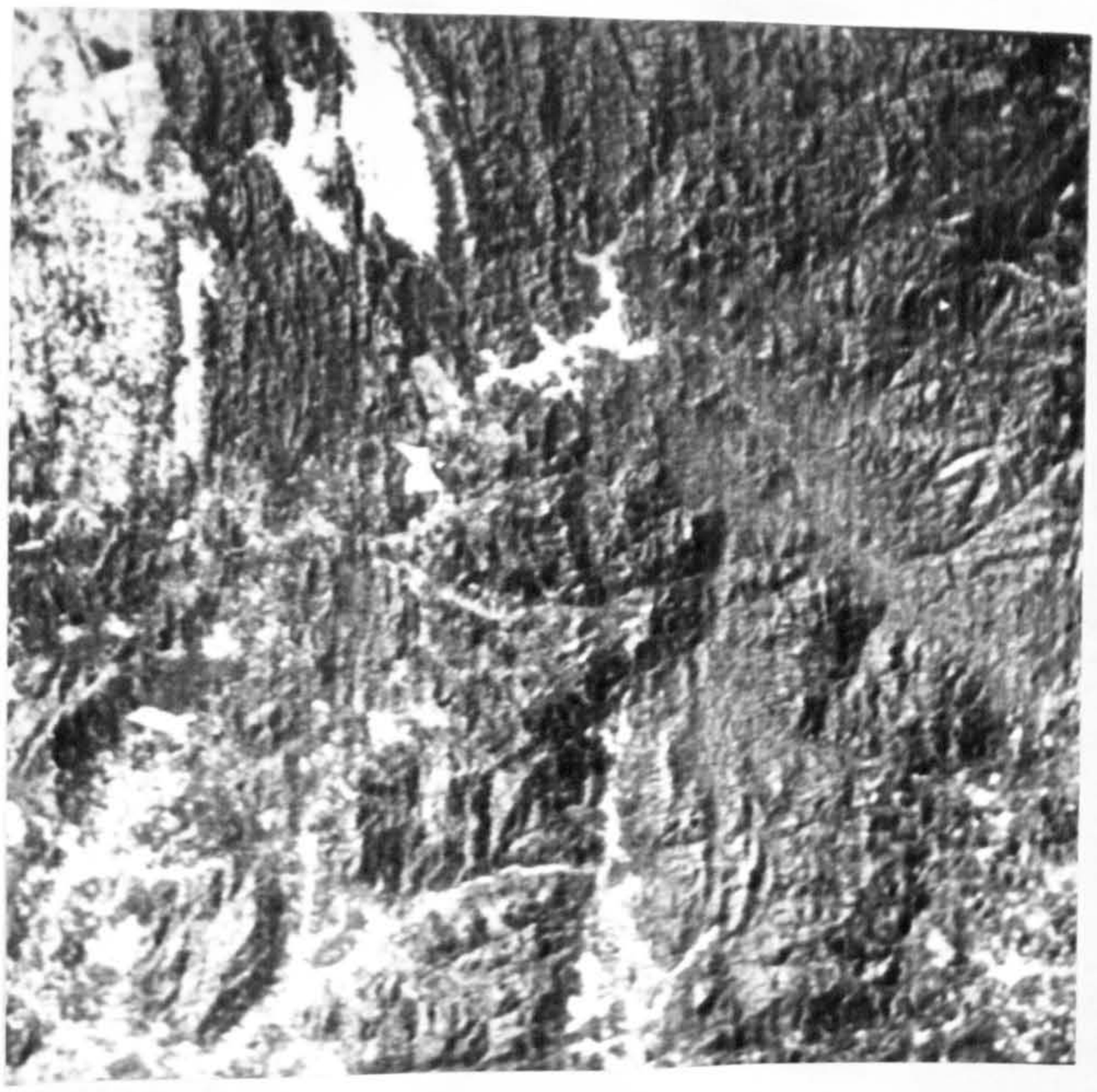

D MSS BANDS 5/7

E MSS BANDS 7/4

Figure 6.22 (continued)

However this was not so, the ratio combination in Figure 6.21F does not contain any new or better information given by this process that is not already known. Other ratio images were also tried and examined including TM bands 2/7 to identify iron bearing rocks (Eldvidge and Lyon, 1985), TM bands 4/2 and TM bands 3/2 which have been found to be among the most useful for lithological discrimination (Bailey and Dwyer, 1982; Saraf et al., 1989) and many other combinations. However, again the vegetation and drift cover proved too heavy and the resulting images do not offer any new feature or better discrimination between cover types.

MSS bands 7/5 (or MSS bands 5/7) is perhaps the most useful band ratio because it is positively related to vegetation amount (Tucker, 1979). This ratio exploits the fact that vigorous vegetation reflects strongly in the MSS band 7 waveband and absorbs in the MSS band 5 waveband (see Figure 3.5), hence the bands 7/5 or bands 5/7 bring out the distribution of vigorous vegetation quite clearly. The MSS band 7/band 5 for the Kedah-Perak area is shown in Figure 6.22A, where generally the lighter the pixel ratio, the more vegetation present within the field of view of the picture element, and for the MSS bands 5/7 (Figure 6.22D) gives the opposite result. Therefore the distribution of green vegetation is well pronounced in both band ratios, and this is very important because it can be used to infer lithological information of this densely vegetated area. Based on tonal variation within the vegetated area on the MSS bands 7/5 ratio image, it is shown that the lightest tone on the image, which

means more vegetation cover, corresponds to the granite terrain. On other hand, the sandstone/conglomerate and the metamorphic rocks appear grey, hence are less densely vegetated than the granite. Water bodies and bare fields appear black and dark grey to black respectively. The shadow effect in higher topography which is apparent on the original images is very much reduced on this ratio image, hence relief impression; drainage and lineaments are much less pronounced. Other ratio images were also tried and examined but they did not contain any new information, except the MSS bands 7/4 which gives much a better result in terms of relief impression and enhancing lineaments (Figure 6.22E).

Combinations of ratio images

Like other processed images, three ratio images can be assigned to different colours and combined to produce a colour composite, and with the colour factor now involved there can be many combinations processed to enhance the different features. Various colour ratio composites of the Landsat TM data sub-scene for the Lochindorb and the MSS data sub-scene for the Kedah-Perak areas were produced with an aim to get a better image which offers better separation or recognition of different geologic features. As mentioned earlier, six of the ratio images of the TM data for the Lochindorb area which show good tonal variations in relation to the different cover types in the area are the TM bands 2/1, 3/1, 3/4, 4/5, 7/1, and 7/4, and the MSS bands 4/5, 4/6, 4/7, 5/6, 5/7, and 6/7 ratio images of the MSS data for the Kedah-Perak area. These ratio

images were combined with different colour combinations to produce several colour ratio composites. In this study, therefore, only the selected ratio images were used in combinations of ratio images in order to make the process more objective, less expensive and less tedious.

Figure 6.23A shows TM band 2/1, 7/1, and 3/1 displayed in blue, green and red respectively for the Lochindorb area. This combination shows overall good colour variation for various cover types which are related to main surface deposits, therefore it able to show general distribution of main themes in the area. Forested areas appear very dark purple to black, green grass displays as blue, bare fields or areas with thin cover types appear pale yellow to yellowish green. Alluvial deposits which are covered by green grass are therefore related to the bluish areas. Most of the peat deposits are shown as pink to reddish pink except the Moidach peat where it generally appears pale red surrounded by dark greenish-reddish pink colour of glacial deposits. Bedrock areas are associated with dark green colour, however its differentiation with other themes especially the glacial deposits is still problematic. Water bodies are shown as black.

Other colour composites of ratio images for Lochindorb area are shown in Figure 6.23(B) and (C) where band 4/5, 7/1, 3/1 and band 3/2, 5/2, 7/4 were displayed in blue, green and red respectively. In terms of surface deposits both combinations offer no additional information than the previous one. Although the colour variation in the bands 3/2, 5/2 and 7/4 combination do reflect the superficial deposits in the

A TM BANDS 2/1(B)-7/1(G)-3/1(R)

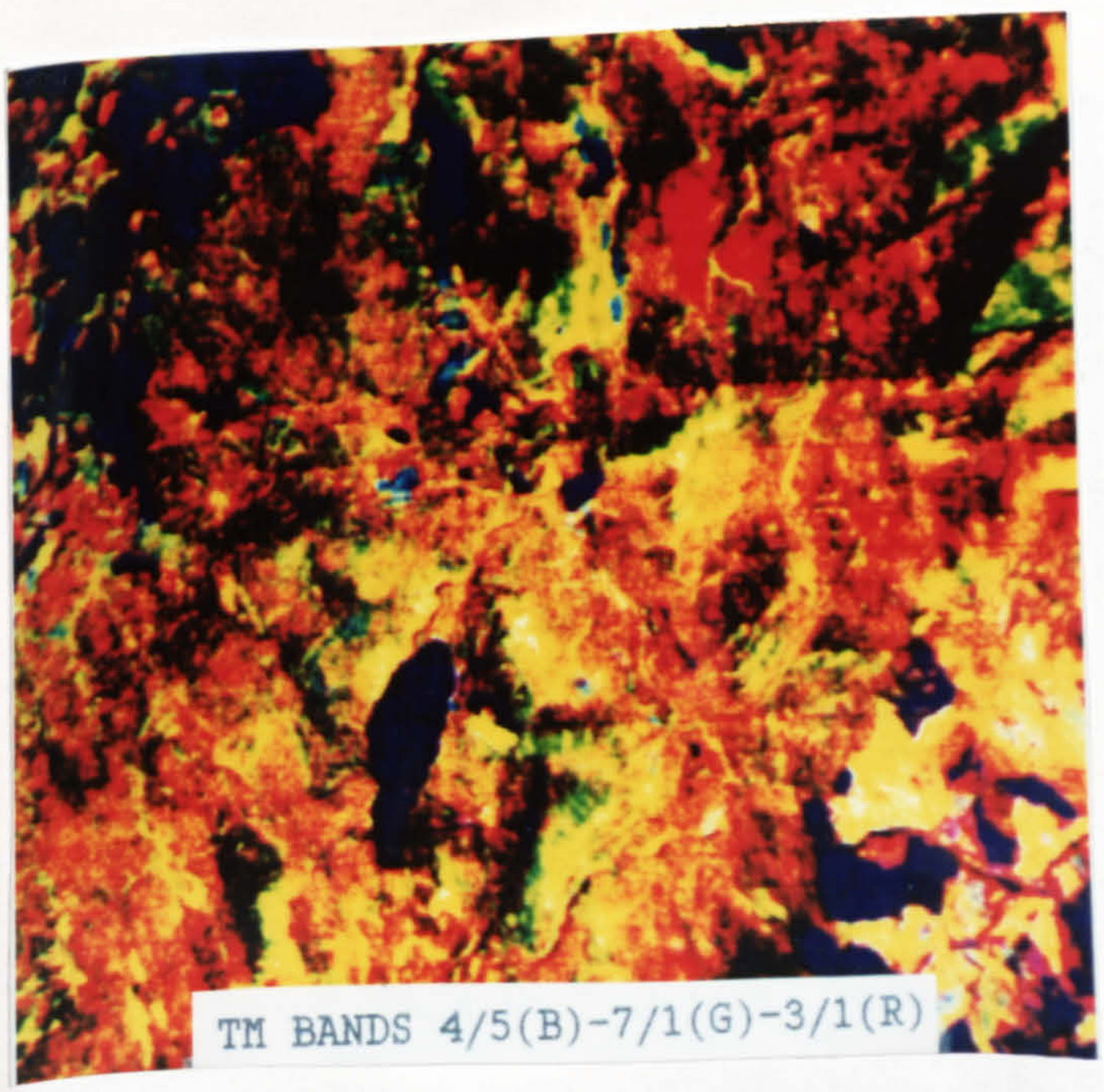

B TM BANDS 4/5(B)-7/1(G)-3/1(R)

Figure 6.23 TM bands-ratio colour composites of the Lochindorb area (A-C). Scale 1:160,000.

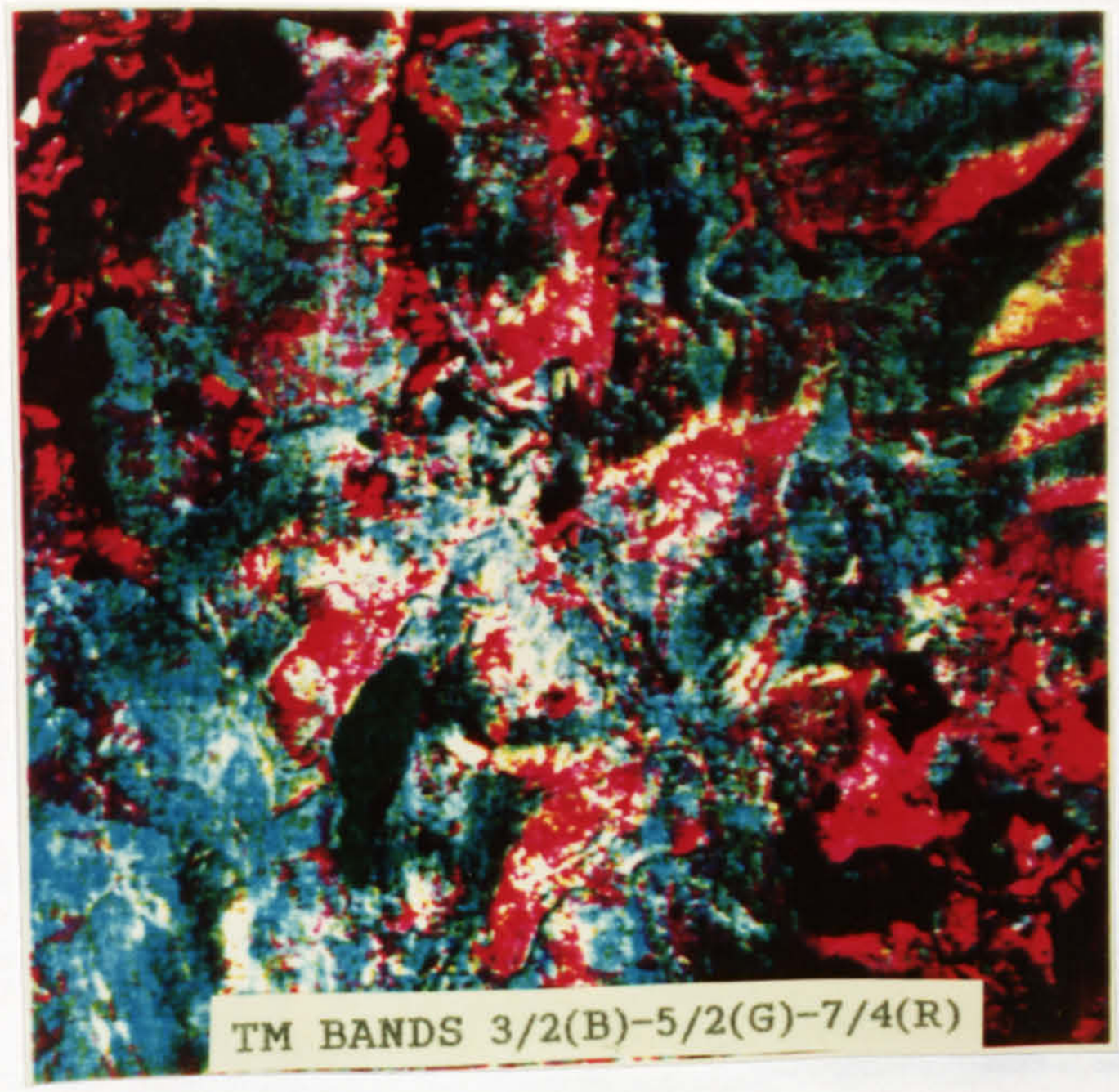

C TM BANDS 3/2(B)-5/2(G)-7/4(R)

Figure 6.23 (continued)

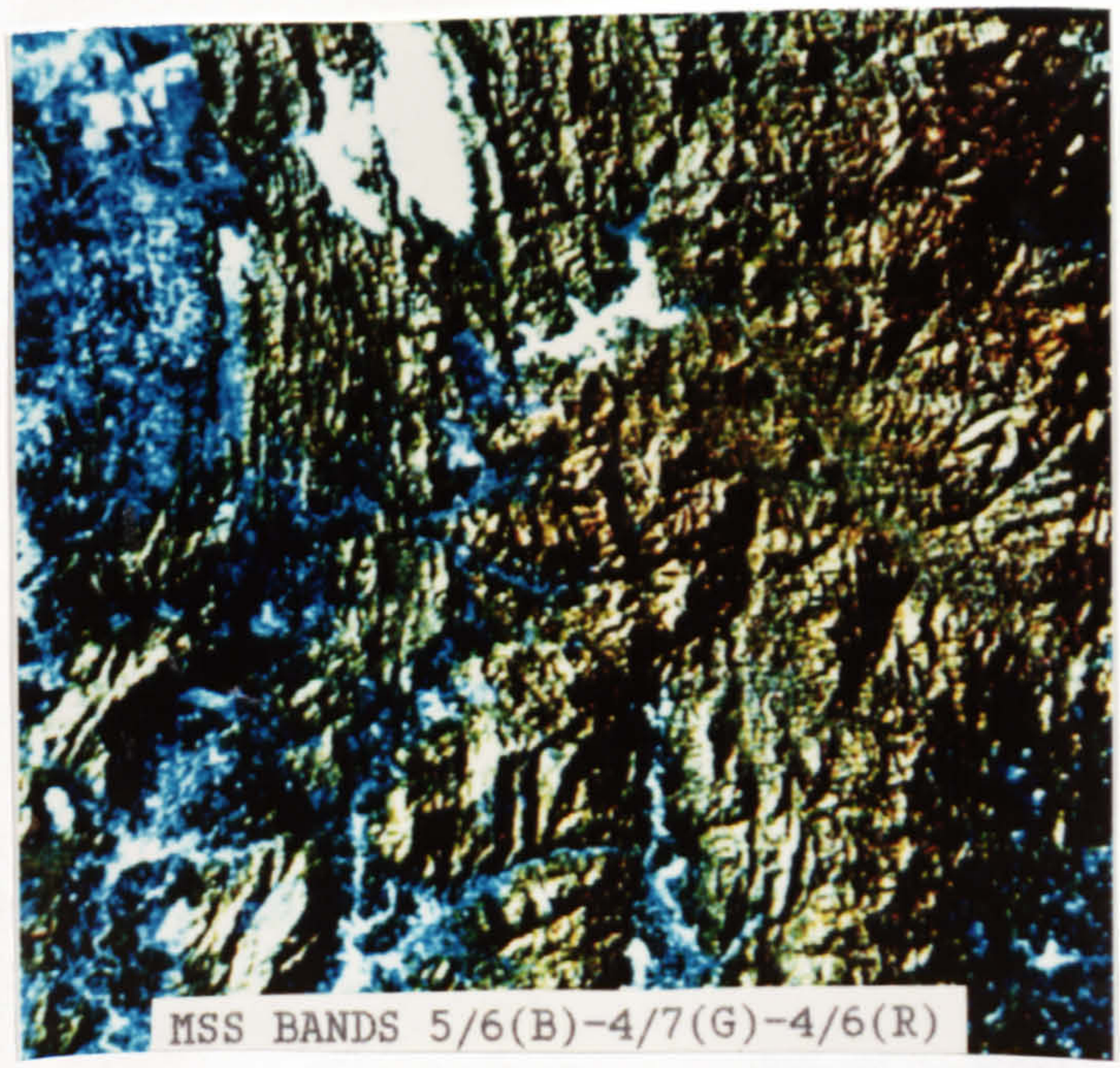

A MSS BANDS 5/6(B)-4/7(G)-4/6(R)

Figure 6.24 MSS band-ratio colour composites of the Kedah-Perak sub-area 1 (A-C). Scale 1:600,000.

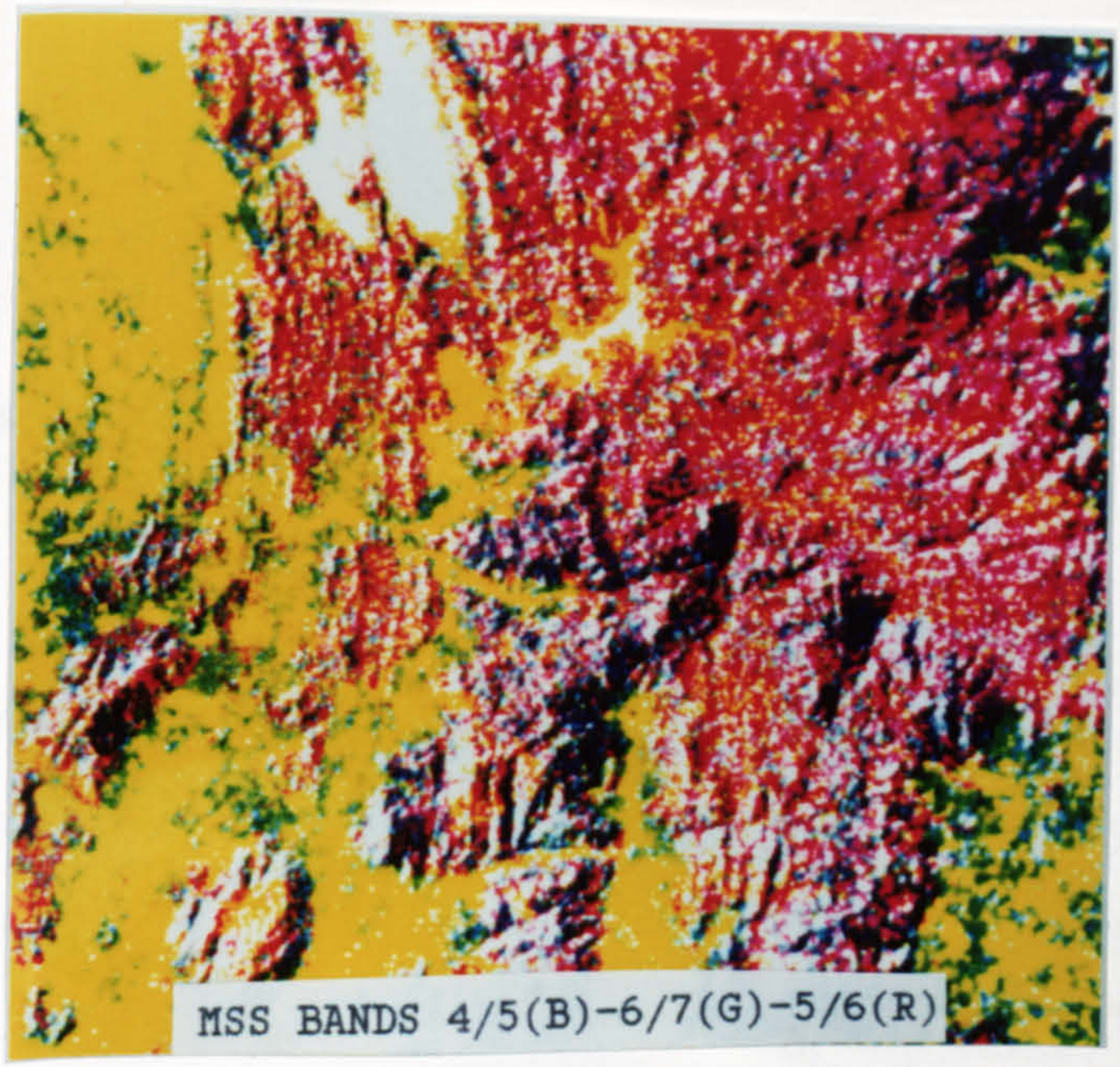

B MSS BANDS 4/5(B)-6/7(G)-5/6(R)

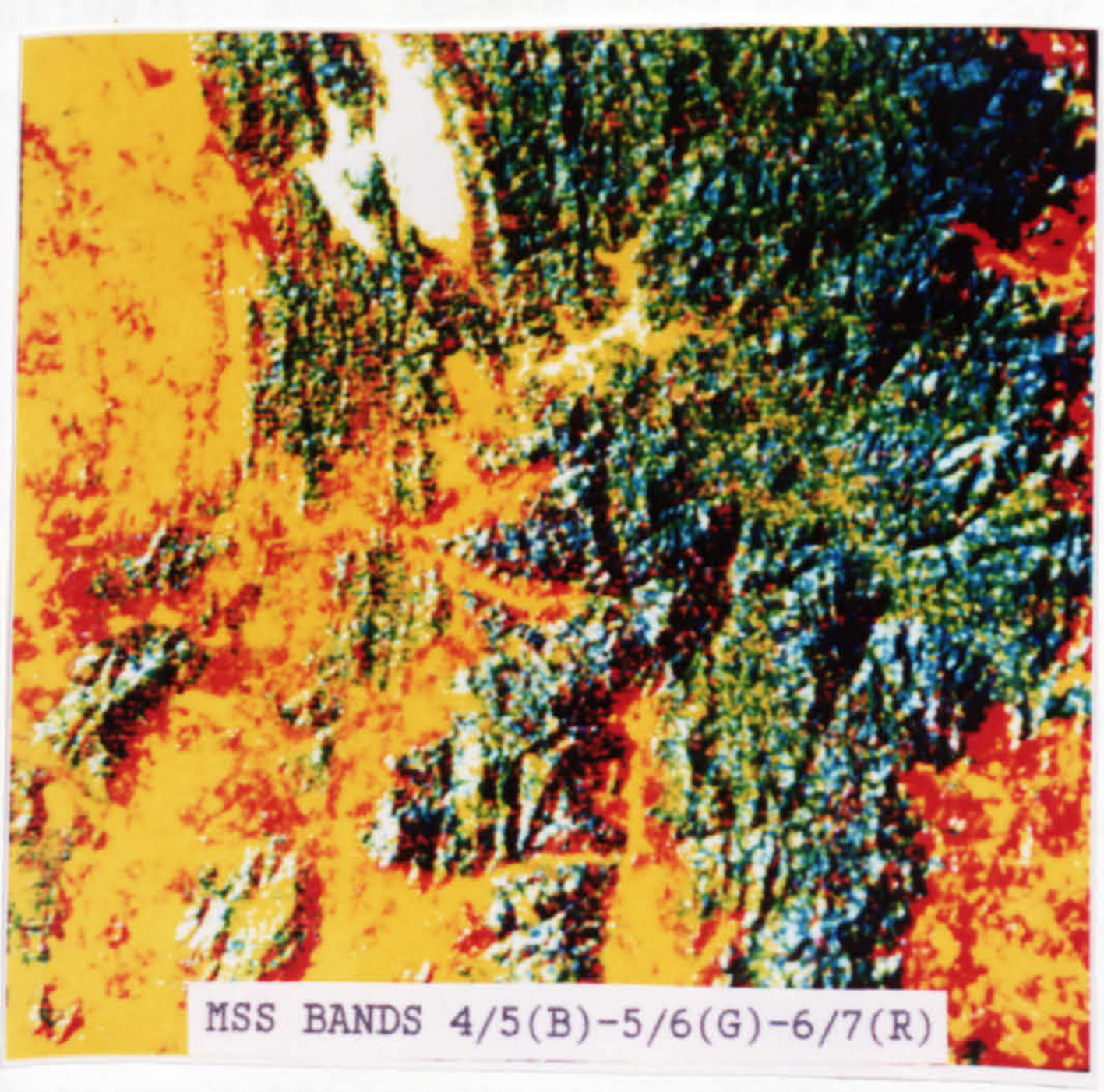

C MSS BANDS 4/5(B)-5/6(G)-6/7(R)

Figure 6.24 (continued)

area, it less informative than the first combination (2/1-7 / 1 - 3/1 combination). In addition, a few other combinations which had been reported in other publications (Podwysocki, 1983; Drury and Hunt, 1989), and which were supposed to enhance various features, were also tried, but the resultant images do not show better results or offer new information.

A few of the MSS ratio combinations produced for Kedah-Perak area are shown in Figure 6.24. Generally the resultant images did not show good colour variations compared with the previous colour composites. Figure 6.24B shows a colour ratio composite of MSS 4/5, 6/7, 5/6 displayed as blue, green and red respectively, and it did show more colour variation in water bodies which may be related to their depth or to suspended sediments in the water. This feature did not appear in other images before. The main rock units appeared in different colours, for example the granite appears purple whereas the metamorphic and sandstone/conglomerate appear orange purple, their boundaries however are not very well defined. The combination of the MSS band 5/6, 4/7, 4/6 with blue, green and red respectively (Figure 6.24A) enhances very well the relief-forming bands of the resistant lithological units and also their structural trends. Therefore, several major lineaments which correspond to several faults are better depicted, and also the relief impression between the granite (higher relief), the metamorphic (subdued relief) and the sandstone/conglomerate (moderate relief) are very well presented. Hence these features can be used to discriminate

between them rather than by their colour differences. Combination of the MSS bands 5/6, 4/7, and 5/7 displayed in blue, green and red respectively also gives a nearly similar result as the MSS bands 5/6, 4/7 and 4/6.

It had been mentioned in many publications that the most common colour ratio composite which aids visual interpretation in geological work is the combination of MSS 4/5, 5/6 and 6/7 which are displayed as blue, green and red respectively. This colour composite for Kedah-Perak area is shown in Figure 6.24C. In addition to this, two other colour ratio composites which had been reported useful in geological applications by previous workers are the combination of MSS 4/5, 5/7, 6/7, MSS 4/5, 4/6, 6/7, and MSS 4/5, 5/7, 7/4 displayed in blue, green and red respectively. Like the MSS 4/5, 5/6 and 6/7, it is evident that none of them produce better results or offer new information which can be used in discriminating of rock units in the area, rather they look much less useful compared to the previous ratioed images in terms of geological information content.

6.2.7 Filtering techniques

As mentioned earlier in the Chapter 5 (section 5.5), a technique called filtering has been developed to enhance linear features. With this aim, and in accordance with one of the objectives of the study, the MSS and TM sub-scene of the Loch Tummel and the MSS data of the Kedah-Perak areas which were chosen for lineament analysis were processed through the technique, in addition to the contrast enhancement (section

the contrast stretched image products of the original bands, it was found that the near-infrared Landsat MSS band 7, and the mid-infrared Landsat TM band 5 for the Loch Tummel, and the Landsat MSS band 7 for the Kedah-Perak areas proved best for structural (lineament) interpretation because of the sharp definition of geologic features. Consequently these images were processed through the filtering technique (section 5.5 in the Chapter 5) in order to enhance lineaments for both areas.

High-pass filtering

The contrast stretched images of the TM band 5 and MSS band 7 of the Loch Tummel sub-scene and the contrast stretched image of the MSS band 7 of the Kedah-Perak sub-scene were passed through the "edge enhancement" filter in the DIAD System as described in the section 5.5.2 in the Chapter 5. The aim of this process is therefore to get an overall effect which is to bring out linear pattern related to topography and fracturing. The edge-enhanced images for the MSS band 7 and TM band 5 for the Loch Tummel are shown in Figure 6.25A and B, and Figure 6.27 shows the edge-enhanced image of the MSS band 7 of the Kedah-Perak area. Generally the edge-enhanced images do show sharper edges and better contrast than the corresponding contrast stretched images. For example, several major lineaments which are related to known faults can be seen more clearly and better represented in the TM as well as MSS edge-enhanced image of the Loch Tummel. However, for the 1024 x 1024 image for the Kedah-Perak area, the edge-enhanced image

looks more noisy and less informative, and not useful for lineament mapping for the area.

Nondirectional filtering

The same data sources, contrast stretched images of TM band 5 and MSS band 7 of the Loch Tummel and MSS band 7 of the Kedah-Perak areas were also processed in the DIAD System through nondirectional filtering (section 5.5.3) with an aim to detect edges and boundaries on the images. After trying several filters (as mentioned in section 5.5.3), it was found that the following filter (Laplacian add back) is the best for producing nondirectional edge enhancement images in these study areas, and therefore this was applied to the data sources:

$$\text{nondirectional filter} = \begin{matrix} 0 & -1 & 0 \\ -1 & 5 & -1 \\ 0 & -1 & 0 \end{matrix}$$

The resultant images for the TM data and MSS data for the Loch Tummel sub-scene are shown in Figure 6.26A and B. Generally the images are good in terms of contrast and show more linear features than the corresponding contrast stretched images, however for the Kedah-Perak area, the resultant images look little bit "noisy". In this study, this image was passed through a low-pass filter which is able to suppress high frequencies detail (section 5.5.1), to make the image appear continuous, less "noisy" and show clearer definition for linear features. It is evident that the resultant image does

A MSS BANDS 7 - EDGE ENHANCED

B TM BANDS 5 - EDGE-ENHANCED

Figure 6.25 Edge-enhanced images for the MSS band 7 (A) and TM band 5 (B) of the Loch Tummel area. Scale 1:320,000. Note that many linear features are better enhanced (bright lines) on the MSS image with snow cover.

A MSS BAND 7 - LAPLACIAN ADD-BACK FILTERED

B TM BAND 5 - LAPLACIAN ADD-BACK FILTERED

Figure 6.26 Laplacian add-back filtered images for the Loch Tummel area: (A) MSS band 7 and (B) TM band 5. A few major lineament which are corresponding to a major fault are better displayed particularly in the TM image. Scale 1:320,000.

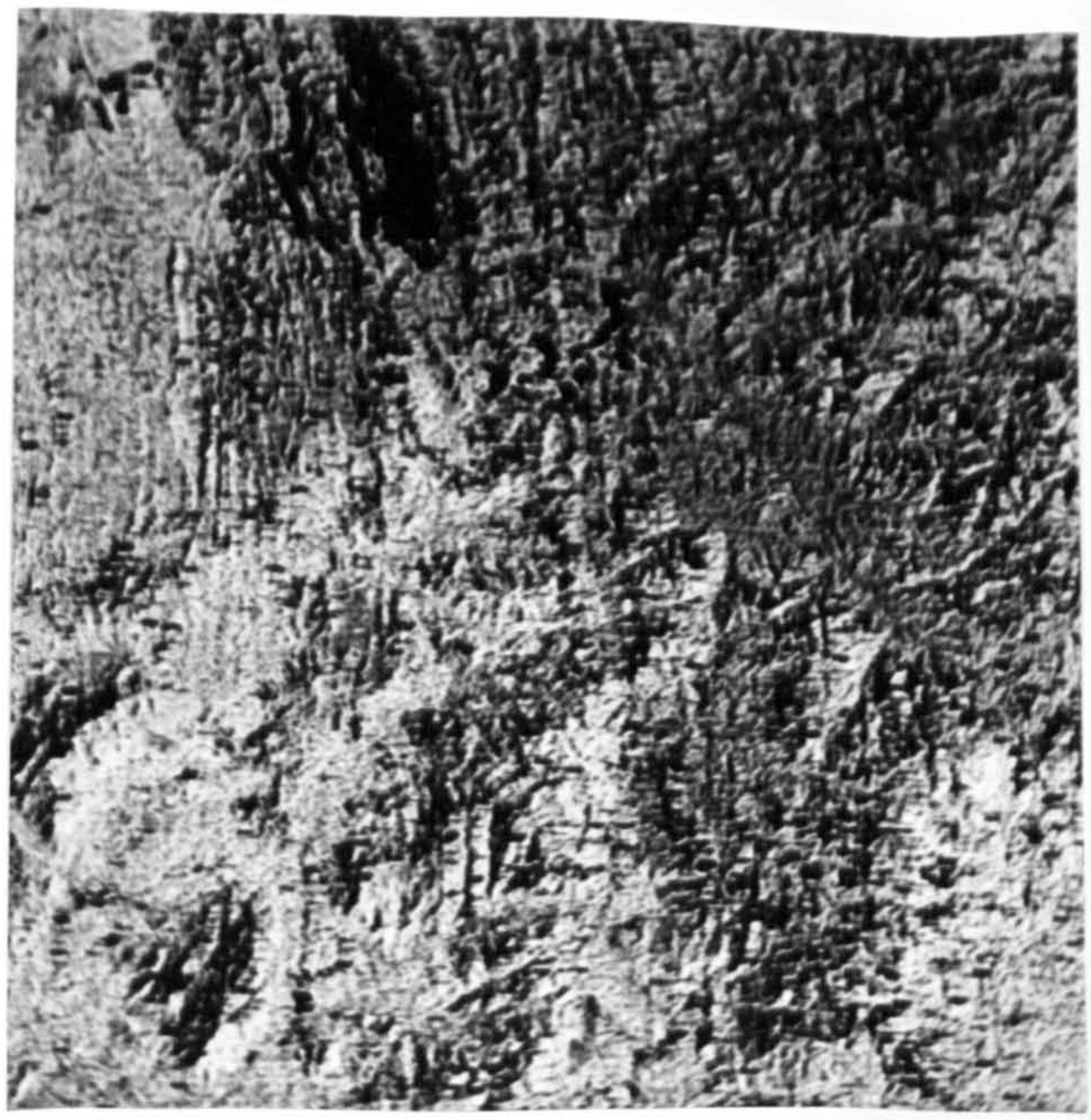

MSS BAND 7 - EDGE-ENHANCED

Figure 6.27 Edge-enhanced image for the MSS band 7 of the Kedah-Perak sub-area 1. Scale 1:300,000. Note that the image looks more noisy and less informative (structurally) than the original band 7 (Figure 6.6D).

MSS BAND 7 - LAPLACIAN ADD-BACK AND "SMOOTH" FILTERED

Figure 6.28 Laplacian add-back filtered image for the Kedah-Perak sub-area 1. Several major lineaments which may be related with geological faults are clearly shown. Scale 1:600,000.

show better contrast and better definition for linear features (Figure 6.28), and a few major lineaments can be seen more clear here than on the contrast stretched images.

Directional filtering

As discussed in Chapter 5, section 5.5.4, directional filtering proved to be of particular value in the enhancement or depiction of features with a preferred orientation, including geological linear features (lineaments). The same data sources (the contrast stretched images of the TM band 5 and MSS band 7 for the Loch Tummel sub-scene, and MSS band 7 for the Kedah-Perak sub-scene) which were found to reveal the most structural information in both study areas, were again used in the process. Four different images were then produced from each data sub-scene by different edge detection processes (two dimensional spatial convolution, see section 5.5.4 in the Chapter 5) in the DIAD System. Several directional filters (as given in section 5.5.4) were tried, and it was found that the three by three kernel filters with the following weighting factor arrangements, as mentioned by Drury (1987) and Mather (1987), produced the best result, hence these were used in enhancing linear features:

```
 -1  0  1
 -2  0  2   North-south enhancement
 -1  0  1

 -1 -2 -1
  0  0  0   East-west enhancement
  1  2  1
```

```
-2 -1  0
-1  0  1    Northeast-southwest
 0  1  2    enhancement


 0 -1 -2
 1  0 -1    Northwest-southeast
 2  1  0    enhancement
```

Some of the resultant images for both areas, the Loch Tummel and Kedah-Perak areas are shown in Figure 6.30 and 6.31, respectively. It is evident that many linear features, appearing as white lines with different length, were enhanced and quite well displayed especially in areas which are related to higher topography for both areas. The results for the Lochindorb area (Figure 6.29), however, show that only very few linear features have been depicted. These may be related to the topography of the area which is less pronounced or the results may well show that only a small numbers of linear features are present in the area. For the Loch Tummel and Kedah-Perak areas, although several linear features, several kilometres long, were well depicted and displayed, it appears that the shorter linear features are much more enhanced and very well depicted whereas many of the longer linear features seem to be under enhanced or undepicted. This makes the images look "noisy" with so many shorter linear features. The reason for this is possibly related to the kernel size used in the process where the 3 x 3 kernel (the only size available in the DIAD System) is theoretically more suitable for structures up to some 100 m in length (Chavez, 1983; Crósta and Moore, 1989). Apart from that, the directional filters enhancing only

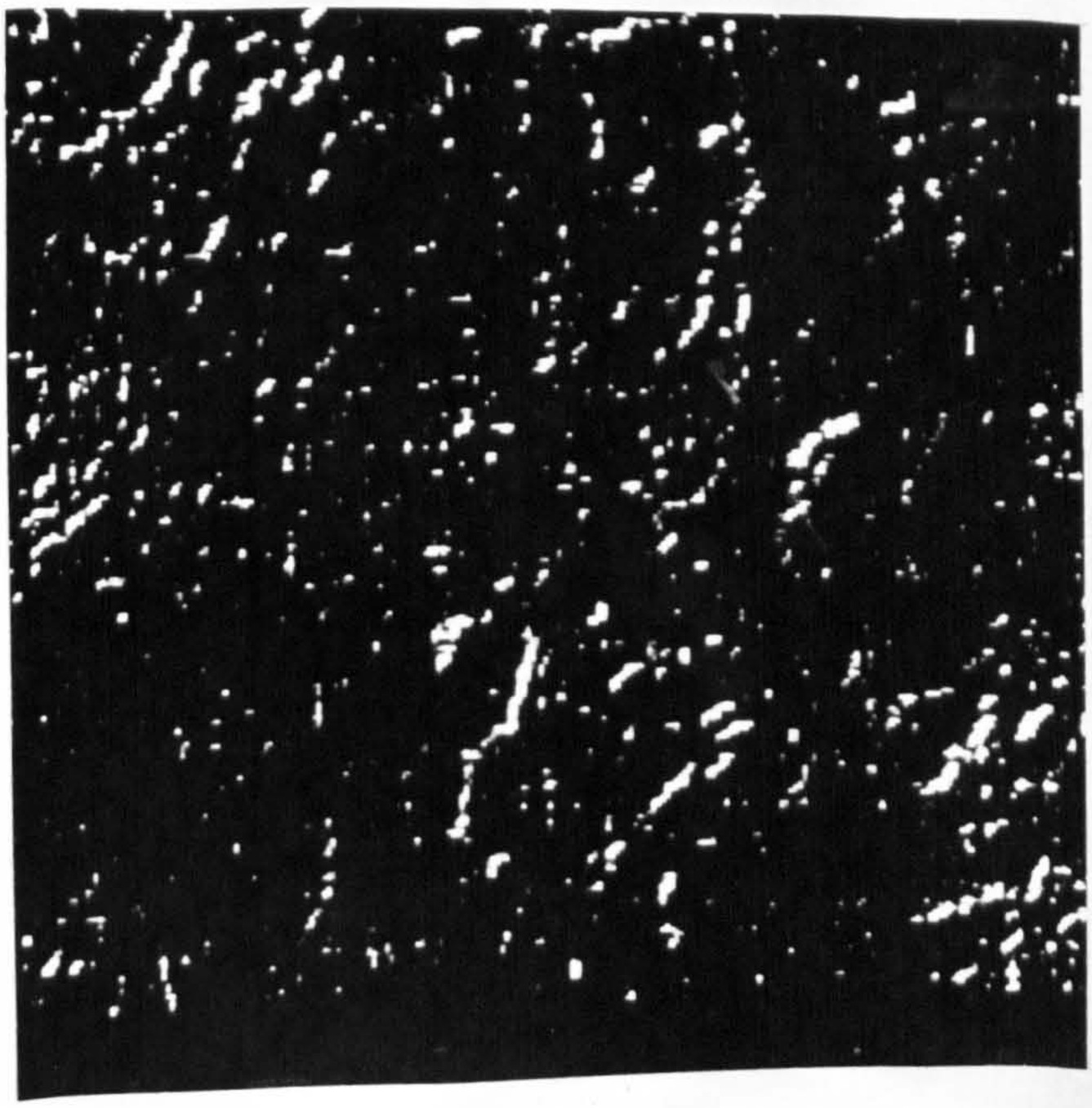

A MSS Lochindorb - NE-SW

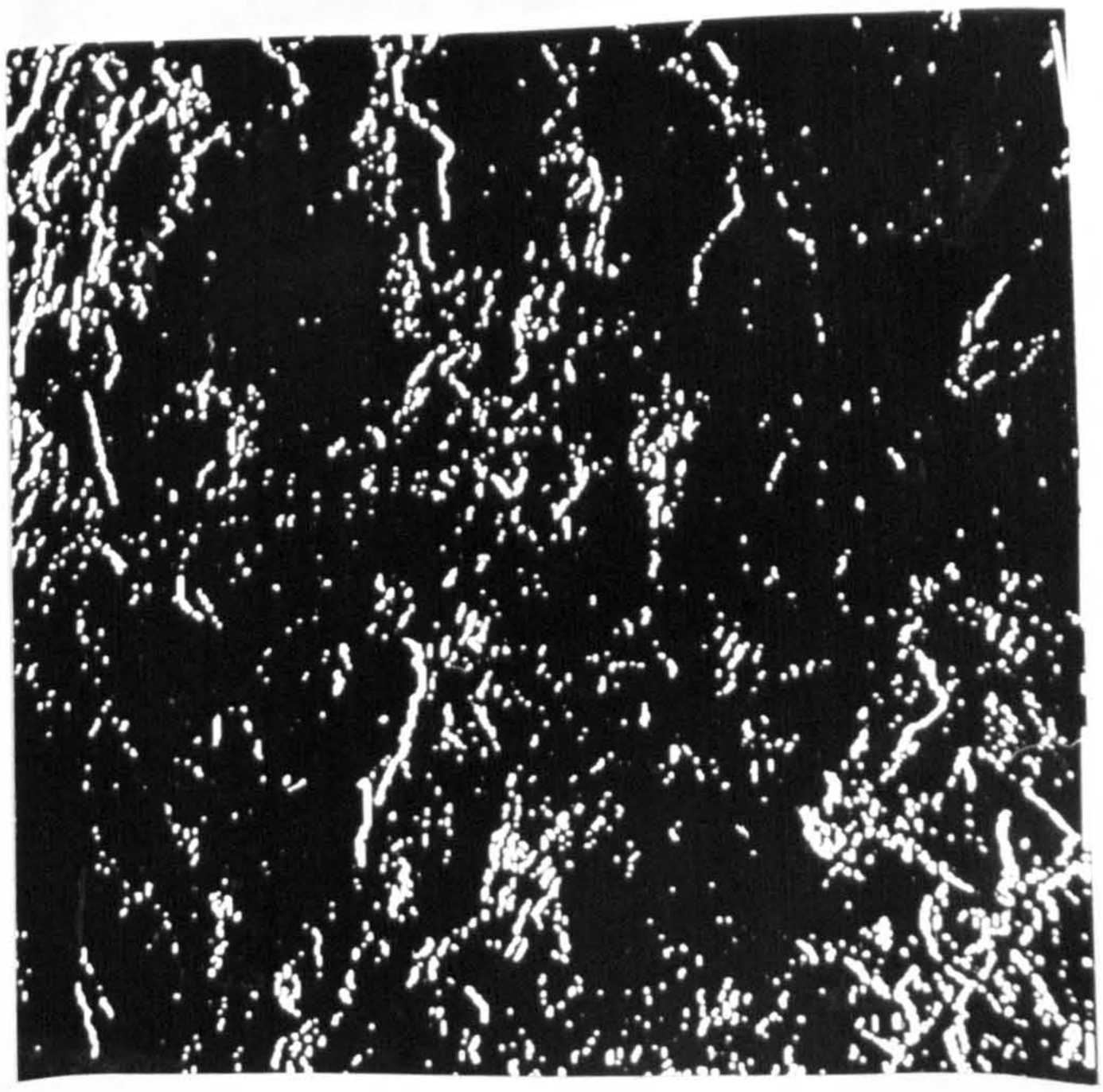

B TM Lochindorb - N-S

Figure 6.29 Directional filtered images for the Lochindorb area: (A) MSS band 7 and (B) TM band 5. Scale 1:160,000. Note that only a few lineaments are shown particularly in the TM image, however, many of them are in fact corresponding to non-geological linear features such as forest and agricultural field boundaries.

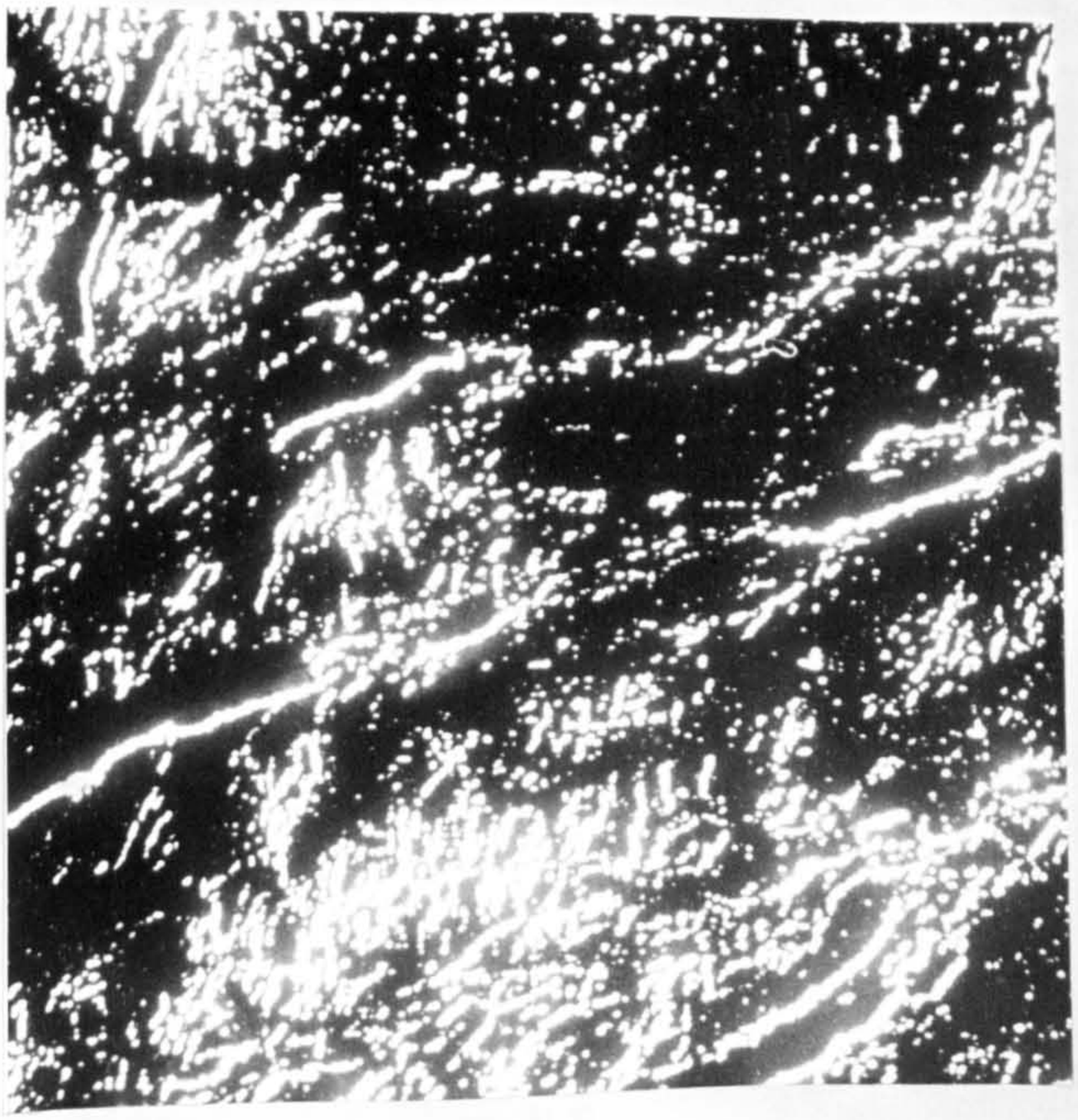

A MSS Loch Tummel - NE-SW

B TM Loch Tummel - NE-SW

Figure 6.30 Directional filtered images for the Loch Tummel area: (A) MSS band 7 and (B) TM band 5. Scale 1:320,000. Linear features are depicted and shown as white lines.

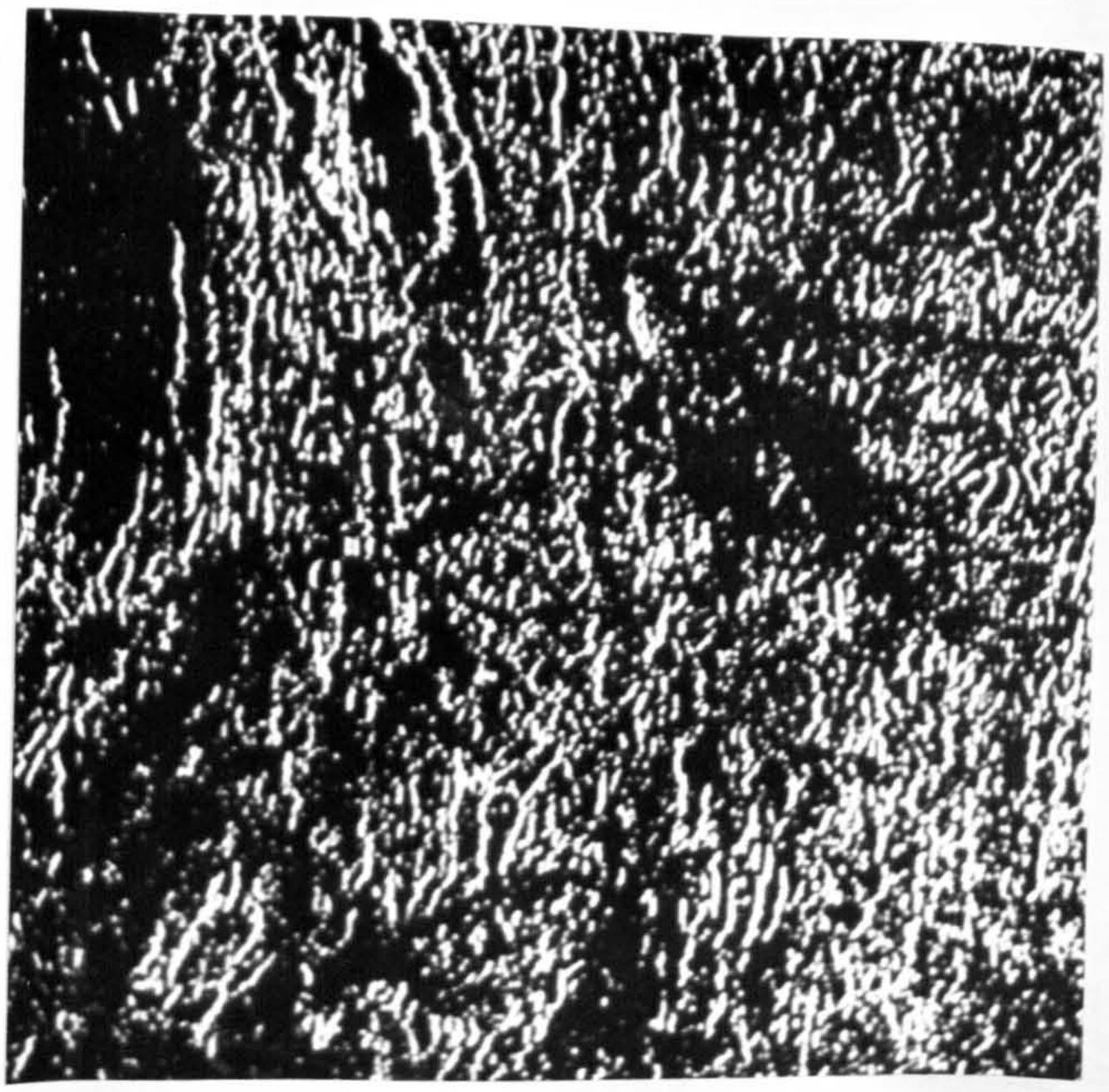

A MSS Kedah-Perak N-S

B MSS Kedah-Perak N-S

Figure 6.31 Directional filtered images (A-D) for the Landsat MSS band 7 of the Kedah-Perak sub-area 1. The following filters are used:

(A) $\begin{matrix} -1 & 0 & 1 \\ -2 & 0 & 2 \\ -1 & 0 & 1 \end{matrix}$ (B) $\begin{matrix} -1 & 0 & 1 \\ -1 & 0 & 1 \\ -1 & 0 & 1 \end{matrix}$ (C) $\begin{matrix} -1 & 2 & -1 \\ -2 & 4 & -2 \\ -1 & 2 & -1 \end{matrix}$ (D) $\begin{matrix} -2 & -1 & 0 \\ -1 & 0 & 1 \\ 0 & 1 & 2 \end{matrix}$

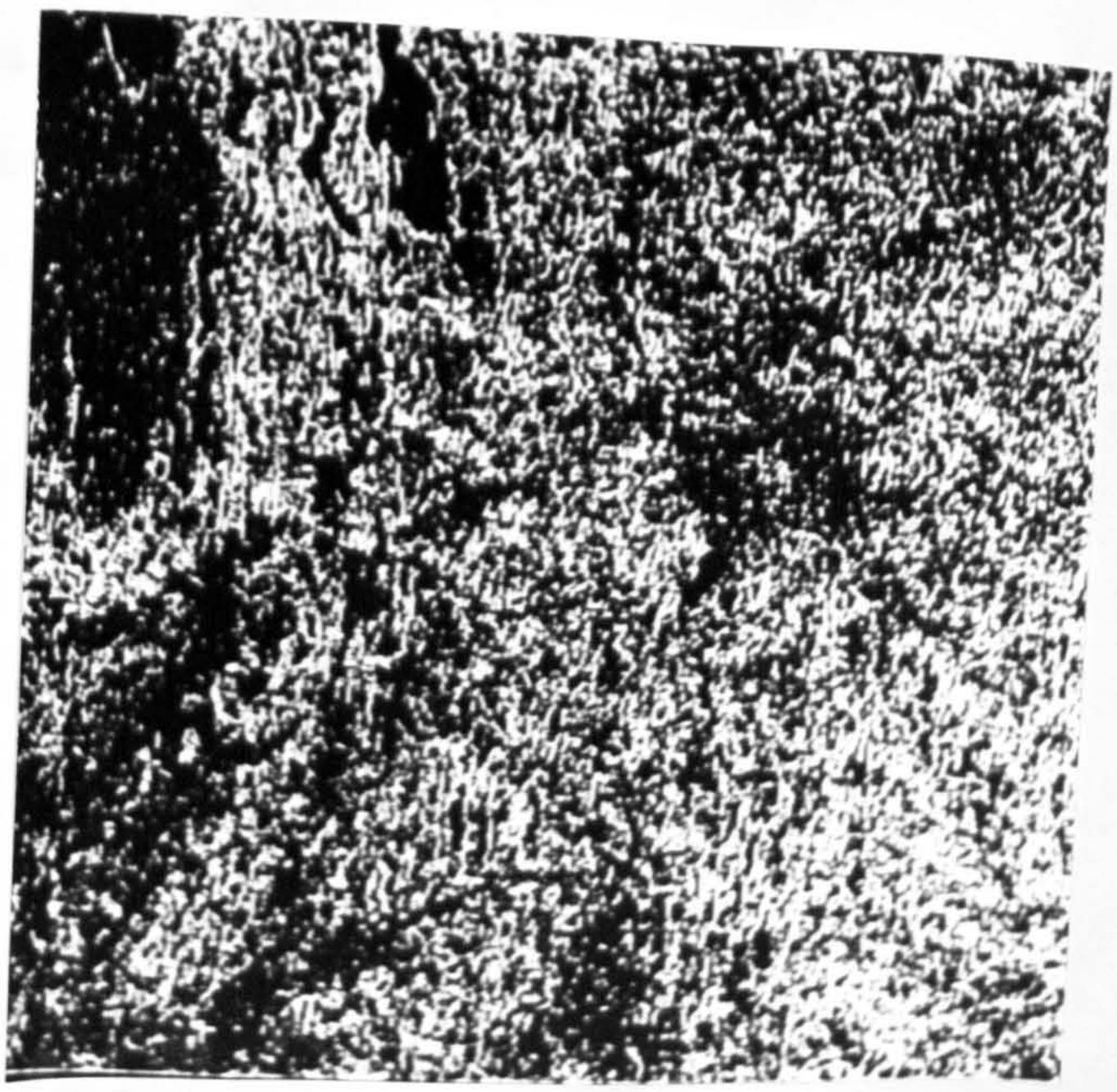

C MSS Kedah-Perak N-S

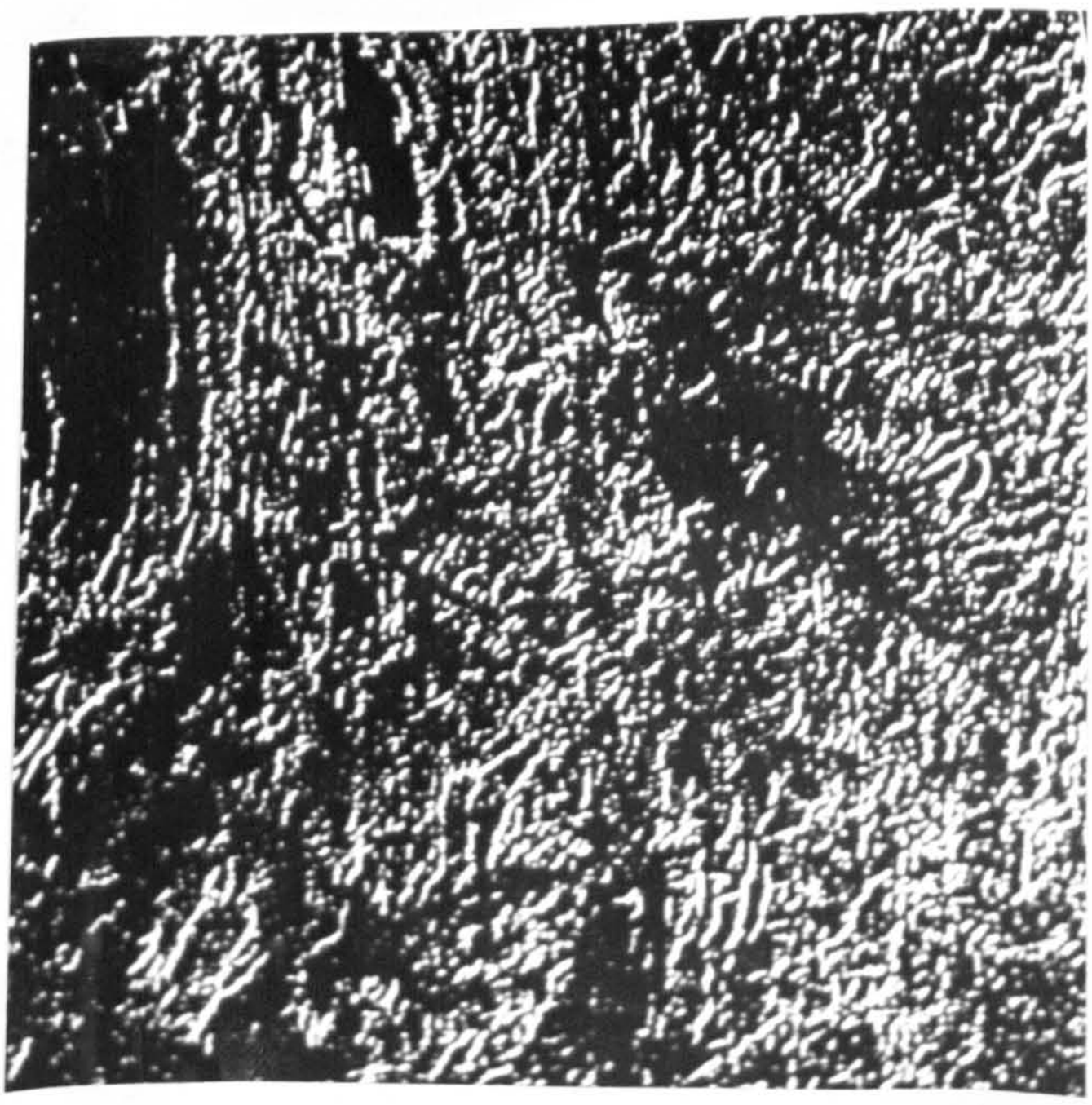

D MSS Kedah-Perak NE-SW

Figure 6.31 (continued)

linear features trending near the specified azimuth such as north-south or southwest (compare Figure 6.31A and 6.31D. In the results, some lineaments are only visible in individual enhanced images; such features are often artifacts of the processing. Therefore, with these conditions in mind, the delineation of lineaments from such images must be made with an objective method if possible, as mentioned in section 8.2 in Chapter 8, in order to minimise possible bias due to this factor.

6.2.8 Other processed images

Two other processes: image subtraction (section 5.4.1), and negative printing were employed on the TM and MSS data set for the Loch Tummel and MSS data set for the Kedah-Perak in order to see whether these could produce better images for lineament interpretation. The algorithms for the operations are available in the DIAD System.

Many image subtracting operations were tried between different bands for each data set. The resultant images did not show ground features any better than were shown on previous images. For example, the TM band 7-4 (Figure 6.32), although it shows good tonal variations and displays a few major lineaments, they are generally less pronounced. Other subtracted images are of poorer quality than the TM band 7-4 image.

In addition to the above processing, several "negative" images of the original bands, particularly the bands which visually proved best for lineament interpretation because of

the sharp definition of geologic features, were produced through the algorithm available in the DIAD System. Some of the resultant images do show some improvement over the original band images particularly in terms of displaying the lineaments. Figure 6.33A shows the negative image of TM band 5 for the Loch Tummel area. Because of the nature of negative images, the image shows opposite grey tones of the positive image (Figure 6.5D), that is the darker areas in the positive images will appear lighter in the negative images and vice versa. Therefore, it is evident that the negative image does display some lineaments, particularly the one which is related to the subdued topography or shadowed areas where in both cases it appears rather dark grey to black in the positive images, deemphasising the details including lineaments, but in the negative images these areas appear much lighter, therefore some details in them may be observed. However, some details which appear in the lighter tones of the positive images may be deemphasised in the negative images because they appear as rather dark grey tones or even black. It appears that the negative image can offer additional information to the corresponding positive image, and therefore it may be used as complimentary to the positive image rather than replace it as a data source for lineament extraction. Negative images of MSS band 7 for sub-areas 1 and 2 of the Kedah-Perak area are shown in Figure 6.33B and C.

TM BANDS 7-4

Figure 6.32 TM band (7-4) image of the Loch Tummel area. Scale 1:320,000.

A TM BAND 5 - NEGATIVE IMAGE

Figure 6.33 Negative images of TM band 5 of the Loch Tummel area (A), MSS band 7 of the Kedah-Perak sub-area 1 (B) and sub-area 2 (C). The images show opposite grey-tones with their corresponding positive images. Scale 1:320,000 (image A) and 1:600,000 (image B and C).

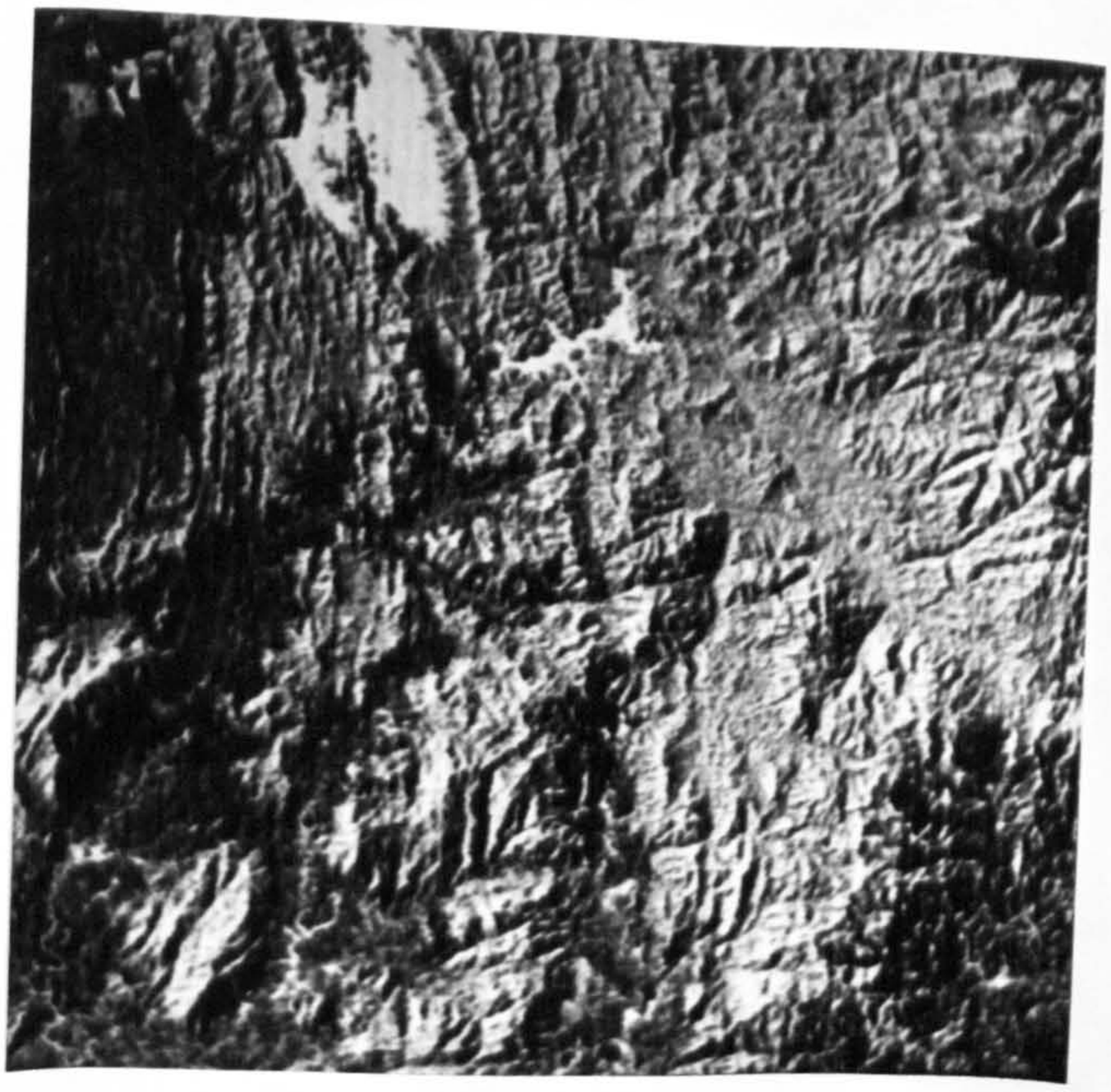

B MSS BAND 7 - NEGATIVE IMAGE

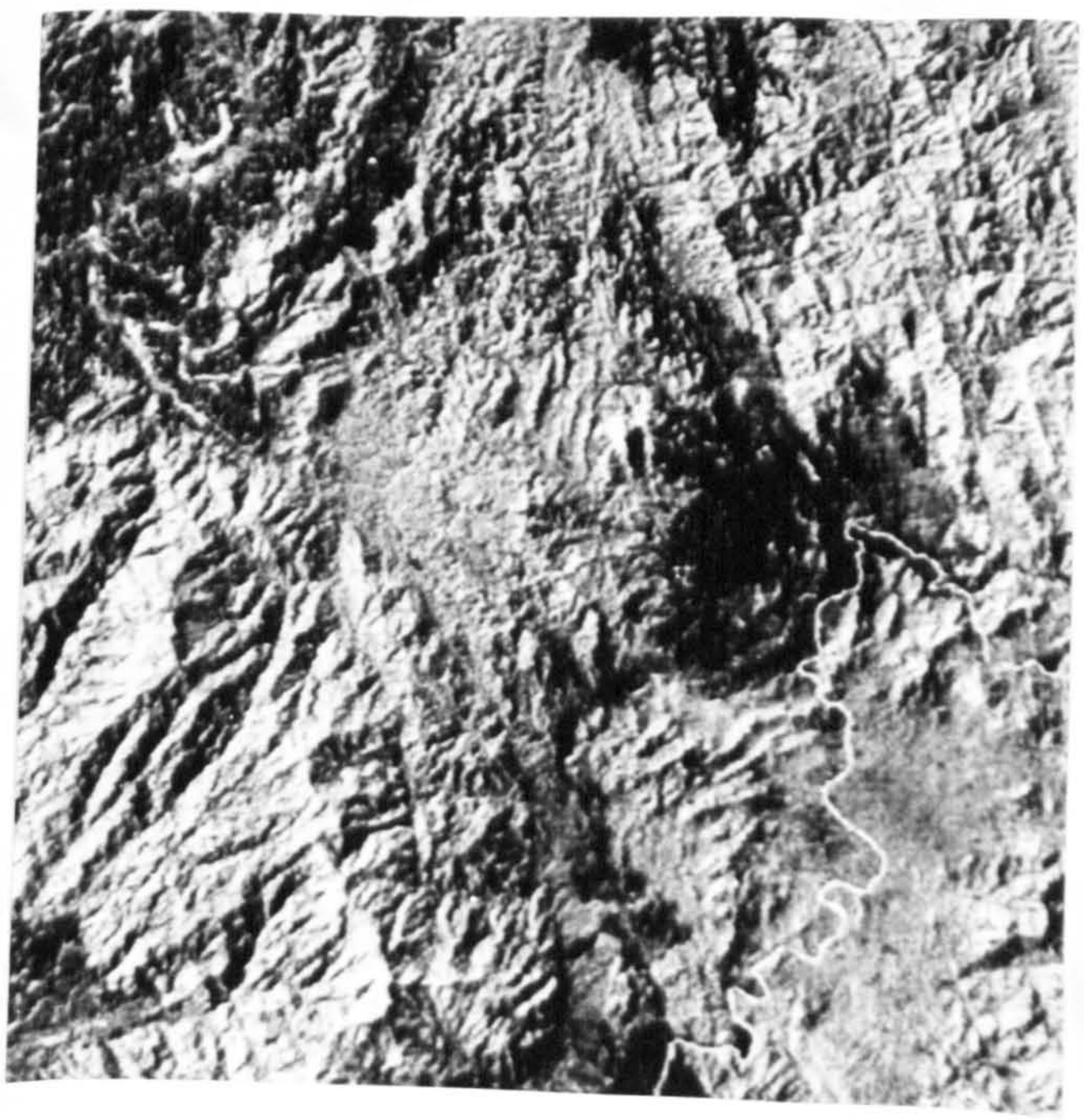

C MSS BAND 7 - NEGATIVE IMAGE

Figure 6.33 (continued)

6.3 Comparison of the geological information content of enhanced image products

A comparison of the geological information content of several enhanced image products, which were selected based on their general assessment in section 6.2, will be carried out in terms of (a) lithological/surface material discrimination (for example, separately involving discrimination between rock and surface material, between different rock units and between different surface material units), and (b) structural discrimination (for example, the identification of lineaments, representing faults and other fractures). Geological interpretation of the data products is a highly subjective process which involves visual integration of various types of information like photo-characteristics (tone, texture), morphological expressions (drainage, rock properties), and covers (surficial material, vegetation, cultivation). Therefore, there is no clear way in which the relative merits of different data products can be accurately compared or assessed. In this study, however, lithological, surface material and structural discrimination (restricted to the identification of lineaments, representing faults or other fractures) were assessed by comparing information on the 1:50,000 drift map (BGS sheet 84E, 1978), the 1: 50,000 and 1: 63,360 geologic maps (BGS sheet 54E, 1974 and BGS sheet 55, 1967) and the 1:500,000 geologic map (Geological Survey of Malaysia, 1985) with spectral/textural units identifiable on the image products which are equivalent to variations in vegetation, soil, rock, etc. for the study areas. This

assessment method was based on the methods which were employed by Rakshit and Swaminathan (1985) and Greenbaum (1987). For the Lochindorb area, however, only surface material discrimination of the data products was assessed because of lack of structural information in the area (as shown in the published map (Figure 2.4 and 2.5) as well as in the processed images (section 6.2.7 and Figure 6.29). However, the overall relief impression and drainage appearance on each data product of the area will be stated. For the Loch Tummel area, only structural discrimination (identification of lineaments) of the image products was assessed. For the Kedah-Perak area, the discussion will be focussed only on the image products of the sub-area 1 rather the sub-area 2, because it contains all the main rock types based on the published map.

In order to carry out this assessment, an overlay of geological boundaries drawn from the corresponding map was superimposed and compared in turn with each selected image and a score assigned in the range 0 to 5 (0, almost nil; 1, poor; 2,fair; 3,good; 4,very good; 5,obvious) according to the perceived discrimination across each of a number of selected points of geological boundaries in the map. For convenience, in this study 50 selected points (based on the points of intersection between boundary lines with N-S and E-W lines drawn at every 2 km interval) on geological boundaries (25 for glacial-peat, 10 for glacial-bedrock, 5 for glacial-alluvium, 5 for peat-alluvium and 5 for peat-bedrock boundaries) for the Lochindorb and 32 points (based on the points of intersection between boundary lines with N-S and E-

W lines drawn at every 10 km interval) on geological boundaries (20 for granite-metamorphic, 3 for granite-sandstone/conglomerate, 3 for metamorphic-sandstone/conglomerate, 3 for granite-shale/mudstone, 3 for sandstone/conglomerate-shale/mudstone) for the Kedah-Perak areas were chosen and used in the comparison process. The number of point selected for a certain unit generally reflects the abundance of that unit in the area, where the bigger the number the more widespread the unit. For the structural discrimination, 25 major faults (on the published map) were chosen and used for the sub-area 1 of Kedah-Perak and 8 fault sections (on the published map) for the Loch Tummel area, and similar scores were assigned according to the prominence of lineaments and the degree of certainty with which they could be identified. One point must be noted and kept in mind throughout the assessment, that in the conversion of slides (which were used during the assessment) to photographs (produced for display) some of the clarity has been loss, hence observation of the image is better with slides. The results of the comparative assessment of geological information on various image products of the Lochindorb, the Kedah-Perak and the Loch Tummel areas is presented in Table 6.7, Table 6.8 and Table 6.9, respectively, and the following discussion will be focused on those results.

Table 6.7 and Table 6.8 show that for both areas, total scores calculated for each image product in each category as a percentage of the maximum possible were found to vary quite widely between the different discrimination categories. For

Image/image combination	Lithology-surface material score			Structure score	Final score	Final ranking	OIF
	glacial/peat	peat/bedrock	glacial/bedrock				
B1	20.4	12.5	7.1	1	13.3	27	
B2	26.5	25.0	14.3	1	21.9	23	
B3	30.6	37.5	21.4	2	29.8	19	
B4	12.2	12.5	28.6	4	17.8	24	
B5	22.4	25.0	42.9	4	30.1	18	
B7	12.2	12.5	21.4	3	15.4	26	
PC1	18.4	12.5	35.7	3	22.2	22	
PC2	14.3	25.0	7.1	1	15.5	25	
DF1	10.2	25.0	50.0	2	28.4	20	
DF2	28.6	37.5	14.3	2	26.8	21	
B1-5-4	63.3	50.0	57.1	3	56.8	7	1
B3-5-4	44.9	75.0(3)	64.3	3	61.4	6	3
B4-5-7	51.0	37.5	78.6(3)	4	55.7	8	5
B1-3-4	79.6(2)	75.0(3)	85.7(2)	3	80.1	3	6
B1-3-5	40.8	62.5	42.9	2	48.7	11	9
B2-3-4	44.9	50.0	57.1	3	50.7	10	13
B2-3-5	34.7	50.0	28.6	1	37.8	15	16
B1-2-3	34.7	37.5	21.3	1	31.3	17	19
PC 3-2-1	44.9	25.0	71.4	2	47.1	13	
PC 4-1-2	36.7	37.5	71.4	2	48.5	12	
PC 5-3-2	51.0	37.5	42.9	1	43.8	14	
PC 5-4-2	34.7	12.5	50.0	0	32.4	16	
DF3-2-1 or DF 3-1-2	100 (1)	87.5(2)	78.6(3)	2	88.7	2	
DF2-3-1	61.2	62.5	64.3	2	62.7	4	
R2/1-7/1-3/1	73.5(3)	100 (1)	100 (1)	2	91.2	1	
R3/2-5/2-7/4	61.2	62.5	64.3	2	62.7	4	
R4/5-7/1-3/1	73.5(3)	50.0	35.7	2	53.1	9	
Actual maximum score (%)	39.2	32.0	28.0				

B, TM bands; PC, principal component; DF, discriminant function; R, TM ratio; OIF, optimum index factor. Numbers in brackets denote rankings in individual categories. * Structure score based on overall relief impression and drainage appearance only: 0, almost nil; 1, poor; 2, fair; 3, good; 4, very good; 5, obvious, and was not counted in the final score.

Table 6.7 Comparison of the geological information content of TM imagery of the Lochindorb area. Scores for lithology-surface material have been re-scaled to percentage success. Actual maximum percentage scores in each category are also shown.

Image/ image combination	LITHOLOGICAL SCORE								
	granite/ metamorphic	granite/ sandstone	metamorphic/ sandstone	granite/ shale	sandstone/ shale	total litho-logical score	Structure score	Final score	Final ranking
B4	34.1	28.6	40.0	25.0	77.7	41.1	58.9	44.1	18
B5	43.2	42.8	40.0	37.5	77.7	48.2	63.3	50.7	17
B6	70.4	28.6	80.0	37.5	88.8	61.1	86.7	65.3	12
B7	79.5	71.4	80.0	50.0	55.5	67.3	100 (1)	72.8	8
PC1	68.2	71.4	40.0	50.0	77.7	64.3	86.7	65.7	11
PC2	52.3	28.6	80.0	50.0	44.4	51.1	95.5(3)	58.5	15
DF1	63.6	85.7(2)	60.0	62.5	66.6	67.7	73.3	68.6	10
DF2	61.4	28.6	80.0	62.5	66.6	59.8	88.9	64.7	13
B7 (addback filtered)	70.4	28.6	60.0	50.0	55.5	52.9	97.2(2)	60.4	14
R7/4	75.0	42.8	60.0	37.5	55.5	55.5	80.0	58.5	15
B4-5-7	86.4	71.4	100(1)	62.5	88.8	78.0	88.9	83.5	3
PC3-2-1	93.2	57.1	80.0	62.5	100(1)	78.5	88.9	83.7	2
PC4-1-2	90.9	85.7(2)	80.0	44.4	77.7	75.7	77.8	76.1	7
PC4-3-2	95.4(3)	71.4	80.0	62.5	77.7	85.1	74.4	76.9	6
DF3-2-1	81.8	42.8	80.0	62.5	88.8	71.2	77.8	72.3	9
R6/7-4/6-4/5	97.7(2)	71.4	40.0	87.5(2)	88.8	77.1	83.3	78.1	5
R5/6-4/7-4/6	79.5	100(1)	80.0	100 (1)	100(1)	91.9	91.1	91.8	1
R4/5-6/7-5/6	100(1)	71.4	60.0	87.5(2)	88.8	84.8	67.8	79.2	4
Actual maximum score (%)	44.0	46.6	33.3	53.3	60.0		72.0		

B, MSS bands; PC, principal component; DF, discriminant function; R, ratio. Numbers in brackets denote rankings in individual categories.

Table 6.8 Comparison of the geological information content of MSS imagery of the Kedah-Perak area. Scores for lithology and structure have been re-scaled to percentage success. Actual maximum percentage scores in each category are also shown.

example, total scores for the glacial deposit-peat, peat-bedrock and glacial deposit-bedrock for the Lochindorb area are 39, 32 and 28 per cent respectively, and for the granite-metamorphic, granite-sandstone/conglomerate, metamorphic-sandstone, granite-shale/siltstone, sandstone/conglomerate-shale/siltstone and the structure category for the Kedah-Perak area are 44, 46, 33, 53, and 60 and 72 per cent respectively. For the purpose of ranking images the method employed by Greenbaum (1987) is adopted here where these differences were ignored and scores re-scaled so that the highest-ranked in each category was equal to 100. An overall score for each image product was obtained from the simple average of the four re-scaled scores. Although the score is not strictly a true mean score, this gave to each discrimination category an equal weighting, which would seem appropriate from a geological interpretation viewpoint (Greenbaum, 1987).

For the Lochindorb area, considering all the image products which were assessed, the band-ratio colour-composite (RCC) TM bands 2/1, 7/1 and 3/1 displayed in blue, green and red respectively (Figure 6.23A), was found to be the best for discrimination between peat-bedrock and between glacial deposit-bedrock. The discriminant analysis colour-composite (DCC), DF 3-2-1 (Figure 6.19A), on the other hand, offers the best discrimination between the glacial and peat (the main deposits in the area). These two images were found to be considerably better than the best band colour-composite combination (based on OIF), TM bands 1,5,4 in Figure 6.7A (except for structural information)). Not only that, two other

band colour-composites, TM bands 1,3,4 (Figure 6.7D, ranked sixth in the OIF) and TM bands 3,4,5 (Figure 6.7B, ranked third in the OIF) were also more informative than the TM bands 1,5,4 combination (Table 6.7). No actual assessments were made for the structural discrimination in each of the image products for the area, however their general impression for this information was observed and the results show that structural information was found to be significantly better on both colour-composite (TM bands 4,5,7 in Figure 6.7C) and black and white single bands (TM band 4 and TM band 5 in Figure 6.3D and E respectively). After further observation between these three image products, the TM band 5 was found to be best overall, the other two were found to be more or less equally good, in terms of structural information. This is probably due to the fact that the TM band 5 is a maximum rock reflectance band, hence it shows sharp definition of rock-type boundaries (Crósta and Moore, 1989) and the human eye is more responsive to features of higher spatial frequency in monochrome than in colour (Drury, 1986a), therefore for structural studies, black and white images are more effective than those in colour.

In Table 6.7, final score and overall rankings show that the single most informative image in this study area is given by band-ratio colour composite TM bands 2/1-7/1-3/1 (Figure 6.23A). The result suggests, as reported by many workers (Rowan et al., 1974; Condit and Chavez, Jr, 1979; Drury, 1987; Sabin, 1987), that the band ratio technique is an effective method of enhancing spectral differences or colour differences

and effectively minimizes the effect of variable degrees of brightness caused by the environmental factors and suppressing differences in albedo variation. The discriminant analysis colour-composite TM DFs 3-2-1 (Figure 6.19A) or DFs 3-1-2 (Figure 6.19C) was placed second (very close with the first rankings) and TM bands 1-3-4 colour-composite (Figure 6.7D) was placed third in the rankings. For the TM DFs combination, the nature of its image products which contain "separable spectral classes" has produced images which offer overall better separation especially between the glacial and peat deposits. The first two images, however, show less structural information than the third image. It is apparent, therefore, that no single image is best in all aspects for geological application in the area, and consequently therefore, a geological interpretation in the area would benefit from using several image products, for example the TM band-ratio 2/1-7/1-3/1 and TM DF 3-2-1 colour composites and the TM band 5. It was found that the image products from principal component analysis seem to be much less informative than many other images, and in one instance the lower-order of the PCC is more informative than the higher-order (for example the principal component 5-3-2 offers better discrimination between the glacial deposit and peat than the PC 3-2-1 , see Table 6.7), however, this lower-order PCC, because of its low variance content, is still much less informative in the final rankings than many other colour-composite images. This result is possibly because of the subtle spectral differences between cover types of these two deposits is better represented in the

lower-order images than in the higher-order which contain mainly spectral responses from rather homogeneous cover types like forest, grass, water bodies and agricultural lands. Therefore in higher-order PCC, for example the PCC 3-2-1 combination, the very high percentage of variance content is possibly contributed mainly by these cover types, consequently these are shown very clearly in the corresponding image (Figure 6.14B). However the discrimination between the two main deposits: the peat and glacial, which was based on the subtle spectral responses of their less uniform cover types, is perhaps much less represented here, hence their spectral differences and boundary delineation are not clearly shown. Among the TM band colour-composites, the TM bands 1-3-4 combination (Figure 6.7D) is ranked highest in terms of geological information content and far better than the best band combination (TM bands 1-5-4) based on the OIF. The characteristics of the TM band 1 (useful for soil/vegetation discrimination), TM band 3 (designed to sense in a chlorophyll absorption region aiding in plant species differentiation) and TM band 4 (useful for determining vegetation types, vigor and biomass content) (see Table 4.4) are possibly more suitable and able to record and show the differences in spectral response between different cover types in the area which are related to the geological units. The TM bands 3-5-4, the second best band combination based on OIF was rated slightly more informative than TM bands 1-5-4 (Table 6.7). Apart from this, the final rankings for band combination, as rated for geological interpretability, are generally consistent with OIF

rankings, however the correspondence is not exact. Therefore, it seems that while the OIF is an easily-computed guide to useful band combinations, the results do not necessarily produce the most informative images for geological interpretation. Nevertheless it is reasonable to expect the overall spectral response as indicated by this method to provide at least a guide to geologically useful band combinations. Therefore in the study area, by observing the first six or seven rankings (often band combinations that are within 2 to 3 rankings of each other appear similar in colour-composite form because there is little difference in their total information content as shown by Chavez et al., 1984) rather than all 20 possible 3 band combinations, the process is made less tedious and inexpensive, for finding the best band colour-composite combination. In the assessment, all the black and white image products were found to be less informative than the colour-composite products in this assessment. Beside the fact that our eye can perceive many more shades of colour than tones of grey (Ray and Fisher, 1957; Yost and Wenderoth, 1967; Billingsley et al., 1970), this may indicate that for the surface material or rock-type discrimination, information provided by spectral characteristics of the terrain are important.

For the Kedah-Perak area, considering all the imagery products which were assessed for their geological information content, the band-ratio colour-composite MSS bands 5/6-4/7-4/6 displayed in blue, green and red respectively (Figure 6.24A) were found to be best for lithological discrimination

between the granite:sandstone/conglomerate, granite:shale/siltstone and sandstone/conglomerate:shale/siltstone, while MSS bands 4/5-6/7-5/6 (Figure 6.24B) were best for discrimination between the granite and metamorphic rocks and the MSS bands 4-5-7 colour composite (Figure 6.10A) was found to be best for discrimination between metamorphic:sandstone/conglomerate. Once again, for similar reasons as mentioned before, the structural information in black and white image products is more informative than the colour-composite products. The top two rankings in this category are of this type of image product, where the contrast stretched MSS band 7 (Figure 6.6D) was found the best followed by the filtered MSS band 7 using the Laplacian convolution filter (Figure 6.28).

In Table 6.8, for this area, the final score and overall rankings show that the single most informative image product is given by the band-ratio colour-composite of MSS bands 5/6-4/7-4/6 as shown in colour in Figure 6.24A. Like other image products for the area, not much information may be gained from its colour (most of the area is covered by dense tropical forest hence it is represented by almost one colour over a large area). Notwithstanding, other image characteristics particularly texture are well enhanced (this is possibly due to the nature of the ratioing process which can effectively minimize the effect of variable degrees of brightness caused by environmental factors, hence it will enhance or display the true surface characteristics better), consequently the impression of relief, drainage pattern and structural features

especially lineaments and strike ridges are better displayed and hence it is very useful for geological interpretation of this particular area. The highest variance content in the principal component combination (PC 3-2-1) (Figure 6.16A) was place second, while the standard false colour-composite of MSS bands 4-5-7 was ranked third (Figure 6.10) (slightly lower than the PC 3-2-1 combination) (Table 6.8). As in the Lochindorb area, given the rankings in individual categories, it is apparent that no single image is best in all respects for geological discrimination, therefore a better interpretation can be made by using several images. The discriminant function combination, for example DF 3-2-1, was placed in a much lower position in the final rankings. The result shows that the vegetation cover in the area has proved too heavy for this technique. The image products from the discriminant analysis seem to be less informative in terms of structural information (fractures, lineaments, faults and drainage pattern), where a large area is covered by dense tropical forest. In this case structural features are more important than colour in order to infer the rock types in the area. Because of this, therefore it is perhaps not surprising that the MSS band 7 (Figure 6.6D), which displays better surface features, was rated slightly more informative than the DFs 3-2-1 in the final rankings despite the fact that our eye can perceive more shades of colour than tones of grey.

The structural assessment results for several image products of the Loch Tummel TM sub-scene are shown in Table 6.9 in order to find out the best two images for lineament

Image/image combination	Structure score	Final ranking
B5	80.9	3
B5 (edge enhancement)	90.5	2
B5 (addback filtered)	100	1
B 7-4	76.2	4
B 3-4-5	66.7	6
B 7-5-4	71.4	5
Actual maximum score (%)	52.5	

B = TM bands.

Table 6.9 Comparison of the structural information content of TM imagery of the Loch Tummel area. Scores have been re-scaled to percentage success. Actual maximum percentage score in the comparison is also shown.

interpretation of the area. The filtered images of the TM band 5 (using Laplacian filter) and high pass (edge enhancement) filter) were found to be best for this purpose. Both images (as shown in Figure 6.26B and Figure 6.25B) were chosen and used in the lineament analysis for the area (as describe in the Chapter 8). Based on visual observation, similar image products for the MSS data for the same area, as shown in Figure 6.26A and Figure 6.25A, were found to be best, and were used for the same purpose.

This method of assessment is not wholly objective because of the nature of the subject which is highly subjective, however it gives a means of obtaining a semi-quantitative estimate of comparative geological interpretation of different data products for two study areas. Another important point must be stressed that the relative importance for geological interpretation of the different bands, principal component analysis, band-ratioing and discriminant analysis will be scene dependent to a large degree. Therefore, the rankings shown in this study will not necessarily be valid elsewhere. Even the results from this study have indicated that the best three images for geological interpretation for the two study areas are not identical even from the same image processing techniques. It has been said that the colour combination can significantly affect the individual's ability to make certain distinctions (Skaley et al., 1977). The example of this phenomenon is demonstrated in Figure 6.19, where in terms of band combination, all of them are the same, however their colour combinations are different and it was evident that the investigator's ability to make certain distinctions between them is different. Hence in many instances, including the TM band colour-composites where the OIF was calculated with the assumption that only band combinations were of importance and the six possible colour combinations for each band combination did not affect information content, several colour combinations of a single three-band combination were generated in order to get better images for interpretation in this study.

6.4 Summary

Examples of the image products of all the image processing techniques employed in this study are presented, and their general assessment is discussed. It is clear that through simple digital image processing such as linear contrast stretch, better images can be produced, and more information can be extracted from them compared to the original (unprocessed) data. Further manipulations of the data can offer better results and/or further information.

The assessment of the geological information content of the image products shows that the ratio colour composites provide the most information on superficial deposits and lithology for the Lochindorb and Kedah-Perak areas, respectively. The advantages of this technique compared to others may have contributed to the result. This reflects why the technique is one of the most commonly used in geological interpretation of remotely sensed data as well as in other fields. For structural information, black and white image products are generally better than the colour composites. The Laplacian add-back filtered images of TM band 5 and MSS band 7 are the best for structural information of the Loch Tummel area, while for the Kedah-Perak area, the contrast stretched MSS band 7 was found to be the best.

CHAPTER 7

INTERPRETATION OF THE IMAGE PROCESSING: lithological and surface material mapping

7.1 Introduction

In this Chapter, interpretation of the digitally processed and enhanced image products which were found to be best for geological mapping (section 6.3) of the Lochindorb and for the Kedah-Perak area will be discussed. For reasons discussed in Chapter 2, interpretation of the image processing for surface material mapping will be concentrated on the Lochindorb area and lithological mapping on the Kedah-Perak area. For the Loch Tummel area, despite its diversity in topography and apparently more outcrops compared with the other two areas, the processed image products for this area showed very little information significant for lithological or surface material mapping, apart from showing alluvial deposits. There are two obvious reasons for this. First, the greater part of the area is covered by one type of surface material, mainly a glacial deposit (boulder clay) which is monotonously covered by mixture of turf, heather and bracken (Chapter 2), and hence gives rather monotonous image character. Second, there is a lot of shadow in the image due to the low sun elevation and relief. As a result, the processed image will show a high response for the area which

faced the sun which will be displayed as brighter tone or different colour, whereas the terrain which faced away from the sun will be in the shadow and will be represented as a low response area or darker tone. Therefore, although the processed image products did show colour variation (e.g. see Figure 6.9), the position of the terrain in respect to the sun is a more dominant factor in controlling this colour or response variation than bedrock or surface materials. Therefore, it is almost impossible to perform lithological mapping using the satellite data for an area with this geological and topographical condition, and also it is less practical to carry out surface material mapping for an area which is dominated only by one type of deposit. In addition to that, the data, particularly the TM for this area, are severely affected by atmospheric interference (see Figure 6.5). Hence the processed images, especially the ones which involved all the original bands or several bands, give spurious results. As a result, no lithological or surface material mapping was carried out for this sub-scene.

For the Lochindorb area, because of the lower resolution of the MSS data, the detail present in it is far less than in the TM, hence making interpretation a lot more difficult (e.g. see Figures 6.2, 6.8 and 6.15). Furthermore, it was found that there is no new information concerning either lithology or surface materials given by the processed MSS data that is not already known from the TM. For this reason, therefore, the discussion will be focused only on the TM data products. The better spatial and spectral resolution of the TM (Chapter 4)

may allow the identification of certain geological units. However, complications introduced by the interaction of the geology, vegetation and drift in the area (as discussed in the Chapter 2) prevent global lithological interpretation. Consequently, after extensive digital analysis and close observation between the image products and the published geological map, it was found that no colour (blue-green-red) combinations of data from any combination of three bands were able to show any consistent correlation between image characteristics and outcropping rock types. The first obvious reason for this is the lack of sufficient variation in mineral contents (the area consists of psammitic granulites, pelitic schists and granites which are mainly composed of quartz, feldspar and a small amount of mica) to give measurable variations in albedo and absorption features on exposed outcrops. Another important factor is the very low percentage of horizontal, bare outcrop compared with what can be seen from oblique views in the field, and with that represented on the solid and drift geological map of the area. Solid geology or bedrock class on the map represents areas with less than 1 m of superficial cover (Kujansuu and Koho, 1982; Whitten and Brooks, 1972; Greenbaum, 1987), whereas any cover (the area is substantially covered by drift deposits) and its associated vegetation on an image obviously masks the underlying rock totally. Field experience showed that the area has a diversity of flora and in other areas its distribution may have a close relation with the geology (MÜhlfeld, 1976; Talvitie, 1979; Kujansuu and Koho, 1982).

However, although the data, TM data in particular, did show considerable diversity in vegetation cover, the pattern bore no relationship with the distribution of mapped rock types. The main reason is probably due to the dominance of exotic glacial deposits, and there is no or very little control exercised by bedrock over vegetation communities. Sometimes the underlying geology can be inferred from its influence on the soil condition and hence the vegetation (Raines and Wynn, 1982; Brooks and McDonnell, 1983) but this proved not to be the case in this region. Due to this fact, it was thought that the only geologically productive use of satellite multi-spectral data for this particular area would be to assess variations in the type of surface material deposits from their vegetation cover. The mapping process for the area therefore was carried out based on this geobotanical view.

Field visits in the area particularly around Carn nan Clach Garbha (356940), Aitnoch (400984), Badahad (380045), Auchlochan (415032), Drumguish (374015) and Kerrow (412997) provided sufficient information on local distribution of surface material as well as vegetation cover types. There are three types of surface material deposit in the area: alluvium which can be classified to several river terraces; glacial deposits which can be divided into three categories, namely glacial sand and gravel, moraines and morainic drift, and boulder clay; and peat deposits which are divided into two types, valley and terrace peat and blanket peat (The Macaulay Institute For Soil Research, 1976; BGS, 1978). These can be

identified on the basis of certain field criteria including distinctive landforms such as hummocky ground moraine, soil profiles, and composition and clast size of the deposits. These criteria, however cannot be resolved on the processed images, and therefore in order to use satellite data to assess variation in the type of surface material deposits from their vegetation cover only a few distinct categories of the deposits are possible to recognise. These are:

a. glacial deposits, thin podzolic mineral soils, thin peat.

b. thick Sphagnum peat.

c. alluvial deposits.

d. screes, both active and stabilised.

In addition to the above mentioned categories, bedrock units which included all rock exposures may also be recognised. In the field, however, no attempt was made to measure the percentage of cover plants found in each category. Notwithstanding this, several general observations in the area were made about the relationships of the vegetation cover associated with specific superficial deposits, to guide image enhancement, and to identify them in various colour or grey tone variations, as follows:

a. Extensive areas of heathland are mainly underlain by the glacial deposits (mainly boulder clay), thin podzolic mineral soils and thin peat. In much drier areas where thin peat is present they are dominated by members of the Heather family (Ericaceae), mainly the Heather itself or Ling and followed by the Heaths (Photograph 7.1). Their densities are much less and their sizes are shorter

than on the thick peat deposits (Photograph 7.9), and they are frequently burned. There are also small communities of Gorse which often forms dense clumps or thickets (Photograph 7.2). Grasses are relatively abundant and often dominant in depressions in the microtopography or where thin peat is absent, especially on higher ground (Photograph 7.9). They include Sheep's Fescue, Common and Brown Bent-grass, Mat-grass, and Purple moor-grass . Cross-leaved Heath or Bog Heather, Heath Rush and Purple moor-grass become more abundant in the wetter areas, mainly on thicker peat deposit (Photograph 7.3 and 7.9), which therefore have more or less similar cover types to the peat deposits in more dry areas. Most of the improved land areas which are dominated by mixed, bright green grasses are underlain by well-drained glacial sand and gravel (Photograph 7.4). This area has a similar cover type to the alluvium. However its location may give an indication about the underlying deposit. Apart from the above cover types, large forested areas are also underlain by this category of deposit which is simply called "glacial deposits" in the following discussion.

b. Alluvium is uniformly covered by mixed green grasses and forms the most important areas of grazing and cultivation in the area (Photograph 7.5). Its location is confined along main drainage channels, such as the Findhorn and Dorback Burn. The unit is also extensively covered by forest.

Photograph 7.1 Glacial deposits (till) are dominated by members of the Heather family (Ericaceae). Here, their densities are much less and their sizes are shorter than on the peat deposits (dry area) - see Photograph 7.3, and they are frequently burned. Grasses are relatively abundant and often dominant on higher ground where thin peat deposits are absent. Location: Slope of the Knock of Braemoray (407010).

Photograph 7.2 Small communities of Gorse which often form dense clumps or thickets on the till deposits. Location: Burnside (403950).

Photograph 7.3 Till deposits are dominated by Cross-leave Heath (Bog Heather) in the wetter areas and thicker peat deposits. Other common cover-types in this area include several types of grasses such as Common and Brown Bent-grass, Mat-grass and Purple moor-grass. These cover-types are more or less similar to the thick peat deposits (on more dry areas) - see Photograph 7.9. Generally, the peat deposits become thicker towards foreground. Location: 2 km NW of Carn Luig (330018).

Photograph 7.4 Most of the improved land areas are underlain by fluvio-glacial sand and gravel deposits. This human influence has made the areas having similar cover-types (mixed of bright green grasses) with areas covered by the alluvial deposits (Photograph 7.5). Location: Kerrow (412997).

c. Thick Sphagnum peat deposits are covered with dense Heather on the drier sites. At some places, this type of peat deposit shows a similar cover type to the glacial deposits (Photograph 7.9), and therefore, it is difficult to separate them. Purple grass-moor, Cotton-grass, Bog Heather and a variety of Rushes are associated with the Bog Mosses (*Sphagnum* species) in saturated areas (Photograph 7.6). This category is called "peat" in the following discussion. Apart from these cover types which form a fairly open habitat, however, there are mounds of thick peat deposits in areas 1 km to the south of Moidach More (415030) on which there are sparse shrubs and birch trees. These cover types may indicate that the peat deposits in this area have reached the final stage in the formation of Histosols (peat) (FitzPatrick, 1983). This unit is called "Moidach peat" in the subsequent discussion. At the time of the field visit the area had been cleared and burned with a few trees left, and was dominated by similar cover types as in the "peat" areas. The Moidach peat forms the largest area of peat deposits in the study area (see Photograph 2.9).

d. Active screes comprise variably lichen-covered bare angular rock fragments and become increasingly grassed down slope. They are confined to the upper slope of the main ridges or hills which are formed mainly by psamitic rocks (Photograph 7.7A). Stabilised screes develop a thin cover of fescue grass with variable amounts of bracken (Photograph 7.7B). This unit occurs only in a fewsmall

Photograph 7.5 Alluvium, confined mainly along main drainage channels, is uniformly covered by mixed green grasses and forms the most important areas of grazing and cultivation. Location: The Findhorn (416936).

A

Photograph 7.6 Cover-types on the thick Bog Mosses (*Sphagnum* species): (A) purple grass-moor, Cotton-grass and Bog Heather, (B) a variety of Rushes, and (C) note that the area is poorly drained (saturated area) - smaller photograph shows the peat deposits of the same area. Location: Photograph A - Drumguish (375014), B - Auchlochan (410021) and C - near the road between Lochindorb - Carn nan Clach Garbha (347953).

B

C

Photograph 7.6 (continued)

areas. For this reason it was not possible to locate it in the image products, and the unit could not be mapped as a separate unit; rather it was included in the bedrock unit.

e. Bedrock is confined to the hill tops or main ridges. Apart from very small percentage indeed of exposed bedrock and more than 50 per cent of them are lichen covered, most of this unit is uniformly covered by mixture of thin heather and thin grass, mainly fescue grass (Photograph 7.8 and 7.9, see also Photograph 2.3, 2.4 and 7.7A). Because of its association with high relief areas, some spectral information from bedrock and its cover types are masked by macro-shadows. However in many cases the shadow is used to infer the location of the bedrock unit based on this association. Although three main rock types (granite, siliceous schist and granulite, and pelitic gneiss and schist) do exist in the area, on the satellite images the individual rock types cannot be separated and recognised. Therefore the "bedrock" category in the following discussion will included the three main rock types.

Therefore three categories of deposits namely "glacial", "peat", "alluvial" deposits together with bedrock will be used and discussed in mapping process using TM data for the Lochindorb area.

A

B

Photograph 7 .7 Active screes comprise of lichen-covered angular rock fragments and become increasingly grassed down slope (A), and a thin cover of fescue grass with variable amount of bracken occur on stabilised screes (B). Location: Photograph A - Creag Ealraich (305944) and B - Craig Tiribeg (360984).

A

B

Photograph 7.8 More than 50% of the exposed bedrock are lichen covered, on top of that, the bedrock in the area is covered by thin heather and grass (mainly fescue grass). See also Photograph 2.3, 2.4 and 7.7A. Location: Photograph A - Drumroy (344967 and B - Huntly's Cave (358046).

Photograph 7.9

Field view of the general correlation between landforms:surface deposits:vegetation cover over the area. (A) bedrock at higher ground (ridge/hill) with thin grass cover, (B) till forms smooth-flowing slopes with thin heather and mixture of grasses cover, (C) thick peat deposits occur at nearly flat and valley-floor areas and covered by Purple grass-moor, Cotton-grass, Bog Heather and variety of Rushes, and (D) the area between (B) and (C) which is made up of till and peat (variable in thickness) occupy an area with gentle to very gentle slopes with dense and long heather cover together with mixture of grasses. Location: western slope of the Carn nan Clach Garbha (350940).

For the Kedah-Perak area, although it was almost completely covered by dense forest, except for agricultural areas and areas which are covered with alluvium, the area is free from other superficial deposits as mentioned in the Chapter 2. Furthermore, most of the soil, sub-soil and clayey mantle, resulting from the humid tropical weathering processes of parent rocks, are *in situ* (Jones, 1970). The physical information of the area like topographic relief, drainage, distribution of vegetation and land use can be seen as a relief impression, texture, colour or grey tone and pattern in the processed image products and should, therefore, have a close relationship with underlying bedrock. Consequently, geological interpretation was carried out in order to test the practical application of Landsat multi-spectral imagery as an input to geological mapping for this particular type of area (i.e. vegetation cover). The interpretation and its comparison with the published map are discussed in section 7.3.

Before the results of surface material mapping for the Lochindorb area, and for lithological mapping for the Kedah-Perak area are discussed, the colour association, photo-characteristics and image characteristics of cover types and rock types for both areas as seen on the most informative images based on their geological information content (section 6.3) will be examined. These characteristics are important because they will be used as the criteria to identify cover types (which are related to certain surface deposits) or to identify certain rock types in the mapping process.

7.2 Surface material mapping of the Lochindorb area

Chapter 6 shows the result of the geological information content of several data products for the Lochindorb area. The final score and overall rankings indicate that the colour-composite combinations of TM bands 2/1-7/1-3/1, DFs 3-2-1, and TM bands 1-3-4 displayed in blue, green and red respectively, are the top three most informative colour-composite images in the area in terms of discrimination between surface material deposits. All these three images are displayed in Figures 7.5, 7.6 and 7.7 respectively . The TM bands 5 and 3 as well as the DF 1, on the other hand, are the top three most informative black and white images (Table 6.7). Colour association and image characteristics in all of these images were examined in relation to cover types as well as with related superficial deposits and bedrock; Table 7.1 summarises the relationships. It is evident that although in these best images the four cover themes do show some differences, they are not very distinctive, hence it. is almost impossible to perform efficient global visual interpretation for surface material mapping in the area. However, an attempt was made to carry out surface material mapping based on visual interpretation of the colour association and image-characteristics of the image products. The interpreted data from the images which were printed at a scale of 1: 70,000 were transferred to a single overlay. The interpretation map is shown in Figure 7.1 which has been reduced to 1: 80,000 scale. The map does show four categories of deposits: glacial deposits, peat, alluvial, and

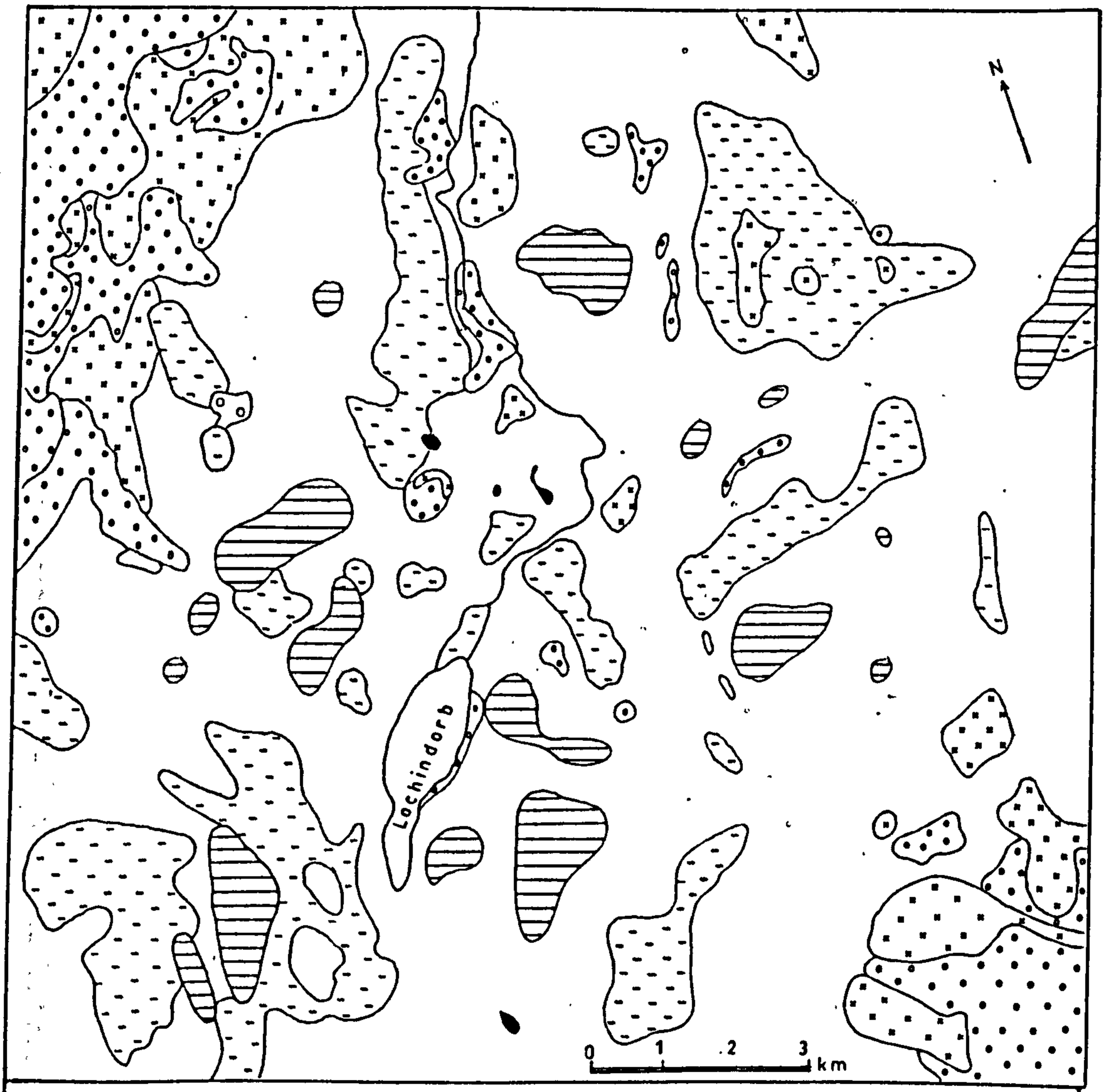

Grass, mainly related to alluvial deposit (near drainage channels) or improved land on the glacial deposits (mainly sand and gravel)

Forrest, mainly coniferous and related to alluvial deposits (near drainage channels) or glacial deposits in other areas. Small area of deciduous and shrubs are related to peat deposits

Peat deposits

Glacial deposits, mainly boulder clay, and sand and gravel

Bedrock, metamorphic and igneous rocks

Figure 7.1 Surface material map of the Lochindorb based on visual interpretation of the TM image products.

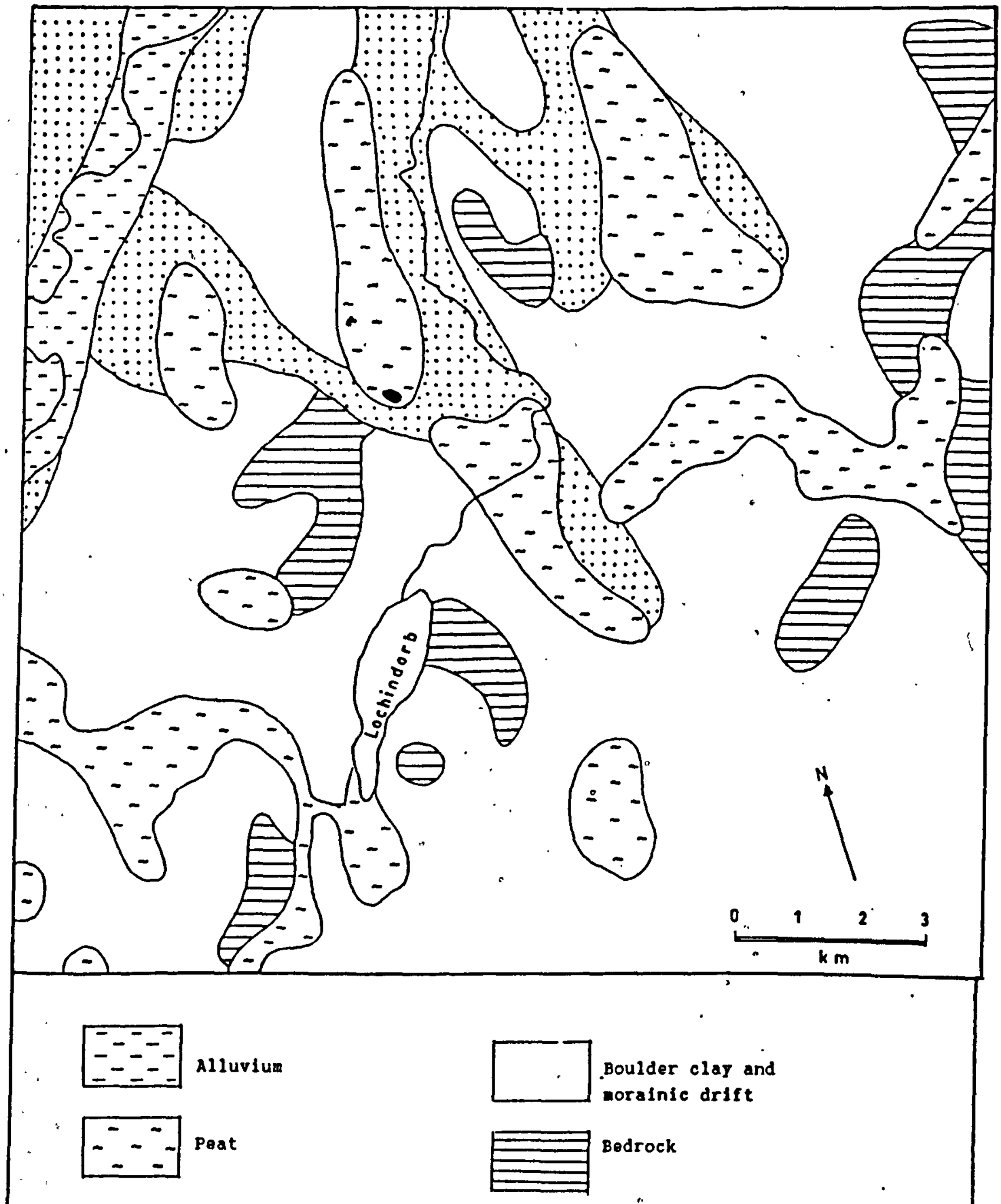

Figure 7.2 The Quaternary map of the Lochindorb area, reduced from the Quaternary map of the United Kingdom 1: 625,000 (BGS, 1977)

bedrock. The Quaternary map for the same area, derived from a 1: 625,000 BGS map is shown in Figure 7.2. Comparison of these two maps indicates good overall agreement (although in detail a number of differences exist),.and apparently the interpreted map shows more detailed information, especially for the peat deposits. However, the published map separates the glacial deposit into two categories: boulder clay (and morainic drift) and glacial sand and gravel. Although the areas which are occupied by these two glacial categories do show colour and texture differences on the images (see Figure 6.7D, 6.23A), these subtle differences are not strong enough to draw a boundary between them. Even with field knowledge of the area, it was still not possible to separate the two types of glacial deposit on the images (based on the image characteristics).

When compared the interpreted map (Figure 7.3), derived from the images scaled 1: 70,000 (Figure 7.5, 7.6 and 7.7) and the published map at nearly similar scale (Figure 7.4), show that the interpreted map is too simple to be of any real use in mapping the superficial deposits of the area. Notwithstanding this, the general distribution and location of the four superficial deposits, particularly the peat in saturated areas, are well indicated, therefore the map (as well as the images) give reasonably a good synoptic cover for the whole of the area. Hence it can be used to pinpoint the rough location where certain type of surface deposits or the bedrock may be present. Therefore, for regional studies and preparation of preliminary map at scale about 1: 80,000 or

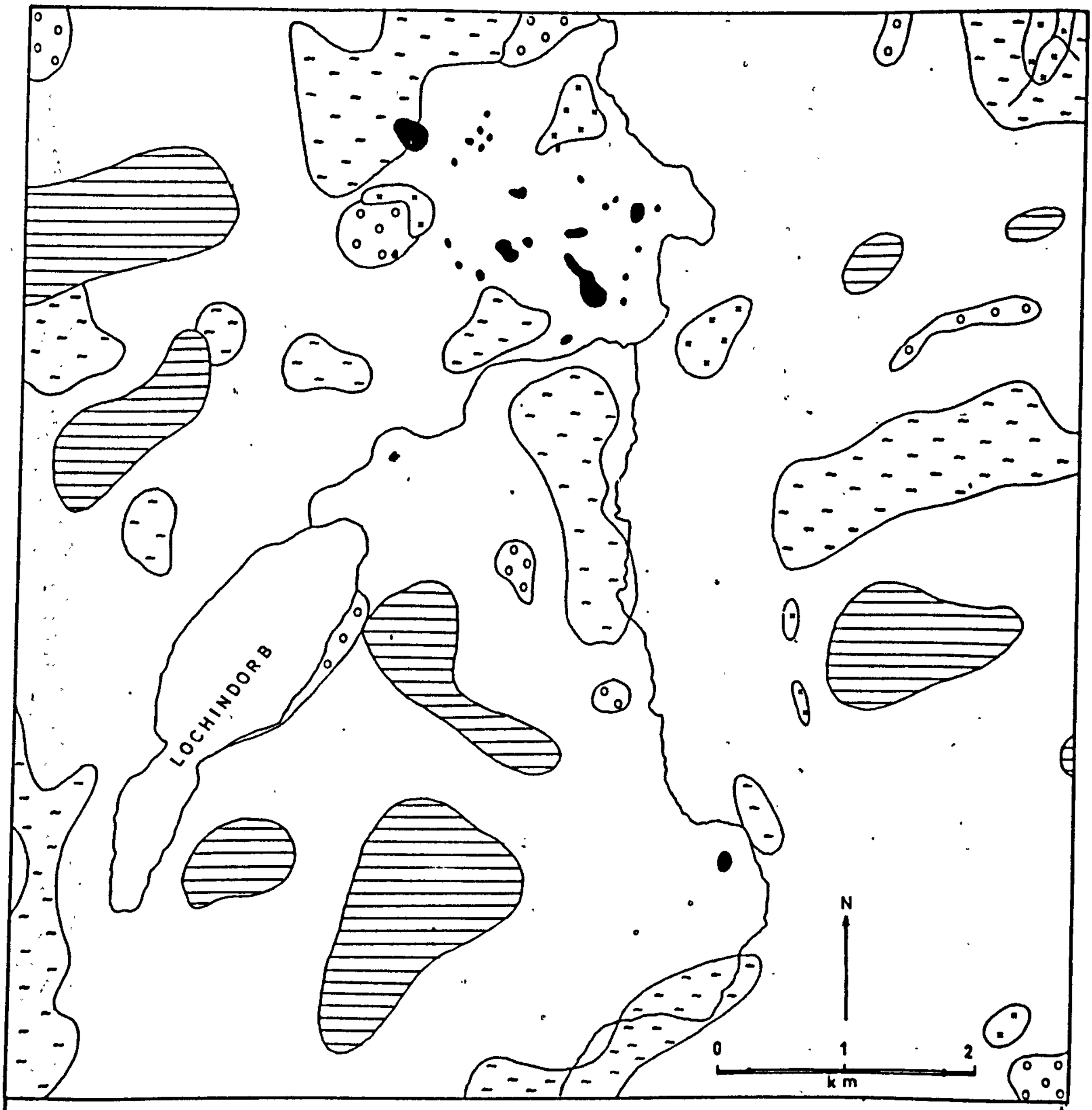

Grass, mainly related to alluvial deposit (near drainage channels) or improved land on the glacial deposits (mainly sand and gravel)

Forrest, mainly coniferous and related to alluvial deposits (near drainage channels) or glacial deposits in other areas. Small area of deciduous and shrubs are related to peat deposits

Peat deposits

Glacial deposits, mainly boulder clay, and sand and gravel

Bedrock, metamorphic and igneous rocks

Figure 7.3 Surface material map of the Lochindorb based on visual interpretation of the TM image products (enlarged from the Figure 7.1).

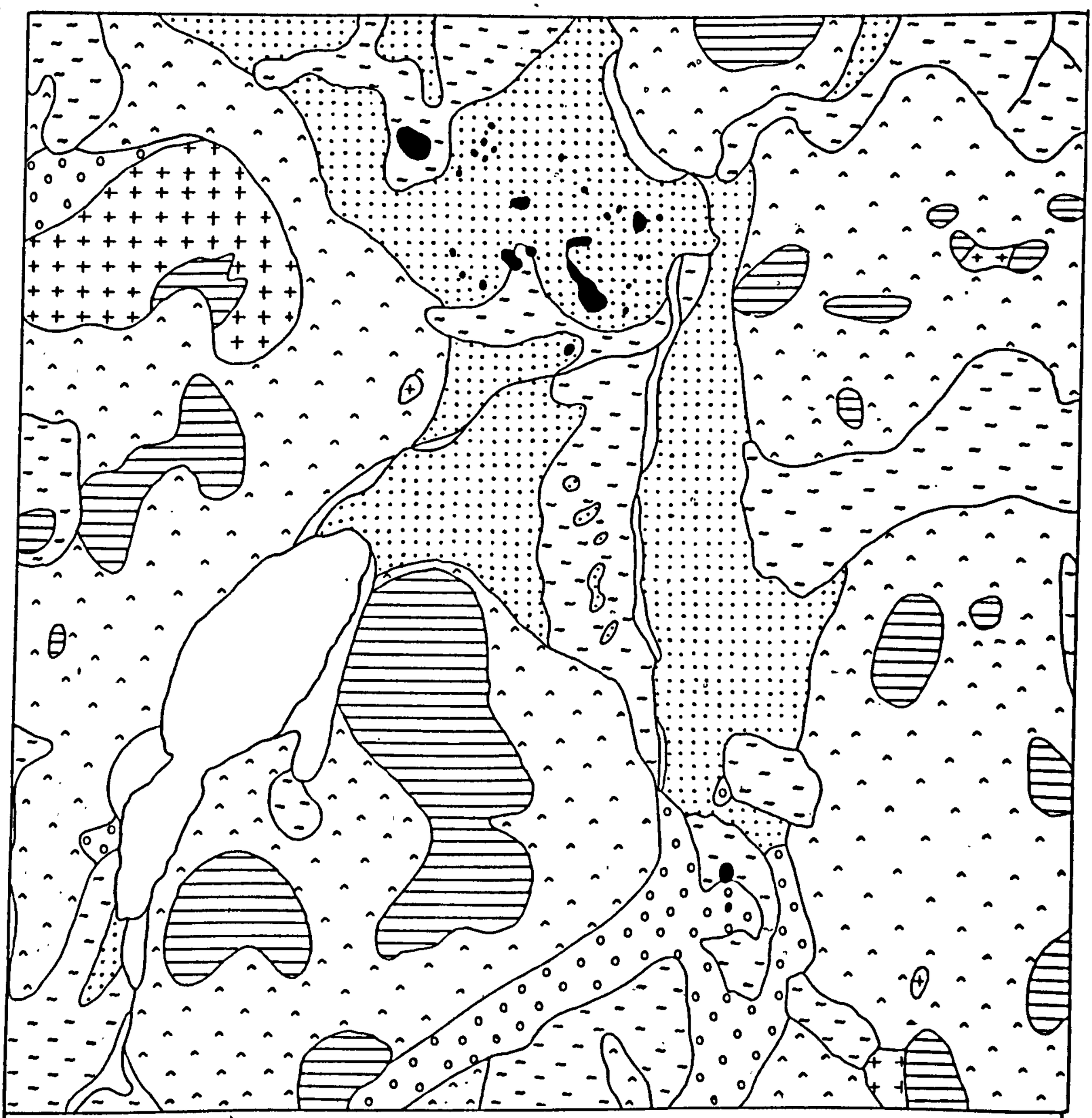

Figure 7.4 Map of the superficial deposits of part of the Lochindorb area (slightly simplified after BGS, 1978).

smaller, the use of satellite data, in this case the TM, is very useful.

This broad information based on multi-spectral data, may be combined or used with information from other sources such as black-and-white aerial photographs for further work including mapping, in order to produce 'better' maps. For aerial photography, although it is poorer spectrally, provides important spatial information which means (a) small units can be more precisely delineated and the boundary between different themes could be more accurately located; (b) textural details like bedding, foliation and jointing, if present, combined together with topographic relief expressed in stereoscopic viewing also assist in separating spectrally similar units; (c) features, particularly man-made ones, which have no geological significance can be identified and discounted. Therefore surface material mapping over a 100 km^2 block within the Lochindorb sub-scene, was carried out based on a combination of multi-spectral information of the TM data, and photo-characteristics for an area containing representative surface material deposits. The result of the interpretation will be discussed in section 7.2.3.

7.2.1 Colour association and image-characteristics of cover types

Colour associations of cover types in the area were summarised in Table 7.1 after close examination based on the top three colour composites in the final rankings (Figures 7.5, 7.6 and

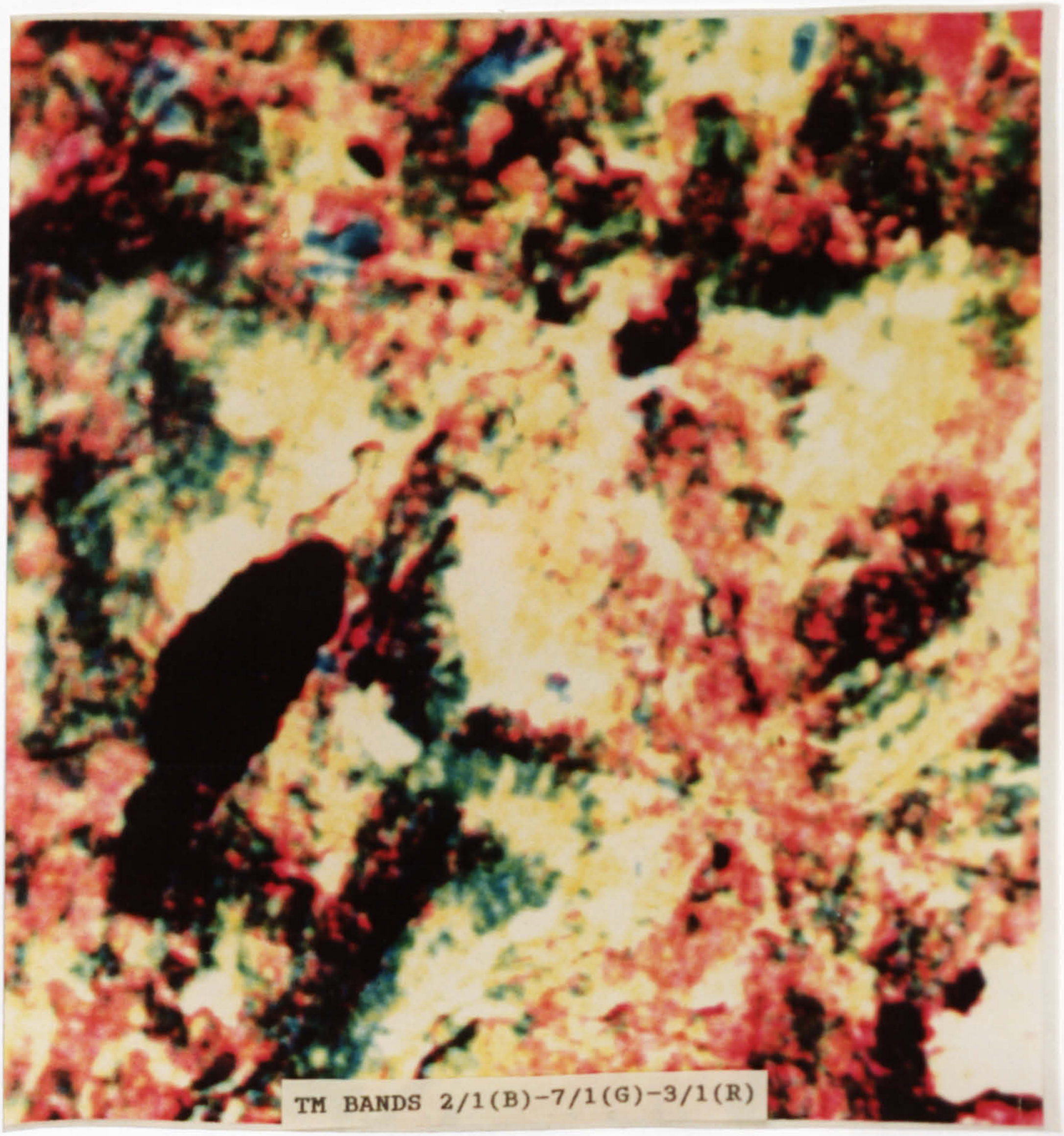

TM BANDS 2/1(B)-7/1(G)-3/1(R)

Figure 7.5 TM band-ratio colour composite of the Lochindorb area (enlarged from Figure 6.19A. The image is ranked first in terms of geological information content compared with other image products in the assessment. Scale 1:50,000.

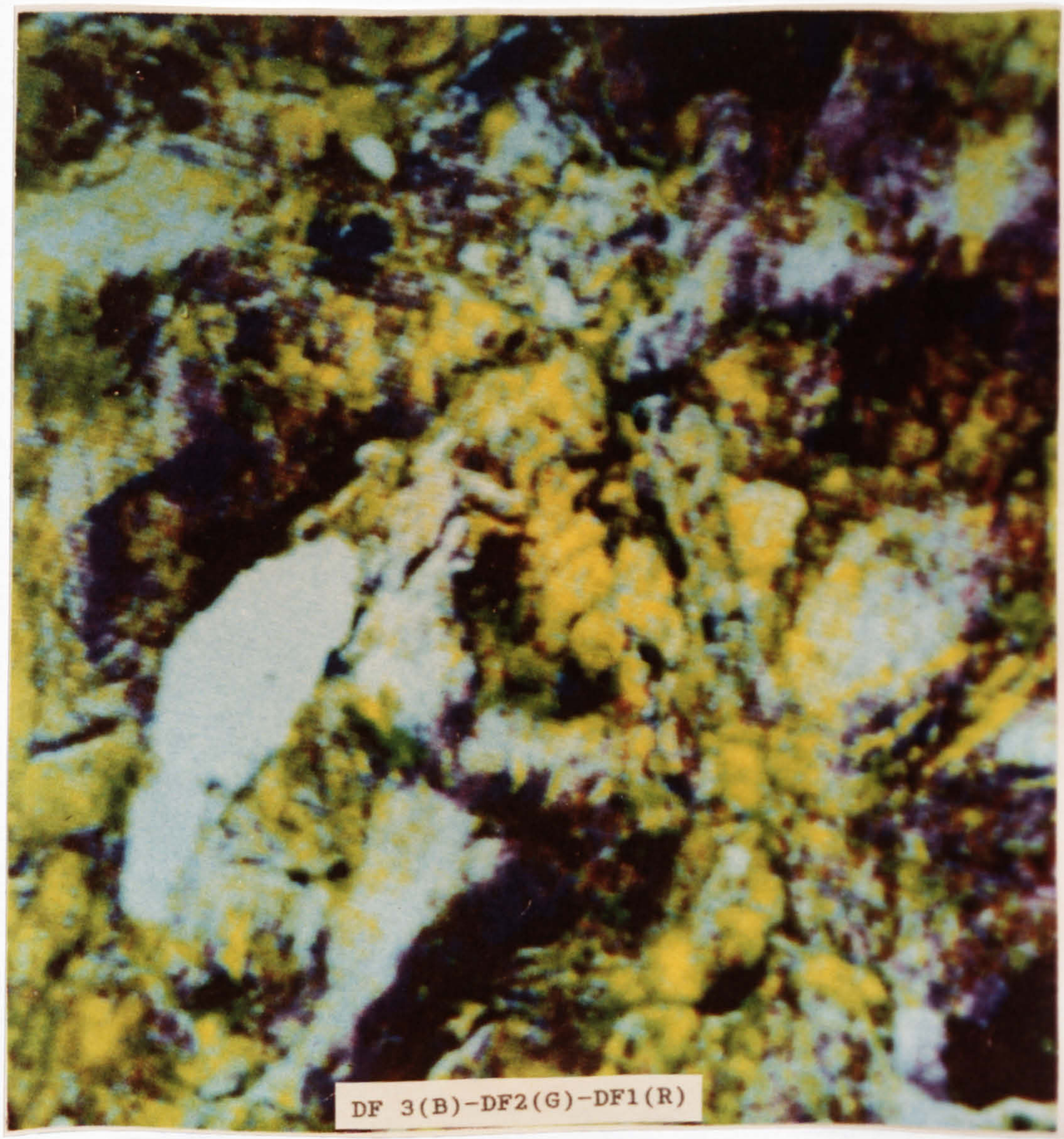

DF 3(B)-DF 2(G)-DF 1(R)

Figure 7.6 TM discriminant function colour composite of the Lochindorb area (enlarged from Figure 6.15A). The image product is rated second in the geological information content among the images produced in the study. Scale 1:50,000.

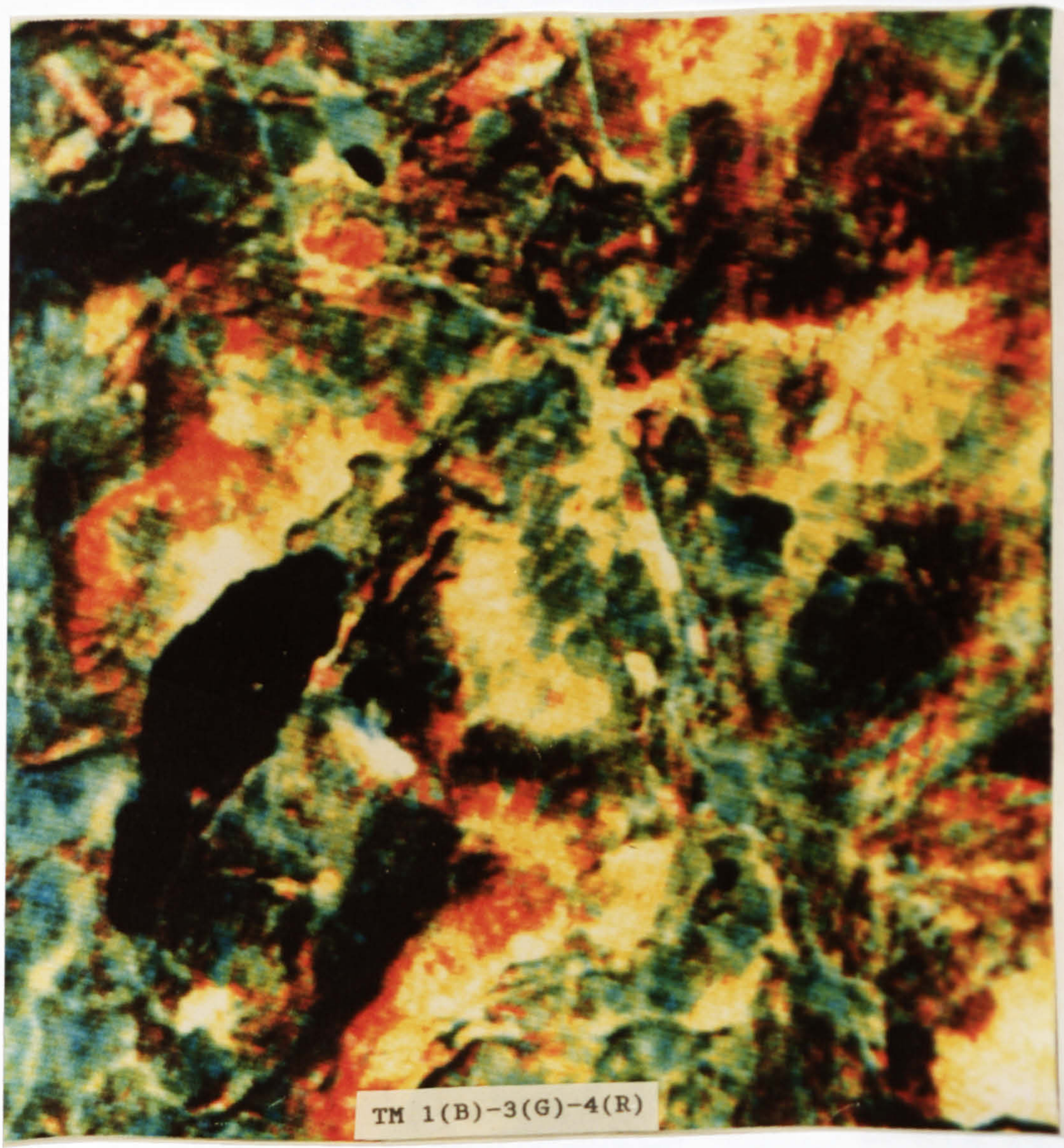

TM 1(B)-3(G)-4(R)

Figure 7.7 TM bands 1-3-4 colour composite combination of the Lochindorb area (enlarged from Figure 6.5E), is the best band combination among other TM band combinations. The combination is chosen based on the basis of experimentation and interpretative experience. Scale 1:50,000.

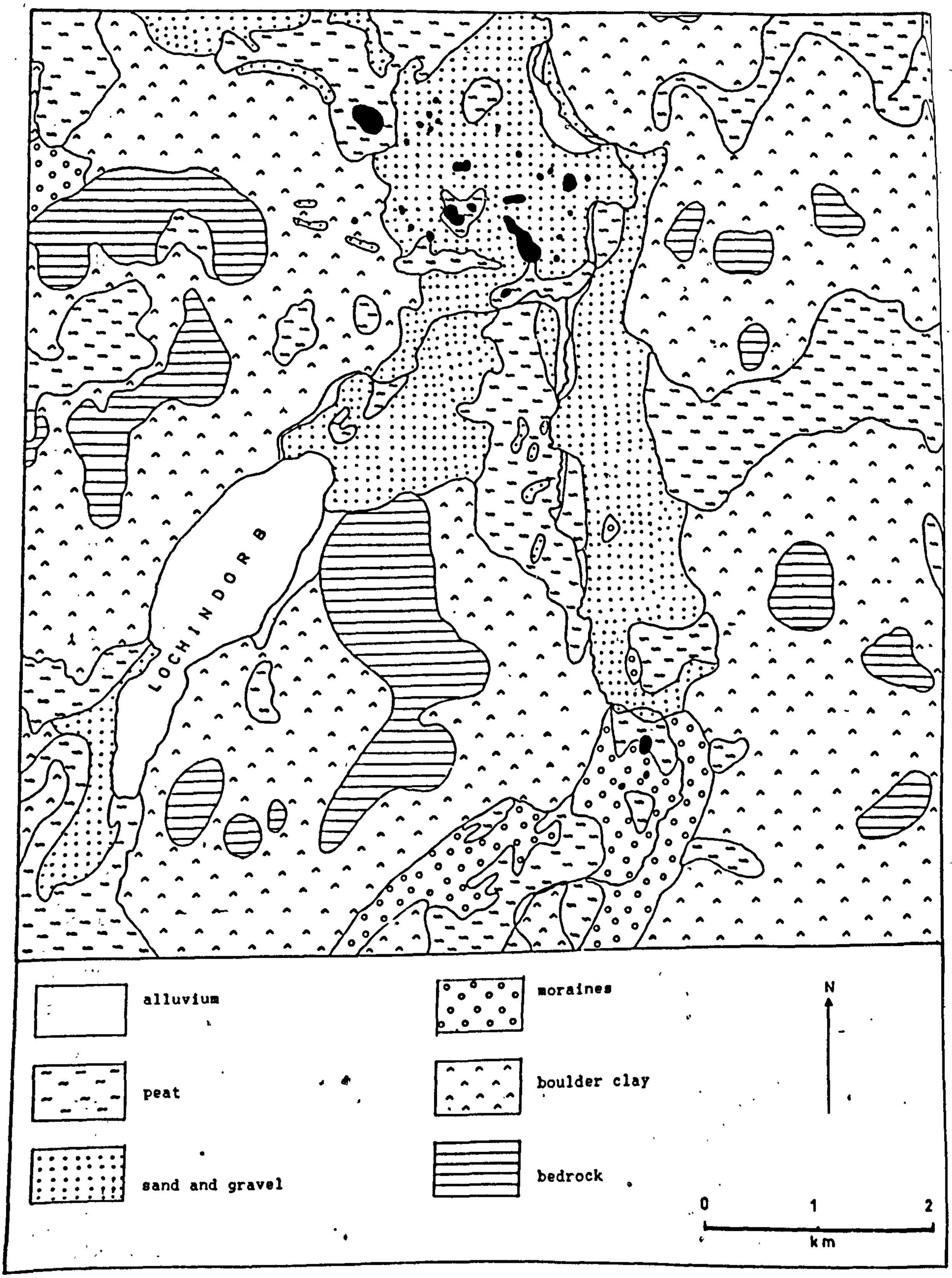

Figure 7.8 Surface material map of part of the Lochindorb area based on the TM imagery, aerial photograph and field visits.

7.7). It was found that among the four cover themes, the peat deposit shows the most distinctive and consistent colour. The colour association of cover types are very useful not only to get a rough idea about their distribution, .location and boundary, but also in many areas to identify certain spectrally similar cover types on aerial photographs. In addition to the colour association, other image-characteristics like relief impression, texture and grey-tone are also important criteria for the discrimination of geological units. In the area, however, only grey-tone can be clearly observed on the image products whereas texture is more uniform, and is not an important criterion. Therefore only the grey-tone element was used together with colour association and photo-characteristics (section 7.2.2) in order to identify, discriminate and separate between cover types which are related to different surface material deposits in this area. Table 7.1 summarises the grey-tone of several cover types which was depicted from the top three individual black and white images in the final ranking (Table 6.7).

7.2.2 Photo-characteristics of cover types

The successful accomplishment of a photo-geological interpretation requires attention to some elements such as outcrops, landforms, drainage, vegetation and cultivation (Mekel, 1978). These elements are expressed in terms of tone, texture, pattern and shape. Interpretation of photographs, therefore relies on these basic characteristics of the surface together with other elements like size (scale) and context

	FIELD OBSERVATION				COLOUR ASSOCIATION AND IMAGE CHARACTERISTICS						CONCLUSION
	Main Cover Type	Associated Landform	Geological Component/ Category of the Deposit	Drainage Condition*	BRC 2/1-7/1-3/1	DFCC 3-2-1	BCC 1-3-4	B5	B3	DF1	Main category of the deposits (in (mapping process)
A	coniferous trees/forest	hill and hill top	mainly related to rock outcrop in hilly area	freely drained	v.dark purple	uniform yellow	dark red-brown	black	black	light grey	bedrock (hilly areas) or glacial deposits (in other areas)
B	deciduous trees, or young pine	gently sloping terrain and hill slope	mostly in the glacial, sand and gravel	freely drained	reddish purple	patches of dark purple	brownish blue-green	medium grey	grey	grey	glacial deposits
C	green grass/ farmland/ grazing field	flat, gently sloping and undulating terrain	mostly in alluvium deposit also on sand and gravel	freely drained	blue to light blue	green	pink to brownish	light grey	dark grey	black	alluvium or glacial deposits
D	less green grass/grazing field	slope and undulating terrain	mostly related to boulder clay deposit	freely to imperfectly drained	greenish & pinkish	v.d.green and dark	yellow & pale-brown	white	white	black	glacial deposits
E	none or very thin veg.(grass) cover	lowland area, slope and hill summit	bare field or burned area or associated with bedrock	freely drained	pale yellow	bluish purple to blue	white to pale yellow	white	white	v.dark grey	alluvium, glacial bedrock (depend on location)
F	mix. grass, sphagnum, stands of heather, shrub with birch trees	flat, depression and mound terrain	thick peat deposit in saturated area	poorly drained	reddish pink	purple	yellow and blue-green	grey	light grey	light grey	peat deposits (saturated areas)
G	heather and mixture of grass	gently sloping and flat terrain	usually associated with boulder clay with thin peat deposit	poory to imperfectly drained	pink with dark green patches	dark yellow	pale brown	dark grey	grey	grey	glacial deposits
H	dense short heather and fescue grass	hill and hill slope	mostly associated with boulder clay or bedrock in hilly area	freely to imperfectly drained	dark green	white to yellow	dark brown	v.d. grey	d.grey to v.d. grey	v.light grey	bedrock and glacial deposits

* based on the Soil Map, Soil Survey of Scotland, sheet 84, 1976.

Table 7.1 Colour associations, image characteristics and field observation of the main surface deposits and bedrock of the Lochindorb area.

(Carroll and Bendelow, 1977; Drury, 1987). All these elements are discussed at length by many authors in several text books. Aerial photographs for the area were interpreted on a similar basis. However because the area is almost completely vegetated, the main element for interpretation are the tonal properties of vegetation/cover types. These characteristics of cover types may be correlated with the distribution of underlying deposits, and the surface material mapping in the area was carried out on this basis. Table 7.2 summarises the photo-characteristics of cover types in the area which were used in the mapping process. With guide and support by the colour associations and image-characteristics of cover types in the colour-composite images (section 7.2.1) the interpretation process was made easier and more reliable.

7.2.3 The interpreted maps and their comparison with the published maps

The information guided by the multi-spectral information in the most informative images (scale 1: 70,000) and photo-characteristics (scale 1:25,000 to 1:30,000) were traced on several overlays, which were transferred to a 1: 40,000 base map to produce a preliminary surface material map. The map was checked through field visits, and correction and reinterpretation were carried out and finally the information was compiled as a final map (Figure 7.9 - in folder). Parts of the map are shown in Figure 7.8 in order to show its relationship with the image (Figure 7.5, 7.6 and 7.7), and its comparison with the published map (Figure 7.4).

PHOTO-CHARACTERISTICS						MORPHOLOGICAL EXPRESSION				COVER		CONCLUSION
Tone			Texture									
Rock/unit	Vegetation	Cultivation	Rock/unit	Vegetation	Cultivation	Resistance	Drainage	Bedding	Jointing	Vegetation	Cultivation	
very light grey	grey to dark grey	grey to light grey	smooth	coarse	smooth	very low	external, persistent, meandering pattern	none	none	dense	intense	alluvium
light grey	very dark grey	grey	eneven	medium rough & speckled	smooth	low	many small drainage	none	none	dense	common (on improved land)	sand and gravel
grey	d.grey to grey with l.grey stripe/patches	grey to light grey	smooth to medium coarse	smooth	smooth	low	many small gullies, parallel pattern on sloping terrain	none	none	dense	rare	boulder clay
-	very dark grey	-	-	smooth	-	moderate	external, low density	none	none	dense	none	morainic drift
very dark grey	light grey	-	smooth	smooth, speckled & matted	banded due to artificial drainage lines	very low	artificial drainage lines	none	none	moderate to low	none	peat
-	grey to dark grey	-	-	smooth	-	moderate to high, forms rolling hill	external, low density	none	several direction, low.density	dense	none	igneous rock (granite)
very light	dark grey	-	medium coarse	smooth	-	high to moderate, forms hilly areas	external, very low density	massive, with few "bedding" traces	low density	sparse to moderate	none	metamorphic rock (psammite, semi pelites, quartzite, gneisses)

Table 7.2 Photo-characteristics of the main surface deposits, bedrock and their cover-types of the Lochindorb area.

All five categories: alluvial, peat, sand and gravel, morainic drift and boulder clay of the superficial deposits mapped in the area are identified. However, four rock units mapped are grouped and represented by only two units in the preliminary interpreted map: metamorphic rock and igneous rock. Although a large proportion of the two rock types was identified (either on aerial photographs - see Table 7.2, or during field visits), they are shown, however, as one category or 'bedrock unit', in the surface material map of the area (Figure 7.8). Apart from that, the interpreted map shows a few minor lineaments and foliation traces which are recognised on aerial photographs (Figure 7.9 - in folder), and are not shown in the published map.

Generally, the interpreted map units correspond very well with the published map. However, one may notice as the most significant differences that there is more boulder clay in the interpreted map than in the published map and vice versa for the bedrock unit (Table 7.3). In general, the larger areas of bedrock which formed topographically elevated ground are correctly identified. This can be found, for example, around Carn Ruigh Chorrach and Carn nan Clach Garbha (Figure 7.9). However, in some rounded hilly areas (for example around Carn Ruigh Thuim and Knock of Braemoray) (Figure 7.9), which are largely covered by superficial deposits, although they form higher ground, it is slope steepness which indicates the boundary between bedrock and the deposits and this is not clearly shown. It is evident that apart from exposed bedrock

	Published Map (BGS, 1978)	Interpreted Map	Differences
Alluvium	3.02%	1.66%	-1.36%
Peat	21.05%	22.67%	+1.62%
Sand and gravel	10.67%	10.92%	+0.25%
Morainic drift	4.82%	5.86%	+1.04
Boulder clay	44.69%	48.73%	+4.04%
Bedrock	13.78%	8.18%	-5.60%

Water bodies occupy nearly 2% of the total mapped area.

Table 7.3 Percentage of the surface material deposits and bedrock in the Lochindorb area: comparison between the published map (Figure 2.5) and the interpreted map (Figure 7.19).

which is usually confined to the hill tops, a number of areas in this situation do not correlate with the published map and are classified as boulder clay on the interpreted map. In addition, a number of lower-lying areas, where bedrock outcrops commonly form small scattered knolls protruding through superficial deposits, also do not correlate with the mapped geology and again are classified as boulder clay. Field visits to such areas, for example around Huntly's Cave, indicate that the area mapped as outcrop comprises less than 40 per cent rock exposure (see Photograph 2.4 and 7.8B) and almost all are heavily vegetation covered. In these two situations, therefore, it is clear that the bedrock covered by thin overburden is mapped as solid in the published map, whereas from a remote sensing viewpoint, the mapped units represent the actual ground surface information. Table 7.3 also shows a higher percentage of morainic drift unit in the interpreted map than on the published map. Although the morainic drift is usually associated with typical hummocky terrain on higher ground and can be easily separated from bedrock on aerial photographs, as in the case of boulder clay, the topographic slope which marks the boundary between the two units is often not clearly shown. Therefore, apart from exposed bedrock which can be identified on the photographs, a number of areas in this situation also do not correlate with the published map and are mapped as morainic drift. Anyway, the sum of increasing percentage in the boulder clay and morainic drift does not exactly correspond to the amount of decreasing percentage in the bedrock class (Table 7.3). This

perhaps indicates that apart from boulder clay and morainic drift, there is a possibility that the mapped outcrop was classified as sand and gravel or peat deposits because these two classes are also associated with bedrock units in a few places.

Apart from the bedrock, alluvium is also considerably less in the interpreted map than in the published map (Table 7.3). In the area, alluvium and peat deposits are closely associated and occurred in low and flat areas near river channels, hence topographically they are very similar, and, sometimes in terms of cover types, both deposits are also very similar. Therefore, in some places, for example along the River Divie, Dorback Burn, Anaboard Burn, and their tributaries, where alluvial deposits occupy small areas, it is most likely that the mapped alluvial deposit is classified as peat or as sand and gravel which occupies larger areas. During field visits to the area, it was found that in a few areas, for example at the bottom end of the Lochindorb (Photograph 7.10), the mapped alluvial deposits (Figure 7.4), consist of about 1 m thick peat rather than alluvial deposit, therefore the area was delineated and classified as peat in the interpreted map (Figure 7.8). The considerably smaller area of alluvial deposits in the interpreted map than on the published map, therefore, may due to the situation where some of the mapped alluvial deposits are classified as peat or sand and gravel because of their resemblance in topography or cover type particularly in narrow strip areas near the drainage channels or because of the fact that some of the mapped

Photograph 7.10 Mixture of grasses in area mapped as alluvium (Figure 7.4) whereas from remote sensing view and field observation the area is classified as peat deposit (Figure 7.8). Location: south-end of the Lochindorb.

alluvial deposits are in fact peat deposits, as in the above example. On the other hand, the sand and gravel deposits, correspond very well with the published map. This unit with its typical uneven and speckled texture which reflects its more or less hummocky terrain on a flat or very gently sloping area, can be easily identified on aerial photographs and separated from peat deposits which in many areas are usually associated with the sand and gravel.

The TM images give good synoptic cover for the entire area, therefore the general distribution of the deposits, based on their cover types, is quite well indicated. It has been shown that for regional studies the use of the TM data is very useful. However, the interpreted map of the TM images is too simple to be of any real use in semi-detailed mapping of superficial deposits in the area at scale about 1:50,000. The obvious reason is that the TM data cannot produce the spatial resolution necessary to depict the differences between the deposits. In addition, the very high percentage of the vegetation cover also prevents direct identification of the deposits. Consequently it makes it very difficult to delineate and map them accurately. Nevertheless, the gross classification based on the multi-spectral information (from the TM) is combined with the spatial information (from the aerial photographs) in order to map superficial deposits in the area. The result shows that the interpreted map shows very good agreement with the mapped area although in detail a number of differences exist.

7.2.4 Summary

In summary, this investigation has demonstrated that the Landsat TM images have not proved to be of practical application for detailed superficial deposits mapping in the Lochindorb area, Scotland. Although the TM resolution is superior to the MSS data, the resolution is still not sufficient for the purpose. In addition, the main problem with this study was that the areas are covered by vegetation which masked the solid as well the drift lithologies. The study, however, has provided some encouragement that, apart from the alluvial deposits, the technique could be used to identify the peat from other deposits as a result from the more direct influence of peat deposits on vegetation cover types than others.

7.3 Geological mapping of Kedah-Perak area

For the Kedah-Perak area, the three most informative images in terms of discrimination between different rock units (see Table 6.8) are shown in Figure 7.10, 7.11, and 7.12. For geological mapping purposes, the same image products which covered sub-area 2 are also displayed (Figure 7.15, 7.16, and 7.17). In all images, it is evident that the most distinctive feature is the difference between the dense vegetation (forest) cover and non-vegetated or less dense vegetation cover which are represented by two different colours. During the assessment process in Chapter 6, it was found that these two terrain categories broadly correspond to certain rock units which have different characteristics. Generally, the

dense forest cover occupied higher ground areas (hilly, mountainous or ridges) which are underlain by high resistance rock types like granite, sandstone, conglomerate and metasandstone. On other hand, the areas which have less or no vegetation cover form lowland, flat or undulating areas and are underlain by more soft rock types like siltstone, mudstone and shale. In fact, a few kilometres west of Pedu and Muda Reservoir these two terrain categories coincide very well with the geological boundary between two sedimentary rock units: siltstone and shale, and sandstone and conglomerate (Figure 7.13). Very large areas are covered by dense vegetation and there is no exposed bedrock which is normally covered with thick saprolite and soil. However the colour and image characteristics seem to have a close relationship with the underlying bedrock. With the help of these criteria, it seems to be possible to differentiate and draw some boundaries between major rock units in the area. Therefore, an interpretation exercise was carried out over the Kedah-Perak area to make use of, and to test, the practical application of the MSS data as an input to geological mapping by using the most informative image products (see Table 6.8). For this purpose, although some knowledge of the mapped geology of the area had been gained in the earlier stage of the study, for example during image products assessment process, this information was ignored as far as possible and an attempt was made to interpret the imagery as objectively as possible. This means that only features distinguishable on the image itself were annotated on the overlay. Colour associations and image-

characteristics of rock types in the area were examined and summarised in a Table 7.4 (section 7.3.1). The interpreted geological map for the area is shown in Figures 7.14 and 7.19, and the map shown was produced without any field visit to the area. First, this is because the aim of this study is to make use and to examine the usefulness of satellite data (the Landsat MSS) for geological application: preparing a small scale preliminary geological map of this particular area solely based on the interpretation of the processed Landsat MSS data. Second, the area was selected at the later stage of the study period due to the "less encouraging" results from the Scottish examples, so with this time constraint and the location of the area which is very far from the University, it was not possible to undertake field visits to the area. The discussion of the result and comparison with the published map (section 7.3.3) do indicate the nature of the interpreted map as a preliminary map where many areas are indicated as "unresolved areas" which simply need clarification and supporting data from field visits.

7.3.1 Colour association and image-characteristics of geological units

Based on the three most informative colour composites in the final rankings (Table 6.8), the colour associations of several image units in the area were observed one after another. In terms of colour, it is evident that in all images the main colour is contributed by the dense forest cover and variation in colour is also mainly related to the variation in

vegetation. These colour variations are sometimes strong enough to be depicted in certain image products. In addition to colour, other image-characteristics of rock types which can be seen on several images, also serve as important criteria in order to differentiate between different geological units and may be used in the mapping process. Among these are relief impression, texture and grey tone. These criteria were examined on the best three individual black and white images in the final rankings (Table 6.8). This observation phase is very important in order to identify and establish a number of classes/units based on spectral and other image characteristics. Finally, after close examination, nine image units were identified and their colour association and image-characteristics are summarised in Table 7.4. These characteristics were observed and used during the interpretation process in order to separate and to draw a boundary between the units. The probable lithological unit for each of the image units are also given in Table 7.4, and were used in the interpreted map of the area.

7.3.2 The interpreted maps and their comparison with the published map

Visual interpretation was carried out on the image products which are printed at scale 1: 250,000, and then were reduced to scale 1: 300,000 for the display (Figure 7.10, 7.11, 7.12, 7.15, 7.16 and 7.17). Image units were discriminated on the image products which are based mainly on a combination of

	IMAGE CHARACTERISTICS							MORPHOLOGICAL EXPRESSION			COVER		CONCLUSION
	Colour			Tone			Texture	Rock/unit	Properties				
	BRC 5/6-4/7-4/6	BCC 457	PCC 321	B7	DF1	PC1		Resistance	Bedding	Jointing/ Lineament	Cultivation	Vegetation	Probable Lithology
A	pale brown	red	bright green to blue-green	grey	dark grey	v.dark grey	coarse	very high	none	multidirection persistent and high density	none	very dense	ig. rock: granite
B	whitish pale-blue	pale blue with red bands	pale blue-green with red patches	light grey	white	v.light grey	fine and speckled	low	massive to well bedded	very low	intense	sparse to scattered	sed. rock: shale, sand-stone
C	greyish pale-blue	pale blue with red patches	pale blue-green with patches	light grey	white	v.light grey	fine and speckled	low	massive	very low density	intense	sparse to scattered	Sed./Met.rock: siltstone, shale, slate
D	pale-brown	red	blue-green	dark grey	grey	dark grey	linear and banded	moderate	well bedded	not persistent low density	none	very dense	Sed. rock: interbedded sandstone-siltstone
E	pale-brown	red	blue-green	dark grey	medium d. grey	dark grey	moderate coarse, banded & linear	moderate to high	well bedded to massive	medium to high density	none	very dense	Met. rock: metasandstone, slate
F	pale-brown	red	blue-green	dark grey	medium d. grey	dark grey	moderate banded & linear	high	well bedded to massive	medium density	none	very dense	Sed. rock: sandstone, conglomerate
G	dark pale-brown	dark red	dark blue-green	v. d. grey	medium l.grey	dark grey	moderate uneven	moderate to high	massive to well bedded	low to medium density	rare to common	very dense	Met. rock: phyllite, slate
H	greenish pale-brown	dark red	dark blue green	dark grey	grey	dark grey	moderate coarse to fine	moderate to low	none	low to medium density	very rare	very dense	Ig. rock: granite
I	dark blue to pale-blue	pale red	bright green	v. l. grey	v.d. grey	white	moderate fine to fine	low to moderate	none	none	common	moderate	Ig. rock: volcanics

* based on the black and white images (B7, DF1 and PC1).

\+ image unit F' (on the map – Figure 7.14) shows similar characteristics as image unit F, however the F' forms a long, persistent and high ridge.

Table 7.4 Colour associations and other image characteristics of rock-types of the Landsat MSS for the Kedah-Perak area. Similar image unit annotation is given on the MSS images in Figure 7.15, 7.16 and 7.17.

image texture, morphological expression (topography, bedding and jointing), colour/tones and cover (cultivation and vegetation). Each unit recognized from the images was unique as summarised in Table 7.4. Interpreted information from the images was transferred to a single overlay and a composite geological interpretation built up. The resulting interpretation map (at scale 1: 250,000) was reduced to a scale of 1: 300,000 and is shown in Figure 7.14 for sub-area 1 and Figure 7.19 for sub-area 2. Slightly simplified data from the regional geological map at an original scale of 1: 500,000 (Geological Survey of Malaysia, 1985) are presented in Figure 7.13 and 7.18 for comparison.

Nine image units which are observed and identified (Table 7.4) were delineated in the study area. The geology of the area, only has four map units which belong to four geological periods and one intrusive rock unit (see Figure 2.11 and 2.12). The four geological period rock units, however, consist of various rock types as shown in Table 2.5. Some of these rock types are indicated in the published map (Figure 7.13 and 7.18).

Image unit A (interpreted as igneous rock, granite) which occurs in a large area, has typical image characteristics such as very high relief impression (high resistant), no bedding traces, multiple direction and high density of lineaments and coarse texture, and corresponds very well with the mapped unit acid intrusive (mainly granite). It is evident that in areas where the unit A forms higher topography and is bounded by other units which form low topography, for example at the

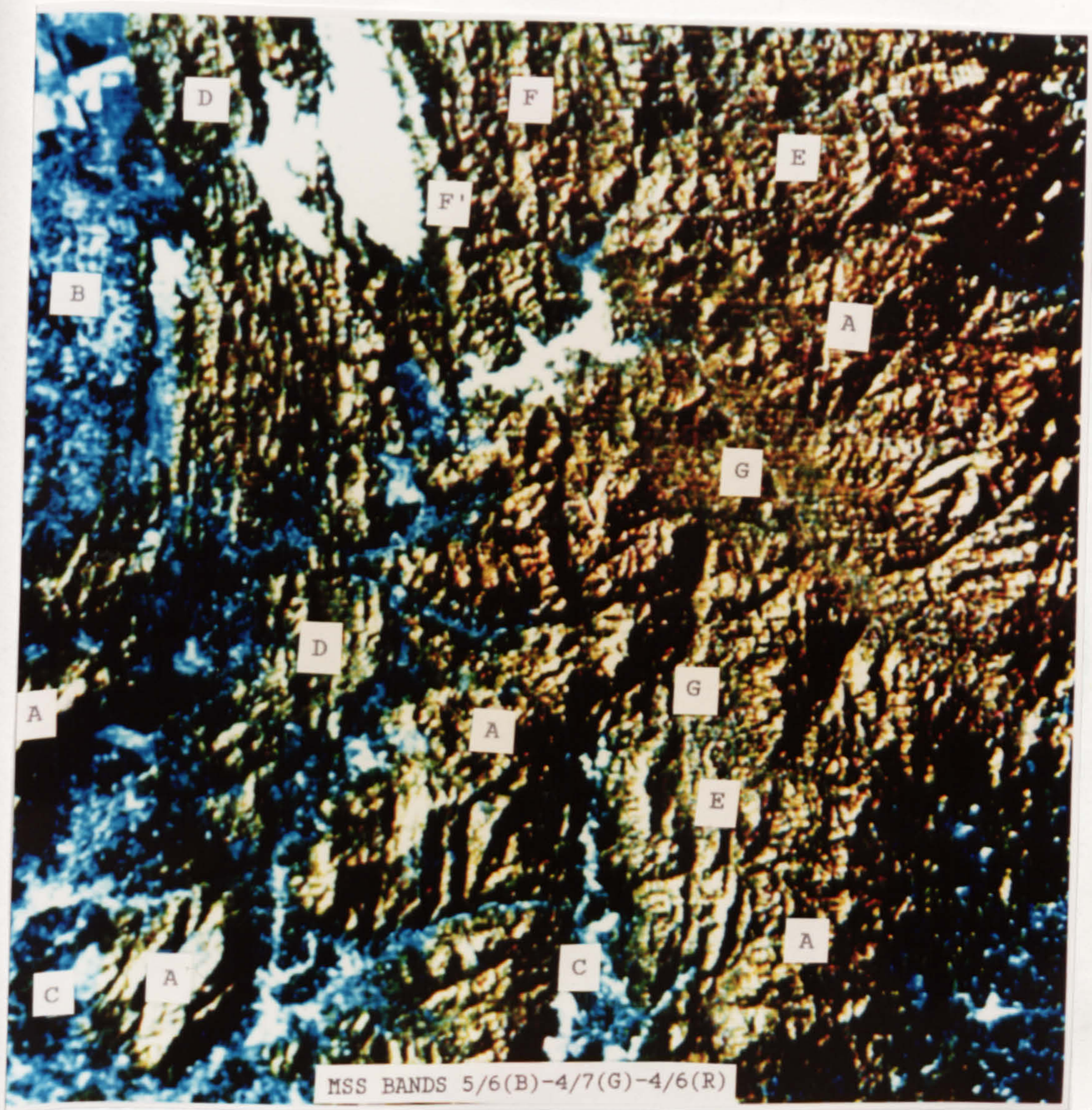

MSS BANDS 5/6(B)-4/7(G)-4/6(R)

Figure 7.10 MSS band-ratio colour composite of the Kedah-Perak sub-area 1. The image is ranked first in the geological information content assessment for the area. Scale 1:300,000. See Figure 7.15 for similar image product of the sub-area 2.

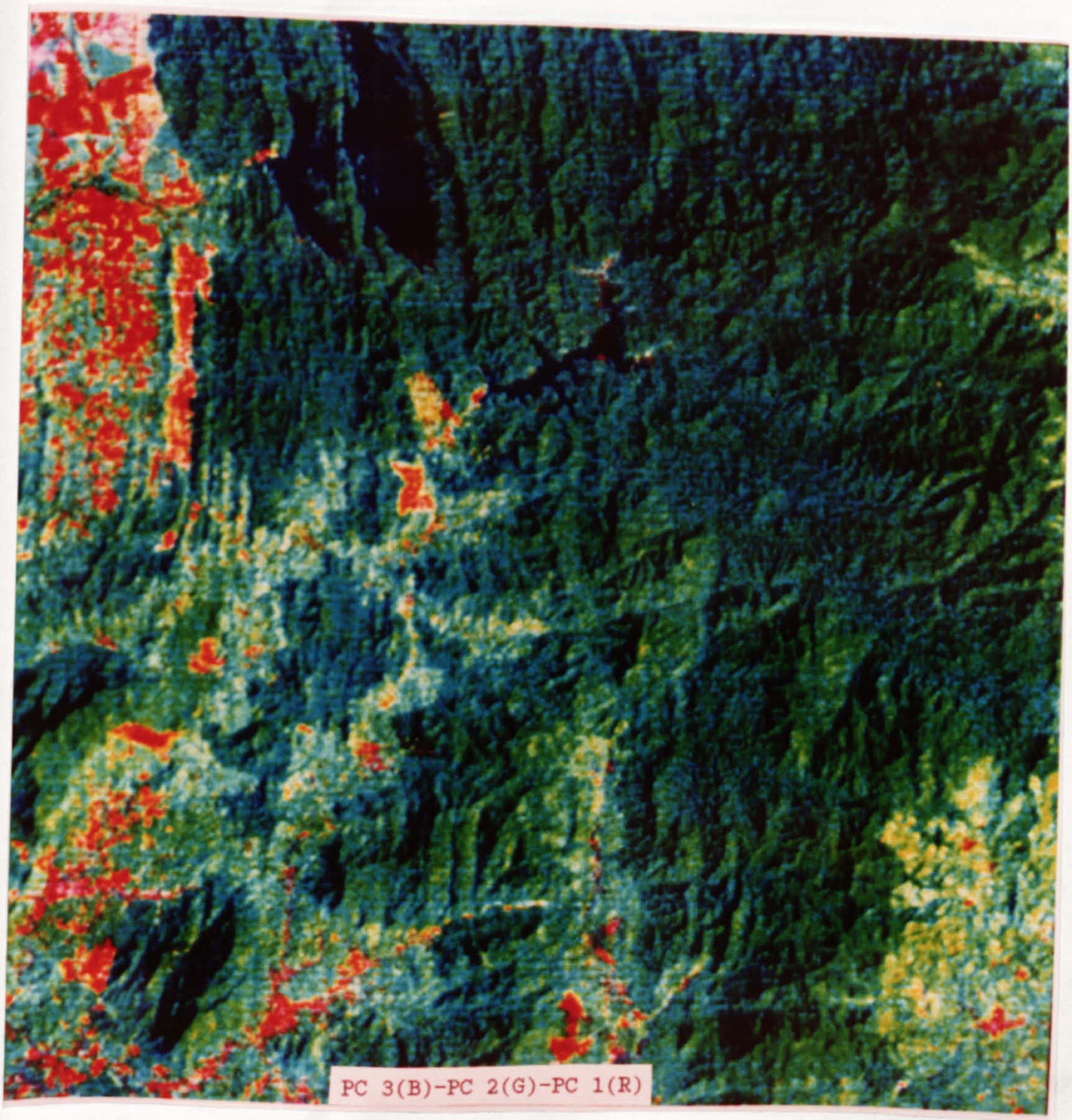

PC 3(B)-PC 2(G)-PC 1(R)

Figure 7.11 MSS principal component colour composite of the Kedah-Perak sub-area 1. This image product is ranked second among other images based on their geological information content for the area. Scale 1:300,000. See Figure 7.16 for similar image product for the sub-area 2.

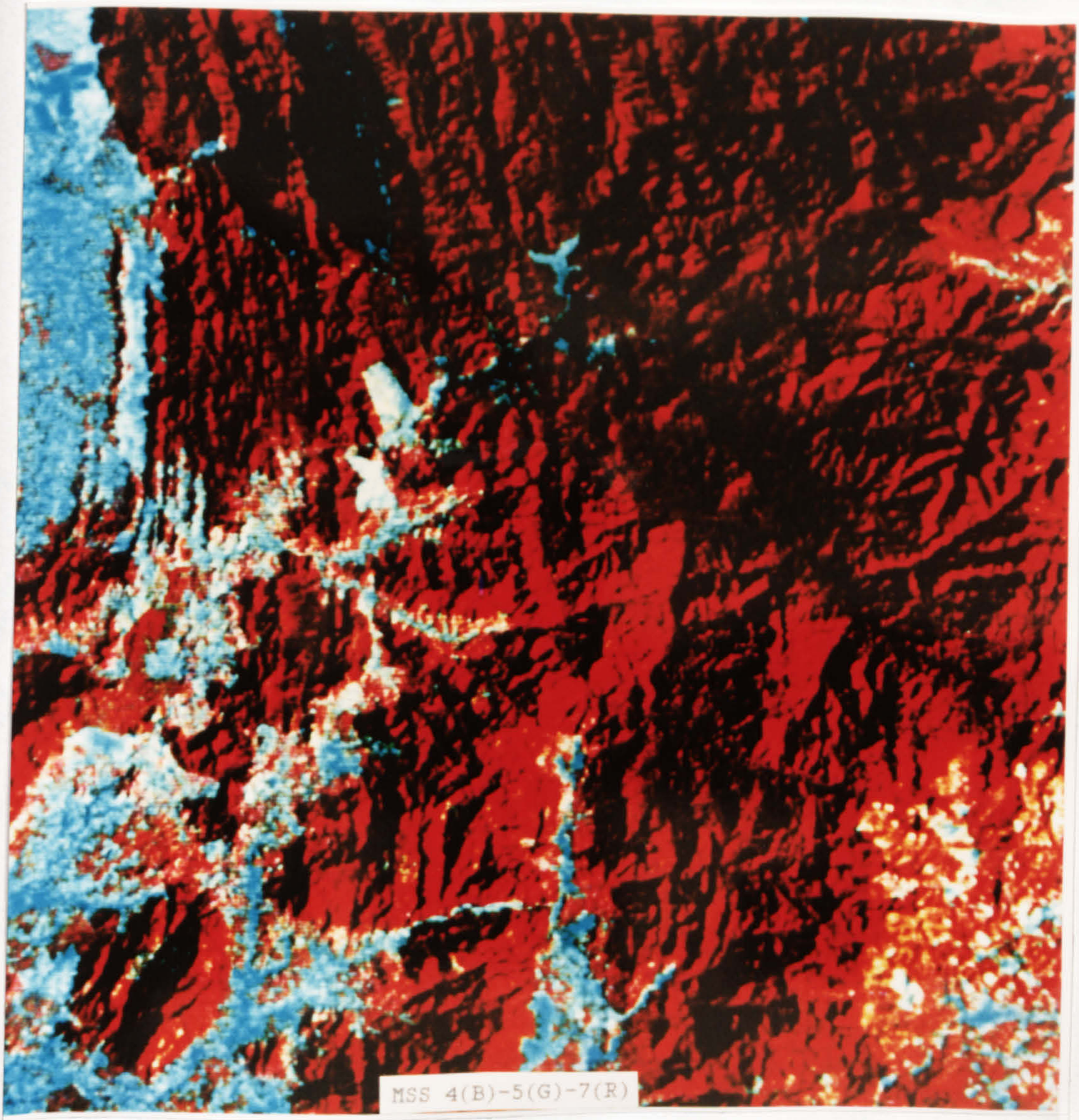

MSS 4(B)-5(G)-7(R)

Figure 7.12 MSS band 4-5-7 colour composite combination of the Kedah-Perak sub-area 1. This standard colour composite is ranked third based on its geological information content among other image products for the area. Scale 1:300,000. See Figure 7.17 for similar image product for the sub-area 2.

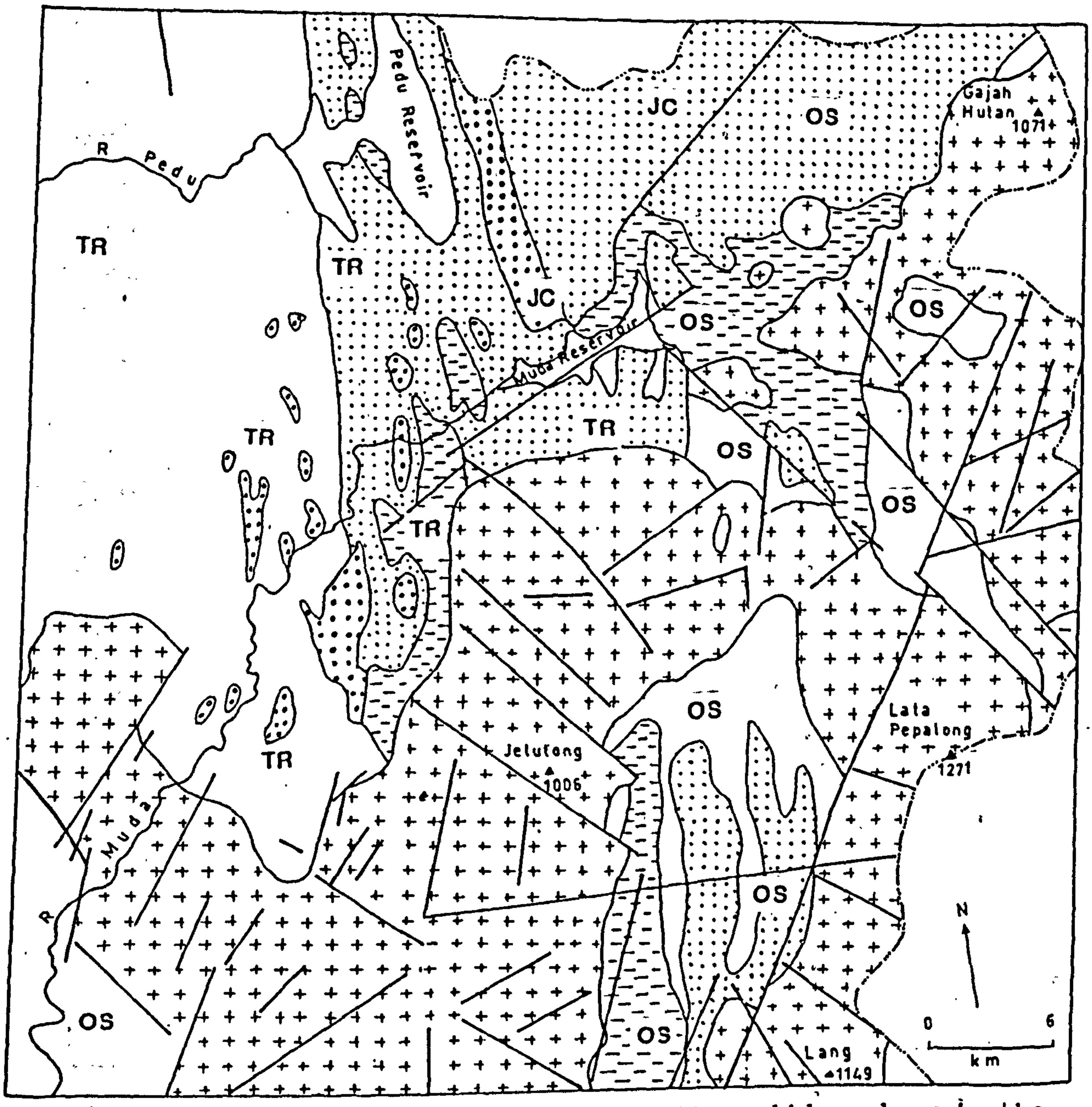

Figure 7.13 Slightly simplified map of the solid geology in the Kedah-Perak sub-area 1 (after Geological Survey of Malaysia, 1985).

Key for Figure 7.13 and 7.18

T	TERTIARY: Isolated continental basin deposits of Late Tertiary age: shale, sandstone, conglomerate and minor coal seams.
JC	CRETACEOUS - JURASSIC: Continental deposits of thick, cross-bedded sandstone with subordinate conglomerate and shale/mudstone.
TR	TRIASSIC: Interbedded sandstone, siltstone and shale; widespread volcanics, mainly tuffs of rhyolitic to dacitic composition. Limestone, conglomerate and chert locally prominent.
OS	SILURIAN - ORDOVICIAN: Schist, phyllite, slate and limestone. Minor intercalations of sandstone and volcanics.

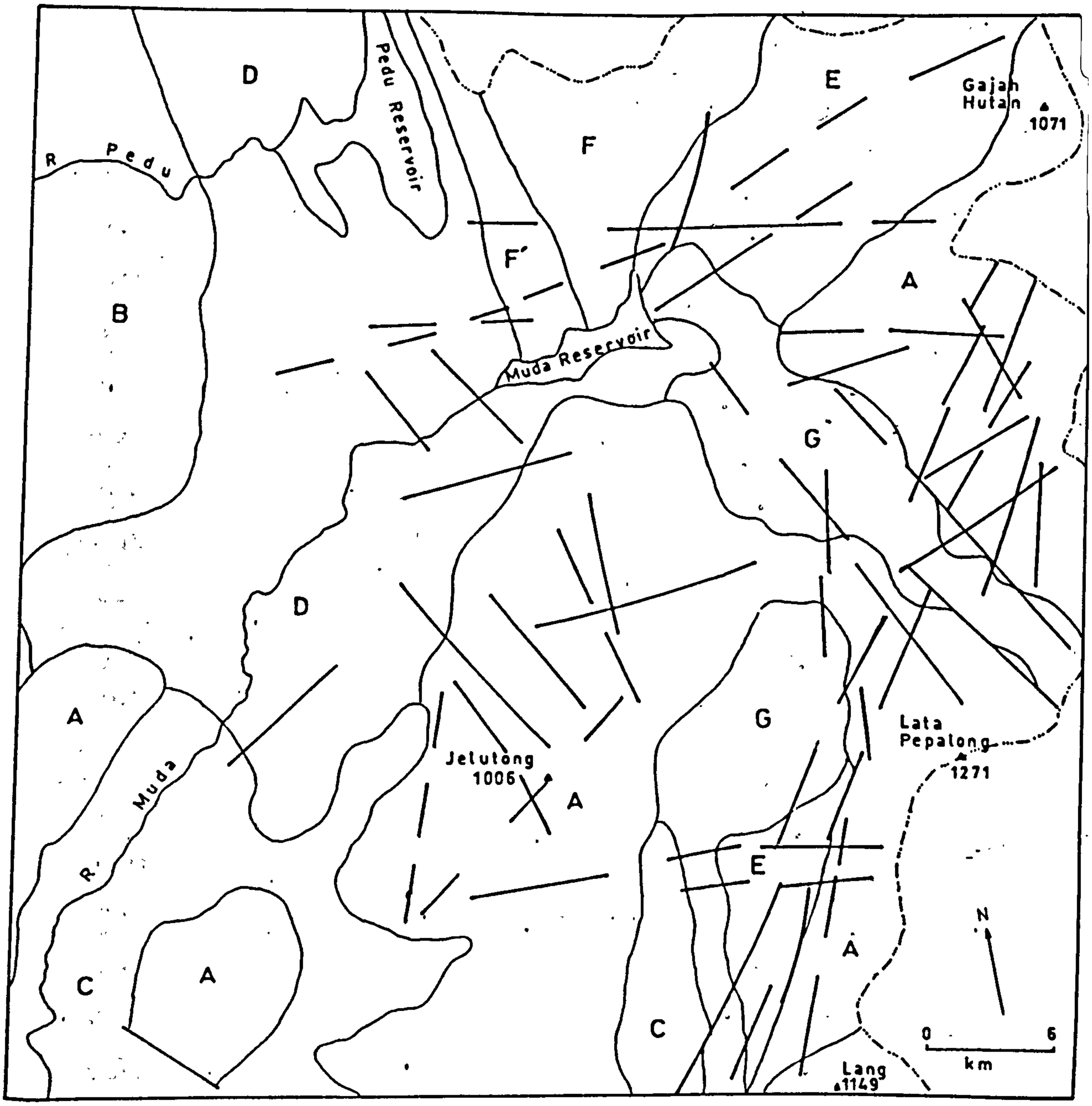

Key for Figure 7.14 and Figure 7.19

IMAGE UNIT	IMAGE CHARACTERISTICS	PROBABLE LITHOLOGY
A	resistance: very high; no "bedding sign"; lineament/jointing: multiple direction, persistent, high density; coarse texture; vegetation: very dense.	Igneous rock - granite
B	resistance: low; massive to well bedded; lineament/jointing: low density; cultivation: intense; texture: fine to speckled.	Sedimentary rock -shale/sandstone
C	resistance: low; massive; lineament/jointing: low density; texture: fine to speckled; cultivation: intense; vegetation: sparse to scattered.	Sedimentary/ metamorphic rock - siltstone/shale/ slate
D	resistance: moderate; well bedded; lineament/jointing: less persistent, low density; texture: linear to banded; cultivation: none; vegetation: very dense.	Sedimentary rock interbedded sandstone - siltstone
E	resistance: moderate to high; massive to well bedded; lineament/jointing: less persistent and medium density; texture: moderate coarse, banded and linear.	Metamorphic rock -schist/meta-sandstone

Figure 7.14 Geological interpretation of the Kedah-Perak sub-area 1 based on the Landsat MSS imagery. Thick lines are major lineaments which may represent geological faults. See Table 7.4 for further detailed characteristics of the image units.

western and southwestern areas of the sub-area 2 (Figure 7.15, 7.16 and 7.17), the unit can be delineated easily and correlates very well with the granite in the published map (Figure 7.18). However, for other areas where the granite does not form higher topography or does not show the above mentioned characteristics, they do not correspond with the mapped geology. For example, at the southwestern corner of the sub-area 1 (Figure 7.10, 7.11, and 7.12) and northwestern corner of the sub-area 2 (Figure 7.15, 7.16, and 7.17), the lowland area with fine to speckled texture, intense cultivation and sparse to scattered vegetation cover is mapped as granite (Figure 7.13 and 7.18), but is interpreted as sedimentary rocks (shale and siltstone) (Figure 7.14 and 7.19). Such areas, which are occupied by rock shattered and deeply weathered rocks, simply need clarification and supporting data, for example from field visits, to resolve it. For an area where unit A is bounded by another unit which also forms higher topography, however, it is still possible to differentiate between them based on their image characteristics. For example, by careful examination of the strike ridges or "bedding traces" of unit D at about the centre of the sub-area 1 (Figure 7.10, 7.11, and 7.12), it was possible to draw its boundary with unit A (Figure 7.14). A similar situation occurs in the northeastern corner of the sub-area 1 where unit E, although it forms higher topography and has similar image characteristics with unit A, and can be identified separately, by close examination of subtle "bedding signs" of unit E.

Image unit B, which has typical image characteristics such as low relief impression (low resistance), very low lineament density, intense cultivation and a few none persistent strike ridges (Table 7.4), is interpreted as sedimentary rock (shale and siltstone), and occupies an area at north-west corner of sub-area 1 (Figure 7.14). When comparing this with the mapped geology (Figure 7.13), the image unit B corresponds to part of the Triassic sedimentary rocks (interbedded shale, siltstone and sandstone, conglomerate locally prominent). Based on the image characteristics, the unit B is therefore likely to represent interbedded shale and siltstone (with occasional sandstone or conglomerate beds which form occasional non persistent strike ridges).

Image unit C also shows similar image characteristics to image unit B such as low relief impression, intense cultivation and sparse to scattered vegetation cover (Table 7.4). The unit C, however, seems to be more uniform, massive and resistant than unit B, and therefore it is interpreted as either sedimentary rock (massive siltstone or shale) or metamorphic rock (slate). When compared with the mapped geology, it was found that at the southwestern corner of the sub-area 1, the unit C is related to igneous rock (Figure 7.13), and it is related to the Silurian - Ordovician metamorphic rock at southwestern corner of the sub-area 2, while an area at the northwestern corner of the sub-area 2 unit C is related to both Triassic sedimentary rocks as well

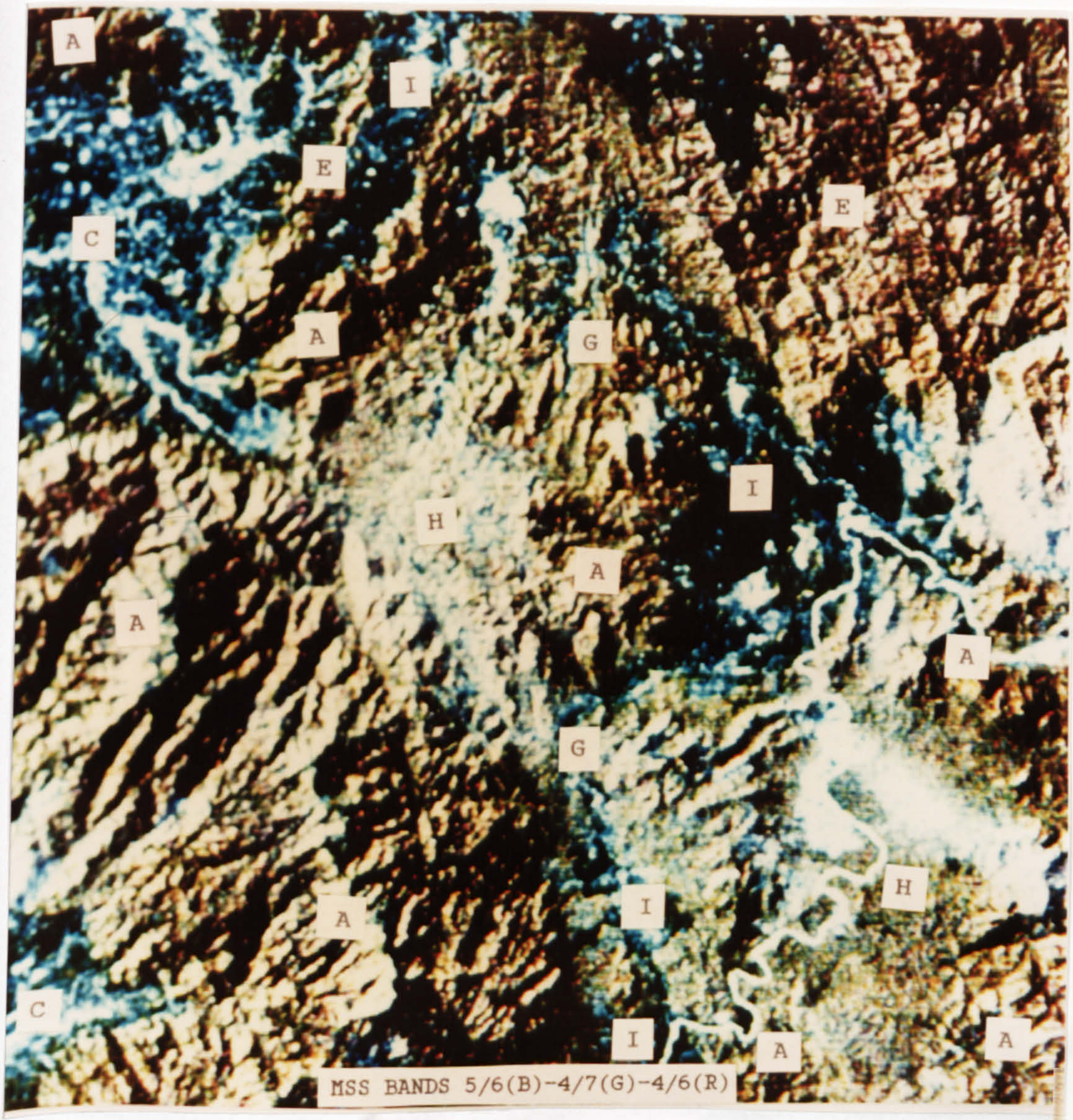

MSS BANDS 5/6(B)-4/7(G)-4/6(R)

Figure 7.15 MSS band-ratio colour composite of the Kedah-Perak sub-area 2. Scale 1:300,000. See Figure 7.10 for similar image product for the sub-area 1.

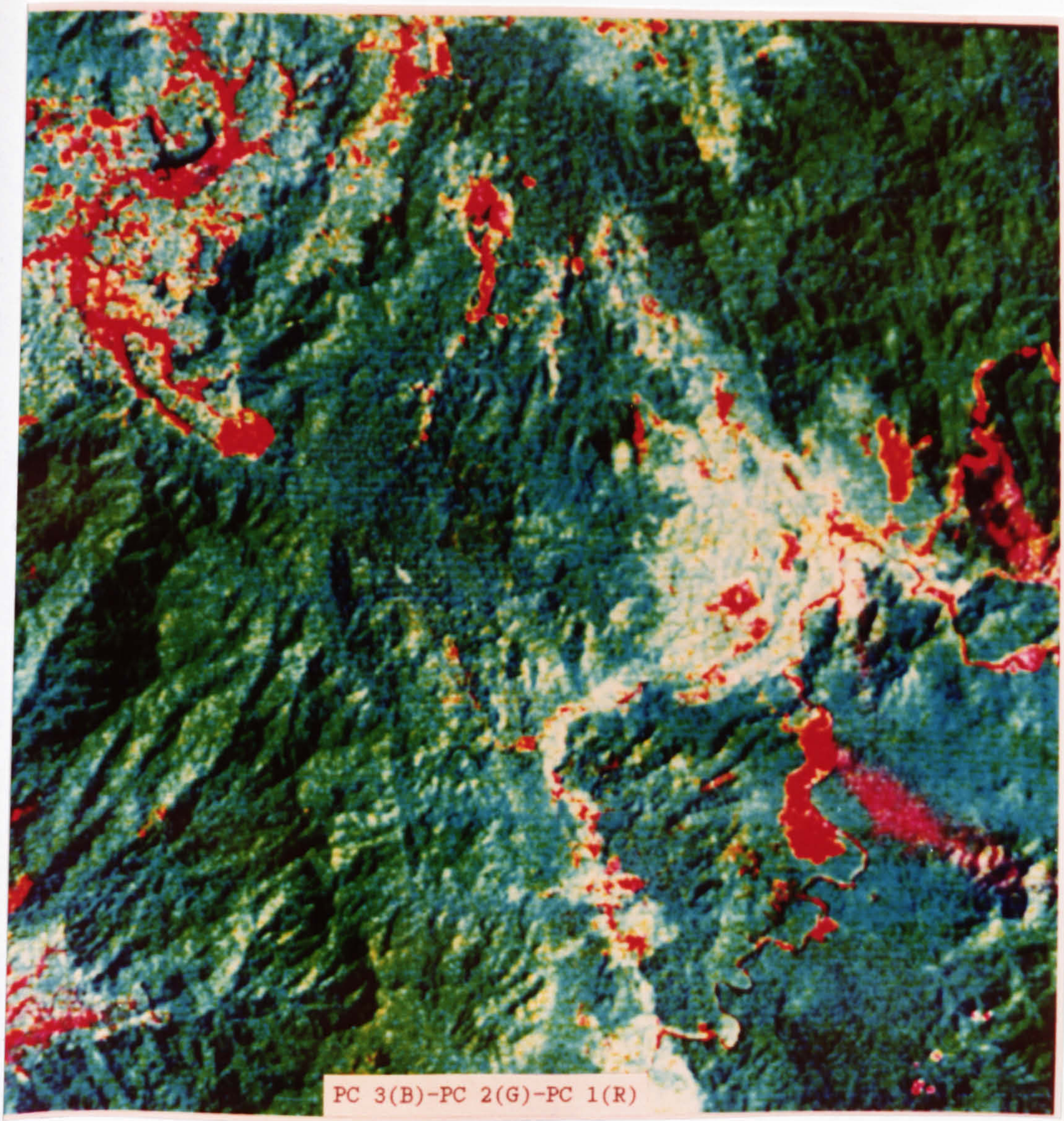

PC 3(B)-PC 2(G)-PC 1(R)

Figure 7.16 MSS principal component colour composite of the Kedah-Perak sub-area 2. See Figure 7.11 for similar image product for the sub-area 1. Scale 1:300,000.

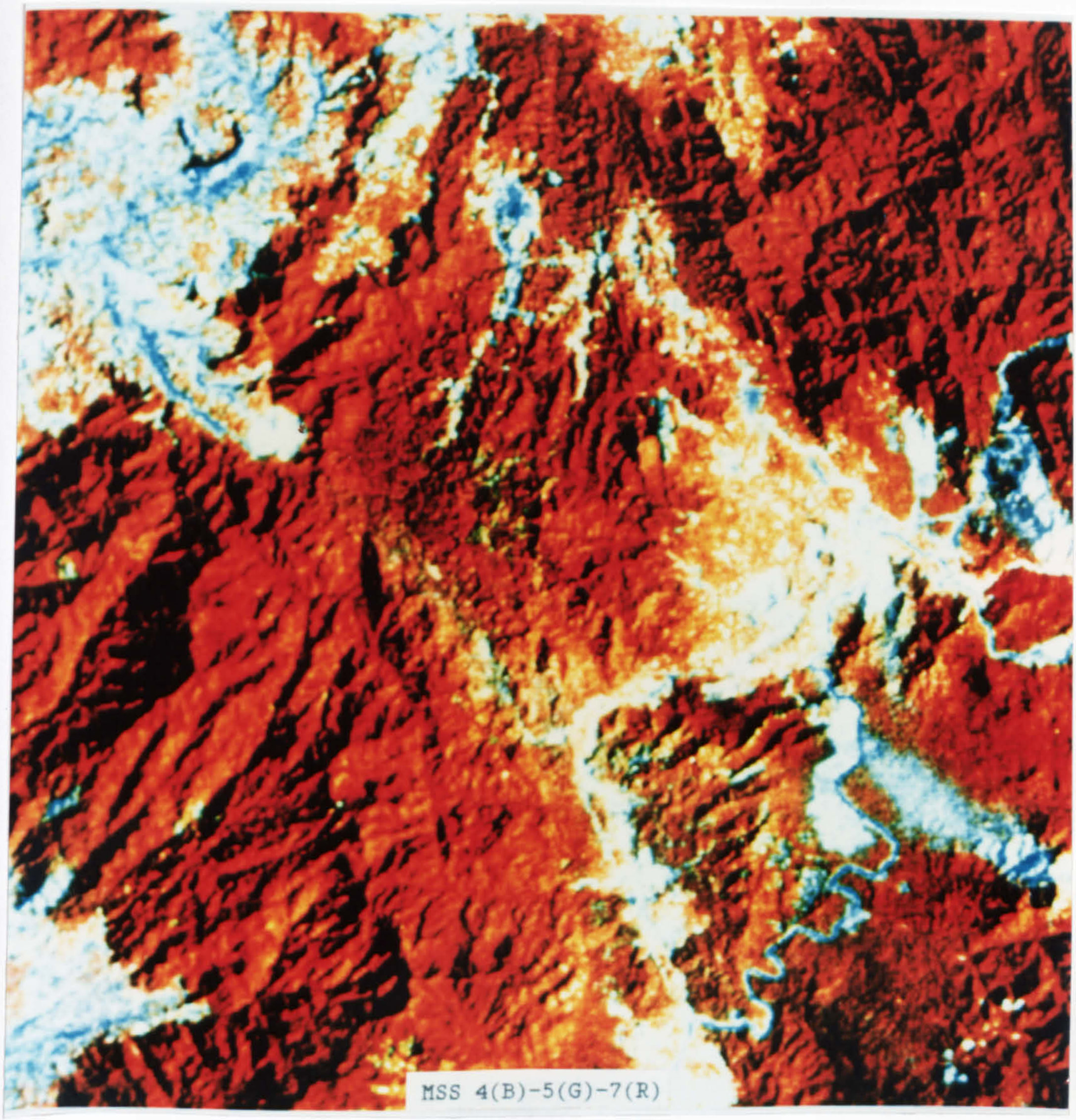

MSS 4(B)-5(G)-7(R)

Figure 7.17 MSS band colour composite of the Kedah-Perak sub-area 2. See Figure 7.12 for similar image product for the sub-area 1. Scale 1:300,000.

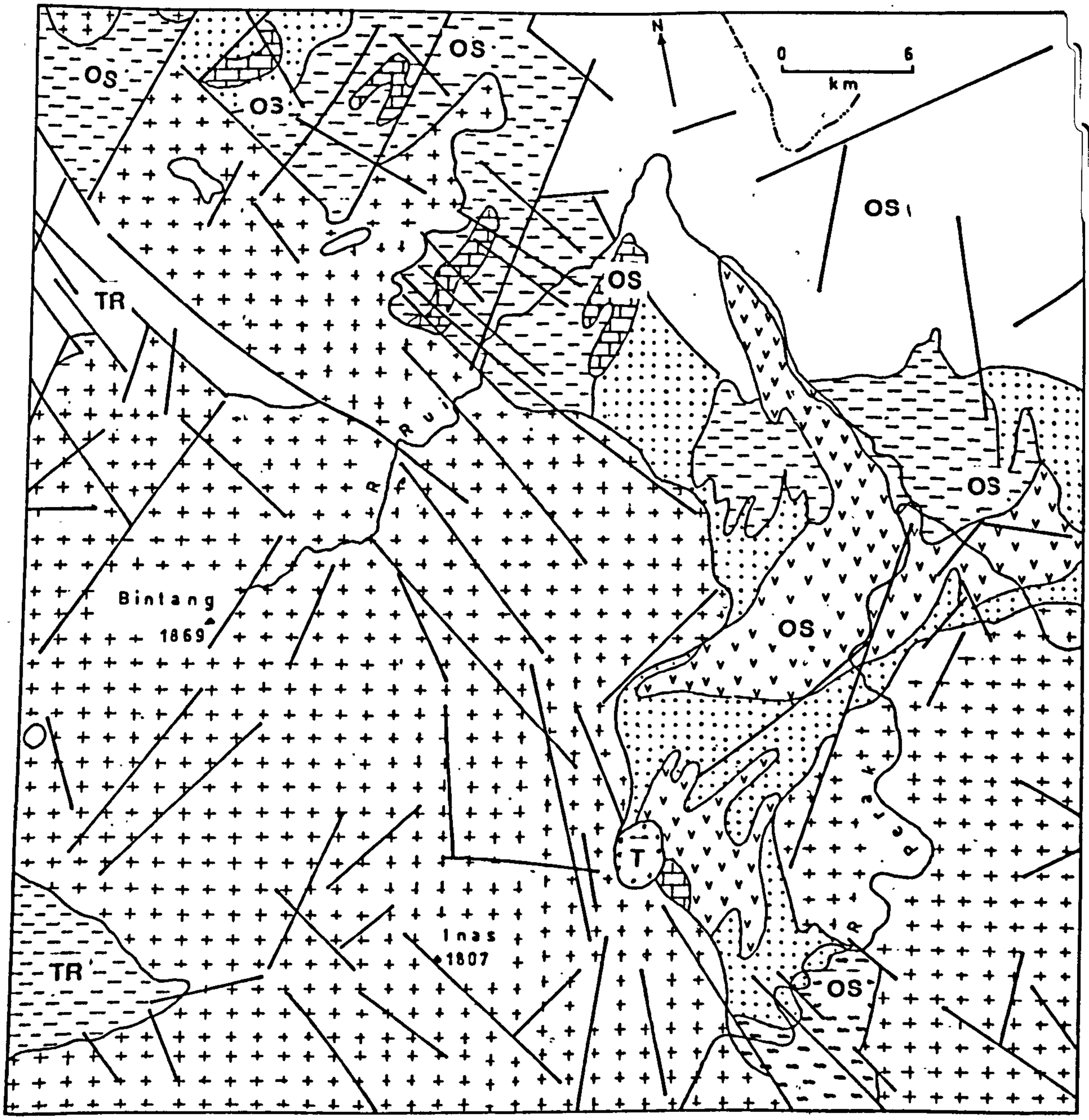

Figure 7.18 Slightly simplified map of the solid geology in the Kedah-Perak subarea 2 (after Geological Survey of Malaysia, 1985).

Key for Figure 7.13 and 7.18 (continued)

- shale, mudstone, siltstone, phyllite and slate
- sandstone/metasandstone
- conglomerate
- limestone/marble
- schist
- acid to intermediate volcanics
- acid intrusive (mainly granite)
- fault
- geological boundary

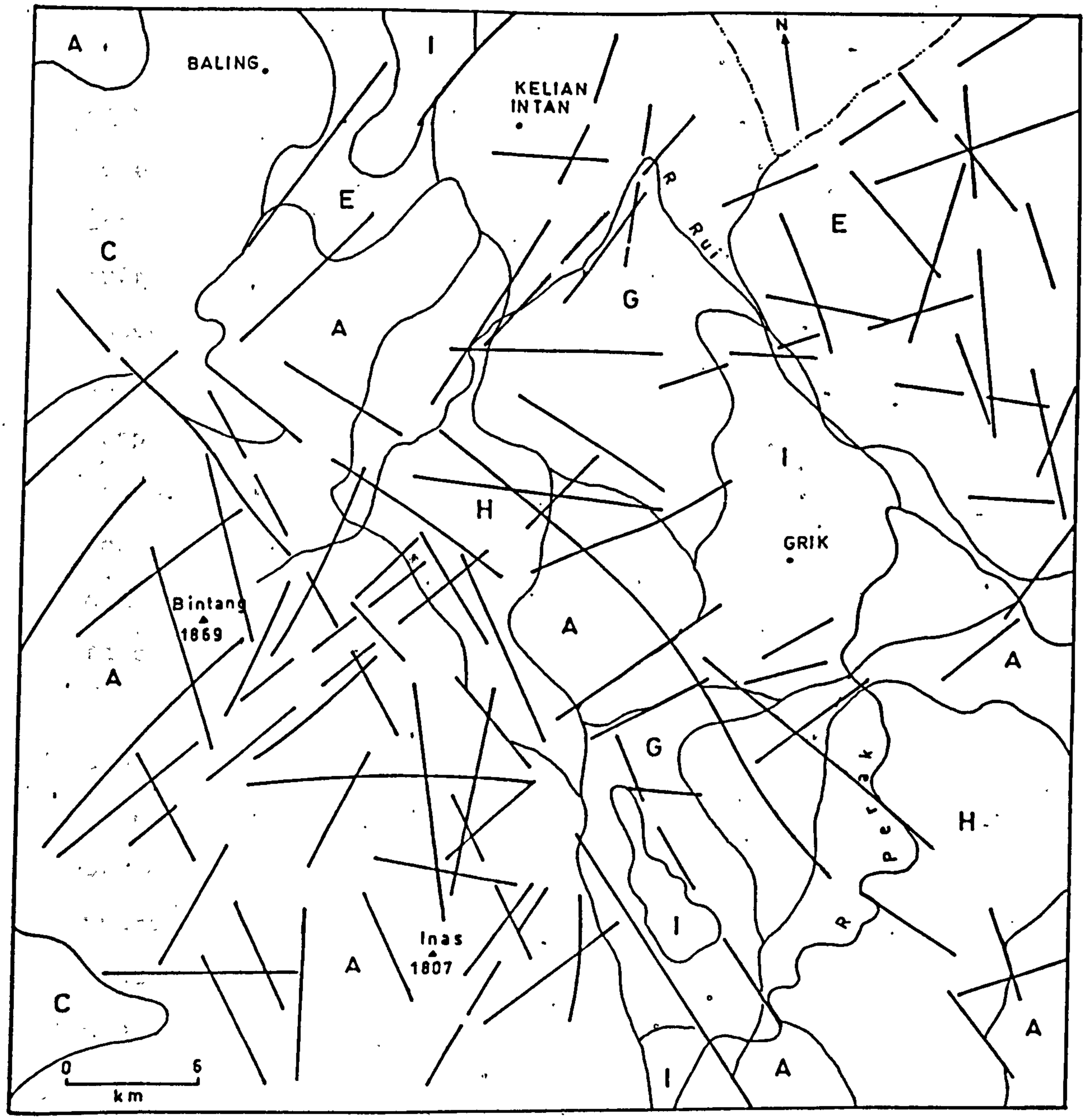

Key for Figure 7.14 and 7.19 (continued)

IMAGE UNIT	IMAGE CHARACTERISTICS	PROBABLE LITHOLOGY
F	resistance: high; well bedded to massive; lineament/jointing: not persistent and low density; texture: moderate linear and moderate banded; cultivation: none; vegetation: dense	Sedimentary rock - sandstone/ conglomerate
G	resistance: moderate to low; massive to well bedded; lineament/ jointing: low to medium density; texture: moderate uneven; cultivation: rare to common; vegetation: very dense	Metamorphic rock - phyllite/slate
H	resistance: moderate to low; no "bedding sign"; lineament/ jointing: multiple direction and medium to low density; texture: medium coarse to fine; cultivation: rare; vegetation: very dense	Igneous rock - granite
I	resistance: low; no "bedding sign"; no lineament/joint; texture: fine; cultivation: common; vegetation: moderate	Igneous rock - extrusive

Figure 7.19 Geological interpretation of the Kedah-Perak sub-area 2 based on the Landsat MSS imagery. Thick lines are major lineaments which may represent geological faults. See Table 7.4 for further detailed image unit characteristics.

as Silurian - Ordovician metamorphic rocks (Figure 7.18). It is evident that the mapped units which occur in the lowland areas do not show their typical image characteristics sufficiently clearly to separate them. Therefore, they are interpreted or classified as one unit (Unit C). The interpreted map, therefore, does not correlate well with the mapped geology and some areas probably incorrectly classified as massive shale or/and siltstone or slate. These areas, as for areas where the granite do not form higher terrain, need clarification and supporting data from field visits in order to correctly identified and map the area.

Image unit D occurs only in the sub-area 1, and its typical image characteristic is persistent parallel ridge (strike ridges) which simply indicates that the unit consists of well bedded rocks. The unit forms moderate relief, and therefore is interpreted as sedimentary rocks (interbedded sandstone and siltstone) (Figure 7.14). When compared with the mapped geology, the unit D corresponds very well with the Triassic sedimentary rocks (mainly consisting of interbedded sandstone and siltstone, and conglomerate locally prominent) (Figure 7.13). Therefore ,units B and D correspond to a similar mapped unit, the Triassic sedimentary rocks. However, based on their image characteristics, unit D is interpreted as interbedded sandstone and siltstone with occasional conglomerate, whereas unit C is interpreted as interbedded siltstone and shale with occasional sandstone.

Although image unit E appears slightly less resistant than unit F, generally these two units show similar image

characteristics such as colour, tones and vegetation. However, in terms of bedding and texture they do show slight differences (Table 7.4), hence it is possible to differentiate unit E (massive to well bedded, and moderate coarse, linear and banded texture) and unit F (well bedded to massive, and moderate linear and banded texture). Unit E is interpreted as a metamorphic rock such as metasandstone and slate whereas unit F is interpreted as a sedimentary rock unit consisting of sandstone and conglomerate. The unit E (Figure 7.14 and 7.19) corresponds with a part of the Silurian - Ordovician metamorphic rocks (mainly consist of metasandstone) (Figure 7.13 and 7.18), whereas unit F (Figure 7.14) corresponds very well with the Cretaceous - Jurassic sedimentary rocks (thick sandstone with conglomerate and mudstone locally present) in the published map (Figure 7.13). At first glance, image unit F also appears to have similar image characteristics as image unit D. The unit D, however, shows much thinner and more obvious strike ridges than in the unit F, therefore unit F should consist of interbedded rocks of much thicker beds which have nearly similar resistance. At the boundary between unit F and unit D, there is one very thick rock unit forming a long, persistent and high ridge. Based on the image characteristics, this very thick unit is designated as F' in Figure 7.14 (interpreted as a part of the image unit F), and is interpreted as a very thick sedimentary rock which possibly consists of conglomerate or sandstone or both. In the published map (Figure 7.13), this unit corresponds very well

with the mapped conglomerate of the Cretaceous - Jurassic sedimentary rocks.

All three image units, viz G, H, and I show subdued relief. The units, however, have different image characteristics, in terms of colour, tone, bedding, lineament and vegetation cover (Table 7.4). Unit G which has a subtle "bedding sign" and nearly massive character is interpreted as a metamorphic rock (phyllite and slate) rather than a sedimentary rock (Figure 7.19). Comparing the mapped geology, image unit G corresponds with a part of the Silurian - Ordovician metamorphic rocks (mainly related to phyllite and slate) (Figure 7.18). The unit E also corresponds with the Silurian - Ordovician metamorphic rocks. Based on their image characteristics, the unit G (low resistance) may consist of slate and phyllite whereas the unit E (high resistance) may consist of phyllite and metasandstone. Both image units H and I do not have a "bedding sign", unit H, however, has moderate coarse texture, moderate lineament density, dense vegetation cover and no cultivation, whereas unit I has fine texture, no lineament, much less dense vegetation cover and is cultivated (Table 7.4). Based on their image characteristics, therefore unit H is interpreted as an igneous rock (granite), and unit I is interpreted also as an igneous rock (intrusive) (Figure 7.19). Comparing the published map (Figure 7.18), the image unit H corresponds with a part of the mapped acid intrusive (granite). For the image unit I, two of them correspond quite well with the Silurian - Ordovician rock unit (consisting of volcanics - rhyolite tuff), whereas the one at the north in

the sub-area 2 is mapped as the Silurian - Ordovician rocks (consisting of slate and phyllite) and the one at the south is mapped as the Silurian - Ordovician rock (consisting of schist) (Figure 7.18). In this area, although the units do not form high relief, some image characteristics such as lack of "bedding sign" and multiple direction and lineament density can still be observed, and hence make it possible to interpret and identify igneous rock in the area. This intrusive rock may represents the granite which has been considerably affected by hydrothermal alteration, and in such areas weathering and erosion may have progressed more rapidly to produce undulating granitic terrain of less pronounced relief (Jones, 1970). However, the two areas which are interpreted as an intrusive rock do not correspond with the mapped geology. Supporting data from field visits are needed for such areas in order to map the areas correctly.

It is evident that no single image unit corresponds with any one of the mapped units. Except for the image unit C, however, combinations of two or three of the image units do correspond quite well with certain mapped units. For example, a combination of the image units B and D corresponds with the mapped Triassic rocks, and a combination of image units E, G, and I corresponds with the mapped Silurian - Ordovician rocks. The interpretation map (Figure 7.14 and 7.19) and correlation between the image units and the mapped units (Table 7.5) have shown four rock types namely interbedded shale, siltstone, sandstone (Triassic Rocks), conglomerate (Cretaceous -

IMAGE UNITS		MAPPED UNITS	
		Lithology	Period
A	granite	acid intrusive, mainly granite	Cretaceous-Triassic
H	granite		
F	sandstone and conglomerate	thick sandstone with conglomerate and mudstone locally present	Cretaceous-Jurassic
F'	thick sandstone or conglomerate or both	conglomerate	
B	shale and siltstone with sandstone	interbedded shale, siltstone and sandstone, conglomerate locally prominent	Triassic
D	sandstone and siltstone with conglomerate		
C	siltstone or shale; or slate		
E	phyllite and metasandstone	mainly metasandstone	Silurian-Ordovician
G	phyllite and slate	mainly phyllite and slate	
I	extrusive igneous rock	volcanic facies: rhyolite tuff	
		schist	

Table 7.5 Correlation between the image units and the mapped units for the Kedah-Perak area.

Jurassic), sandstone and conglomerate (Cretaceous - Jurassic) and metasandstone (Silurian - Ordovician) were identified and delineated on the Landsat images. In addition to these, a very large area of the granite (Acid intrusive), volcanics (Silurian - Ordovician) and interbedded siltstone and shale (Triassic) were also delineated. It was not possible to delineate each of the rock types (facies) which occupy only a small area, and as a result, for example, schist, phyllite, slate, limestone and with minor sandstone and volcanics (Silurian - Ordovician) areas are classified as one image unit, G. In addition, a number of lowland areas which are underlain by the Triassic, Silurian - Ordovician and Acid Intrusive were not delineated to correspond with the mapped geology. Two other small areas, one area corresponds with the schist (Silurian - Ordovician) while the other corresponds with the phyllite and slate (Silurian - Ordovician) were classified together as image unit I (extrusive igneous rock). It was also not possible to identify and to delineate the Late Tertiary to Quaternary deposit (Lawin Basin Deposit) which occupies a small area in the sub-area 2 (Figure 7.18).

Beside rock types, many lineaments were observed on the Landsat images. Some of them coincide very well with the known faults. From the images, many lineaments (possibly representing fault lines not previously mapped) were delineated. The lineament analysis of the area is discussed in the Chapter 8.

7.3.4 Summary

In summary, this study (which should be seen as a preliminary attempt in lithological mapping from space using Malaysian example) has demonstrated that the Landsat MSS images are useful for lithological interpretation at scale 1:250,000 in Kedah-Perak area, Malaysia. Geologic features, including main rock units, are readily interpreted despite the dense vegetation cover. The study has shown that for this area (which is almost completely covered by dense vegetation), the textural information are more important that the spectral in order to identify and separate between different rock types.

CHAPTER 8

INTERPRETATION OF THE IMAGE PROCESSING: lineament mapping and analysis

8.1 Introduction

Linear features (lineaments) on the surface of the earth have attracted the attention of geologists for a long time (e.g. Hobbs ,1904 and 1911 and Rich, 1928). Early lineament interpretations were made from aerial photographs. After the second World War particularly in the sixties, numerous articles dealing with the detection and geological interpretation of linear patterns on aerial photographs appeared (e.g. Kaiser, 1950; Blanchet, 1957; Kupsch and Wild, 1958; Lattman, 1958; Henderson, 1960; Brown, 1961; Lattman and Matzke, 1961; Haman, 1961; Mollard, 1962; Boyer and McQueen, 1964; Allum, 1966; van der Meer Mohr, 1967; Renner, 1968; Norman, 1969; Rumsey, 1971; Tjia, 1971). More recently, since space photographs were made and data became available from satellites, geologists have been interested in tracing lineaments from such images. The synoptic view of topography provided by satellite images, most particularly by those from the Landsat series, when taken under favourable atmospheric conditions, can be considered equivalent to controlled, mosaics of aerial photographs. This imagery has led to an upsurge of interest in lineament analysis.

As a result a considerable number of papers on lineament interpretation have been published. Many authors have used lineament interpretations to delineate fractures and fracture systems in different parts of the world (e.g. Viljoen et al., 1975; Sesören, 1976; Johnson and Frost, 1977; Offield, 1977; Ramberg, et al., 1977; Kim, 1979; Iranpanah and Esfandiari, 1980; Csillag, 1982; Cochrane and Tianfeng, 1983; Moore and Waltz, 1983; Stefouli and Osmaston, 1984; Bellis et al., 1985; Isiorho, 1985; Parsons and Yearley, 1986; Maude, 1987), or to map of previously unknown faults or structures (e.g. Johnston et al., 1975; Reeves et al., 1975; Johnson and Frost, 1977; Gold, 1980; Williams, Jr, 1983; Sabin, 1987), or to carry out structural analysis of global or regional tectonics (e.g. Molnar and Tapponier, 1975; Cardamone et al., 1976; Dikkers, 1977; Frost, 1977; Braun, 1982; Marrs and Raines, 1984; Zilioli and Antoninetti, 1987). In addition, the potential economic importance of the linear structural features in terms of, for example, ground water exploration (e.g. Moore and Hinkle, 1977; Vincent and Scot, 1978), base metal deposits and petroleum exploration (e.g. Halbouty, 1976; Offield et al., 1977; Rowan and Lathram, 1980; Turner et al., 1982; Ahmed, 1983), has promoted numerous investigations of linear features on the Landsat images (Short and Lowman (1973). Given the importance, it must be stated that lineaments are often very subtle and vary in the characteristics that enable them to be seen on Landsat images, and many are preferentially enhanced by varied illumination conditions. Hence their recognition is subjective, and such interpretation can be variable (Siegal

and Short, 1977; Moore and Waltz, 1983). In addition to that, the results obtained from lineament analyses can vary considerably in their information content because of the effects of several factors such as ability of interpreters, the data source and the definition (Tomes et al., 1974; Siegal and Short, 1977; Burns et al., 1976; Burns and Brown, 1978; Huntington and Raiche, 1978; Parsons and Yearley, 1986; Koopmans, 1986 and 1988). Therefore, along with this upsurge there has been a growth of disquiet over reliability in identification of lineaments and hence the validity of their interpretation has been questioned (Podwysocki et al., 1975; Wise 1982 and 1983; Moore and Waltz, 1983; Wheeler, 1983).

Furthermore, the image analysis developed for a certain region may not be applicable in other regions (Kim, 1979). It would be useful, therefore, to develop a methodology which minimises possible bias and variation in mapping, and the delineation of lineaments must be recognised by an objective method. In this case, the Loch Tummel and the Kedah-Perak areas were selected to examine the use of images for lineament mapping and analysis. A few important points such as the recognition and the definition of lineaments, the data source, the basis of analysis and the method of interpretation will be discussed first. This is followed by the results of lineament mapping and analysis for the study areas and these are discussed in section 8.2 and 8.3.

8.1.1 Recognition and terminology of lineaments

The earliest descriptions and recognition of spatial relationships among linear features that may be related to underlying geologic structures was given by Hobbs (1904), who introduced the term "lineament" to characterize such relationships among (a) *crests of ridges or boundaries of elevated areas*, (b) *the drainage lines*, (c) *coast lines*, and (d) *boundary lines of formations, petrographic rock types, or lines of outcrops* (p. 485), and defined the term lineament as: "*significant lines of landscape/the Earth's face that reveal the hidden architecture of the rock basement*" (Hobbs, 1912, p. 227). With the increased usage of aerial photographs and satellite images, much confusion has arisen regarding the term and its definition for a "linear feature" or "lineament" found on images or photographs. Numerous definitions of lineaments exist, the main variations being in terms of length and the type of data source of detection (e.g. air photographs, satellite images etc.) Siegal and Short (1977) showed the great diversity of names and non-systematic nomenclature for linear features that is now used, and they found that linear features are often referred to as: *linears, lineations, linear elements, shadow linears, lineaments, faults, photo-lineaments, linear structural features, fracture traces, cultural linears, megajoints, topographic lineaments, structural lineaments, transgressive linear features, mesofractures, and microfractures*. This shows that there is often little agreement as to what linear features are, partly because the criteria for their recognition are not clearly established and partly because the definitions are inadequate. O'leary et al. (1976) examined in full the terminology and definitions which have been used for the

linear features. They defined the word lineament as "*a mappable, simple or composite linear feature of a surface, whose parts are aligned in a rectilinear or slightly curvilinear relationship and which differs distinctly from the patterns of adjacent features and presumably reflects a subsurface phenomenon.*" (O'leary et al., 1976, p. 1467). In their conclusion they proposed to use the word lineament which could be applicable to the earth sciences in general and to geologic remote sensing in particular, rather than linear or lineation having distinctly different meaning from structural elements on the images. Their terminology has been used in this sense by, for instance Dikkers (1977), Frost (1977), Johnson and Frost (1977), Kim (1979), Moore and Waltz (1983), Lake et al. (1984), Isiorho (1985), Maude (1987), Zilioli and Antoninetti (1987).

Some lineaments are particularly noticeable due to their narrow linearity, and the way they appear to cut across other features on images. In many instances, however, the recognition of lineaments on the images is extremely difficult because they often appear as subtle features and vary in the characteristics by which they are recognised. Therefore the diagnostic characteristics used in their photo-identification often vary from one lineament to another. According to Tunstall (1975), an image consists of basic units or points, and if a point is to be assigned to a lineament the point has to fulfil certain criteria, for example one point must be adjacent to at least another similar one and they must form a linear feature, and the points must share a property common to all members of the feature, and not shared with points outside

the line. These characteristics are based on the relief, pattern, texture and tones of the images. There are also lineaments which, strictly speaking, are not themselves composed of identifiable points, but form the boundary between two areas which differ in image characteristics such as tone, texture, relief and pattern, to be recognised as, for example vegetation alignments, linear topographic features, relief change lines, dark tonal lines, textural lines and linear drainage channels (Renner, 1968; Stefouli and Osmaston, 1984). Therefore lineaments are usually manifested by a variety of surface features, and may be distinguished on Landsat images on the basis of one or more of the following criteria (Short and Lowman, 1973):

a. lines of variable length, straightness, and continuity, as set apart by tonal contrasts in the image.

b. bands of variable width which contrast in tone to the areas immediately adjacent.

c. alignments of topographic forms.

d. alignments of drainage patterns.

e. co-alignment of cultural features, e.g., farms, road patterns, etc. with underlying structural and/or surrounding topographic control.

The above properties and characteristics were used in this study to recognise the lineaments, and the definition by O'leary et al. (1976) was adopted to delineate them on the images.

8.2 Data selection and approach in delineation of lineaments

In accordance with the objective of the study, the Landsat TM and MSS data were obtained for the Loch Tummel and the Landsat MSS data for the Kedah-Perak area (see Table 4.5 in Chapter 4). The TM band 5 (Figure 6.5D) and the MSS band 7 (Figure 6.4) of the Loch Tummel, and the MSS band 7 for the Kedah-Perak area (Figure 6.6D) were found the best in terms of contrast and definition of geological features (section 6.2.2 in the Chapter 6). These images were digitally processed (section 5.5 in the Chapter 5) in order to enhance lineaments for both areas. The structural assessment results for several image products of the Loch Tummel area, see Table 6.9, has indicated that the filtered image of the TM band 5 using the Laplacian convolution filter was found to be the best (Figure 8.1B) and edge enhancement filter (8.2B) was the second best for this purpose. Based on visual observation, the same image products for the MSS of the Loch Tummel area were found the best two for lineament mapping (Figure 8.1A and 8.2A). Table 6.8 (section 6.3 in the Chapter 6) shows that the contrast stretched of MSS band 7 (Figure 8.9) and filtered MSS band 7 image using the Laplacian convolution filter (Figure 8.10) were found the first and second best respectively in enhancing lineaments for the Kedah-Perak area. These image products therefore were used in this study for lineament mapping. In addition to the above mentioned non-directional enhancement image products, four different images were also produced for each data sub-scene by different directional filters (north-south, northeast-southwest, east-west, northwest-southeast) as

mentioned in section 5.5.4 and 6.2.7. These directionally processed images were also used for lineament mapping and analysis for both areas (Figures 6.30 and 6.31). All the image products were produced at scale 1: 130,000 for the Loch Tummel and 1: 250,000 for the Kedah-Perak areas.

Lineaments were mapped by photo-interpretation from the best two of the computer enhanced images for both areas, the Loch Tummel and Kedah-Perak. This method does not imply any automated technique for computer extraction of lineaments, but the use of appropriate enhanced images where lineaments can be more easily traced. Therefore, in this particular study, all lineaments with an arbitrary minimum length of 1 km for the TM and the MSS data for the Loch Tummel area as well as for the MSS data for the Kedah-Perak area, were traced on transparent paper placed over the images by visual interpretation. This interpretation method has been criticized as subjective by Moore and Waltz (1983), who argued in favour of machine processing, due to inter- and intra-operator variance. Whilst computer processing does avoid such problems, however, it raises the issue of adequacy of algorithms for lineament identification. Fully automated methods require an inordinate amount of computer processing of the image, adequate algorithms for lineament identification which at the present time are still being developed and would still not produce an accurate map devoid of cultural effects (Podwysocki et al., 1975; Parsons and Yearly, 1986). This means that the machine method still requires some interaction to eliminate cultural effects, for example by comparing the

output with the topographic map. It was thought that the visual interpretation method can still be retained if the problems of subjectivity can be resolved. In this study, the problem of inter-operator variance stressed by Moore and Waltz (1983) was avoided by using only one operator. The intra-operator variance was minimized by following a standard method for lineament mapping (Parson and Yearley, 1986), as follows: a transparency with a grid was placed on the image. By this means the image was divided into small units of equal size, where each of the units could be examined separately, for example in this study using magnifying glass, thereby assuring a near-uniform observation of all of the study area. The size of the grid was quite arbitrary and one of 2 cm side (equivalent to a ground distance of about 2.5 km for the Loch Tummel and 5 km for the Kedah-Perak areas) was selected for convenience.

This method was applied to the two best images examined to map the lineaments. The two interpretations produced for each of the data sets were then superimposed and all lineaments present on both interpretations were traced onto a new overlay. The four directionally filtered images of each data set were also interpreted visually and followed the same method. Photo-interpretation of lineaments detectable on conventional Landsat images necessarily implies some limitations due to the characteristics of the satellite sensor system (Zilioli and Antoninetti, 1987). Therefore, the use of the directionally enhanced images for lineament mapping is essential in order to minimise these limitations. The

interpretations, however, show that some lineaments are only apparent in one enhanced image; such features are often artifacts of the processing. Because of this, in this study, each of the four images produced for each of the data sets was interpreted separately. Four interpretations produced for each of the data sets were then compared and all lineaments present on more than one of the interpretations were traced onto a new overlay. By adopting this procedure, the lineament mapping was considered to be more objective. The two new overlays for each of the data sets were combined and all lineaments were traced onto a final interpretation. The results which include only the most definite lineaments are shown in Figure 8.3, 8.4, 8.11 and 8.12. Three points need to be mentioned. First, care is needed in the interpretation of the results of such analysis to exclude man-made features, therefore, the final maps were screened to remove lineaments related to cultural features such as railways and roads by comparing with the topographic maps and geological maps of the areas. Secondly, when comparing or superimposing two interpretations, all lineaments which fell within approximately 130 m (1 mm on the 9 x 9 inch images of 1: 130,000 scale images of the Loch Tummel data sets) and within approximately 250 m (1 mm on the 9 x 9 inch images of 1: 250,000 scale of the Kedah-Perak data set) of each other and deviated by no more than approximately 3 degrees are considered contiguous, and where two lineaments overlap by more than half their length they are considered to be coincident. Thirdly, the negative images of the TM band 5 and MSS band 7 for the Loch Tummel, and the MSS band 7 for the

Kedah - Perak areas were used as a complementary data source in the lineament mapping because they can offer additional information, as described in section 6.2.8.

In this study, lineament directions and lengths were measured and grouped in 5° interval classes and rose diagrams for the lineaments were constructed. Several studies (Blackstone, 1975; Offield et al., 1977; O'leary et al., 1977) have used rose diagrams or histograms, which show azimuth-frequency of lineaments, to reveal the significant trend of lineaments. In such studies, the number of lineaments found in any direction is used as a frequency for each azimuth. Due to the method of interpretation described above, visually distinct lineaments are shown as single continuous lines and less distinct ones as composite structures composed of many short aligned portions. It is therefore perhaps unreasonable to produce a rose diagram only by cumulating the frequencies of lineaments within different azimuth ranges by number, as this tends to bias the distribution towards the less visually distinct structures. Therefore, in this analysis, the rose diagrams have been constructed by aggregating the total length of lineaments within given azimuth ranges of 5°, as was done in Henderson (1960) and Raines (1978). In this way more weight is given to long lineaments, which are more likely related to geological structures such as faults, than are short ones. For comparison, however, the rose diagrams shown in this study were taken from the lineament interpretation and show the azimuthal distribution of lineaments calculated by both length as well as by number of observations.

8.3. Lineament mapping and analysis of Loch Tummel area

A total of 735 lineaments, 398 from the TM and 337 from the MSS data sets of the Loch Tummel, with a total length of 946 km (413 km from the MSS and 612 km from the TM data) were traced. Only the lineaments with minimum length of about 2 km are shown in Figure 8.3 and 8.4. Length, orientation and frequency of the total lineaments were measured and counted, and summarised in Figure 8.5. Comparison between these two maps indicates a very good overall agreement, particularly in terms of lineament trends, although in detail a number of differences exist which may related to spatial resolution and natural cover of the two data sets.

8.3.1 General lineament pattern and distribution

Except in a few lowland areas, where exposures are extremely bad due to substantial alluvial and drift cover, the distribution of lineaments on the maps is probably a fairly accurate reflection of occurrence and density of the fractures. In the interpreted maps (Figure 8.3 and 8.4), although they are ubiquitous, they are most frequent, particularly in the TM data, in half of the area from NE to SW and also in the central part of the area, while the MSS lineament map shows higher intensity of lineaments at the lower central area. Apart from the topography, another factor affecting the general lineament pattern is the lack of lithological controls in the Grampian Division ('Young' Moines) which is composed of a thick and monotonous psammitic

A MSS BAND 7 - LAPLACIAN ADD-BACK FILTERED

Figure 8.1 Laplacian add-back filtered images for the Loch Tummel area: (A) MSS band 7 and (B) TM band 5. The images are found best for structural (lineament mapping). Scale 1:160,000.

B TM BAND 5 - LAPLACIAN ADD-BACK FILTERED

Figure 8.1 (continued)

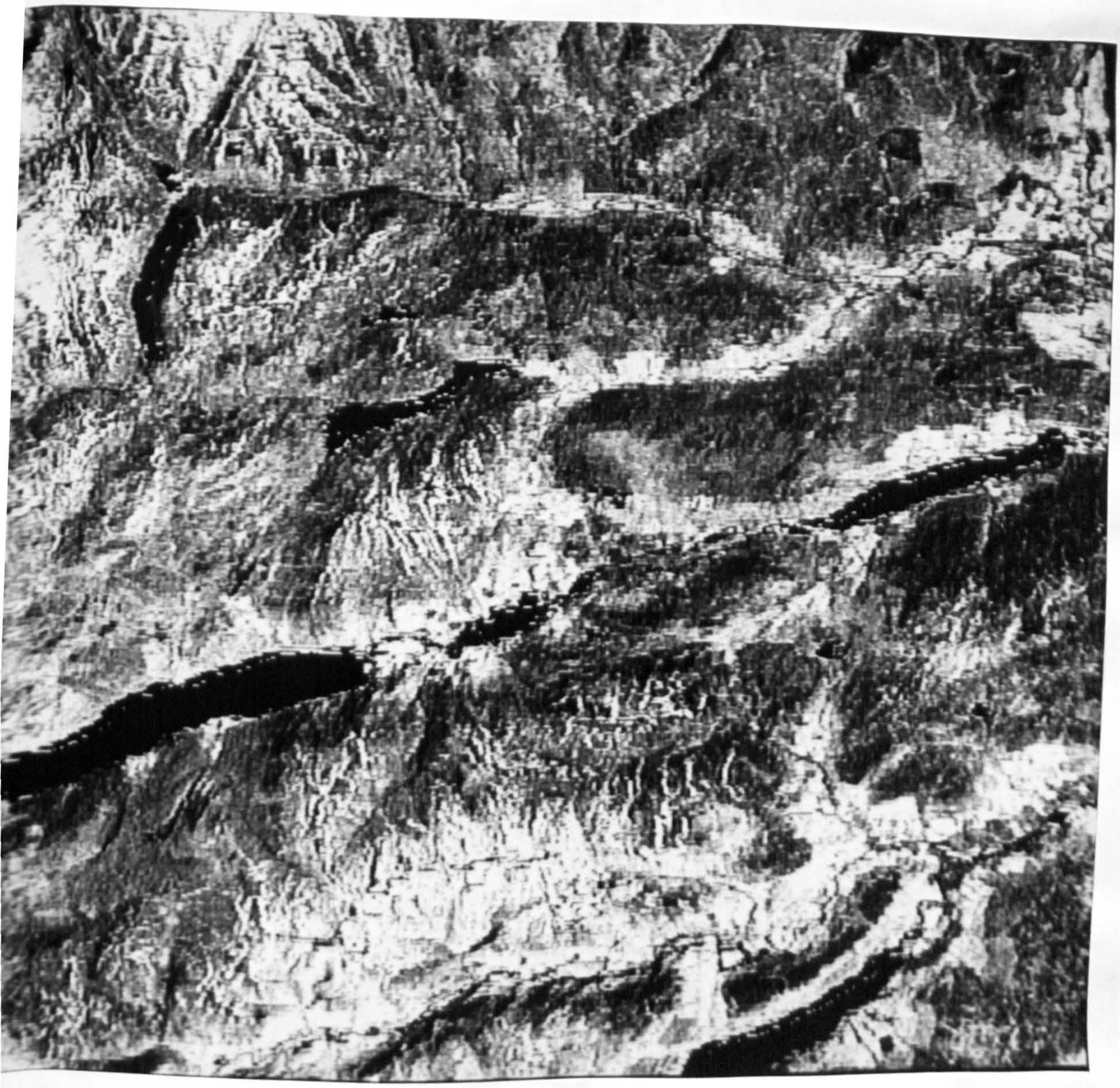

A MSS BAND 7 - EDGE ENHANCED

Figure 8.2 Edge-enhanced images for the MSS band 7 (A) and TM band 5 (B) of the Loch Tummel area. The images are ranked second in the assessment of the geological (structural) information content of the image products of the area. Scale 1:160,000.

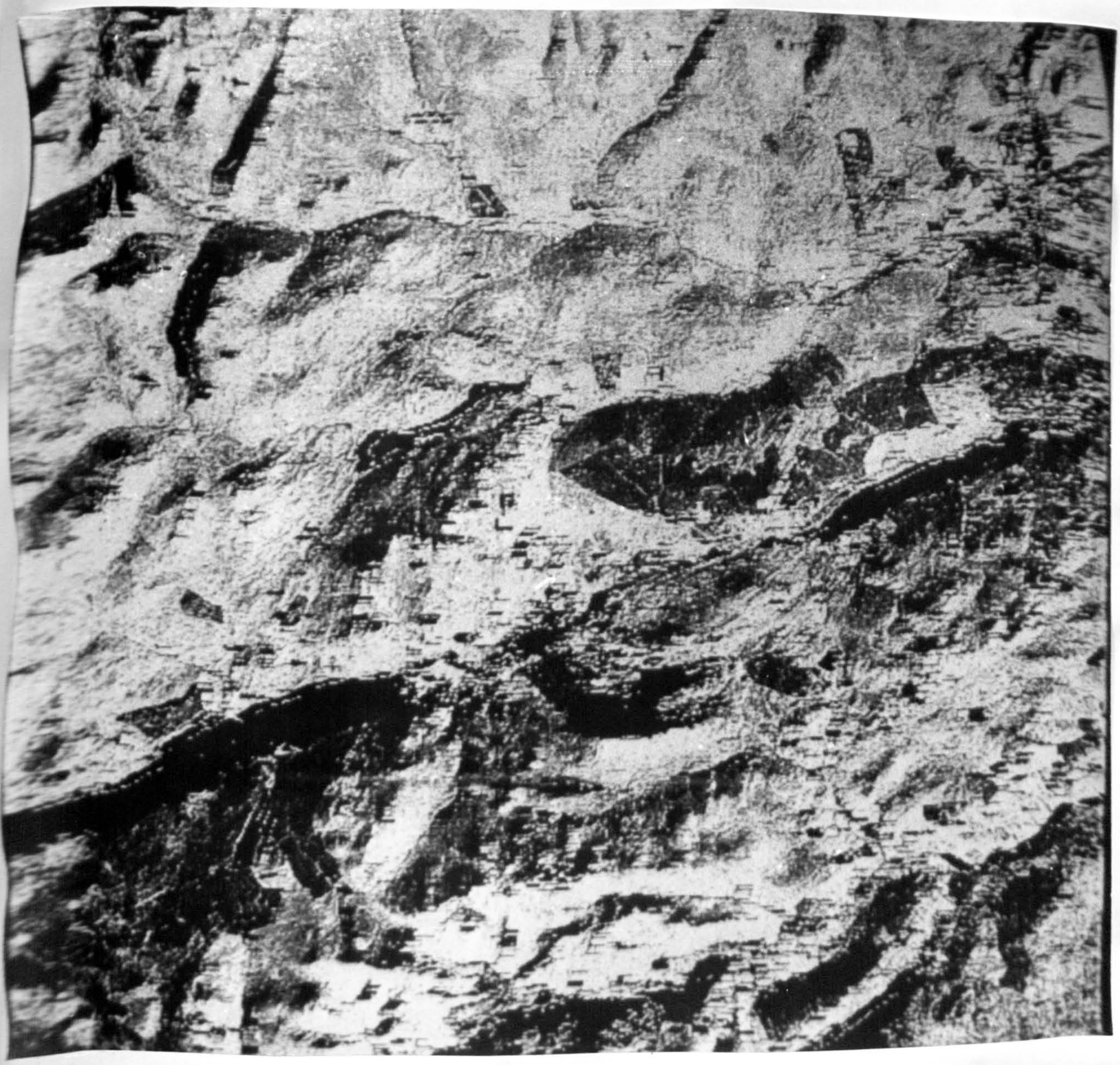

B TM BAND 5 - EDGE ENHANCED

Figure 8.2 (continued)

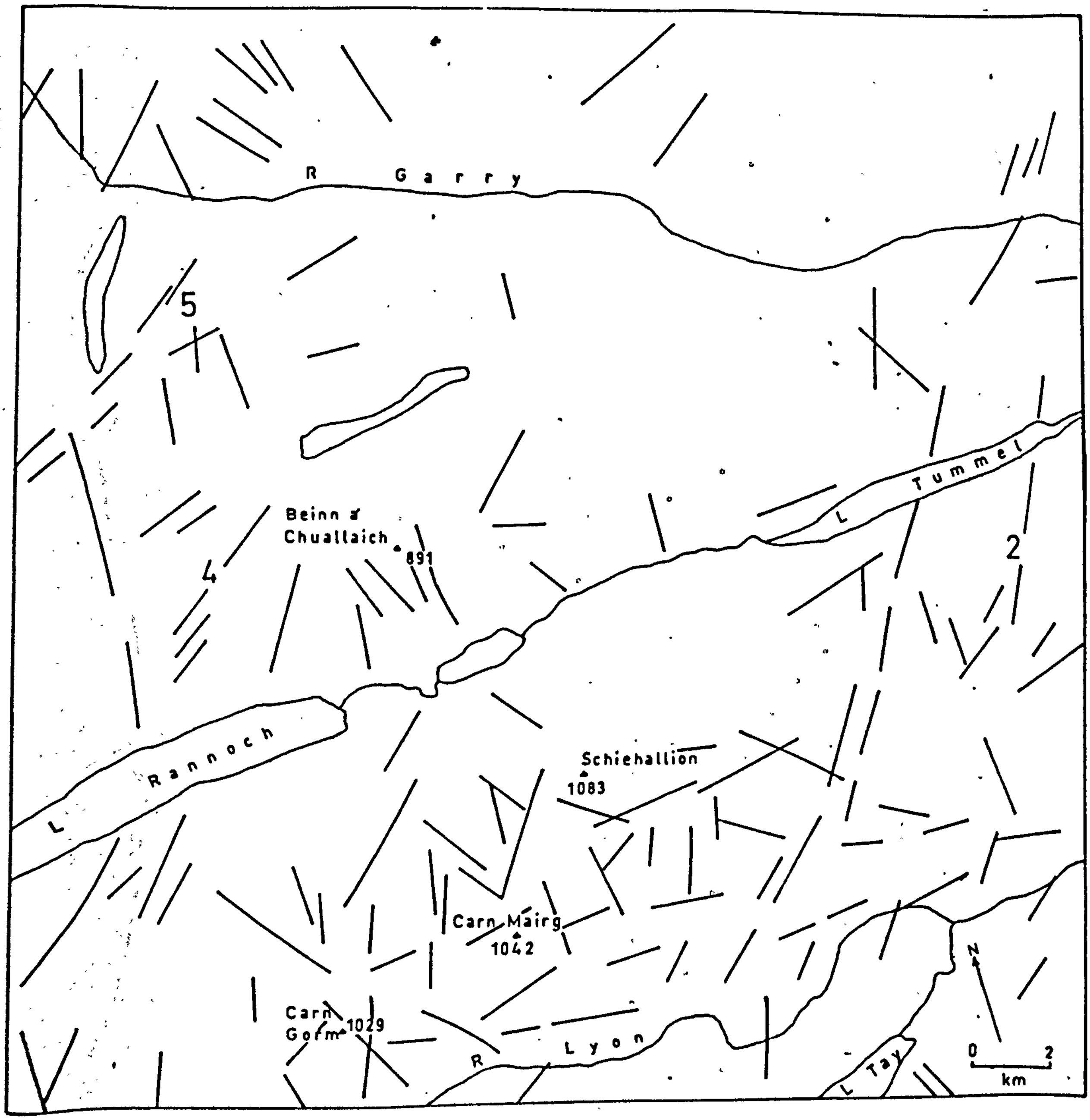

Figure 8.3 Lineament map of the Loch Tummel area derived from the Lands at MSS images. Three new lineament trends (2, 4, and 5) depicted on the images are also shown.

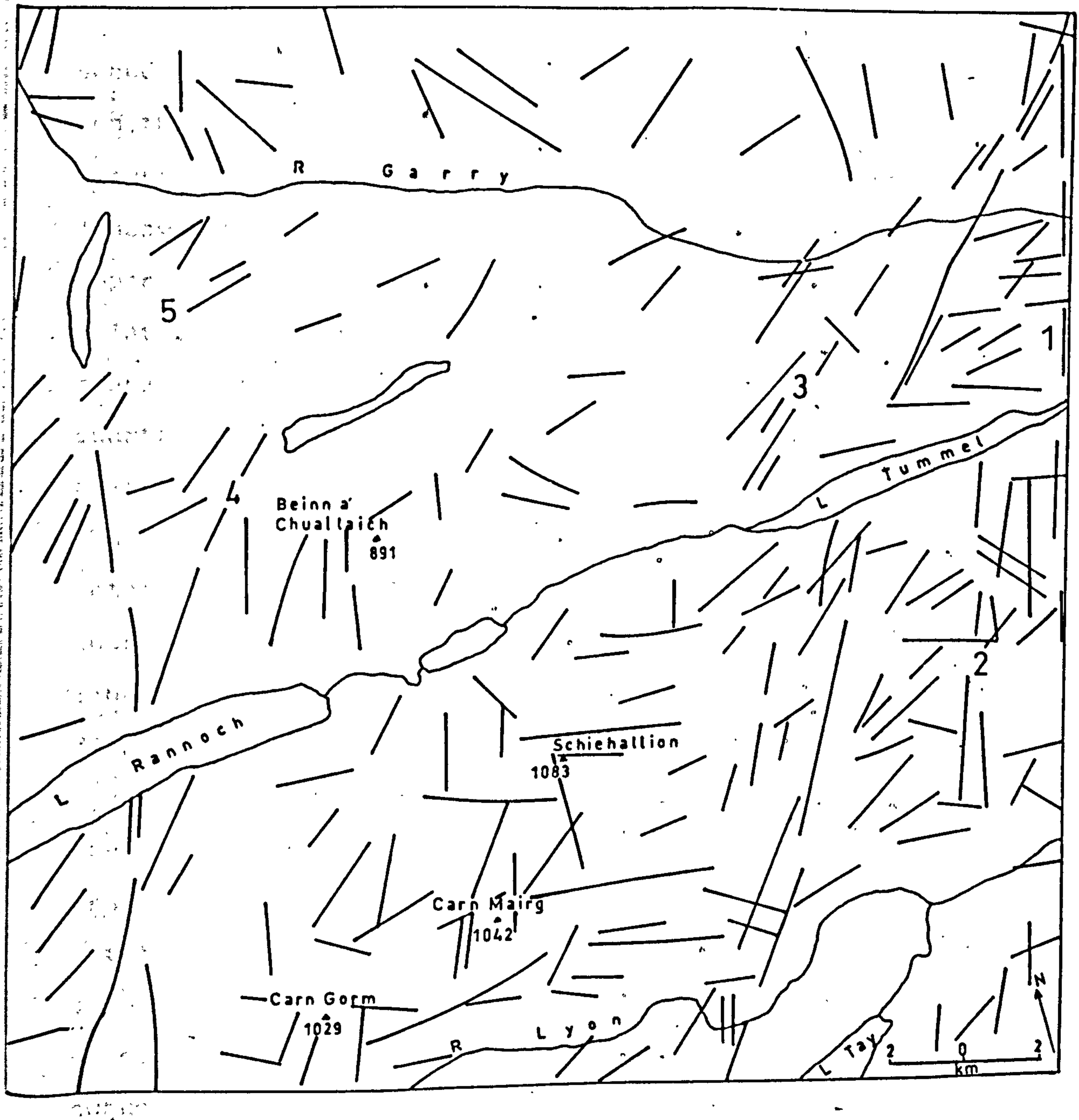

Figure 8.4 Lineament map of the Loch Tummel area derived from the Landsat TM images. Five new lineament trends (1, 2, 3, 4, and 5) depicted on the images are also shown.

sequence which covers almost all the area between the Tummel and the Garry, west of the Loch Tay Fault (see Table 2.3 and Figure 2.7). This may help explain the apparent scarcity of lineaments in these areas. On the other hand, the areas which apparently have a higher intensity of lineaments are generally related to the areas underlain by the Dalradian which is characterized by a greater diversity of rocks including quartzites and limestones. The TM lineament map reflects this relationship better than the MSS. For example, in the NE area the MSS map (Figure 8.3) shows almost similar lineament intensities on the west and east of the Loch Tay Fault, whereas in the TM lineament map (Figure 8.4) the difference in lineament intensity on either side of the fault is better displayed.

A significant proportion of the lineaments within the area of the interpretation is dominated by a major NE-SW trend. From the MSS interpretation (Figure 8.5A), one major but broad peak concentration of lineaments is found between 010°-050°, within which the 045°-050° direction had the highest 5° concentration with total length of 36 km. In terms of number, lineaments are concentrated most in the 015°-020° directions with 7.4% of the total lineaments. Two other peaks of lineament directions, which are lower than the previous peak, occurred in the 275°-285° and 315°-335° directions. In comparison with the MSS, a lineament analysis of the TM data (Figure 8.5B), it was found that the major peak of lineament concentration is in the 035°-060° direction within which the 045°-050° direction is the highest (similar to the MSS data)

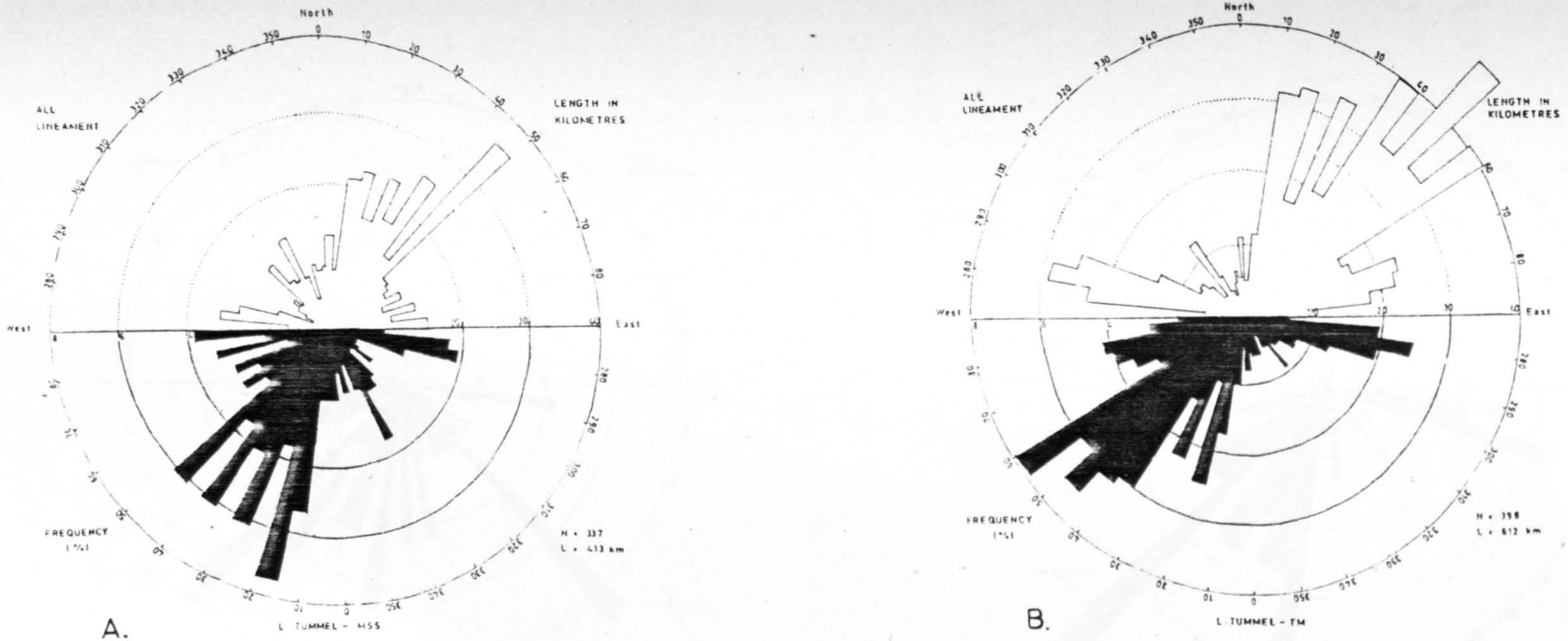

Figure 8.5 Rose diagrams of the lineament calculated by both length as well as number of observation on the MSS (A) and (B) on the TM data, Loch Tummel area. Rose diagrams (C) and (D) show the azimuthal distribution of the lineaments with more than 2 km length derived from the same data.

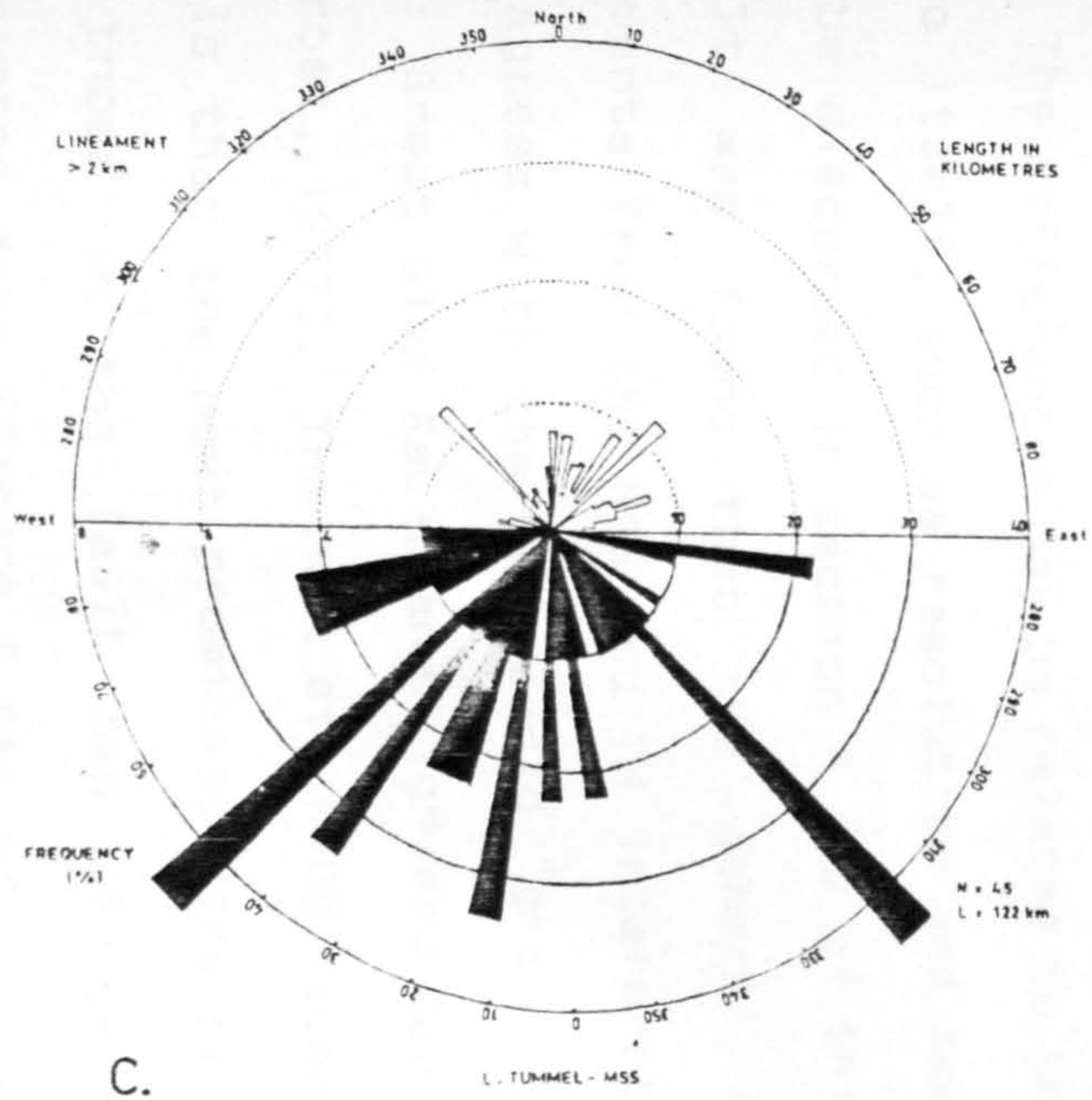

C.

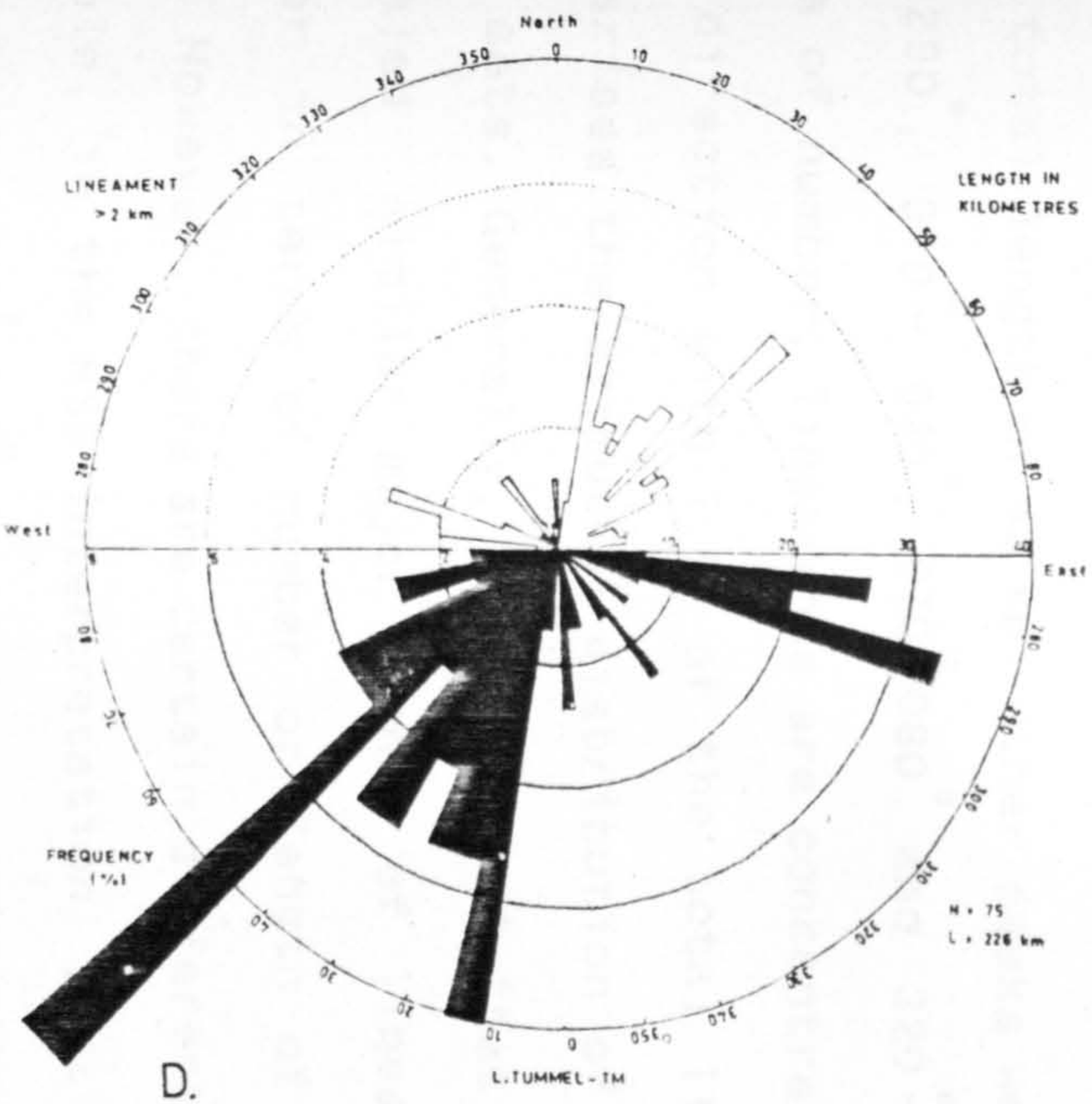

D.

Figure 8.5 (continued)

with total length of 48 km. Other peaks were also found in the 275°-290°, 010°- 020°, 070°-080° and 320°-325° directions. In terms of number, lineaments are concentrated most in the 055°-060° direction with 7.8% of the total lineaments. Table 8.1 summarises the azimuthal distribution of lineaments for both data sets. Generally, it is evident that both data sets have revealed similar major trends of lineament concentration, either in terms of number or length of lineaments, in the area. However, there are certain differences between them. For example, in the MSS interpretation, particularly in terms of number, the 330°-335° direction appears to be more important as compared with the TM data. However, in terms of length, in the TM interpretation, the concentration of longer lineaments is in the 320°-325° direction which may related to this trend is fairly well represented (although less obvious than in the MSS). The differences may be related to the nature of the data source itself, such as resolution and temporal effects which will be discussed in section 8.3.2 of this chapter.

It was found that the general orientation of the lineaments from the MSS and TM interpretations of the study area agrees with the Caledonoid "grain" (020° - 059°) in the block: Great Glen Fault and Highland Boundary Fault (Johnson and Frost, 1977). The most striking aspect of the interpreted maps is that the most prominent directions agree quite well with those in the fault map (Figure 8.6B) and in the interpreted data (Figure 8.6A) of the region. Although the Figures show the data from a much larger area and at regional

DATA	MAJOR PEAK						LENGTH GROUP
	By Length			By number of observation			
	First	Second	Others	First	Second	Others	
TM	035-060 (055-060)	275-285 (280-285)	010-020 070-080	035-060 (055-060)	275-290 (280-285)	065-080	< 2 km
MSS	010-050 (055-060)	315-335 (280-285)	275-285	010-050 (015-020)	275-285 (280-285)		
TM	045-050	285-290	010-025	045-050	275-290 (285-290)	010-025	2-3 km
MSS	035-040	010-015	065-075	010-040 (010-015)	315-320	065-080	
TM	010-015 030-035	285-295 (290-295)	320-325	010-015 030-035	280-295	320-325	3-5 km
TM	045-050	010-015	285-290	045-050	010-015	275-285	> 2 km
MSS	315-320	045-050	065-075	315-320 045-050	010-015	065-080	
TM	035-060 (045-050)	275-290 (280-285)	010-020 070-080	035-060 (055-060)	275-290 (280-285)	010-020 070-080	total
MSS	010-050 (045-050)	275-285 (275-280)	315-335	015-050 (015-020)	275-285 (280-285)	320-335	

bers in bracket show the mode of lineament concentration in a broad peak.

ble 8.1 The azimuthal distribution of lineaments for both Landsat MSS and TM of the Loch Tummel area. See Figure 8.6 for comparison with the published data of the area.

scale compared with the study area, nevertheless, the results show the main features of the fault pattern are clearly brought out in the lineament maps, and this is perhaps not surprising but it should be emphasised that the lineament maps were constructed largely without reference to any fault map. When compared with the mapped faults (Figure 8.7), the most prominent amongst them coincides with the line of the Loch Tay Fault (025° - 040°), the Killin Fault (020°) and the Tyndrum Fault (030°). All these faults are accepted as being wrench faults with substantial (sinistral) displacements and smaller NE-SW trending faults probably belong to this wrench-fault regime (Johnson and Frost, 1977), which most likely corresponds very well with the major trend of lineaments in the interpretation maps. Some minor faults, many trending in the NW-SE (310°-330°) direction, and a few faults trending NNW-SSE to N-S and E-W have been reported in the region (Smith, 1961; Johnston and Frost, 1977), and it is tempting to regard the NW-SE faults as the complementary set to NE-SW wrench faults in a conjugate shear system (Smith, 1961). The minor peak concentrations of lineaments in the 330°-335° direction of the MSS data and in the 320°-325° direction of the TM data may be related to the minor faults trending 310°-330°. However, both interpreted data (Figure 8.5), and the published data (Figure 8.6A) show a decreased intensity of lineaments in this direction as compared with the fault map data (Figure 8.6B). Both interpretation maps also show good agreement with the NNW-SSE to E-W faults. Therefore, when comparing the

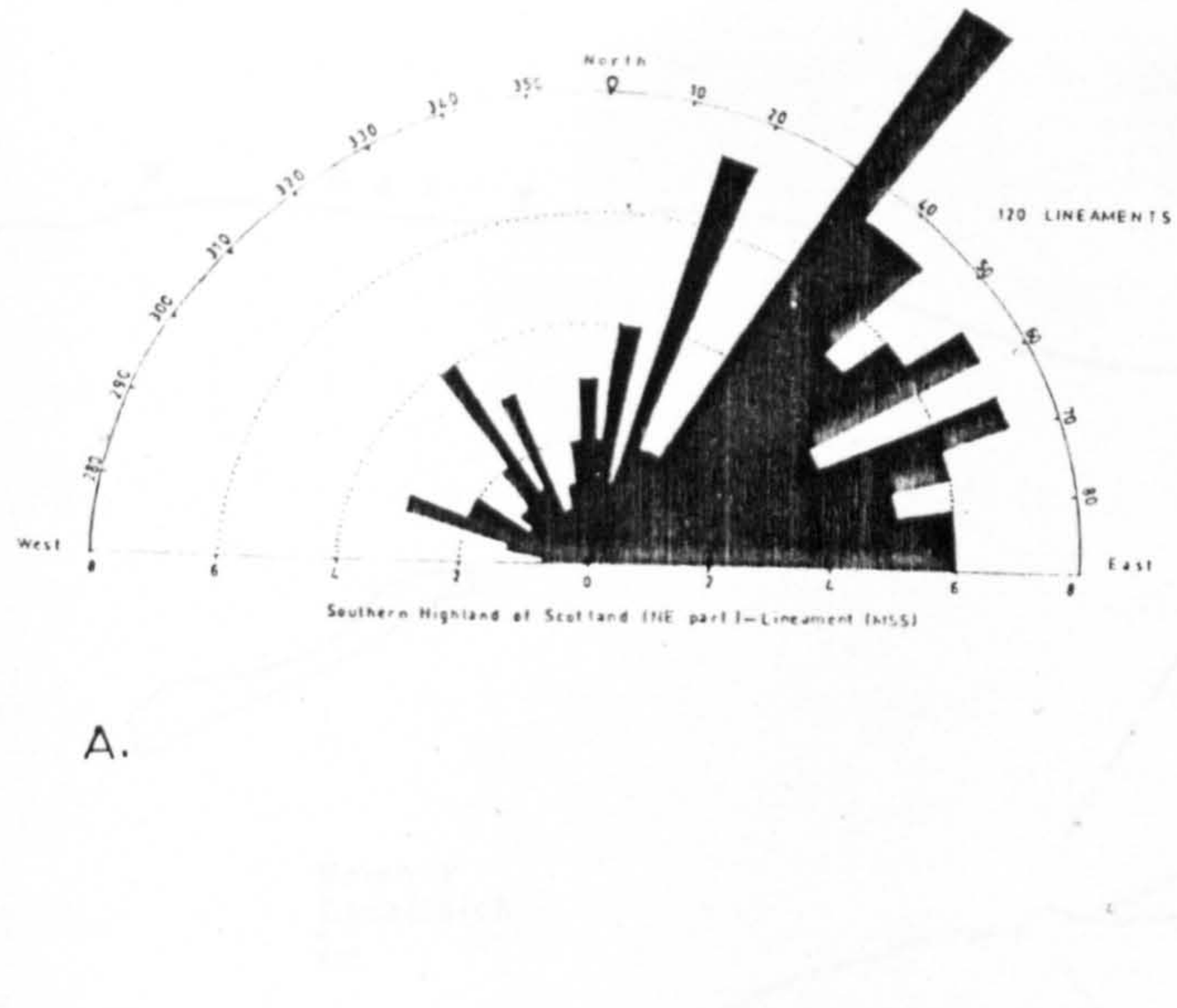

Figure 8.6 Rose diagrams of frequency of Landsat lineaments (A) and mapped faults (B) in Southern Highland of Scotland (NE part of region) (Figure 1 and 3 of Johnson and Frost, 1977).

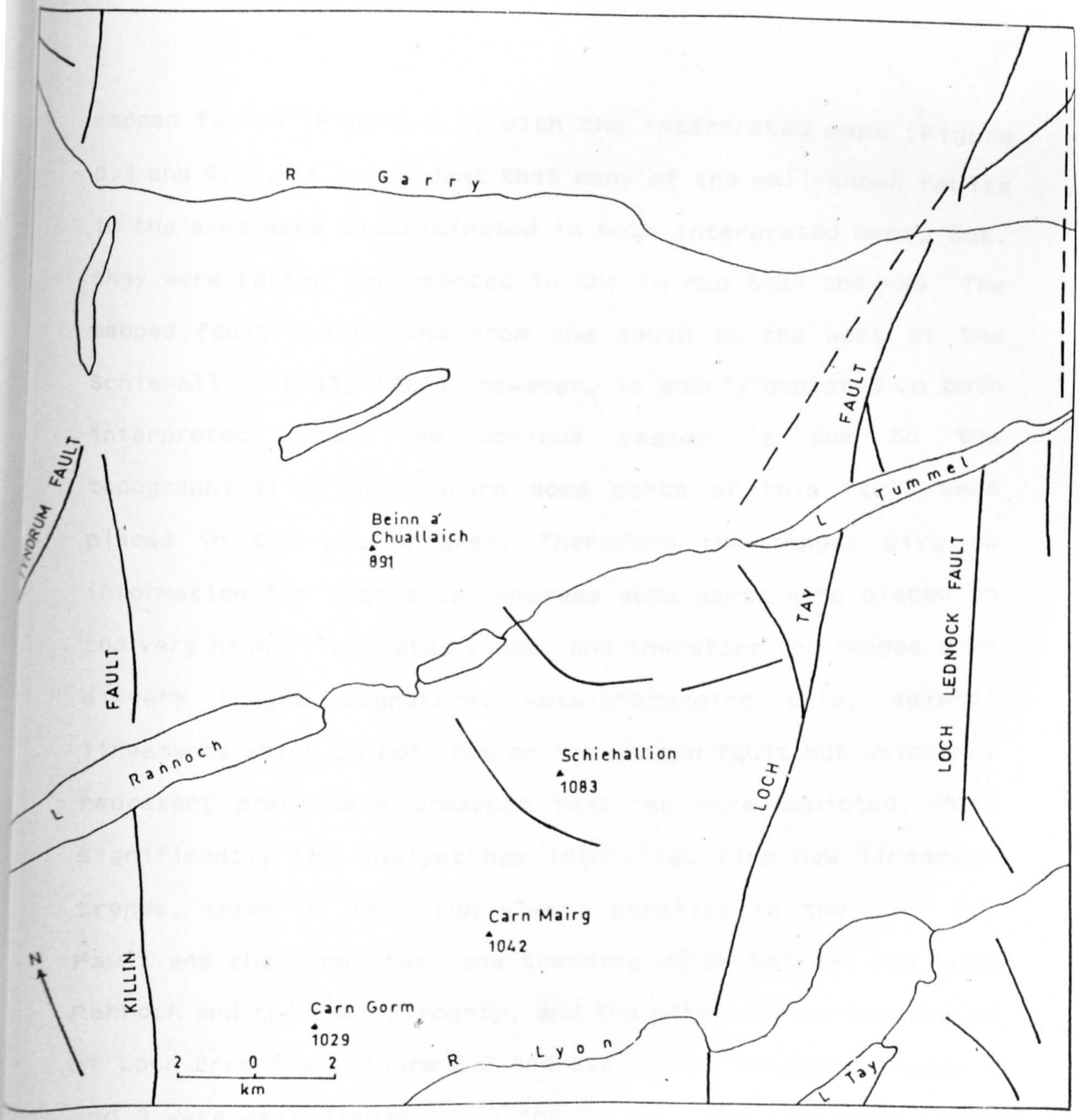

Figure 8.7 Mapped faults in the Loch Tummel area (after BGS, 1967; Johnson and Frost, 1977). The interpreted fault lines depicted on the Landsat and TM as well as on aerial photographs are also shown. The Loch Lednock Fault (the interpreted fault based on the MSS imagery interpretation) (Saraf et al., 1987) is well depicted in this study.

mapped faults (Figure 8.7) with the interpreted maps (Figure 8.3 and 8.4), it is evident that many of the well-known faults in the area were discriminated in both interpreted maps, but, they were better represented in the TM map than the MSS. The mapped fault which runs from the south to the west of the Schiehallion (BGS, 1967), however, is poorly depicted on both interpreted maps. The obvious reason is due to the topographical effect, where some parts of this fault were placed in the shadow area. Therefore the images give no information for that area, whereas some parts were placed on the very high illuminated slope, and therefore the images give a very bright signature. Notwithstanding this, several lineaments which do not show on the mapped fault but which may represent previously unmapped features were depicted. Most significantly the analyst has identified five new lineament trends, three of them run almost parallel to the Loch Tay Fault and the other two, one trending NE-SW between the Loch Rannoch and the Loch Errochty, and the other one is located NW of Loch Errochty (Figure 8.3 and 8.4). The lineament trends 1 and 3 were well displayed in the TM map, the lineament trend 5 was better depicted in the MSS map than the TM and vice versa for the trend 2, whereas trend 4 was well displayed on both interpreted maps. These lineament trends were further studied by using aerial photographs. Table 8.2 summarises the characteristics of the lineaments, their geological interpretation and correlation with the published geologic map. The result shows that only the trends 1, 2 and 3 possibly represent new fault lines, while the other two trends

correspond with the lamprophyre which occurs as dykes in the area. The lineament trend 2, however, was found to correspond with the Loch Lednock Fault, the interpreted fault based on the MSS imagery interpretation (Saraf et al., 1987). A small segment, perhaps the continuation of the lineament trend 1, was also depicted south of the Loch Tummel (Figure 8.4). The continuation of the trend to the further south of the loch, however, was not shown. Based on its location and photo-characteristics, the lineament trend 1, therefore, was interpreted as a new NNE-SSW trending fault which runs from south of the Loch Tummel in the south and merges with the Loch Tay Fault to the north of the Loch Tummel (Figure 8.4). The lineament trend 3 was also interpreted as a new NE-SW trending fault line which runs almost parallel to the Loch Tay Fault which extends from west of Loch Tummel in the south to north of Loch Tummel in the north (Figure 8.4). From the TM data, it appears that the trend merges with the Loch Tay Fault. This feature, however, was not depicted on the aerial photographs, on which its northeast line terminates in the drift cover in the Garry River valley.

8.3.2 Lineament length and frequency

In this study, the lengths of lineaments have been divided into four groups to see if length plays an important role in relation to certain orientations. The groups were quite arbitrary, and the lineaments with lengths: less than 2.0 km, 2.1 - 3.0 km, 3.1 - 5.0 km, more than 5 km, were selected for

LINEAMENT TREND	PHOTO-CHARACTERISTICS	CORRELATION WITH THE PUBLISHED MAP	CONCLUSION/ INTERPRETATION
1, 2, AND 3	appear as straight lines, largely coincide with the alignment of drainage (trenches or valleys) and generally show linear tone differences, in some places they show darker tone (dark line) than the surrounding areas.	unmapped linear features (trends)	new fault lines
4 and 5	appear as narrow straight and curved lines (walls), discordantly cutting across the "bedding" traces of country rock, dark tone, in many instances they show parallelism to each other.	lamprophyres - occur mainly as dykes	igneous rock dykes

Table 8.2 The photo-characteristics, geological correlation with the map and interpretation of a new (major) lineament trends on the Landsat TM and MSS images of the Loch Tummel area.

LENGTH	< 2 km	2-3 km	3-5 km	> 5 km	TOTAL
MSS	73.4%	10.1%	1.3%	0%	84.8%
TM	81.2%	14.6%	2.8%	1.5%	100%

Table 8.3 Percentage frequency of lineaments for Landsat TM and MSS of the Loch Tummel as a function of length.

convenience. The frequency of each group has been summarized in Figure 8.8 and Table 8.1.

Totals of 398 and 337 lineaments on the TM and MSS data set respectively, were depicted for the area. A majority of the lineaments depicted on both data sets was less than 2.0 km length. For example, 81 and 73 per cent of the lineaments defined on the TM and MSS, respectively, are included in this group (Table 8.3). However, by analyzing the mapped lineament on each image separately, it was found that 87 per cent of the total lineaments mapped on the MSS were in this category, whereas for the TM data the figure was only 81 per cent. This may give an indication that, despite its lower resolution, a larger number of lineaments at 2.0 km and less were mapped on the MSS than on the TM. This discrepancy can be explained in part by the different cover conditions at the times of imaging. The snow in the MSS data enhances very subtle small linear features patterns (Harris, 1987; Sabin, 1987; Iranpanah, 1989) which are lost in the 'noise' of high spatial frequency cover variations seen in the TM image. These variations, however, become less significant at larger scales, hence the number of longer lineaments detected on the TM was larger than that on the MSS (Table 8.3). There are only 1.5 per cent of the total lineaments defined on the TM with lengths more than 5 km, and no lineament in this group was defined on the MSS. Apart from the lower spatial resolution in the MSS, the very low frequency for longer lineaments mapped in the images can be related to two factors. First, although a few lineaments with several kilometres length were

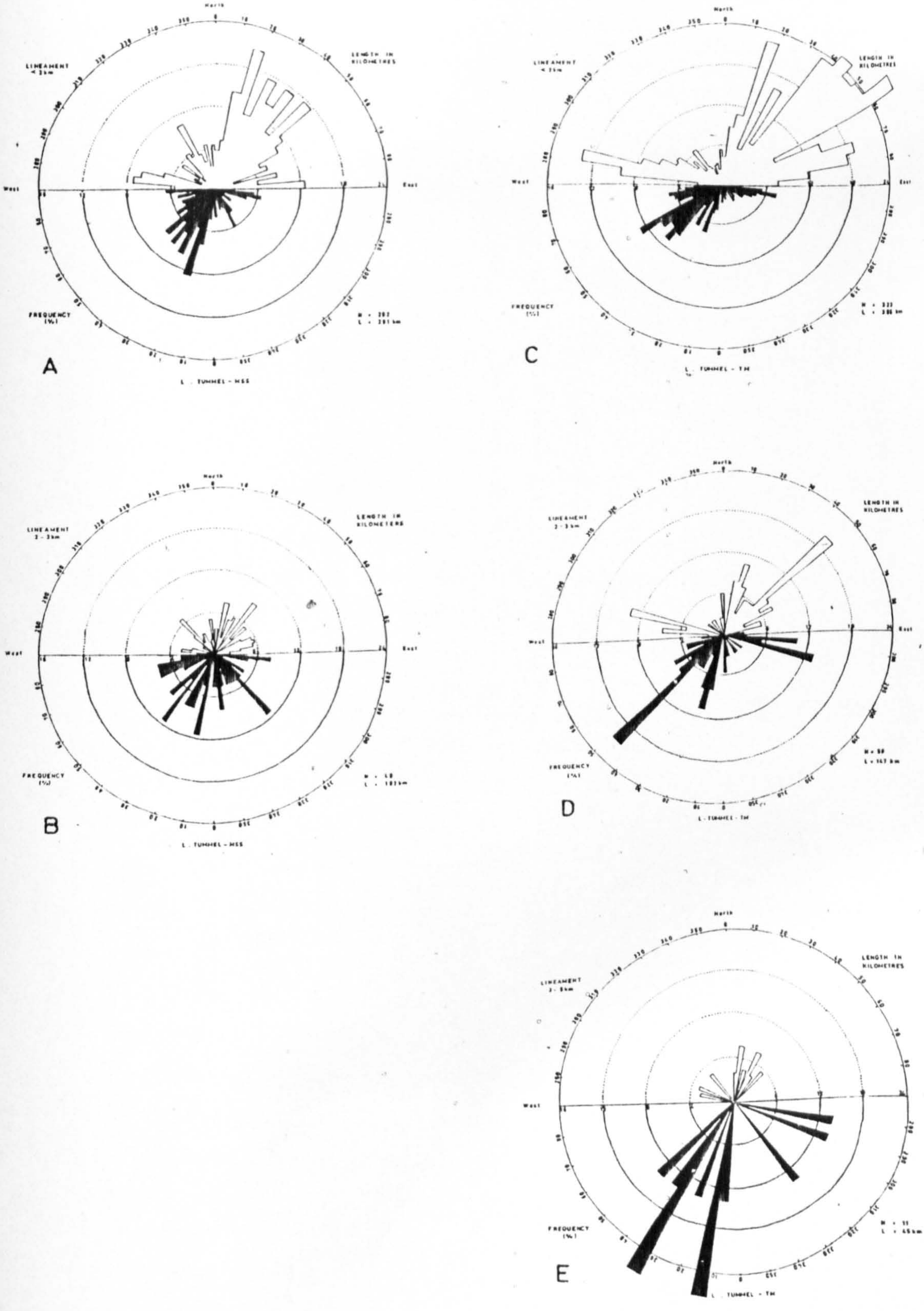

Figure 8.8 Rose diagrams of the Landsat MSS lineaments with less than 2 km (A) and 2 - 3 km length (B); and of the Landsat TM lineaments with less than 2 km (C), 2 - 3 km (D) and 3 - 5 km length (E), calculated by both length as well as number of observation.

defined, the kernel size used in the process is theoretically more suitable for structures up to some 100 m in length (Chavez, 1983; Crósta and Moore, 1989). Therefore the shorter lineaments were enhanced and very well depicted, whereas many of the longer lineaments were under enhanced or undepicted. Second, despite the existence of several major (long) faults in the area, there is a substantial drift cover and this, has made them less obvious and also discontinuous, so that they appear on the images as several shorter lineaments rather than as a continuous line. Thus the TM image has only 15 per cent more lineaments than the MSS data. Therefore, despite its lower spatial resolution than the TM, the MSS data is still very useful in this particular case. Generally, both data sets pick out one major orientation range from 15^{o}-60^{o}, but some data sets pick out one orientation in preference to others in certain length groups. For example, the MSS shows two preferred orientations with ranges from 0^{o}-5^{o} (in group length of 2-3 km) and 315^{o}-335^{o} (in all group lengths), where both orientations were absent or less preferred on the TM. Again these differences can be explained in part by the differences in the nature of image cover. In relation to this, the preferred orientation of 315^{o}-335^{o} is more or less coincident with the sun azimuth (162^{o}) of the TM data (see Table 4.5). The directional dependency of Landsat lineament analysis on the sun azimuth direction as well as the scan direction is well known from the literature. Therefore, shadow enhancement will be at a minimum for lineaments running parallel or subparallel to the sun azimuth direction, and these will be under

represented on the TM. On the other hand, lineaments in directions perpendicular to the sun azimuth direction will be additionally enhanced. Although the images used in this analysis were processed to overcome this angular dependence, its effect is still evident. For the MSS data set, the differences in the nature of image cover may again be used to explain the occurrence of lineaments in the 315°-335° direction as well as for the 0°-5° direction. Table 8.1 summarises the first three main orientations in all length groups, for total lineaments and also for lineaments with length more than 2 km. Differences were noted in lengths and frequencies of lineaments, but they are nearly uniform and do not show certain trends which can differentiate between the two data sets.

8.3.3 Summary

In summary, this study has indicated that both of the Landsat data, the TM and MSS, are useful for structural (lineaments) interpretation in Loch Tummel area, Scotland. Geologic features, particularly lineaments, are readily interpreted despite extensive drift and vegetation cover. Therefore, the technique (mapping linear features) has proved especially useful in the area where drift cover inhibits the identification of fractures by other means including ground survey. It is apparent that the TM is better than the MSS in spatial as well as spectral resolution and offers an improvement in the ability to map lineaments, particularly for longer ones.

8.4 Lineament mapping and analysis of Kedah-Perak area.

The total numbers of lineaments mapped are 710 (339 from the sub-area 1 and 371 from the sub-area 2) with a total length of about 2900 km. Only the lineaments with a minimum length of about 2 km are shown in Figures 8.11 and 8.12. After plotting all lineaments, their orientations are determined, lengths are measured, and from these data several rose diagrams have been prepared for analysis, interpretation and comparison with the published data.

8.4.1 Lineament analysis and orientation

It is evident that a large proportion of the lineaments in the area is dominated by two major NE-SW and NW-SE trends (Figure 8.13A). These trends were also well depicted in both sub-areas as shown in Figure 8.13B and 8.13C). Beside that, both sub-areas also show the lineaments in a more or less E-W direction. In addition to these, sub-area 1 shows another lineament trend in NNE-SSW direction. An attempt was made to plot rose diagrams for different length groups of lineaments to see if length plays an important role in relation to certain orientations (Figure 8.14). The frequency of each group has been summarized in Table 8.4. It is evident that although the apparent shift of the lineament peak from one length group to another length group does exist, the major orientations for the whole area as well as in each sub-area are well depicted in each length groups. Therefore, there is

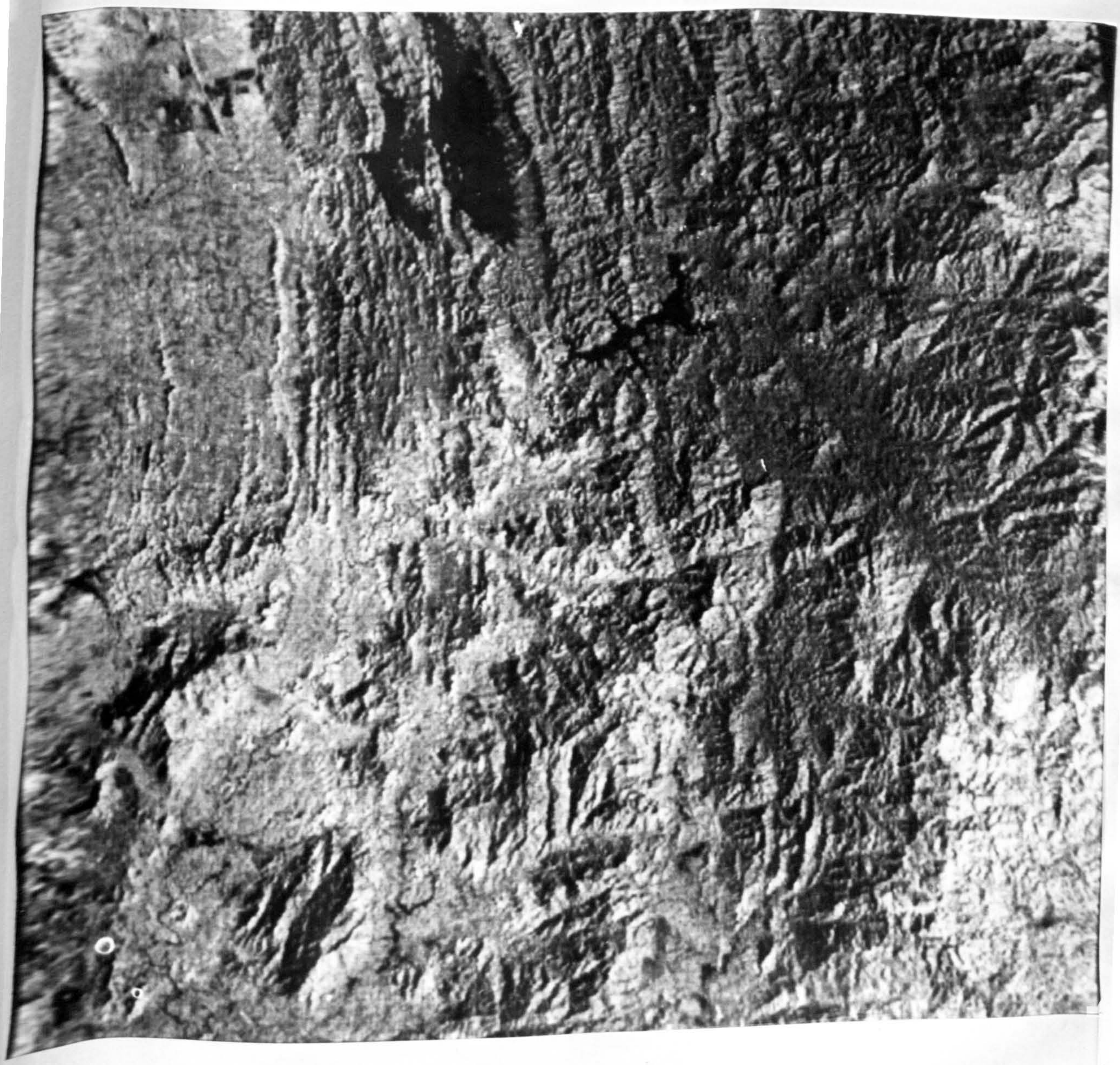

A Band 7 (0.8-1.1μm)

Figure 8.9 Linear contrast stretched of Landsat MSS band 7 of the Kedah-Perak sub-area 1 (A) and sub-area 2 (B). The band 7 is found best particularly for lineament analysis compared with other images. Scale 1:300,000.

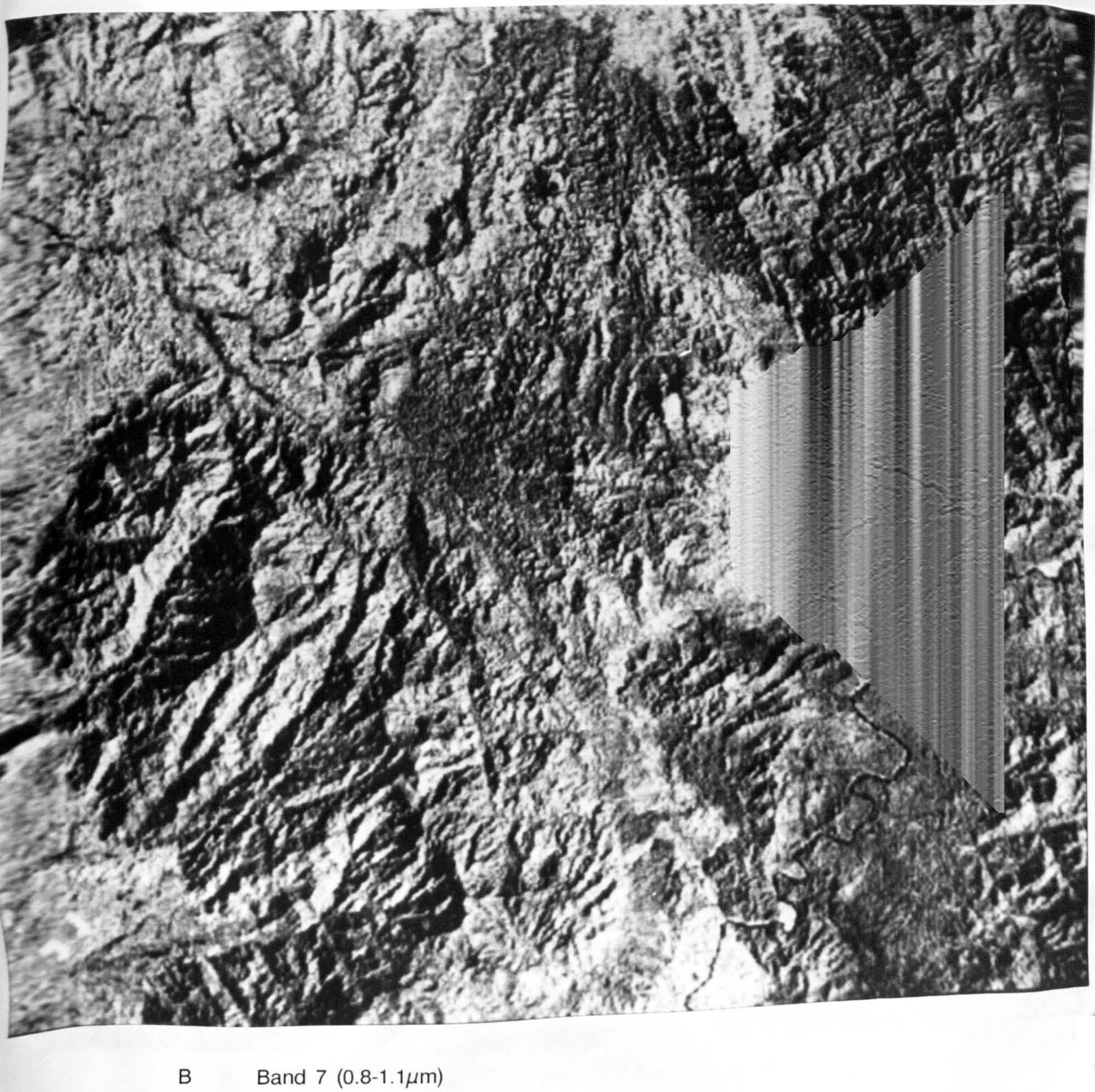

Figure 8.9 (continued)

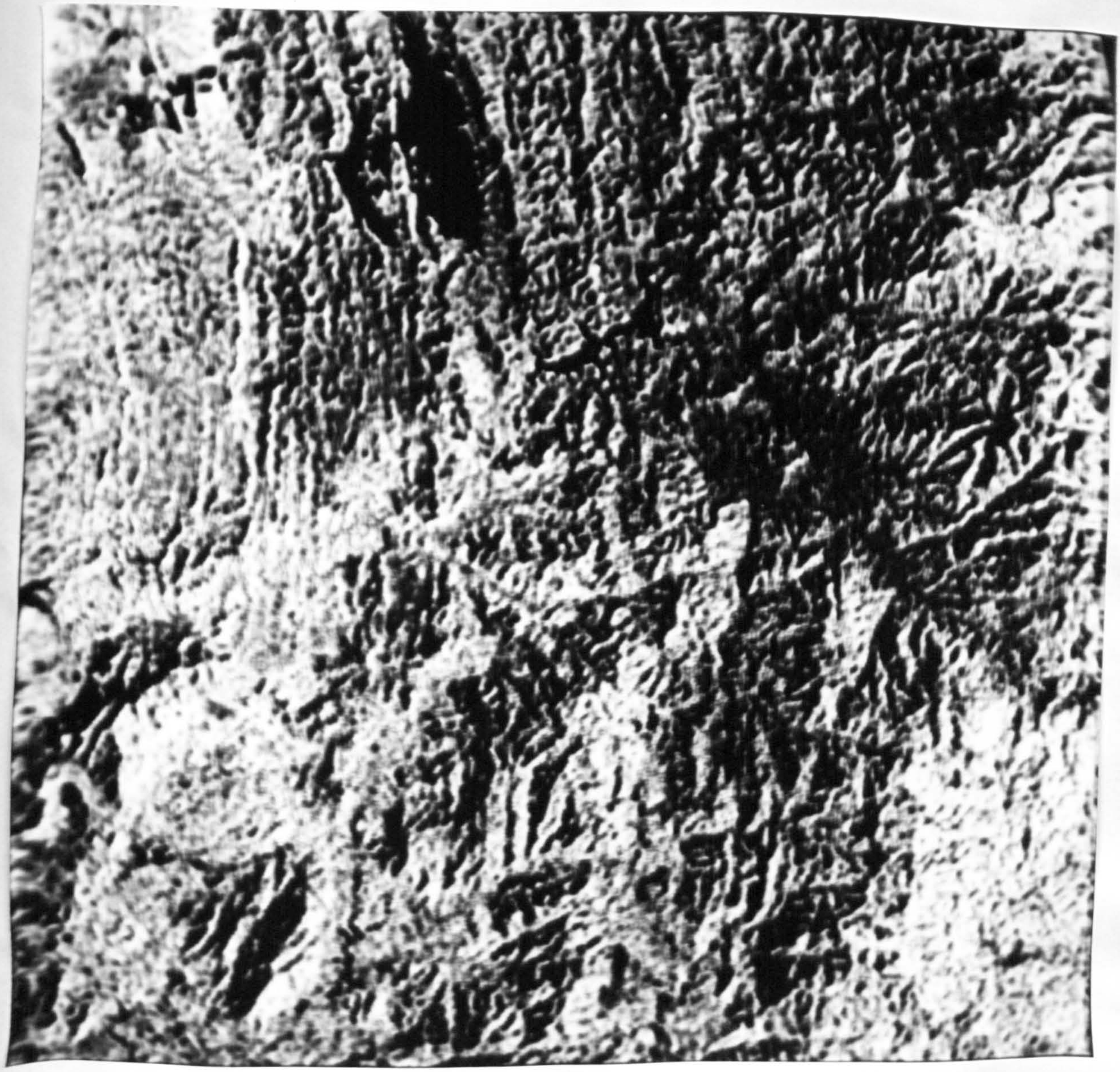

A MSS BAND 7 - LAPLACIAN ADD-BACK FILTERED

Figure 8.10 Laplacian add-back filtered images of the Landsat MSS band 7 for the Kedah-Perak sub-area 1 (A) and sub-area 2 (B). Scale 1:300,000. The image products are rated second best for lineament mapping of the area.

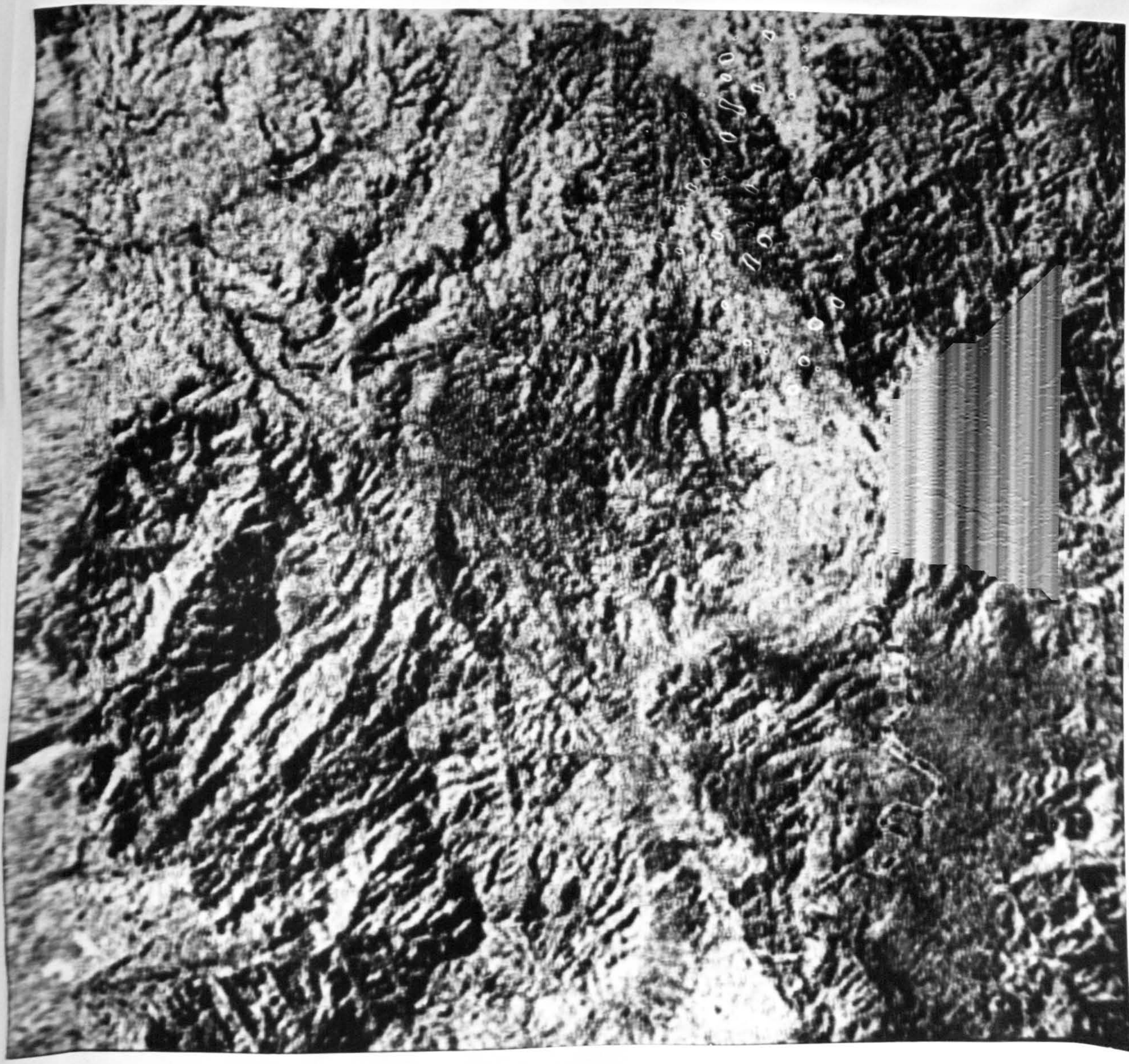

B MSS BAND 7 - LAPLACIAN ADD-BACK FILTERED

Figure 8.10 (continued)

Figure 8.11 Lineament and circular feature map of the Kedah-Perak sub-area 1 derived from the Landsat MSS images. See Figure 8.13 for comparison with the mapped fault of the area.

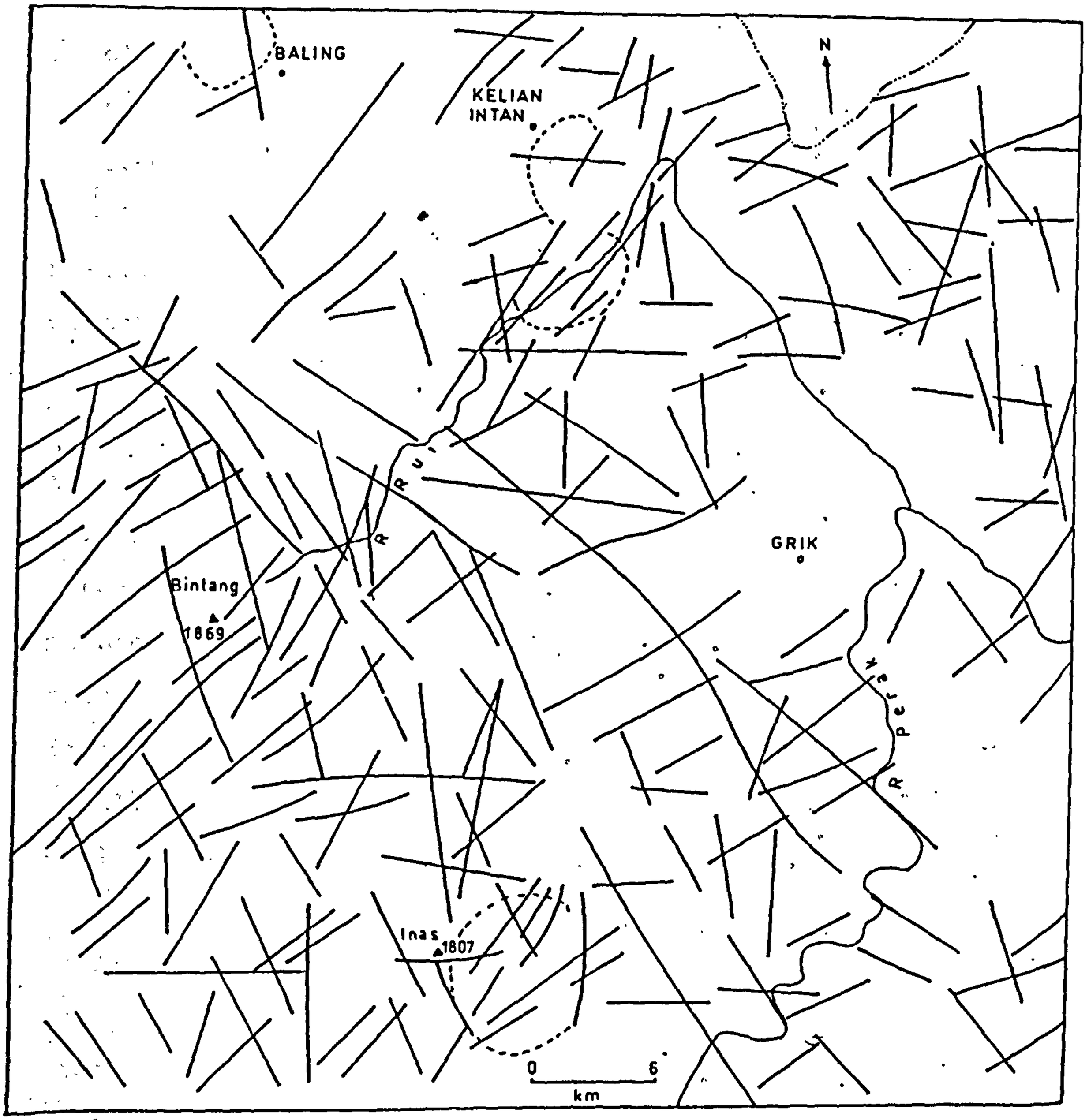

Figure 8.12 Lineament and circular feature map of the Kedah-Perak sub-area 2 derived from the Landsat MSS images. See Figure 8.14 for comparison with the mapped fault of the area.

no clear evidence that the length of the lineaments plays an important role in relation to certain orientations in the area. When all rose diagrams were examined, it was found that the lineaments in SE-NW direction are poorly represented. The possible reason for this is the sun azimuth because this direction coincides with the sun azimuth direction, which is 128° (see Table 4.5). Therefore, the lineaments in this direction may be under-represented, and those perpendicular to it over-represented. However, the rose diagram for the mapped faults (Figure 8.15B) also shows very few faults in this direction (128°) and many faults occur in the direction perpendicular to it. This will indicate that the poorly represented mapped lineament in the 128° and the higher concentration in the direction perpendicular to it is not totally due to the sun azimuth direction, rather it may well reflect the actual lineaments in the area.

The lineaments mapped in this study were compared with faults mapped in the Geological Map of Peninsular Malaysia in scale of 1: 500,000 (Geological Survey of Malaysia, 1985). Similar measurements were carried out for faults mapped. Comparisons were carried out in terms of their orientations, number, length and also their locations.

First, comparison was made between two sets of rose diagrams with respect to their total numbers and lengths in each 5 degree interval. As shown in Figure 8.13A and 8.15B, the two sets of rose diagrams are more or less concordant in both of their numbers and lengths, and it can be concluded that the main features of the fault pattern are clearly

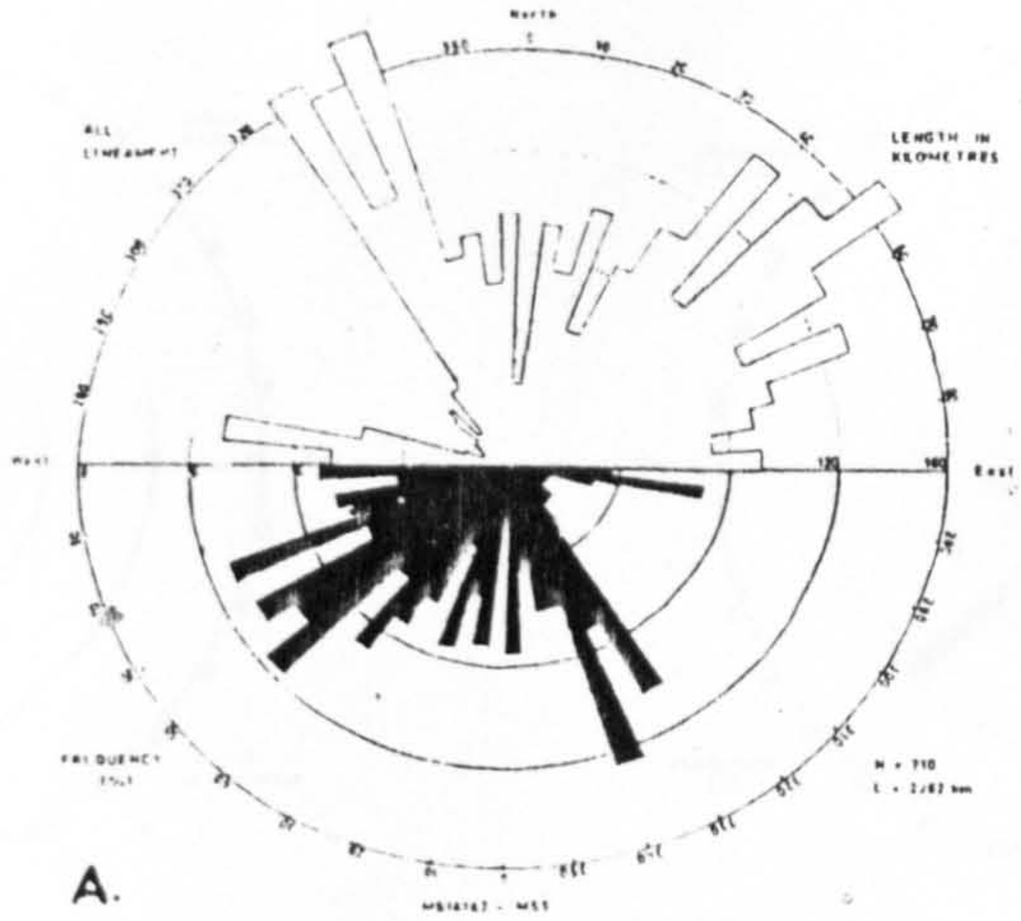

A.

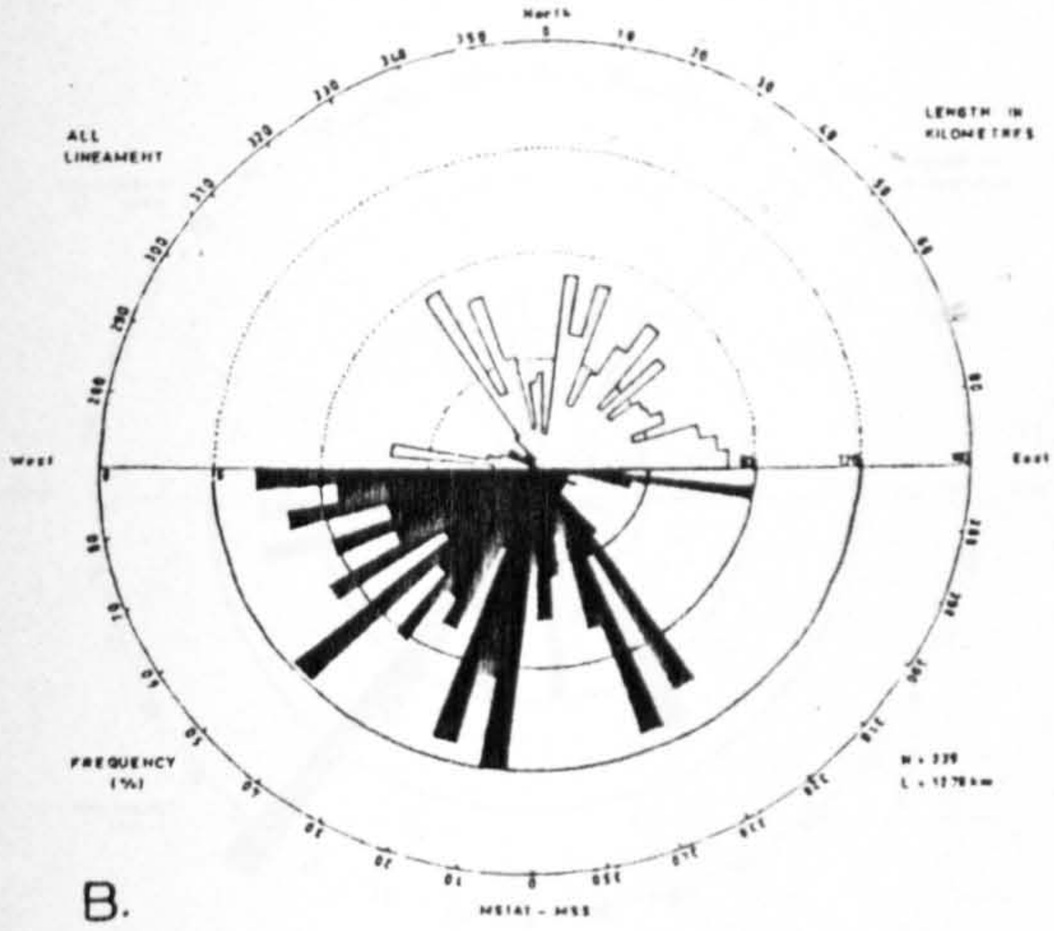

B.

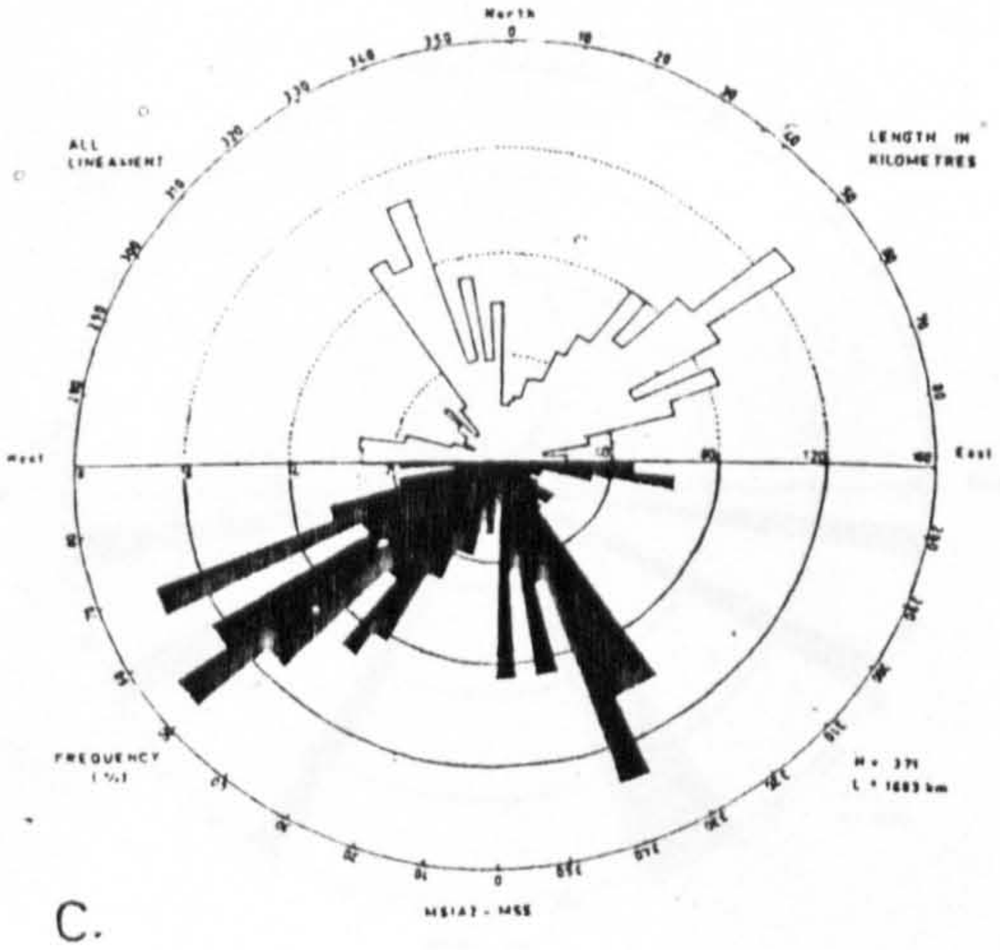

C.

Figure 8.13 Rose diagrams of the lineaments calculated by both length as well as number of observation on the Landsat MSS for the Kedah-Perak area (A), Kedah-Perak sub-area 1 (B) and Kedah-Perak sub-area 2 (C).

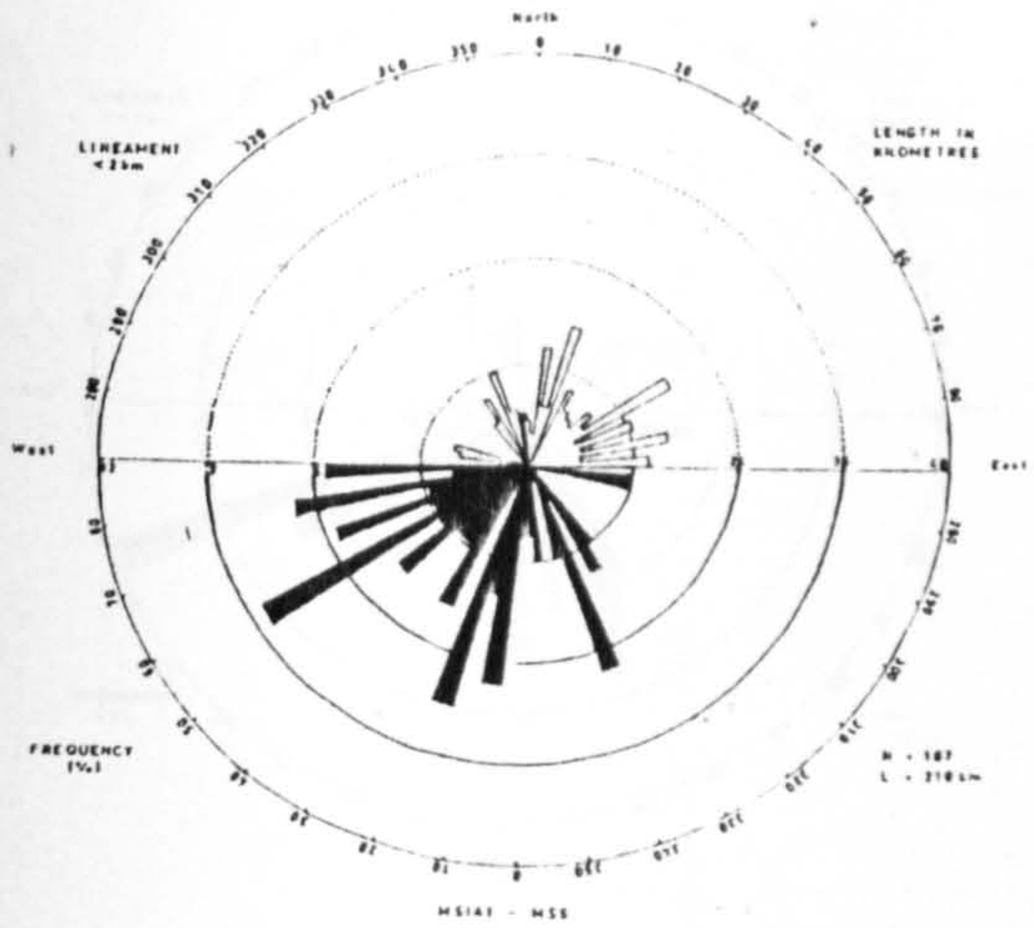

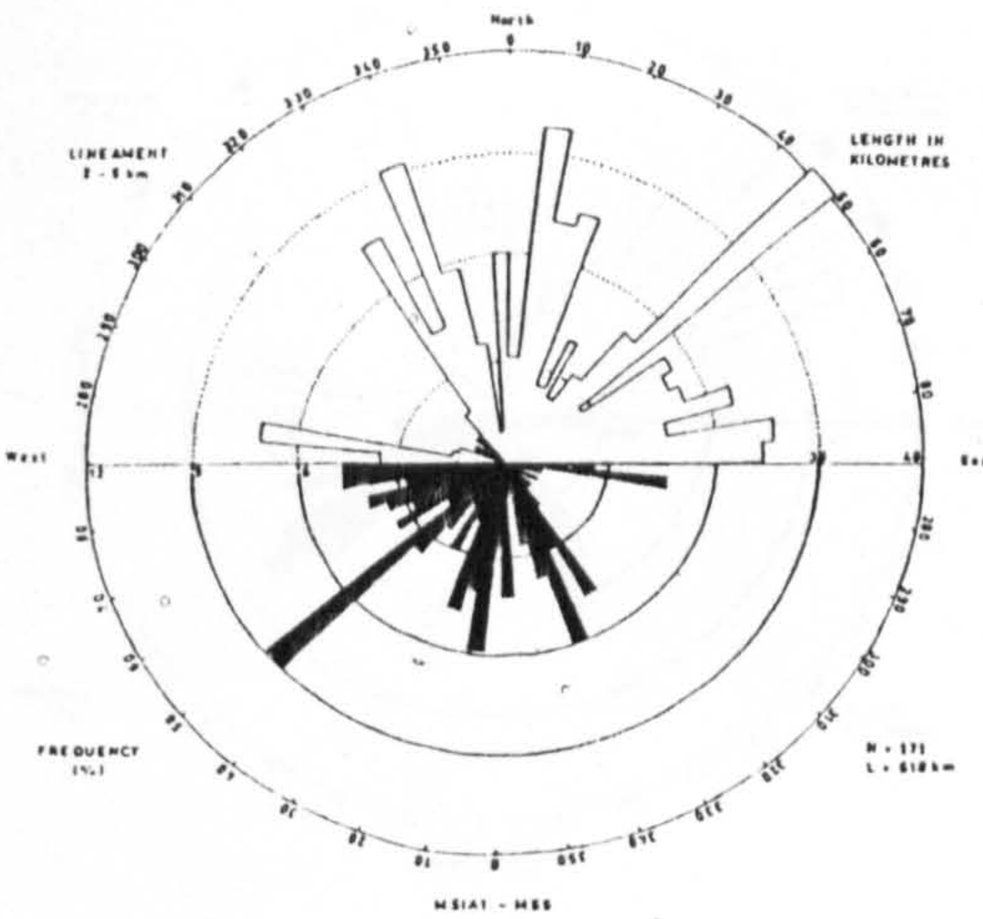

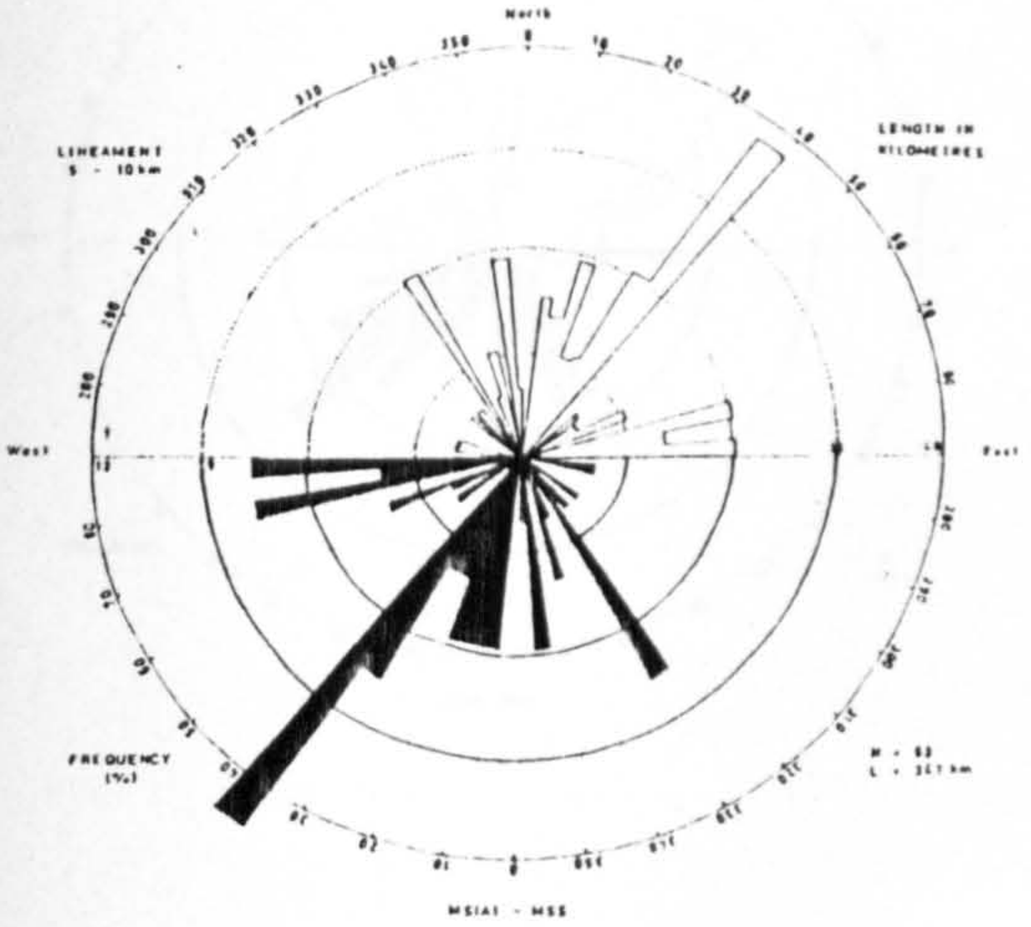

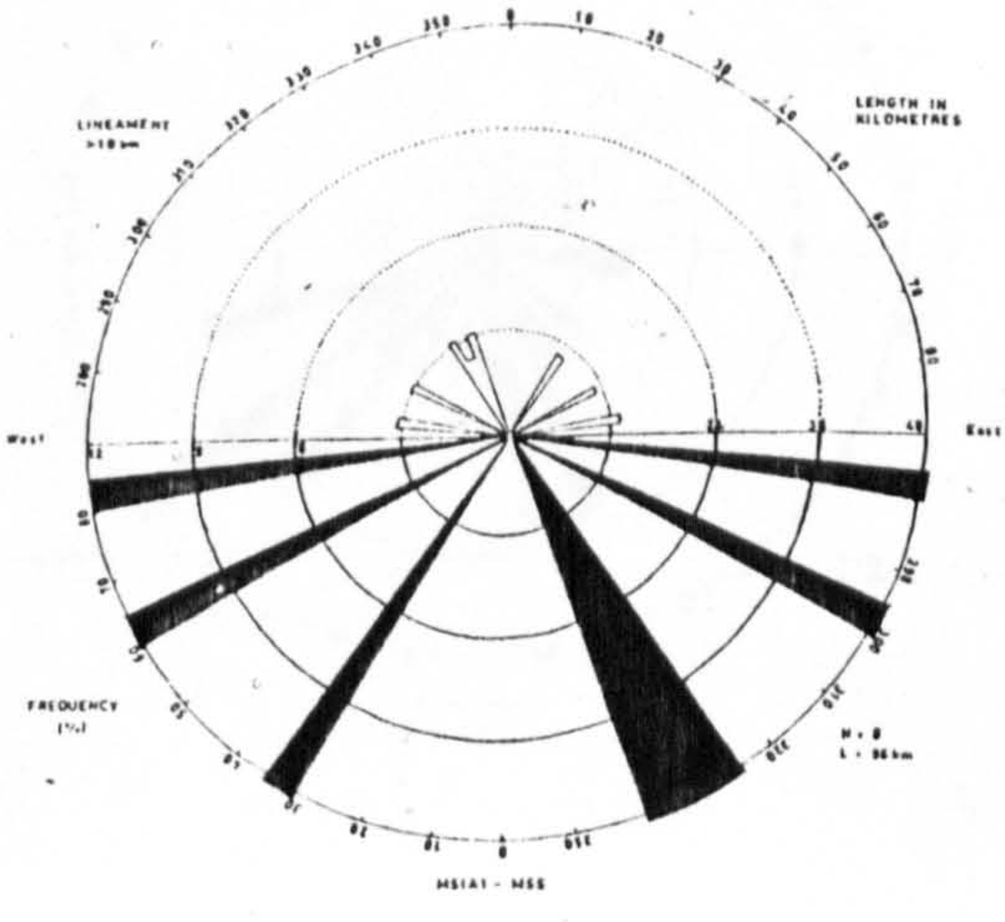

Figure 8.14 Rose diagrams of the Landsat MSS lineaments with less than 2 km, 2 - 5 km, 5 - 10 km, and more than 10 km length of the Kedah-Perak area, calculated by both length as well as number of observations.

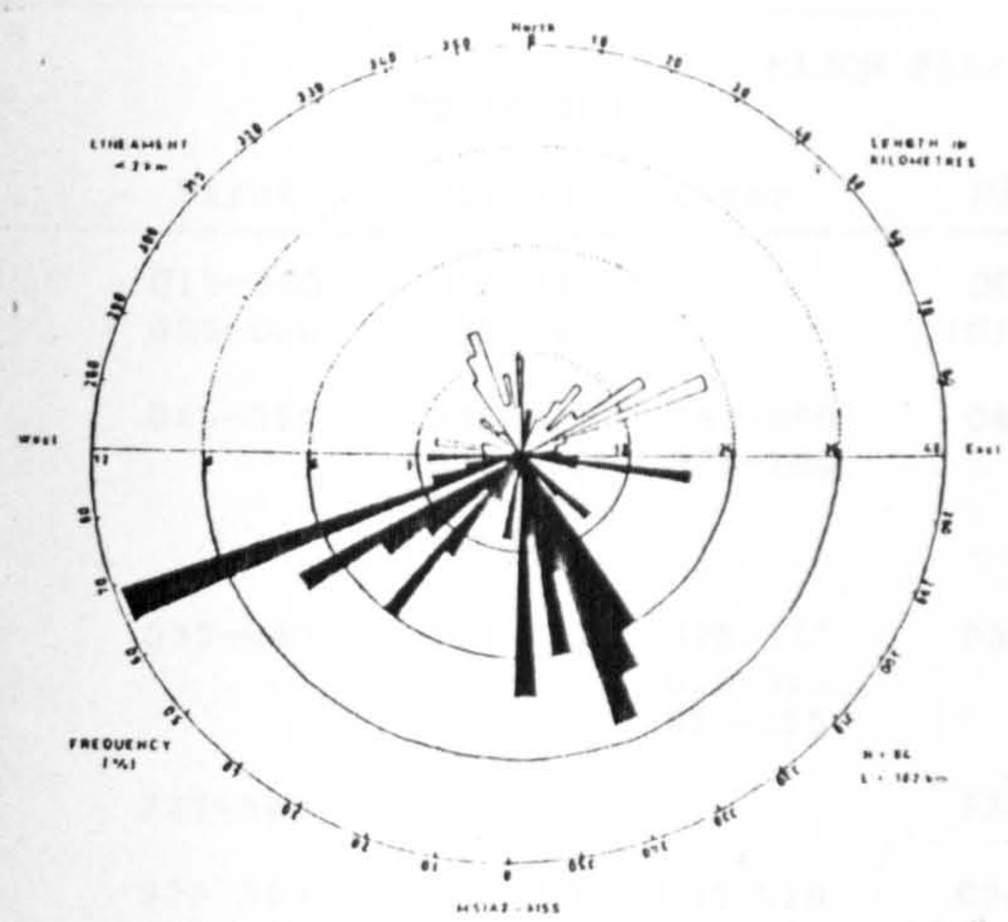

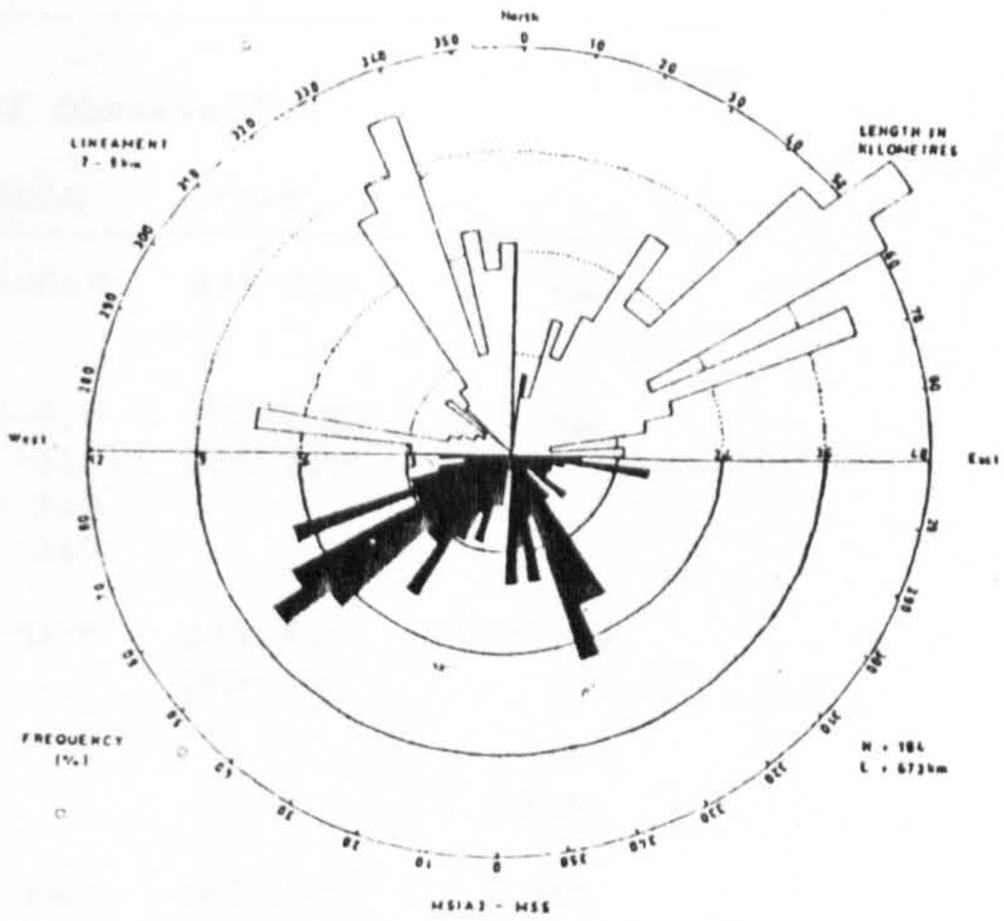

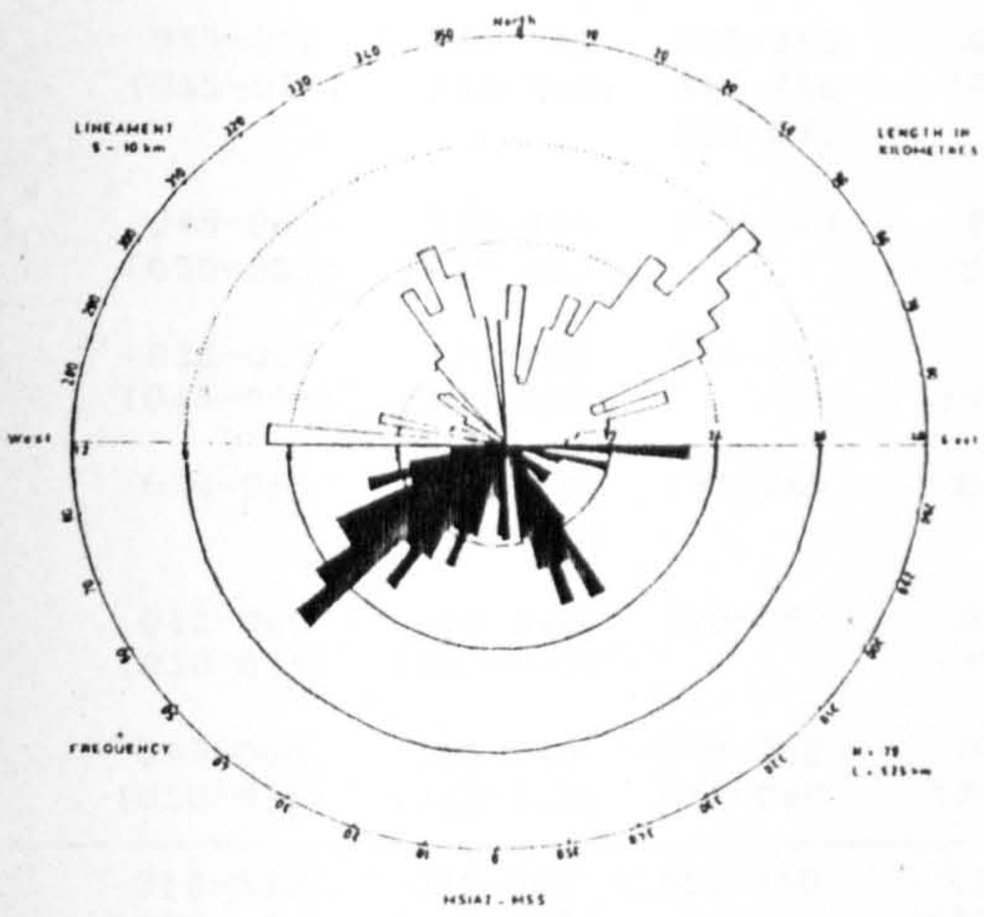

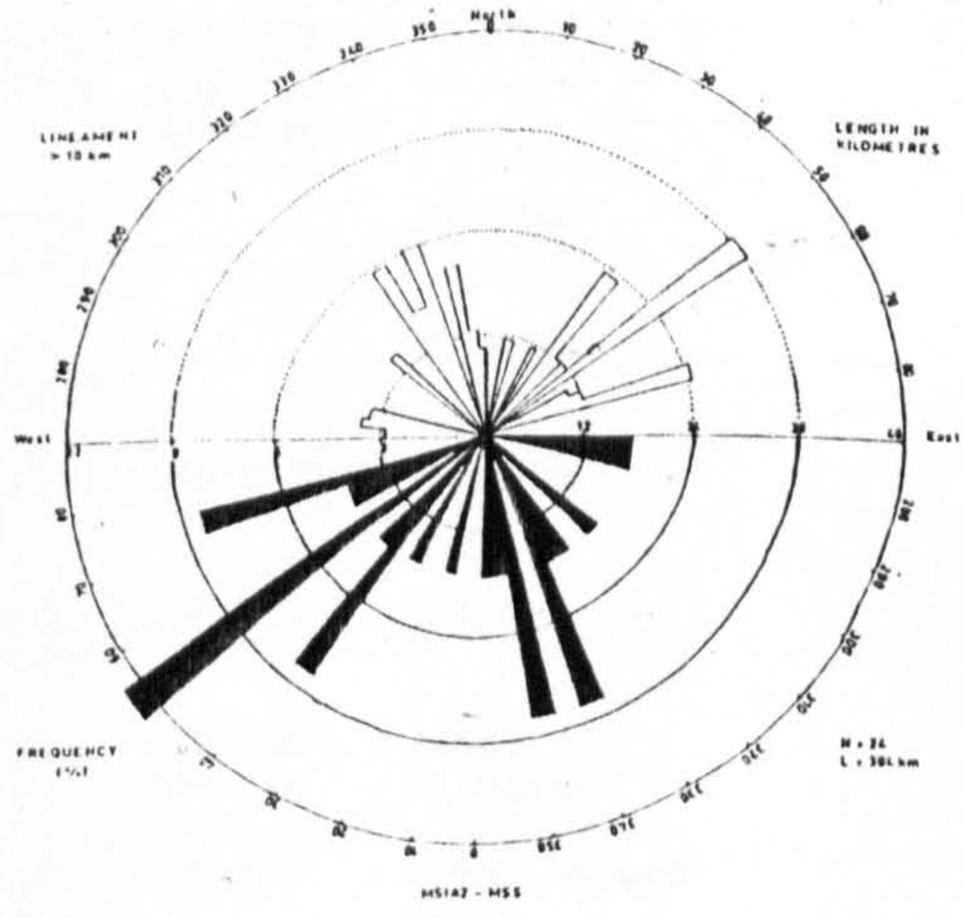

Figure 8.14 (continued)
Rose diagrams of the Landsat MSS lineaments of different length groups for the Kedah-Perak sub-area 2.

AREA/ DATA	MAJOR PEAK By Length			By Number of Observation			LENGTH GROUP
	First	Second	Other	First	Second	Other	
	015-020 055-060	325-340 (335-340)		005-020 (015-020)	055-060	325-340	< 2 km
	045-050	005-020 (005-010) 325-340 (335-340)	080-090 275-280	045-050	005-020 (005-010) 325-340 (335-340)	080-090 275-280	2-5 km
MSIA1 (MSS)	035-040	080-090	325-330 005-015 350-355	035-040	075-090	325-330 005-020	5-10 km
	325-340			325-340			> 10 km
	325-340 (325-330)	080-090	005-020 030-040	035-050 (045-050)	325-340 (325-330)	005-020 080-090	> 2 km
	325-340 (325-330)	005-020 (005-010)	075-090 035-040 275-280	005-020 (005-010)	325-340 (335-340)	045-050 085-090	total lineament
MSIA1 (Map)	030-035	310-325 (315-320)	055-060 270-275	015-060 (055-060)	310-325 (310-320)		total mapped fault
	055-070 (065-070)	325-340 (335-340)	355-360 275-280 030-035	055-070 (065-070)	325-340 (335-340)	355-360 275-280 035-040	< 2 km
	045-060 (050-055)	325-340 (335-340)	275-280	045-060 (050-055)	325-340 (335-340)		2-5 km
MSIA2 (MSS)	035-065 (045-050)	325-345 (335-340)	270-275	045-065 (045-050)	325-345 (325-330)		5-10 km
	050-055	325-350 (335-340)	275-285	050-055	335-350	070-075	> 10 km
	045-060 (050-055)	325-340 (335-340)	270-280	045-060 (050-055)	330-345 (340-345)	270-280	> 2 km
	045-060 (050-055)	325-340 (335-340)	270-280 070-080	325-340 (335-340)	045-070 (050-055)	355-360 270-280	total lineament
MSIA2 (Map)	315-330 (325-330)	020-040 (030-035)	355-360	315-330 (320-330)	030-050 (030-035)	355-360	total mapped fault
MSIA1& MSIA2 (MSS)	325-340 (335-340)	035-055 (050-055)	275-280 005-020	325-340 (335-340)	045-070 (045-050)	275-280 005-015	total lineament
MSIA1 & MSIA2 (Map)	315-330 (325-330)	020-035 (030-035)	355-360	315-330 (320-330)	010-050 (030-035)	355-360	total mapped fault

Numbers in bracket show the mode of lineament concentration in a broad peak.

Table 8.4 The azimuthal distribution of lineament derived from Landsat MSS of the Kedah-Perak area. For comparison, the distribution of the mapped faults (Geological Survey of Malaysia, 1985) is also given.

brought out in the lineament map, if we are only interested in the statistics of their trend. However, in terms of the total numbers and lengths, the mapped lineaments are many times as large as those of faults. It was found, that the minimum length of the faults shown in the published map is about 2 km. Furthermore, large lineaments of the order of five kilometres and more is interpreted to represent faults, because these lineaments are too large to be joints without displacements, although it is not always possible to prove this in the field because of the absence of outcrops due to the advanced stage of weathering (Tjia, 1971; Ibrahim Abdullah, 1984). Therefore, it was thought that it would be more appropriate to compare the rose diagram of the faults with the rose diagram of the lineaments with a minimum length of about 2 km, rather than with the total lineaments. As illustrated in Figure 8.15, the two rose diagrams are more or less concordant in both of their numbers and lengths. Therefore, again, if we are only interested in the statistics of their trends, it can be concluded that the mapped lineaments are more or less closely related to faults. The rose diagrams for each sub-area and their corresponding faults also gave similar results (Figure 8.15C-F). When compared with the structural trendlines map (Figure 8.16), the preferred directions of the mapped lineaments coincide well with the line of the Bok Bak Fault System, which belongs to the Northwest Domain of the Geological Domains of Peninsular Malaysia, where 325° and 035° are the most common fractures trends (Burton, 1970; Tjia and Zaiton Harun, 1985). The preferred directions also correspond

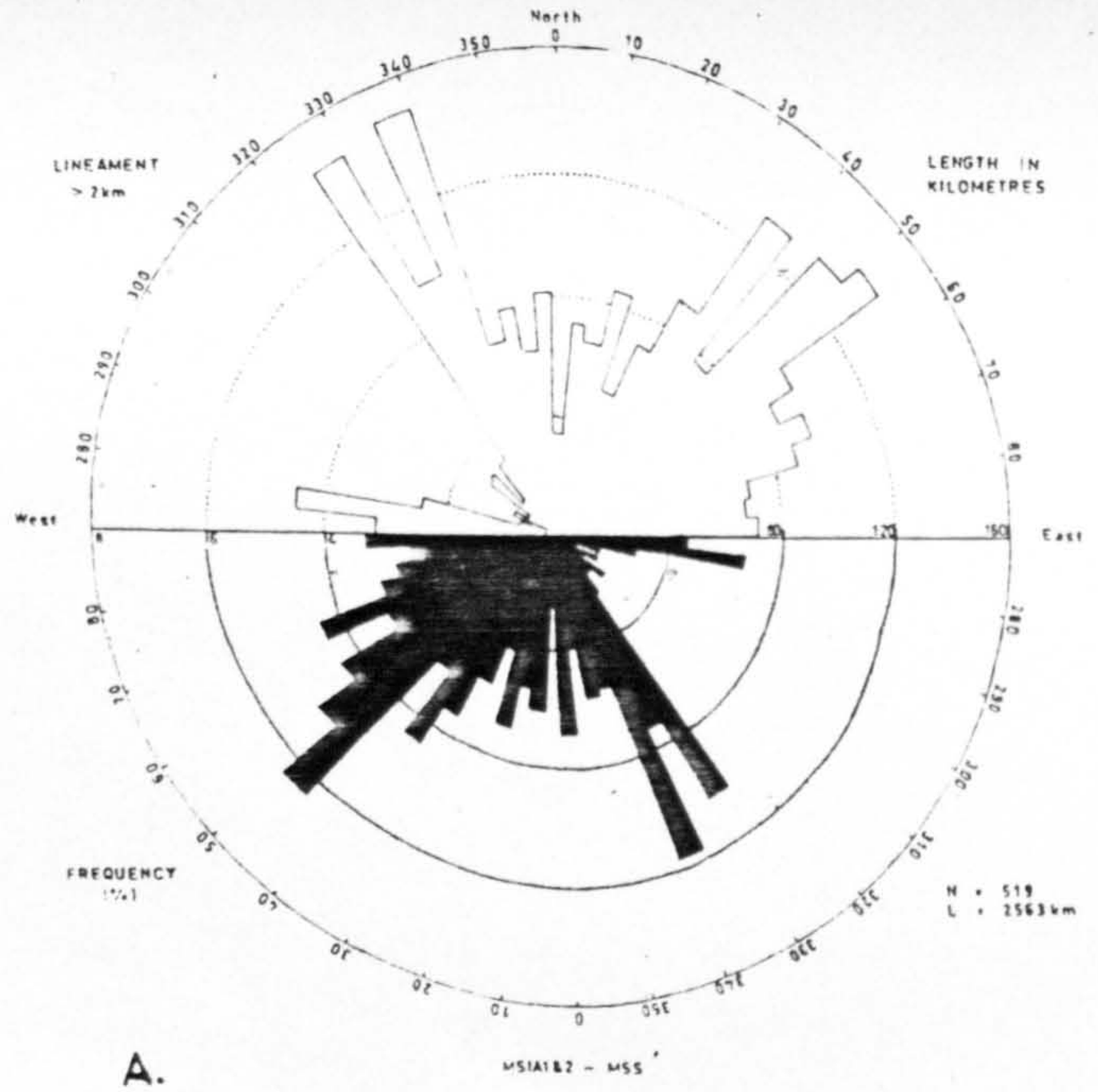

A.

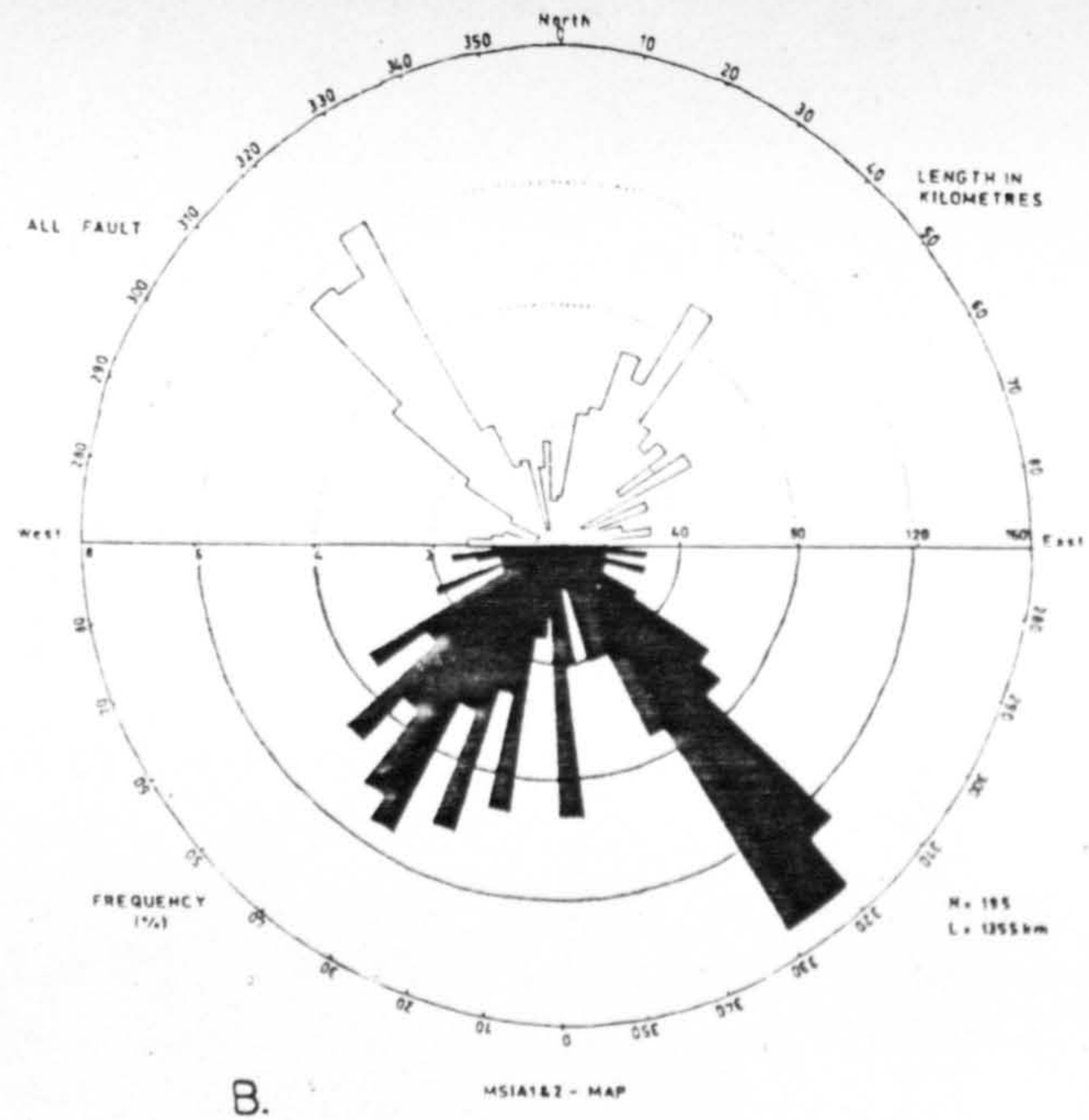

B.

Figure 8.15 Rose diagrams of the Landsat MSS lineaments with more than 2 km length (A) and mapped faults (B), calculated by both length as well as number of observation, of the Kedah-Perak area. Rose diagrams (C) and (D), (E) and (F) show the azimuthal distribution of the lineaments with more than 2 km length and mapped faults for the Kedah-Perak sub-area 1 and 2 respectively.

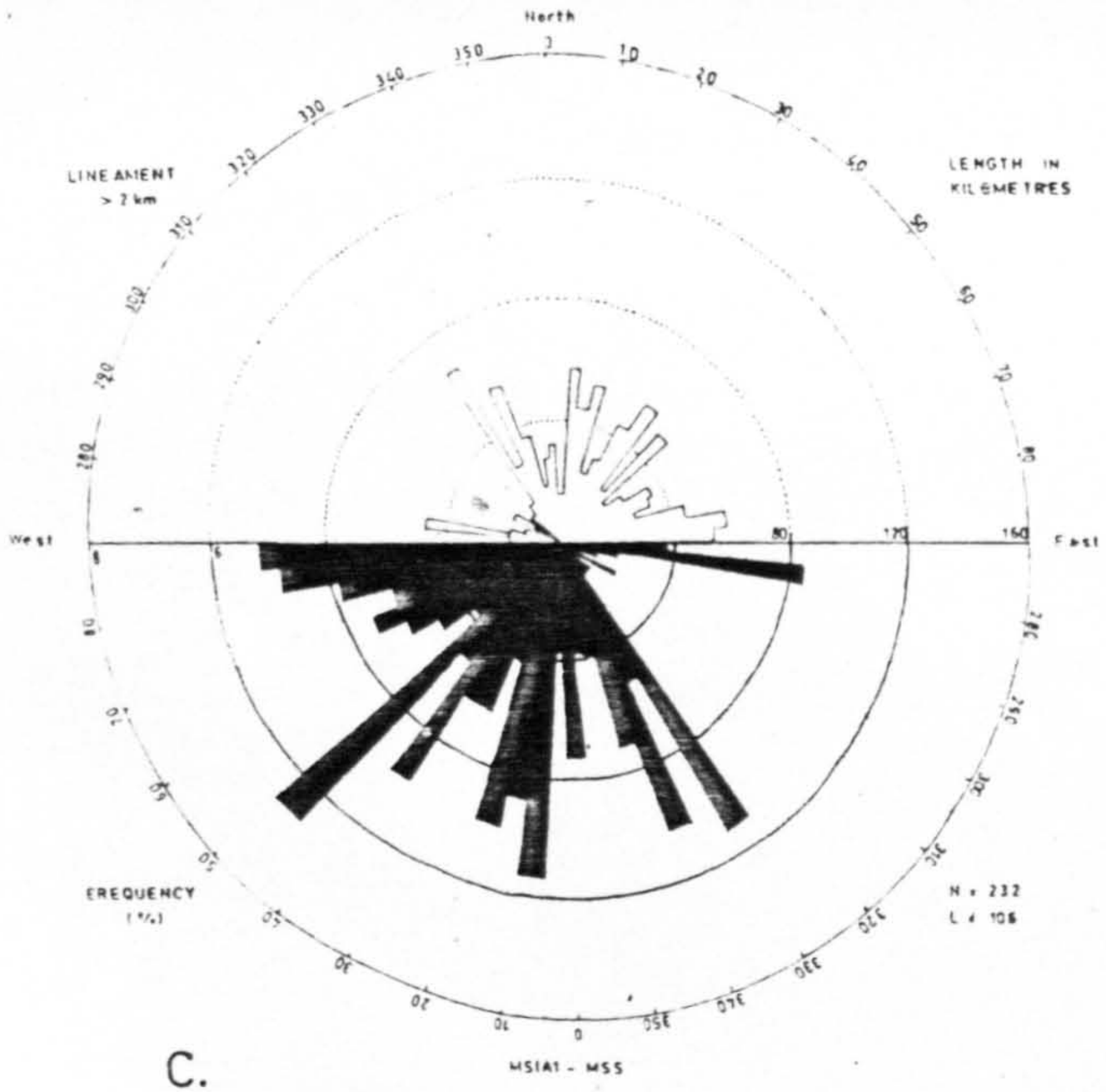

C.

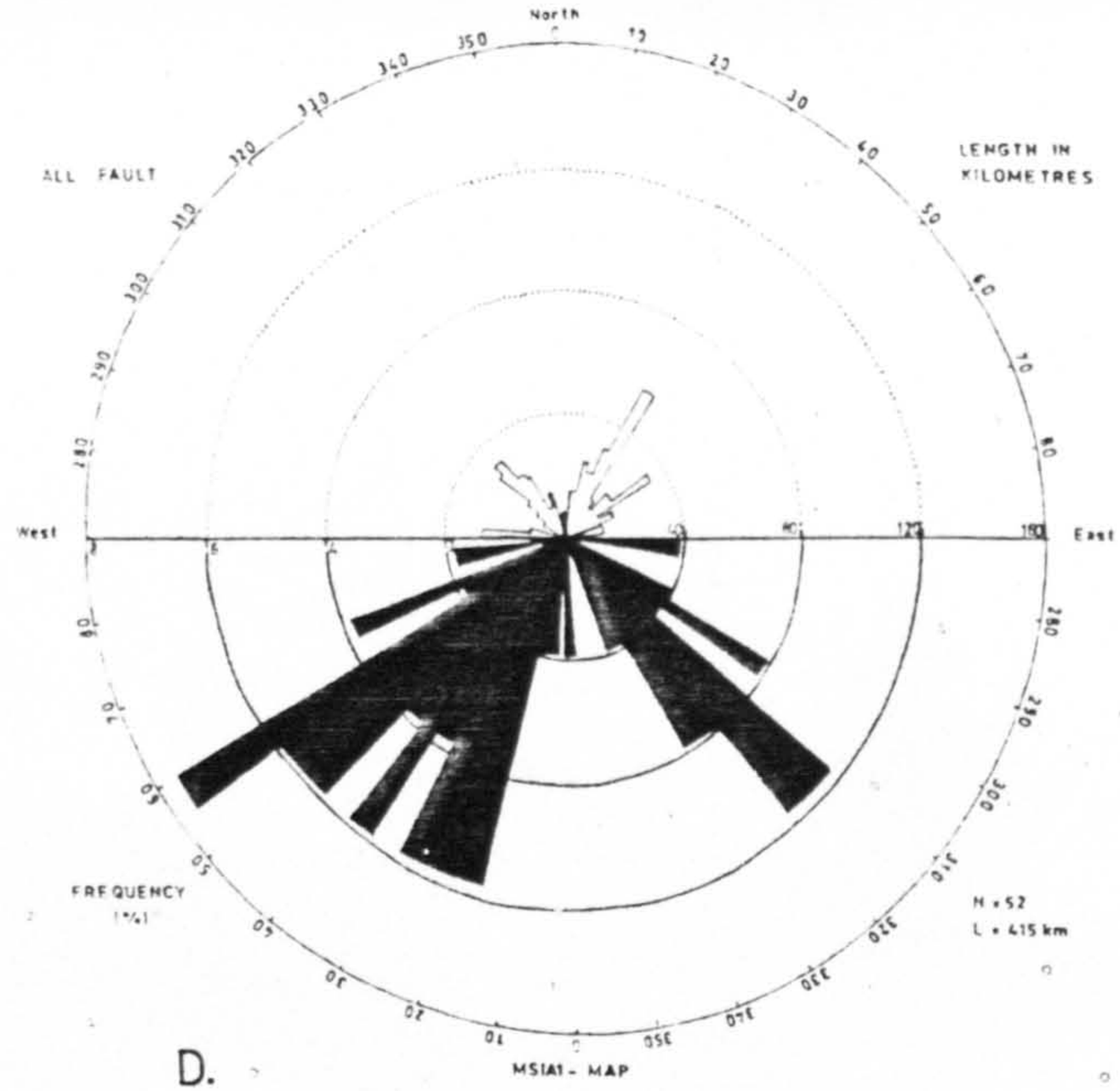

D.

Figure 8.15 (continued)
Rose diagrams of azimuthal distribution of Landsat MSS lineaments with more than 2 km length and mapped faults of the Kedah-Perak sub-area 1.

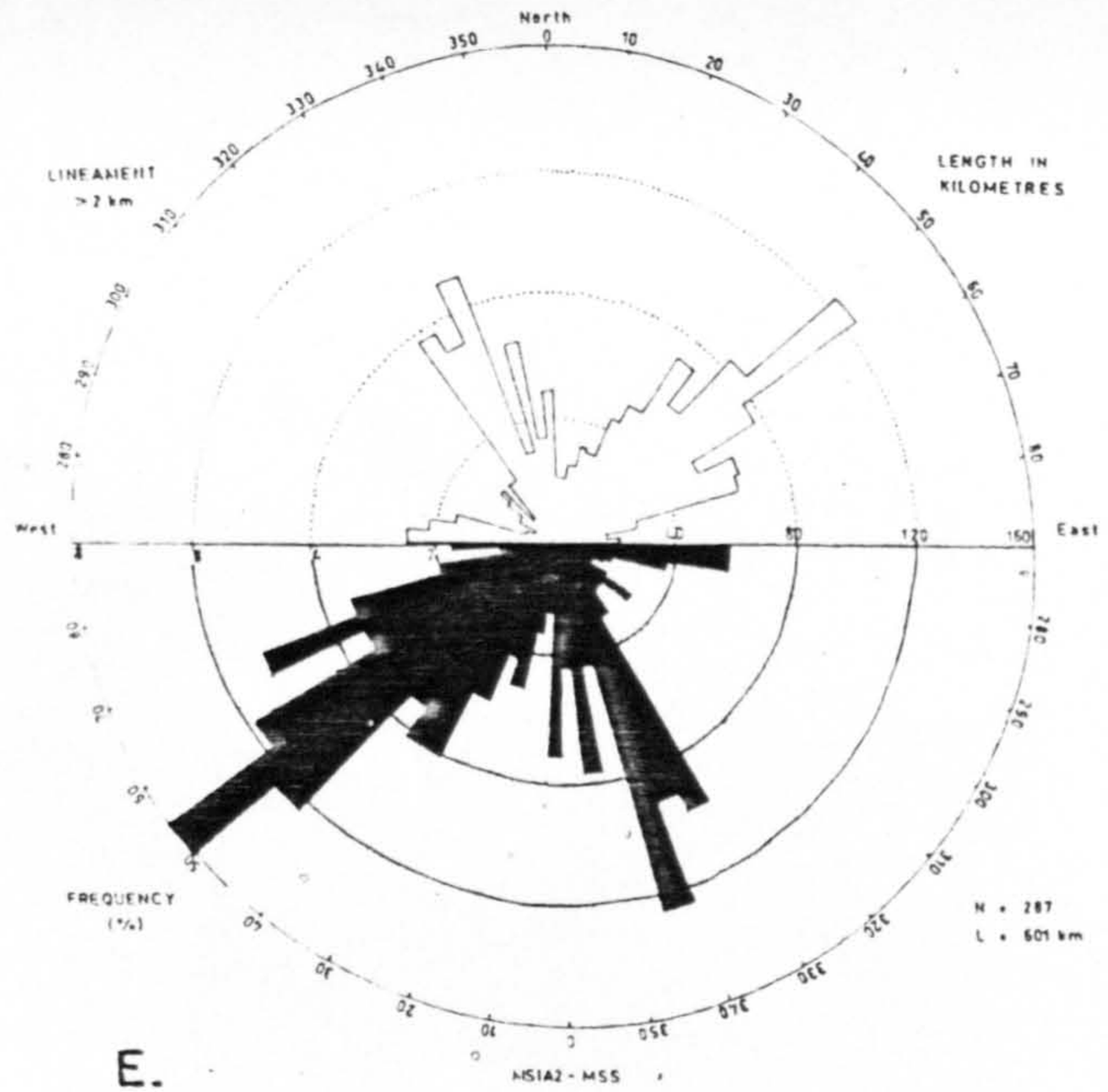

E.

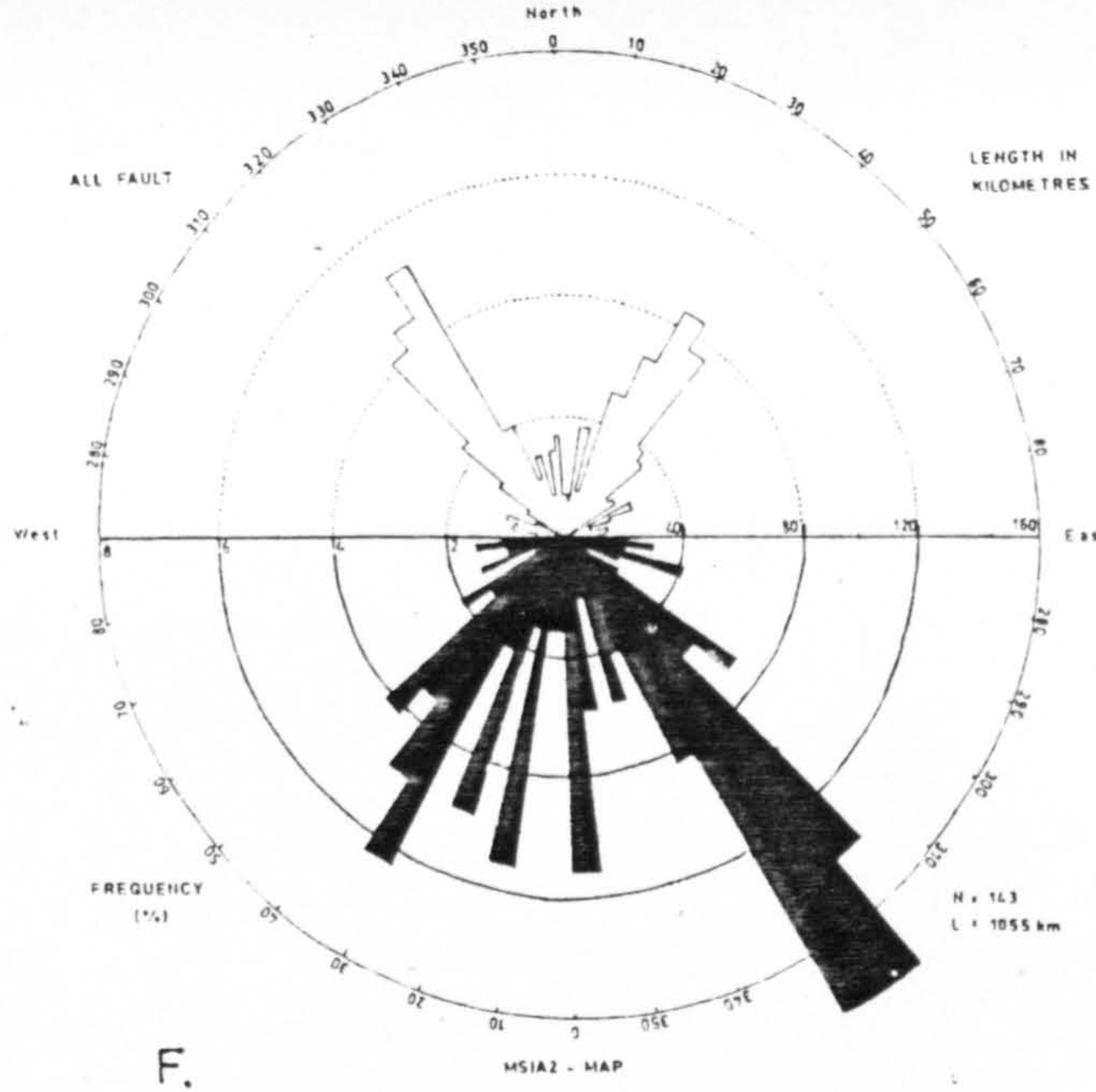

F.

Figure 8.15 (continued)
Rose diagrams of azimuthal distribution of Landsat MSS lineaments with more than 2 km length and mapped faults of the Kedah-Perak sub-area 2.

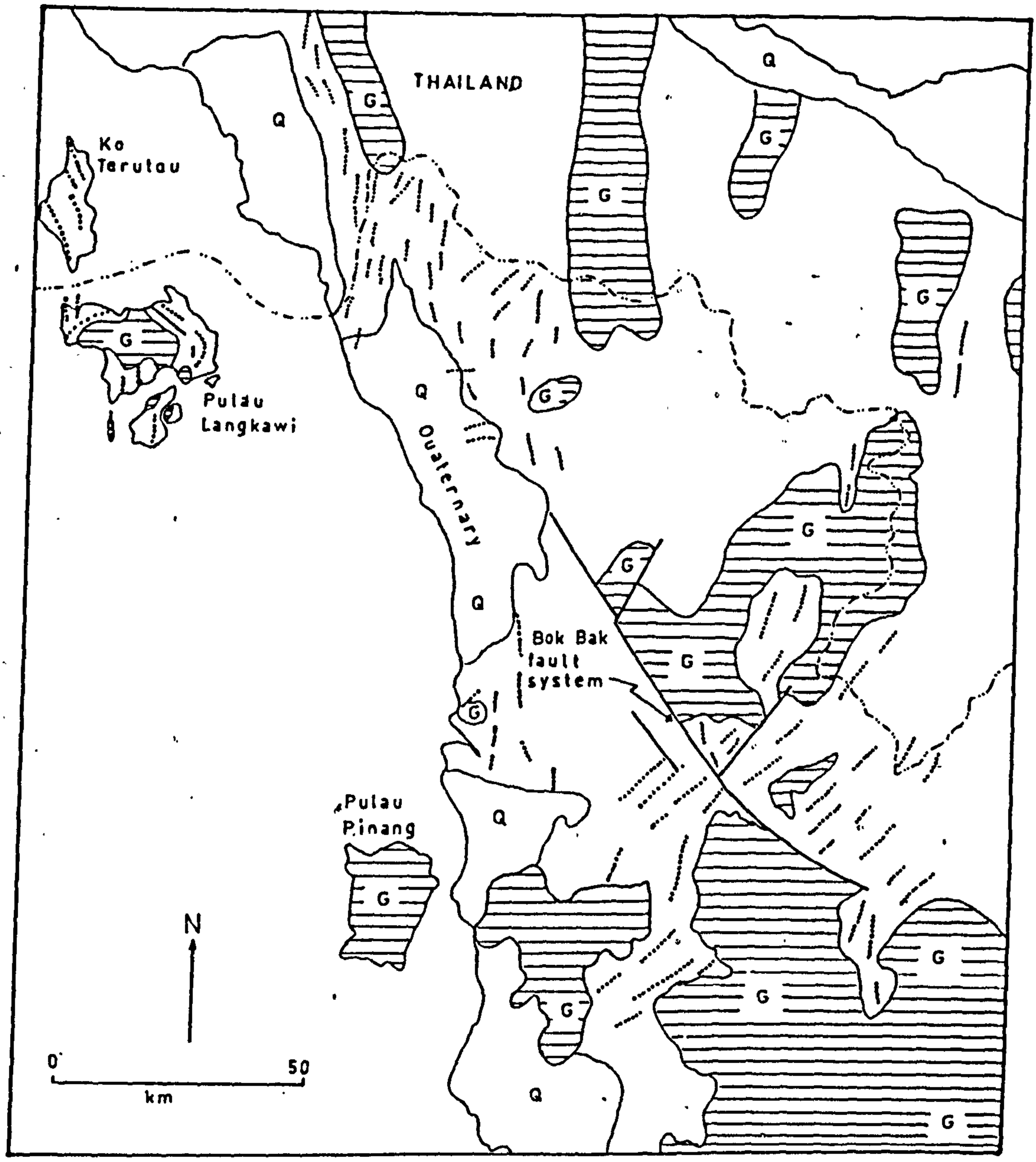

Figure 8.16 The structural trendlines of the Northwest domain of the Malaysia Peninsular (Fig. 2 of Tjia and Zaiton Harun, 1985). The domain has northerly and northeasterly strikes. Note that the Bok Bak Fault system is the major structural element in the area.

with the two main directions of faulting, particularly in areas underlain by the granite, with mean directions of 323° and 032° (Burton, 1970). Therefore, based on orientation, it is evident that the main features of the fault pattern are clearly brought out in the lineament map.

The total numbers and lengths of mapped lineaments, however, are respectively, 2.7 and 1.9 times as large as those of faults. Thus, if most of the faults agree with the lineaments in terms of location, the results may imply that the known faults must be extended or that the lineaments traces are longer than the actual faults. An attempt was carried out to check and compare the mapped lineaments and the mapped faults with respect to their locations. An overlay of the interpreted lineaments was superimposed with an overlay of the mapped faults drawn from the map. For this purpose, the published map was enlarged from scale of 1: 500,000 to the same scale as the original interpreted lineament map, which is 1: 250,000. However, it was difficult to get an accurate registration between the two overlays, and it is difficult to prove the identity between the maps of different data source. Therefore, only the interpreted map for sub-area 1 was checked (because it has less dense lineament and fewer number of mapped faults than sub-area 2) and the following conditions were adopted in this particular study in order to check and compare the location between the lineaments and the faults. All lineaments which fell within approximately 500 m (2 mm on the 9 x 9 inch images of 1: 250,000 scale) of each fault and deviated by no more than 5° were considered contiguous, and

only where a lineament overlaps a fault by more than half of its length was it considered to be coincident. The result shows that 62 per cent (36 out of 58) of the mapped faults were revealed and are coincident with the interpreted lineaments. The mapped faults which do not coincide or are not identified on the interpreted lineaments include 10 faults with length less than 5 km and 6 faults which occur in the lowland area. Thus faults are more likely to be identified and to coincide with the interpreted lineaments if they occur in the higher ground and are longer in length. However, the results indicate that a large number of the mapped faults were revealed in the interpreted lineaments and in several cases, as shown in Figure 8.17, the mapped faults should be extended. However, a large number of lineaments, particularly the shorter ones, were not coincident with the faults, and they are more likely represent joints rather than faults. Despite this, a few prominent lineaments are shown in Figure 8.17 which are also not coincident with the known faults. Based on their size and their prominence, they may well represent fault lines not previously mapped or reported, rather than joints. For the sub-area 2, although the locations were not checked between the mapped faults and the interpreted lineaments, it is evident that a large number of faults were revealed on the lineament map and some known faults should be extended (Figure 8.18). As in the sub-area 1, several prominent lineaments were found which show no association with the known faults. These are interpreted as a fault lines not previously mapped or reported (Figure 8.18).

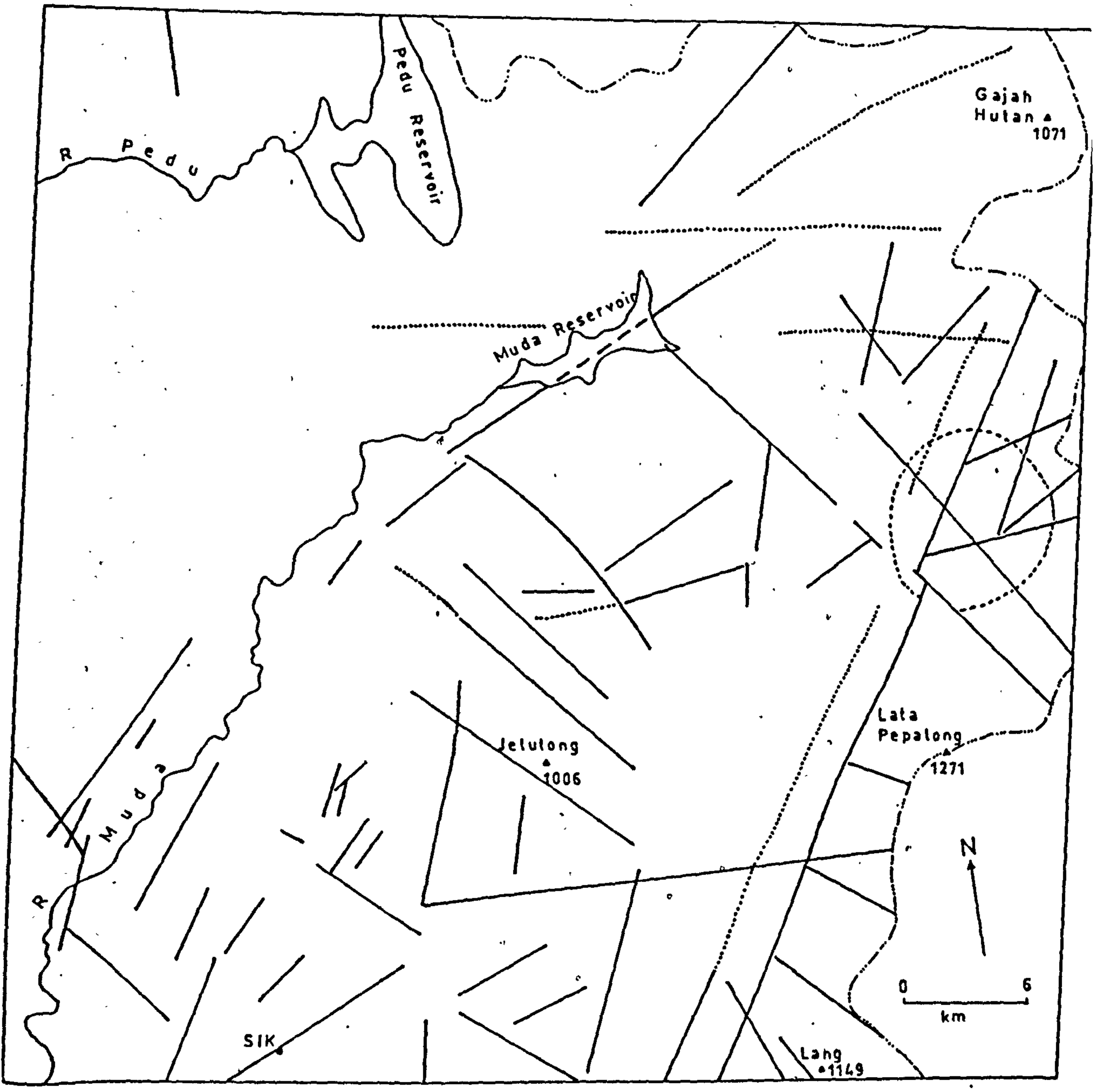

Figure 8.17 Mapped faults in the Kedah-Perak sub-area 1 (Geological Survey of Malaysia, 1985). Several major lineaments which are well depicted on the Landsat MSS, and are not corresponding to any mapped faults, are interpreted as new fault lines in the area. A major circular feature, which are well displayed in the images is also shown.

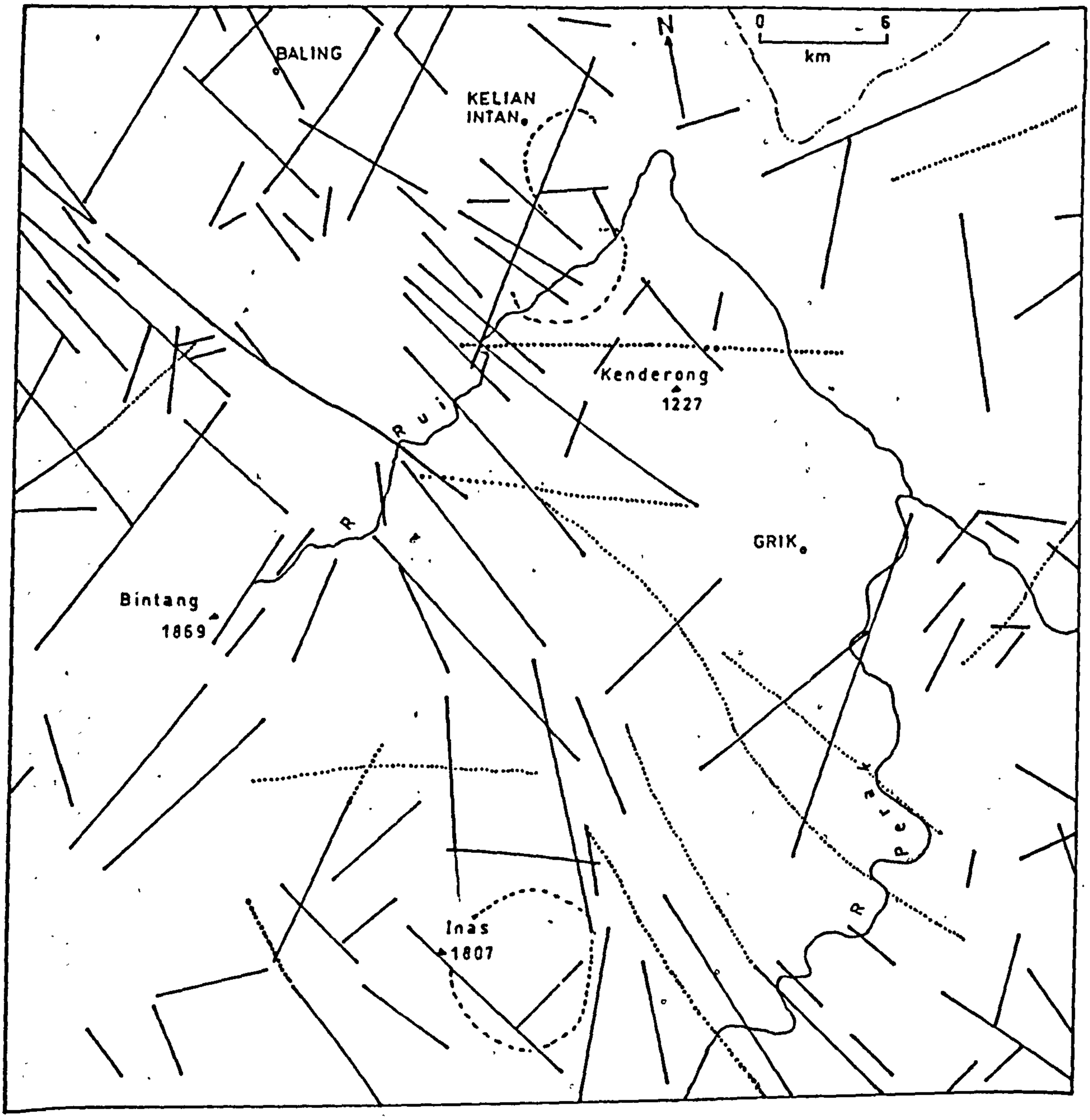

Figure 8.18 Mapped faults in the Kedah-Perak sub-area 2 (Geological Survey of Malaysia, 1985). Dotted lines represent several major lineaments on the Landsat MSS which do not correspond to any mapped faults, and are interpreted as new fault lines in the area. In addition, a few circular features which are depicted on the images are also shown.

8.4.2 Lineaments and fracture analysis

Based on their length and the results in section 8.4.1, the mapped lineaments can be interpreted as fractures ranging from joints to faults. A number of basic criteria is now available for fracture analysis as a result of intensive laboratory experiments on rock deformation and corroborated by field evidence. Comprehensive texts about fracture analysis have been written by Handin and Hager (1957), Hill (1963) and Badgley (1965), and can be summarized as follows.

Brittle fracturing of rocks results from compression under confining pressures or from tension. All stresses acting upon a body can be combined or resolved into three stresses working along orthogonal lines, the so-called principal or normal stresses. P indicates the maximum principal stress, Q the intermediate principal stress, and R represents the minimum principal stress. If fractures result from this stress system, two first order shear planes are formed, symmetrically arranged around the P-direction and making a dihedral angle of 25 to 30 degrees with the P direction, while their intersection parallels Q. Relaxation of P may result in fractures perpendicular to P, these are tension fractures. Extension fractures are possible in planes parallel to those of P and Q, that is normal to R under certain ratios of P and R. It is possible that during the compression history of an area the original R-stress may occasionally exceed the original P-stress and in this way form second order shears which are arranged with dihedral angle of 25 to 30 degrees to

the new maximum principal stress direction(= original R-direction) and intersecting each other along lines parallel to the original Q direction. Figure 8.19 shows the various fractures, their possible displacements as a result of an east-west directed maximum compression, as used by Tjia (1972) in order to name the fractures represented by lineaments.

The total number of lineaments were measured in sub-areas 1 and 2, and are shown as length/frequency rose diagrams (Figure 8.13B and C). Based on the assumption that the majority of the long and straight topographic elements indeed represent fractures, lineament analyses carried out based on topographic maps at scale 1: 250,000 or 1: 253,440 by Tjia (1972) indicate that Peninsular Malaysia may be divided into seven tectonic domains, where each domain is characterized by one or more dominant structural trends (Figure 8.20). The area covered by the sub-area 1 and part of the sub-area 2, therefore, are included in the tectonic domain 1, while a portion of the area covered by the sub-area 2 is included in the tectonic domain 3. It is clear that each of the structural strikes is interpreted as a result of a regional compression perpendicular to it as summarised in the Table 8.5.

By using the above structural information of the area and the basic criteria in fracture analysis, nearly all the maximum frequencies in Figure 8.13B and C may be interpreted as one particular type of fracture as a result of one particular compression. For example, the lineaments in Figure 8.13B have been interpreted as follows: tension (75^{o}-90^{o}),

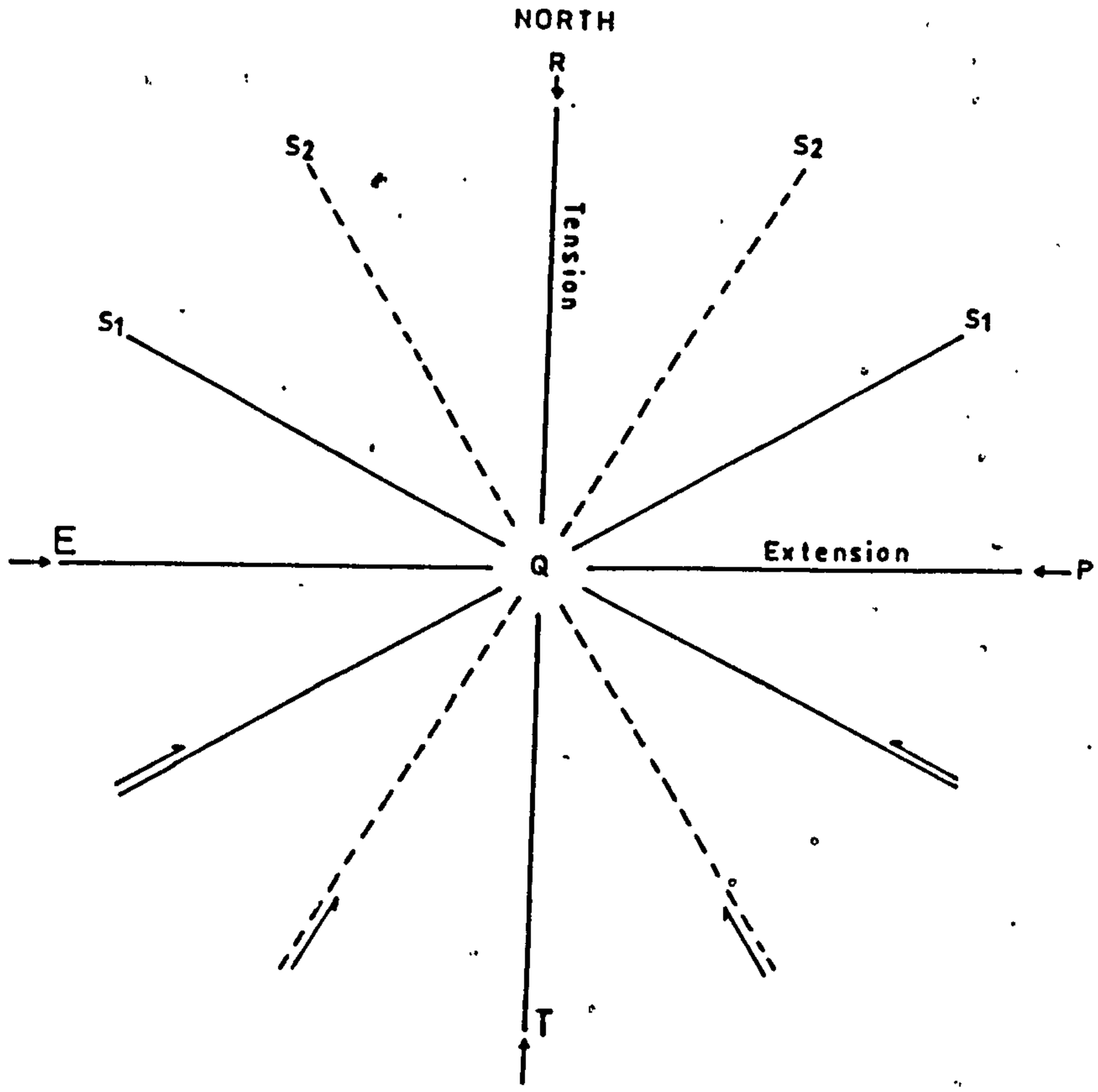

Figure 8.19 Potential fracture orientations as a result of east-west directed maximum compression. T = tension, E = extention, S1 = first order shear, S2 = second order shear. P, Q, and R are respectively maximum, intermediate, and minimum principal stresses. The relative movements on the various fractures are indicated by small arrows (after Tjia, 1971 and 1972).

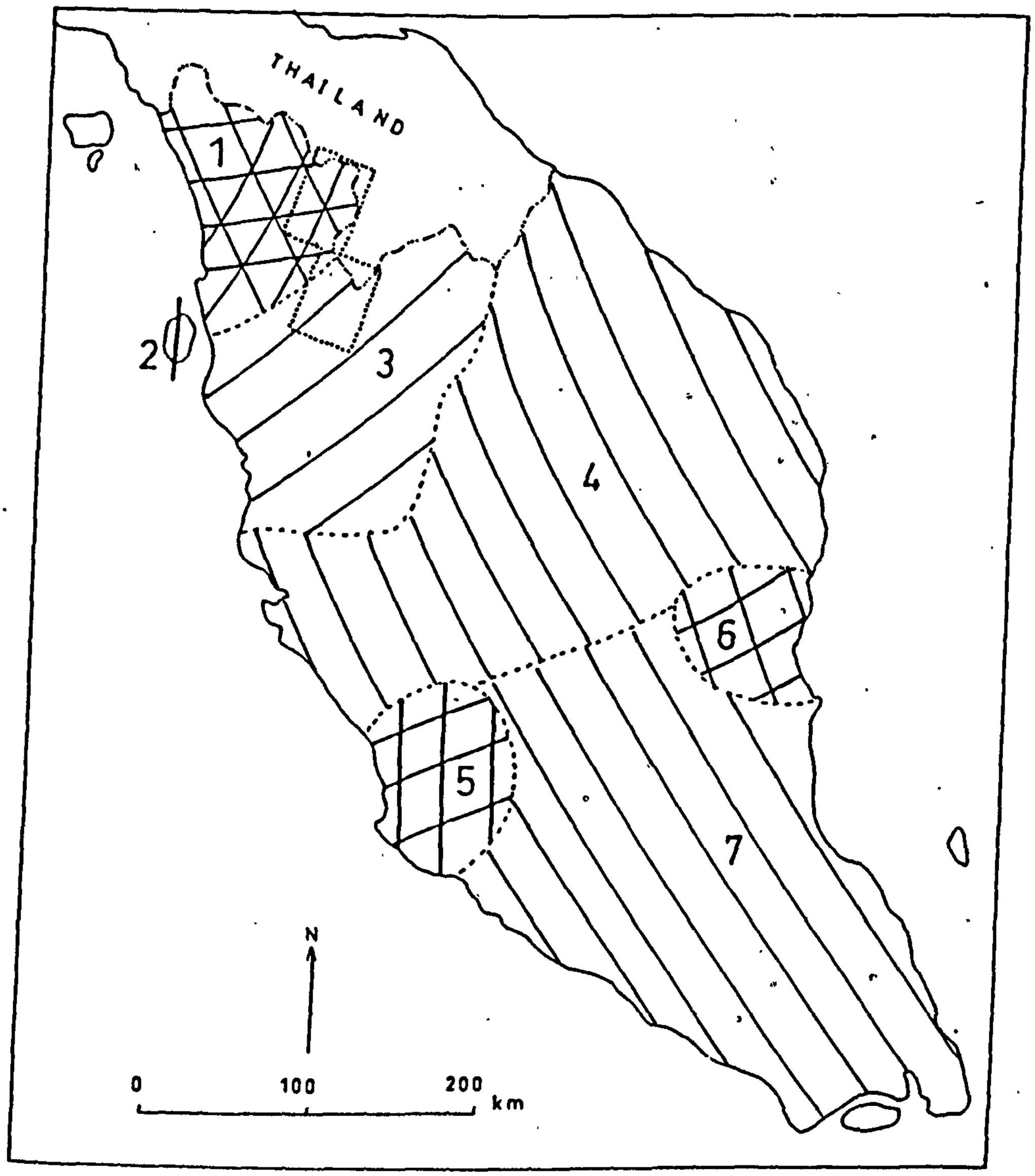

Figure 8.20 Seven morphotectonic domains of Peninsular Malaysia. Heavy solid lines represent structural trends based on lineament pattern and fold axes (after Tjia, 1972 and 1978). The study area is included in the domains 1 and 3, where the domain 1 has more than one structural directions.

TECTONIC DOMAIN	AGE	STRIKE	COMPRESSION DIRECTION
1	Early Paleozoic	80^0 30^0	$P_1 = 350^0$ $P_2 = 300^0$
	Late Paleozoic and Mesozoic	340^0	$P_3 = 70^0$
2	Early Mesozoic	0^0	$P = 90^0$
3	Late Paleozoic	55^0	$P = 325^0$
4	Late Paleozoic and Mesozoic	345^0	$P = 75^0$
5	Early Paleozoic Early Mesozoic	80^0 0^0	$P_1 = 350^0$ $P_2 = 90^0$
6	Late Paleozoic Early Mesozoic	60^0 330^0	$P_1 = 330^0$ $P_2 = 60^0$
7	Late Paleozoic and Mesozoic	320^0	$P = 50^0$

Table 8.5 Structural strikes in Peninsular Malaysia (Tjia, 1972 and 1978).

first order shears (325°-340° and 005°-020°), and second order shears (275°- 280°) and so on. Table 8.6 summarises the (main) interpreted fracture types in the study area.

The results for the sub-area 1 show very similar directions to those interpreted by Tjia (1972). This indicates that both data sources, the topographic map and Landsat imagery, give very similar information for fracture analysis for this particular scale and area. The differences in terms of area covered by the sub-area 1, compared with the whole area of the tectonic domain 1, can be used to explain the differences between the results of the two analyses. For the sub-area 2, the results of analysis show a lack of similarity with the results interpreted by Tjia (1972). There are two possible reasons for this finding. First, the area covered by the sub-area 2 is only about 10 per cent of the total area of the tectonic domain 3, therefore the results may not represent the characteristics of the tectonic domain 3. Second, the area is adjacent to the tectonic domain 1 and also close to the tectonic domain 2 (Figure 8.20), therefore there are possibilities that the area is still affected or influenced by the principal compressions in these domains. Consequently, the lineaments in 70°-80° and 35°-40° directions are perhaps more or less related to the principal compression in the domain 1 (070°), and the lineaments in 270°-280° are possibly related to the principal compression in the domain 2 (approximately in east-west direction) (Tjia, 1972, Figure 4).

AREA	LINEAMENT PEAK	FRACTURE TYPE	COMPRESSION DIRECTION
	325-340	S1	
	005-020	S1	P1 = 350
	075-090	T1	
Kedah-Perak			
sub-area 1	035-040	T2	
(Domain 1)	275-280	S2	P2 = 300
	060-070	E3	P3 = 070
	045-060	T1	
	325-340	E1	P1 = 325
Kedah-Perak	270-280	S	
sub-area 2	035-040	S	P = 070
(Domain 3)	070-080	E	(Domain 1)
	270-280	E	P = 090 (Domain 2)

- Compression directions are taken from Tjia, 1972 and 1978.
- See Figure 8.19 for the fracture types annotation.

Table 8.6 Several interpreted fracture types (based on the fracture analysis and the related regional compression) in the Kedah-Perak area.

For the sub-area 1, generally the mapped faults (Figure 8.15D) show quite similar results with both the Landsat (Figure 8.13B) and the topographic map analyses by Tjia (1972). The differences in information content between the plotted faults which represent faults, and the plotted lineaments, either from Landsat or topographic map which represent either joints or faults may be used to explain some differences which occur between the plotted faults and the plotted lineaments. Despite differences in terms of information content, the plotted faults (Figure 8.15F) also show similarity with the plotted lineaments taken from Landsat for the sub-area 2 (Figure 8.13C). However, the plotted faults show a lack of similarity with the results found by Tjia (1972). The probable reasons are, first, the plotted faults (Figure 8.15F) are not representive of the whole area of the tectonic domain 3, and second, the plotted lineaments represent a wide range of fracture types ranging from joints to faults, whereas the plotted faults only represent mapped faults. Therefore, there are differences in terms of information content between these two data sets, which explains the different results.

8.4.3 Lineaments and rock type

It has been reported that the occurrence and concentration of rock fractures are governed by rock type, thickness of uppermost weathered mantle and brittleness of rocks by Harris et al. (1960). They also found that brittle rocks such as siliceous dolomites or limestones commonly show a high

concentration of fractures, and the concentration of deformational fractures was approximately inversely proportional to the thickness of the uppermost mantle. Their finding is supported by Henderson (1960), who reported that high concentrations of lineaments were associated with the thinning of soil cover close to the outcrops. Apart from rock types and covers, the high concentration of fractures coincides exactly with positive structures and low concentrations within depressions (Gol'braykh et al, 1966). In the lineament analysis of Peninsular Malaysia, Tjia (1972) reported that many lineaments are very well displayed in areas underlain by the granite, whereas in other areas they are poorly shown. Kim (1979) also reported that extremely low concentrations of lineaments occurred in the volcanic area of the northern part of the Korean Peninsula. In this study, the density maps of lineaments for the two sub-scenes were produced and were overlapped with the published map of the distribution of rock types, in order to test the above conclusions and findings.

As shown in Figures 8.21, clear relationships between rock types and concentrations of lineaments are undetectable. Notwithstanding this, it may be recognized easily that high concentrations of lineaments are mostly related to higher terrains underlain by the granite (G) and that low concentrations of lineaments are usually related to lower terrains of the Triassic Rocks (TR) and the Silurian-Ordovician Rocks (OS). However, it is evident that the lineament density is low in places where the granite forms

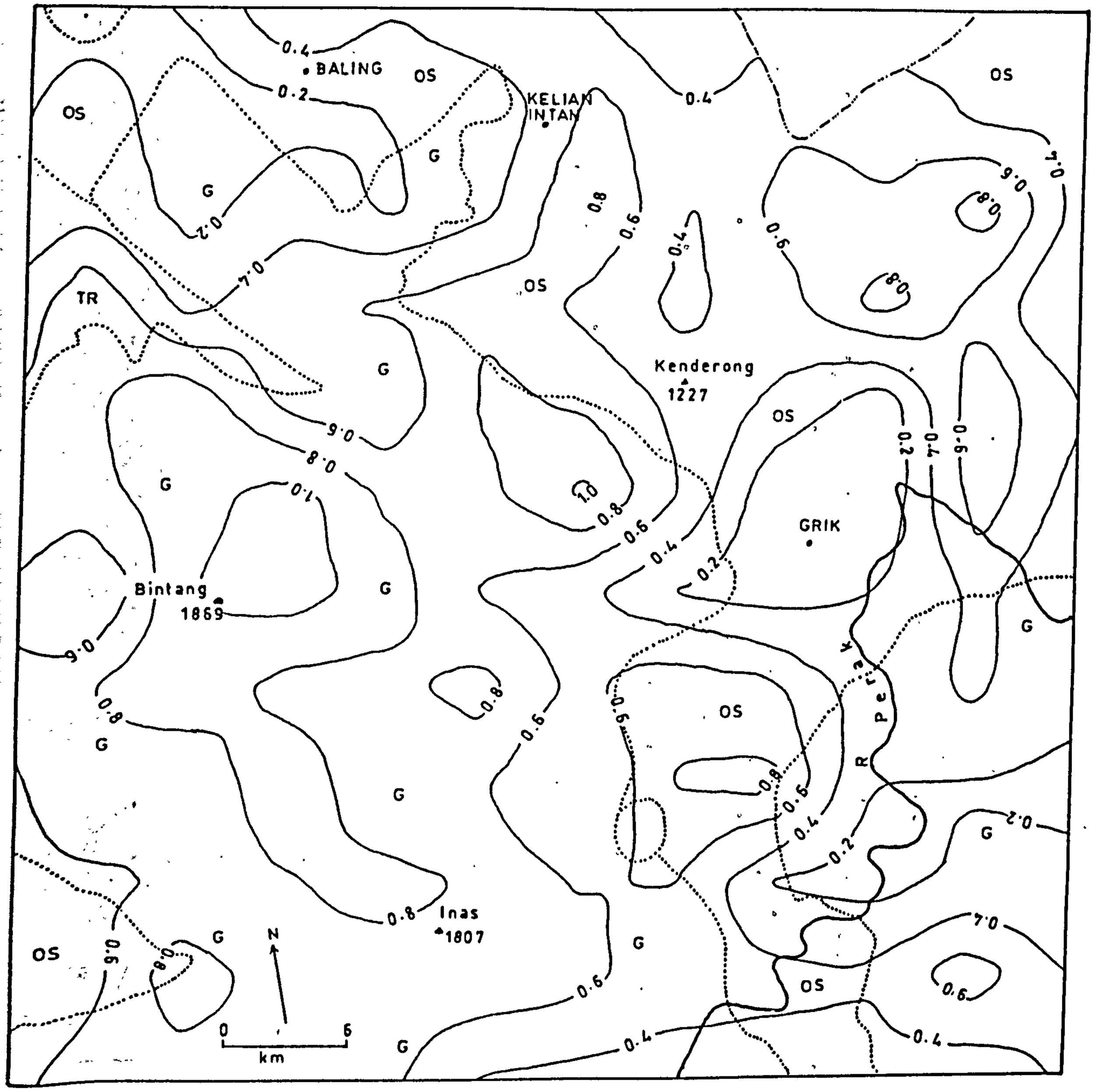

B

Figure 8.21 (continued)
Relationship between the rock types and the density of lineaments seen on Landsat MSS image for the Kedah-Perak sub-area 2. The geological boundaries are taken from the map by Geological Survey of Malaysia (1985). G = granite, T = Tertiary, TR = Triassic, and OS = Ordovician - Silurian .

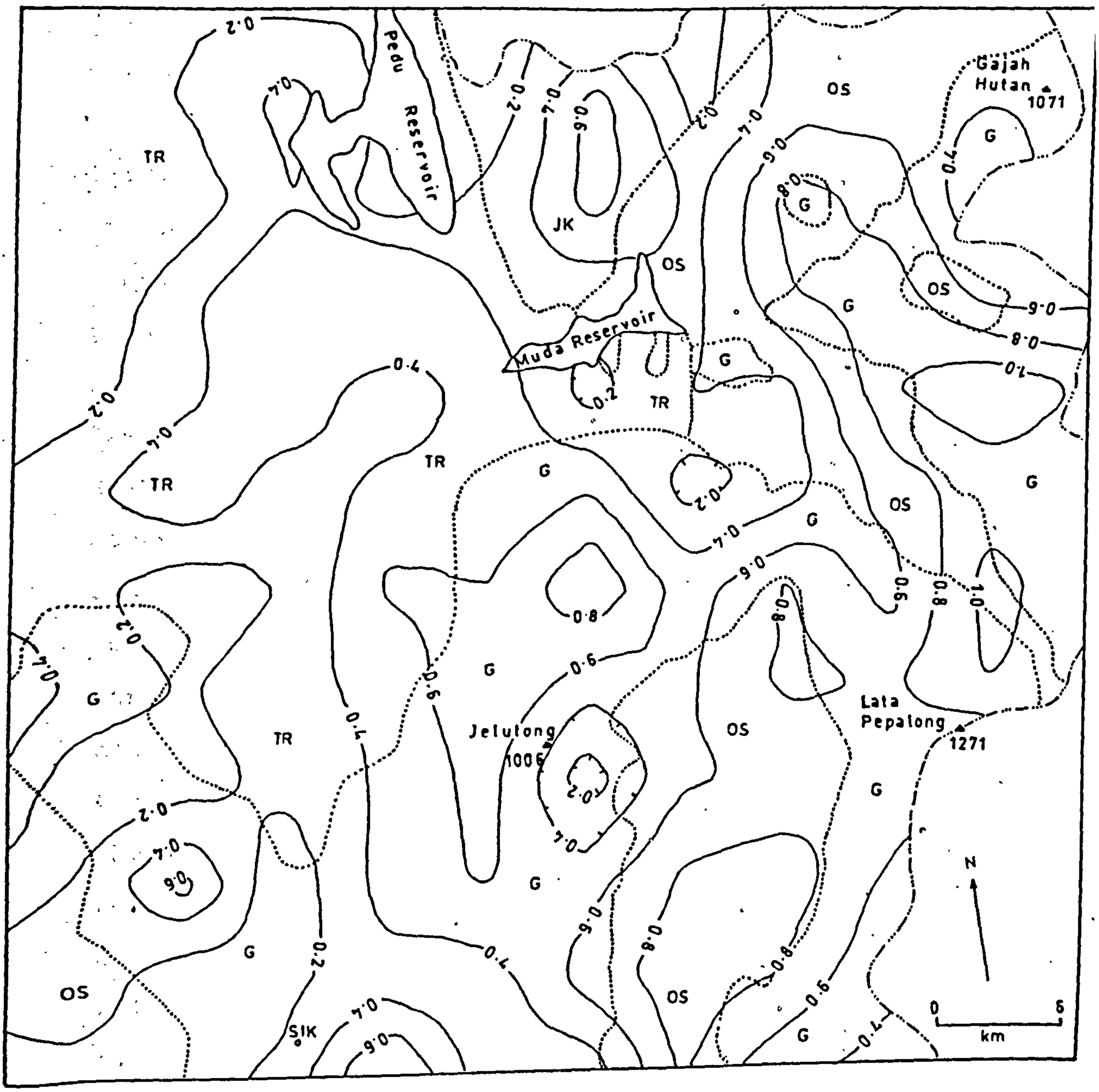

A

Figure 8.21 Relationship between the rock types and the density of lineaments depicted on Landsat MSS of the Kedah-Perak sub-area 1 (A) and sub-area 2 (B). The geological boundaries are taken from the map by Geological Survey of Malaysia (1985). G = granite, JK = Jurassic - Cretaceous, TR = Triassic, and OS = Ordovician - Silurian.

lowland areas. On the other hand, the lineament density is high in places where the Triassic and Silurian-Ordovician Rocks form highland areas. Therefore, the high lineament concentrations in the area are closely related to higher terrain which is formed by more resistant rocks such as granite and sandstone, whereas low lineaments concentrations are associated with lower terrain which is mainly formed by less resistant rock types such as shale and slate. Around Grik, the area mapped as volcanics in the Silurian-Ordovician Rocks was found to have an extremely low lineament concentration. Although in some areas the causes of lineament concentrations remains unclear, they seems to have some structural significance. For example, two areas in the east and southeast part of the sub-area 1, which are occupied by the Silurian-Ordovician rocks, may represent a depression, whereas the area in the northeast corner of the sub-area 1 may represent a positive structure such as horst. Therefore, high or low concentrations of lineaments in these area may be related to particular structures as reported by Gol'braykh et al. (1966). However, structural and lithologic "lows" with few yisible lineaments are certainly common. But their lowland and deepened positions may be due to close fracturing and followed by deep weathering, hence a contradiction occurs between visible evidence and actuality. Therefore, in order to know the relations between rock types and concentrations of lineaments and its related geological structures, more detailed studies, supported by field data, at larger scale are needed in this area.

8.4.4 Lineaments and mineral deposits

It has been long recognized that, in many mineral provinces, mining districts were not randomly distributed but tended to occur in linear zones or belts. It has been said that areas with numerous fracture intersections are good prospecting targets because channels, such as faults or joints are conduits for ore-forming solutions (Riley, 1959 and Sabin, 1987). Local fracture patterns are mappable on enlarged Landsat images, hence are being used on a worldwide basis in exploration. Many studies, on the relationships between Landsat fracture patterns and ore deposits, have been reported (Halbouty, 1976; Offield et al., 1977, and Ahmed, 1983). Apart from linear fractures, circular features and intersections of circular features with fractures may also be related to mineralized areas (Nicolais, 1974, as quoted by Sabin, 1987). Mineral occurrences and ore deposits in the study area are in many cases genetically related to acid intrusive, and most of the primary ore deposits appear to be associated either directly or indirectly with the granite (Jones, 1970). The occurrences of minerals have reported for the area by the Geological Survey of Malaysia (GSM, 1976). However, only cassiterite is likely to be of economic interest, whereas minor occurrences of other minerals, have been reported, but none of these has been found in sufficient quantity to be of economic significance (Jones, 1970). As in other areas of Malaysia, in addition to their occurrence in primary deposits, the cassiterite in particular are also found considerable

quantities as alluvial placers (Wan Fuad Wan Hassan, 1989), which have accumulated along the drainage channels of the area. These secondary deposits have formed as a result of weathering and transportation of material from the areas of primary mineralization.

In this study, a lineament density map which represents the concentrations of lineaments per unit area (25 km^2) was constructed and the map compared with that of the mineral distribution map. Apart from a few small secondary tin deposits, there is almost no mineral deposit shown in the mineral distribution map for the area covered by sub-area 1, therefore the comparison was carried out only for the sub-area 2. As shown in Figure 8.22, there is only one place where the concentration of lineaments and the occurrence of circular features are apparently coincide with the distribution of mineral deposits, whereas in other areas this relationship is not obvious or none. This may indicate that the majority of ore deposits in the area are not closely related to the concentrations of lineaments and circular features. The mineralized area near Kelian Intan (Figure 8.22), which coincides with the concentration of lineaments and one circular feature is the largest primary mineral deposit that has been reported in the area, and is currently being mined whereas other deposits may be small, secondary deposits and with no potential or unknown potential economic interest (Jones, 1970; GSM, 1976). Therefore, the lack of close correlation between the concentrations of lineaments and the

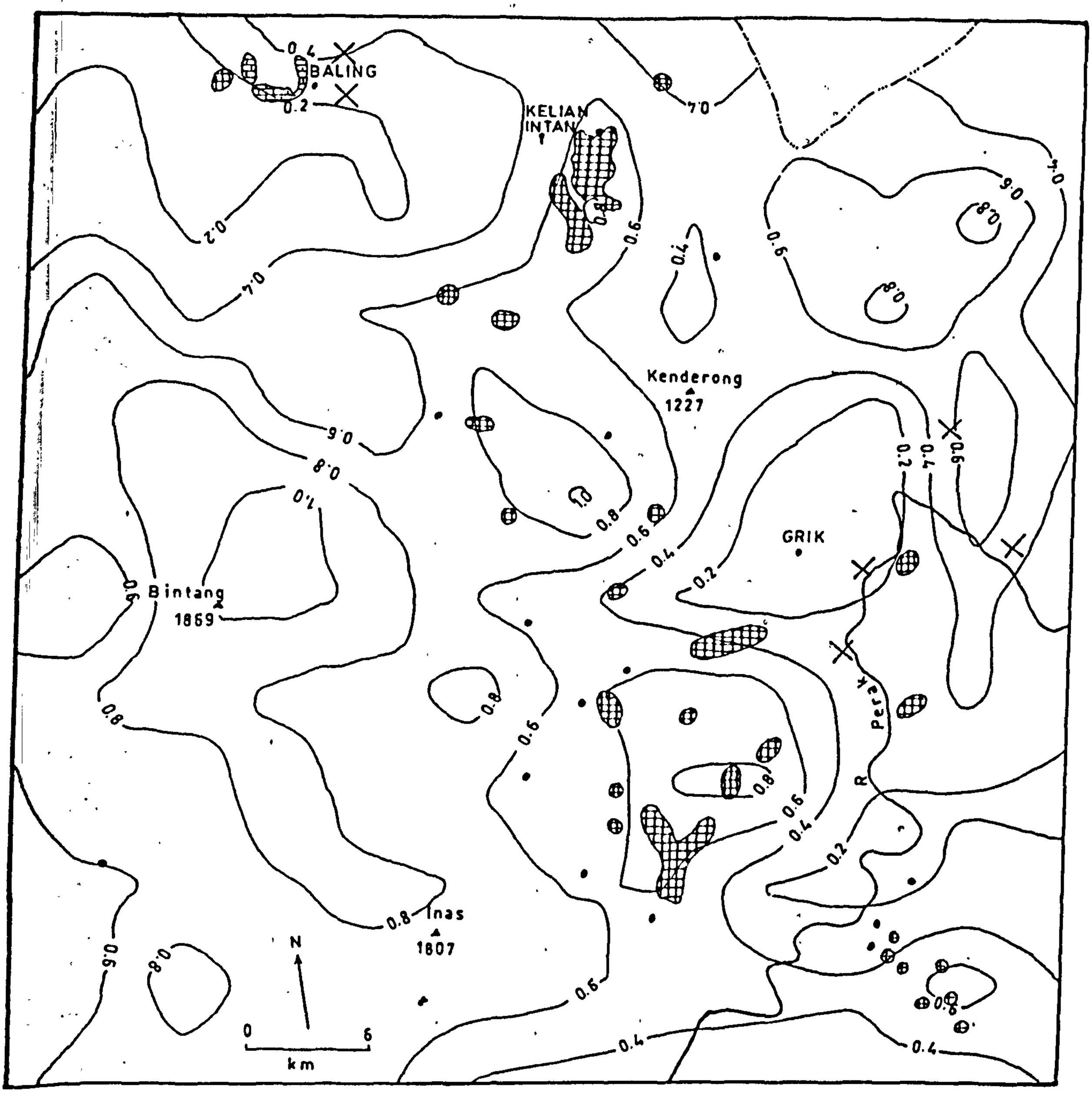

TIN-ORE (cassiterite) & ALLUVIAL ORE-MINERALS

BASE METAL, MINOR METAL & OTHER ORE-MINERALS

Limestone area

Quarry site

Figure 8.22 The relationship between the mineral deposits and lineament density as depicted on the Landsat MSS images of the Kedah-Perak sub-area 2. The information about mineral deposits are taken from the map by Geological Survey of Malaysia (1976).

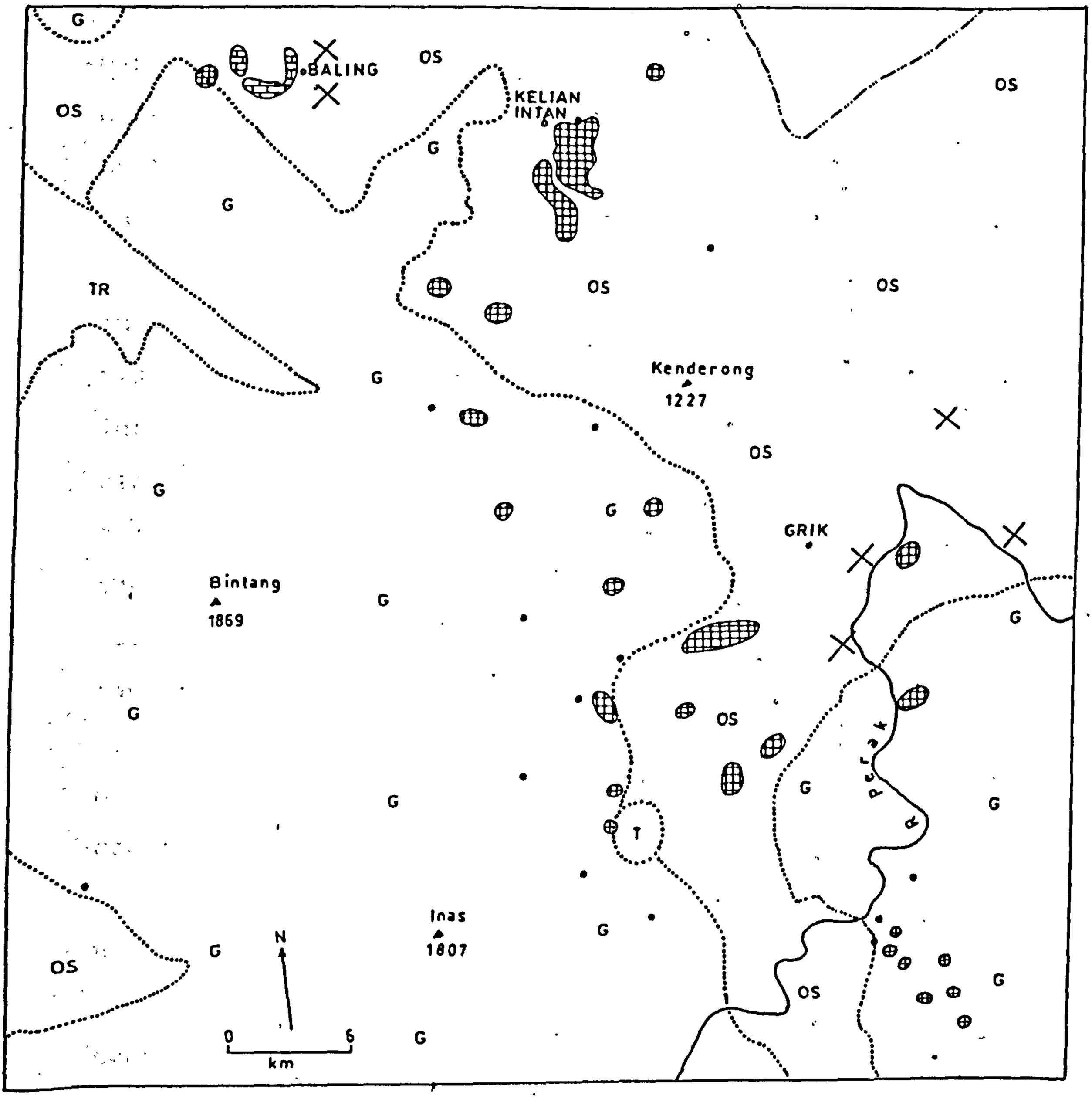

- TIN-ORE (cassiterite) & ALLUVIAL ORE-MINERALS
- BASE METAL, MINOR METAL & OTHER ORE-MINERALS
- Limestone area
- Quarry site
- G Granitic and intermediate intrusive rocks
- T Tertiary,
- TR Triassic and
- OS Ordovician-Silurian rocks

Figure 8.23 The distribution of mineral deposits and intrusive igneous rock (granite) in the Kedah-Perak sub-area 2. The distribution of mineral deposits and the lithological boundaries are taken from the map by Geological Survey of Malaysia (1976 and 1985), respectively.

mineral deposits does not necessarily mean that the deposits have no relation with the lineament, rather it may well be due to the lack of large primary and economical mineral deposits in the area. It is interesting to note that the locations of most primary mineral deposits appear to be associated with the intrusions of granite (Figure 8.23), as reported by Jones (1970) and Wan Fuad Wan Hassan (1989). Apart from fractures including several new interpreted fault lines, several circular features were observed and recorded. Because there is evidence that large mineral deposit in the area is related to the concentration of lineaments and circular feature, the location and recognition of faults and extension fractures, fault intersection patterns and such other regional feature will, therefore, facilitate the planning of mineral exploration programmes and the location of new mineral deposits.

8.4.5 Summary

In summary, this investigation has demonstrated that the Landsat MSS images are very useful for structural (lineaments) interpretation in Kedah-Perak area, Malaysia. Despite the dense vegetation cover, the study has shown that remote-sensor data can be used in locating known features and additional previously unknown features which may be of economic importance in the area. Hence, lineament analyses from satellite data of the area can provide a new, rapid and stimulating overview for regional structural studies and mineral prospecting.

CHAPTER 9

CONCLUSIONS AND RECOMMENDATIONS

9.1 General remarks on geological remote sensing

Remote sensing from space platforms is neither a panacea nor an all-purpose system that will revolutionize the geological sciences. It is merely another tool available to geologists to study certain problems. Therefore, digitally enhanced satellite images are sources of geological information that are complementary, and not an alternative, to traditional methods of investigation. With remote-sensing techniques it is possible to obtain certain lithological and structural information more efficiently and cost-effectively for large areas than can be achieved on the ground, and occasionally such techniques can provide unique information not otherwise obtainable. It is common that satellite images attract our attention to certain features which can be interpreted. The same features can be inspected and interpreted on the ground. From here then the correction and extrapolation to the image interpretation can be made. Therefore, a close integration of ground truthing and image interpretation is required in order to obtain good results.

Except in a very rare case where it is possible to predict the occurrence of certain rock types purely by their appearance on the imagery (Pontual, 1987), many factors such

as described in section 5.1 may result in a different spectral response than the laboratory measurement (Siegal and Goetz, 1977; Williams, 1983). Furthermore, in geological remote sensing, spatial relationships as well as spectral signatures are important (Goetz and Billingsley, 1974), and textural information (Gurney and Townshend, 1983; Offield and Elgy, 1987), at present, is best analyzed by the human eye (Brunner and Veck, 1985). The inhomogeneity of most geologic units and the similarity of their spectral signatures in the wavelength bands measured by widely available remote sensing systems pose inseparable problems, and except for a very rare case (Goetz and Rowan, 1981), unsuccessful attempts and inability of all the automated classification schemes (despite using an ideal or nearly ideal areas) to portray correctly the lithologic units reflect the above facts (Blodget et al., 1975; Siegal and Abrams, 1976; Podwysocki et al., 1977; Guha and Mallick, 1985; Drury, 1986b). Subsequently, following the above points and the unsuccessful results of the techniques applied in the early stage of this study, the computer-aided classification and mapping of the computerized processing of digital images were not employed in this study. Instead, it was felt that visual interpretation of the processed images, through some techniques which have been developed with the aim of improving development of the images for visual interpretation (Robinson, 1977; Condit and Chavez, 1979; Moik, 1980; Blodget and Brown, 1982; Hunt et al., 1986; Curlis et al., 1986), was the better way of preparing thematic maps. This methodology permits the geologist to utilize more effectively his or her field

experience and also to utilize special complementary image characteristics such as texture, geomorphology and lineament pattern, an interaction which is difficult to transfer/understand by computer for automated classification techniques.

It has been shown that through a simple interactive digital processing of images from CCTs, for example contrast stretched images, a definite improvement over the originals can be achieved and significant extra information can be extracted from the images. Sophisticated image processing, involving spatial filtering and multi-spectral manipulation of the data can provide further information not retrievable from standard photographic images. Although image enhancement, particularly contrast, can be increased by photographic means (Best and Smith, 1978; Dean and Spencer, 1982; Shazly, 1987), manipulating digital data directly in the computer has the advantage that the stretching or increase in contrast is absolutely controlled (Goetz and Billingsley, 1974). Therefore digital processing is much more common and widely used in dealing with the remote sensing data. Hence, before the interpretation, the data were digitally processed in different ways with the aim of getting better products. Interpretation directly from a video screen is best suited to sub-scenes, but by taking photographs of a digitally enhanced image, the user can generate a hard copy (with different scales) of a scene with good contrast and better definition than standard product photographs from the EROS Data Center as shown by Rothery (1985) and Spray and Burges (1985).

9.2 Mapping lithology and superficial deposits from satellite images

When Landsat images became widely available (see Landsat Data Users Handbook, 1979), it appeared that these images, which retain their visual quality at enlargements up to 1:250,000 for MSS and 1:50,000 for TM data, would make possible the production of geologic maps of the previously unmapped parts of the world or to produce larger scale maps for the areas covered by regional scale maps. However, in general, lithological interpretation from satellite remote sensing data is difficult because (a) most of the Earth's land surface areas are not exposed or have only small outcrops surrounded by superficial cover or vegetation (Allum, 1984); (b) the weathered surface may have a different spectral response curve than the laboratory spectrum of a crushed version of the same rock types (Williams, 1983); (c) the scale of satellite remote sensing pixels commonly involves spatial variation of surface type within a pixel (Allum, 1984); (d) the relatively broad wavebands used in most remote sensing satellites are not sufficiently sensitive to narrow band absorption features (Harris, 1987); (e) too much or too little relief (Leith and Alvarez, 1985); (f) cloud-cover; and (g) the lack of ground observations, all commonly render it very difficult to make a full geologic interpretation of a satellite image. The usefulness of satellite data as a mapping tool for lithological mapping in area of large outcrops or areas of rock outcrops which are more or less uniform, however, has

been demonstrated . In some areas, indirect measures of the geology, particularly related to mineral exploration, can be obtained by analysis of the vegetation cover, and this has been demonstrated and can be particularly successful where the vegetation (natural) and bedrock geology are closely correlated. In such areas, satellite sensors gather spectral data for mixed assemblages of plant species (i.e. plant communities) and only rarely are single species responses measured, because of the spatial integration effect of large pixels.

In the study areas, lithological interpretation from Landsat imagery is difficult or not possible because of masking by superficial deposits and vegetation. As a result, a number of analytical techniques were shown to have very limited use for geological discrimination under these conditions although their benefits under ideal conditions were confirmed. In addition, the areas are poorly exposed and most outcrops, for example in the Lochindorb area, are considerably smaller than the area sampled by individual pixels. Weathered surfaces may have reflectance properties that differ markedly from those of fresh rock surfaces, and few outcrops are completely bare of vegetation. Rocks contain a variety of minerals, and a single rock classification may cover a range of mineral components and differing proportions of the components. On the other hand, different rocks may contain similar major mineral components which give similar spectral signatures, in the wavelength bands measured by Landsat, for different rock types. Therefore, most pixel-sized areas

contain superficial deposits or vegetation or both as well as rock outcrops, so that each reflectance value constitutes the sum of the reflectance from all the constituents plus a background albedo contribution from the surrounding area. Therefore, it is only under very rare circumstances that reflectance values can be used to determine rock types in the study areas. For this reason, textural information, contributions from topographic relief, lineament and drainage patterns are found more important than spectral information in discriminating rock types, particularly for an area with almost complete vegetation cover such as the Kedah-Perak area. Because of the vegetation cover, it is also difficult to map superficial deposits in the Lochindorb area. Although there is a good relationship between the vegetation cover and superficial deposits, farming activities nowadays allow agriculture to be planned with little regard to the geology, so that it is rarely possible to make accurate geological interpretations based on vegetation; better geological interpretation by remote sensing may be achieved in areas of natural vegetation. Therefore, for geological remote sensing, it is expected it would be more successful in areas with harder bedrock, unvegetated drift, high relief, natural vegetation or at least less varied and less intensive agriculture.

9.2.1 Concluding remarks on the superficial deposits mapping of the Lochindorb area

For the Lochindorb area, as reported for many other areas (Davis et al., 1987; Podwysocki et al., 1983; Rothery, 1987b; Crósta and Moore, 1989), the Landsat MSS data have not proved useful for semi-detailed mapping (scaled about 1: 80,000 to 1: 50,000) because of the limited spatial resolution. As a result, all the MSS image products for this area show poor quality (blurred due to large scale) and contain much less and offer no new information to that obtained from the TM. The improved spatial and spectral resolution of the Landsat TM allows the superficial deposits to be discriminated (to a certain degree) at a scale as detailed as 1: 50,000. In the area, TM visible band 3 (0.63-0.69 μm) provided good spectral resolution for glacial-peat and peat-bedrock categories. Spectral information for differentiating glacial deposits from bedrock was provided by TM infrared band 5 (1.55-1.75 μm). The band 5 which was found the best by Crósta and Moore (1989) for geological applications was found slightly more informative than band 3, hence it became the best overall among the original TM images. A study from central Snowdonia, a comparatively well exposed area for Britain, by Greenbaum (1987) showed that the airborne MSS band 10 (2.08-2.35 μm) which coincides with TM band 7 was found best for structure and ranked second in discriminating between solid and solid/drift amongst original bands. The low information content of TM band 7 in this study (see Table 6.7), which is supposed to be higher because its principal application is for

the discrimination of rock types (Table 4.4), indicates that spectral reflectance from vegetation is dominant and more important than the reflectance from rock outcrops or bare areas. Among other black and white image products, however, the difference between glacial deposits and bedrock is best shown in the discriminant function 1 (DF 1). Notwithstanding this, if we want to use only black and white image products for geological interpretation for this area, the contrast stretched TM bands 5 and 3 are considered to be the optimum because of their information content is easy to produce.

Since nearly all the interpretation is based on vegetation (as a result of the more direct influence of the deposits on vegetation cover types in certain areas), colour composite images of the area considerably enhanced the units. The best amongst the image products produced in this study is provided by the TM band-ratio colour-composite (RCC) 2/1, 7/1, and 3/1 displayed as blue, green and red respectively. The advantages of the technique (as mentioned in section 5.4.1) have made it possible to enhance spectral differences between cover types, outcrops and superficial deposits, and it is widely used in geological interpretation of remotely sensed data. Podwysocki et al. (1983), for example, have used a colour-ratio-composite image composed of TM 5/7, 5/2, and 3/4 to reveal kaolin quarries and to distinguish these from gravel and granitic rock quarries in Macon, Georgia. In another study, Podwysocki et al. (1983) used a colour ratio composite from a 24-channel Bendix multi-spectral scanner which is equivalent to Landsat TM bands 5/1, 3/4, and 5/7, and successfully distinguished

between altered and unaltered rocks in Utah. Ratio-contrast stretching of images from airborne thematic mapper bands which are coincident with Landsat TM ratios 7/4, 5/2, and 3/2, projected through blue, green and red filters, respectively, was found to produce a wide spread of colours and be useful for visual discrimination for Assynt, Sutherland (Drury, 1986b). Except for the combination mentioned by Drury (1986b), all other colour composite combinations that were supposed to enhance various features do not produce useful results for the area. One of the possible reasons is that all the said combinations were produced for a well exposed terrain with no or little vegetation cover, so it is evident that similar combinations do not work for an area with dense vegetation which dominates the spectral characteristics. For the TM 7/4, 5/2, and 3/2 combination (Figure 6.23C), even though it is not as good as the TM 2/1, 7/1, and 3/1 combination (Figure 6.23A), its colour variations more or less coincide with the distribution of superficial deposits, particularly peat, in the area. This is because the two areas, Assynt and Lochindorb, are similar physiographically, but the Assynt area is more exposed, contains a greater variety of rocks and has poorer soil development (Drury, 1986b), than Lochindorb, hence producing different results.

The discriminant function colour-composite 3, 2, 1 was found good to discriminate glacial from peat deposits. The ability of the technique to separate spectral classes (groups of pixel) which may belong to certain categories and translate the information along new axes is evident in the image (Figure

6.19). There is a high possibility that this technique will provide better results if applied to area with more rock exposed and less vegetation cover.

The principal component colour composites (PCCs) have been reported very useful in other areas by previous authors (Fontanel et al., 1975; Donker and Mulder, 1977; Jacobberger et al., 1983; Canas and Barnett, 1985; Greenbaum, 1987; Drury, 1986b). In this study the PCCs were found less informative than many other image products, and in one instance the lower-order of the PCC is more informative than the higher-order (Table 6.7). Again these results can be explained in part by the dominance of vegetation cover in the Lochindorb area compared with the areas studied by others, and by the differences in terms of spectral information content between the PC images as described in section 6.3.

Among the TM band colour-composites (BCC), the combination of TM bands 1, 3, and 4, displayed in blue, green and red respectively, (which was empirically selected) is found the best. The combination is similar to what was used by Tibaldi and Ferrari (1988) in their geological study of the Gregory Rift, Kenya. However, the combination is different from the colour composite combinations which have been found best for other areas (Drury, 1986b; Greenbaum, 1987; Kaufmann, 1988; Drury and Hunt, 1989; Davis et al., 1989; Crósta and Moore, 1989; Qari, 1989; Saraf et al., 1989). The TM band 7 (2.08-2.35 μm) with its principal application for rock discrimination (Table 4.4), should always be included in the colour composite combinations for geological purposes, and

this is most likely true (although not always) for arid and semi-arid areas which are well exposed with no or little vegetation cover. However, it is rarely used for the areas with the opposite conditions, as in the UK, examples. The TM 1-3-4 combination is better than the best band combination (BCC 1-4-5) based on the optimum index factor (OIF) (section 5.4.4). This result agrees with what has been found by Greenbaum (1987), that the OIF will not necessarily be a true indicator of geological information content particularly when spectral response is mainly from vegetation as in the Lochindorb area. Therefore, band selection based mainly on statistical methods or generalized recipes cannot always take into account the more subtle, qualitative information that provides the key to skilful geological interpretation. Interpreter judgement should, therefore, remain a major factor in band selection for colour composite images, as suggested by Drury and Hunt, 1989.

Delicate textural and topographical information, useful for structural interpretation, was provided by TM bands 4 and 5, and TM bands (BCC) 4-5-7 colour-composite, where the TM band 5 was found to be best overall. This may relate to two factors: first, TM band 5 is a maximum rock reflectance band, hence it shows sharp definition of rock-type boundaries (Crósta and Moore, 1989); second, the human eye is most responsive to features of higher spatial frequency in monochrome than in colour (Drury, 1986a). Therefore for structural studies, black and white images are more effective than those in colour. It is evident that in the area, apart

from very minor lineaments, no major new structural features have been shown on the image products of the area since the work of Horne (1923).

It was not possible to perform lithological mapping of the area, even with the information of vegetation pattern. Based on information from field visits, it was found that a correlation does exist (although not very obvious) between cover-types and superficial deposits (as discussed in section 7.1). Therefore, superficial deposits mapping was carried out in the area based on their cover types by interpreting (mainly the colour association) the best image products and by spatial extrapolation based on ground truthing data from selected locations. The RCC 2/1-7/1-3/1, DCC 3-2-1, BCC 1-3-4, and TM band 5 are considered optimum for geological interpretation in the area.

Although the interpreted map contains more information than the published 1: 625,000 map, it cannot differentiate between different types of glacial drift. Apart from the nature of the deposits in the area which is covered by vegetation, the now obvious reason for this is that the TM data cannot produce the resolution necessary to depict the differences (largely topographic) between the deposits. Consequently, despite using the best image products for interpretation, comparison with the published drift map at a scale 1: 50,000 shows that the interpreted map contains much less detail and shows no new information. The actual maximum scores of the geological information content in image products are low: 39%, 32%, and 28% respectively for the glacial:peat,

peat:bedrock and glacial:bedrock discrimination, and may well reflect the information content in the interpreted map. Notwithstanding this, the map gives a reasonably good synoptic cover of the general distribution of the deposits, particularly peat. In this aspect, therefore, the result shows that TM imagery can be used for the preparation of "simple" superficial deposits maps at scales from 1: 50,000 to 1:80,000 or preliminary maps at a scale of about 1:200,000, or for regional study to supplement information on surface materials distribution shown in published geological maps at similar scales. However, in Scotland as well in the rest of the U.K. the conditions are: all the areas are covered by regional geologic maps at scales 1:250,000; only about 10% of the areas are not covered by geologic maps at scales 1:63,360 or 1:50,000; some areas which are considered to be of outstanding geological interest are covered by an 'intermediate' 1: 25,000 scale; and since the 1960's the standard large scale map for recording field survey has been produced at 1:10,000 scale, particularly for the coalfield and geologically important areas (BGS, 1987). Therefore, although the usefulness and importance of satellite data in regional lithological surveys have been demonstrated in many regions, particularly in arid and semi-arid environments where the synoptic view and broad sensor range have provided valuable new insights into geology (e.g Rowan et al., 1974; Viljoen et al., 1975; Rothery and Milton, 1981; Blodget and Brown, 1982; Rothery, 1987a and 1987b; Davis and Berlin, 1989; Bagheri and Kiefer, 1989) the use of multi-spectral satellite data, in this case the TM, for

geological applications (to map surface material deposits) in the region is very limited and has not proved notably successful. Another geological study (lithological mapping) using Landsat MSS for the Scottish example of Glen Coe also gives unsuccessful results (Abdelhamid and Vaughan, 1988). Therefore, it is evident that for Britain, the impact of satellite remote sensing for lithological mapping (solid and drift) has been rather less because of different objectives and constraints (Greenbaum, 1987). The low resolution of the remote sensing multi-spectral data is the greatest drawback for lithological interpretation, and certainly does not contain the level of detail found on aerial photographs. Substantial glacial deposits and vegetation over the area are other major problems in this field. In other geological studies such as measurement of sediment and turbidity patterns, determination of vegetation stress, mapping recent deposits (river, lake or coastal deposits), and shoreline changes, the Landsat MSS and TM data can still play an important role in providing valuable information for the region.

It has been recognized that aerial photographs are the best option for detailed geological mapping. Although multi-spectral images are useful for achieving a gross classification of the geology, the lack of textural and contextual information makes it difficult for the interpreter to comprehend the underlying nature of the observed spectral variations. On the other hand, although aerial photographs are poorer spectrally, they provide very good spatial

information. The combination of aerial photographs and multi-spectral data in the mapping of superficial deposits for the Lochindorb area has produced a 'better' map than the map derived from the multi-spectral data alone. It appears that almost all the information can be interpreted from the aerial photographs alone. However, working together with the multi-spectral data, which give a very good general picture of the area (and also in some instances the colour association of cover types is more useful than the grey tones in identifying the superficial deposits particularly peat) has made the mapping task easier and time saving. It is evident that the map derived from the TM images and aerial photographs contains many details, and with information from field visits (ground truth), spatial extrapolation and correction can be made to produce a superficial deposits map of the area (Figure 7.9). The map shows very close agreement with the published drift map at a scale of 1:50,000. The differences between them are most likely related to the differences in their information content: the published map may show the subsurface information whereas the interpreted map solely shows the surface information.

9.2.2 Concluding remarks on the lithological mapping of the Kedah-Perak area

In all processed images, the most distinct feature shown is the difference between vegetated and non-vegetated or less densely vegetated areas which is represented by two distinct colours or grey tones. The two terrain categories broadly

correspond to two lithological groups. This relationship, although vague, has made it possible to trace a major geological boundary to a certain degree.

As for the Lochindorb or other areas, contrast stretching of the MSS data shows a definite improvement over the originals. The best among black and white images in terms of lithological information content are the DF 1 and MSS band 7. However, the MSS band 7 shows better textural and structural information than the DF 1, and hence becomes the single most informative black and white image for geological interpretation for the area. MSS band 7 was also found very informative for geological studies (by visual interpretation) in other areas (e.g. Welby, 1976; Iranpanah, 1977; Sesören, 1984; Rakshit and Swaminathan, 1985) because the effect of vegetation is less, whereas relief impression and drainage, and contrast between surface and water bodies is more pronounced or prominent compared with other MSS bands.

The MSS ratio colour composite (RCC) 5/6, 4/7, and 4/6 was found the best compared to other colour composites. Despite the fact that they show less colour difference (most likely because the vegetation cover is too dominant and therefore controls the spectral characteristics of the area rather than the rocks), the technique enhances textural information very well in this dissected tropical terrain, and this can be used as a criterion to discriminate between rock types, together with the spectral information. In this area, the RCC 5/6, 4/7, and 4/6 combination provides good contrast among terrestrial features and offers good separation between

major rock units; granite:sandstone, granite:shale, and sandstone:shale. The most common MSS ratio combination, MSS bands 4/5, 5/6, and 6/7 and other combinations, have been reported very useful for geological mapping (Goetz and Billingsley, 1974; Blodget et al., 1975; Blodget and Brown, 1982; Warner, 1985), but as mentioned in section 6.2.6 have not proved useful in this area which is covered by dense tropical forest, in contrast to those arid or semi-arid areas with no or little vegetation cover. Notwithstanding this, a similar technique (ratioing), although in a different combination, has been found very useful for geological interpretation for both study areas, the Lochindorb and Kedah-Perak.

Principal component analysis has produced images with good geological information content for the area. However, like other image products, the technique was also unable to enhance subtle spectral differences because of the extensive, dense vegetation cover, but its colour definition of vegetation cover and textural information are better displayed and hence useful for interpretation. Overall the PCC 3-2-1 is the most informative among other PC combinations, and it provides good discrimination between the sandstone and shale units. The same PC combination has also been reported very useful for geological applications in other areas (Moik, 1980; Jacobberger et al., 1983; Canas and Barnett, 1985). Lower order PC combinations, for example using PC components 4-3-2, may give better discrimination as reported in other areas (Townshend, 1984). However, despite showing good colour

variation, the overall image definition is poorly displayed due to the low variance content.

In addition, the MSS colour composite (BCC) using bands 4-5-7 combination, was also found useful in this study. It provides good information where the metamorphic and sandstone units can be separated. Although the BCC 4-5-7 is slightly less informative than the PCC 3-2-1 combination (Table 6.8), it is faster, easier (no complication involved) and cheaper to produce the BCC than the PCC or any other colour composites. Therefore, in many cases the BCC, particularly the bands 4-5-7 combination, is more commonly used in the basic geological interpretation of Landsat MSS data than the PCC or other colour composite products (e.g Cole, 1977; Blodget and Brown, 1982; Almashoor and Tjia, 1987; Alizai and Ali, 1988). In addition the BCC image usually provides enough detail to map the major geologic units (Goetz et al., 1973). In general, therefore, for geological mapping, automatic classification schemes are not required and subsequently, expensive computer processing is unnecessary (Goetz and Billingsley, 1974). The Landsat BCC 4-5-6 combination was found very useful in delineating ultramafic rocks in New Zealand (Brooks and McDonnell, 1983), but has not proved useful in this study. Other colour composite images, for example from discriminant analysis, do not provide sufficient geological information, particularly textural, for interpretation, and they are not useful in this area.

It is evident that for lithological interpretation in this area, textural information is far more important than the

colours or grey tones which appear rather uniform and/or similar for large areas due to the vegetation cover. This is quite different from other areas such as the arid and semi-arid zones, where the spectral information is commonly used to differentiate between rock units (e.g. Cole, 1977; Blodget and Brown, 1982; Davis and Berlin, 1989). However, other studies indicate that lithological interpretation of satellite imagery from a tropical region has been possible based on surface characteristics rather than on spectral signatures. For example, Sabin (1983) has used topographic characteristics to differentiate and delineate terrain categories which correlate with major rock types, and Wadge and Dixon (1984) have used an overall tone (brightness), amplitude and wavelength of local repetitive brightness variation (texture) and the orientation of directional aspects of the texture (fabric) to differentiate and map several limestone formations. Therefore, for an area with dense vegetation cover, as in humid tropical regions, spectral information from remote sensing data have a very limited use to differentiate rock types. On the other hand, the relationship between rock type and surface roughness, which is determined by the response of rocks to weathering, and is depicted as a "texture unit" on remote sensing imagery plays a major role in lithological interpretation in such areas. In this study, the spectral information (tone or colour), however, is useful to separate between vegetated and non-vegetated or less densely vegetated terrain which is broadly related to certain main rock types in the study area. In the area, optimum lithologic

interpretations can be made if the three images: RCC 5/6, 4/7, and 4/6; PCC 3-2-1; and BCC 4-5-7, are used in concert.

Large areas are covered by dense tropical forest. Apart from alluvial deposits which are confined along the main river valleys, and *in situ* soil and saprolite overlying the unweathered bedrock, the area is free from other superficial deposits. These factors have resulted in a good relationship between the physical features (topographic relief, drainage, distribution of vegetation and land use) with underlying bedrock which can be interpreted on the images. Nine image units were observed, identified and discussed, and some of them correspond very well with the mapped units. Generally, the major rock units like granite, sandstone, conglomerate and metasandstone which occupy large areas, form rugged and high-relief topography and correlate well with the corresponding mapped units, whereas the mapped units that cannot be distinguished on the Landsat images, or show no correlation with the image units, are located in areas of smooth and low-relief topography and occupy a small area. This clearly indicates that in this area the spectral separation was low and dependence upon texture was high. The study shows that it was not possible to delineate each of the rock types (facies) which occupy a small area including the Tertiary unit of Lawin Basin Deposit (Figure 7.18) because of a lack of textural as well as spectral characteristics. In many cases, it is possible to map alluvial deposits with less difficulty compared with other rock units because of their location along drainage channels and around water bodies, land-use

patterns (highly cultivated) and smooth-lowland topography. The deposits, although they are identified, have not been mapped in this study because they cover only a small strips along the main river valleys.

The result of the study has provided some encouragement that the remote sensing technique could be used to discriminate certain major solid lithologies at a scale of 1: 250,000 despite the low resolution of the MSS data and the almost complete vegetation cover. However, "unresolved" areas remain in the interpreted map and clarification and additional data from field visits are simply needed in order to confirm the interpretation or correctly identify the areas. Therefore, it is believed that the types of Landsat analyses discussed do not and will not replace geologic field work but can be useful as part of a geologic program involving regional studies of the area. Remote sensing imagery, the Landsat MSS images in this study, display and attract our attention to specific features (for example lineaments, "bedding signs", topographic relief and vegetation cover) which are used in the interpretation. Similar features can also be visited and inspected on the ground to get the "ground-truth" information from which the correction and extrapolation can be made. In this way a more accurate map can be produced. With more experience in the geographic area, coupled with better images (no cloud cover and good quality), with good spatial and moderately high spectral resolution such as Landsat TM and SPOT, much more detailed information could be derived from the images of the area.

9.3 Mapping lineaments from satellite imagery

Lineaments are in general well displayed on satellite data. It is well known, however, that there is a directional dependence with respect to the Sun azimuth and the scan line direction for passive remote sensing systems (Kim, 1979; Maude 1987; Zilioli and Antoninetti, 1987), and with look direction for active remote sensing system (Koopmans, 1986 and 1988) at which in general there is under representation. By applying certain methods of digital image processing such as directional filtering, it is possible to enhance the lineaments in certain directions including the one which is under-represented, and thus the directional dependence effect. can be minimized. Direct lineament mapping is believed to have the advantage of more effective discrimination between tectonic and non-tectonic features than strictly automatic methods. Therefore, the images were analyzed through visual interpretation rather than automated machine processing techniques, to produce lineament maps. Although the method has been criticized as subjective, by adopting certain ways of extracting lineaments from the images (as discussed in section 8.2), the lineament mapping can be made more objective. In a study like this, in addition to the above mentioned factors, numerous biases and errors may influence the final interpretation. Such factors include a varying degree of vegetation cover and exposed rock, and confusion between geological lineaments and man-made lineaments. Hence, care has been taken to minimize (if not eliminate) such errors by a

screening method (cross-checking between the interpreted data, Landsat images, topographic maps and existing geological maps). However, human weaknesses and disposition can, of course, never be ruled out, as emphasized for instance by Wise (1976).

The interpretation of digitally enhanced Landsat images has revealed novel information concerning the distribution and trend of lineaments in the study areas. In general, the significance of the lineaments observed in Landsat images is still a matter of debate. For instance, the importance of the individual lineaments cannot be simply derived from their intensity of expression, and the distinction between lithological and fracture lineaments can be difficult particularly in a terrain of less strong relief and which is generally poorly exposed. However, most of the lineaments recognised on the prints are generally quite clear and frequent, and no painstaking effort has been made to pick out subtly expressed lineaments (possibly reflecting lithological contacts, foliation etc). Moreover, most major lineaments recorded are clearly expressed and commonly coincide with mapped faults where such data exist. Thus, these lineaments should have a tectonic origin, largely representing faults, whereas the minor lineaments are interpreted as possible expressions of joints and fractures.

The uses of lineament analysis are economic as well as academic. Such analysis may give a quick and reliable indication of certain features of the subsurface geology as a prelude to any sort of fieldwork or survey. Such techniques

are most significant in an age where time is money and results are required quickly. Significant areas may be pin-pointed for further more exact study. If we consider the economic applications as well as the purely academic applications of geological mapping, the lineament analyses are not only significant in terms of the whole gambit of rock deformation, but are also related to such matters as hydrology, petroleum exploration, mineralisation and ore body location.

Landsat imagery has proven valuable in the determination of regional fault and fracture patterns, but in the final analysis, the ultimate meaning of the lineaments seen on the satellite imagery can be proved only by field visits and/or by subsurface geological investigations.

9.3.1 Concluding remarks on the lineament analysis of the Loch Tummel area

The potential of synoptic coverage of Landsat TM and MSS data in providing structurally related information was assessed in the Loch Tummel area. The relative merits of TM versus MSS data were examined. Lineament maps (original scale 1: 130,000) derived from the two data sources are presented and compared with the published data and map.

A few significant observations and conclusions resulting from this study are given below:

1. The MSS band 7 (0.8-1.1 μm) and TM band 5 (1.55-1.75 μm) were found to produce the best results for structural interpretation because of the sharp definition of 'rock-type' boundaries. These bands were also reported best,

by Viljoen et al., (1975), Sesören (1976), Kim (1979), Drury (1986a), Maude (1987), and Cròsta and Moore (1989), in other areas for structural interpretation. Both images were further processed by means of filtering techniques in order to enhance the lineaments for preparing the lineament maps. The Laplacian add-back filtered and edge-enhanced images of these two bands are considered to be optimum for lineament mapping in the area and are used together with the directionally filtered images of similar bands (MSS band 7 and TM band 5). It was found that the negative prints of the two bands can provide additional (complementary) information to the corresponding positive images in lineament extraction.

2. The most prominent lineament direction (NE-SW) agrees quite well with those in the fault map, therefore the main features of the fault pattern are clearly brought out in the lineament map in both data, the TM as well as MSS. However, the mapped fault in the direction of 315-335° is less represented in the lineament maps, particularly the TM's data. The regional lineament map derived from Landsat MSS data by Johnson and Frost (1977) which includes the study area also showed a similar result. This is most likely because of the effect of directional dependency of lineament analysis of satellite data on the sun azimuth and the difference in natural surface cover between these two data sets.
3. Apparently, a larger number of shorter lineaments (2 km or less) were mapped on the MSS (despite its lower

resolution) than on the TM. Other studies have clearly shown this discrepancy (Lake et al., 1984, Table 1). This can be explained in part by the snow cover in the MSS data which enhances subtle small linear feature patterns, as reported by Harris (1987), Sabin (1987) and Iranpanah (1989), which are lost in the 'noise' of high spatial frequency cover variation seen in the TM image. However, for longer lineaments, the better resolution TM is superior than the MSS.

4. The generally high density of lineaments in the region, which is predominantly drift-covered or consists of very uniform Moinian lithology (for half of the area), may be an illustration of the ability of satellite imagery to "spot" lineaments under such difficult circumstances, a problem well known to workers on the geology of Scotland (Johnson and Frost, 1977).

5. This analysis confirms many well-known features but also reveals a few previously unrecognised major lineament trends, which are interpreted (with photogeological evidence) as 'new' fault lines, thus updating the existing structural geologic map of the area.

6. Given the differences in land cover conditions between the two image data sets, however, it was very difficult to evaluate objectively the relative merits and/or demerits of the TM in comparison with the MSS except in very general terms, in this study. Generally the TM provides a good improvement over the MSS because (a) it depicts/displays longer lineaments (which is more

important from geological point of view), and (b) two of the new interpreted faults are depicted better on the TM image than on the MSS, and (c) although a larger number of shorter lineaments apparently were mapped on the MSS than on the TM, the TM is still able to display a quite large number of shorter lineaments (despite lacking snow cover which has been reported to emphasize geological structures. Therefore the results generally agree with the conclusion given by other workers, for example Settle et al. (1983), Townsend (1987), that the higher spatial resolution offered by Landsat TM data would provide a large improvement in the ability to map lineaments.

9.3.2 Concluding remarks on the lineament analysis of the Kedah-Perak area

The potential of synoptic coverage of Landsat MSS data in providing structure related information was assessed in the Kedah-Perak area. Many lineaments are present and well displayed in the area which has a high-relief and dissected terrain. Therefore, lineaments (believed to represent fractures of some kind) seen on Landsat images have been mapped, and a lineament map (original scale 1: 250,000) is presented. Mapped lineaments are analyzed and compared to fault patterns on the published geological maps.

A few significant observations and conclusions resulting from this study are as follows:

1. Among four bands of Landsat MSS data, lineaments are best displayed on the MSS band 7. The Laplacian add-back

filtered image of this band is rather defocused, but able to enhance major lineaments in the area. These two image products are considered to be optimum for lineament mapping purposes for the area. Lineaments are also derived from directionally filtered images as well as from the negative print of the MSS band 7.

2. Compilations of all lineaments show two dominant trends, one NW-SE and one NE-SW. These directions coincide well with a major fault system, the Bok Bak and with two main directions of faulting in the area. This indicates that the main features of the fault pattern are clearly brought out in the lineament map. Furthermore, a good correlation (in terms of location) exists between image lineaments and previously mapped faults.

3. New prominent lineaments which are probably faults were delineated and recorded along with new circular features, thus, updating the structural geologic map of the area.

4. Tectonically, sub-areas 1 and 2 belong to two different tectonic domains. The results of fracture analysis, although they show similarity with the previous study , however, do not clearly reflect the difference between these two domains, because the areas do not exactly represent two different tectonic domains. Notwithstanding this, the results show that with satellite imagery, such analysis can be done quickly in order to get similar or even better results than using topographical maps.

5. Except for the volcanics in the Silurian-Ordovician Rocks, a clear relationship between rock types and

concentrations of lineaments is undetectable in the area. The higher concentrations of lineaments, however, appear to be correlated with the higher terrains formed by more resistant rocks, particularly granite and sandstone. There is also a possibility that high and low concentrations of lineaments are related to geological structures as reported by Gol'braykh et al., 1966.

6. The concentrations of lineaments and circular features appear to be correlated, at least, with main ore deposits.

9.4 Future recommendations

9.4.1 Geological remote sensing in Scotland (U.K.): lithological mapping

In Britain, the main requirement of satellite remote sensing data is for detailed geological maps (Greenbaum, 1987). On the other hand, large areas are poorly exposed, covered in drift and vegetation which make the area less than ideal for remote sensing work. This study indicates that the low resolution of the most widely available satellite data such as Landsat MSS and TM over the area is the greatest problem because it is simply not sufficient for semi-detailed/detailed geological interpretation in this area of Great Britain. Other constraints, include the scarcity of cloud-free and snow-free scenes of this part of the world, and the choice of season for the acquisition of data is reported to be important (Drury, 1986a and 1986b; Greenbaum, 1987) for vegetation discrimination in getting indirect geological information.

Therefore, for future mapping of lithology and superficial deposits using remote sensing data, consideration should be given to several matters in order to achieve better results. These include;

1. Acquiring a good spatial resolution of remote sensing data.

SPOT data:

Preliminary studies have indicated that fine ground resolution (10 m for panchromatic and 20 m for multi-spectral bands) makes the SPOT data clearly superior to Landsat TM for geological interpretation (Bailey and Dwyer, 1984; Chavez and Berlin, 1984; Metz et.al., 1984), and when combined with the stereoscopic capabilities should make SPOT a very useful tool for geologic mapping (NRSC, 1987; Lillesand and Kiefer, 1987). At present, more areas of the U.K. are covered by good quality of SPOT than by the Landsat TM scenes (NRSC, 1987). With these advantages, the SPOT data should be used in future geological remote sensing and may give better results than the Landsat data. The SPOT data, however, record only a few of the potentially useful parts of the EM spectrum (Chevrel et al., 1981) (Table 9.1). Therefore, for an area which contains large amounts of clay (e.g. in hydrothermal zones) and carbonate (e.g. in limestone units) minerals, it is likely that the Landsat TM (with higher spectral resolution) would have provided a better spectral separation of such rocks than would the SPOT data (Bailey and Dwyer, 1984; Borengasser and Taranik, 1985; Chavez and Bowell, 1988). However, in any poorly exposed, heavily vegetated and drift covered areas, it

	Approximate satellite equivalent							
	ATM		LANDSAT TM		LANDSAT MSS		SPOT	
Band	Edges (μm)	Band	Edges (μm)	Band	Edges (μm)	Band	Edges (μm)
1	0.42-0.45						
2	0.45-0.52	1	0.45-0.52				
3	0.52-0.605	2	0.52-0.60	4	0.5-0.6	1	0.50-0.59
4	0.605-0.625						
5	0.63-0.69	3	0.63-0.69	5	0.6-0.7	2	0.61-0.68
6	0.695-0.75			6	0.7-0.8		
7	0.76-0.90	4	0.76-0.90			3	0.79-0.89
8	0.91-1.05			7	0.8-1.1		
9	1.55-1.75	5	1.55-1.75				
10	2.08-2.35	7	2.08-2.35				
11	8.50-13.0	6	10.4-12.5				
Resolution:	4-10m*	30m (band 6: 120m)		80m		20m (panchromatic (0.51-0.73 μm): 10m)	

* Hamblin and Crofts (1984), Lynn (1984) and Greenbaum (1987).

Table 9.1 List of ATM bands with approximate equivalent with Landsat Thematic Mapper, Landsat Multi-spectral Scanner and SPOT (Adopted from Williams, 1984).

is believed that spatial resolution is more important, and required for more successful results than the spectral resolution, in geological interpretation of remotely sensed data. Therefore, large areas of the U.K. would benefit from the high spatial resolution of SPOT data and only a few areas would need higher spectral resolution for identification and discrimination between different geological units. At present the SPOT data are more costly to acquire compared to the Landsat data, and like the Landsat, the number of good scenes per year is not high and there is a possibility that some areas will have no SPOT data coverage in coming years. These factors all limit the usage of SPOT data in practice.

Airborne Thematic Data (ATM):

Airborne multi-spectral imagery (e.g. from Daedalus ATM 11-channel scanner, Bendix 24-channel scanner, NASA NS-001 8-channel scanner) which has high spatial resolution and moderately high spectral resolution is another possible data source that should be used in future work. Many areas in the U.K. are covered by the Daedalus ATM 11-channel data (Table 9.1), following the Natural Environment Research Council (NERC) ATM campaigns (Williams, 1984). In addition to its high resolution, the other advantages of ATM are that it can provide cloud-free and snow-free data which are difficult to get by orbital satellite systems because of the frequent occurrence of clouds, and the ability to acquire the data under the most favourable climatic conditions. The ATM data have proved to be superior to satellite data in various

geological studies including lithology (Lyon, 1972; Podwysocki et al., 1983) and structure (Rothery et al., 1986) in arid and semi-arid areas. In U.K., ATM data have not proved sufficiently successful to be of practical application in assessing sand and gravel resources over low-lying cultivated areas of the Warwick-Redditch area, Warwickshire (Hamblin and Crofts, 1984). However, in the upland areas, although the ATM data cannot produce the resolution needed for detailed mapping (scale 1:10,000), they show some encouragement particularly in discriminating superficial deposits based on their vegetation cover types (Drury, 1986b; Smithurst and Vaughan, 1987), and more successful results have been reported for Snowdonia, a comparatively well exposed area for Britain and where man's influence is minimal (Greenbaum, 1987). These studies have indicated that the ATM could be used to discriminate geological units, and particularly promising is its potential for discriminating superficial deposits. Although the region is well covered by geological maps, the drift mapping over large areas has not been done to modern standards (Will, per. comm., 1987, BGS, Edinburgh). The data, therefore, should be acquired and used in future geological study, particularly in preparation of drift maps program at scale of 1: 50,000 or even 1: 25,000 to overcome the low spatial resolution of the Landsat imagery and perhaps the low spectral resolution of the SPOT data. The ATM data, however, have a disadvantage because the coverage is on an experimental basis only and very limited in coverage compared to satellite data.

2. Acquiring remote sensing data in a particular season

In this study as well as studies by other workers, it has been indicated that geological interpretation is largely based on vegetation. In this area there is a seasonal variation in vegetation, and the expression of geobotanical features varies depending on the seasonal condition of the vegetation (Elvidge and Lyon, 1983). From this point, it is important, therefore, to acquire remote sensing data in certain months which can provide the best vegetation discrimination. Guha and Mitchell (1966) have suggested that for detection of heavy metals in vegetation (stressed vegetation study) in the region, the month of May is the best. For the Highlands of Scotland, Drury (1986b) suggested that the optimum times for vegetation discrimination are from late June through August. In general, therefore, it would probably be better to acquire imagery in the early part of the growing season when the effects of cultivation are less pronounced in order to get more geological information from soil/rock/vegetation cover. The late October acquisition date of the Landsat TM imagery used in this study is less than ideal. However, the dieback in vegetation which has started by that time of year has made possible the discrimination of cover types, particularly over peat and alluvial deposits. Having data from the early growing season, together with the early to middle-autumn, a multi-temporal analysis might have enabled the best possible discrimination of vegetation cover, and the outcome results should be better than the present work.

3. Combining radar with visible and infrared data

The utility of airborne and satellite-based radar imagery, which contains information on the morphology and roughness of a given terrain and on the relative reflectivity of its constituent materials, to detect and depict subtle geologic features has been amply demonstrated by numerous studies. Furthermore, several studies have indicated that where radar imagery is available, it can be used in a complementary way with other data to produce very encouraging results (McDonough and Martin-Kaye, 1984; Koopmans, 1986; Alizai and Ali, 1988). With the advantages of radar systems and since radar images are so different from those of other spectral regions, it might seem appropriate to use them together with other data. Therefore, it is suggested that for future study, radar imagery (if available) should be used together with other data. At present, however, only limited portions of the earth are covered by airborne as well as by satellite-based radar images (Sabin, 1987, Figure 6.17) and because of some difficulties, the data quality of SIR-B which cover the U.K, for example, are not able to be used to its expected potential (Mather, 1987; Harris, 1987). However, the development of several future satellite-based radar systems will increase this potential source of geological information.

In summary, it is perhaps through further study and understanding of the interrelationships that exist between vegetation and geology, particularly superficial deposits coupled with a good spatial resolution and moderately high spectral resolution (acquired in the months which are optimum

for geological uses), plus unique information from radar imagery that will make the role of satellite multi-spectral imagery in lithological mapping become more important and largely complementary to that of aerial photography for this region.

9.4.2 Geological remote sensing in Malaysia: lithological mapping

Despite the heavily vegetated terrain, the result of the study has demonstrated the value of the Landsat MSS for geological interpretation of Malaysia. With better images (cloud-free and good quality) and use of full resolution of the data (compared to what has been used in the study where the images were sampled at every two pixels to cover a larger area for preliminary and regional study), much more detailed information could be derived from the Landsat MSS images of the area. However, persistent cloud cover hampers the acquisition of cloud-free aircraft or satellite images in the visible spectrum. This is one of the reasons why the geology of large areas of Malaysia is inadequately mapped (at scales 1: 63,360 to 250,000 or larger). It is most likely that the availability of cloud-free Landsat TM and SPOT images over the area will also be very limited as shown by Landsat MSS, hence the potential benefit offered by these images may not be realised. The limitation, however, does not apply to aircraft and satellite radar systems because of their ability to penetrate cloud cover. Although radar does not penetrate foliage in heavily vegetated areas to any significant extent,

geologic features are commonly enhanced on radar images because of its ability to enhance subtle topographic features (Ford, 1980; Ford et al., 1983; Sabin, 1987). Radar imagery, therefore, is more useful in tropical areas where other images are difficult to acquire. The value of satellite radar system for geologic mapping is enormous as has been demonstrated in many parts of the world including tropical regions (Elachi, 1980; Froidevaux, 1980; Sabin, 1983; Wadge and Dixon, 1984; Koopmans, 1986; Mackenzie and Ringrose, 1986). At the moment, however, Malaysia is covered by only one swath of radar images from a space shuttle mission (orbit 30 of SIR-A). With the development of several future satellite-based radar systems, the availability of this very useful geological data source should increase. The availability of complete satellite radar coverage of Malaysia would facilitate the preparation of regional geologic maps, and may give better results in delineating lithological boundaries because it contains better textural and structural information which are very important in the region. Aircraft radar images could be acquired for more detailed interpretations at larger scales. As mentioned earlier (section 1.2), it is likely that most of the remaining mineral resources which have been not explored will be hidden beneath vegetation such as the tropical forest. Malaysia has large mineral reserves particularly in the Main Range (central belt of Malaysia Peninsular), and considerable exploration potential. If Malaysia was covered by good remote sensing imagery (most likely radar images), mineral exploration as

well as geological mapping could proceed much faster than it is at present.

In addition to the cloud cover, dense tropical ever-green rain forest which masks the geology of the area is another major problem facing the interpretation of lithology from remote sensing imagery. Unlike the Scottish example, Malaysia has no obvious seasonal variation in vegetation. Therefore, for geological applications, seasonal remote sensing data are not important in the area. Although the vegetation covers in general are uniform, however, Jones (1970 and 1981) reported that in certain areas, the natural forest varies considerably with rock-type, for example (1) the limestones support low scrubby vegetation where *Taxotrophis ilicifolia* and *Zizyphus sp.* are common with occasional high trees amongst which *Hopea ferria* with its bright green to reddish foliage is most characteristic; (2) the clastic sediments are covered by high dark-green forest in which the giant dipterocarp *Shorea sericeiflora* is most conspicuous; and (3) on the abnormally dry quartzite ridges the characteristic growth consists only of scrubby species of *Callophyllum* and *Eugenia sp.* ,hence frequently geological boundaries can be accurately traced by sharp differences in forest type. In recent study in Kalimantan, Indonesia, Thorp et al., (1990) suggested that vegetation can be used to recognize certain alluvial formations which are associated with "white sands" and "kerangas" heath forest, however, accurate boundary drawing is not possible and the vegetation does not have a unique association with one deposit (e.g. "white sands") only. Notwithstanding, this gives an

indication that there is a possibility of using vegetation to discriminate lithology in humid areas as has been widely used in semi-arid areas. With this view, it is recommended that for future development of the geobotanical technique in the area, the establishment of the relationship between image characteristics and vegetation species community in "typical areas" should be focused. The established characteristics should be valid and be applicable to other areas in the country which experience the same (tropical) climate. Further, perhaps with better spectral resolution combined with good spatial resolution data may make the role of satellite multi-spectral imagery in mapping lithology become more important and produce better results in the region.

9.4.3 Geological remote sensing: lineament mapping

In this study, although lineaments are well displayed on both Landsat MSS and TM images, the TM is better. Drury (1986b) stated that regional structural studies are best served by Landsat TM or SPOT data. Therefore, use of SPOT data for the Scottish example and of TM or SPOT data for the Malaysia example should improve the results of the study. The potential of radar images for structural mapping has been demonstrated (Blom et al., 1984; Nielsen and Stern, 1985; Schultejann, 1985), and in many cases structural features are better depicted on radar imagery than in visible and near-infrared spectral bands (Berlin et al., 1980; Koopmans, 1986; Lillesand and Kiefer, 1987; Sabin, 1987). Therefore, radar imagery (if available) is another potential data source or likely to be

the best option for structural studies particularly for Malaysia which has persistent cloud cover. In addition to the use of higher spatial resolution data or radar imagery, the following points should be considered for future work:

1. There is a directional dependence with respect to Sun azimuth and scan line direction on Landsat and SPOT data, and with regard to look direction on radar imagery. In addition to the use of filtering techniques to minimize this effect, by combining information from radar imagery in which its look direction is perpendicular to the Sun azimuth and scan line direction of Landsat or SPOT, or by combining information from Landsat and SPOT imagery which has different scan-line direction, complimentary information will be provided and the confidence level will be increased for the determination of structures.

2. The results in this study, as well as many reported elsewhere (Harris, 1987; Sabin, 1987; Iranpanah, 1989) show that structural features are enhanced in images taken in the winter season (when the solar elevation angle is low and the present of snow cover). Apart from this, Drury (1986a) reported that, over agricultural terrain, Landsat TM imagery from the early part of the growing season provided the best structural discrimination. Had data from the two periods been available, they might have enabled the best possible extraction of structural information over the Scottish terrain to be obtained.

3. In this study, only a 3 x 3 kernel size is available and has been used to produce directional filtered images for

lineament analyses. It has been said that this kernel size is suitable for structures up to some 100 m length (Chavez, Jr., 1983, and Crósta and Moore, 1989), hence shorter lineaments are well enhanced whereas longer lineaments are under enhanced. For this reason, several kernel sizes should be made available in image processing systems so that the one which produces optimum lineament enhancement will be selected to give the best possible results. In the absence of this facility, resampling of the original image data might simulate a larger kernel size.

4. In this study, the 1024 x 1024 image size of the TM data (Loch Tummel area) and MSS data (Kedah-Perak area) were used for large area (small scale) mapping. For detailed (larger scale) mapping, a full resolution detail of the data should be used instead, which means that four 512 x 512 TM images instead of one 1024 x 1024 TM image of the Loch Tummel and eight 512 x 512 MSS images, instead of two 1024 x 1024 MSS images of the Kedah-Perak have to be interpreted. For the Loch Tummel and surrounding areas, detailed lineament studies are desirable and important in order to study the structure as well as tectonics of a complex fracture-zone. For the Kedah-Perak area, more detailed lineament studies are necessary at a local scale in order to establish the relations between rock types and concentrations of lineaments and their structural meaning. Further investigation, for example by geophysical survey, of the circular features as well as major fault interaction zones in the area as to their economic potential, is suggested.

References

ABDELHAMID, G. A. A., and VAUGHAN, R. A., 1988, Interpreting the geology of Glen Coe using Landsat MSS ,data and aerial photographs. In *Remote Sensing: Moving Towards 21st Century,* 1988 International Geoscience and Remote Sensing Symposium (Edinburgh: European Space Agency), 745-746.

ABRAMS, M. J., 1980, Lithological mapping. In *Remote Sensing In Geology,* edited by B. S. SIEGAL and A. R. GILLESPIE (New York: Wiley), 381-418.

AHMED, F., 1983, Relationships of mineral deposits and lineament analysis of the Red Sea region, northeastern Sudan. *Advance Space Research,* 3, 71-79.

ALIZAI, S. A. K., and ALI, J., 1988, Comparison of Landsat MSS and SIR-A data for geological application in Pakistan. *International Journal Remote Sensing,* 9, 85-94.

ALLISON, L. J., and SCHNAPF, A., 1983, Metrological satellites. Chapter 14 of *Manual of Remote Sensing,* edited by R. N. COLWELL, 2nd edition (Fall Church: American Society of Photogrammetry).

ALLISON, I., MAY, F., and STRACHAN, R. A., (Eds.) 1988, *An Excursion Guide to the Moine Geology of the Scottish Highlands* (Edinburgh: Scottish Academic Press), 270 p.

ALLUM, J. A. E., 1966, *Photogeology and regional mapping* (New York: Pergamon Press), 107 p.

_____, 1970, Assessment of satellite photographs for geological mapping and research. *Journ. Brit. Interplanetary Soc.,* 23, 297-306.

_____, 1984, The choice of satellite-borne or air-borne remote sensing for geology and mineral exploration. *Geoscience Canada,* 11, 208-209.

ALMASHOOR. S. S., and TJIA, H. D., 1987, A prominent fault across the Malaysia-Thai boundary: a preliminary report. *Warta Geology, Newsletter, Geol. Soc. Malaysia,* 13, 35-37.

ANDERSON, J. G. C., 1948, Stratigraphical Nomenclature of Scottish Metamorphic Rocks. *Geological Magazine,* 85, 89.

_____, 1956, The Moinian and Dalradian Rocks between Glen Roy and the Monadhliath Mountains, Inverness-shire. *Trans. R. Soc. Edin.,* 23, 429-458.

ANDERSON, J. G. C., and OWEN, T. R., 1980, *The Structure of the British Isles,* second edition (Oxford: Pergamon Press), 251 p.

ANDERSON, J. R., HARDY, E. E., ROACH, J. T., and WITHER, R. E., 1976, A land use and land cover classification for use with remote sensor data. *US Geological Survey Professional Paper 964,* Washington, DC.

ANDERTON, R., BRIDGES, P. H., LEEDER, M. R., and SELLWOOD, B. W., 1983, *A Dynamic Stratigraphy of the British Isles* (London: George Allen and Unwin).

ANUTA, P. E., 1977, Computer-assisted techniques for remote sensing data interpretation. *Geophysics,* 42, 468-481.

ASP, 1983, *Manual of Remote Sensing,* second edition (Fall Church, Virginia: American Society of Photogrammetry).

BADGLEY, P. C., 1965, *Structural and Tectonic Principles* (Tokyo: John Weatherhill, Inc.).

BAGHERI, S., and KIEFER, R. W., 1989, Updating regional geology of the South Central Alborz Mountains of Iran based on Landsat digital data. *Geocarto International,* 4, 35-42.

BAILEY, G. B., and ANDERSON, P. D., 1982, Applications of Landsat imagery to problems of petroleum exploration in Quaidam Basin, China. *American Association Petroleum Geologists Bulletin,* 66, 1348-1354.

BAILEY, G. B., and DWYER, J. L., 1984, Evaluation of SPOT simulator data for geologic mapping in the Split Mountain Region, Uintah County, Utah. In *SPOT Simulation Applications Handbook.* Proceedings of the 1984 SPOT Symposium (Arizona: American Society of Photogrammetry), 47-55.

BAIRD, W. J., 1988, *The Scenery of Scotland The Structure Beneath* (Edinburgh: National Museum of Scotland), 36 p.

BANDAT, H. F. VON, 1962, *Aerogeology* (Houston, Texas: Gulf Publ. Comp.), 350 p.

BARRETT, E. C., and CURTIS, L. F., 1982, *Introduction to Environmental Remote Sensing*, second edn. (New York: Chapman and Hall).

BARROW, G., GRANT WILSON, J. S., and CUNNINGHAM, E. H., 1905, The geology of the country round Blair Atholl, Pitlochry and Aberfeldy. *Memoirs of the Geological Survey Scotland* (HMSO), 156 p.

BARZEGAR, F., 1979, Rock type discrimination using enhanced Landsat imagery. *Photogrammetric Engineering and Remote Sensing*, 45, 605-610.

BAUER, M. E., CIPRA, J. E., ANUTA, P. E., and ETHERIDGE, J. B., 1979, Identification and area estimation of agricultural crops by computer classification of Landsat MSS data. *Remote Sensing of Environment*, 8, 77-92.

BEGNI, G., 1982, Selection of the optimum spectral bands for the SPOT satellite. *Photogrammetric Engineering and Remote Sensing*, 48, 1613-1620.

_____, 1988, SPOT image quality. Twenty months of experience. *Int. J. Remote Sensing*, 9, 1409-1414.

BELLISS, S. E., FOWLER, A. D. W., and MCDONNELL, M. J., 1985, Linear features in Wairarapa: quantitative study using Landsat imagery. *New Zealand Journal of Geology and Geophysics*, 28, 359-367.

BERHE, S. M. and ROTHERY, D. A., 1986, Interactive processing of satellite images for structural and lithological mapping in northeast Africa. *Geological Magazine*, 123, 393-403.

BERLIN, G. L., SCHABER, G. G., and HORSTMAN, K. C., 1980, Possible fault detection in Cottonball Basin, California: an application of radar remote sensing. *Remote Sensing of Environment*, 10, 33-42.

BERNSTEIN, R., 1983, Image geometry and rectification. In *Manual of Remote Sensing*, edited by R. N. COLWELL (Fall Church: American Society of Photogrammetry), 873-922.

BERNSTEIN, R., and FERNEYHOUGH, D. G. JR., 1975, Digital image processing. *Photog. Eng. and Remote Sensing*, 41, 1465-1476.

BERNSTEIN, R., LOTSPIECH, J. B., MYERS. J., KOLSKY, H. G., and LEES, R. D., 1984, Analysis and processing of Landsat-4 sensor data using advanced image processing techniques and technologies. *IEEE Transactions on Geoscience and Remote Sensing*, GE-22, 192-221.

BEST, R. G., and SMITH, J. R., 1978, Photographic contrast enhancement of Landsat imagery. *Photogrammetric Engineering and Remote Sensing*, 44, 1023-1026.

BGS, 1954, *Geological Map (Solid) of the Nairn*, sheet 84, scale 1:63,360.

_____, 1964, *Geological Map (Solid) of the Kingussie*, sheet 64, scale 1:63,360.

_____, 1967, *Geological Map (Solid) of the Blair Athole*, sheet 55, scale 1:63,360.

_____, 1974, *Geological Map (Solid) of the Loch Rannoch*, sheet 54E, scale 1:50,000.

_____, 1977, *Quaternary Map of the United Kingdom*, 1st edition, scale 1:625,000.

_____, 1978, *Geological Map (Drift) of the Nairn*, sheet 84E, scale 1:50,000.

_____, 1987, *Catalogue of Printed Maps.*

BILLINGSLEY, F. C., (ed.), 1983, Data processing and reprocessing. Chapter 17 of *Manual of Remote Sensing*, edited by R. N. COLWELL (Fall Church: American Society of Photogrammetry).

BILLINGSLEY, F. C., GOETZ, A. F. H., and LINDSLEY, J. N., 1970, Color differentiation by computer image processing. *Photographic Science and Engineering*, 14, 28-35.

Birnie, R. W., and Francica, J. R., 1981, Remote detection of geobotanical anomalies related to porphyry copper mineralization. *Economic Geology*, 76, 637-647.

Black, S. M., 1987, Interactive digital image processing as an aid in the mapping of brittle structures using satellite sensor image data. In *Advances In Digital Image Processing*, Proceedings RSS Annual Meeting 1987 (Nottingham: Remote Sensing Society), 343-354.

Blackstone, D. L., 1975, Mapping of linear structural elements from remote sensing imagery. *Contribution to Geology*, 14, 1-6.

Blanchet, P. H., 1957, Development of fracture analysis as exploration method. *American Association Petroleum Geologists Bulletin*, 41, 1748-1759.

Blodget, H. W., and Brown, G. F., 1982, Geological mapping by use of computer-enhanced imagery in western Saudi Arabia. *U. S. Geological Professional Paper 1153* (Washington D. C.: U. S. Printing Office), 10 p.

Blodget, H. W., Brown, G. F., and Moik, J. G., 1975, Geological mapping in northwestern Saudi Arabia using Landsat multi-spectral techniques. *NASA Earth Resources Survey Symposium, July 1975, Houston, Texas.* NASA TM X-58168, 971-989.

Blom, R. G., and Daily, M. I., 1982, Radar image processing for rock-type discrimination. *IEEE Trans. on Geoscience and Remote Sensing*, GE-20, 343-351.

Blom, R. G., Crippen, R. E., and Elachi, C., 1984, Detection of subsurface features in Seasat radar images of Means Valley, Mojave Desert, California. *Geology*, 12, 346-349.

Boorder, H. de., 1981, Structural-geological interpretation of SLAR imagery of the Colombian Amazones. *Trans. Instn. Min. Metall. (Section B: Appl. Earth Sci.)*, 90, B145-B152.

Borengasser, M. X., and Taranik, J. V., 1988, Structural geology and regional tectonics of the Mineral County area, Nevada, using Shuttle Imaging Radar-B and digital aeromagnetic data. *Int. J. Remote Sensing*, 9, 967-980.

BORENGASSER, M. X., KLEINER, E. F., VREELAND, P., PETERSON, F. F., KLIEFORTH, H., and TARANIK, J. V., 1987, Geological and vegetational applications of Shuttle Imaging Radar-B, Mineral County, Nevada. *Photogramm. Eng. Remote Sensing,* 54, 71-76.

BOULTER, J. F., 1979, Interactive digital image restoration and enhancement. *Computer Graphics and Image Processing,* 11, 301-312.

BOWERS, S. A., and HANKS, R. J., 1965, Reflection of radiant energy from soil. *Soil Science,* 100, 130-138.

BOYER, R. E., and MCQUEEN, J. E., 1964, Comparison of mapped rock fractures and airphoto linear features. *Photogrammetric Engineering,* 30, 630-635.

BRADBURY, P. A., HAINES-YOUNG, R. H., MATHER, P. M., and MACDONALD, A., 1985, The use of remotely-sensed data for landscape classification in Wales: the status of woodlands in the landscape. In *Advance Technology for Monitoring and Processing Global Environmental Data* (Reading: Remote Sensing Society), 401-411.

BRAUN, O. P. G., 1982, A structural synthesis of Brazil, based on the study of major lineaments derived from remote sensing imagery interpretation. *Photogrammetria,* 37, 77-108.

BROOKS, R. R., 1972, *Geobotany and biogeochemistry in mineral exploration* (New York: Harper and Row), 290 p.

_____, 1983, *Biological methods of prospecting for minerals* (New York: Wiley).

BROOKS, R. R., and MCDONNELL, M. J., 1983, Delineation of New Zealand ultramafic rocks by computer processing of digital data from satellite imagery. *New Zealand Journal of Science,* 26, 65-71.

BROWN, C. W., 1961, Comparison of joints, faults and airphoto linears. *Am. Assoc. Petroleum Geologist Bull.,* 45, 1888-1892.

BRUNNER, J. S., and VECK, N. J., 1985, Image texture encoding for geological mapping. In *Advance Technology for Monitoring and Processing Global Environmental Data* (Reading: Remote Sensing Society), 331-339.

Burns, K. L., and Brown, G. H., 1978, The human perception of geological lineaments and other discrete features in remote sensing imagery: signal strengths, noise levels and quality. *Remote Sensing of Environment*, 7, 163-176.

Burns, K. L., Shepherd, J., and Berman, M., 1976, Reproducibility of geological lineaments and other discrete features interpreted from imagery: measurement by a coefficient of association. *Remote Sensing of Environment*, 5, 267-301.

Burton, C. K., 1964, The older alluvium of Johore and Singapore. *J. Trop. Geogr.*, 18, 30-42.

_____, 1965, Wrench faulting in Malaya. *Journal of Geology*, 73, 781-798.

_____, 1970, *Geology and Mineral Resources of the Baling Area, Kedah and Perak*. Geological Survey Malaysia, District Memoir 12, 150 p.

_____, 1973, Mesozoic. In *Geology of the Malay Peninsula*, edited by D. J. Gobbett and C. S. Hutchison (New York: John Wiley), p. 97-141.

Byrne, G. F., Crapper, P. F., and Mayo, K. K., 1980, Monitoring land-cover change by principal component analysis of multitemporal Landsat data. *Remote Sensing of Environment*, 10, 175-184.

Canas, A. A. D., and Barnett, M. E., 1985, The generation and interpretation of false-colour composite principal component images. *International Journal Remote Sensing*, 6, 867-881.

Cannon, H. L., 1960, Botanical prospecting for ore deposits. *Science*, 132, 591-598.

Cardamone, P., Casnedi, R., Cassinis, G., Cassinis, R., Marcolongo, B., and Tonelli, A., 1976, Study of regional linears in central Sicily by satellite imagery. *Tectonophysics*, 33, 81-96.

Carroll, D. M., Evan, R., and Bendelow, V. C., 1977, Air photo-interpretation for soil mapping. *Soil Survey Technical Monograph No. 8* (Harpenden: The Soil Survey), 85 p.

CHAHINE, M. T., 1983, Interaction mechanisms within the atmosphere. Chapter 5 of *Manual of Remote Sensing*, edited by R. N. COLWELL (Fall Church: American Society of Photogrammetry).

CHAVEZ, P. S., 1983, Geological application (sub. ed. R. S. WILLIAMS). In *Manual of Remote Sensing*, second edition, edited by R. N. COLWELL (Falls Church, Virginia: American Society of Photogrammetry), 1667-1953.

CHAVEZ, P. S., and BAUER, B., 1982, An automatic optimum kernel-size selection technique for edge enhancement. *Remote Sensing of Environment*, 12, 23-38.

CHAVEZ, P. S. JR., and BERLIN, G. L., 1984, Digital processing of SPOT Simulator and Landsat TM data for the SP Mountain Region, Arizona. In *SPOT Simulation Applications Handbook*. Proceedings of the 1984 SPOT Symposium (Arizona: American Society of Photogrammetry), 56-66.

CHAVEZ, P. S. JR., BERLIN, G. L., and SOWERS, L. B., 1982, Statistical method for selecting Landsat MSS ratios. *Journal Applied Photographic Engineering*, 8, 23-30.

CHAVEZ, P. S., JR. and BOWELL, J. A., 1988, Comparison of the spectral information content of Landsat TM and SPOT for three different sites in the Phoenix, Arizona Region. *Photogrammetric Engineering and Remote Sensing*, 54, 1699-1708.

CHEVREL, M., COURTOIS, M., and WEILL, G., 1981, The SPOT satellite remote sensing mission. *Photogrammetric Engineering and Remote Sensing*, 47, 1163-1171.

COCHRANE, G. R. and TIANFENG, W., 1983, Interpretation of structural characteristics of the Taupo volcanic zone New Zealand from Landsat imagery. *International Journal Remote Sensing*, 41, 111-128.

COLE, M. M., 1977, Landsat and airborne multi-spectral and thermal imagery used for geological mapping and identification of ore horizons in Lady Annie–Lady Loretta and Dugald River areas, Queensland, Australia. *Trans. Inst. Min. Metall.*, Section B, B195-B215.

COLLINS, W., CHANG, S. H., RAINES, G., CANNEY, F., and ASHLEY, R., 1983, Airborne biogeochemical mapping of hidden mineral deposits. *Economic Geology,* 78, 737-749.

COLWELL, R. N., (ed.), 1960, *Manual of Photographic Interpretation* (Fall Church: American Society of Photogrammetry), 868 p.

_____, 1968, Remote sensing of natural resources. *Scientific American,* 218, 54-69.

_____ (ed.), 1983, *Manual of Remote Sensing,* second edition (Fall Church, Virginia: American Society of Photogrammetry).

CONDIT, C. D. and CHAVEZ, P. S., 1979, Basic concepts of computerized digital image processing for geologists. *U. S. Geological Survey Bulletin 1462,* 16 p.

CORNILLON, P., 1982, *An Overview of Environmental Satellites and Sensors* (University of Rhode Island: NOAA/Ses Grant), Marine Memorandum 72.

COURTIER, D. B., 1974, Geology and mineral resources of the neighbourhood of Kulim, Kedah. *Geol. Surv. Malaysia Map Bull. 3,* p. 4.

CRAIG, G. Y., (Editor), 1983, *The Geology of Scotland,* second edition (Edinburgh: Scottish Academic Press), 472 p.

CR STA, A. P. and MOORE, J. McM., 1989, Geological mapping using Landsat Thematic Mapper imagery in Almeria Province, south-east Spain. *International Journal Remote Sensing,* 10, 505-514.

CSILLAG, F., 1982, Significance of tectonics in linear feature detection and interpretation on satellite images. *Remote Sensing of Environment,* 12, 235-245.

CURLIS, J. D., FROST, V. S., and DELLWIG, L. F., 1986, Geological mapping potential of computer-enhanced images from the shuttle imaging radar: Lisbon Valley Anticline, Utah. *Photogrammetric Engineering and Remote Sensing,* 52, 525-532.

CURRAN, P. J., 1980, Multi-spectral remote sensing of vegetation amount. *Progress in Physical Geography,* 4, 315-341.

_____, 1985, *Principles of Remote Sensing,* (London: Longman Scientific and Technical), 282 p.

_____, 1987, On defining remote sensing. *Photogrammetric Engineering and Remote Sensing,* 53, 305-306.

DARCH, J. P., and BARBER, J., 1983, Multitemporal remote sensing of geobotanical anomaly. *Economic Geology,* 78, 770-782.

DAVIS, P. A. and BERLIN, G. L., 1989, Rock discrimination in the complex geologic environment of Jabal Salma, Saudi Arabia, using Landsat TM data. *Photogramm. Engineering and Remote Sensing,* 55, 1147-1160.

DAVIS, P. A., BERLIN, G. L., and CHAVEZ, P. S. JR., 1987, Discrimination of altered basaltic rocks in the Southwestern United States by analysis of Landsat TM data. *Photogrammetric Engineering and Remote Sensing,* 53, 45-55.

DEAN, K. G., and SPENCER, J. P., 1982, Evaluation of photographic enhancements of Landsat imagery. *Remote Sensing of Environment,* 12, 381-390.

DIAD, 1988, *DIAD Systems User's Manual.*

DIKKERS, A. J., 1977, Sketch of a possible lineament pattern in northwest Europe. *Geologie en Mijnbouw,* 56, 275-285. GM

DONKER, N. H. W., and MULDER, N. J., 1977, Analysis of MSS digital imagery with the aid of principal component transform. *ITC Journal,* 1977-3,

DOZIER, J., and FREW, J., 1981, Atmospheric corrections to satellite radiometric data over rugged terrain. *Remote Sensing of Environment,* 11, 191-205.

DRURY, S. A., 1986a, Remote sensing of geological structure in temperate agricultural terrains. *Geological Magazine,* 123, 113-121.

_____, 1986b, Geological application of airborne thematic mapper data: Assynt, Sutherland. *NERC Special Topic: Remote Sensing, report.* Natural Environment Research Council, Swindon.

_____, 1987, *Image Interpretation in Geology,* (London: George Allen and Unwin), 243 p.

DRURY, S. A., and HOLT, R. W., 1980, The tectonic framework of the South Indian craton: a reconnaissance involving Landsat imagery. *Tectonophysics,* 65, T1-T15.

DRURY, S. A., and HUNT, G. A., 1989, Geological uses of remotely-sensed reflected and emitted data of lateritized Archaean terrain in Western Australia. *Int. J. Remote Sensing,* 10, 475-497.

EGGER, A. J., 1979, Large scale circular features in North Westland and West Nelson, New Zealand; possible structural control for porphyry molybdenum-copper mineralisation?. *Economic Geology,* 74, 1490-1495.

ELACHI, C., 1980, Spaceborne imaging radar: geologic and oceanographic applications. *Science,* 209, 1073-1082.

_____, 1982, Radar images of the earth from space. *Scientific American,* 247, 54-61.

_____, 1983, Microwave and infrared satellite remote sensors. Chapter 13 of *Manual of Remote Sensing,* edited by R. N. COLWELL, 2nd edition (Fall Church: American Society of Photogrammetry).

ELACHI, C., BROWN, W. E., CIMINO, J. B., DIXON, T., EVANS, D. L., FORD, J. P., SAUNDERS, R. S., BREED, C., MASURSKY, H., MCCAULEY, J. F., SCHABER, G. G., DELLWIG, L., ENGLAND, A., MACDONALD, H., MARTIN-KAYE, P., and SABIN, F., 1982, Shuttle imaging radar experiment. *Science,* 218, 996-1003.

ELIASON, E. M., CHAVEZ, P. S., and SODERBLOM, L. A., 1974, Simulated "true colour" images from ERTS data. *Geology,* 2, 231-234.

ELVIDGE, C. D., and LYON, R. J. P., 1983, Geobotanical exploration and regional geobotany. In *Manual of Remote Sensing,* 2nd edition, edited by R. N. COLWELL (Fall Church: American Society of Photogrammetry), 1893-1898.

———————, 1985, Estimation of the vegetation contribution to the 1.65/2.22 μm ratio in airborne thematic mapper imaging of the Virginia Range, Nevada. *International Journal Remote Sensing,* 6, 75-88.

FISCHER, W. A., 1975, History of remote sensing. In *Manual of Remote Sensing,* first edition, edited by R. G. REEVES (Fall Church, Virginia: American Society of Photogrammetry), 27-50.

FITZPATRICK, E. A., 1983, *Soils. Their Formation, classification and Distribution* (London and New York: Longman), 228-229.

FONTANEL, A. C., BLANCHET, C., and LALLEMAND, C., 1975, Enhancement of Landsat imagery by combination of multi-spectral classification and principal component analysis. *Proceedings NASA Earth Resources Survey Symposium, July, 1975, Houston, Texas.* NASA TM X-58168, 991-1012.

FORD, J. P., 1980, Seasat orbital Radar images for geological mapping: Tennessee-Kentucky-Virginia. *Amer. Asso. Pet. Geol. Bull.,* 64, 2064-2094.

FORD, J. P., CIMINO, J. P., and ELACHI, C., 1983, Space shuttle Columbia views of the world with imaging radar: the SIR-A experiment. *JPL Publication No.82-95* (Pasadena: Jet Propulsion Laboratory).

FRASER, S. J., and GREEN, A. A., 1987, A software defoliant for geological analysis of band ratios. *Int. J. Remote Sensing,* 8, 525-532.

FREDEN, S. C., and GORDON, F. JR., 1983, Landsat satellites. Chapter 12 of *Manual of Remote Sensing,* edited by R. N. COLWELL, 2nd edition (Fall Church: American Society of Photogrammetry).

FROIDEVAUX, C. M., 1980, Radar, an optimum remote-sensing tool for detailed plate tectonic analysis and its application to hydrocarbon exploration (an example in Irian Jaya, Indonesia), in *Radar geology - an assessment* (California Institute of Technology: Jet Propulsion Laboratory Publication 80-61), 457-501.

FROST, R. T. C., 1977, Tectonic patterns in the Danish Region (as deduced from a comparative analysis of magnetic, Landsat, bathymetric and gravity lineaments). *Geologie en Mijnbouw*, 56, 351-362.

FROST, V. S., PERRY, M. S., DELLWIG, L. F., and HOLTZMAN, J. C., 1983, Digital enhancement of SAR imagery as an aid in geologic data extraction. *Photogrammetric Engineering and Remote Sensing*, 49, 357-364.

FUSSELL, J., RUNDQUIST, D., and HARRINGTON, J. A., JR., 1986, On defining remote sensing. *Photogrammetric Engineering and Remote Sensing*, 52, 1507-1511.

_____, 1987, On defining remote sensing, a response. *Photogrammetric Engineering and Remote Sensing*, 53, 1096.

GAUSMAN, H. W., 1974, Leaf reflectance of near infrared. *Photogrammetric Engineering and Remote Sensing*, 40, 183-191.

GEMMELL, A. M. D., 1975, Quaternary studies in north-east Scotland: an introduction. In *Quaternary Studies In North-east Scotland*, 1-13.

Geological Survey of Malaysia (GSM), 1976, *Mineral Distribution Map of Peninsular Malaysia*, 7th edition, scale 1:500,000.

_____, 1985, *Geological Map of Peninsular Malaysia*, 8th edition, scale 1:500,000.

GILLESPIE, A. R., 1980, Digital techniques of image enhancement. In *Remote Sensing in Geology*, edited by B. S. SIEGAL and A. R. GILLESPIE, (New York: Wiley), 139-226.

GOBBETT, D. J. and HUTCHISON, C. S., (eds.), 1973, *Geology of the Malay Peninsula* (New York: John Wiley).

GOBBETT, D. J., and TJIA, H. D., 1973, Tectonic history. In *Geology of the Malay Peninsula*, edited by D. J. GOBBETT and C. S. HUTCHISON (New York: John Wiley), 305-331.

GOETZ, A. F. H., BILLINGSLEY, F. C., GILLESPIE, A. R., ABRAMS, M. J., SQUIRES, R. L., SHOEMAKER, E. M., LUCCHITTA, IVO., and ELSTON, D. P., 1975, Applications of ERTS images and image processing to regional problems and geologic mapping in northern Arizona. *Jet Propulsion Laboratory Technical Report 32-1597,* 188 p.

GOETZ, A. F. H., and BILLINGSLEY, F. C., 1974, Digital image enhancement techniques used in some ERTS application problems. *Third Earth Resources Technological Satellite Symposium, Dec., 1973, Washington, D. C.,* NASA SP-351, 1971-1992.

GOETZ, A. F. H., and ROWAN, L. C., 1981, Geological remote sensing. *Science,* 211, 781-791.

GOETZ, A. F. H., ROCK, B. N., and ROWAN, B. N., 1983, Remote sensing for exploration: an overview. *Economic Geology,* 78, 573-590.

GOL'BRAYKH, I. G., ZABALUYER, V. V. and MIRKIN, G. R., 1966, Tectonic analysis of mega-jointing: A promising method of investigating covered territories. *International Geology Review,* 8, 1009-1016.

GOLD, D. P., 1980, Structural geology. In *Remote Sensing in Geology,* edited by B. S. SIEGAL and A. R. GILLESPIE (New York: Wiley), 419-484.

GONZALEZ, R. C., and WINTZ, P., 1977, *Digital Image Processing* (Reading, Massachusetts: Addison-Wesley).

GREENBAUM, D., 1987, Lithological discrimination in central Snowdonia using airborne multi-spectral scanner imagery. *International Journal Remote Sensing,* 8, 799-816.

GRIFFITHS, J. C., and ROSENFELD, M. A., 1954, Operator variation in experimental research. *Journal of Geology,* 62, 74-91.

GUHA, P. K., and MALLICK, S. B., 1985, Digital MSS and spectral reflectance data in lithologic discrimination. *ITC Journal,* 1985-1, 42-46.

GUHA, M. M., and MITCHELL, R. L., 1966, Trace and major element composition of the leaves of some deciduous trees, II Seasonal Changes. *Plant and Soil,* 24, 90-112.

GURNEY, C. M., and TOWNSHEND, J. R. G., 1983, The use of contextual information in the classification of remotely sensed data. *Photogrammetric Engineering and Remote Sensing,* 49, 55-64.

GUSTAFSON, G. C., 1982, *Applied Geography* (Englewood Cliffornia: Prentice-Hall), p. 170.

HACKMAN, R. J., 1966, Geologic evaluation of radar imagery in southern Utah. *U. S. Geological Survey Professional Paper 575-B,* B115-B160.

HALBOUTY, M. T., 1976, Application of Landsat imagery to petroleum and mineral exploration. *American Association Petroleum Geologists Bulletin,* 60, 745-793.

_____, 1980, Geological significance of Landsat data for 15 giant oil and gas fields. *American Association Petroleum Geologists Bulletin,* 64, 8-36.

HAMAN, P. J., 1961, Lineament analysis on aerial photographs. *West Canadian Research Publication,* Series 2 no. 1.

HAMBLIN, R. J. O., and CROFTS, R. G., 1984, Multi-spectral survey of an area of scattered drift deposits between Warwick and Redditch. *International Journal Remote Sensing,* 5, 729-732.

HANDIN, J., and HAGER, R. V., 1957, Experimental deformation of sedimentary rocks under confining pressure: test at room temperature on dry samples. *Am. Assn. Petrol. Geologists Bull.,* 41, 1-56.

HARALICK, R. M., and FU, K. S., 1983, Pattern recognition and classification. In *Manual of Remote Sensing,* edited by R. N. COLWELL (Fall Church: American Society of Photogrammetry), 793-805.

HARRIS, A. L., and PITCHER, W. S., 1975, The Dalradian Supergroup. In *A Correlation of the Precambrian Rocks in the British Isles., Spec. Rep. Geol. Soc. London,* 6, 52-75.

HARRIS, R., 1987, *Satellite Remote Sensing: an introduction* (London and New York: Routledge and Kegan Paul), 220 p.

HARRIS, J. F., TAILOR, G. L., and WALPER, J. L., 1960, Relation of deformational fractures in sedimentary rocks to regional and local structure. *Am. Assoc. Petroleum Geologist Bull.*, 44, 1853-1873.

HENDERSON, G., 1960, Airphoto lineaments in Mpanda area, Western Province, Tanganyika, Africa. *American Association Petroleum Geologists Bulletin*, 44, 53-71.

HILL, E. S., 1963, *Elements of Structural Geology*, (New York: John Wiley & Sons), 259-261.

HINXMAN, L. W., 1908, *Bathymetrical survey of the fresh water lochs of Scotland* (Murray and Pullar), 1, 164 p.

_____, 1915, The geology of Mid-Strathspey and Strathdearn. *Memoir Geological Survey of Scotland* (HMSO).

HOBBS, W. H., 1904, Lineaments of the Atlantic border region. *Geological Society American Bulletin*, 15, 483-506.

_____, 1911, Repeating patterns in the relief and in the structure of the land. *Geological Society America Bulletin*, 22, 123-176.

_____, 1912, *Earth Features and Their Meaning* (New York: Macmillan Co.), 506 p.

HOFFER, R. M., 1978, Biological and physical considerations in applying computer-aided analysis techniques to remote sensor data. In *Remote Sensing - the quantitative approach* (New York: McGraw-Hill), 227-289.

HOLDERMANN, F., BOHNER, M., BARGEL, B., and KAZMIERCZAK, H., 1978, Review of automatic image processing. *Photogrammetria*, 34, 225-258.

HOLZ, R. K., 1973, *The Surveillant Science* (Boston, Massachusetts: Houghton Mifflin), p. 5.

HORD, R. M., 1982, *Digital Image Processing of Remotely Sensed Data* (New York: Academic Press, Inc.).

HORLER, D. N. H., BARBER, J., and BARRINGER, A. R., 1980a, Effects of cadmium and copper treatments and water stress on the thermal emissions from peas (*Pisum sativum L.*): controlled environment experiments. *Remote Sensing of Environment*, 10, 191-199.

_____, 1980b, Effects of heavy metals on the absorbance and reflectance spectra of plant. *International Journal Remote Sensing*, 1, 121-136.

HORNE, J., 1923, The geology of the Lower Findhorn and Lower Strath Nairn. *Memoir of Geological Survey, Scotland* (HMSO).

HOTELLING, H., 1933, Analysis of a complex of statistical variables into principal components. *Journal Educational Psychology*, 24, 417-441.

HUNT, G. R., and SALISBURY, J. W., 1970, Visible and near-infrared spectra of minerals and rocks-I. Silicate minerals. *Modern Geology*, 1, 283-300.

_____, 1970, Visible and near-infrared spectra of minerals and rocks I. Carbonates. *Modern Geology*, 2, 23-30.

_____, 1975, Visible and near-infrared spectra of minerals and rocks-XI. Sedimentary rocks. *Modern Geology*, 5, 211-281.

_____, 1976, Visible and near infrared spectra of minerals and rocks: XII. Metamorphic rocks. *Modern Geology*, 5, 219-228.

HUNT, G. R., SALISBURY, J. W., and LENHOFF, C. J., 1971, Visible and near-infrared spectra of minerals and rocks-III. Oxides and hydroxides. *Modern Geology*, 2, 195-205.

_____, 1973, Visible and near-infrared spectra of minerals and rocks-VII. Acidic igneous rocks. *Modern Geology*, 4, 217-224.

_____, 1974a, Visible and near-infrared spectra of minerals and rocks-VIII. Intermediate igneous rocks. *Modern Geology*, 4, 237-244.

_____, 1974b, Visible and near-infrared spectra of minerals and rocks-IX. Basic and ultrabasic igneous rocks. *Modern Geology,* 5, 15-22.

HUNT, G. A., DRURY, S. A., and ROTHERY, D. A., 1986, Techniques for choosing the optimum Thematic Mapper channel combination for lithological mapping in semi-arid terrains. In *Mapping from Modern Imagery,* Proceedings RSS Annual Meeting 1986 (Edinburgh: Remote Sensing Society), 637-646.

HUNTINGTON, J. F., 1969, Methods and applications of fracture trace analysis in the quantification of structural geology. *Geological Magazine,* 106, 430-451.

HUNTINGTON, J. F. and RAICHE, A. P., 1978, A multi-attribute method for comparing geological lineament interpretations. *Remote Sensing of Environment,* 7, 145-161.

HUTCHISON, C. S., 1973, Metamorphism. In *Geology of the Malay Peninsula,* edited by D. J. GOBBETT and C. S. HUTCHISON (New York: John Wiley), 253-303.

IBRAHIM ABDULLAH, 1984, Lineamen kepulauan Langkawi: implikasinya terhadap geologi struktur. *Sains Malaysiana (Earth Science),* 13, 45-62.

INGEBRITSEN, S. E., and LYON, R. UJ. P., 1985, Principal components analysis of multitemporal image pairs. *International Journal of Remote Sensing,* 6, 687-696.

IRANPANAH, A., 1977, Geologic applications of Landsat imagery-delineation of major geologic features in north-central Iran. *Photogrammetric Engineering and Remote Sensing,* 43, 1037-1040.

_____, 1989, Thematic mapping of basement-related cross-strike structural discontinuities and their relationship to potential oil-bearing structures. *Photogrammetric Engineering and Remote Sensing,* 55, 1491-1496.

IRANPANAH, A, and ESFANDIARI, B., 1980, Interpretation of structural lineaments using Landsat-1 images. *Photogrammetric Engineering and Remote Sensing,* 46, 225-229.

ISIORHO, S. A., 1984, Radar geology of the Shelleng-Numan area in Nigeria. An evaluation. *International Journal Remote Sensing,* 5, 519-531.

_____, 1985, The significance of lineaments mapped from remotely sensed images of the 1:250 000 Lau Sheet in the Benue trough of Nigeria. *International Journal Remote Sensing,* 6, 911-918.

JACOBBERGER, P. A., ARVISON, R. E., and RASHKA, D. L., 1983, Application of Landsat multi-spectral scanner data and sediment spectral reflectance measurements to mapping of the Meatiq Dome, Egypt. *Geology,* 11, 587-591.

JENSEN, J. R., 1983, Biophysical remote sensing. *Annals of the Association of American Geographers,* 73, 111-132.

_____, 1986, *Introductory Digital Image Processing - A Remote Sensing Perspective* (Englewood Cliffs, New Jersey: Prentice Hall), 379 p.

JENSEN, J. R., and HODGSON, M. E., 1983, Remote sensing brightness maps. *Photogrammetric Engineering and Remote Sensing,* 49, 93-102.

JENSON, H., GRAM, G. C., PORCELLO, L. J., and LEITH, E. N., 1977, Side looking airborne radar. *Scientific American,* October, 1977.

JOHNSON, M. R. W., 1983, Chapter 3: Torridonian-Moine and Chapter 4: Dalradian. In *Geology of Scotland,* edited by G. Y. Craig (Edinburgh: Scottish Academic Press), 49-104.

JOHNSON, M. R. W., and FROST, R. T. C., 1977, Fault and lineament patterns in the southern Highland of Scotland. *Geologie en Mijnbouw,* 56, 287-294.

JOHNSTON, J. E., MILLER, R. L., and ENGLUND, K. J., 1975, Applications of remote sensing to structural interpretations in the southern Appalachian. *Journal Research U. S. Geological Survey,* 3, 285-293.

JOHNSTONE, G. S., 1966, *British Regional Geology, The Grampian Highlands,* 3rd edition (Edinburgh: HMSO), 107 p.

_____, 1975, The Moine Succession. In *A Correlation of the Precambrian Rocks in the British Isles, Spec. Rep. Geol. Soc. London,* 6, 30-42.

JOHNSTONE, G. S., SMITH, D. I., and HARRIS, A. L., 1969, The Moinian Assemblage of Scotland. In *North Atlantic - geology and continental drift,* edited by M. KAY. *Mem. Am. Assoc. Pet. Geol.,* 12, 159-180.

JOHNSTONE, W. E., 1953, Photogeology and mineral exploration. *Mining Magazine,* 88, 265-270.

JONES, C. R., 1970, Geology and Mineral Resources of the Grik Area, Upper Perak. *Geological Survey Malaysia, District Memoir 11,* 144 p.

_____, 1981, Geology and mineral resources of Perlis, North Kedah and the Langkawi Islands. *Geol. Surv. Malaysia District Memoir 17,* p. 19.

KAISER, E. P., 1950, Structural significance of lineaments [abs.]. *Geological Society America Bulletin,* 61, 1475-1476.

KAUFMANN, H., 1988, Mineral exploration along the Aqaba-Levant structure by use of TM data. *Int. J. Remote Sensing,* 9, 1639-1658.

KAYAN, I., and KLEMAS, V., 1978, Application of Landsat imagery to studies of structural geology and geomorphology of the Mentese Region of southwestern Turky. *Remote Sensing of Environment,* 7, 51-60.

KIM, S. K., 1979, Analyses of lineaments extracted from Landsat images of the Korean Peninsula. *Journal of Earth Science,* Nagoya University, 26/27, 49-74.

KOOPMANS, B. N., 1983, Side-looking radar, a tool for geological surveys. *Remote Sensing Review 1983,* 1, 19-69.

_____, 1986, A comparative study of lineament analysis from different remote sensing imagery over areas in the Benue Valley and Jos Plateau Nigeria. *International Journal Remote Sensing,* 7, 1763-1771.

_____, 1988, A comparative analysis of dyke lineaments mapped from Shuttle Imaging Radar and Large Format Camera photography in hyperarid areas of the Eastern Desert, Egypt, and Red Sea Hills, Sudan. *Int. J. Remote Sensing,* 9, 981-995.

KUJANSUU, R., and KOHO, S., 1982, On the suitability of the Landsat data for the general geological mapping of quaternary deposits in northern Lapland. *Photogrammetric Journal of Findland,* 9, 65-75.

KUPSCH, W. O. and WILD, J., 1958, Lineaments in the Avonlea area, Saskatchewan. *American Association Petroleum Geologists Bulletin,* 42, 127-134.

LABOVITZ, M. L., MASUOKA, E. J., BELL, R., NELSON, R. F., LARSEN, C. A., HOOKER, L. K., and TROENSEGAARD, K. W., 1985, Experimental evidence for spring and autumn windows for the detection of geobotanical anomalies through the remote sensing of overlying vegetation. *International Journal of Remote Sensing,* 6, 195-216.

LAI, K. H., 1987, Photogeology of the Padang Terap-Saba Yoi-Yaha area. *Geol. Surv. Malaysia Annual Report.*

LAKE, S. D., MUNDAY, T. J., and DEWEY, J. F., 1984, Lineament mapping and analysis in the Wessex Basin of southern England: a comparison between MSS and TM data. In *Satellite Remote Sensing - review and preview,* Proceedings RSS Annual Conference 1984 (Reading, UK: Remote Sensing Society), 361-374.

LAMBERT, R. ST. J., and MCKERROW, W. S., 1976, The Grampian orogeny. *Scottish Journal Geology,* 12, 271-292.

Landsat Data Users Handbook, 1979 (washington, D. C.:U. S. Government Printing Office), 533 p.

LATHRAM, E. H., 1972, Nimbus IV view of the major structural features of Alaska. *Science,* 175, 1423-1427.

LATTMAN, L. H., 1958, Technique of mapping geologic fracture traces and lineaments. *Photogrammetric Engineering,* 24, 568-576.

LATTMAN, L. H., and MATZKE, R. H., 1961, Geological significance of fracture traces. *Photogrammetric Engineering,* 27, 435-438.

LATTMAN, L. H., and RAY, R. G., 1965, *Airphotographs in Field Geology* (New York: Holt, Rineart and Winston), 221 p.

LEITH, W. and ALVAREZ, W., 1985, Structure of the Vakhsh fold-and-thrust belt, Tadjik USSR: geologic mapping on a Landsat image base. *Geological Society America Bulletin,* 96, 875-885.

LILLESAND, T. M., and KIEFER, R. W., 1987, *Remote Sensing and Image Interpretation,* second edition (New York: John Wiley and Sons), 721 p.

LINTZ, J. JR., and SIMONETT, D. S., (eds), 1976, *Remote Sensing of Environment* (Reading, Massachusetts: Addison-Wesley Publishing Company), p. 1.

LO, C. P.,1986, *Applied Remote Sensing* (London: Longman Scientific and Technical).

LONGSHAW, T. G. and GILBERTSON, B., 1974, Computerised interpretation of ERTS-1 data in South Africa. *South African Journal Science,* 70, 114-117.

_____, 1975, Multi-spectral aerial photography as exploration tool-II: an application in the Bushveld Igneous Complex, South Africa. *Remote Sensing of Environment,* 4, 147-163.

LOWMAN, P. D., 1965, Space photography - a review. *Photogrammetric Engineering,* 31, 76-86.

_____, 1973, Geologic uses of Earth orbital photography. In *The Surveillant Science,* edited by R. K. Holz (Boston: Houghton Mifflin Company), 170-182.

LUNDEN, B., and WESTER, K., 1988, Landsat TM and SPOT HRV survey mapping of bedrock outcrops. In *Remote Sensing: Moving Towards the 21st Century,* 1988 International Geoscience and Remote Sensing Symposium (Edinburgh: European Space Agency), 483-484.

LYNN, D. W., 1984, Surface material mapping in the English Fernlands using airborne multi-spectral scanner data. *Inst. J. Remote Sensing,* 5, 699-713.

LYON, R. J. P., 1970, The multiband approach to geological mapping from orbital satellites: is it redundant or vital?. *Remote Sensing of Environment*, 1, 237-244.

_____, 1972, Infrared spectral emittance in geological mapping: airborne spectrometer data from Pisgah Crater, California. *Science*, 175, 983-985.

_____, 1975, Mineral exploration applications of digitally processed Landsat imagery. *Proceedings of the First Annual William T. Pecora Memorial Symposium, held in Sioux Falls, South Dakota in October 1975*, 271-292.

_____, 1977, Mineral exploration applications of digitally processed Landsat imagery. *U.S. Geological Survey Professional Paper 1015.*

LYON, J. P., and LEE, K., 1970, Remote sensing in exploration for mineral deposits. *Economic Geology*, 65, 785-800.

Macaulay Institute For Soil Research, 1976, see Soil Survey of Scotland.

MACDONALD, H. C., 1969, Geologic evaluation of radar imagery from Darien Province, Panama. *Modern Geology*, 1, 1-63.

_____, 1980, Techniques and applications of imaging radars. In *Remote Sensing in Geology*, edited by B. S. SIEGAL and A. K. GILLESPIE (John Wiley and Sons), 297-336.

MACKENZIE, J. S., and RINGROSE, P. S., 1986, Use of Seasat SAR imagery for geological mapping in a volcanic terrain: Askja Caldera, Iceland. *International Journal Remote Sensing*, 7, 181-194.

MARRS, R. W. and RAINES, G. L., 1984, Tectonic framework for Powder River Basin, Wyoming and Montana, interpreted from Landsat imagery. *American Association Petroleum Geologists Bulletin*, 68, 1718-1731.

MATHER, P. M., 1976, *Computational methods of multivariate analysis in physical geography* (Chichester: Wiley).

_____, 1987, *Computer Processing of Remotely-Sensed Images, an Introduction* (New York: John Wiley and Sons), 352 p.

MAUDE, R., 1987, Lineaments in enhanced Landsat images from a portion of west Wales. *Geological Journal,* 22, 107-118.

McCAULEY, J. F., SCHABER, G. G., BREED, C. S., GROLIER, M. J., HAYNES, C. V., ISSAWI, B., ELACHI, C., and BLOM, R., 1982, Subsurface valleys and geoarcheology of the eastern Sahara revealed by shuttle radar. *Science,* 218, 1004-1020.

McDONOUGH, M., and MARTIN-KAYE, P. H. A., 1984, Radargeologic interpretation of Seasat imagery of Iceland. *International Journal Remote Sensing,* 5, 433-450.

MEER MOHR, H. E. C. VAN DER. 1967, Fracture analysis from aerial photographs. *Proceeding 1st Congress International Society Rock Mechanics, Lisbon,* 59-61.

_____, 1969, Geological interpretation of hyperaltitude photographs from Gemini spacecraft. *Photogrammetria,* 24, 167-174.

_____, 1974, The use of ERTS-1 multi-spectral imagery for geological mapping. *ITC Journal,* 74/3, 385-394.

MEKEL, J. F. M., 1978, The use of aerial photographs and other images in geological mapping. In *ITC Textbook of Photo-Interpretation Volume 8* (Enschede: International Institute for Aerial Survey and Earth Sciences), 396 p.

METZ, R. A., BLAKE, D. W., and WOTRUBA, P. R., 1983, Review of SPOT imagery simulation at the Copper Canyon Cu-Au mining area, Lander County, Nevada. In *SPOT Simulation Application Handbook,* Proceedings of the 1984 SPOT Symposium (Arizona: American Society of Photogrammetry), 83-91.

MILLER, V. C., 1961, *Photogeology* (New York: McGraw-Hill), 243 p.

MILTON, N. M., COLLINS, W., CHANG, S. H., and SCHMIDT, R. G., 1983, Remote detection of metal anomalies on Pilot Mountain, Randolph County, North Carolina. *Economic Geology,* 78, 605-617.

MOIK, J. G., 1980, Digital processing of remotely sensed images. *NASA Special Publication SP-431* (Washington D. C.: NASA).

MOLLARD, J. D., 1962, Photo analysis and interpretation in engineering geology investigations: a review. *Reviews in Engineering Geology,* 1, 105-128.

MOLNAR, P., and TAPPONNIER, P., 1975, Cenozoic tectonics of Asia: effects of a continental collision. *Science,* 189, 419-426.

MOORE, J. D., and HINKLE, F., 1977, High-yield wells and springs along lineaments interpreted from Landsat imagery in Madison County, Alabama, USA. In *Karst Hydrogeology,* edited by J. S. JOLSON and F. L. DOYLE, 447-486.

MOORE, G. K. and WALTZ, F. A., 1983, Objective procedures for lineament enhancement and extraction. *Photogrammetric Engineering and Remote Sensing,* 49, 641-647.

MORRISELY, L. A., WEINSTOCK, K. J., MOUAT, D. A., and CARD, D. H., 1984, Statistical analysis of Thematic Mapper simulator data for the geobotanical discrimination of rock types in south west Oregon. *IEEE Transactions on Geoscience and Remote Sensing,* GE-22, 525-529.

MÜHLFELD, R., 1976, Relationship between vegetation, soil, bedrock and other geologic features in moderate humid climate (Central Europe) as seen on ERTS-1 imagery. *Geol. Jb.,* A-33, 21-35.

MYERS, V. I., 1975, Crops and soils. Chapter 22 in *Manual of Remote Sensing,* edited by R. G. REEVES (Fall Church, Virginia: American Society of Photogrammetry), 1715-1814.

_____, 1983, Remote sensing applications in agriculture. In *Manual of Remote Sensing,* edited by R. N. COLWELL, 2nd edition (Fall Church: American Society of Photogrammetry).

NASA, 1977, *Landsat Data User's Handbook* (Greenbelt, Maryland: NASA-TM-74722).

National Remote Sensing Centre (NRSC), 1987a, *SPOT Users Guide,* Fanborough, UK.

_____, 1987b, *Users Guide,* Fanborough, UK.

NIELSEN, K. C., and STERN, R. J., 1985, Post-Carboniferous tectonics in the Anadarko Basin, Oklahoma: evidence from side-looking radar imagery. *Geology,* 13, 409-412.

NOAA, 1986, *Landsat Data Users Notes,* Issue No. 35, South Dakota, USA.

NORMAN, J. W., 1969, Linear geological features as an aid to photogeological research. *Photogrammetry,* 25, 177-187.

NRSC - see National Remote Sensing Centre.

O'LEARY, D. W., FRIEDMAN, J. D. and POHN, H. A., 1976, Lineament, linear, lineation: Some proposed new standards for old terms. *Geological Society American Bulletin,* 87, 1463-1469.

OFFIELD, R. B., and ELGY, J., 1987, Geological mapping from remotely sensed data using tonal, textural and contextual features. In *Advances in Digital Image Processing,* Proceeding RSS Annual Conference, Nottingham 1987: Remote Sensing Society), 533-537.

OFFIELD, T. W., 1977, Structure mapping on enhanced Landsat images. *Geophysics,* 42, 482-500.

OFFIELD, T. W., ABBOTT, E. A., GILLESPIE, A. R. and LOGUERCIO, S. O., 1977, Structure mapping on enhanced Landsat images of southern Brazil: Tectonic control of mineralization and speculations on metallogeny. *Geophysics,* 42, 482-500.

OLSON, C. E., JR., 1960, Elements of photographic interpretation common to several sensors. *Photogrammetric Engineering,* 26, 651.

PARSON, A. J., and YEARLEY, R. J., 1986, An analysis of geologic lineaments seen on Landsat MSS imagery. *International Journal Remote Sensing,* 7, 1773-1782.

PASADENA, P. R., and CAEN, J. L. B., 1984, Surficial deposits of two Algerian playas as seen on SIR-A, Seasat and Landsat coregistered data. *Z. Geomorph.,* 28, 483-498.

PEACH, B. N., and HORNE, J., 1930, *Chapters on the Geology of Scotland* (Oxford).

PIASECKI, M. A. J., 1980, New light on the Moine rocks of the Central Highlands of Scotland. *J. Geol. Soc. London,* 137, 41-59.

PIASECKI, M. A. J., and VAN BREEMEN, O., 1979a, A Morarian age for the 'younger Moines' of central and western Scotland. *Nature,* 278, 734-736.

_____, 1979b, The 'Central Highland Granulites': cover-basement tectonics in the Moine. In *The Caledonides of the British Isles - Reviewed, Spec. Publ. Geol. Soc. London,* 8, 139-144.

PODWYSOCKI, M. H., GUNTHER, F. J., and BLODGET, H. W., 1977, *Discrimination of Rock Types by Digital Analysis of Landsat Data,* NASA X-923-77-17, 44 p.

PODWYSOCKI, M. H., MOIK, J. G., and SHOUP, W. C., 1975, Quantification of geologic lineaments by manual and machine processing techniques. *NASA Earth Resources Survey Symposium, Houston, Texas, June 1975,* NASA TM-X-58168, 885-903.

PODWYSOCKI, M. H., SALISBURY, J. W., BENDER, L. V., JONES, O. D., and MIMMS, D. L., 1983, Analysis of Landsat-4 TM data for lithologic and image mapping purposes. *NASA Conference Publication 2326,* 2, 35-39.

PODWYSOCKI, M. H., SEGAL, D. B., and JONES, O. D., 1983, Mapping of hydrothermally altered rocks using airborne multi-spectral scanner data, Marysvale, Utah, Mining District. *Advance Space Research,* 3, 101-112.

PODWYSOCKI, M. H., SEGAL, D. B., and ABRAMS, M. J., 1983, Use of multi-spectral scanner images for hydrothermal alteration in the Marysvale, Utah, mining area. *Economic Geology,* 78, 675-687.

PONTUAL, A., 1987, The effect of weathering minerals on the spectral response of rocks in Landsat TM imagery. In *Advances In Digital Image Processing,* Proceedings RSS Annual Conference, Nottingham 1987 (Nottingham: Remote Sensing Society), 549-558.

PRATT, W. K., 1978, *Digital Image Processing,* (New York: Wiley), 750 p.

PRESS, N. P., and NORMAN, J. W., 1972, Detection of ore bodies by remote-sensing the effects of metals on vegetation. *Inst. Mining and Metall. Trans.*, Section B, 81, 166-168.

PRICE, R. J., 1983, *Scotland's Environment During the Last 30,000 Years* (Edinburgh: Scottish Academic Press), 224 p.

PROST, G., 1980, Alteration mapping with airborne multi-spectral scanners. *Economic Geology*, 75, 894-906.

QARI, M. Y. H. T., 1989, Lithological mapping and structural analysis of Proterozoic rocks in part of the southern Arabian Shield using Landsat images. *Int. J. Remote Sensing*, 10, 499-503.

RAINES, G. L., 1978, Porphyry copper exploration model for northern Sonora, Mexico. *Journal Research U.S. Geological Survey*, 6, 51-58.

RAINES, G. L., and CANNEY, F. C., 1980, Vegetation and geology. In *Remote Sensing in Geology*, edited by B. S. SIEGAL and A. R. GILLESPIE (New York: John Wiley and Sons), 365-380.

RAINES, G. L., OFFIELD, T. W., and SANTOS, E. S., 1978, Remote sensing and subsurface definition of facies and structure related to uranium deposits, Powder River Basin, Wyoming. *Economic Geology*, 73, 1706-1723.

RAINES, G. L., and WYNN, J. C., 1982, Mapping of ultramafic rocks in a heavily vegetated terrain using Landsat data. *Economic Geology*, 77, 1755-1769.

RAJ, J. K., 1982, A reappraisal of the Bok-Bak fault zone. *Warta Geologi, Newsletter, Geol. Soc. Malaysia*, 8, 35-41.

RAKSHIT, A. M., and SWAMINATHAN, V. L., 1985, Application of digitally processed and enhanced Landsat imagery for geological mapping and mineral targeting in the Singhbhum Precambrian mineralized belt, Bihar-Orissa. *International Journal Remote Sensing*, 6, 457-471.

RAMBERG, I. B., GABRIELSEN, R. H., LARSEN, B. T., and SOLLI, A., 1977, Analysis of fracture patterns in southern Norway. *Geologie en Mijnbouw*, 56, 295-310.

RAY, R. G., 1960, Aerial photographs in geologic interpretation of mapping. *U. S. Geological Survey Professional Paper 373,* 230 p.

RAY, R. E., and FISCHER, W. A., 1957, Geology from the air. *Science,* 126, 725-735.

RAYNER, D. H., 1976, *The Stratigraphy of the British Isles* (Cambridge: Cambridge Univ. Press), 459 p.

REBILLARD, P., and BALLAIS, J. L., 1984, Surficial deposits of two Algerian playas as seen on SIR-A, Seasat and Landsat coregistered data. *Z. Geomorph. N. F.,* 28, 483-498.

REEVES, R., (ed.), 1975, Terrain and minerals: assessment and evaluation. In *Manual of Remote Sensing,* edited by R. G. REEVES, first edition (Fall Church, Virginia: American Society of Photogrammetry), 1107-1351.

RENNER, J. G. A., 1968, *The structural significance of lineaments in the Eastern Monsech area, Province of Lerida, Spain* (Delft: ITC Publications, Series B, No. 45), 29 p.

RICH, J. L., 1928, Jointing in limestone as seen from the air. *American Association Petroleum Geologists Bulletin,* 12, 861-862.

RICHASON, B. F., JR., 1978, *Introduction to Remote Sensing of the Environment,* first edition (Dubuque, Iowa: Kendall/Hunt), p. 4.

RILEY, C. H., 1959, *Our Mineral Resources* (New York: John Wiley & Sons), 338 p.

RINGROSE, P. S., and DAVENPORT, C. A., 1988, Enhancement of glacial fractures by analysis of TM data: Glen Roy, Scotland. In *Remote Sensing: Moving Towards 21st Century,* 1988 International Geoscience and Remote Sensing Symposium (Edinburgh: European Scape Agency), 741-744.

ROBINSON, J. E., and CARROLL, S., 1977, Software for geologic processing of Landsat imagery. *Computer and Geosciences,* 3, 459-464.

ROSENFELD, A., and KAK, A. C., 1976, *Digital Picture Processing* (New York: Academic Press).

ROTHERY, D. A., 1985, Interactive processing of satellite images for geological interpretation—a case study. *Geological Magazine,* 122, 57-63.

_____, 1987a, Decorrelation stretching and related techniques as an aid to image interpretation in geology. In *Advances in Digital Image Processing,* Proceedings RSS Annual Conference 1987 (Nottingham: Remote Sensing Society), 194-203.

_____, 1987b, Improved discrimination of rock units using Landsat Thematic Mapper imagery of the Oman ophiolite. *Journal Geological Society London,* 144, 587-597.

ROTHERY, D. A., and DRURY, S.A., 1984, The neotectonics of the Tibetan Plateau. *Tectonics,* 3, 19-26.

ROTHERY, D. A., HUNTER, W. M., DRURY, S. A., and HUNT, G. A., 1986, Large scale geological mapping using airborne thematic mapper imagery in Western Australia. In *Mapping from Modern Imagery* (Proceeding RSS Annual Meeting 1986 (Edinburgh: Remote Sensing Society), 359-368.

ROTHERY, D. A., and MILTON, E. J., 1981, Lithological discrimination in an ophiolite terrain: Landsat MSS imagery and reflectance measurements in Oman. In *Geological and Terrain Analysis Applications of Remote Sensing,* edited by J. A. ALLEN and M. J. BRADSHAW (Remote Sensing Society), 3-23.

ROWAN, R. L., 1975, Application of satellites to geological exploration. *American Scientist,* 63, 393-403.

ROWAN, L.C., GOETZ, A. F., and ASHLEY, R.P., 1977, Discrimination of Hydrothermally Altered and Unaltered Rocks in Visible and Near-Infrared Multi-spectral Images. *Geophysics,* 42, 522-535.

ROWAN, L. C., and LATHRAM, E. H., 1980, Mineral exploration. In *Remote Sensing In Geology,* edited by B. S. SIEGAL and A. R. GILLESPIE, (New York: Wiley), 553-605.

ROWAN, L. C., WETLAUFER, A. F., GOETZ, A. F., BILLINGSLEY, F. C., and STEWART, J., 1974, Discrimination of rock types and detection of hydrothermally altered areas in south-central Nevada by the used of computer-enhanced ERTS images. *U.S. Geological Survey Professional Paper 883,* 35 p.

RUMSEY, I. A. P., 1971, Relationship of fractures in unconsolidated superficial deposits to those in the underlying bedrock. *Modern Geology,* 3, 25-41.

SABIN, F. F. JR., 1983, Geologic interpretation of space shuttle radar images of Indonesia. *American Association Petroleum Geologists Bulletin,* 67, 2076-2099.

_____, 1987, *Remote sensing-principles and interpretation,* second edition (New York: W. H. Freeman and Company), 449 p.

SABIN, F. F., BLOM, R., and ELACHI, C., 1980, Seasat radar image of the San Andreas fault, California. *American Association Petroleum Geologists Bulletin,* 64, 619-628.

SANTISTEBAN, A., and MUNOZ, L., Principal components of a multi-spectral image: application to a geological problem. *IBM J. Res. Develop.,* 22, 444-454.

SARAF, A. K., CRACKNELL, A. P., and MCMANUS, J., 1987, Remote sensing for geobotanical studies in the Central Grampian Highlands of Scotland. In *Advances in Digital Image Processing,* Proceedings RSS Annual Conference 1987 (Nottingham: Remote Sensing Society), 225-232.

_____, 1989, Geological application of airborne Thematic Mapper data in Sutherland, north-west Scotland. *International Journal Remote Sensing,* 10, 545-555.

SCHULTEJANN, P. A., 1985, Structural trends in Borrego Valley, California: interpretations from SIR-A and SESAT SAR. *Photogrammetric Engineering and Remote Sensing,* 51, 1615-1624.

SEGAL, D. B., 1983, Use of Landsat multi-spectral scanner data for the definition of limonitic exposure in heavily vegetated areas. *Economic Geology,* 78, 711-722.

SESUREN, A., 1976, Lineament analysis from ERTS (Landsat) images of the Netherlands. *Geologie en Mijnbouw,* 55, 61-67.

_____, 1984, Geological interpretation of Landsat imagery of the Bangladesh Ganges delta. *ITC Journal,* 3-1984, 229-232.

SETTLE, M., and TARANIK, J. V., 1982, Use of the space shuttle for remote sensing research: recent results and future prospects. *Science*, 218, 993-995.

SETTLE, M., CHAVEZ, P., EVERETT, J. R., KAHLE, A. B., KIEFFER, H. H., KITCHO, C. A., MILTON, N. M., and MOUAT, D. A., 1983, Thematic Mapper data analysis. In *Frontier For Geological Remote Sensing From Space*, Report of the Fourth Geosat Workshop (Arizona: American Society of Photogrammetry), 21-26.

SHAZLY, H. EL., 1987, Discrimination of geological features using digital and photographical enhancements of Landsat MSS data. *Journal of African Earth Sciences*, 6, 119-126.

SHEFFIELD, C., 1985, Selecting band combinations from multi-spectral data. *Photogrammetric Engineering and Remote Sensing*, 51, 681-687.

SHORT, N. M., 1982, *The Landsat Tutorial Workbook*, NASA reference publication 1078 (Washington: NASA Scientific and Technical Information Branch), 553 p.

SHORT, N. M. and LOWMAN, P. D., 1973, *Earth observations from space-outlook for the geological sciences* (New York: Goddard Space Flight Center), Report X-650-73-316.

SIEGAL, B. S., and ABRAMS, M. J., 1976, Geologic mapping using Landsat data. *Photogrammetric Engineering and Remote Sensing*, 42, 325-337.

SIEGAL, B. S., and GOETZ, A. F. H., 1977, Effect of vegetation on rock and soil type discrimination. *Photogrammetric Engineering and Remote Sensing*, 43, 191-196.

SIEGAL, B. S., and GILLESPIE, A. R., 1980, *Remote Sensing In Geology* (New York: Wiley and Sons, Inc.).

SIEGAL, B. S., and SHORT, N. M., 1977, Significance of operator variation and the angle of illumination in lineament analysis on synoptic images. *Modern Geology*, 6, 75-85.

SIEGRIST, A. W., and SCHNETZLER, C. C., 1980, Optimum spectral bands for rock discrimination. *Photogrammetric Engineering and Remote Sensing,* 46, 1207-1215.

SIMONETT, D. S., (ed.), 1983, The development and principles of remote sensing. In *Manual of Remote Sensing*, second edition, edited by R. N. Colwell (Fall Church, Virginia: American Society of Photogrammetry), p. 2-13.

SINGH, A., and HARRISON, A., 1985, Standardised principal components. *International Journal of Remote Sensing,* 6, 883-896.

SKALEY, J. E., FISHER, J. R., and HARDY, E. E., 1977, A color prediction model for imagery analysis. *Photogrammetric Engineering and Remote Sensing,* 43, 45.

SLATER, P. N., 1979, A re-examination of the Landsat MSS. *Photogrammetric Engineering and Remote Sensing,* 45, 1479-1485.

_____, 1980, *Remote Sensing: Optics and Optical Systems* (Reading, Mass.: Addison-Wesley).

SMITH, D. I., 1961, Patterns of minor faults in the south-central Highlands of Scotland. *Bulletin Geological Survey Great Britain,* 17, 145-152.

SMITH, J. A., 1983, Matter-energy interactions in the optical region. Chapter 3 of *Manual of Remote Sensing,* edited by R. N. COLWELL (Fall Church: American Society of Photogrammetry).

SMITH, H. T. U., 1943, *Aerial Photographs and their Applications* (New York: Appleton-Centry-Crofts). 372 p.

SMITH, W. L.; 1977, Remote sensing applications for mineral resources. In *Remote Sensing Application for Mineral Exploration,* edited by W. L. SMITH (Stroudburg, Pennsylvania: Dowden Hutchinson and Rodd, Inc.).

SMITHURST, L. J. M., VAUGHAN, R. A., and STONE, P., 1987, An evaluation of remote sensing techniques for lithological discrimination and lineament analysis in the Ballantrae Complex, SW Scotland. In *Advances in Digital Image Processing,* Proceedings RSS Annual Conference 1987 (Nottingham: Remote Sensing Society), 580-592.

Soil Survey of Scotland, 1976, *Systematic Soil Survey Map,* sheet 84 and part sheet 94, scale 1:63,360.

Southworth, C. S., 1985, Characteristics and availability of data from earth-imaging satellites. *U. S. Geol. Surv. Bull. 1631* (Washington, D. C.: U.S. Geol. Surv.), 102 p.

Spray, J. G., and Burges, L. A., 1985, Landsat MSS imagery applied to geological investigation of the Norseman area granitoid-greenstone terrain, southeast Yilgarn Block, Western Australia. *Geological Magazine,* 122, 587-594.

Stefouli, M., and Osmaston; H. A., 1984, The remote sensing of geological linear features using Landsat: matching analytical approaches to practical applications. In *Satellite Remote Sensing-review and preview,* Proceeding RSS Annual Conference 1984 (Reading: Remote Sensing Society), 227-236.

Styles, P. J., 1988, The production of anaglyphs from SPOT-HRV panchromatic data for geomorphological mapping. In *Remote Sensing: Moving Towards the 21st Century,* 1988 International Geoscience and Remote Sensing Symposium (Edinburgh: European Space Agency), 485-487.

Suits, G. H., 1983, The nature of electromagnetic radiation, Chapter 2 in *Manual of Remote Sensing,* edited by R. G. Reeve (Falls Church, VA: American Society of Photogrammetry).

Sultan, M., Arvidson, R. E., and Guinness, E. A., 1987, Lithologic mapping in arid regions with Landsat thematic mapper data: Meatiq dome, Egypt. *Geological Society America Bulletin,* 99, 748-762.

Swain, P. H., and Davis, S. M., 1978, *Remote Sensing: the Quantitative Approach* (New York: McGraw-Hill).

Swaminathan, V. L., Kamath, D. S., Rakshit, A. M., Chakrebarty, D. K., and Kurien, T. K., 1983, Application of remote sensing techniques in mineral resources survey - a case study pertaining to Singhbhum shear zone, Bihar, India. *Advance Space Research,* 3, 55.

Talvitie, J., 1979, Remote sensing and geobotanical prospecting in Findland. *Geological Society Findland Bulletin,* 51, 63-73.

TARANIK, J. V., 1978, Principles of computer processing of Landsat data for geological application. *U. S. Geological Survey Open File Report 78-187* (Washington D. C.: U. S. Department of Interior).

TAYLOR, M. M., 1974, Principal components colour display of ERTS imagery. *Third Earth Resources Technological Satellite Symposium, Dec., 1973, Washington, D. C.*, NASA SP-351, 1877-1898.

THOMAS, I. L., BENNING, V. M., and CHING, N. P., 1987, *Classification of Remotely Sensed Images* (Bristol: Adam Hilger).

THORP, M. B., THOMAS, M. F., MARTIN, T., and WHALLEY, W. B., 1990, Late Pleistocene sedimentation and landform development in western Kalimantan (Indonesian Borneo). *Geologie en Mijnbouw*, 69, 133-150.

TIBALDI, A., and FERRARI, M., 1988, Potential of Landsat TM image for crystalline rock type discrimination: Gregory Rift, Kenya. *Geocarto International*, 3, 3-12.

TJIA, H. D., 1971, Lineament pattern on Penang Island, West Malaysia. *J. Trop. Geogr.*, 32, 56-61.

_____, 1972, Lineamen-lineamen Malaysia Barat. *Ilmu Alam* (Kuala Lumpur), 1, 24-31.

_____, 1973, Geomorphology. In *The Geology of the Malay Peninsula*, edited by D. J. GOBBETT and C. S. HUTCHISON (New York: John Wiley).

_____, 1978, Structural geology of Peninsular Malaysia. *3rd. Regional Conference on Geology and Mineral Resources of Southeast Asia*, Bangkok, Thailand in Nov., 1978, 673-682.

TJIA, H. D., and ZAITON HARUN, 1985, Regional structures of Peninsular Malaysia. *Sains Malaysiana (Sains Bumi)*, 14, 95-107.

TOMES, B. J., MARRS, R. W. and PARKER, R. B., 1974, Comparison of ERTS, Skylab 190 A and 190 B Sensors, and aircraft photographs for lineation mapping. *Contribution to Geology*, 12, 61-68.

TOWNSEND, T. E., 1987, A comparison of Landsat MSS and TM imagery for interpretation of geologic structure. *Photogrammetric Engineering and Remote Sensing*, 53, 1245-1249.

TOWNSHEND, J. R. G., (Ed.) 1981, *Terrain Analysis and Remote Sensing* (London: George Allen and Unwin).

_____, 1984, Agricultural land-cover discrimination using thematic mapper spectral bands. *Int. J. Remote Sensing*, 5, 681-698.

TUCKER, C. J., 1979, Red and photographic infrared linear combinations for monitoring vegetation. *Remote Sensing of Environment*, 10, 127-150.

TUNSTALL, K. W., 1975, Recognizing patterns: are there processes that precede feature analysis? *Pattern Recognition*, 7, 95-106.

TURNER, R. E., RAINES, G. L., KLEINKOPF, M. D., and LEE-MORENO, J. L., 1982, Regional northeast trending structural control of mineralization, northern Sonora, Mexico. *Economic Geology*, 77, 25-37.

U. S. GEOLOGICAL SURVEY, 1979, *Landsat Data User's Handbook* (revised, Sioux Falls, South Dakota).

VILJOEN, R. P., VILJOEN, M. J., GROOTENBOER, J., and LONGSHAW, T. G., 1975, ERTS-1 imagery: an appraisal of applications in geology and mineral exploration. *Minerals Science Engineering*, 7, 132-168.

VINCENT, R. K., and SCOTT, G. N., 1978, Ground water exploration in Northwestern Tamil Naidu, India, with Landsat data. *Proceedings of the 12th Inter. Sympos. Rem. Sensing Environment*, 3, April 1978, 1053-1060.

WADGE, G., and DIXON, T. H., 1984, A geological interpretation of Seasat-sar imagery of Jamaica. *J. of Geology*, 92, 561-581.

WAN FUAD WAN HASSAN, 1989, Some characteristics of the heavy detrital minerals from Peninsular Malaysia. *Geol. Soc. Malaysia Bull.*, 24, 1-12.

WARNER, T. A., 1985, Rock discrimination in the Orange Free State using digitally processed Landsat imagery. *South African Journal of Photogrammetry, Remote Sensing and Cartography,* 14, 259-270.

WATSON, A. I., 1984, The physical basis of remote sensing. *Proceedings Univ. Dundee Summer School "Remote Sensing Application In Civil Engineering" Dundee Aug-Sept 1984,* 9-13.

_____, 1987, A new method of classification for Landsat data using the 'watershed' algorithm. *Pattern Recognition Letters,* 6, 15-19.

WELBY, C. W., 1976, Landsat-1 imagery for geologic evaluation. *Photogrammetric Engineering and Remote Sensing,* 42, 1411-1419.

WHEELER, R. L., 1983, Linesmanship and the practice of linear geo-art: discussion. *Geological Society America Bulletin,* 94, 1377-1378.

WHITTEN, D. G. A., and BROOKS, J. R. V., 1972, *Dictionary of Geology,* reprinted 1985 (Middlesex: Penguin Books).

WHITTOW, J. B., 1977, *Geology and Scenery In Scotland*, reprinted 1982 (Middlesex: Penguin Books), 362 p.

WILLIAMS, D. F., 1984, Overview of NERC airborne thematic mapper campaign of September 1982. *Int. J. Remote Sensing,* 5, 631-634.

WILLIAMS, R. S. JR., (Sub-editor), 1983, Geological applications. In *Manual of Remote Sensing*, second edition, edited by R. N. COLWELL (Falls Church: American Society of Photogrammetry), 1667-1951.

WILLIAMS, R. S. JR., and CARTER, W. D., (ed.) 1976, ERTS-1: A new window on our planet. *U.S. Geological Survey Professional Paper 929* (Washington: U. S. Government Printing Office), 362 p.

WISE, D. U., 1976, Linesmanship: Guidelines for a thriving geological artform. In *Proc. First Internat. Conf. In the New Basement Tectonics, Utah 1974,* Utah Geol. Ass. Paper Publ., 5, 635-636.

_____, 1982, Linesmanship and the practice of linear geo-art. *Geological Society America Bulletin,* 93, 886-888.

_____, 1983, Linesmanship and the practice of linear geo-art: reply. *Geological Society America Bulletin*, 94, 1379.

WRIGHT, G. G. and BIRNIE, R. V., 1986, Detection of surface soil variation using high resolution satellite data: result from the UK SPOT-simulation investigation. *Int. J. Remote Sensing*, 7, 757-766.

YOST, E. F., and WENDEROTH, S., 1967, Multi-spectral colour aerial photography. *Photogrammetric Engineering*, 33, 1020-1032.

ZIEGLER, P. A., 1982, *Geological Atlas of Western and Central Europe.* Shell Petroleum, 130 p.

ZILIOLI, E., and ANTONINETTI, M., 1987, Geostructural evolution of the Southern Alps: lineaments trends detected on Landsat images. *Remote Sensing of Environment*, 23, 479-492.

SUPERFICIAL DEPOSITS MAP OF THE LOCHINDORB AREA, SCOTLAND.

(BASED ON VISUAL INTERPRETATION OF TM IMAGERY AND AERIAL PHOTOGRAPHS, AND FIELD VISITS)

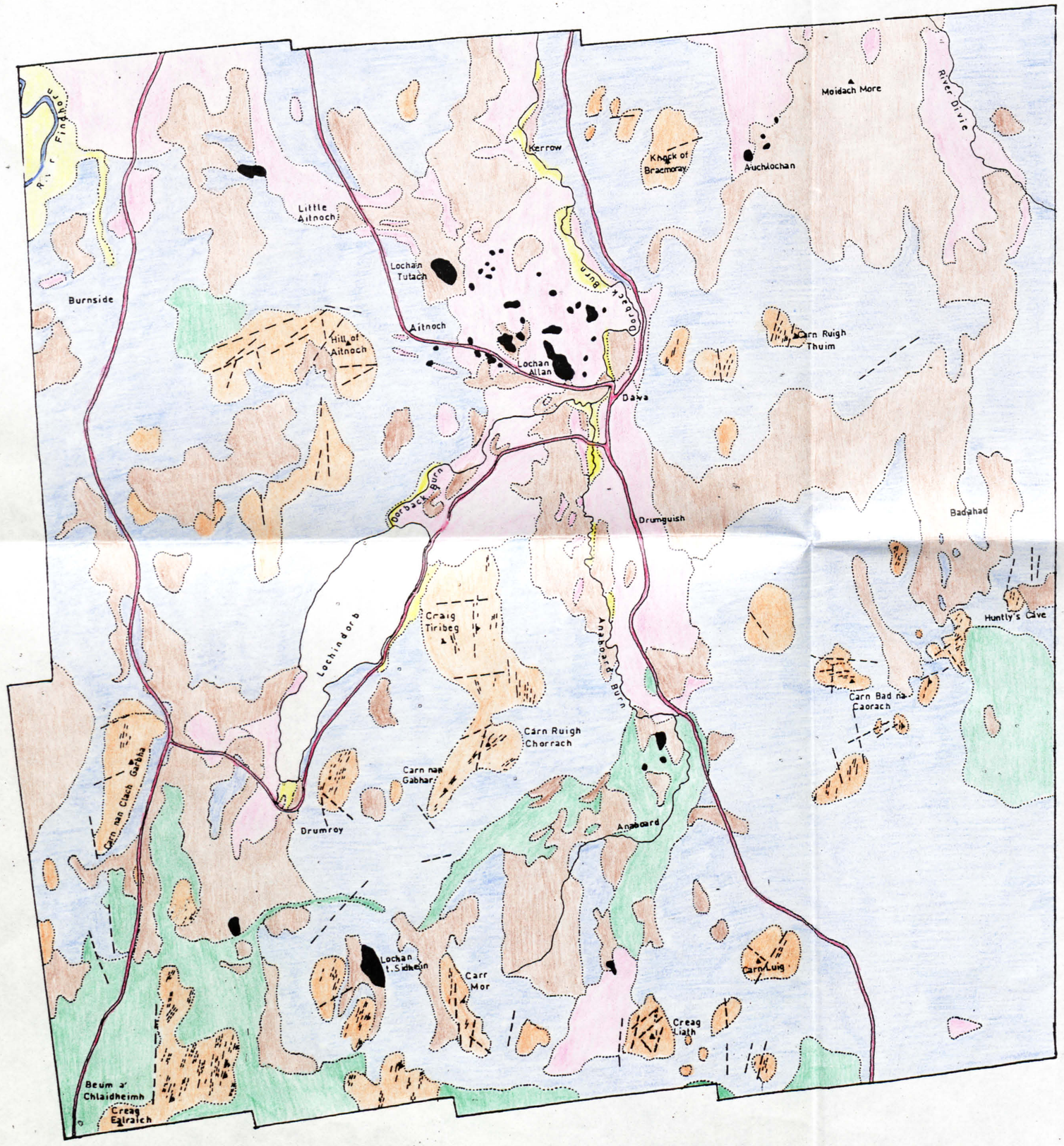

EXPLANATION

DRIFT

	Freshwater alluvial floodplains and terraces at different levels	RECENT and PLEISTOCENE
	Peat	
	Glacial sand and gravel	
	Moraines and morainic drift	
	Boulder clay and undifferentiated drift	

SOLID

	Granite with local basic modification	LATE-SILURIAN to DEVONIAN
	Psammites and semi-pelites with subordinate quartzites	GRAMPIAN DIVISION ('Young Moine')
	Psammitic and siliceous gneisses, interbanded with belts of quartzite and pelitic gneiss	CENTRAL HIGHLAND DIVISION ('Old Moine')

	Bedding traces		River
	Dip direction		Main road
	Lineament		Loch
	Geological boundary	▲	Hill summit

Age of the units are based on the drift map, sheet 84 E, BGS (1978), and Allison et al., (1988).

1 0 1 2 km

N

Figure 7.9

M A Juhari, Stirling University, 1990